Discovery of Small Molecule Epigenetic Modulators

Moses Moustakim
Keble College
Trinity Term 2018

Synthesis for Biology and Medicine Centre for Doctoral Training, Structural Genomics Consortium and Chemistry Research Laboratory

A thesis submitted in partial fulfilment of the requirements of the degree of Doctor of Philosophy

Abstract

Target validation is increasingly becoming a central tenet to successful execution of drug discovery campaigns. An emerging approach towards the development of novel therapies for previously untreated diseases is the development of small molecule chemical probes which can be used as early stage tools for pertinent biological questions to be explored about a molecular target within the context of disease.

A number of proteins which regulate epigenetic mechanisms have been correlated with disease onset and progression. Despite disease links, there remains a paucity in the understanding by which many of these pathologically relevant proteins exert their phenotypic effect when dysregulated. The discovery of novel chemical probes will facilitate further understanding of the underlying biology of these epigenetic targets.

This thesis reports on the discovery and development of chemical probes and inhibitors of epigenetic proteins. A series of synthetic medicinal chemistry efforts is described towards the multi-faceted improvements of lead compounds by means of potency, selectivity and cell activity against their cognate targets.

In chapter 1 the associated concepts, primary literature and core principles of the subsequent chapters are comprehensively examined. In chapter 2 a report on the discovery of the first chemical probe for the bromodomains of p300/CBP Associated Factor (PCAF) and General Control Nonderepressible 5 (GCN5) proteins, previously untargeted and disease relevant protein domains is described. Following this, chapter 3 describes the development of inhibitors of the second macrodomain of polyadenosine diphosphate ribosylating protein 14 (PARP14) building on the understanding of SAR around the target and reporting the most potent ligand described to date. Chapter 4 then goes on to describe the discovery a chemical probe for the YEATS domain containing proteins ENL and Af9. Up to this date there have been no reported inhibitors or chemical probes for the YEATS domain containing proteins despite numerous links to cancers.

The final chapter 5 describes the outputs from the industrial placement period of my doctoral training during which synthetic methodology and total synthesis research at Vertex Pharmaceuticals was carried out. In this chapter the substrate scope of an additive free UV-A promoted photocyclisation of aryl-enamines to spiroindolines is described. The utility of this additive-free complexity building reaction is demonstrated through the formal synthesis of an alkaloid natural product (±)-horsfiline.

One foot in front of the other.

Acknowledgements

I would like to first thank my supervisors Paul Brennan and Darren Dixon for providing me a supportive and encouraging environment to explore scientific interests. I am very grateful for the intellectual input and mentorship that both Darren and Paul have provided to me over the past three to four years. I would also like to extend a thank you to the directors and administrators of the Synthesis for Biology and Medicine Centre for Doctoral Training (SBM CDT) who have been an invaluable source of support in navigating many processes over the doctoral degree. I would also like to thank Keble College, the EPSRC and industrial partners of the SBM CDT for funding my DPhil.

The Structural Genomics Consortium (SGC), Target Discovery Institute (TDI) and Nuffield Department of Medicine (NDM) have been excellent environments to conduct scientific research. I feel very fortunate to have been able to make use of the well-equipped facilities in these institutes and I am very grateful to the those who strive to ensure the future funding of these institutes.

Within the SGC/TDI I would like to say thank you to the people who have helped me learn some of the biological techniques relevant to the work in this thesis including; Apirat Chaikuad (ITC/protein expression), Finnian Wolfreys (protein expression), Cynthia Tallant Blanco (ITC/protein expression), Octovia P. Monteiro (AlphaScreen) and Matthias T. Ehebauer (protein expression).

I would also like to extend thanks to those who have been involved in the biochemical and biophysical screening assays which supported the development of the medicinal chemistry projects described in this thesis in addition to those involved in cellular experiments. In particular I would like to thank Octovia P. Monteiro, James Bennett, Thomas Christott, Charline Giroud, Marion Schüller, Catherine Rogers, Jennifer Ward and Andrew Lewis.

Thank you to those who helped enable my internship at Vertex Pharmaceuticals; Mike Mortimore, Jeremy Green, Michael Boyd and Brian Ledford. I would also like to thank all of the Vertex employees I had the pleasure of working alongside during my tenure at the Boston laboratories. A mention goes out to Jacob Bush and Andi Grote for being great lab partners.

I would like to thank the members of the Brennan group laboratory who have helped to make this an enriching period of my training. There have been a number of group members who I have had the

pleasure of working alongside over the years, I would like to thank (in no particular order); Miranda Wright, Gian Filippo Ruda, Saleta Vazquez Rodriguez, Tamas Szommer, Robert Quinlan, Vincent Fagan, Stephane De Cesco, Mark McLaughlin and many others for the numerous social and academic activities we were able to enjoy together.

More broadly I would like to extend thanks to the support staff of both the NDM and SGC whose tireless work have enabled the research to continue unhindered in both departments. I would like to thank the NDM finance team, the NDM administration team, Ross Macrae, Darren Blase, Andrew Keepence-Keyte, Ling Jinks, Omar Rivas Rosiles, Christopher Sluman, David Damerell, Brian Marsden and many more.

I would like to thank my parents Rita and Mohamed for instilling an early sense of resilience and encouraging an interest in higher education in the first place. Without their encouragement I would not have been able to have recovered from failing my GCSEs to eventually engaging in doctoral study. I would like to thank my brothers for their support and our friend Antar for being the strongest person we knew.

Finally, I am eternally grateful to my partner Yasemin, who knew me long before the journey towards a doctoral degree. I am extremely appreciative of the compassion and support she has shown me over the many years. Her understanding of the time I needed to commit to the laboratory was essential to the completion of this work. I am also excited to be sharing the experience with her in the next stage of our lives.

Table of Contents

List of Figures

List of Schemes

List of Tables

Abbreviations

5-HT	5-hydroxytryptamine receptor
α-KGDH	α-ketoglutarate dehydrogenase
ADME	Absorption, distribution, metabolism and excretion
Ac	Acetyl
ADP	Adenosine diphosphate
ADPR	Adenosine diphosphate ribosylating
AlphaScreen	Amplified luminescent proximity homogeneous assay screen
ALT	Alternate lengthening of telomeres
ALL	Acute lymphoblastic leukaemia
ART	Adenine diphosphate ribosyltransferase
ATAD2	ATPase family, AAA domain containing 2
BAF	BRG1/BRM associated factor
BAZ2A	Bromodomain adjacent to zinc finger domain A
BAZ2B	Bromodomain adjacent to zinc finger domain B
BBB	Blood brain barrier
BET	Bromodomain and extra-terminal
Boc	*tert*-Butoxycarbonyl
Bn	Benzyl
BRD	Bromodomain
Bcl-2	B-cell lymphoma 2 protein
BCP	Bromodomain containing protein
BRD2-4	Bromodomain containing proteins 2-4
BRD7	Bromodomain-containing protein 7
BRD9	Bromodomain-containing protein 9
BRET	Bioluminescence resonance energy transfer
CBP	CREB binding protein
CCL2	Chemokine (C-C motif) ligand 2

CECR2	Cat eye syndrome critical region 2 protein
CETSA	Cellular thermal shift assay
clogP	Calculated partition coefficient
clogD	Calculated distribution coefficient
c-Myc	Myeolocytomatosis viral oncogene homologue
DBU	1,8-Diazabicyclo[5.4.0]undec-7-ene
ΔT_m	Change in melting point (thermal shift)
DDR	DNA damage response
DMF	*N, N*-dimethylformamide
DMSO	Dimethylsulfoxide
DPF	Double plant homeodomain finger
DOT1L	Disruptor of telomeric silencing 1-like
DSF	Differential scanning fluorimetry
dTAG	Degradation tag
E	Glutamic acid
EC_{50}	Half maximal effective concentration
ER	Endoplasmic reticulum
Et	Ethyl
EA	Ethyl Acetate
EDG	Electron donating group
EWG	Electron withdrawing group
F	Phenylalanine
FALZ	Foetal Alzheimer antigen
FRET	Förster resonance energy transfer
G_1	Growth phase 1
GCN5	General control non-depressible protein 5
GNAT	GCN5-related *N*-acetyltransferase
GST	Glutathione S-transferase
H	Histidine

HATU	1-[Bis(dimethylamino)methylene]-1H-1,2,3-triazolo[4,5-b]pyridinium 3-oxide hexafluorophosphate
Hdm2	Huma double minute 2 homolog
HEK293	Human embryonic kidney 293
HIV	Human immunodeficiency virus
HPLC	High performance liquid chromatography
HRMS	High resolution mass spectrometry
HTRF	Homogenous time resolved resonance fluorescence
iART	Inactive adenine diphosphate ribosyltransferase
IBS	Illustrator for biological sequences
IC_{50}	Half maximal inhibitory concentration
IL1-α	Interleukin 1 α
IL-6	Interleukin 6
IL-8	Interleukin 8
ITC	Isothermal titration calorimetry
K	Lysine
KAc	Acetyllysine
Kappa-κ	κ opioid receptor
KCr	Crotonyllysine
K_D	Dissociation constant
KD	Knockdown
KDa	Kilo Dalton
KDM	Lysine demethylase
KO	Knockout
L	Leucine
LED	Light emitting diode
LiHMDS	Lithium bis(trimethylsilyl)amide
LRMS	Low resolution mass spectrometry
M	Methionine

MDCK-MDR1	Madin darby canine kidney-multi drug resistance gene 1
MCP-1	Monocyte chemoattractant protein 1
MCF7	Michigan Cancer Foundation-7
Mp	Melting point
MLLT1	Mixed lineage leukaemia protein 1
MLLT3	Mixed lineage leukaemia protein 3
MLL	Mixed lineage leukaemia
MKL-1	Megakaryotic leukaemia 1
MMP 9	Matrix metallopeptidase 9
MOZ	Monocytic leukaemia zinc finger
MSC	Mesenchymal stem cell
Mu-μ	Mu opioid receptor
MW	Molecular weight
NAD^+	Nicotinamide adenine dinucleotide
NanoBRET	Nanoluciferase bioluminescence resonance energy transfer
NCI	National cancer institute
NER	Nucleotide excision repair
NF-κB	Nuclear factor κB
NP	Nucleoprotein
OPRL1	Opioid receptor-like 1
p21	Clyclin-dependent kinase inhibitor 1 (protein of 21 Kilo Dalton molecular weight)
p300	E1A binding protein (protein of 300 Kilo Dalton molecular weight)
p53	Tumour suppressor protein (protein of 53 Kilo Dalton molecular weight)
PAF1	Polymerase associated factor 1
PARG	Poly(ADP)ribose glycohydrolase
PART	Polyadenine diphosphate ribosyltransferase
PB1-5	Polybromo protein 1-5
PCAF	p300/CBP associated factor
Pgp	Permeability glycoprotein

Ph	Phenyl
PLK4	Polo like kinase 4
POI	Protein of interest
PROTAC	Proteolysis targeting chimera
PTEN	Phosphatase and tensin homolog
RING	Really interesting new gene
S	Serine
siRNA	Small interfering RNA
SAGA	Spt-Ada-GCN5-Acetyltransferase complex
SAHA	Suberoylanilide hydroxamic acid
SCA7	Spinocerebellar ataxia type 7
SEC	Superelongation complex
SEM	Standard error of mean
SGC	Structural Genomics Consortium
shRNA	Short hairpin RNA
SMARCA	SWI/SNF related, matrix associated, actin dependent, regulator of chromatin, subfamily A
STAT6	Signal transducer and activator of transcription 6
STD-NMR	Saturation transfer difference nuclear magnetic resonance
TAF1	Transcription initiation factor TFIID subunit 1
Tat	Transactivator of transcription
TEA	Triethylamine
TES	Triethylsilyl
TBS	*tert*-butyldimethylsilyl
THF	Tetrohydrofuran
TNF-α	Tumour necrosis factor α
TRIM24	Tripartite motif-containing 24
TRIM28	Tripartite motif-containing 28
T_m	Melting point (biomolecule)

UCC	Urothelial carcinoma
W	Tryptophan
Wnt	Wingless-type MMTV (mouse mammary tumour virus)
YD	YEATS Domain
ZF	Zinc Finger

List of Data and Experiments Contributed by Others

Chapter 2

- Differential Scanning Fluorimetry (DSF) assays were carried out by Oleg Fedorov and Octovia P. Monteiro (SGC/TDI).
- NanoBRET experiments were carried out by collaborators Danette Daniels and Jacqui Mendez-Johnson (Promega Corporation).
- Pharmacokinetic studies were carried out at Charles River Laboratories.
- MDCK-MDR1 permeability assays were carried out at Cyprotex.
- Expression of recombinant PCAF and GCN5 protein was carried out by Apirat Chaikuad (SGC, PCAF) and Matthias T. Ehebauer (PCAF/GCN5, ODDI).
- Homogenous Time Resolved Resonance Fluorescence (HTRF) assays were carried out by the author and Emma Murphy (ODDI).
- Previous inhibitors described were synthesised by Peter G. K. Clark (Oxford Chemistry) and Laura Trulli (Oxford Chemistry).
- Expression and purification of recombinant *Pf*GCN5 protein, Isothermal Titration Calorimetry (ITC) with *Pf*GCN5 and crystallography with *Pf*GCN5 was carried out by Raymond Hui, John R. Walker, Yu-Hui Lin and Chung-Feng D. Hou (SGC Toronto).
- Cellular viability studies using PBMCs were carried out by Hongbing Yang and Lucy Dorrell (Oxford NDORMS).
- Parasitic growth inhibition assays were carried out by Michael Duffy (Uni. Of Melbourne).
- *In vivo* PK studies were carried out through UCB Pharma Ltd.

Chapter 3

- Previous compounds in the carbazole series were synthesised by collaborators Kerstin Reidel and Franz Bracher at Ludwig-Maximillans University (LMU, Munich).
- Primary assays such as AlphaScreen, BLI and ITC were carried out by Marion Schüller.
- Expression and purification of recombinant PARP14 MD2 protein was carried out by Marion Schüller.

Chapter 4

- Expression and purification of ENL and Af9 YD proteins was carried out by Thomas Christott and Paul Smith.
- Primary binding assays such as AlphaScreen were carried out by Octovia P. Monteiro and Thomas Christott.
- BLI experiments were carried out by James Bennett.
- ITC experiments were carried out by the author and Thomas Christott.
- NanoBRET experiments were carried out by Vicki Gamble and Gillian Farnie.
- Cell proliferation studies were carried out by Catherine Rogers and Kilian Huber.
- Pharmacokinetic studies were carried out at UCB Pharma Ltd.

Chapter 5

- Additional compounds **444**-**449** and **451**-**452** included in the substrate scope section of this chapter were synthesised by Jacob Garwin.

1. Introduction

1.1 Overview

1.1.1 Drug Discovery

There exists a number of approaches to interrogate the structure, role, function and relevance of a particular biomolecule to the onset and progression of disease states. These approaches that can be employed to engage with a therapeutically relevant biomolecule include the development of antibodies,[1] peptidic drugs,[2] conjugates,[3,4] small interference RNAs,[5–9] CRISPR gene editing technologies[10–16], intrabodies[17,18] and small molecules.[15,19–21] Since the advent of the chemical sciences as a discipline for research, significant efforts have been applied towards the development of new chemical agents capable of alleviating human diseases.

Over the past century there has been significant advances made in the fashion in which small molecule drugs are discovered, developed and approved. Whilst the occurrence of a number of diseases in the human population such as infectious, cardiovascular, oncological and inflammatory amongst others have been challenged by the development of small molecule therapeutics, there exists a constant evolution of disease which must be met by small molecule drug discovery efforts of increasing levels of complexity and success. As the process of drug discovery and development becomes increasingly complex there are more significant criteria that need to be achieved in order for a small molecule therapeutic to be produced, vended and administered to patients legally and acquire drug status. A cornerstone of the likelihood that a small molecule will transition through the drug discovery process (Figure 1.1) and avoid attrition is the efficacy of the drug candidate within the context of the disease it is intended to treat.

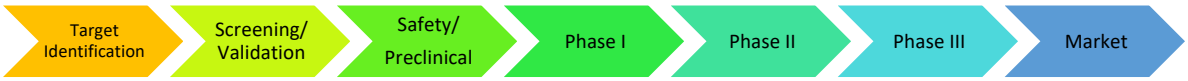

Figure 1.1 Drug discovery and development pipeline.

Currently in 2018 one of the largest market economies for the consumption and sales of pharmaceuticals including small molecule drugs is the USA.[22] As such there is vested interest for small and large pharmaceutical companies to ensure that their discovery and development process of a given candidate is compliant with the Food and Drugs Administration (FDA). Due to the lethality of some diseases which are tackled by small molecule therapies such as cancer, a distinct and clearly defined mechanism of action (MOA) by which a small molecule imparts its beneficial effect is not always required for approval of a candidate as a drug. However herein lies a potential pitfall embedded in the drug discovery pipeline- a lack of detailed molecular understanding about the mechanism by which a molecule imparts its effect can lead to failures in efficacy. Due to the complexity of the biological relationships which are disturbed when a small molecule is introduced to cells/organisms in the context of a disease- some of the early assays/markers for efficacy can drastically simplify phenotypic observations in the drug discovery process which can later lead to false positive data. As such there is a drive and necessity to mitigate this pitfall through the use of complementary small molecule chemical tools that are capable of generating a deeper understanding of given biological targets. These tools then equip researchers to pursue and 'de-risk' biological targets of interest in the drug discovery pipeline.

1.1.2 Target Validation and Chemical Probes

There exists a contentious debate about approaches to small molecule drug discovery. Many of the dated and now generic small molecule drugs exert their beneficial therapeutic effects due to 'poly-pharmacology'. These drug molecules are known to engage and perturb a number of biological targets, it is thought that the interaction with a number of these targets might lead to a single desired pharmacological outcome in combination. However, as the expansive network of biological interactions in a given disease are uncovered and further characterised, the generation of new ways to manipulate single biological targets, at will, represents a pursuit of increasing value.

New biological targets for drug discovery are uncovered in a number of ways; often a loose genetic link is reported in literature publications such as correlations of mRNA transcript levels,[23] proteomics[24–26] or direct activity (e.g. phosphorylation activity on a substrate) with a given disease. In addition to this form of data, often emerging technologies are leveraged such as small interference RNA and/or CRISPR-Cas9 to manipulate the levels of a protein target which may then result in some phenotype commensurate or antagonistic to a disease state.

Small molecule chemical tools which are highly qualified at discerning the relevance of a given biological target within the context of a disease have been described as Chemical Probes (Figure 1.2)[27] within the biological and chemical sciences. A number of definitions of chemical probes have been reported. Generally, it is agreed that a chemical probe is reported to be a small molecule capable of engaging a biological target with high binding affinity (low nM IC_{50}/K_D range). Moreover, there is a requirement for the molecule to also display selectivity for the chosen target and a demonstration of the ability to engage with its cognate target in a cellular context at reasonable or useable concentrations.[28,29] An additional tenet of the criteria for chemical probes is the availability of a structural similar but distinct and inactive negative control compound which can be used to complement the action of a probe molecule and drive

confidence that any observed phenotypes are attributable to target engagement/modulation. Taken together these reagents serve as powerful tools to elucidate new biology around pathologically relevant targets.[30]

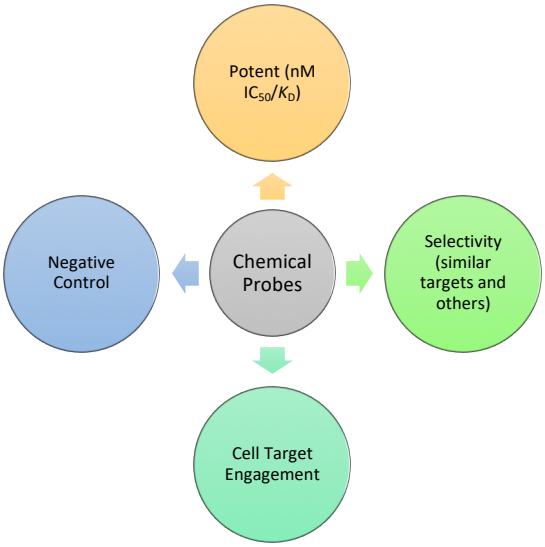

Figure 1.2 Key criteria of chemical probes

As chemical probes continue to be discovered and developed, this catalyses further (dis)interest of the pharmaceutical industry in a particular drug target owing to the (in)validation data generated by researchers on the target. As such both validation and invalidation can serve purposeful ends, to garner interest in a previously 'risky' but relevant target, or, to discourage incorrect investment of research resources in a target that will ultimately not lead to the discovery of new drugs.

There are a number of forums in which the current growing list of chemical probes are curated, allowing researchers to make informed decisions about the type of biological experiments they wish to carry out. One of these growing communities is the Chemical Probes Portal.[29] The Chemical Probes Portal is a knowledge based resource in which chemical probes reported in the literature are reviewed and curated by a scientific advisory board (SAB) using a combination of a star system and comments. The pooled expertise provided by the SAB allows for correct

identification of high quality chemical probes. Moreover, specific insights are also offered into the proper use[30] of given chemical probes where their value and utility may only be apparent under certain circumstances.[30] The cost of drug discovery is increasing and can be attributed in part to the costs generated through attrition. The development of new chemical probes is a potential solution to the rising cost of drug discovery.

1.2 Bromodomain Inhibition

1.2.1 Epigenetics

Deoxy-Ribo-Nucleic Acid (DNA) is packaged up into higher order structures termed 'chromatin'. Chromatin consists of DNA wound around an octamer of subunit proteins, histones. The fundamental repeating unit of chromatin is termed the 'nucleosome' which consists of the octameric cluster of histone proteins (2x H2A, 2x H2B, 2x H3 and 2x H4). In order for transcriptional machinery to efficiently access genes located on the nucleosome, a regulatory mechanism by which the DNA is made more or less accessible is thought to be evident. The accessible form of chromatin is known as 'euchromatin', whereas the transcriptionally inactive and closed form of chromatin is denoted 'heterochromatin'.[31] The negatively charged phosphate back bone of DNA typically drives a strong electrostatic interaction with corresponding positively charged surface histone protein residues such as Lysines (K) and Arginines (R). Direct DNA modifications are also proposed to have some role in epigenetic regulation[32] along with the RNA splicing[33] and non-coding RNA,[34,35] histone lysine residues are one of the most commonly identified sites of epigenetic regulation.[36,37] When these Lysine residues are modified (typically with small chemical changes), their inherent ability to interact with DNA are somewhat altered, which in turn, can alter expression of genes about that specific loci.

The molecular mechanism by which histone proteins are modified in order to modulate gene expression is thought to be the underlying 'epigenetic code'. The study of these mechanistic changes to histone proteins and more broadly chromatin architecture which underpin control of gene transcription is referred to as '*epigenetics*'. The definition of *epigenetics* has been a contentious subject with most discrepancies in the reported definitions hinged on the issue of heritability of epigenetic changes. One of the first uses of the term was reported by C. H. Waddington in 1942 where he gave the definition '[…]between genotype and phenotype, and connecting them to each other, there lies a whole complex of developmental processes[…]'.[38] Whilst other definitions and references to the term have emerged over the past half century,[39,40] for the purposes of later discussions in this thesis, the reported definition including heritability will be used; 'An epigenetic trait is a stably heritable phenotype resulting from changes in a chromosome without alterations in the DNA sequence'.[41] There exists a number of protein families that are known to add, remove and interact with these modified chromatin chemical signatures. Specific protein families have been studied in detail for their structure and function. These families have been broadly and metaphorically divided into 'writers' (proteins capable of adding an epigenetic chemical mark), 'erasers' (proteins capable of removing an epigenetic chemical mark) and 'readers' (proteins capable of binding/interacting with an epigenetic chemical mark). A number of these epigenetic proteins exert their effect on a number of areas of the nucleosome (Figure 1.3).[42] Furthermore, a number of these proteins also contain multiple domains, exist in multiple protein complexes exerting multiple functions on varying sites modification. A number of these proteins which bear similarity in structure also share functional redundancy and exert similar or opposing effects on sites of modification.

Increasingly, it has become apparent when the function of a number of these epigenetic proteins is mis-regulated, there is a genetic and pharmacological correlation with the onset and progression of a number of disease states such as inflammation[43–47], cancers[48,49] and infectious disease.[50,51]

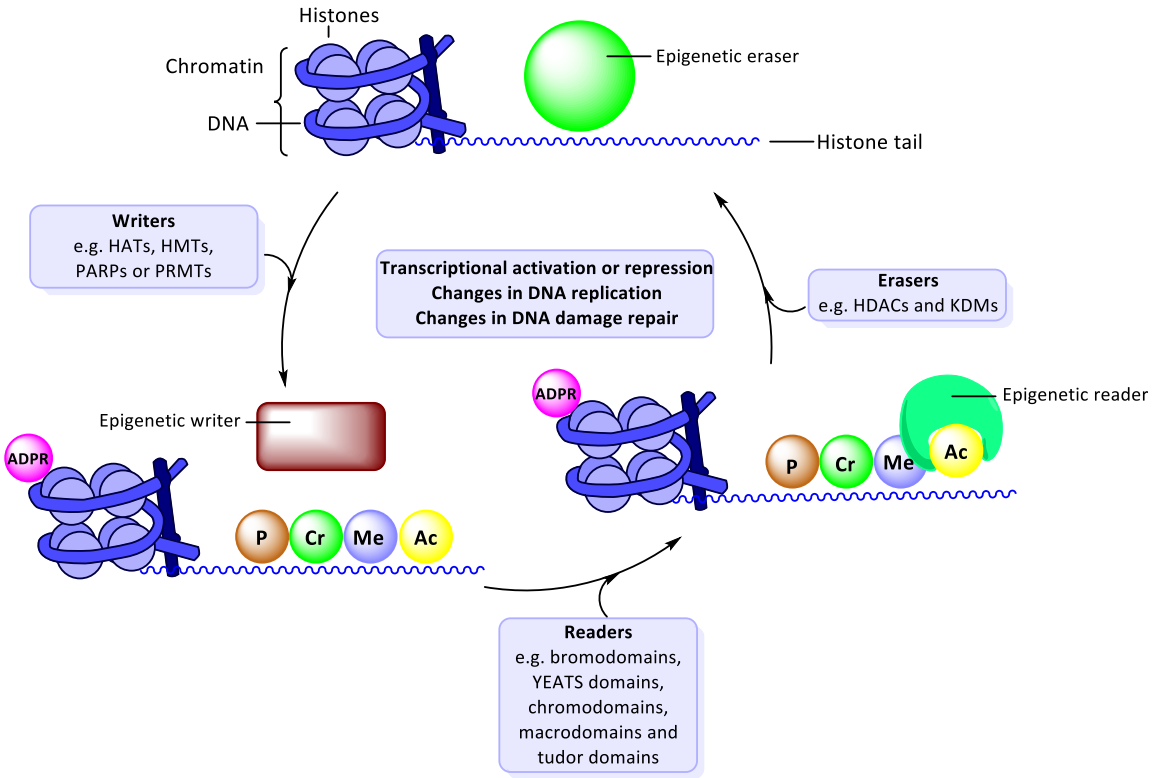

Figure 1.3 Chromatin structure with interacting and modulating proteins. Figure adapted from Falkenberg et. al.[42] *ADPR- adenosine diphosphate ribose, P- phosphate, Cr- crotonyl, Me- methyl, Ac- acetyl. Writers: HAT- histone acetyltransferase, HMT- histone methyl transferase, PARP- poly adenosine diphosphate ribosylating protein, PRMT- protein arginine methyl transferases. Erasers- HDAC- histone diacetyl transferase, KDM- lysine demethylase.*

1.2.2 Lysine Modifications

There are a number of sites of modification on histone proteins which correlate with epigenetic protein interactions.[52–55] Typically, a number of these sites are located on peptidic sites flanking the outer region of individual histone units.[56] These peptidic 'histone tails' which are located close to the surface of the octameric nucleosome, typically contain multiple Lysine residues. Whilst a number of other amino acid residues have been identified as sites for epigenetic modifications (e.g. arginines) the chemical marks which are usually added, removed or interacted with typically occur on lysine residues and are listed below;

- Lysine methylation[57]

- Lysine acylation (acetylation, propionylation, crotonylation, butyrylation, succinylation, phosphoglycerylation, malonylation)[58]

- Lysine conjugation (glycation, pupylation, sumoylation, ubiquitination)

Of the myriad of chemical modifications (figure 1.4) available for epigenetic gene control, lysine acylation has a significant impact on the net charge of the surface of histones (the conversion of a positively charges K residue to a neutral amide).[59] Upon neutralisation of a K residue to the cognate acylated variant, electrostatic interactions with negatively charged DNA are then believed to be weakened and DNA becomes more 'loosely' bound to histones. This net remodelling of chromatin allows for genes located adjacent to become transcriptionally accessible, accessible to modifications and accessible to damaging agents.

In addition to this charge mediated change to chromatin structure, the actual acetyllysine (KAc) mark itself facilitates the binding of KAc 'reading' proteins such as bromodomains.[37,60] Bromodomain containing proteins exist as part of larger nuclear complexes and are capable of recruiting transcription factors and other complexes when bound to chromatin which in turn activates transcription.[61]

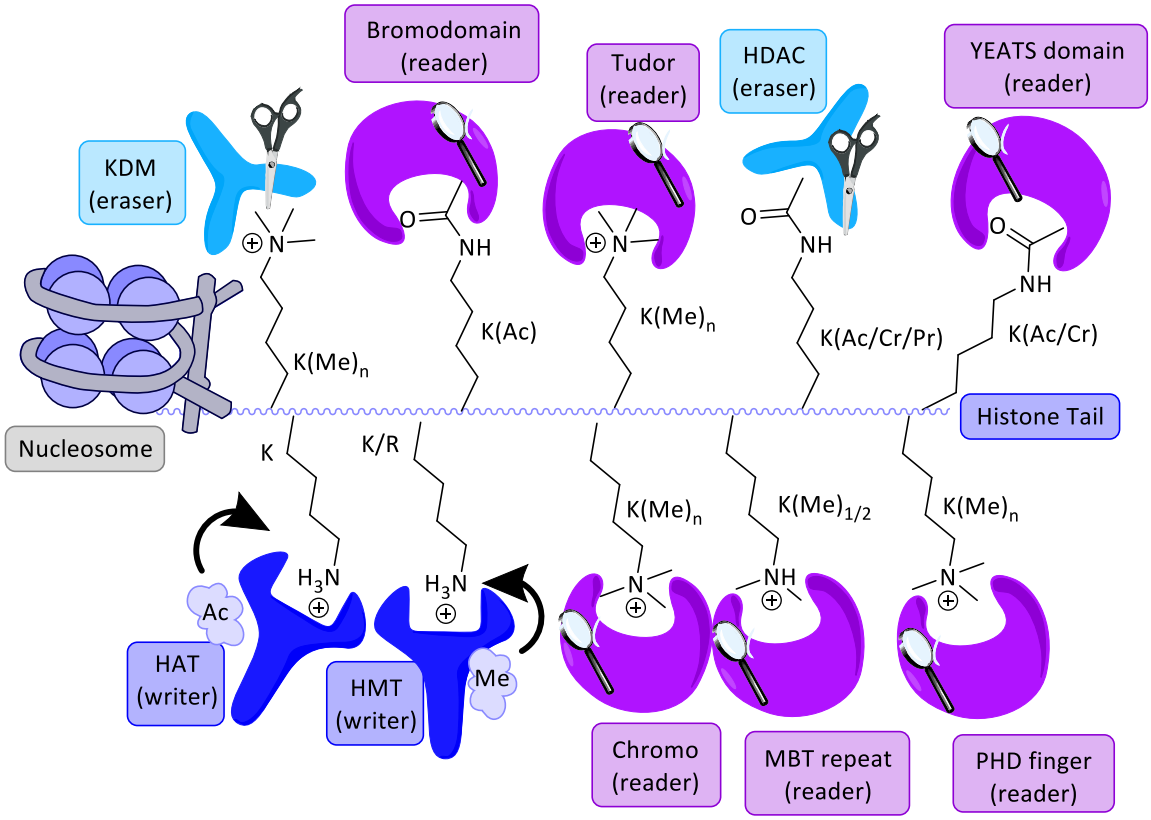

Figure 1.4 Lysine modifying and interacting proteins. Figure adapted from SGC site.[59]

Addition of the acetyl mark to lysines is effected by the histone acetyltransferases (HATs or KATs, Figure 1.6)[62–64] utilising acetyl-coenzyme A (Ac-CoA) as a co-factor, whereas removal or 'erasing' of this epigenetic mark is carried out by histone deacetylases (HDACs or KDACs).[65–67] Due to their intricate nature in regulating transcription, HDACs have received considerable attention in the development of small molecule inhibitors of various family members for the treatment of cancers.[68] Whilst HATs have been genetically linked to a variety of diseases, there has been a paucity of high quality small molecule inhibitors of HAT domains until recently, for example Abbvie's report of the first potent CBP/p300 HAT inhibitor, **1** A-485 (Figure 1.5).[69–71]

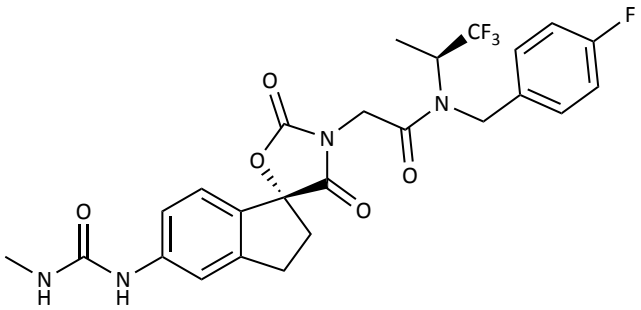

1 A-485
CBP IC_{50} 3 nM
p300 IC_{50} 10 nM

*Figure 1.5 Abbvie CBP/p300 HAT inhibitor **1** A-485.*

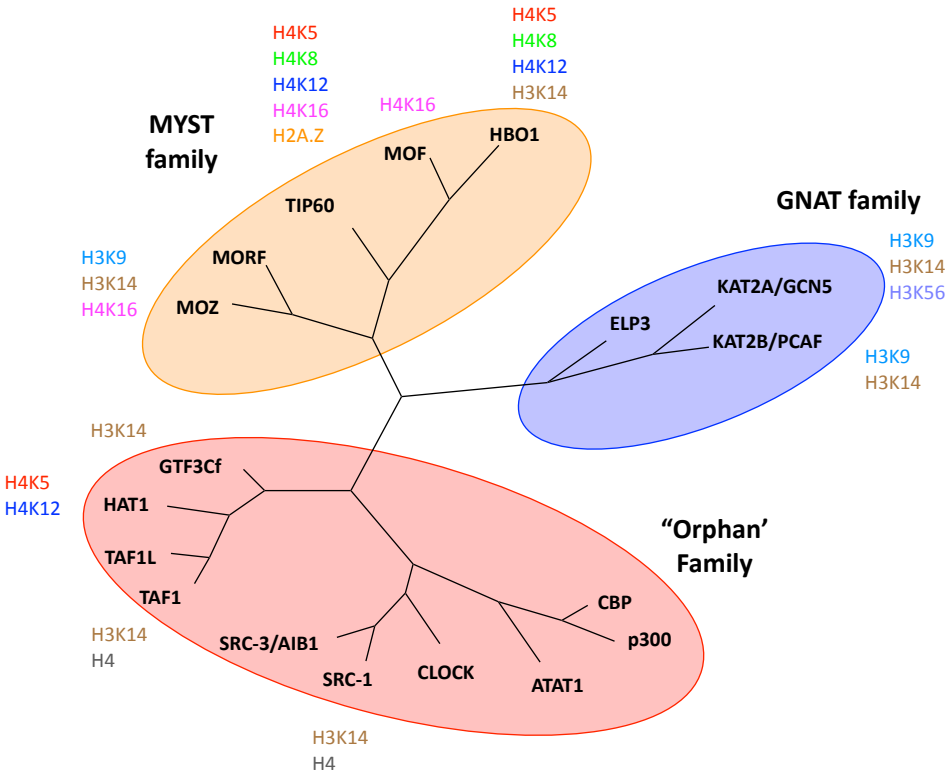

Figure 1.6 Histone Acetyltransferase (HAT) phylogenetic tree. Figure adapted from Di Cerbo et. al.[64]

1.2.3 Bromodomains

One epigenetic family of proteins capable of interacting with acylated K residues are termed Bromodomains (BRDs, Figure 1.7)[72]. The structure of BRDs typically features a 110-amino acid sequence comprised of four α-helices (αZ, αA, αB and αC) in a bundle linked by loops, two of which (ZA and BC) comprise the BRD KAc binding site. This acyllysine interacting module is typically part of a larger multi-domain protein sequence and so the term *Bromodomain*

containing proteins (BCPs) is used. Within the human genome there exists 48 known BCPs which are clustered into eight sub families based on BRD sequence similarity.[37,48,73–80] Many BCPs contain multiple BRD and so to date there have been 61 BRDs identified in humans.[76] The KAc binding site across the various BCPs is largely conserved with key features being a highly conserved asparagine (N) residue and tyrosine (Y) residue along with four structural water molecules which operate in a hydrogen bond network with bound substrates (KAc). For most 'typical' BRDs, the key residue involved in KAc recognition is an asparagine (48 examples), however there exists a number of 'atypical' BRDs where this residue is replaced with a Tyr (8 examples), Thr (4 examples) or an Asp (1 example). Despite weak and non-specific interactions reported for most BRDs and KAc histone substrates, the necessity for a large number of diverse BCPs within the human genome may be indicative of the KAc recognition element of BRDs functioning in concert with other chromatin interacting elements in order to propagate the functional effect of chromatin 'reading'.[52,81,82]

A

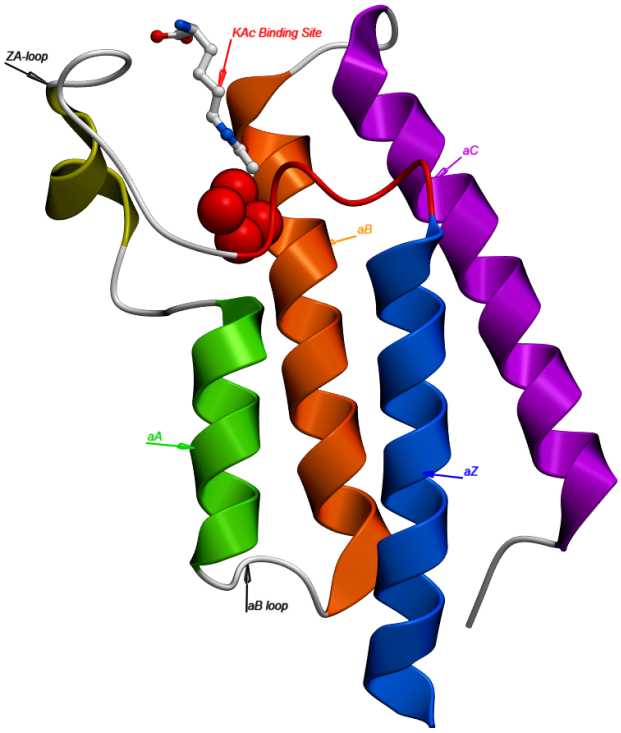

B

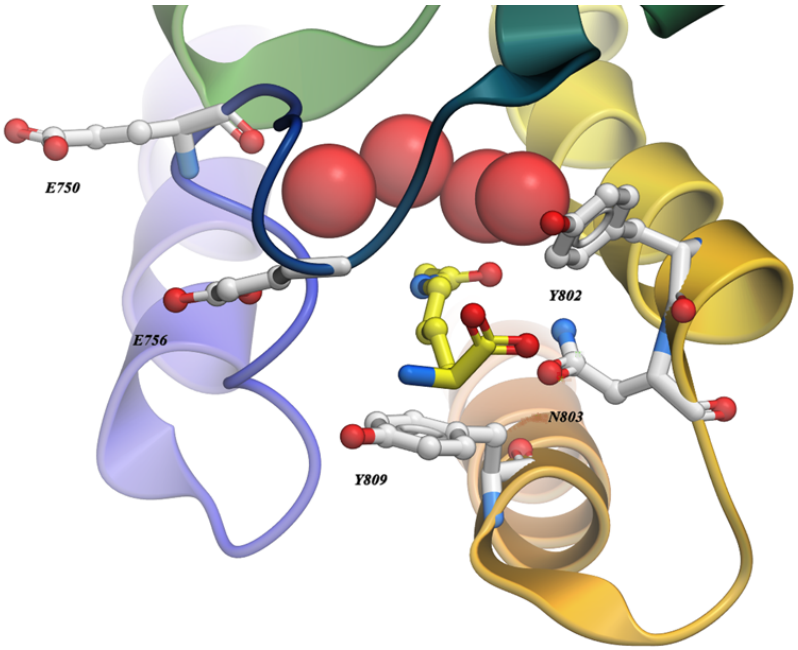

Figure 1.7 A) Co-crystal structure of PCAF BRD with KAc (PDB ID 5FE0). Helices (αA in green, αB in orange, αC in purple, αZ in blue) and loops (all loops shown in grey) denoted. B) KAc binding site of PCAF BRD with KAc bound. Key residues; E750, E756, Y809, Y802 and N803 are displayed in grey sticks. Four structural water molecules are depicted at the rear of the KAc binding site as red balls.

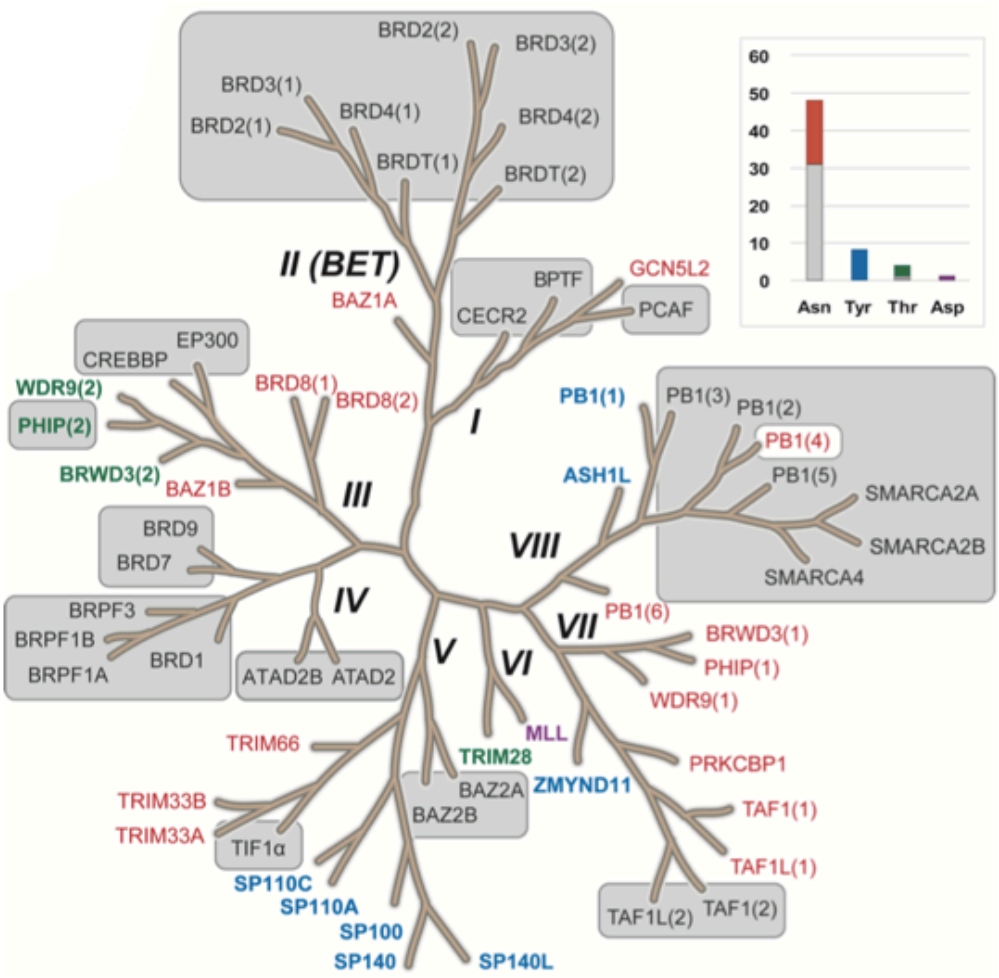

Figure 1.8 BRD Phylogenetic tree clustered by subfamily and annotated in colour by key recognition residue in KAc binding site (Asn in red, Tyr in blue, Thr in green and Asp in purple). BCPs within grey boxes are those for which BRD inhibitors have been previously reported. Figure adapted from Moustakim et. al.[76]

1.2.4 PCAF

The p300/CBP Associated Factor (PCAF/KAT2B) is a BRD containing histone acetyltransferase (HAT)[83] protein deriving from the BRD Sub Family *I* in terms of sequence homology (Figure 1.8). The HAT domain of PCAF belongs to the GCN5-related *N*-acetyltransferase (GNAT) subfamily of HAT proteins which largely contain BRDs as an additional structural element. In addition to this catalytic domain, an *N*-domain (PCAF homology domain) also exists as part of the overall sequence. Both PCAF and its homologue, GCN5, are known to bind H3KAc14 via their corresponding BRDs, however both acetylate K16 and K8 of H4.[84] Additionally, PCAF BRD recognizes H4KAc8/H4KAc20 and H3KAc14/H3KAc9.[85][86] Despite similarities in structure and

KAc binding preference, both PCAF and GCN5 have distinct functions in global histone acetylation and gene expression through knockout studies.[87,88] Dysregulation of PCAF has been correlated with cancer,[89–91] HIV infection[89,92–95] and neuroinflammation.[79,89] Despite these links to a variety of diseases there exists a gap in the understanding of the underlying biology. Additionally, the domain specific functional contributions of the BRD and the HAT domain in disease are poorly understood.

1.2.4.1 PCAF in Cancer

Within the context of cancer, PCAF has been shown to acetylate Lin28B, an RNA binding protein in lung adenocarcinoma-derived H1299 cells, initiating Lin28B cytoplasmic translocation and changes to miRNA levels.[96] Dysregulation of PCAF has been linked to all-trans-retinoic-acid (ATRA) induced granulocytic differentiation in leukemic cell lines such as acute promyelocytic leukaemia (APL) with marked over expression found in bone marrow stem cells from APL patients.[97] In gastric cancer (GC) PCAF has been shown to be a tumour suppressor, downregulation being correlated with poor patient prognosis. PCAF suppresses GC via an interaction with AE1 and p16 which promotes AE1 degradation and p16 nuclear translocation.[98] PCAF activity has been shown to prevent growth of hepatocellular carcinoma through promotion of cell autophagy.[99]

Homeobox domain-containing transcription factor (HOXB9) plays essential roles in embryonic development and oncogenic progression. PCAF has been shown to interact with and acetylate HOXB9 (K27), providing an opposing effect to the HDAC, SIRT1, which in turn supresses lung adenocarcinoma through downregulation of HOXB9 target gene, JMJD6.[100]

PCAF acetylates p53 and histones at p53 promoter regions which transactivates p53 target genes in a number of breast tumour cells.[101] Acetylation of both p53 and HIF-1α is a key

mechanism of PCAF mediated regulation. Acetylation of p53 at K320, in turn controls the rates of transcription of p53 target genes under 'hypoxia-like' conditions.[102]

In both embryonic development, injury and cancer cell progression, the process of epithelial to mesenchymal transition (EMT) plays a major role in transcriptional regulation. It has been found that PCAF acetylates a key transcriptional suppressor involved in EMT, ZEB1, which in turn suppresses transcriptional events at key EMT promoter regions.[103] PCAF also displays repressive activity on tumour suppressor protein PTEN, which contains lipid phosphoinositol phosphatase activity blocking G1 phase events within the cell cycles to supress tumour formation. PCAF expression correlates with acetylation of PTEN which supresses its catalytic activity and perturbs the ability to block the cell cycle at G1.[104]

Reports also suggest that PCAF may have E3 ligase activity in addition to HAT and BRD activity. Downregulation of PCAF decreases ubiquitination of glioma-associated oncogene-1 (Gli1) which facilitates hepatocellular carcinoma progression.[99] In a similar vein, knockdown of PCAF in HeLa or U2OS cells has been shown to stabilize the oncoprotein Hdm2, which is a RING finger E3 ligase, through ubiquitination. Stabilization of Hdm2 then allows for regulation of p53, which Hdm2 is a key regulator of.[105] PCAF has also been identified as an E3 ligase responsible for ubiquitination of Class II Transactivator (CIITA) which in turn regulates Major Histocompatibility Class II (MHC II) genes transcription.[106]

Finally, PCAF has been shown to be targeted by a number of viral proteins such as adenoviral E1A, Epstein-Barr virus encoded EBNA2 and HIV-Tat which can in turn activate oncogenes resulting in cell immortalization and oncogenic transformations.[107]

1.2.4.2 PCAF in Inflammation

PCAF acetylates NFκB on the p65 subunit at K122 and K123[108] to mediate inflammation and has been linked to regulation of vascular inflammation and essential to intimal hyperplasia

development through regulation of CCL2, IL-6 and TNF-alpha.[109] PCAF also acetylates megakaryocytic leukaemia 1 (MKL1) which in turn activates the transcription of pro-inflammatory NFκ-B target genes.[110] Acetylation of H3K9 by PCAF has been shown to be essential for osteogenic differentiation of mesenchymal stem cells (MSCs), knockdown of PCAF correlating with a reduction of bone formation in vitro and in vivo.[111]

1.2.4.3 PCAF in Neuropathology

In neuroscience, PCAF KO mice have been shown to develop resistance to amyloid toxicity suggesting that suppression of PCAF may offer therapeutic opportunities towards amyloid related pathologies.[112] However, PCAF KO mice have also been demonstrated to function normally until two months of age, after which show short term memory deficits which become exacerbated with time. Correlating with increases in plasma corticosterone levels, PCAF knockout mice also show exaggerated responses to acute stress and conditioned fear.[113] These findings are also in agreement with rat studies which showed that PCAF KO or small molecule inhibition of the HAT domain is linked to impairment of short and long term memory in object-in-place studies.[114]

1.2.4.4 PCAF in Infectious Disease

The bromodomain of PCAF was the first protein from this epigenetic family to be successfully crystallised in 1999 by the Zhou group.[85] This seminal work paved the way for efforts in structural biology surrounding these reader domain containing proteins. The Zhou group later showed that the BRD of PCAF is an essential regulator of the lifecycle of HIV-1. The human immunodeficiency virus type 1 (HIV-1) expresses a protein, trans-activator protein (Tat), which stimulates transcription and promotes replication in infected host cells.[92] The expressed Tat protein is acetylated in host cells and is then associated with both CBP and PCAF putatively via their BRDs. Tat is acetylated at Lys-50 and engages with the PCAF BRD which then in turn

outcompetes HIV-1 TAR RNA:KAc50 Tat interactions.[115] Structural analysis studies of both KAc50 Tat and PCAF demonstrated that their exists key residues which when mutated, disrupt the PCAF:KAc50 Tat interaction, namely Tat: Y47 and R53, PCAF: V763, Y802 and Y809 both *in vitro* and *in vivo*.[95] Many of these structural studies have been complemented or are in agreement with computational studies.[93]

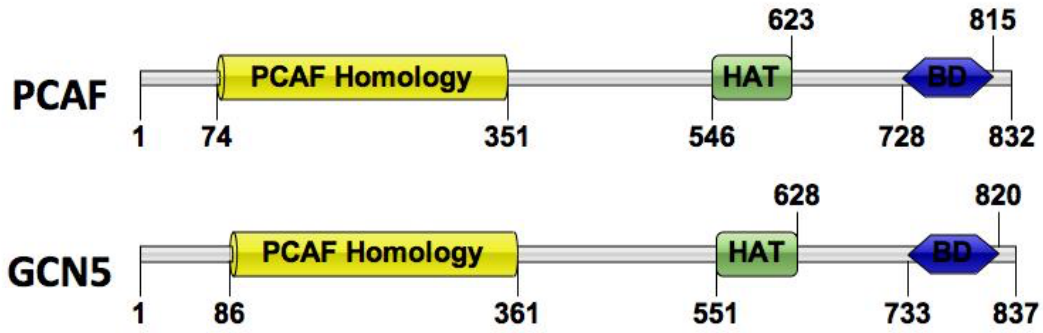

Figure 1.9 Protein domain sequence map of PCAF and GCN5. Protein map was generated using IBS.[116] *PCAF homology domain shown in yellow. HAT domains shown in green. C-terminal Bromodomain signified in blue.*

1.2.5 GCN5

The General Control Nonderepressible 5 (GCN5/KATA) is a closely related paralogue of PCAF (73% sequence similarity) which also functions as a Histone Acetyltransferase (HAT, deriving from the GNAT subfamily)[83] and a bromodomain (BRD) containing protein. GCN5 is known to acetylate and bind to similar sites of Histone H3 that PCAF does. GCN5 was recently shown to be able to catalyse histone succinylation with the α-KGDH complex[117] and has been correlated with diseases such as cancer[118–121] and viral infections.[122,123]

1.2.5.1 GCN5 in Cancer

High levels of GCN5 expression correlate with human colon adenocarcinoma progression. Increased mRNA levels have been linked to transcription factors, c-Myc and proapoptotic E2F1. Knockdown studies of c-Myc indicate that c-Myc mediated colon cancer cell suppression

operates through decreased GCN5 expression and can be rescued by ectopic GCN5 expression.[121] GCN5 expression also positively correlates with human glioma and proliferation of cell nuclear antigen PCNA and matrix metallopeptidase (MMP9). By analogy, knockdown of GCN5 inhibits glioma cell proliferation which also correlates with an increase in the expression of p21.[120]

In leukaemia, GCN5 has been linked to topoisomerase inhibitor resistant cancers. It has been reported that Early Drug Resistant Population (EDRP) cells harbour increased GCN5 levels, inhibition of GCN5 was shown to be lethal to EDPR cancer cells.[124] Within t(1;19) translocated acute lymphoblastic leukaemia (ALL) a fusion of transcription factors occurs to produce- E2A-PBX1 which in turn can promote cell transformation *in vitro* and *in vivo*. The E2A portion of the fusion protein is acetylated by GCN5 which provides a stabilising effect to the fusion protein in cells.[125] Overexpression of GCN5 correlates with non-small cell lung cancer progression. GCN5 is also found to regulate expression of E2F1, cyclin D1 and cyclin E1 *in vivo*[126] along with the transcription factor c-Myc through its acetylase activity.[127]

1.2.5.2 GCN5 in Inflammation

Within inflammation, GCN5 is required in T-lymphocytes for normal development, clonal expansion and differentiation. Deletion or loss of GCN5 function ablates T-cell functioning, IL-2 production and Th1/Th17 differentiation revealing the potential of GCN5 as a target for autoimmune disease therapies.[128] It has been found that mutation studies of GCN5 within the context of endoplasmic reticulum (ER) stress that GCN5 is a regulator of prolonged ER-stress induced apoptosis via modulation of Bcl-2 expression.[129] In Osteoporosis, lower levels of GCN5 and corresponding acetyltransferase activity on H3K9 have been linked to suppression of Wnt signalling which in turn leads to bone defect formation during osteoporosis.[130]

1.2.5.3 GCN5 in Neuropathology

Mice with knockout GCN5 neural stem cell and precursor cells (NSC) have been shown to exhibit reduced growth in brain mass (25% reduction). In addition, knockout of GCN5 also inhibits precursor cell proliferation and overall phenotypes match those of knockout c- or n-Myc suggesting GCN5 is a key Myc transcriptional cofactor.[131] Loss of function GCN5 results in acceleration in cerebellar and retinal degeneration in mouse models of spinocerebellar ataxia type 7 (SCA7) despite not altering the expression of known target genes of Atxn7 (faulty gene in SCA7).[132]

1.2.5.4 GCN5 in Infectious Disease

GCN5 has been linked to acetylation of HIV-1 integrase which facilitates the integration step of the HIV-1 replication cycle. Knockdown GCN5 cell lines exhibit diminished infectivity when treated with HIV-1 commensurate with a decrease in HIV-1 acetylation.[122]

1.2.6 Dual PCAF/GCN5 Pathologies

Interestingly both PCAF and GCN5 have been reported to have similar roles in certain pathologies and dissociable roles in others. PCAF and GCN5 have been correlated with acetylation of the nucleoprotein (NP) of Influenza virus A. Both proteins have been shown to acetylate the NP at different K sites which in turn has opposing effects on viral RNA polymerase activity- PCAF acetylating K31 (repressive) whereas GCN5 acetylates K90 (anti-repressive).[133]

PCAF and GCN5 have been shown to have differing levels of essentiality during early embryogenesis. Knockdown GCN5 mice display diminished embryo viability with 25% of mice dying before birth. This is in contrast with knockdown PCAF mice which develop with minimal abnormalities.[88] In the cell cycle, PCAF and GCN5 have been reported to have differential levels of control in phase transitions (such as G1/S phase transitions). Mutation studies reveal that cells expressing inactive PCAF do not exhibit abnormal growth rates, whereas mutations to GCN5 cause delayed growth rates to DT40 cells. This suppression in growth rates correlates with

changes in acetylome profiles on histones.[134] In DNA Damage Repair (DDR) both PCAF and GCN5 have been reported to activate nucleotide excision repair (NER) through RPA1 acetylation at K163 following UV-induced DNA damage.[135]

In yeast, loss of GCN5 or other components of the GCN5 HAT complex, SAGA, confer sensitivity to HDAC inhibition which correlates with an increased expression of genes involved in oxidative stress response and metabolism. This activity was also observed in human cell lines when either GCN5 or PCAF was knocked down suggesting that a combination of PCAF/GCN5 and HDAC inhibitors may have benefits in cancer therapy.[136] Chemical inhibition of both PCAF and GCN5 has been shown to suppress neuroblastoma cell growth both *in vitro* and *in vivo*.[137] PCAF and GCN5 have been found to be upregulated in urothelial carcinoma (UC). siRNA knockdown studies of both PCAF and GCN5 in UC cell lines (UCCs) demonstrate differential levels of essentiality- GCN5 being consistently upregulated in a number of cell lines, with PCAF levels being variable. As a consequence, single knockdown of GCN5 or double knockdown of PCAF and GCN5 elicits inhibition of cell proliferation in a number of UCCs, whereas PCAF KO alone has minimal effects.[138] Shotgun proteomics reveal polo-like kinase 4 (PLK4) as a substrate for both PCAF and GCN5, acetylating PLK4 K45 and K46- which is a regulator of centrosome duplication. Downregulation of PCAF and GCN5 results in PLK4 over activity and over amplification of centrosomes.[139] Within cancer cell progression, there exists a telomerase-independent mechanism in telomere maintenance termed alternative lengthening of telomeres (ALT). It is reported that within this mechanism, PCAF and GCN5 have opposing effect with GCN5 having a direct effect on ALT cells via repression of telomere recombination whereas PCAF is a telomere promoter in ALT cells.[140] Overexpression of both PCAF and GCN5 correlates with central nervous system tumour (CNST) progression. Benign tumours correlate with decreased levels of PCAF/GCN5 suggesting essentiality of both PCAF/GCN5 in CNST carcinogenesis.[141]

Despite the disease links, both PCAF and GCN5 dysregulation has been reported to have gain of function or loss of function effects depending on cell types and tissues of origin. During the initiation of work on these targets there had only been a few disclosed small molecule chemical structures of PCAF inhibitors mostly bearing moderate PCAF activity without any information on GCN5 activity.[79,90–92,95] Within the patent literature there existed a number of claims of the application of PCAF inhibitors for the treatment of disorders such as cancer, viral infection and inflammation without the disclosure of small molecule chemical structures.[89]

1.2.7 Malarial Bromodomains

Recent advances in understanding how malarial parasites regulate their life cycle and successfully invade and disrupt host organisms has been linked to epigenetic mechanisms.[50,142–145] Of particular note is that one of the most deadly parasitic unicellular organisms in terms of malaria related mortality is *Plasmodium falciparum* (*Pf*) which also expresses a similar orthologue to human PCAF and GCN5, *Pf*GCN5. Increasingly, interest surrounding the essentiality of certain *Pf* epigenetic proteins, including *Pf*GCN5 may present new avenues towards anti-malarial drug discovery.[146,147] A recent report applied human BRD chemical probes to screening for anti-*Pf* activity which revealed a number of inhibitors bearing affinity for *Pf* BRD containing proteins which then conferred anti-*Pf* proliferation activity to the compounds.[148]

1.2.8 Current Bromodomain Probes and Inhibitors

Of the eight human sub-families of BRD containing proteins, a significant amount of attention has been focussed on the therapeutic potential of the Bromodomain and Extra Terminal (BET) proteins deriving from sub family *II* (comprised of BRDT, BRD2, BRD3 and BRD4 all containing two BRDs).[37,60,153–156,74,75,78,82,149–152] Catalysed by this intense research there are now more than 20 clinical trials recruiting or active in 2018 focussed on BET inhibition for the treatment of cancers or cardiovascular diseases including representative pan-BET inhibitors; **2** I-BET762, **3** CPI-

0610, **4** OTX015 and **5** RVX-208 (Figure 1.10).[48,157] The oncology focus of BETi is thought to stem from the repressive effect of BRD4 inhibition on *c-MYC* expression (known oncogene).[158,159]

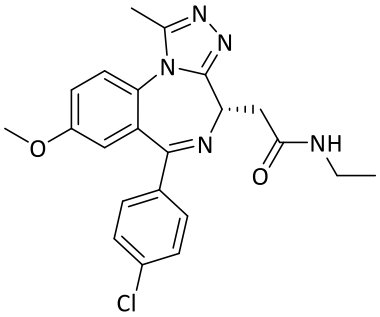

2 I-BET762 (GlaxoSmithKline)
NCT01587703 Solid Tumours and Multiple Myeloma
NCT01943851 Haematological Malignancies

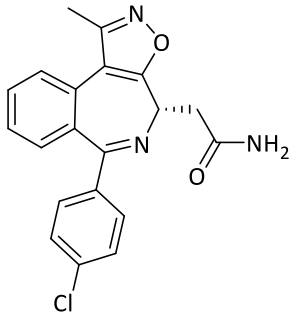

3 CPI-0610 (Constellation Pharmaceuticals)
NCT02157636 Multiple Myeloma
NCT01949883 Lymphoma
NCT02158858 Acute leukaemia and others

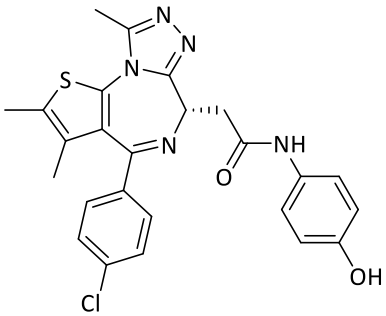

4 OTX015 (OncoEthix)
NCT01713582 Haematological Malignancies

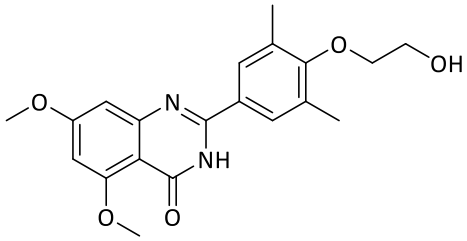

5 RVX-208 (Resverlogix Corp.)
NCT01728467 Atherosclerosis

*Figure 1.10 Representative bromodomain Inhibitors **2** I-BET762, **3** CPI-0610, **4** OTX015 and **5** RVX-208 all in clinical trials for oncology or cardiovascular diseases.*

However there remains seven other sub families of BCP referred to as the non-BET proteins which individually have been linked to a variety of diseases. Despite the highly conserved BRDs displaying good *ligandability* for fragment like small molecules such as the co-solvents DMSO and NMP, achieving single BRD selectivity remains a challenge.[160] The development of selective novel chemical probes for these non-BETs with allow for a robust interrogation of the biology underlying these epigenetic protein targets.[76,77]

1.2.9 non-BET bromodomain chemical probes

Of the BCP deriving from sub families I and III-VIII there now exists a number of chemical probes and inhibitors developed for the corresponding BRDs.

Most of the subfamilies of non-BET BCP now have a chemical probe or inhibitor targeting at least one family member (Figure 1.11). There have been a number of BCP for which chemical probe discovery efforts have been applied with a degree of success across the sub families;

- Sub-family I: CECR2[161]
- Sub-family III: CBP/p300[162–168]
- Sub-family IV: BRD7/9[80,169–174], BRPF1/2/3[175–181], ATAD2A/B[182,183], ATAD2A[184]
- Sub-family V: BAZ2A/B[185,186], TRIM24[177]
- Sub-family VI: None
- Sub-family VII: TAF1[187,188]
- Sub-family VIII: SMARCA/PB1[189]

Whilst sub-family VI has received a paucity of attention this is perhaps owing to the atypical nature the BRDs of both family members MLL and TRIM28.[76]

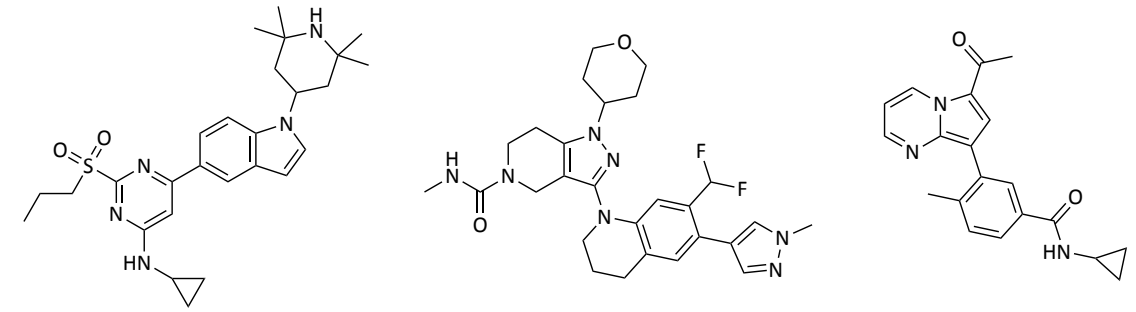

6 NVS-CECR2-1 **7** GNE-781 **8** TP-472

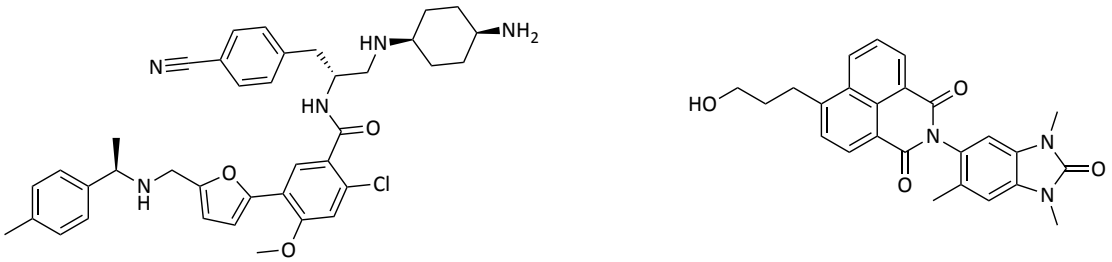

9 BAY-850 **10** BAY-299

*Figure 1.11 Representative non-BET BRD chemical probes and inhibitors. **6** NVS-CECR2-1 (CECR2 chemical probe), **7** GNE-781 (CBP/p300 chemical probe), **8** TP-472 (BRD7/9 chemical probe), **9** BAY-850 (ATAD2A chemical probe), **10** BAY-299 (TAF1/BRD1 chemical probe).*

A number of these non-BET BRDs previously linked to specific diseases have in fact been invalidated as potential therapeutic targets owing to the lack of essentiality of the BRD within the context of the associated disease. This has been the case for SMARCAs[190], ATAD2A/B[182,184] and TRIM24.[191] More recently new strategies have emerged to address these issues through the use of PROTAC technologies[192,193] to induce E3 ligase mediated full length protein degradation, recent examples have been applied to both BRD9[194] and TRIM24[195] inhibitors. It is envisaged that this PROTAC strategy will likely be incorporated as an additional facet to chemical probe development as more reports demonstrate its value.

1.3 Macrodomain Inhibition

1.3.1 Polyadenosine-diphosphateribose polymerases, PARPs

The PARPs[196] are ADP-ribosyl transferase (ART) enzymes known to post-translationally modify substrate proteins.[197] Many of the PARP proteins are capable of transferring poly-ADP ribose (PAR) to their substrates, typically from NAD^+ to a glutamate or aspartate residue. However of

the 17 known human PARP proteins, only PARP1, PARP2, PARP5A and PARP5B have been shown to demonstrate true PARP activity, the remaining PARPs exist as a subset of family members only capable of transferring a single ADP-ribose unit at a time. These members are referred to as the mono(ADP-ribose)transferases (mARTs), additionally two PARPs (PARP9 and PARP13) are reported to harbour inactive ART domains (Figure 1.12).[198]

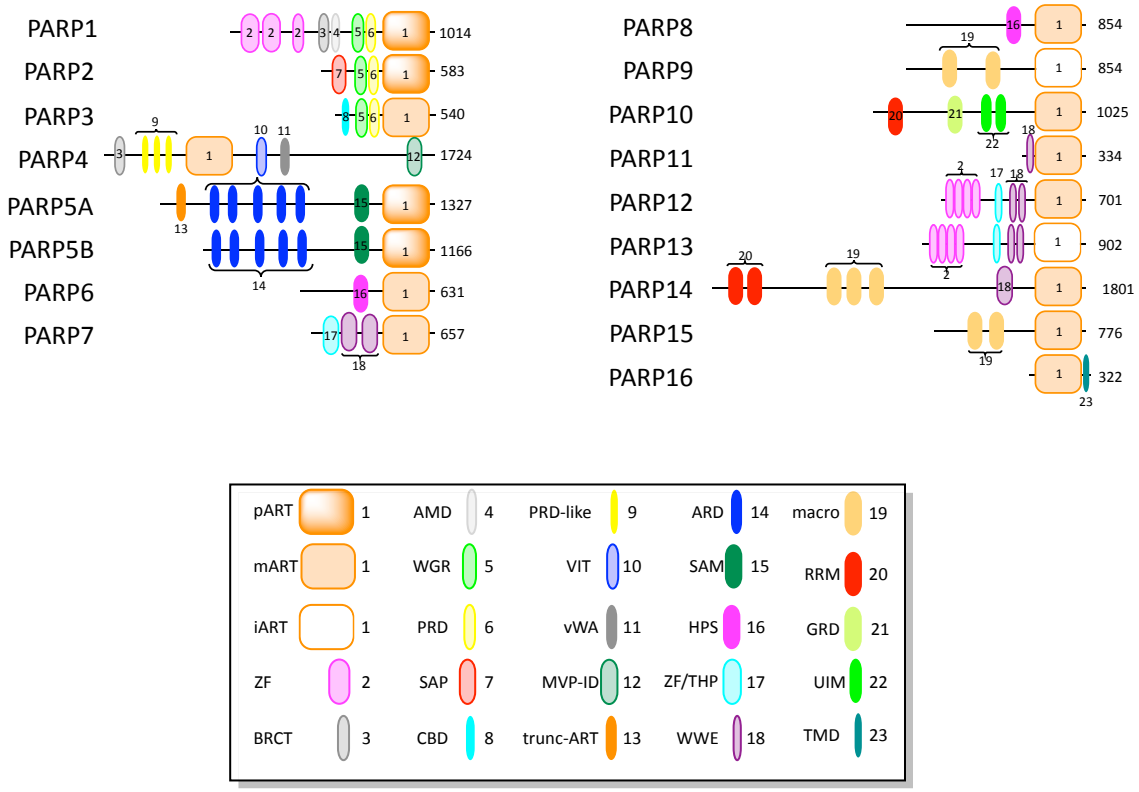

Figure 1.12 PARP protein domain maps. Figure adapted from Hottiger et. al.[199] *pART- poly ADP ribosyltransferase domain, mART- mono ADP ribosyltransferase domain, iART- inactive ADP ribosyltransferase domain, ZF- zinc finger, BRCT- BRCA1 carboxy-terminal domain, AMD- automodification domain, WGR- tryptophan-glycine-arginine repeat domain, PRD- PARP regulatory domain, SAP- SAF/Acinus/PIAS-DNA-binding domain, CBD- co-activator binding domain, PRD-like- PARP regulatory like domain, VIT- vault protein interface alpha-trypsin domain, vWA- von Willebrand type A domain, MVP-ID- major-vault particle interaction domain, trunc-ART- truncated ADP ribosyltransferase domain, ARD- ankyrin repeat domain, SAM- sterile alpha motif domain, HPS- histidine-proline-serine region domain, ZF/THP- zinc finger/threonine-histidine-proline domain, WWE- tryptophan-tryptophan-glutamic acid repeat domain, macro- macrodomain, RRM- RNA binding/recognition motif, GRD- glycine rich domain, TMD- trans-membrane domain, UIM- ubiquitin interaction motif.*

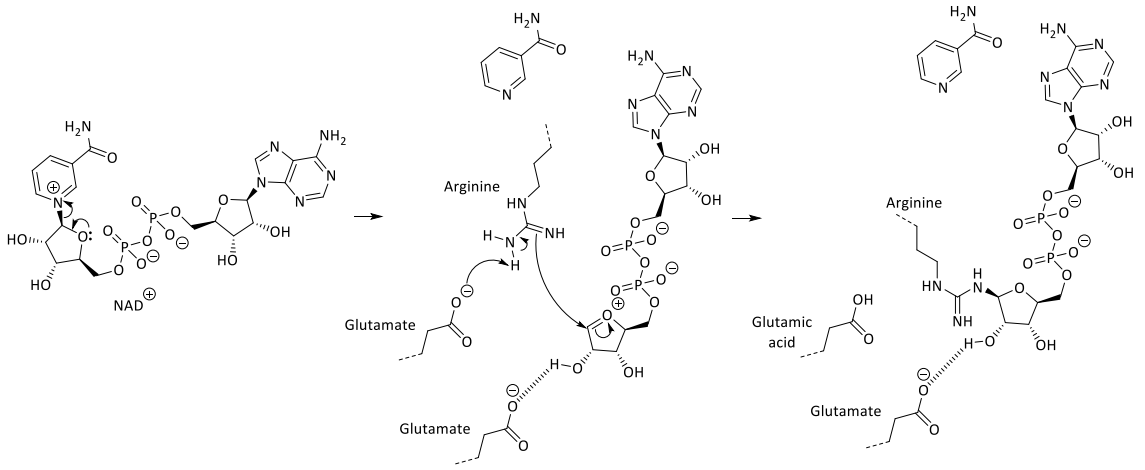

Scheme 1.1 Mechanism of mono-ART of an arginine residue by NAD⁺.

The mechanism of mono-ADP ribosylation (mAR) is dependent on the co-factor Nicotinamide adenine dinucleotide (NAD^+) as a source of ADP (Scheme 1.1). The charged NAD^+ unit is proposed to collapse to form an oxonium species and nicotinamide. Within the active site of the mART a substrate residue such as an arginine acts as a competent nucleophile as the side chain of a conserved glutamate facilitates deprotonation and nucleophilic attack. An adjacent glutamate residue participates in H-bond interactions with the 3' OH of the nucleotide in order to fix the ADP unit in position. After ADP transfer the substrate protein freely dissociates. mART has been shown to occur on arginine,[200] serine[201,202] cysteine,[203] lysine,[54] phosphoserine[204] and asparagine[205] residues. Misregulation of a number of these mARTs have been correlated with the onset and progression of disease.[206] Many of these PARP proteins, and mARTs more specifically, are multi-domain proteins fulfilling additional roles in a cellular context (Figure 1.12)[207]. There exists a gap in understanding about the domain specific contributions of the catalytic ART domains to disease correlations.

1.3.2 PARP14

Of the subset of mARTs, Polyadenosine-diphosphateribose polymerase 14 (PARP14/mART8) is the largest protein (Figure 1.13). Also harbouring a WWE domain, two (RNA binding) RRM repeat domains and three (ADP-ribose binding) macrodomains.[199] PARP14 has been correlated

with a number of diseases, namely cancers such as hepatocellular carcinoma and B-cell lymphoma.[208] PARP14 also functions as a regulator of IL-4 mediated proliferation and survival in B-cells.[209] Metabolic studies of cancer progression have also linked PARP14 as an inhibitor of pro-apoptotic kinase JNK1 which in turn stimulates pyruvate kinase M2 isoform (PKM2) thus enabling increased rates of glycolysis in cancer cells (Warburg effect)[210] which in some instances has been linked to increases in *MYC* expression.[211] PARP14 promotes homologous recombination DNA repair, conversely depletion of PARP14 is linked to sensitivity to DNA damaging agents and accumulation of DNA strand breaks.[212] PARP14 is essential for Th cell differentiation in mice and depletion of PARP14 diminishes STAT6-dependent antibody (Ab) responses.[213] PARP14 is also reported to function in concert with HDAC2 and HDAC3 to regulate the transcription of STAT6 target genes following activation by IL-4.[214] Suppression of PARP14 has been shown to diminish Th17 cell differentiation both *in vitro* and in models of allergic airway inflammation.[215] It has been reported that both PARP14 and another family member PARP9 cross-regulate macrophage activation- silencing of PARP14 induces pro-inflammatory genes M(IFN γ) cells and suppresses anti-inflammatory genes M(IL-4) cells.[216] The effect of PARP14 on STAT6 has also been explored in the context of inflammation models of atopic dermatitis (AD) demonstrating that KO PARP14 can cause progressive like symptoms in AD. KO PARP14 mice with overactive STAT6 expressing T cells showed an increase in mortality rates relative to mice with overactive STAT6 alone.[217]

Despite significant links to cancers[210,218,219], inflammatory diseases[220,221][222] and antimicrobial responses[223], as is the case for many PARPs/mARTs, the domain specific contributions of PARP14 underlying these disease links are poorly understood.

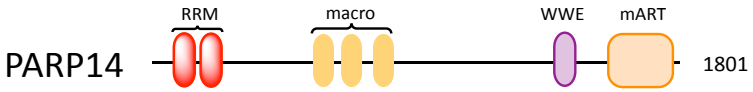

Figure 1.13 PARP14 domain architecture. WWE- tryptophan-tryptophan-glutamic acid repeat domain, RRM- RNA binding/recognition motif, macro- macrodomain, mART- mono ADP ribosyltransferase domain.

1.3.3 Macrodomains

PARP14 contains three consecutive macrodomains within its overall sequence. Macrodomains consist of 130-190 amino acid sequences conserved between many organisms responsible for binding to both free and protein-linked ADPR (ADP ribose). These ADPR reading modules are proposed to have co-evolved with NAD+ dependent enzymes such as PARPs and sirtuins[197,224,225] Of the PARPs (which fall into the Macro2A-like macrodomains), only three contain macrodomains within their overall sequence (PARP9, PARP14 and PARP15). There are 12 different macrodomain containing proteins in humans (16 macrodomains in total), split into four classes- MacroD-type, MacroH2A-like, ALC1-like and PARG-like (Figure 1.14). These posttranslational reading domain containing proteins are amongst a unique class of proteins which have the ability to potentially read and transfer ADPR (write/erase), thus cleaving the glycosidic ADPR bonds (erase) in ADP-ribosylated substrates.[226–234]

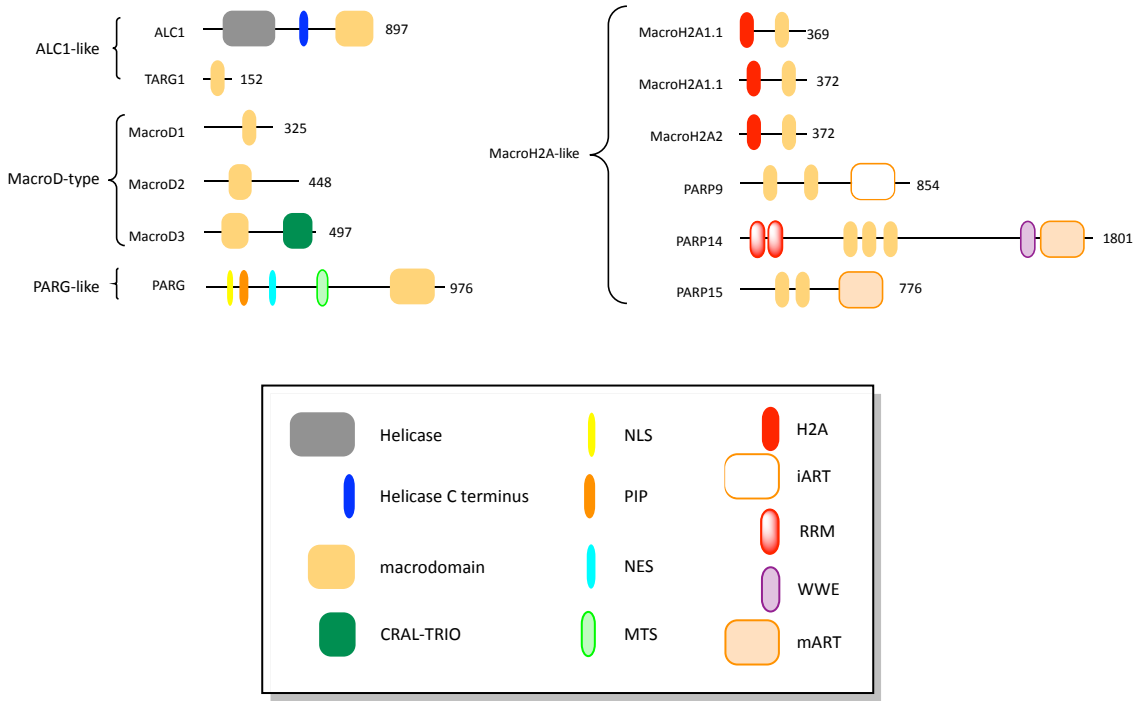

Figure 1.14 Macrodomain containing protein domain map. CRAL-TRIO- cellular retinaldehyde-binding protein-triple functional domain protein, NLS- nuclear localisation signal, PIP- PCNA interacting protein, NES- nuclear export signal, MTS- mitochondrial targeting sequence, H2A- histone 2A, iART- inactive ADP ribosyltransferase domain, RRM- RNA binding/recognition motif, WWE- tryptophan-tryptophan-glutamic acid repeat domain, mART- mono ADP ribosyltransferase domain.

1.3.4 Current Macrodomain Inhibitors

There exists a significant opportunity to delineate the structure and function of macrodomains (MD) within the context of PARP14 biology. At present, many of the disclosed PARP inhibitors in the clinic lack selectivity.[206,235] Of the few PARP14 inhibitors disclosed to date, most have targeted the catalytic ADP ribosyl transferase (ART) domain.[236–240][241] Recently a PARP14 MD2 **11** GeA-69 (Figure 1.15) was disclosed by Schüller and co-workers, which displays a novel allosteric mode of binding.[242] Work was carried out to characterise the potency and nature of binding through biochemical, biophysical and crystallographic studies. In addition to this, information on the cell activity of the compound **11** was acquired through a DNA damage response assay. However there remained no structure activity relationship data around this novel inhibitor **11.** Therefore, there remained a significant opportunity in developing this

interesting hit compound into more developed and potent inhibitors of PARP14 MD2. This recent work also forms the basis of SAR studies around further macrodomain inhibitors described in a later chapter within this thesis.

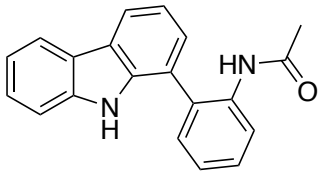

11 GeA-69

*Figure 1.15 PARP14 macrodomain inhibitor, **11** GeA-69.*

1.4 YEATS Domain Inhibition

1.4.1 Non-acetyl lysine acylations

There are a number of post-translational epigenetic marks that occur on histone Lysine residues which in turn remodel chromatin structure and associated complexes, thereby regulating gene expression about that specific loci. One of the more well studied post-translational marks of histone proteins is lysine acetylation.[37,243,244]

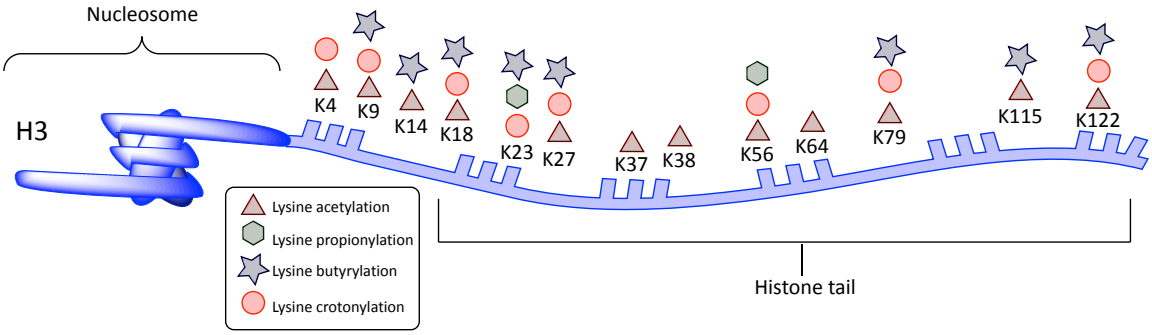

Figure 1.16 Epigenetic histone lysine acyl modifications of histone 3 (H3). Figure adapted from Zhao et. al.[245]

Although the relative distribution of histone lysine acylation is skewed towards acetylation, there exists other acyl- marks which have been characterised as competent regulatory marks within epigenetic mechanisms such as propionylation, butyrylation and crotonylation (Figure 1.16).[246–248]

1.4.2 Human YEATS domain containing proteins

A well characterised and studied epigenetic protein class that interacts with modified histone K residues such as KAc are bromodomain containing proteins,[85,151] other KAc reading domains have recently been identified such as Double Plant Homeodomain Finger (DPF) domains[249] and YEATS (Yaf9, ENL, AF9, Taf14, Sas5) domains (YD).[245]

The YDs have been identified as a relatively tolerant acyllysine binder, containing over 100 family members spread across more than 70 eukaryote species from yeast to humans,[250] showing binding affinity for KAc as well as other epigenetic marks such as crotonyl-, propionyl- and butyryl-lysine. There appears to be a preference for crotonyl marks, despite being a much less abundant mark than acetyllysine.[247,248,251] Due to the non-overlapping pattern of histone lysine acylations occurring at different sites depending on the type of acyl mark conferred, specific marks may therefore bestow a specific effect to local chromatin architecture. Misregulation of the YDs have been correlated with a number of human cancers.[245,252–254] Of the four YD containing proteins in the human genome; YEATS1 (ENL/MLLT1), YEATS2, YEATS3 (Af9/MLLT3) and YEATS4 (GAS41) a number of co-crystal structures have been solved with acyllysine histone peptides including Af9[246,248,255], YEATS2[251] and ENL[252]. The YEATS domain features an 'open-ended' pocket and is believed to interact with crotonyllysine residues through a π- π- π sandwich interaction in the centre of the binding site (Figure 1.17).[245]

1.4.3 ENL

The eleven-nineteen-leukaemia protein (ENL/MLLT1/YEATS1) is one of the four human YEATS domain containing proteins which is fused to mixed-lineage leukaemia (MLL) in some rearranged leukaemias and has been correlated to Acute Myeloid Leukaemia (AML) and the development of Wilms tumour when mutated.[252,253,256] ENL has been linked to the histone methyltransferase DOT1L[257–259] which is essential for MLL-fusion leukaemia[260–263] and also associates with the Af4

sub component in certain rearranged leukaemia.[264] Furthermore mutations of the YEATS domain of ENL has been shown to increase the affinity for PAF1 which in turn transforms hematopoietic cells.[265]

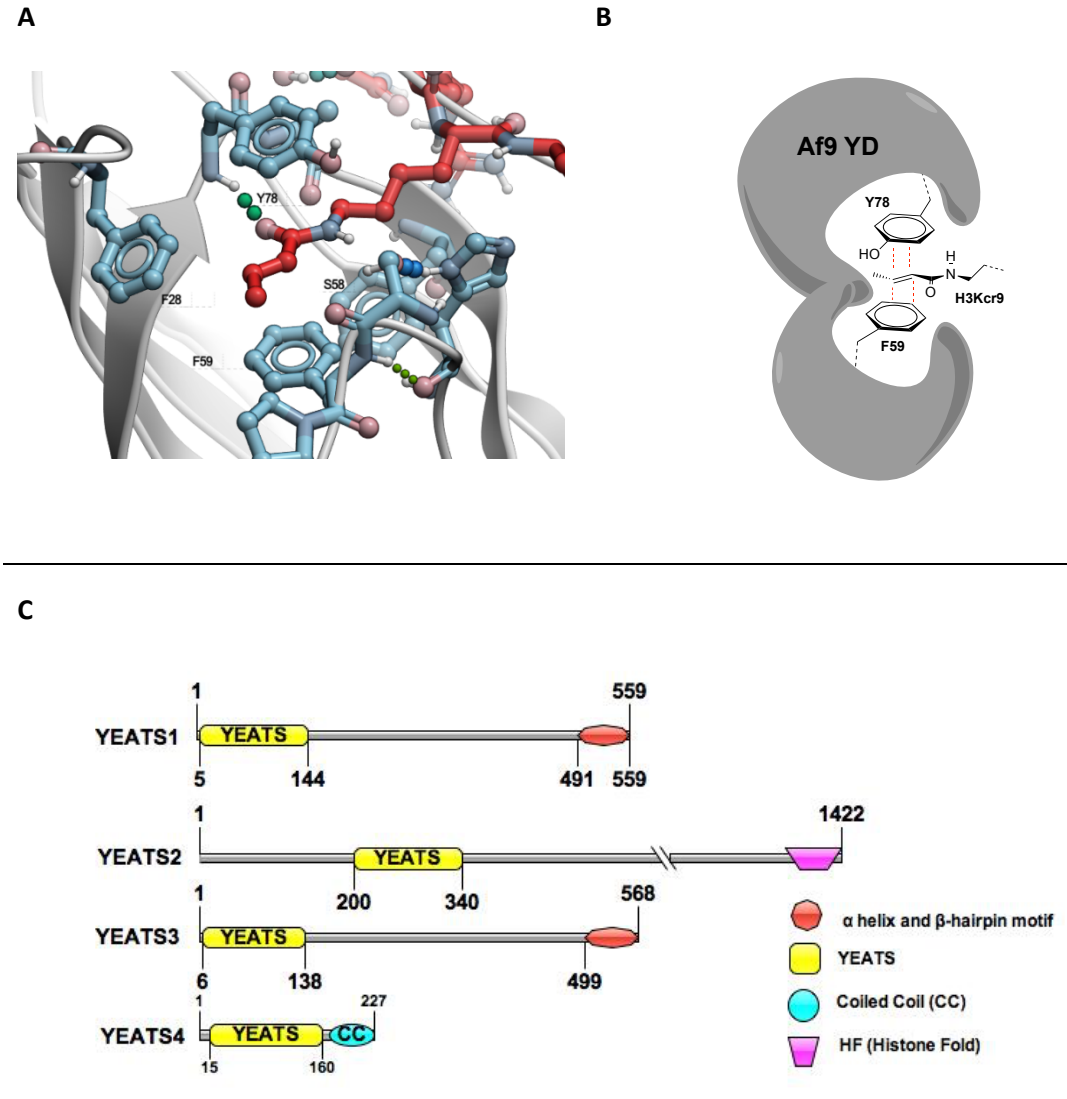

Figure 1.17 A) Af9 YEATS domain co-crystal structure with H3KCr9 peptide (PDB ID 5HJB). Af9 depicted as grey ribbons and light blue sticks. H3KCr9 depicted as red sticks. B) The aromatic π-π-π stacking interaction of Af9 YD residues Y78 and F59 with crotonylated lysine residue (H3KCr9). C) Human YEATS Domain containing protein map. Generated using IBS.[116]

1.4.4 Af9

The human ALL1-fused gene from chromosome 9 (Af9/MLLT3/YEATS3) protein is another similar YEATS domain containing protein to ENL (YD sequence similarity 88%). Similar to ENL, Af9 shares similar roles in chromatin regulating complexes, eg. Super-Elongation Complex (SEC).[245] However, dissimilar to ENL, Af9 is located on different regions of chromatin, which Chromatin Immunoprecipitation studies identify as 89% enrichment of ENL (MV4; 11) at promoter regions of DNA as opposed to 21% for AF9 (HeLa). Despite this difference, translocations leading to the Af9-MLL fusion protein is the most frequent type found in AML (~30%).[245] Af9 shows a preference for binding to H3KAc9 over H3KAc27 and H3KAc18 and mediates recruitment of DOT1L which in turn methylates H3K79.[255] Due to an aromatic π-π-π stacking interaction, also evident in ENL, the YD of Af9 binds to crotonylated histone lysines with a higher affinity than to acetyllysine.[246,248] Recently it has been shown that both ENL and Af9 share a 'KILK' like motif interaction which is present in the extra-terminal (ET) domain of BRD3 and thought to be responsible for the recruitment of chromatin-remodelling complexes such as NuRD, BAF and INO80.[266]

1.4.5 Current YEATS domain inhibitors

There are no known YEATS domain containing protein chemical probes or inhibitors available at this juncture. The closest form of small molecule modulation of a YEATS domain containing protein was reported by Erb and co-workers[253] who showed that using a 'bump and hole' approach[267] with a dTAG system[268] they were able to recruit an E3 ligase to the transfected FKBP-tagged mutant ENL with a PROTAC[193] molecule which showed degradation of the mutant protein.

1.5 Natural Product Synthesis

1.5.1 Flow Chemistry applied to spirocycle synthesis

There exists a number of natural products, chemotherapeutics and future drug candidates that feature spiroindolines or spiro-oxindoles as a structural motif embedded in their core (Figure 1.18).[269] Due to the biological significance of a number of these examples, there is value in the generation of new simplified methods of synthetic access to these scaffolds.

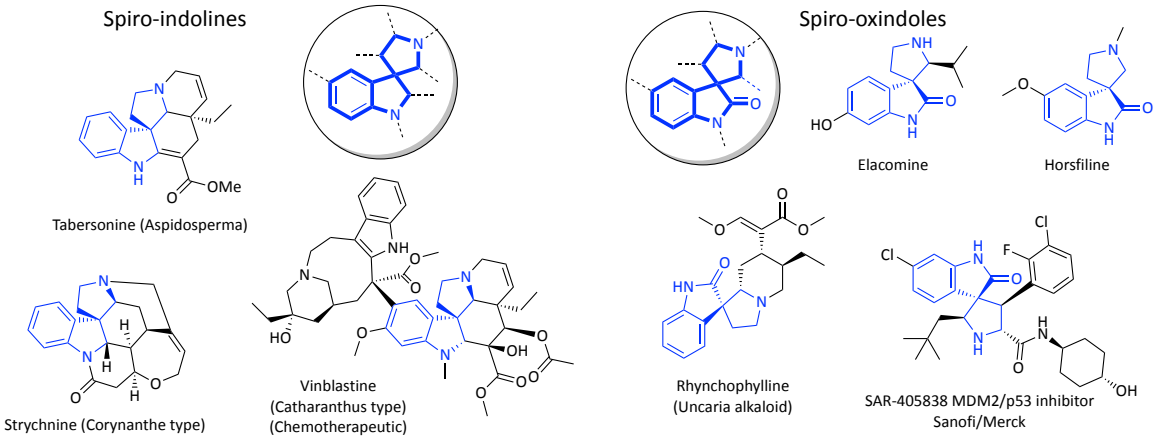

Figure 1.18 Spiroindolines and spiro-oxindoles featured in natural products and drug candidates.

Early reports by Schultz et. al. concerned the use of UV-A promoted cyclisation of aryl-enamines to spiroindolines (Scheme 1.2). Despite this early report, there has been little work carried out since exploring the scope of this useful transformation. Due to first-hand experience of these photocyclisations being hindered by extended reaction times, batch to batch variability and poor conversions, it was envisaged that alternative methods for energy input may offer advantages.

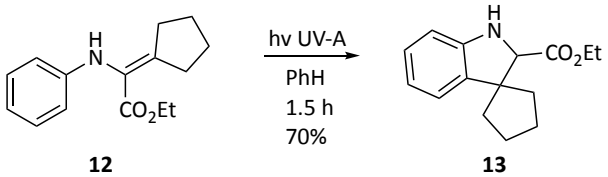

*Scheme 1.2 Shultz's report of UV-A promoted cyclisation of aryl-enamines such as **12** to spiroindolines **13**.*

The use of flow chemistry as applied to photochemistry potentially offers a number of synthetic advantages such as precise heat control, consistent light penetration, control over: reaction times, reagents, scalability and integration with additional parameter control (cooling/heating/reagents).[270–272] When applied to the aforementioned example of UV-A promoted photocyclisations of aryl-enamines to spiroindolines, flow chemistry could enable a new expedient method towards alkaloid natural products such as horsfiline, a spiro-[3, 3']-oxindole (Figure 1.18).[273]

1.6 Biological Methods

Across the various projects that will be described in subsequent chapters (chapters 2-4), a number of biological methods were employed to gain further insight (both qualitative and quantitative) into the interactions of generated small molecule modulators. In order to rank order and build structure activity relationships within chemical series, assay outputs then guide subsequent synthetic and medicinal chemistry efforts. Typically, at the onset of a medicinal chemistry project, the initial or primary assay chosen will be dictated by virtue of the properties of the biomolecule (intended biological target). Often, *in vitro* assays require the generation of stable, well characterised target biomolecule(s) with appropriate appendages or biological tagging systems enabling use of the target in a given assay. This recombinant mutant biomolecule production tends to require a series of optimisation steps in order to appropriate the optimised form of the biomolecule for the assay. As certain assays may be incompatible with certain target biomolecules (instability in assay format/tractability of mutant biomolecule required), access to multiple assays capable of providing interaction readouts is advantageous. Many assays can be considered 'biochemical' in nature or 'biophysical'. Biochemical assays rely upon the interactions of chemical entities in the same phase (likely solution), providing some quantifiable read out that can then be potentially perturbed by the introduction of small molecule modulators which can then affect the assay read out in a concentration dependent

manner. There are a number of innate advantages of a biochemical assay format, namely the ability to screen a number of potential modulators in a high throughput fashion and the high levels of sensitivity associated with interaction phenomena such as Fluorescence. Biophysical assays rely upon direct detection of a binding event incurred by a biomolecule and a potential modulator. The recorded biophysical output can be in the form of heat changes associated with the interaction or changes in the physicochemical properties of the biomolecule. Moreover, if multiple orthogonal assays are able to provide data that is in agreement, this enhances the validity of the assays themselves and any small molecule: biomolecule interactions observed.

In addition to *in vitro* binding assays a number of cellular assays will be briefly described which enable access to information on cellular target engagement, cell membrane permeability, phenotypic biomarkers and pharmacokinetics.

1.6.1 AlphaScreen

Amplified Luminescent Proximity Homogenous Assay Screen is a flexible technology platform centred on the fact that all of the components are 'homogenous' or within solution phase. The technology centres on the proximity of two beads attached to the interacting components of the assay. The two interacting partners are expressed tagged with either a terminal His_6 tag that has a specific affinity for Ni^{2+} ions or a biotin tag which has a high affinity for Streptavidin. Of the two beads, the 'donor bead' which contains phthalocyanine as a photosensitizer is derivatised with Streptavidin, whereas the 'acceptor bead' is derivatised with Ni^{2+} ions. Irradiation at a predetermined wavelength of light which excites the 'donor bead' to an excited state (~680 nm), which in turn is able to emit high energy radiation capable of generating singlet oxygen, only capable of travelling certain distances (limited by the half-life of $^1O_2$: ~200 nm). As singlet oxygen decays down to its ground state, a high energy photon of light is released which in turn can excite an 'acceptor bead', which once excited is capable of emitting light at a defined wavelength (520-620 nm). Any perturbation of the processes that underpin the net

chemiluminescent transfer of energy result in a change in acceptor bead signal. As a result, potential modulators of the interaction under study- be that a protein: substrate, protein: protein or protein: small molecule interaction, are capable of being screened for their ability to interrupt interactions leading to efficient chemiluminescent energy transfer in a dose dependent manner (Figure 1.19). As such, approximations of ligand IC_{50} values against the protein target can be estimated.[274,275]

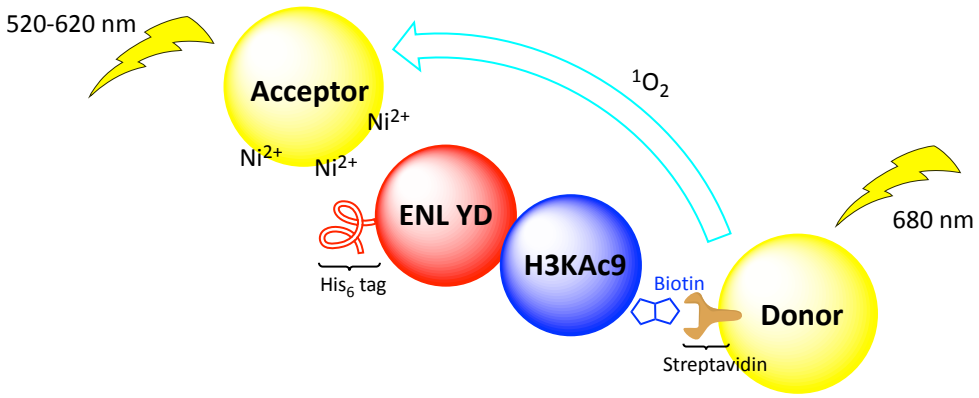

Figure 1.19 AlphaScreen biochemical assay principles depicted measuring the interaction of ENL YD and modified histone peptide H3KAc9. Figure adapted from PerkinElmer.[275]

1.6.2 Differential Scanning Fluorimetry, DSF

When considering the target biomolecule of interest, specifically proteins, an appreciation of the physico-chemical properties can be used to infer the ability of another interacting partner to bind to the protein. Isolated, pure, recombinant protein is known to have a melting point (T_m) or point at which the non-covalent intramolecular bonding interactions which underpin the secondary and tertiary structure begin to break, allowing for the protein to unravel into disordered linear sequences in solution. Generally, folded proteins in polar solutions (aqueous buffers) present polar or charged amino acid residues close to the surface, whereas a number of the more lipophilic and neutral residues are likely to be found 'buried' within the protein. As a protein is denatured into disordered linear chains, a number of the lipophilic residues become 'solvent exposed' and thus can be selectively monitored through the addition of dye molecules

sensitive to this process (Figure 1.20A).[276,277] When a small molecule capable of interacting with the protein in a productive fashion is introduced, stabilisation of the protein through binding results in a 'shift' in melting point (T_m) of the protein, denoted the thermal shift (ΔT_m) (Figure 1.20B). The degree of thermal shift correlates with both affinity of a ligand and concentration; however, a caveat is that thermal shifts are also proportional to the logP of a ligand which affects the enthalpic and entropic contributions to binding and the observed ΔT_m.[278] Despite this, the DSF assay benefits from low requirements of protein loadings, no requirement of protein modifications and that it is amenable to high throughput screening.[220,278–280]

A

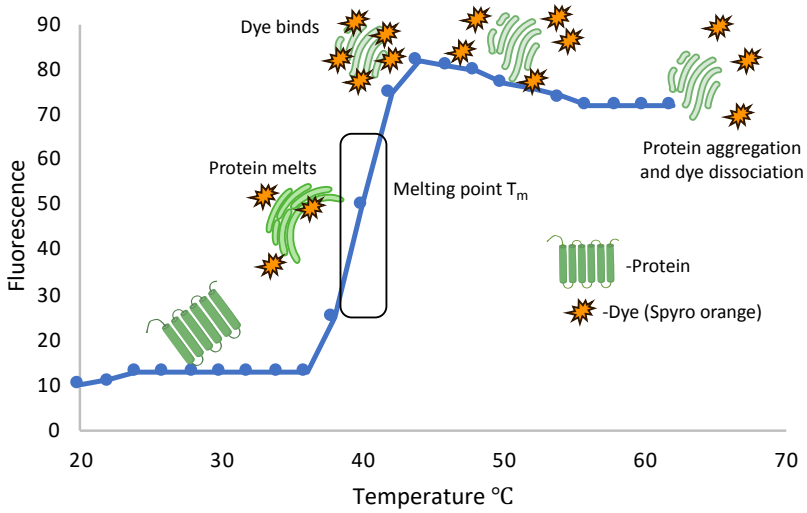

B

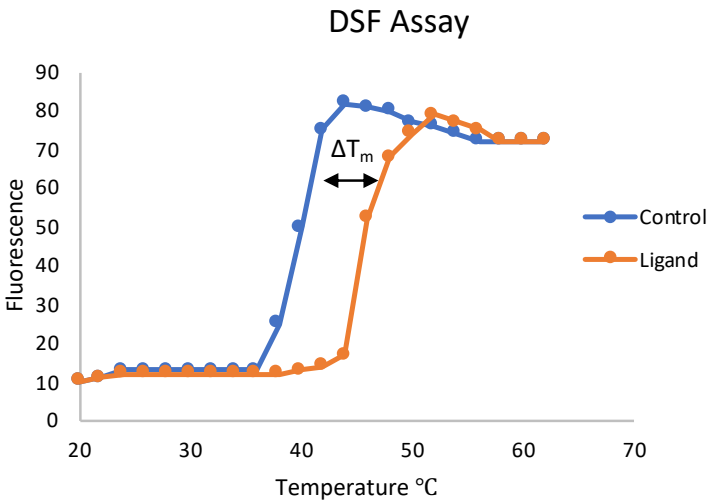

Figure 1.20 A) Differential Scanning Fluorimetry (DSF) Principles. Figure adapted from Argonne National Laboratory site.[277] *B) Example DSF assay output with thermal shift range denoted by 'ΔT_m'.*

1.6.3 Isothermal Titration Calorimetry, ITC

ITC or Isothermal Titration Calorimetry is a biophysical assay used to determine the energetic changes associated with interactions within a solution as one interacting partner is titrated into a solution of the other. Energetic changes in solution can be monitored accurately using modern micro-calorimeters equipped with a reference cell. As accurate concentrations of both solutions can be predetermined, information on the nature and thermodynamics of binding can be inferred from the observed pattern of heat evolution or consumption including; binding mechanisms, affinity and stoichiometry (Figure 1.21).[281] A key advantage of ITC is that whilst the exact concentrations of both interacting partners should be known- any errors in calculations are accounted for by the nature of the assay (assuming the mode of binding is known). The assay is highly endogenous and does not require tagging, however required protein loadings are high, the assay is low throughput and labour intensive relative to other assays which limits the use of this biophysical assay with poorly expressing proteins.

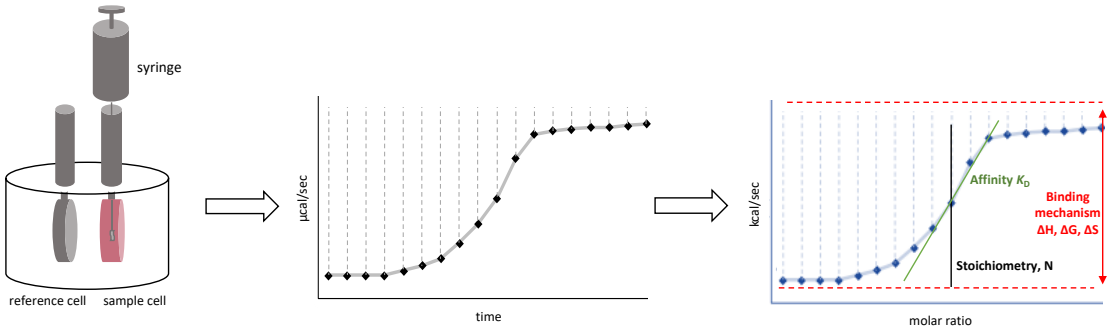

Figure 1.21 ITC components and principles. Figure adapted from 2bind.[281]

1.6.4 Homogeneous Time Resolved Fluorescence Assay, HTRF

Another assay that can be used to measure the interactions of biomolecules is a Homogeneous Time Resolved Fluorescence Assay (HTRF).[282] Based on Fluorescence Resonance Energy Transfer (FRET), the key event underpinning this biochemical assay is the transfer of long-lived

fluorescence irradiation from a Tris-bipyridine europium cryptate donor to an allophycocyanine acceptor moiety. Through conjugation to complementary streptavidin: biotin templating system, a wide variety of biochemical interactions can be explored including competitive displacements using small molecule ligands and inhibitors.

1.7 Cellular Assays

1.7.1 Nano Luciferase Bioluminescence Resonance Energy Transfer Assay, NanoBRET

An assay used to investigate interactions between biomolecules or small molecules and biomolecules within a cellular context is the nanoBRET system developed by Promega Corporation.[283] Transient overexpression of a biomolecule of interest with a fused terminal Nano Luciferase sequence along with overexpression of a Halo tagged substrate biomolecule is carried out. A chloroalkane fluorescent ligand is then introduced which is covalently alkylated on the Halo tag sequence. Additionally, a NanoLuc substrate- furimazine, is introduced to the cellular system which undergoes an oxidative degradation process catalysed by the NanoLuc sequence to form furimamide which in turn releases a photon of light.[284] When the protein of interest and Halo tagged moiety are in close proximity, efficient Bioluminescence Resonance Energy Transfer (BRET) is then transferred to the covalently attached Halo tag ligand (Figure 1.22).[285] Longer wavelength emission (580-620 nm) of the Halo tag ligand can then be monitored whilst potential modulators of the interaction under study are introduced in a dose dependent manner. The nanoBRET assay offers the advantage of high intensity of fluorescence from the NanoLuc sequence emission coupled with narrow ranges of bioluminescence emissions- which minimizes overlap with emission from the corresponding acceptor fluorophore. Any disruptions of the interaction of the biomolecule of interest and the Halo tagged substrate biomolecule can be traced to changes in the BRET efficiency (Acceptor/Donor ratio). Dose dependent screening of potential small molecule inhibitors allows for identification of potent molecules that indeed engage with their target in a cellular context. By analogy the

use of a 'tracer' tool compound is also possible if a cell permeable small molecule hybrid of a protein of interest (POI) ligand conjugated to a fluorescent dye is used in place of a transiently expressed substrate-Halo tagged mutant biomolecule. As depicted (Figure 1.22), protein-protein interactions (PPIs) such as BRD and modified histone interactions can be screened in a cellular context with potential inhibitors. For such an example, the assay typically relies upon sufficient modifications (acetylation) being present on the mutant histone protein- as such additional additives are sometimes required such as pan-HDAC inhibitors (SAHA) to shift acetylation equilibrium in favour of the binding interaction investigated.

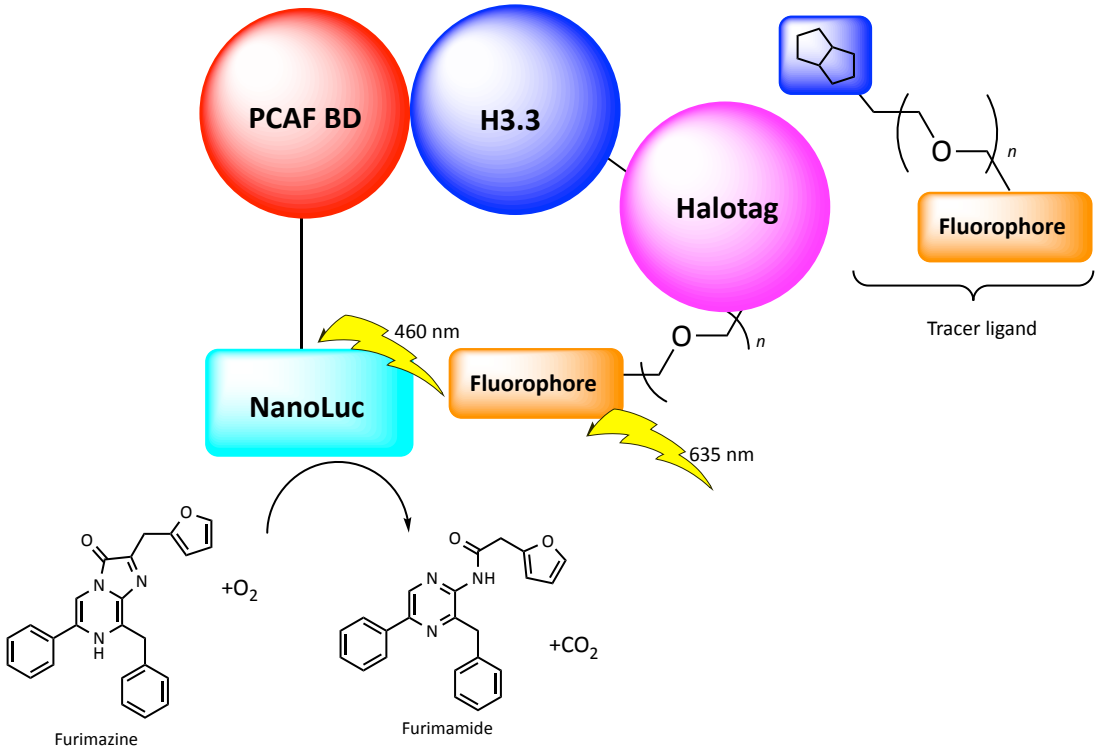

Figure 1.22 NanoBRET assay protocol depicted exemplified by the study of the protein: protein interaction between modified H3.3 and PCAF BRD. Figure adapted from Promega Corporation[285]

1.7.2 Cellular Thermal Shift Assay, CETSA

Another measure of the ability for a small molecule to engage with its target in a cellular context is a Cellular Thermal Shift Assay (CETSA, Figure 1.23).[286] The assay relies upon the principle that soluble proteins in cell lysate have a quantifiable melting point temperatures, above which the

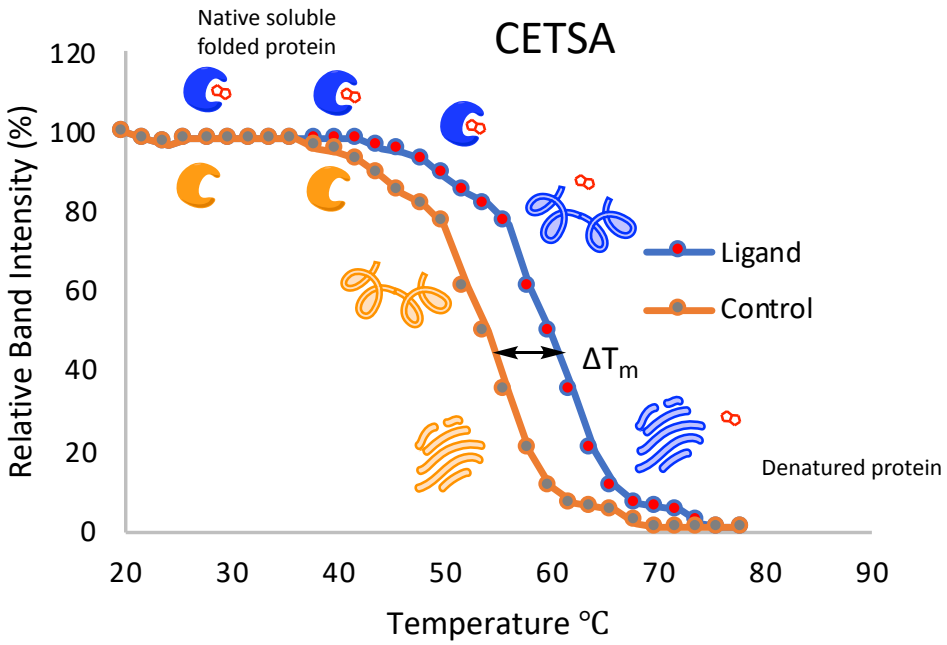

Figure 1.23 Cellular Thermal Shift Assay (CETSA) protein destabilisation curves with or without ligand dosing. ΔT_m denotes observed thermal shift due to ligand stabilisation.

tertiary and secondary structure of the protein begins to become destabilised. Upon complete destabilisation the protein begins to become less soluble and forms aggregates which are then separable from the soluble fraction of cell lysate. When intact (or permeabilised) cells are incubated with a ligand for a given biomolecule, if the ligand is able to permeate cells, engage with and bind to its cognate biomolecule substrate, this interaction may confer a degree of net stabilisation to the protein. If ligand and biomolecule interactions are stabilising in nature, then a shift in the melting point (T_m) of that protein is induced which can be analysed and quantified in a dose dependent manner by Western Blot Analysis. Whilst this assay can be hindered by the fact that not all target biomolecules become less soluble upon denaturation, it can provide a highly endogenous means of validating both cell permeability and cell target engagement.

1.7.3 MDCK-MDR1 Permeability Assay

The Madin Darby Canine Kidney (MDCK)-MDR1 Multi Drug Resistance permeability assay is an assay used to ascertain the ability of small molecules to permeate cell membranes and also predict whether or not molecules are P-glycoprotein (P-gp) inhibitors or substrates.[287] Using Madin Darby Canine Kidney (MDCK) cells stably transfected with the MDR1 gene (encodes P-gp- a major efflux transporter in many cell types), data is reported as both the product of unidirectional and bidirectional studies (x 10^{-6} cm/s) enabling confirmation of the effect of MDR1 overexpression on cell permeability.

1.7.4 BioMAP Diversity PLUS Assay

A cellular assay developed by DiscoverX/eurofins in order to investigate *in vitro* models of inflammatory disease in the context of small molecule inhibition is BioMAP Diversity PLUS.[288] Through the use of 12 separate primary human co-culture systems, predictions about the effects of a small molecule can be made which pertain to both efficacy and safety based on multiple tissues and inflammatory disease states.

1.7.5 NCI-60 Panel

A widely used cellular assay used to investigate the effects of small molecules on a panel of cancer cells is the National Cancer Institute (NCI) Human Tumour Cell Line 60 Panel.[289,290] The NCI offers free comprehensive screening of well characterised cancer cell lines measuring the effect of compound incubation on cancer cell proliferation. Additionally, data on previously screened compounds is available free of charge along with algorithm software in order to correlate cancer cell growth signatures between compounds, allowing for potential elucidation of mechanisms of action and molecular targets.

1.7.6 *in vitro* and *in vivo* Pharmacokinetic profiling

In subsequent chapters data is discussed whereby selected compounds have been profiled for metabolic stability *in vitro* using primary human and/or rat liver microsomes and hepatocytes. Data has been generated in collaboration with a number of companies including Cyprotex and UCB Pharma. Additionally, *in vivo* pharmacokinetic profiling was also carried out in rats to measure oral metabolic stability of selected compounds along with blood brain barrier (BBB) permeability and bioavailability.

1.8 Thesis Objectives

In this thesis a number of disease relevant protein targets that have been previously discussed are chosen for chemical probe and inhibitor design campaigns. Using a combination of synthetic and medicinal chemistry high quality chemical probes and inhibitors will be generated for PCAF/GCN5, PARP14 and ENL/Af9 to further the understanding of their underlying biology. These chemical probe and inhibitor discovery projects will be enabled by many of the biochemical, biophysical and cellular techniques outlined.

In addition to these chemical probe and inhibitor projects a total synthesis based project will be carried out focussed on the synthesis of the natural product (±)-horsfiline, using novel flow photochemistry methods previously discussed.

2. Bromodomain Inhibition

2.1 Introduction

2.1.1 Project Origin

The p300/CBP Associated Factor (PCAF/KAT2B) and General Control Non-depressible 5 (GCN5/KAT2A) proteins are bromodomain containing proteins deriving from phylogenetic sub family I (Figure 2.1). PCAF (KAT2B) has been reported to associate with other histone acetyltransferases (HATs) and bromodomain containing proteins CBP[291,292] and p300[292] during transcription and also been linked to cancer progression[89–91], neuroinflammation[79,89], inflammatory disease[89,293,294] and HIV infection[89,92–95]. These multi-domain proteins contain a catalytic acetyltransferase domain (HAT) and a C-terminal bromodomain, which in PCAF has been predicted to be highly druggable.[73] In order to investigate the origins of these disease links and the domain specific contribution of the BRD to PCAF/GCN5 pathology, a chemical probe discovery programme was initiated. Owing to high sequence similarity in the bromodomain, it was envisaged that developing selective inhibitors between PCAF and GCN5 would pose as a challenge and may not be desired owing to significant overlap in the biology underlying these two protein targets.

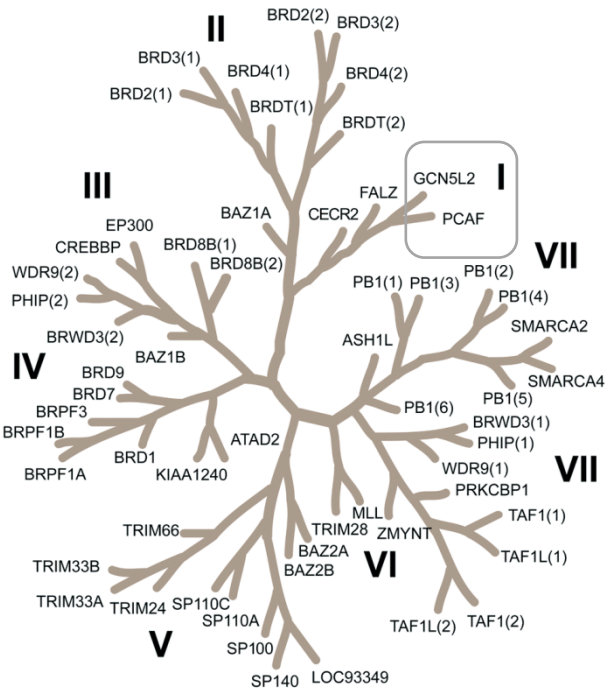

Figure 2.1 Phylogenetic tree of bromodomain containing proteins. PCAF and GCN5 are shown in a grey rectangle box. Figure extracted from Muller et. al.[72]

2.1.2 Chemical Starting Points

One of the first reported inhibitors, compound **14**, of the PCAF BRD was from Wang *et. al.* focussed on the development of disruptors of HIV-1 replication owing to the reported dependence of the HIV-1 virus on the human BRD containing protein.[94] This line of inquiry was also pursued by Hu[295] without significant increases in potency, compound **15** displays modest PCAF BRD inhibitory activity in a fluorescence polarisation assay (PCAF IC_{50} 0.93 μM, EC_{50} 11.5 μM, Figure 2.2A), however there were no studies carried out indicating compound selectivity or direct evidence of target engagement in a cellular context. Whilst the focus of these two inhibitor discovery reports was on targeting PCAF BRD, there were no investigation into GCN5 BRD activity of compounds **14** or **15**, which may indeed significantly contribute to the disruption of the HIV-1 lifecycle. Recently a number of compound structures were disclosed by Genentech and Constellations Pharmaceuticals[90,91,296] including compound **16**, which are potent PCAF BRD inhibitors. Despite significant increases in potency compared to prior reports in the primary

literature, no indication of selectivity or cell activity of these compounds were disclosed at the time. More recently a crystallography campaign against the PCAF BRD was conducted by colleagues at the University of Oxford/Structural Genomics Consortium leading to the identification of a number of weak fragment-like PCAF BRD ligands.[297]

An original subset of potential inhibitors of PCAF/GCN5 BRD were developed by P. G. K. Clark and L. Truilli based on [1,2,4]triazolo[4,3-a]phthal-azine derivatives.[149] Substituted compound **17** was found to be a moderately active PCAF BRD inhibitor displaying weak activity in a DSF assay (PCAF BRD ΔT_m +1.7 °C) and reasonable activity by ITC (PCAF BRD K_D 1 μM). Despite this initial work, there remained significant progress to be made in order to discover sub-micromolar inhibitors of PCAF BRD. In addition to this, there was no structural information on the mode of binding to PCAF BRD and if indeed these weak inhibitors adopt a similar binding mode to that of acetylated histone lysines. Furthermore, there was a lack of information regarding activity of this chemical series against GCN5 BRD, selectivity over other BRD family members, or cell target engagement activity. A well characterised pan-BRD inhibitor, **18** Bromosporine, was reported to bind to PCAF BRD with moderate potency (PCAF BRD K_D 5 μM).[298] Despite no structural evidence about the mode of binding of **17** with PCAF BRD, or indeed GCN5 BRD, numerous BRD co-crystal structures with other targets had been solved with this promiscuous ligand and so it represented a possible chemical starting point for the development of PCAF/GCN5 BRD chemical probes. Additionally, the [1,2,4]triazolo[4,3-a]phthal-azine **19** which shares a similar core to compound **17** had been extensively profiled for binding interactions with other BRDs such as BRD4.

Compounds such as Bromosporine **18** and **19** could be examined in the binding sites of other BRDs and arising information could be used to infer likely interactions between these starting points and PCAF/GCN5 BRD binding site residues. Using this information, additional analogues of

compounds such as **17** could be designed aimed at improving PCAF/GCN5 BRD potency, whilst selectivity could later be 'dialled in' to the chemical series.

A

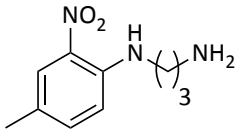

14
PCAF IC_{50} 1.6 µM
HIV-1 EC_{50} 2.76 µM

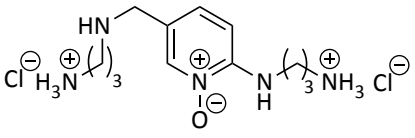

15
PCAF IC_{50} 0.93 µM
HIV-1 EC_{50} 11.52 µM

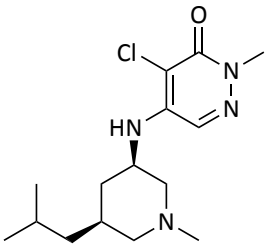

16
PCAF IC_{50} 13 nM

B

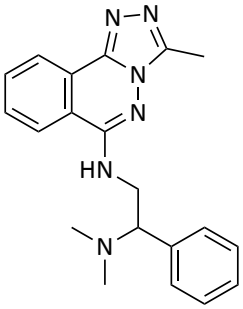

17

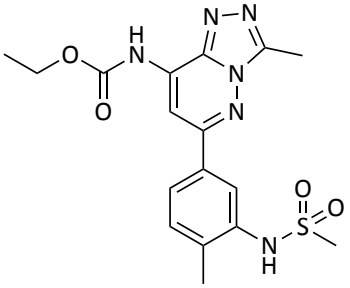

18 Bromosporine

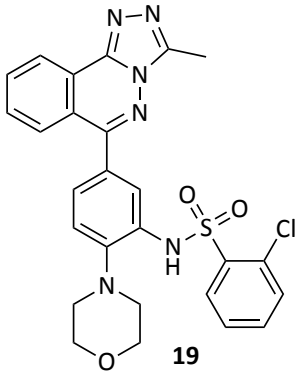

19

Figure 2.2 A) Previous reported PCAF BRD inhibitors. B) PCAF BRD inhibitor chemical starting points.

2.1.3 Aims

The aim of the research project outlined in this chapter was to advance weakly active fragment like inhibitors of the PCAF BRD to a potent probe molecule. Due to GCN5 and PCAF structural similarity in the BRD, in addition to overlapping biology in some instances, a dual probe molecule was the primary aim. Newly identified inhibitors would be optimised for potency, selectivity and cell activity using data derived from a number of *in vitro* and cellular assays leading to the identification of the first PCAF/GCN5 chemical probe.

2.2 Chemical Methods

2.2.1 Initial SAR/Synthesis

Initially it was envisaged that an inspection of BRD binding modes of the moderately potent PCAF BRD ligand Bromosporine **18** and a similar [1,2,4]triazolo[4,3-a]phthal-azine derivative compound **19** with other BRDs might provide initial clues as to how these compounds might interact with PCAF/GCN5 BRD. A co-crystal structure of Bromosporine **18** with BRD4(1) (Figure 2.3, PDB ID 5IGK) provided insights to the nature of interactions underpinning this chemical series. Interactions of Bromosporine **18** with BRD4(1) centre on a H-bond interaction network with the triazolopyridazine core and essential residue N140. The N-H bond of the ethyl carbamate in the core makes a complementary H-bond with the carbonyl O atom of N140. Concomitantly, the methyl group of the triazole KAc mimetic makes contacts with the terminal region of the BRD4(1) pocket which is occupied by four largely conserved structural BRD water molecules. The sulfonamide engages in polar interactions with K91 along the entrance of the BRD4(1) KAc binding site close to the ZA loop.

A separate inspection of a co-crystal structure of [1,2,4]triazolo[4,3-a]phthalazine derivative **19** with BRD4(1) also shows similar interactions of the KAc mimetic triazole with N140 (Figure 2.4, PDB ID 4NQM). The methyl group of **19** occupies the terminal water region of the KAc binding site. Interestingly, dissimilar to Bromosporine, the reverse sulfonamide of **19** is orientated towards W81 where it H-bonds with the tryptophan N-H.

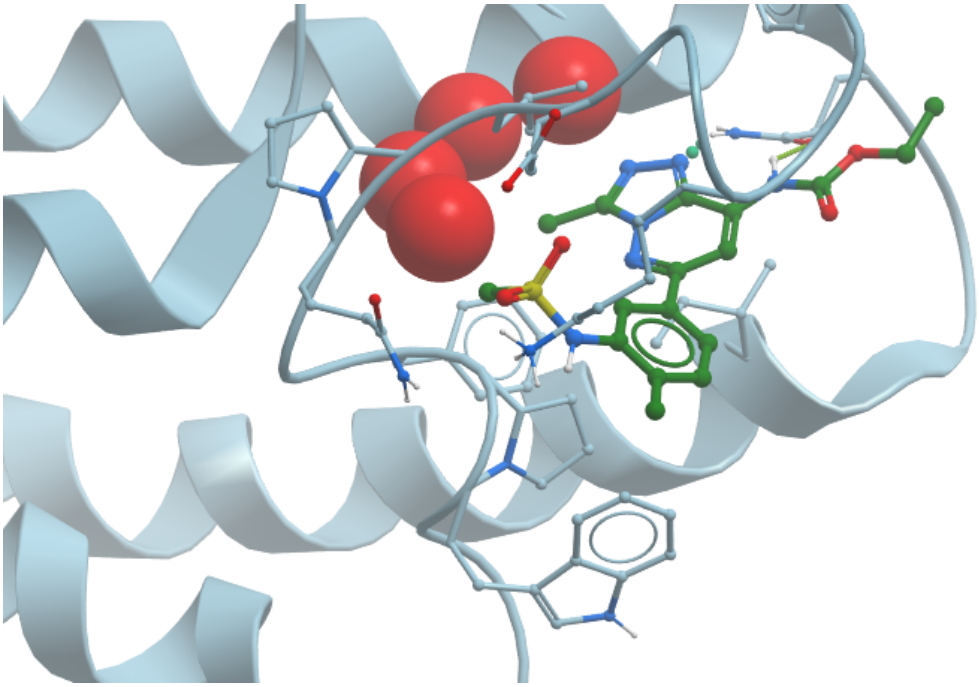

*Figure 2.3 Co-crystal structure of Bromosporine **18** (green sticks) with BRD4(1) (light blue). PDB ID 5IGK. Key residues are depicted as light blue sticks. Four conserved BRD structural waters are depicted as red balls.*

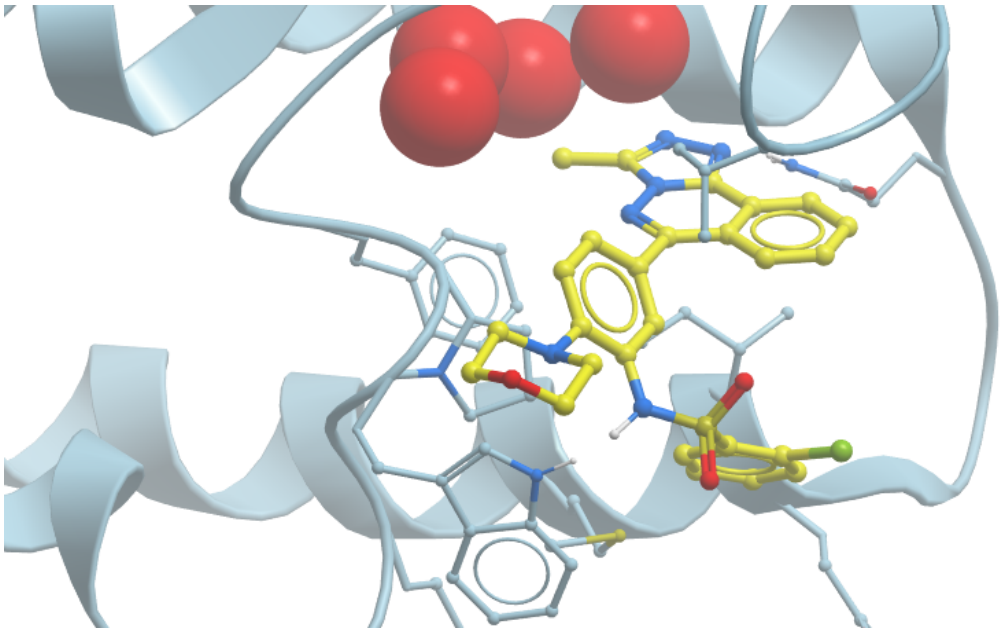

*Figure 2.4 Co-crystal structure of compound **19** (yellow sticks) with BRD4(1) (light blue). PDB ID 4NQM. Key residues are depicted as light blue sticks. Four conserved BRD structural waters are depicted as red balls.*

Taken together it was envisaged that due to the conserved similarities in the BRD KAc binding site of BRD4(1) and PCAF/GCN5 both the Bromosporine series and [1,2,4]triazolo[4,3-a]phthalazine series might bode as promising chemical starting points for potent PCAF/GCN5 inhibitors. Whilst differences between BRD4(1) and PCAF/GCN5, mostly attributable to the entrance of both binding sites, might offer opportunities towards developing selectivity over BRD4(1) starting from these promiscuous chemotypes.

An overlay of previously obtained crystal structures of BRD4(1) (PDB ID 5IGK, Figure 2.5A) and PCAF BRD with acetyllysine (PDB ID 5FE0, Figure 2.5B) reveals a number of notable differences in the BRDs. A number of key KAc recognition residues are conserved between BRD4(1) and PCAF such as N803 (PCAF) and N140 (BRD4). However key residues close to the entrance of the PCAF BRD such as E750 and E756 appear as Q85 and L92. Equally whilst the typical 'WPF' shelf is present in both PCAF (W746, P747, F748) and BRD4(1) (W81, P82, F83), a key residue close to the conserved asparagine in both proteins is significantly different- Y809 in PCAF and I146 in BRD4(1).

A

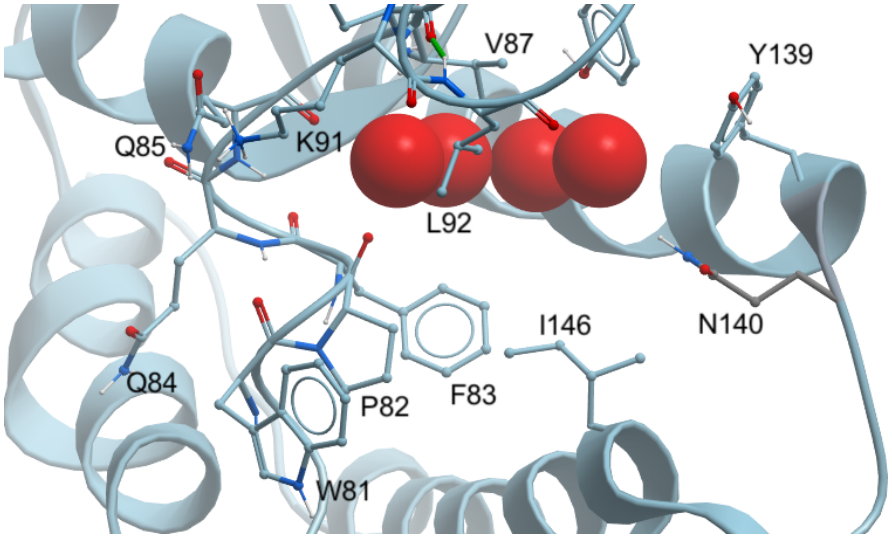

B

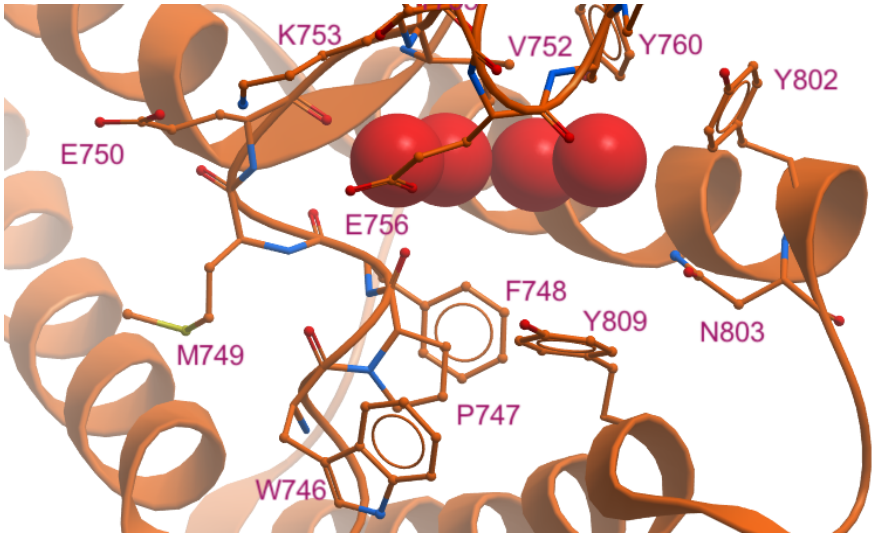

C

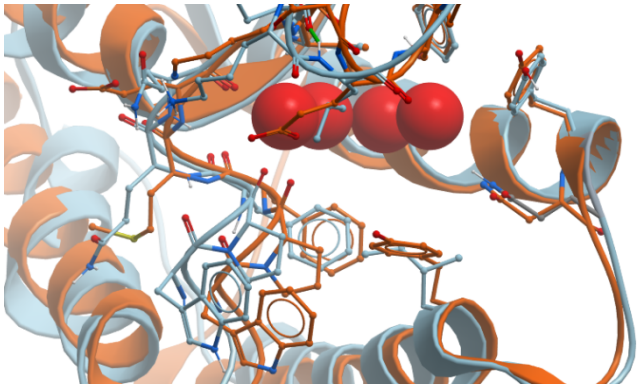

Figure 2.5 A) BRD4(1) BRD structure (light blue) (from PDB ID 5IGK). Key residues are shown as blue sticks in KAc binding site. Conserved water molecules are shown as red balls. Residue labels displayed in black font. B) PCAF BRD structure (orange) (from PDB ID 5FE0). Key residues are shown as orange sticks in KAc binding site. Conserved water molecules are shown as red balls. Residue labels are displayed in purple font. C) Structural superposition of BRD4(1) BRD structure (from PDB ID 5IGK) with PCAF BRD structure (from PDB ID 5FE0).

The initial PCAF/GCN5 inhibitor discovery was progressed using biophysical assays: DSF and ITC. Unfortunately, due to the low binding affinity (STD-NMR PCAF BRD K_D H3KAc36 402 µM, H3KAc9 1051 µM, H3KAc14 128 µM)[86] of acetylated histone peptides to PCAF or GCN5 BRDs- a high throughput biochemical assay which would typically require prior identification of a tagged ligand as part of the assay components, such as AlphaScreen was not available at the onset of the project. Furthermore, it was rationalised that the primary SAR generation would be applied to optimising potency for the PCAF BRD, in part owing to better studied pathology and structural biology compared with GCN5. Prior to the generation of a focussed PCAF BRD library, it was rationalised that as both the [1,2,4]triazolo[4,3-a]phthalazine **17** and Bromosporine **18** (PCAF BRD ITC K_D 5 µM, Figure 2.2)[298] displayed moderate activity for the PCAF BRD that perhaps a merged combination of both structures might lead to more potent PCAF BRD inhibitors such as **20**-**22** (Figure 2.6 and Figure 2.7).

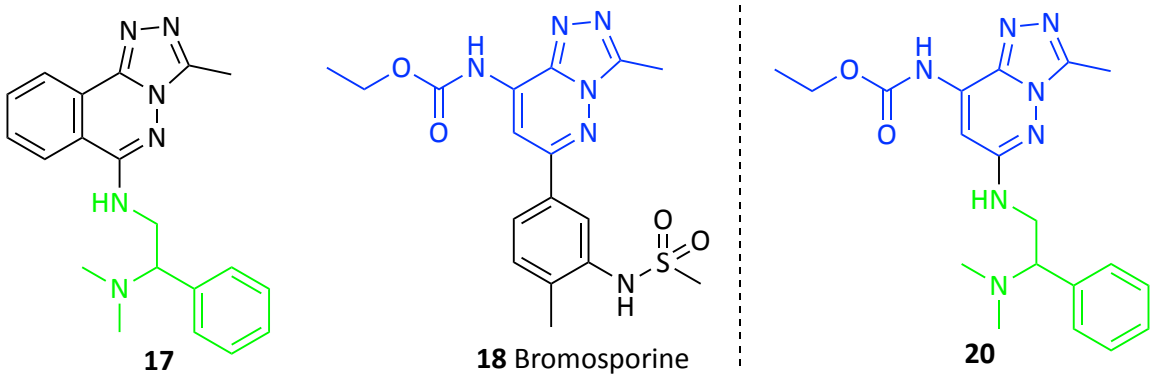

*Figure 2.6 Merging of Bromosporine **18** scaffold with [1,2,4]triazolo[4,3-a]phthalazine derivative **17** to give analogue **20**.*

Despite challenging chemistry underpinning this chemical series, a few derivatives were accessible which were synthesised and screened for PCAF BRD activity through DSF and BromoSCAN assays. Whilst one of the compounds **21** displayed promising activity by DSF against PCAF BRD, activity did not translate into improved binding relative to **17** by ITC (Figure 2.7).

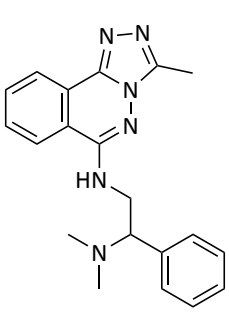

17 PCAF K_D 1 µM

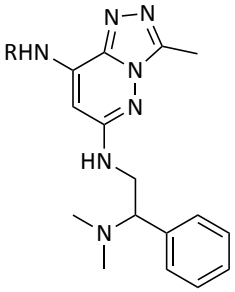

20 R= CO_2Et PCAF K_D >10 µM ΔT_m℃ +0.0

21 R= Boc PCAF K_D 2.8 µM ΔT_m℃ +4.7

22 R=H PCAF K_D >10 µM ΔT_m℃ +2.6

*Figure 2.7 Compounds **20**-**22** screened for PCAF BRD activity by DSF and ITC.*

Instead further efforts were then applied to exploring the SAR directly around reasonably potent hit molecule **17**. It was observed from previously obtained co-crystal structures of the PCAF BRD with KAc that there are a number of charged residues present close to the entrance of the KAc binding site including glutamic acid residues E750 and E756.[297] It was envisaged that the focussed library of PCAF BRD inhibitors, featuring a 1,2-diamine embedded in the structures would be capable of engaging in salt-bridge interactions as in compound **17**. SAR studies to enhance these potential salt-bridge interactions could then be explored. Additionally, owing to the multiple degrees of freedom exhibited by the 1,2-diamine aliphatic chain, areas for optimisation and SAR studies also focussed on substitutions to the aliphatic chain in order to minimize degrees of freedom. It was also notable that the PCAF BRD KAc binding site features an aromatic residue Y809 which is in close proximity to the conserved N803. This aromatic region of the PCAF BRD binding site could make constructive π- π interactions with the flat heterocyclic back bone of the [1,2,4]triazolo[4,3-a]phthalazine series.

2.2.2 *in silico* docking

In order to advance the chemical series based on **17** in an efficient manner, a library was designed based on docking scores generated from hypothetical inhibitors docked into the binding site of a previously obtained co-crystal structure of the PCAF Bromodomain (PDB ID

5FE0) with fragment compounds.[297] The docking software package Molsoft ICM-Virtual Ligand Screening[299] enabled approximately 12,000 virtual ligands to be docked into the PCAF BRD binding site based on enumeration chemistry involving a nucleophilic aromatic substitution reaction with commercially available 1,2-diamines and **23** 6-chloro-3-methyl-[1,2,4]triazolo[3,4-a]phthalazine (Scheme 2.1). Docking results did not offer significant insights into notable ligands for synthesis and rankings of early *in vitro* binding activities did not seem to correlate well with docking scores. However, the docking studies provided a rapid way of filtering out any potential ligands unable to accommodate reasonable ligand poses in the PCAF BRD. Nonetheless, an inspection of the top scoring docked ligands was made and results were filtered based on building block tractability and chemical diversity. A subset of approximately 100 compounds were chosen for synthesis.

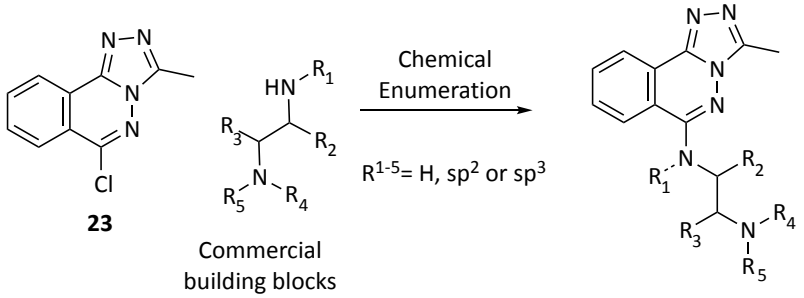

*Scheme 2.1 Chemical enumeration of 6-chloro-3-methyl-[1,2,4] triazolo[3,4-a]phthalazine **23** with various commercially available 1,2-diamines.*

2.2.3 SAR/Synthesis

Construction of the [1,2,4] triazolo[4,3-a] phthalazine core of synthesised derivatives was initiated by a scalable (~20 g) tandem S_NAr/condensation of commercially available 1,4-dichlorophthalazine **24** with acethydrazide in respectable yields (62%). The corresponding 6-chloro-3-(trifluoromethyl)-[1,2,4] triazolo[3,4-a] phthalazine **25** was also obtained via a two-step process; S_NAr of 1,4-dichlorophthalazine **24** with hydrazine to give **26** followed by concomitant trifluoroacetylation/condensation to give compound **25** (43% over two steps). Compounds **23** or

25 were then submitted into a KI/HCl catalysed S_NAr reaction with various 1,2-diamines to provide products in low to excellent yields (8-94%, SI). Compounds were then screened for PCAF BRD activity by DSF and ITC.

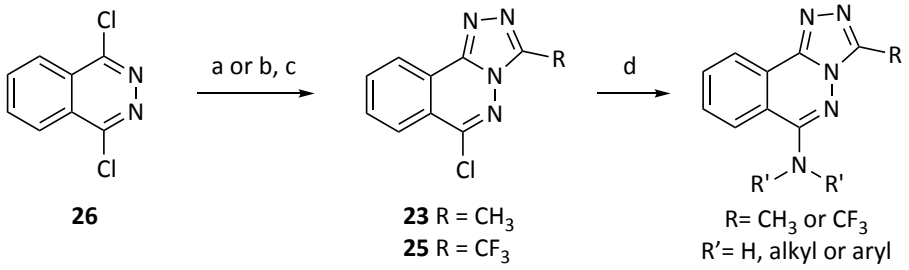

Scheme 2.2 Synthesis of [1,2,4] triazolo[4,3-a] phthalazine derivatives. Reagents and conditions: a) Acethydrazide, DMF 120℃, 16h, 62%; b) $N_2H_4{\cdot}H_2O$, EtOH, 120℃, 10 min, quant.; c) TFA, 100℃, 2h, 43%; d) R'_2NH (1.5–2.0 equiv), KI (0.1 equiv), HCl (0.05 equiv), EtOH or iPrOH, reflux, 3 days, 8–94%.

As can be observed in the SAR displayed in Table 2.1 (compounds **27**-**36**) the chain length of the 1,2-diamine was sensitive to atom spacing, with the sequentially homologated **27**-**29** exhibiting a linear decrease in potency. The largest substituent at R^2 tolerated was a methyl group, additionally groups larger than a methyl such as *N*,*N*-dialkyl substituents (position R^4) also diminished binding activity. Compound screening led to the initial discovery of compound **30**, which was shown to have good potency against the PCAF BRD (ITC K_D 0.30 μM). Stoichiometry of binding by ITC of racemate-**30** showed that activity lay in a single enantiomer. Activity was later attributed to compound (*S*)-**30** after synthesis using single enantiomer building blocks- (**30** PCAF ITC K_D 0.30 μM, BRD/**30** 2:1; PCAF (*S*)-**30** ITC K_D 0.28 μM, BRD/(*S*)-**30** 1:1).

Table 2.1 Amino-substituted triazolophthalazines are potent PCAF BRD Inhibitors.

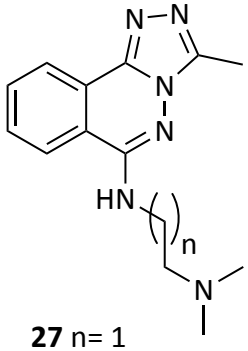

27 n= 1
28 n= 2
29 n= 3

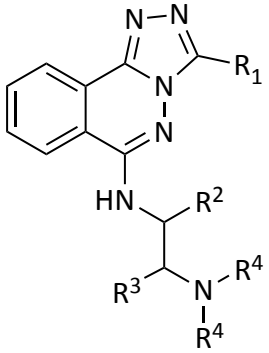

30-**35**, (*S*)-**36**

#	R^1	R^2	R^3	R^4	n	ΔT_m°C[a]	K_D (μM) (ITC)
17	Me	H	Ph	Me	1	1.7	1.0
27	Me	H	H	Me	1	8.5[b]	8.0 ±0.65
28	Me	H	H	Me	2	*ND*	>30
29	Me	H	H	Me	3	*ND*	>30
30	**Me**	**Me**	**H**	**Me**	**1**	**5.6**	**0.30 ±0.039**
(*S*)-30	**Me**	**Me**	**H**	**Me**	**1**	**7.4**	**0.28 ±0.029**
31	Me	Et	H	Me	1	3.3	1.8 ±0.23
32	Me	*i*Bu	H	Me	1	0.85	>30
33	Me	Me	H	Et	1	0.0	>30
34	Me	H	Me	Me	1	4.6	7.3 ±1.1
35	Me	H	Et	Me	1	*ND*	6.9 ±1.4
(*S*)-36	CF_3	Me	H	Me	1	0.65	>30

[a] Compound concentration 10 μM, unless stated otherwise; [b] Compound concentration 100 μM; *ND*: not determined.

The [1,2,4] triazole motif of compound (*S*)-**30** was seemingly required as the key KAc mimetic region from inspection of the binding mode in co-crystal structures of similar derivatives with BRD4 (Figure 2.4).[149] Therefore, the next site of optimisation in this chemical series was on the backbone of the [1,2,4] triazolo[4,3-a] phthalazine core. A number of derivatives of compound (*S*)-**30** were designed and synthesised however much of the chemistry employed in order to access these derivatives suffered from a lack of regioselectivity in the key triazole forming step. Whilst efforts were employed towards enhancing the regioselectivity of this step unfortunately only non-separable regioisomeric mixtures were obtained of target molecules deriving from non-symmetrical phthalazine cores (Figure 2.8).

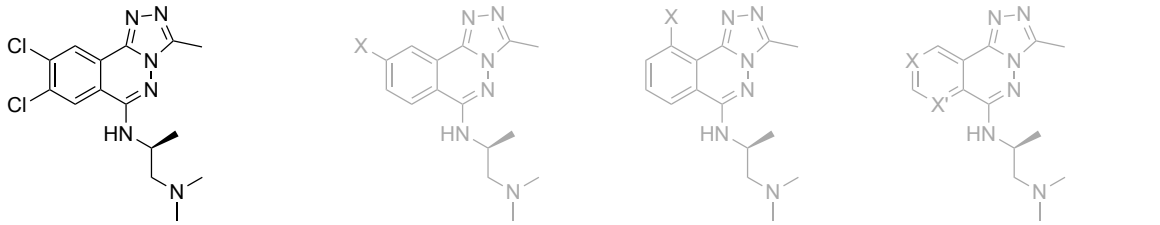

37 K_D 300 nM | X= Me, OMe, F or Cl | X= F, Cl or Me | X= CH X'= N or X= N X'= CH

Figure 2.8 Functionalisation of the [1,2,4] triazolo[4,3-a] phthalazine back bone leads to regioisomeric mixtures of non-symmetrical phthalazines. Non-regioisomerically pure obtained target compounds depicted in grey.

Nonetheless, compounds derived from a symmetrical phthalazine core such as **37** were successfully obtained and displayed potent PCAF BRD activity, however without significant improvements on the non-functionalised (*S*)-**30**. These observations may be rationalised as the backbone aromatic ring of the phthalazine core of **30** likely occupies a similar area of the PCAF BRD KAc pocket as is depicted for compound **19** with BRD4(1) (Figure 2.4). In both proteins these areas are largely solvent exposed regions of the KAc binding site far distinctly far from any potential interacting protein residues.

Instead, after a closer inspection of the SAR around the chemical series (Table 2.1) it was notable that a phenyl substituent placed at position R^3 as in compound **17** was seemingly tolerated considering the apparently tight SAR around this 1,2-diamino motif. It was envisaged that a merging of the substitution patterns of compounds **17** and (*S*)-**30** could potentially increase overall potency and addition of the aromatic substituent might serve as a useful chemical handle to introduce diversity.

Docking studies of potential hybrid compounds indicated that *ortho*- or *meta*- substitutions on the aromatic substituent at R^3 would infer a steric clash with the seemingly narrow KAc binding site pocket, therefore *para*- substituted aromatics were chosen for synthesis. An initial set of seven substituents were chosen (position R^3, Table 2.2) in order to efficiently explore a variety of different potential interactions concurrent with differing physico-chemical properties (R= -Cl, -F, $-CF_3$, $-CO_2Me$, Me, -OMe and H).

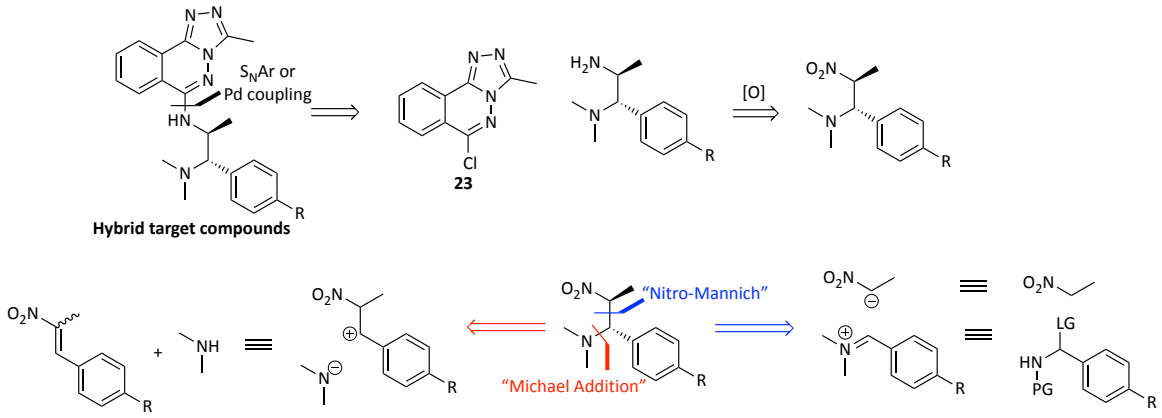

Figure 2.9 Synthetic strategies towards hybrid target PCAF inhibitor compounds. R= Cl, F, CF_3, CO_2Me, Me, OMe and H. PG= Protecting Group. LG= Leaving group.

Strategies towards the synthesis of hybrid target compounds are depicted (Figure 2.9). The target structural motif can be strategically disconnected to reveal a late stage S_NAr or Pd mediated cross coupling of chloride **23** with threo-configured diamines **59**-**65**. Whilst compound **23** is readily prepared from the condensation and cyclisation of 1,4-dichlorophthalazine **24** with acethydrazide, a synthetic route towards diamines **59**-**65** was sought. Disconnection of diamines **59**-**65** reveals two reasonable synthetic options; bond-formation via a 'nitromannich' strategy from an *in situ* prepared benzylimine reacted with a nitro-enolate nucleophile or via a 'Michael addition' strategy using nitro-olefins with dimethylamine as a nucleophile. At this juncture the preferred relative stereochemistry or indeed absolute stereochemistry desired of target compounds was not known. It was therefore decided that synthesis of target compounds would be carried out using racemic methods and where possible any formation of diastereomeric mixtures would be separated using standard chromatography. Target compounds would then be profiled for PCAF/GCN5 binding activity as racemic mixtures and any interesting compounds that showed promise would then be separated to single enantiomers via chiral HPLC.

The chosen strategy for the synthesis of hybrid target compounds was a 'Michael addition' strategy in part due to the well-studied nature of the reaction and due to the amenability, if necessary, to exchange *N*-nucleophiles for other heteroatoms later if SAR permitted. Starting from the corresponding *p*-substituted benzaldehydes (compounds **38**-**44**) a non-selective aza-

Henry reaction with nitroethane was employed furnishing approximately 1:1 mixtures of *E*/*Z* olefins (**45**-**51**). Compounds **45**-**51** were then submitted into a highly diastereoselective conjugate addition via treatment with an excess of dimethylamine in THF, furnishing (*S**, *S**)-nitroalkanes **52**-**58**. Subsequent reduction of nitroalkanes **52**-**58** to the corresponding amines **59**-**65** was completed under hydrogenative conditions using either Pd/C or Raney Nickel. Submission of amines **59**-**65** into the previously described S_NAr reaction allowed for the synthesis of final compounds **66**-**72** in low to moderate yields. As the conjugate addition of amines into nitro-olefins such as **45**-**51** is known to deliver highly diastereo-enriched thermodynamic products with threo relative stereochemistry, compounds **66**-**72** were assigned accordingly in this fashion.[300]

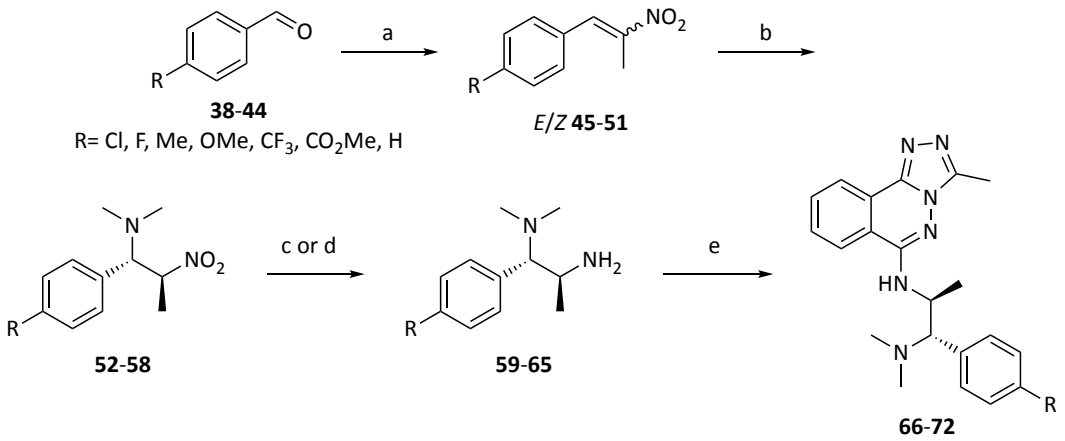

*Scheme 2.3 Synthesis of threo-substituted derivatives **66**-**72**. Reagents and conditions: a) NH_4OAc (0.2 eq), $EtNO_2$, reflux, 1:1 E/Z, quant.; b) Me_2NH (5 eq), THF, rt 16 h, dr 4.6:1 - 33:1; c) H_2 (1 atm), Pd/C (10%), MeOH, rt, 16 h, 11-15% over two steps, single diastereomer; d) H_2 (1 atm), Ra/Ni (0.3 eq), MeOH, rt, 16 h, 25-28%, over two steps, single diastereomer; e) **23** (0.8 eq) KI (0.1 eq), HCl (0.05 eq), EtOH or iPrOH, reflux, 3 days 16-79%.*

2.3 Biological Methods

2.3.1 Potency

Compounds were screened by ITC and compared with previous hit compound, (*S*)-**30**, for binding activity against the PCAF BRD. Gratifyingly, the hybrid compounds (**66**-**72**) all displayed

superior binding activity to PCAF BRD relative to (*S*)-**30** (Table 2.2). Interestingly it was found that despite a variety of substituents placed in the *para* position of the aromatic ring, no notable increases in potency were observed relative to unsubstituted hybrid compound **72** (R= H, Table 2.2).

*Table 2.2 PCAF BRD binding affinity of compounds **66**-**72** measured by ITC*

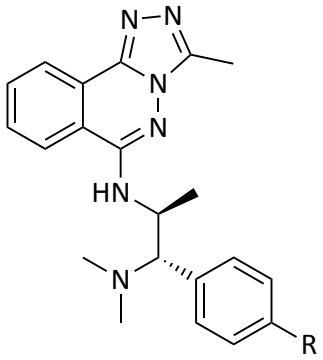

#	R	Configuration	K_D (nM) (ITC)
66	F	(1*S**, 2*S**)	195 ±23
67	CO_2Me	(1*S**, 2*S**)	133 ±15
68	Me	(1*S**, 2*S**)	160 ±54
69	Cl	(1*S**, 2*S**)	223 ±78
70	CF_3	(1*S**, 2*S**)	163 ±117
71	OMe	(1*S**, 2*S**)	179 ±48
72	H	(1*S**, 2*S**)	168 ±27
***L*-72/*L*-Moses**	**H**	**(1*S*, 2*S*)**	**126** ±15
***D*-72/*D*-Moses**	H	(1*R*, 2*R*)	>30,000

Compound **72** was resolved by chiral stationary phase chromatography to separate enantiomers as stoichiometry of binding with racemate **72** by ITC suggested that most of the activity lay in one enantiomer (*N*= ~0.5), after which it was found that the binding activity was attributed to a single enantiomer, the levorotatory, threo configured *L*-**72** (dubbed *L*-Moses, PCAF BRD ITC K_D 126 nM) whereas the opposite enantiomer, *D*-Moses was seemingly inactive against PCAF BRD (*D*-Moses PCAF BRD ITC K_D >50 μM). Binding activity of *L*-Moses was also confirmed by a Homogeneous Time-Resolved Resonance Fluorescence (HTRF) assay based on the displacement of a biotinylated tool compound **73** (Figure 2.10) from GST-tagged recombinant PCAF BRD

protein, demonstrating good potency (PCAF K_i 47 nM) which also corresponded to exquisite selectivity over BRD4 (>4,500-fold selectivity). Binding of *L*-Moses to recombinant PCAF BRD via ITC was primarily driven by enthalpic contributions (ΔH -9.19 kcal/mol) with minimal changes in entropy upon binding (ΔS +0.721 cal/mol. K).

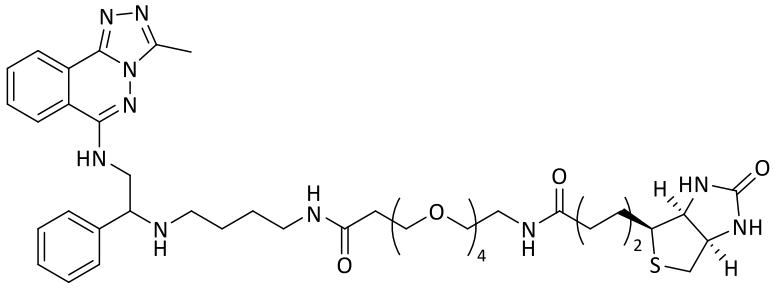

*Figure 2.10 Biotinylated tool molecule **73** for use in PCAF BRD HTRF assay.*

It is noteworthy that the binding affinities of *L*-Moses in the various *in vitro* assays seem to differ slightly which may or may not fall outside of experimental error. Reported potency by HTRF and BromoSCAN seem to be in relative agreement (HTRF PCAF K_i 47 nM, BromoSCAN PCAF K_D 48 nM). As HTRF and BromoSCAN assays involve competitive displacement of another assay component (often a tagged ligand)- there are multiple interactions which may be disrupted by introduced small molecule inhibitors, thus enhancing the sensitivity of the assay. ITC measurements report dissociation constants for the binding interaction of a small molecule and biomolecule. Due to the highly endogenous nature of the assay, the biomolecule under study does not require tagging, and so the assay output can be attributed more closely with the true molecule: biomolecule interactions in solution. The exhibited binding affinity of *L*-Moses with PCAF BRD by ITC was found to be in the low nanomolar range and only approximately two to three-fold different to the values reported in BromoSCAN and HTRF (PCAF BRD K_D 126 nM). A number of other analogues (examples **74**-**116**, SI) were synthesised and characterised for PCAF/GCN5 binding activity prior to the identification of *L*-Moses, DSF results for PCAF/GCN5 compounds (48 selected examples) and PCAF BRD ITC results (47 selected examples) for derivatives are listed (Table 2.3 and Table 2.4 respectively).

Table 2.3 DSF results of selected compounds with PCAF and GCN5

# (10 µM)	PCAF ΔT_m (°C)	GCN5L2 ΔT_m (°C)
29	**0.9**	**0.3**
30	**5.6**	**2.5**
(S)-**30**	7.4	4.0
31	**3.3**	**1.1**
32	**0.9**	**1.1**
33	**0**	**0**
34	**4.6**	**1.0**
(*S*)-**36**	0.7	0.2
78	1.1	0.1
79	1.0	0
81	0.6	0.1
82	0.4	0.1
83	2.7	0.4
84	3.7	0.7
85	2.9	1.1
86	0.5	0
87	0.2	0.3
88	0.2	0
89	1.1	0.5
91	0.6	0.1
92	0.7	0.3
93	0.8	0.1
94	0.9	0
95	0	0.1
98	0.5	0.2
100	0.4	0.2
101	7.3	2.4
102	0.3	0.2
66	8.3	4.4
67	9.6	6.3
68	7.8	4.3
69	6.2	2.7
70	9.1	7.2
71	10.3	6.8
72	7.9	5.0
106	1.0	0.3
107	0.8	0
108	0.7	0.2
109	3.7	0.9
110	0.02	0.2
112	0.4	0.1
113	0.4	0.2
114	0.4	0.1
115	0.1	0.1
116	0	0.2
75	2.8	0.9
76	0.7	0.2
77	3.8	1.5

Table 2.4 ITC results of selected compounds with PCAF.

#	PCAF K_D (μM) [+]	
27	7.98	±0.65
28	>30	-
29	>30	-
30	0.298	±0.039
(*S*)-**30**	0.284	±0.029
31	1.76	±0.23
32	>30	-
33	>30	-
34	7.30	±1.1
35	6.90	±1.4
(S)-**36**	>30	-
81	>30	-
82	>30	-
84	4.30	±0.31
85	1.13	±0.24
87	>30	-
89	>30	-
90	>30	-
91	>30	-
92	0.321	±0.039
93	>30	-
94	>30	-
95	>30	-
96	2.3	±0.93
97	>30	-
98	>30	-
100	>30	-
101	0.168	±0.023
66	0.195	±0.040
67	0.133	±0.015
68	0.160	±0.054
69	0.223	±0.078
70	0.163	±0.117
71	0.179	±0.048
72	0.168	±0.027
107	>30	-
108	>30	-
109	>30	-
110	>30	-
111	>30	-
112	>30	-
113	>30	-
114	>30	-
115	>30	-
75	18.2	±0.13
L-**72**/L-Moses	0.126	±0.015
D-**72**/D-Moses	>30	-

[+] Compound concentration: 30 μM, Protein concentration: 280-320 μM.

2.3.2 Selectivity

Having achieved good potency against PCAF BRD, *L*-Moses was then profiled in a selectivity panel of 48 recombinant human BRD by DSF. *L*-Moses showed the largest thermal shift for PCAF with no significant shifts observed for other BRDs, other than the highly homologous GCN5 (PCAF BRD DSF +5.4°C ΔT_m, GCN5 BRD DSF +3.7°C ΔT_m, Figure 2.11). By ITC *L*-Moses displayed potent activity against recombinant GCN5 (GCN5 BRD K_D 550 nM). Interestingly, dissimilar to PCAF BRD, binding of *L*-Moses to GCN5 BRD is made up of more significant entropic contributions to free energy of binding as opposed to enthalpic ones (ΔH -4.97 kcal/mol and ΔS +11.99 cal/mol. K). The corresponding enantiomer *D*-Moses displayed no measurable activity against PCAF or GCN5 pertaining to the potential utility of this stereoisomer as a useful negative control molecule. An additional measure of selectivity, the DiscoverX BromoSCAN assay[301] was also used to profile *L*-Moses against 48 recombinant human BRDs. Data was in agreement with that observed through DSF, *L*-Moses demonstrated potent activity against PCAF (PCAF K_D 48 nM) and GCN5 (GCN5 K_D 220 nM) with no measurable activity against any other BRD screened other than very weak binding to BRPF1 (BRPF1 K_D 6.3 μM) corresponding to excellent PCAF selectivity (86-fold vs BRPF1).

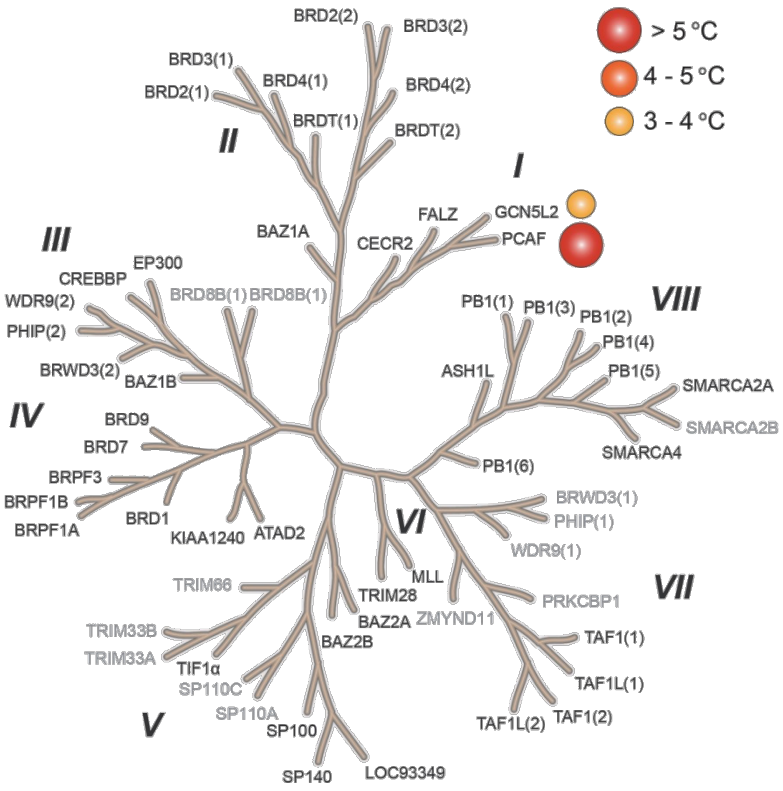

Figure 2.11 DSF selectivity panel of L-Moses against 48 human recombinant bromodomain proteins. BCP in black text included in selectivity screen. Grey BCP not included in screen.

Despite seemingly excellent PCAF/GCN5 selectivity within the family of BRD some efforts were made to profile *L*-Moses against other cellular target proteins to understand wider selectivity. This additional profiling would reveal any broader off-targets and also allow for any conferred cellular phenotypes through *L*-Moses mediated PCAF/GCN5 BRD inhibition to be attributed to a target effect with greater confidence. In a eurofins GPCR/ion channel panel containing 130 non-family targets, *L*-Moses showed no measurable activity against all potential off targets (<60% at 10 μM) except for opioid receptors (mu-μ IC_{50} 100 nM, OPRL1 IC_{50} 840 nM, kappa-κ IC_{50} 1,100 nM,) and the 5-HT transporter (IC_{50} 220 nM).

2.3.3 Cell Activity

In order to determine the cell target engagement activity of *L*-Moses a number of cell-target engagement-based assays were explored. Using Promega's NanoBRET[283] target engagement assay system *L*-Moses was shown to displace NanoLuc-tagged truncated PCAF BRD from Halo-tagged H3.3 in HEK293 cells in a dose-dependent manner corresponding to nanomolar activity (EC_{50} 260 nM). Encouragingly in the same NanoBRET assay the negative control, *D*-Moses, showed no activity at 5 μM (Figure 2.12).

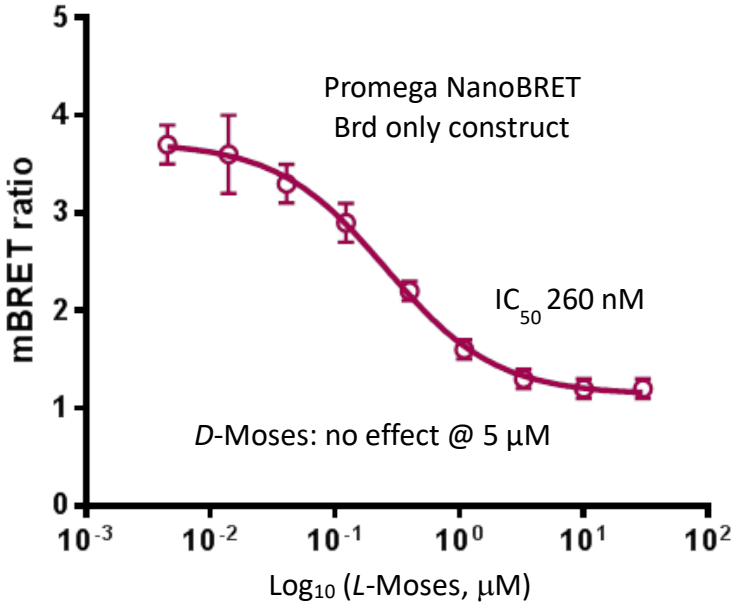

Figure 2.12 NanoBRET dose response of L-Moses in HEK293 cells transfected with NanoLuc tagged PCAF BRD and Halo tagged H3.3

Additional evidence of target engagement within a cellular context was also obtained in the form of competitive pull-down studies using an immobilized form of *L*-Moses. Derivative compound **105** which contains an appropriate amine chain appendage onto the aryl motif of *L*-Moses was acylated following treatment with an excess of *N*-hydroxysuccinimide (NHS) activated sepharose beads (Scheme 2.4).

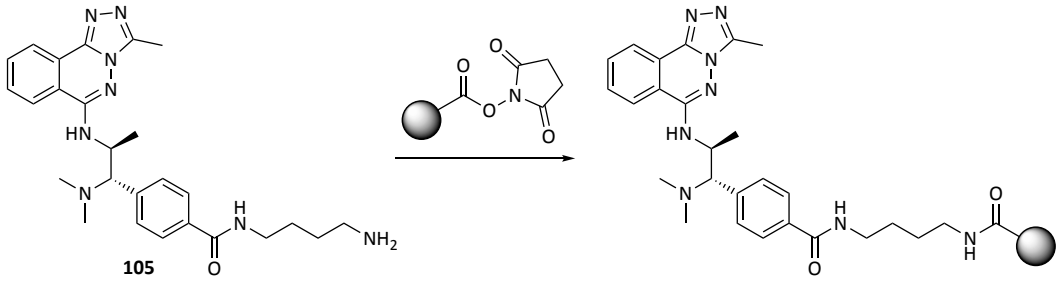

*Scheme 2.4 Attachment of compound **105** onto immobilised beads.*

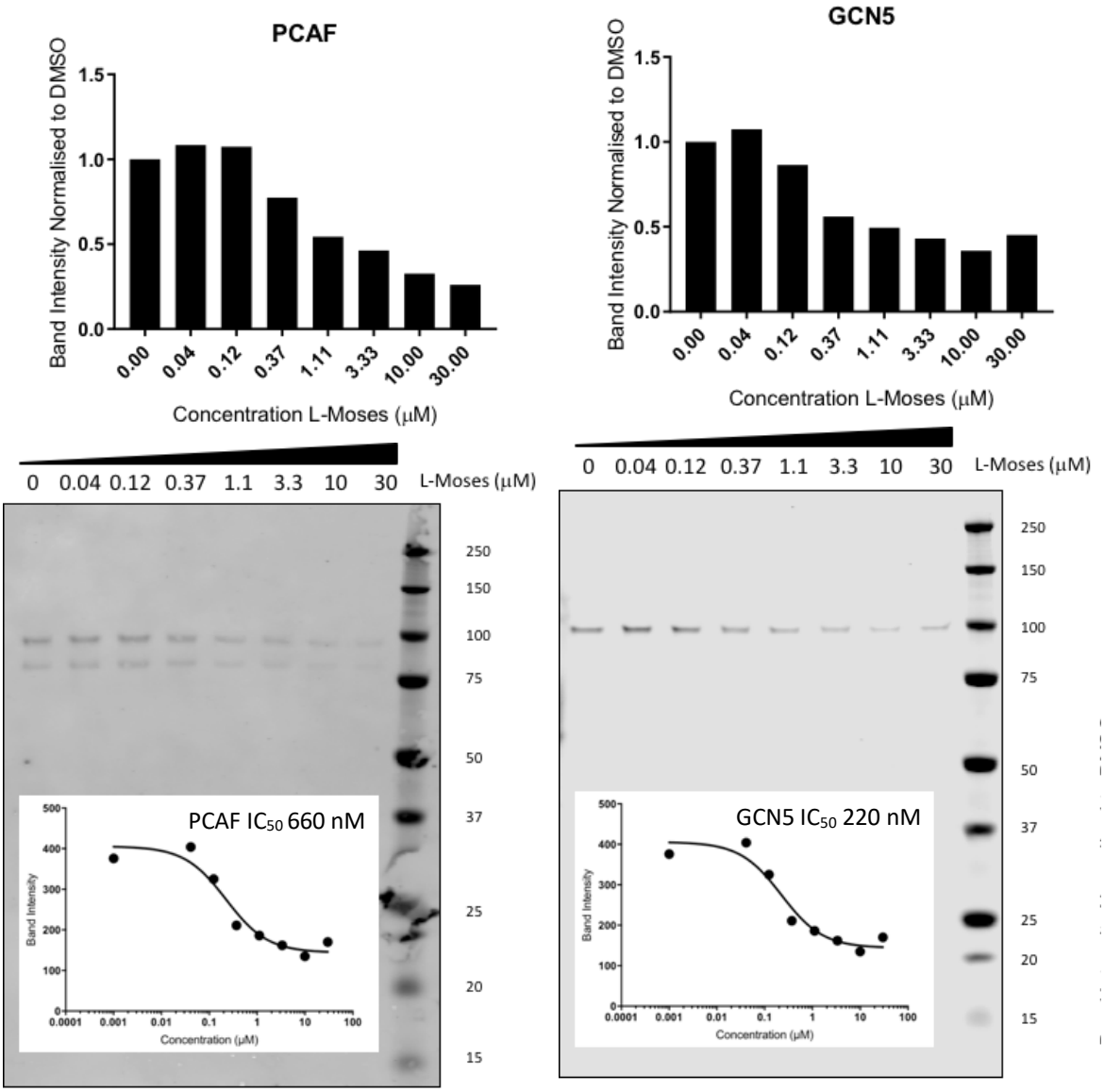

*Figure 2.13 Competitive pull-down studies using immobilised L-Moses against endogenous PCAF and GCN5. Pull down studies carried out on 5 mg of MCF7 cell lysates with immobilised L-Moses, **105**. Lysates were incubated with free L-Moses at indicated concentrations at 4°C for 30 minutes prior to pull down. Blots were probed for PCAF (Cell Signalling #3378 MW= 93 KDa) and GCN5 (Cell Signalling #3305 MW= 94 KDa).*

Compound *L*-Moses was able to competitively displace immobilized **105** from endogenous PCAF and GCN5 in cell lysates (MCF7 cells) in a dose dependent manner corresponding to sub-μM target engagement activity (PCAF IC_{50} 660 nM, GCN5 IC_{50} 220 nM, Figure 2.13). There are some discrepancies in the reported binding affinity values between this assay and the NanoBRET assay. However, it is noted that the assay readout using lysate competitive pull-down studies can be the source of variability, in addition to the fact that the NanoBRET assay examines the effect on a mutant protein and so is relatively artificial.

2.3.4 Cellular Phenotype

Having characterised and validated cell target engagement activity of *L*-Moses, attention then turned towards what effect PCAF/GCN5 BRD inhibition would have in a disease context. Using the DiscoverX BioMAP Diversity PLUS[288] phenotypic profiling assay which is a set of disease relevant assays comprised of 12 individual human primary cell-based co-culture systems which model predictions of activity in multiple tissues and disease models in a dose dependent manner (0.3, 1.1, 3.3 and 10 μM, Appendix Figure 1.).

L-Moses did not show demonstrable cytotoxicity in the BioMAP assay after 72-hour treatment of cells. In addition to this, little to no activity was seen in the biomarker readouts. A few changes that were noted include increased MCP-1, IL-8 and IL1-α in macrophages/venular endothelial cells. Additionally, in the lung fibroblast tissue remodelling readout, *L*-Moses caused a decrease in Col-1 was observed at the top concentration (10 μM). Despite reported links of both PCAF and GCN5 to inflammation, this cellular assay panel may not be optimal for studying inflammation related readouts due to the relatively short treatment window of 72 hours, which may not be sufficient time for inhibition of these epigenetic proteins to exert an obvious phenotypic effect. Or it may be that the BRD of PCAF/GCN5 does not have an effect in the biological processes involved in the readout of this assay.

Additionally, *L*-Moses was profiled in the National Cancer Institute (NCI-60) panel which examines the effects of a compound on a variety of well characterised cancer cell lines after 72 hour treatment.[289] It was found that *L*-Moses treatment did not exert a measureable effect on cell proliferation/apoptosis (Figure 2.14). This may suggest that PCAF/GCN5 BRD small molecule inhibition is not relevant to oncology. However, PCAF/GCN5 is a multi-domain containing protein and whilst there may be genetic links to various disease indications, the domain specific contribution of the bromodomain may not be essential to disease progression. Furthermore, whilst the concentration used in the NCI-60 panel (10 μM) likely far exceeds the concentration required to inhibit PCAF/GCN5 BRD in a cellular context using *L*-Moses, the fixed time at which a read out is taken (72 hours) may again not be optimal for investigating the effects of inhibition of these epigenetic proteins. Indeed, whilst the bromodomain is likely to be the key contributor to overall chromatin binding, the acetyltransferase domain (HAT) likely also has an affinity for unmodified histone tails, in addition to the poorly characterised PCAF Homology *N*-domain and so PCAF/GCN5 BRD inhibition may not completely displace PCAF/GCN5 and its associated complexes from chromatin. If sufficient chromatin displacement of PCAF/GCN5 is not carried out through small molecule treatment, then it may not be possible for an effect on transcriptional regulation to take place.

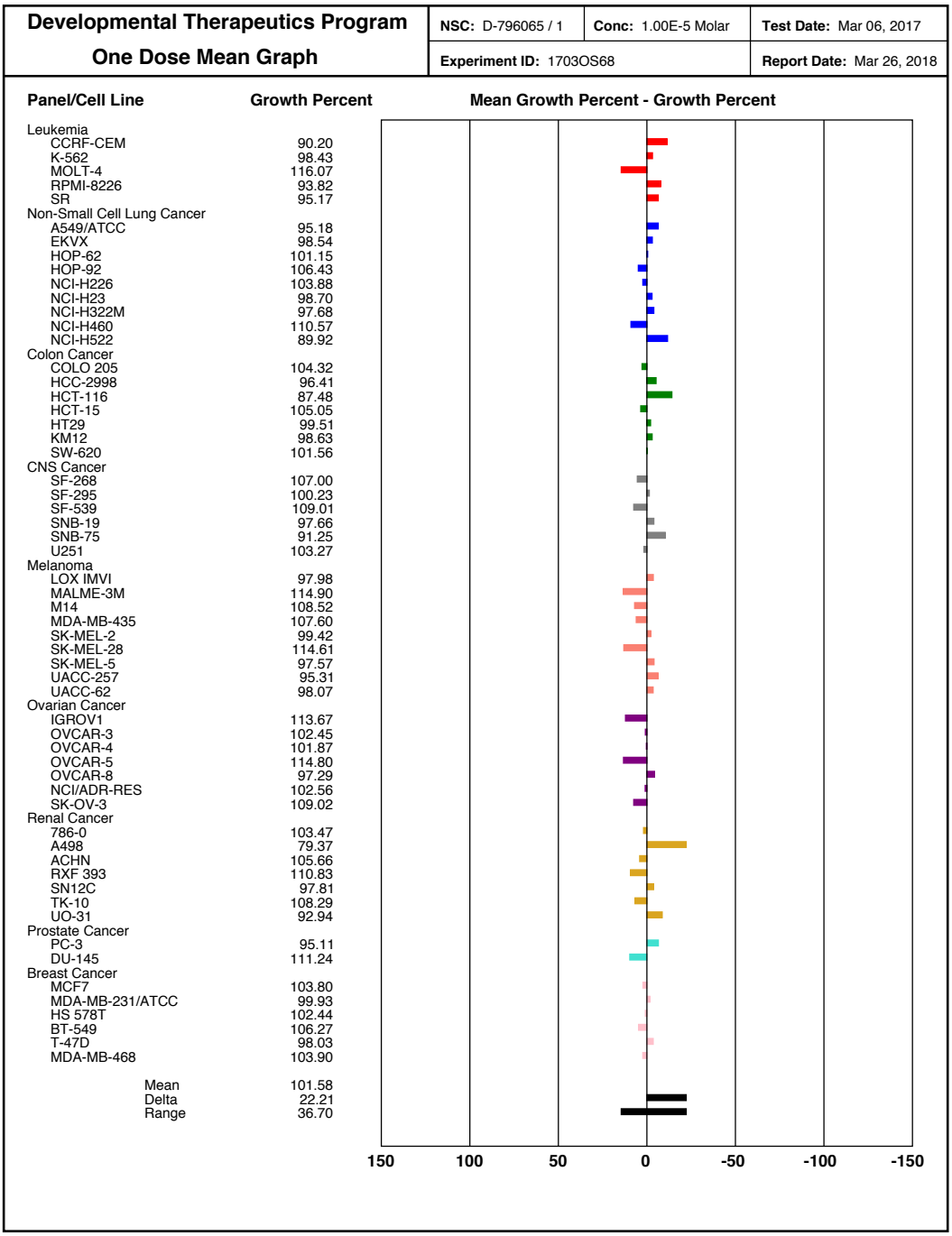

Figure 2.14 NCI-60 panel data on L-Moses treatment at 10 μM for 72 hours.

2.3.5 Pharmacokinetic Studies and Permeability studies

An investigation into the *in vitro* metabolic stability of the probe molecule *L*-Moses was carried out to inform the suitability of the probe in an *in vivo* context for exploring PCAF/GCN5 BRD inhibition. **72**/*DL*-Moses and a fluoro derivative **66** were exposed to samples of liver microsomes

and analysed for metabolic degradation by LC-MS at consecutive time points (0, 5, 15, 30 and 45 minutes, Table 2.5).

*Table 2.5 in vitro metabolic stability data of compound **66** and **72**/DL-Moses after treatment with human and mouse liver microsomes*

#	Metabolic Stability (Human)				Metabolic Stability (Mouse)			
	CL_{int} (μL/min/mg protein)	SE CL_{int}	$t_{1/2}$	n	CL_{int} (μL/min/mg protein)	SE CL_{int}	$t_{1/2}$	n
72	35	2.2	40	5	37	2.6	38	5
66	29	2.0	48	5	21	1.3	65	5

Following treatment of compound **66** and **72**/*DL*-Moses with human liver microsomes it was found that both compounds display moderate resistance to metabolic degradation (**72**/*DL*-Moses $t_{1/2}$ 40 mins, compound **66** $t_{1/2}$ 48 mins). This data was encouraging as throughout the chemical probe discovery campaign pharmacokinetics had not been a parameter that had been characterised or indeed optimised. Interestingly compound **66** displayed slightly more stability in mouse liver microsomes than human microsomes (compound **66** $t_{1/2}$ 65 mins).

Cell permeability data on the probe molecule was generated using a commercial MDCK-MDR1 assay at Charles River Laboratories. It was found that the lead probe molecule *L*-Moses displays good permeability with an efflux ratio <2 (Efflux ratio 1.18). Negligible differences were observed in the A-B/B-A ratios in MDR1 overexpressing cells in the presence of a P-gp inhibitor (A-B/B-A 59/70 10^{-6} $cm.s^{-1}$) suggesting that the probe is not a P-gp substrate or inhibitor.

As an additional measure of metabolic stability an *in vivo* rat pharmacokinetic study was carried out on the probe molecule, **72**/*DL*-Moses, to examine oral metabolic stability. In addition to this, an examination of the blood-brain-barrier (BBB) permeability (using intraperitoneal injection) of the lead probe molecule was also carried out. This study was carried out in rats in order to inform dosing for future models of inflammation using rats, the overall *in vivo* oral stability (**72**/*DL*-Moses rat oral $t_{1/2}$ 49 min) was encouraging having not optimised the compound for PK properties. Additionally, the probe molecule displayed good BBB permeability after IP dosing of

rats and exposure times of 45 minutes (Brain/Plasma ratio: 2.3) pertaining to the potential utility in using the probe molecule to study PCAF/GCN5 related neuropathology.

2.4 Chiral Synthesis

In order to access sufficient quantities of both enantiomers *L*-Moses and *D*-Moses it was envisaged that the racemic synthesis followed by chiral resolution using chiral stationary phase HPLC would need to be replaced by an asymmetric route to either stereoisomer either through an enantioselective synthetic step or synthesis from chiral building blocks. One potential catalyst controlled enantioselective step to form the intermediate *N*, *N*-dimethyl-2-nitro-1-phenylpropan-1-amine required to synthesise *DL*-Moses could be an enantioselective nitro-mannich reaction of nitroethane with the corresponding *N*-protected benzylimines.[302] However many of the available methods in the literature, whilst tuneable for enantioselectivity, unfortunately largely deliver the undesired relative stereochemistry of products (erythro- instead of the desired threo- diastereoisomers).

It was found that an asymmetric synthesis starting from the commercially available (1*R*,2*S*)-(-)-norephedrine **117** was able to deliver *L*-Moses as a single stereoisomer over seven discrete steps (Scheme 2.5). Initially (1*R*,2*S*)-(-)-norephedrine **117** was Boc-protected through treatment with Boc anhydride in quantitative yields to give **118**. Alcohol **118** was then treated with thionyl chloride and pyridine under kinetic conditions to afford cyclic sulfamidite which was then immediately submitted into a periodate oxidation with catalytic amounts of ruthenium to give cyclic sulfamidate **119** in reasonable yields (48%) over two synthetic steps (Figure 2.15).

Submission of sulfamidate **119** into an S_N2 reaction with dimethylamine which proceeds with complete selectivity for C-O bond cleavage at the benzylic position allows for inversion of stereochemistry stereospecifically delivering Boc-protected **120** as a single stereoisomer (48% isolated yield). Deprotection of **120** with trifluoroacetic acid (TFA) gave free amine **121** in

quantitative yields which was then submitted into a S_NAr reaction with 6-chloro-3-methyl-[1,2,4] triazolo[3,4-a] phthalazine **23** in isopropanol to furnish *L*-Moses (30% isolated yield, Scheme 2.5). Synthesis of the corresponding negative control, *D*-Moses, was also completed asymmetrically starting from commercially available (1*S*,2*R*) -(-)-norephedrine.

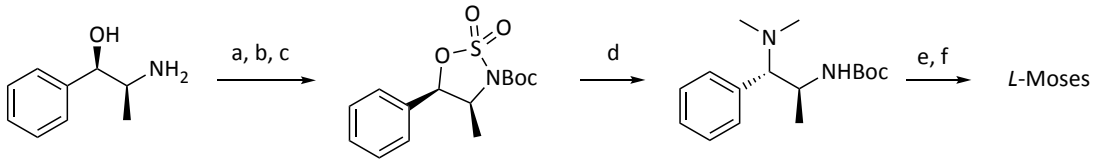

(1*R*,2*S*)-(-)-norephedrine **117** **119** **120**

*Scheme 2.5 Asymmetric synthesis of L-Moses starting from (1R,2S)-(-)-norephedrine **117**. A) Boc_2O, DIPEA, CH_2Cl_2, RT, 16 h, quant. B) $SOCl_2$, Pyridine, MeCN, 2h, -40 °C to 0 °C; c) $NaIO_4$ (1.5 equiv), $RuCl_3 \bullet 3H_2O$ (0.05 equiv), MeCN, 1 h, 0 °C, 48% (over two steps); d) Me_2NH (3 equiv), THF, RT, 16 h, 63%; e) TFA, CH_2Cl_2, quant.; f) **23** (0.8 equiv), KI (0.1 equiv), HCl (0.05 equiv), iPrOH, reflux, 3 days, 30%.*

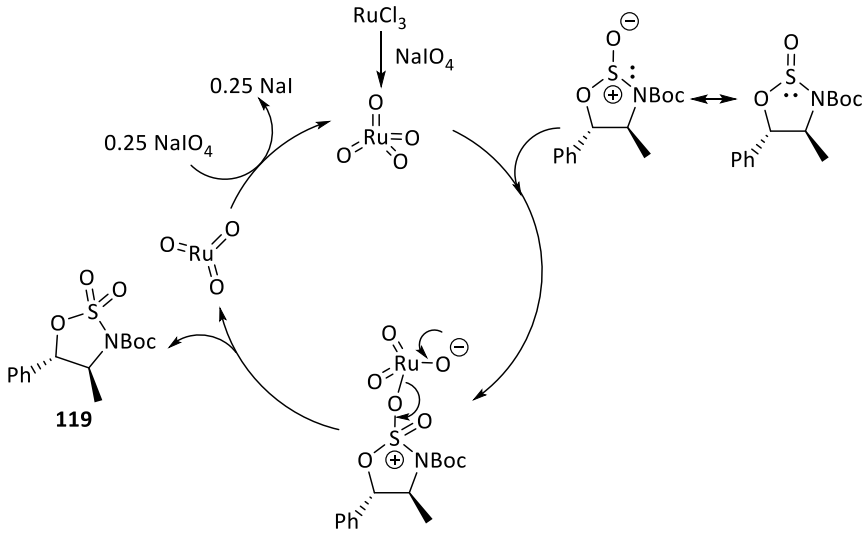

*Figure 2.15 Putative mechanism for the Ruthenium oxidation of sulfamidite to sulfamidate **119**.*

2.5 Other Inhibitors of PCAF/GCN5

The work described culminated in the publication of the first discovered chemical probe for PCAF/GCN5.[303] Subsequently, Humphreys and co-workers at GSK published their efforts on the development of a PCAF/GCN5 chemical probe (Figure 2.16).[304] The reported lead compound GSK4027 **122** along with enantiomeric negative control GSK4028 **123** represents an analogous

chemical probe to *L*-Moses which can be used in conjunction to explore PCAF/GCN5 associated biology. GSK4027 **122** is a potent (PCAF IC_{50} 40 nM, TR-FRET) and selective (≥70-fold) PCAF/GCN5 chemical probe. Cell target engagement was also demonstrated through a NanoBRET displacement assay of full length Nano-Luc tagged PCAF from Halotagged H3.3 (PCAF EC_{50} 60 nM).

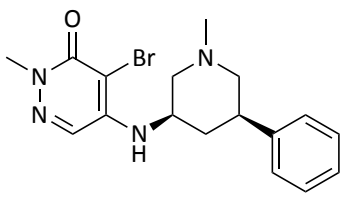

122 GSK4027
PCAF (TR-FRET) IC_{50} 40 nM
PCAF K_i (BROMOscan) 1.4 nM
GCN5 K_i (BROMOscan) 1.4 nM
PCAF NanoBRET EC_{50} 60 nM

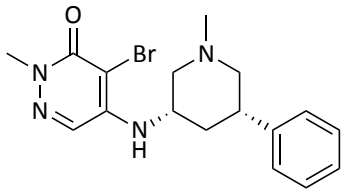

123 GSK4028
negative control

Figure 2.16 GSK4027 ***122*** *a PCAF/GCN5 chemical probe alongside negative control GSK4028* ***123****.*

2.6 Malarial Bromodomains

Despite previous reports of co-crystal structures being readily obtained of PCAF BRD with fragment sized inhibitory compounds,[297,304] efforts to obtain a co-crystal structure of PCAF BRD or GCN5 BRD with *L*-Moses were unsuccessful. Colleagues from SGC Toronto's parasitology group noted that human PCAF BRD and GCN5 BRD share a high degree of similarity with *Pf*GCN5 BRD, the BRD containing protein deriving from the malarial parasite species, *Plasmodium falciparum* (42% overall sequence similarity with PCAF in BRD, 45% overall sequence similarity with GCN5 in BRD). Moreover, a number of epigenetic proteins within the *Pf* proteome have been shown to be essential for the lifecycle of the parasite[50] and so we sought to explore the binding activity of *L*-Moses with *Pf*GCN5 BRD. Unsurprisingly due to high sequence homology, *L*-Moses shows potent binding to *Pf*GCN5 (*Pf*GCN5 K_D 280 nM), with negative control *D*-Moses showing no activity against *Pf*GCN5. In order to further understand the interaction of *L*-Moses with *Pf*GCN5 BRD and more broadly insights into the interactions present with human PCAF and

GCN5, *L*-Moses was successfully co-crystallised with *Pf*GCN5 (Figure 2.17, PDB ID 5TPX). From the obtained structure binding activity was rationalised as *L*-Moses indeed binds directly in the KAc binding site, cooperating in a H-bond network between the four-conserved water molecules at the rear of the binding site. Additionally, the triazole motif of *L*-Moses H-bonds with N1436 and a salt-bridge interaction is present between the dimethylamine motif of *L*-Moses and E1389 (equivalent to E756 in PCAF). Notably an edge to face π-π stack was observed between the phenyl substituent of *L*-Moses and tryptophan W1379 (PCAF conserved as W746, average distance 4.5 Å) which may explain the necessity of the phenyl substituent in hybrid compounds synthesised against PCAF BRD.

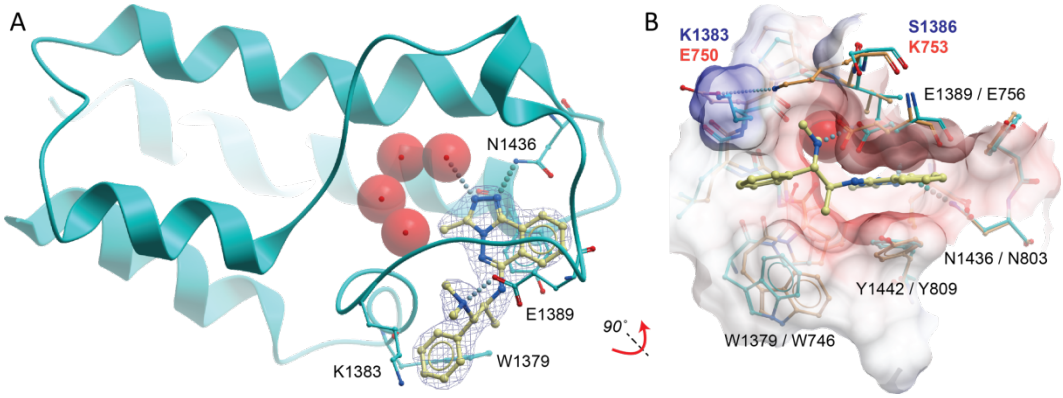

Figure 2.17 A) L-Moses (pale yellow sticks) binds to the KAc binding site of PfGCN5 (cyan) B) Overlay of co-crystal structure of L-Moses (pale yellow sticks with PfGCN5 (PfGCN5 cyan sticks, PDB ID 5TPX) with PCAF structure (PDB ID 5FTZ, orange sticks). Comparison of sequence homology (black text for same residues, Red text PCAF differences, Blue text PfGCN5 differences). Figure extracted from Moustakim et al.[303]

Structural differences between PCAF and *Pf*GCN5 within the KAc binding site hinge mainly on the presence of a salt bridge in PCAF between E750 and K753 which is not present in *Pf*GCN5 (residues non-conserved; K1383 and S1386). Differences such as this may provide insights on how species-selective inhibitors may be designed and synthesised using *L*-Moses as a chemical starting point. It was rationalised that elaboration of *L*-Moses through ligand growth at the dimethylamino motif might extend into the open region of the KAc binding site in *Pf*GCN5 flanking K1383 and S1386, whereas in PCAF elaboration would induce a protein: ligand clash via

the salt bridge between E750 and K753. To explore this, compounds **124**-**133** were synthesised and screened against recombinant PCAF BRD by HTRF and recombinant *Pf*GCN5 by ITC (Table 2.6).

Table 2.6 Characterisation of potential PfGCN5 selective inhibitors

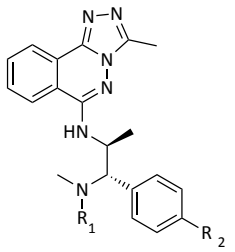

#	R_1	R_2	*Pf*GCN5 BRD K_D (μM)	PCAF BRD IC_{50} (μM)
124	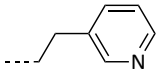	H	3.6	6.1
125	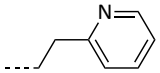	H	4.7	7.6
126	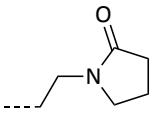	H	8.5	20
127	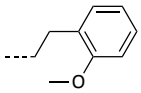	H	18	8.5
128		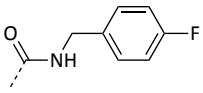	0.31	0.29
129		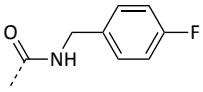	0.69	1.2
130		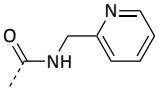	0.34	0.56
131		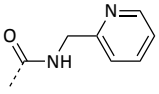	0.93	0.86
132	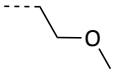	H	11.1	30
133		H	0.56	1.4
***L*-Moses**	**H**	**H**	0.28	0.047

Despite rational design of potential *Pf*GCN5 inhibitors, most of the designed inhibitors exhibited weaker activity against both PCAF and *Pf*GCN5 relative to *L*-Moses. Seemingly the simplest

modification- the replacement of the dimethylamino motif of *L*-Moses with a *N, N*-ethylmethylamino substituent gave compound **133** which displays retained sub- activity μM against *Pf*GCN5 (*Pf*GCN5 K_D 0.56 μM) but weaker activity against PCAF BRD (PCAF BRD IC_{50} 1.4 μM) relative to *L*-Moses. However, despite displaying activity against the human isoforms (PCAF/GCN5) of *Pf*GCN5, *L*-Moses was generally not found to exhibit cytotoxicity in a variety of human cell lines, as such, selectivity over the human isoforms may not be necessary when searching for more potent *Pf*GCN5 BRD inhibitors to disrupt the *Pf* life cycle.

In order to explore the functional effect of *Pf*GCN5 inhibition, *L*-Moses was screened against red blood cells infected with *Pf*GCN5 (blood stage). Interestingly *L*-Moses showed sub-μM parasite killing activity against blood stage *Pf* (*L*-Moses *Pf* IC_{50} 0.47 μM) (Figure 2.18). Whereas the corresponding PCAF/GCN5 negative control probe molecule, *D*-Moses, displays weaker *Pf* growth inhibitory activity (*D*-Moses *Pf* IC_{50} 2.48 μM) suggesting that this *Pf* inhibitory effect is an on-target effect. This may also indicate that the BRD of *Pf*GCN5 is essential to the life cycle of the parasite. Indeed, recent reports of cross-screening efforts with BRD inhibitors against *Pf* growth inhibitory activity suggest this may be the case.[148]

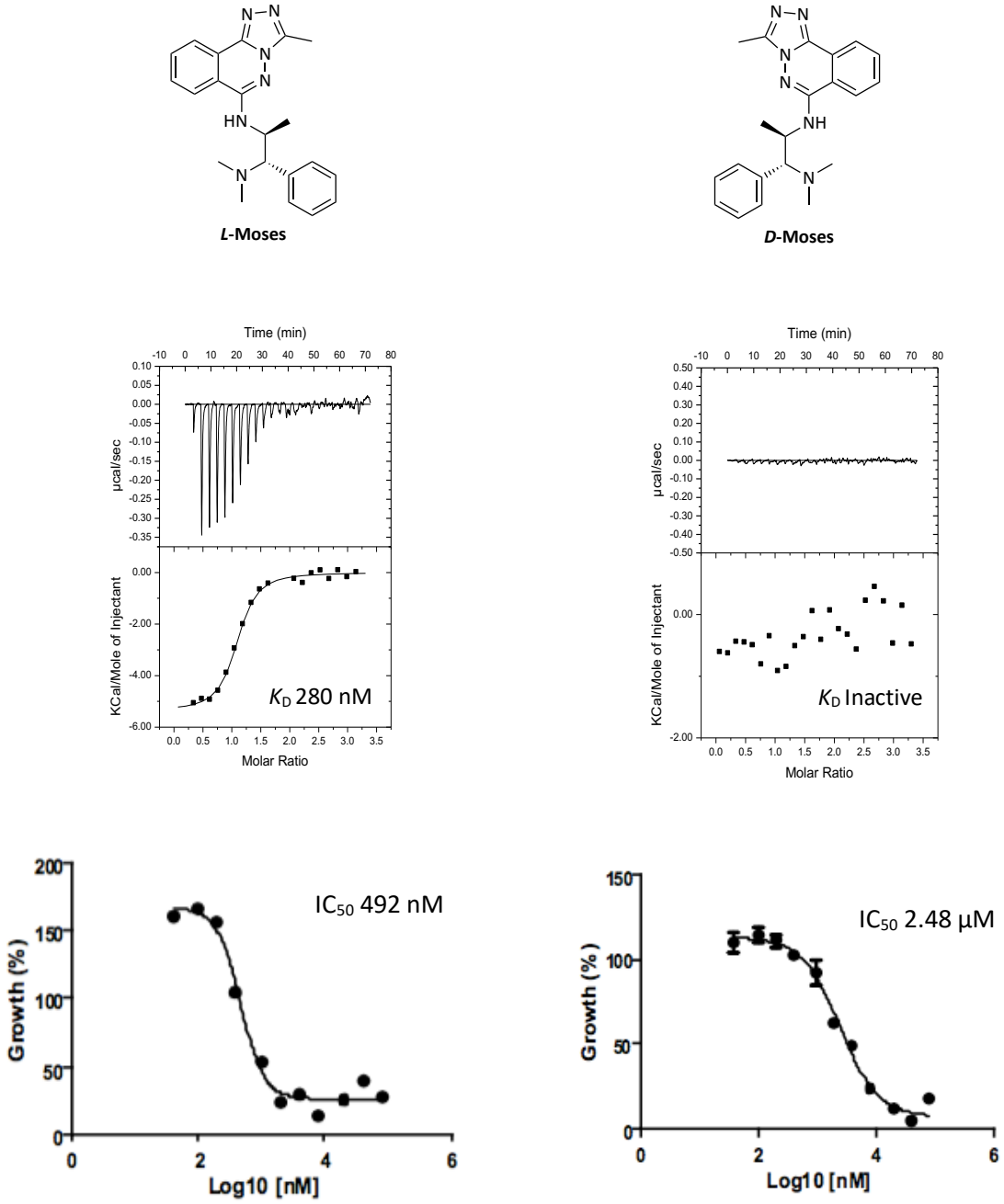

Figure 2.18 Comparison of binding activities of L-Moses and D-Moses against PfGCN5 BRD by ITC alongside comparison of growth inhibition against Pf of L-Moses and D-Moses in the red blood stage of the Pf lifecycle.

2.7 Conclusions and Future Work

This chapter has described the discovery and development of the first PCAF/GCN5 chemical probe. Aided by an initial *in silico* screen (~12k compound library), a number of promising

chemical starting points were identified based on known promiscuous KAc mimetics. A focussed set of PCAF/GCN5 BRD inhibitors were chosen for synthesis based on the commercial availability of starting materials, synthetic tractability, chemical diversity and docking score. After the synthesis of approximately 100 analogues and biophysical characterisation of binding with recombinant PCAF/GCN5, a potent and ligand efficient inhibitor was identified, dubbed *L*-Moses. The identified molecule was profiled by ITC where nanomolar binding was evident to both PCAF BRD and GCN5 BRD. The corresponding enantiomer, *D*-Moses, was found to be inactive against both PCAF and GCN5. This data was validated by DSF, HTRF and BromoSCAN. Selectivity was ascertained for PCAF/GCN5 in a BromoSCAN panel and a DSF panel of 48 recombinant BRD demonstrating excellent PCAF/GCN5 selectivity. Additionally, broader target selectivity was displayed in a eurofins GPCR/ion channel panel demonstrating good selectivity over most targets other than a subset of opioid receptors. Evidence of target engagement within a cellular context was confirmed through a NanoBRET displacement assay of Nano-Luc tagged PCAF BRD from halotagged H3.3 in HEK293 cells where nanomolar cell activity was measured (EC_{50} 260 nM). In addition, MCF7 cells treated in a dose dependent manner with *L*-Moses were lysed and evidence of competitive displacement over an immobilised form of *L*-Moses used to pull down PCAF/GCN5 was observed corresponding to sub-μM activity. In order to deliver sufficient quantities of both enantiomers of the probe molecule, an asymmetric synthesis was designed and achieved using sulfamidate chemistry[305] giving access to *L*-Moses and *D*-Moses as single enantiomers starting from the commercially available single stereoisomers of the alkaloid norephedrine.

Structural insights into the observed activity of *L*-Moses against PCAF/GCN5 BRD were acquired through obtaining a co-crystal structure of *L*-Moses with the highly homologous *Pf*GCN5 from *Plasmodium falciparum*. The observed mode of binding rationalised potency and selectivity for human PCAF/GCN5 and binding activity of *L*-Moses with *Pf*GCN5 was characterised in the nanomolar range (*Pf*GCN5 BRD 0.28 μM). Potent binding with *Pf*GCN5 translated into activity in

a cellular disease context, with *L*-Moses displaying sub-μM (*Pf* IC_{50} 0.47 μM) activity against *Plasmodium falciparum* when treated in the blood stage, pertaining to the potential essentiality of *Pf*GCN5 BRD to the life cycle of the parasite.[50]

Surprisingly, despite efforts made towards identifying a phenotype elicited from treatment of relevant human cell lines or human disease models with *L*-Moses, obvious beneficial effects remained elusive. Profiling of *L*-Moses mediated PCAF/GCN5 BRD inhibition was carried out examining the potential in oncological indications (NCI-60 panel) and inflammation (BioMAP Diversity PLUS panel). However, no obvious effect was reported when relevant cell lines were treated for 72 hours with high concentrations of the lead probe, *L*-Moses (up to 10 μM). This may indicate a lack of relevance of PCAF/GCN5 BRDs within the context of diseases associated with the full-length endogenous proteins. If PCAF/GCN5 small molecule inhibition using the probe *L*-Moses is insufficient at incapacitating either PCAF or GCN5 at exerting their transcriptional regulatory effects, then indeed other domains such as the HAT or PCAF Homology *N*-domain may be the truly relevant targets. There lies the possibility that in fact the BRDs of PCAF/GCN5 act in concert with another chromatin associating domain which has an affinity for chromatin (such as the HAT domain, Figure 2.19A). If this is the case, then treatment with BRD inhibitors may not fully displace PCAF/GCN5 and associated complexes from chromatin and so related transcriptional events and pathologies may ensue (Figure 2.19B). This is in contrast with other HAT domain containing proteins such as CBP/p300 for which a number of bromodomain inhibitors and chemical probes exist.[29] Recent reports suggest that the epigenetic cross talk between chromatin interacting domains of CBP/p300 is relatively complex. The two CBP/p300 BRD inhibitors I-CBP112 **134** and SGC-CBP30 **135** which have been characterised to bind to the KAc binding site of their targets (Figure 2.20)[162,163] in fact exert opposing effects on p300 HAT activity as demonstrated by Cole *et. al*.[306]

An additional notion is that PCAF and GCN5 BRD inhibition may in fact have opposing roles in the phenotypic assays examined, which when explored using a dual PCAF/GCN5 probe, may in fact lead to inconclusive phenotypic effects due to the antagonism of dual target inhibition.

A

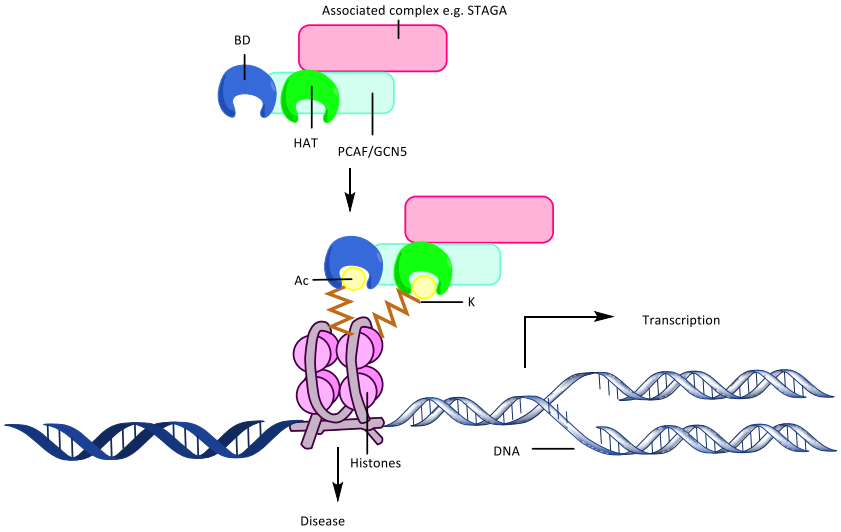

B

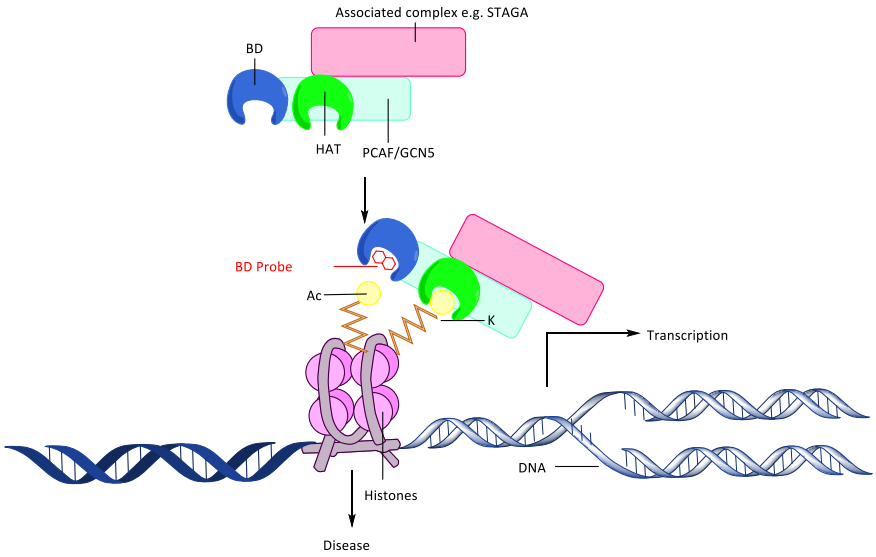

Figure 2.19 A) Association of PCAF/GCN5 and related complexes to acetylated chromatin driving transcriptional events. B) Displacement of BRD of PCAF/GCN5 using a BRD probe which is insufficient at displacing the full-length proteins and associated complexes.

Nonetheless, *L*-Moses represents a useful chemical probe to the epigenetic community which is now disseminated free of charge through the Structural Genomics Consortium[28] and also purchasable through chemical suppliers such as Tocris Bioscience.[307] It is envisaged that through this dissemination process other researchers will be able to run well designed biological experiments, of which there are numerous, aimed at trying to further the understanding of PCAF/GCN5 BRD associated biology in conjunction with analogous probes such as GSK4027 **122**.[304] These studies may be complemented by the generation of PROTAC variants of both *L*-Moses and GSK4027 **122** in order to study full length PCAF/GCN5 degradation. In other BRD containing targets such as TRIM24, it has been shown that BRD inhibition does not recapitulate the phenotypes of full length protein KO/KD studies. In lieu of this, conversion of a TRIM24 probe molecule to a PROTAC variant led to demonstrable phenotypic effects in relevant cell lines.[195] The outputs of the work described in this chapter were featured in a communication article published in early 2017.[303,308]

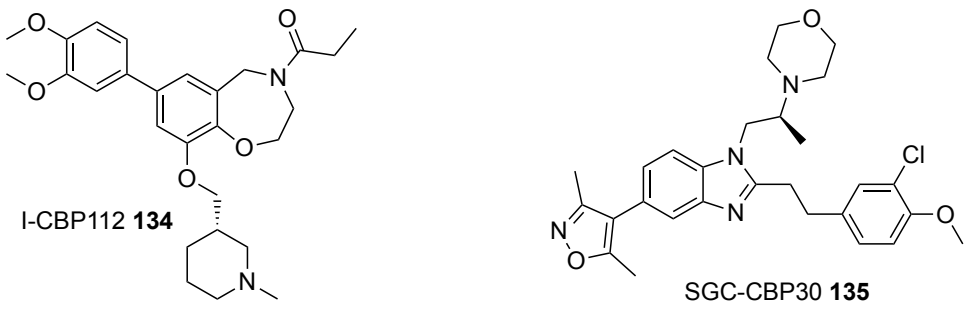

*Figure 2.20 CBP/p300 BRD inhibitors I-CBP112 **134** and SGC-CBP30 **135**.*

3. Macrodomain Inhibition

3.1 Introduction

3.1.1 Project Origin

The polyadeonosine diribose phosphate polymerases (PARPs) are a group of proteins capable of transferring poly-ADP ribose to substrate proteins.[197,220,309] Of these proteins, a subset exist as mono-ADP Ribose transferase (mARTs), characterised by the mechanistic ability to transfer one ADP-ribose unit at a time to a given substrate (Scheme 3.1).[196,310,311] PARP14 (ART8) is the largest of this subset and contains three macrodomains (ADP ribose binding domain) which prior to the project had been targeted in inhibitor development, owing to the disease links underpinning PARP14 and the lack of understanding about the domain specific contributions of the three macrodomain modules to PARP14 function or pathology.[240,241,312] Overexpression of PARP14 has been correlated with B-cell lymphoma progression, hepatocellular carcinoma and overall poor patient prognosis.[208] PARP14 has also been shown to promote a higher rate of glycolysis in cancer (Warburg effect)[210] which has been shown to be regulated by high *MYC* expression.[211]

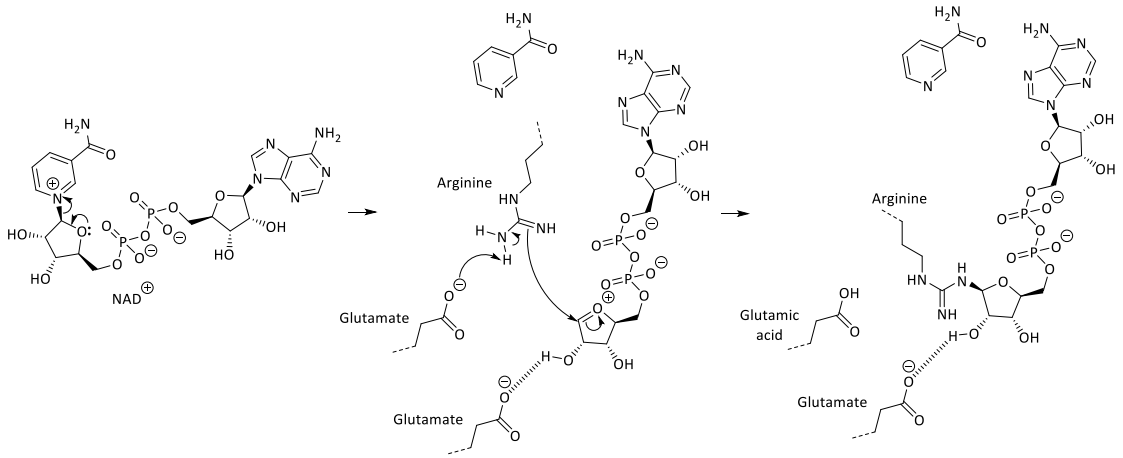

Scheme 3.1 Mechanism of mono-ART of an arginine residue by NAD⁺.

3.1.2 Chemical starting points

Through a collaboration between Novartis, Ludwig Maximillans University (LMU) and the Structural Genomics Consortium (SGC) a medium throughput screen was conducted by Schuller et al (~50k compounds) which uncovered carbazole GeA-69 **11** as a sub-μM inhibitor of the second macrodomain (MD2) of PARP14.[242] The binding activity of carbazole **11** was confirmed by ITC, BLI and AlphaScreen. Interestingly a close structural analogue, carbazole **137**, was successfully co-crystallised with PARP14 MD2 (PDB ID 5O2D) which revealed an allosteric binding mode of this chemical series. It was envisaged that the second macrodomain of PARP14 might in fact be the most promising to target through small molecule inhibition in order to deliver a functional effect (Figure 3.1). Indeed, the second macrodomain of PARP14 was found to bind most potently to ADP-ribosylated peptides *in vitro* (PARP14 MD1/ADPR-peptide K_D 137 ± 7 μM, PARP14 MD2/ADPR-peptide K_D 6.8 ± 0.1 μM, PARP14 MD3/ADPR-peptide K_D 15 ± 0.9 μM). In addition to this, PARP14 is one of the two PARP macrodomain containing proteins with a functionally active ART domain (PARP9 ART domain being ineffectual) and so targeting this protein may be promising in terms of uncovering useful functional effects.[309]

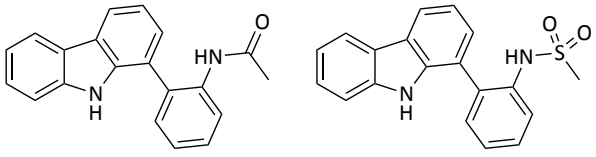

11 GeA-69
PARP14 MD2 IC_{50} 0.71 μM
PARP14 MD2 K_D 0.86 μM

137
PARP14 MD2 IC_{50} 0.9 μM
PARP14 MD2 K_D 2.1 μM

*Figure 3.1 Identified PARP14 MD2 inhibitor carbazole **11** and analogue **137**.*

A comparison of previously obtained co-crystal structure of PARP14 MD2 and ADP-ribose bound reveals that carbazole **137** induces a 'loop-shift', the displacement of which prevents ADP-ribose binding to PARP14 MD2.

A

B

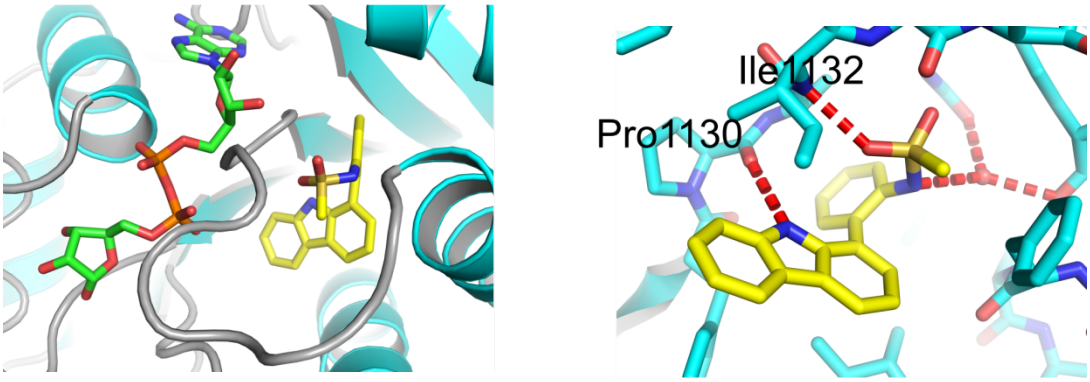

*Figure 3.2 A) Overlay of co-crystal structure of **137** (yellow sticks) with PARP14 MD2 (cyan) (PDB ID 5O2D) with ADP-ribose (green sticks) from co-crystal structure (PDB ID 3Q71); B) Co-crystal structure of **137** (yellow sticks) and PARP14 MD2 (cyan) with H-bonds shown as red dotted lines. Figure extracted from Moustakim et. al.*[313]

Both carbazole **11** and **137** showed good selectivity for PARP14 MD2 over the other two macrodomains (MD1 and MD3). It was envisaged that targeting the macrodomain with the greatest affinity for isolated ADP-ribosylated peptides would bode the most promising avenue towards developed inhibitors exerting a phenotypic effect. As a measure of cell-target engagement Schüller et. al.[242] developed a laser micro-irradiation assay which demonstrated that carbazole **11** indeed does permeate cells and engage with the target but only at high compound concentrations (>100 μM). Therefore, there remained a need to improve the cellular potency of this carbazole chemical series which might translate from improvements in *in vitro* binding to PARP14 MD2.

3.1.3 Aims

The aim of this work was to progress the novel allosteric inhibitor reported by Schüller *et. al*.[242] which shows sub-μM *in vitro* potency and selectivity for PARP14 MD2 through SAR studies and medicinal chemistry.

3.2 Chemical and Biological Methods

3.2.1 SAR/Synthesis

At the onset of this work, the previously identified carbazole hit compound **11** and corresponding sulfonamide **137** were structurally segmented into separate rings A-D (Figure 3.3).

Through a collaborative effort with colleagues from the Department of Pharmacy, Ludwig-Maximilians University and a co-worker at the SGC (Marion Schüller), medicinal chemistry and screening efforts were combined on this chemical series. Co-workers at Ludwig-Maximilians University largely focussed efforts on the optimisation and SAR studies of rings A-C. Significant efforts were expended on analogue synthesis in order to identify novel PARP14 MD2 inhibitors with increased potency relative to compounds **11** and **137**. Synthesised potential PARP14 MD2 inhibitors were then profiled at the SGC by M. Schüller using ITC, BLI or AlphaScreen. Unfortunately, it was found that rings A-C were not tolerant to structural changes with most modifications relative to initial hit compounds **11** and **137** ablating PARP14 MD2 inhibition.

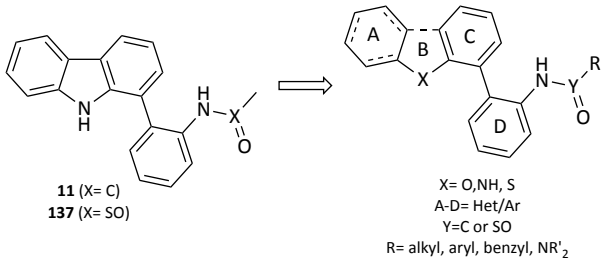

*Figure 3.3 PARP14 MD2 SAR studies of **11** and **137**.*

Our follow-on efforts from these SAR learnings were centred on the replacement of the acetamide of compound **11** or the methanesulfonamide of **137** in order to explore other areas of the PARP14 MD2 binding site and potentially identify new interactions. Additionally, a small number of compounds were synthesised with modifications focussed on ring D such as a fluoro-, methyl- and cyano- substituent as in compounds **138**-**140** (Table 3.1) maintaining single digit μM

PARP14 MD2 activity. It was found from previously synthesised analogues in LMU that sequential homologation of the sulfonamide motif in **137** to the corresponding ethane-, propane- and butane- analogues (examples **141**-**143**) maintained binding affinity for PARP14 MD2. Similarly, homologation of the acetamide in compound **11** into analogues **144** (ethanamide) and **145** (propanamide) also seemed to retain binding activity. However interestingly further homologation to the *n*-pentanoyl derivative **146** was inactive which may be attributable to a steric clash with the protein or an accruing entropic penalty induced by longer flexible alkyl chains. Notwithstanding, these observations suggested that there might be adequate room within the PARP14 MD2 binding site for ligand growth. It was found that replacement of the acetamide and methanesulfonamide of compound **11** and **137** with a 2-phenylacetamide in compound **147** and a phenylmethanesulfonamide as in compound **148** furnished single digit μM PARP14 MD2 inhibitors (compound **147** IC_{50} 7.6 ± 0.3 μM, compound **148** IC_{50} 3.6 ± 0.3 μM, Figure 3.4). This was slightly unexpected as compound **146** bearing the smaller aliphatic substituent was seemingly inactive.

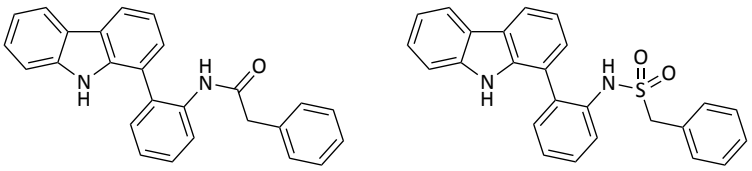

147
PARP14 MD2 IC_{50} 7.6 μM

148
PARP14 MD2 IC_{50} 3.6 μM

*Figure 3.4 Compounds **147** and **148** chosen for further optimisation.*

In parallel with efforts at LMU by K. Reidel (synthesis of compounds **141**-**143**, **154**-**164**), the structural motifs in compounds **147** and **148** were then explored further by the author as they potentially represented suitable vectors for exploring interactions with residues such as F1144 (Figure 3.2B) in addition to being sites of facile introduction of chemical diversity. Compound **149** was coupled with the corresponding 2-phenylacetyl chlorides or phenymethanesulfonyl chlorides under standard conditions with Pyridine to form the corresponding amides and sulphonamides (Scheme 3.2). Where a particular 2-phenylacetyl chloride was not available, the

corresponding carboxylic acid was used in its place and coupled using standard HATU coupling methodologies.

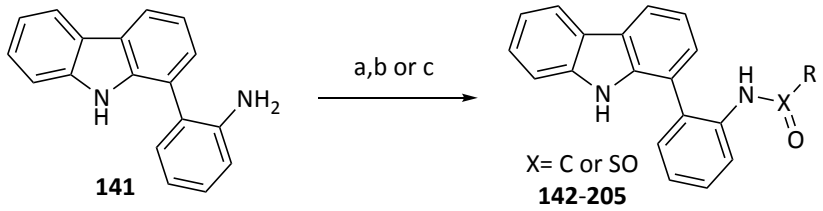

*Scheme 3.2 Derivatisation of aniline **141** to form amides and sulfonamides **142-205**. a) RCOCl (1.1 eq), Pyridine (1.3 eq), CH_2Cl_2, rt, 16 h. b) RSO_2Cl (1.1 eq), Pyridine (1.3 eq), CH_2Cl_2, rt, 16 h. c) RCO_2H (1.1 eq), HATU (1.2 eq), DIPEA (2 eq), CH_2Cl_2, rt, 16 h.*

Final compounds were then evaluated for PARP14 MD2 binding activity using AlphaScreen by M. Schüller. Potent compounds were then selected for further characterisation by BLI or ITC. A comparison of compounds synthesised by collaborators at LMU (K. Reidel), (compounds **141**-**143**, **154**-**164)** and compounds synthesised at the SGC by the author (**138**-**140**, **144**-**153**, **165**-**205**) allowed PARP14 MD2 SAR to be elucidated. As shown in Table 3.1, many of the modifications to rings A-D did not confer increased binding activity relative to initial hit compound **11**. Additionally it was found that 2- or 4- substituted phenylacetamide or phenylmethanesulfonamide groups such as a 2-F or a 2-Cl (as in compounds **179** and **180**) or 4-Me, 4-F, 4-OMe, 4-CN, 4-Cl or 4-CF_3 (as in compounds **181**-**186**) did not show improvements in binding relative to compounds **147** and **148**. Interestingly a 3-cyano substituted phenylmethanesulfonamide derivative, compound **197** (PARP14 MD2 IC_{50} 0.66 μM), showed a increase in potency relative to the parent sulfonamide **148**, also showing improvements in binding activity relative to the initial lead acetamide **11**. Interestingly the corresponding 3-cyano phenylacetamide **196** exhibited diminished binding activity which may be explained the difference in the ability of an amide or sulfonamide motif to engage in the H-bond acceptor interactions demonstrated in the previously obtained co-crystal structure of PARP14 MD2 and compound **137**. Despite a number of other analogues of **11** and **137** also being

Table 3.1 Binding affinity characterisation data of carbazole series for PARP14 MD2

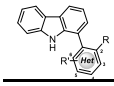	R	R'	IC_{50} (μM)	K_D (μM)	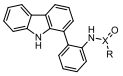	R	X	IC_{50} (μM)
11	**-NHAc**	**H**	**0.72**	**0.86**	**144**	-Et	C	1.0
137	-$NHSO_2Me$	H	0.9	2.1	**145**	*n*-Pr	C	0.9
154[a]	-NHAc	3-aza	>50	n.d.	**146**	*n*-Bu	C	>50
155[a]	-NHC(O)NH-*t*Bu	H	7.2	n.d.	**165**	-CH_2CH_2OMe	SO	8.6
156[a]	-$NHC(S)CH_3$	H	10.5	n.d.	**166**	5-Methylisoxazo-4-yl	SO	>50
157[a]	-NHEt	H	>50	n.d.	**167**	-NMe_2	SO	2.5
158[a]	-NEtAc	H	>50	n.d.	**168**	Ph	SO	>50
138	-$NHSO_2Me$	4-Me	1.1	n.d.	**160**[a]	-CF_3	C	1.1
139	-$NHSO_2Me$	4-CN	n.d.[b]	5.2	**161**[a]	-Cyclopropyl	C	1.2
140	-NHAc	6-Me	1.7	1.6	**162**[a]	-Cyclohexyl	C	>50
150	-$NHSO_2Me$	5-CF_3	>50	n.d.	**163**[a]	-2-furyl	C	>50
151	-NH_2	4-Me	>50	n.d.	**164**[a]	-Ph	C	1.9
152	-NH_2	5-CF_3	>50	n.d.	**147**	**-CH_2Ph**	**C**	**7.6**
153	-NH_2	6-Me	>50	n.d.	**148**	**-CH_2Ph**	**SO**	**3.6**
141[a]	-$NHSO_2Et$	H	1.2	n.d.	**169**	2-OMe-Ph	C	>50
142[a]	-$NHSO_2$*n*-Pr	H	2.9	n.d.	**170**	3-OMe-Ph	C	12.7
143[a]	-$NHSO_2$*n*-Bu	H	3.3	n.d.	**171**	4-OMe-Ph	C	9.0
159[a]	-$NHC(O)CH_2NMe_2$	H	5.5	n.d.				

[a]*Synthesised by K. Reidel.* [b]*Data was not obtained due to solubility issues in the AlphaScreen assay.*

Table 3.2 Binding affinity characterisation data of carbazole series for PARP14 MD2

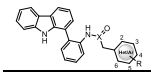	R/Het	X	IC_{50} (μM)[a]	K_D (μM)	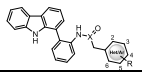	R/Het	X	IC_{50} (μM)[a]
172	3-aza	C	1.1	1.5[a]	**185**	4-Cl	C	6.2
173	3-aza-4-Me	C	1.0	2.7[a]	**186**	4-CF_3	SO	8.1
174	3, 6-aza	C	2.1	3.9[a]	**187**	3,4-OMe	C	4.3
175	4-aza-3-CN	C	2.4	n.d.	**188**	3,4-dioxole	C	6.9
176	3-aza-4-CN	C	3.5	n.d.	**189**	2-F-5-CN	SO	1.2 (K_D 1.3)
177	3-aza-4-OH	C	6.6	n.d.	**190**	2,5-Me	C	44.6
178	2-F	SO	2.4	n.d.	**191**	3,4-Cl	C	6.3
179	2-F	C	2.8	n.d.	**192**	3-OMe	C	6.6
180	2-Cl	C	4.4	n.d.	**193**	3-F	C	4.2
181	4-Me	C	8.7	n.d.	**194**	3-F	SO	1.4
182	4-F	C	>50	n.d.	**195**	3-CF_3	C	7.1
183	4-OMe	C	6.2	n.d.	**196**	3-CN	C	2.1
184	4-CN	SO	6.2	n.d.	**197**	**3-CN**	**SO**	**0.66 (K_D 0.55)**

[a]*No error of fit obtained for these K_D values. n.d. denotes not determined.*

synthesised (Scheme 3.2) and screened (compounds **165**-**205**, see supporting information) compound **197** was found to be the most potent PARP14 MD2 inhibitor (Table 3.1 and Table 3.2).

3.2.2 *in silico* docking

As diffractable crystals of sulfonamide **197** and PARP14 MD2 remained elusive despite attempts to co-crystallise the compound by M. Schüller, an evaluation of docked poses through the use of ICM was carried out to try and understand the nature of binding.[299] Using simple ligand minimisation of carbazole **197** in PARP14 MD2 it is unclear how 3-CN substituted **197** would make favourable interactions with PARP14 MD2. However, as this form of docking studies does not allow for side chain movement to accommodate ligand poses, docking studies using SCARE (SCan Alanines and Refine) docking were conducted. As depicted in Figure 3.5, the optimal docked pose of 3-CN phenylacetamide **197** features a rotation of the side chain of F1144, inducing a complementary π-π stack interaction. Furthermore, additional hydrophobic interactions are possible between the ligand and side chains of M1108 and L1137.

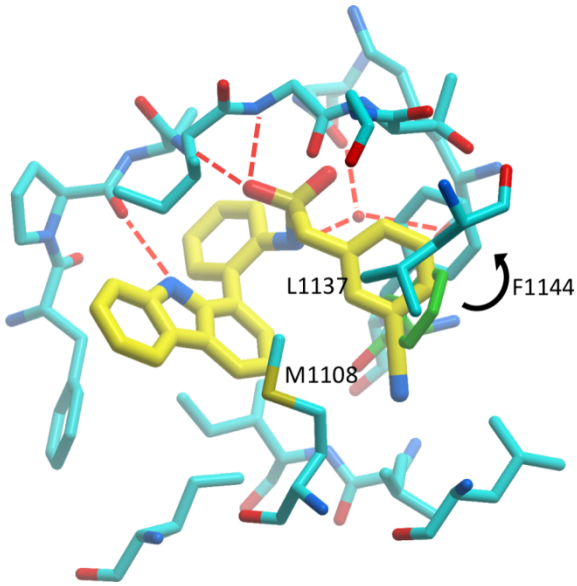

*Figure 3.5 3-cyano substituted carbazole **197** (yellow sticks) is predicted to bind to PARP14 MD2 (aqua sticks) similarly to initial hit compound **137**. SCARE docking predicts that F1144 side chain moves (original residue position in green) to accommodate the phenylmethanesulfonamide substituent of **197** (final position of F1144 side chain in aqua) and induces a complementary π-π stacking interaction.*

3.3 Conclusions and Future Work

The work described in this chapter centres on the development of an allosteric inhibitor scaffold deriving from a screening hit (compound **11**, GeA-69) against the second macrodomain (MD2) of PARP14. Prior work identified compound **11** as a sub-μM inhibitor of PARP14 MD2 and a co-crystal structure with a similar sulfonamide analogue **137** rationalised the nature of inhibition as allosteric through the induction of a PARP14 MD2 loop movement which then perturbs the ADPR binding site. Through a collaborative effort with collaborators at Ludwig-Maximilians University, compound **11** was strategically divided into sections (rings A-D, Figure 3.5) and analogues focussed on improving the potency of original hit **11** were then synthesised and screened. It was found that the SAR around rings A-D of initial hit **11** was very sensitive to modifications, with the parent compound showing superior PARP14 MD2 binding activity as compared with the various synthesised analogues. Interestingly it was found that the acetamide of **11** and methanesulfonamide of **137** were potentially replaceable with larger substituents without completely diminishing PARP14 MD2 activity. The introduction of a 2-phenylacetamide

or phenylmethanesulfonamide as in compounds **147** and **148** were promising points for compound elaboration and binding pocket exploration. A number of analogues of compounds **147** and **148** were then synthesised ultimately leading to the identification of carbazole **197** which features a 3-CN substituted phenylmethane sulfonamide motif. Carbazole **197** is a potent (IC_{50} 0.66 μM) inhibitor of PARP14 MD2 as characterised by AlphaScreen and confirmed through BioLayer Interferometry (BLI) also displaying nanomolar inhibition (PARP14 MD2 0.55 μM). Flexible docking studies through the use of SCARE docking demonstrated that carbazole **197** likely induced side chain movement in F1144 in order to accommodate the bulky 3-CN phenylmethanesulfonamide substituent, also inducing a potential π-π stacking interaction.

Future work in this series involves advancing 3-CN substituted **197** into an even more potent 'lead-like' structures. Advances in potency may be derived from the introduction of additional interactions with the binding pocket of PARP14 MD2, or the optimisation of current interactions. Nonetheless in order to rationally circumvent the tight SAR highlighted in this carbazole series, crystallographic structural information may be required in order to design improved ligands.

Additionally, selectivity profiling of carbazole **197** across the family of human macrodomains should be carried out to explore if this newly identified lead MD2 inhibitor still retains the selectivity for PARP14 MD2 that the initial hit exhibits. Furthermore, it would be of interest to explore the effect of compound **197** in the laser irradiation functional assay described by Schüller *et*. *al*.[242] to understand the utility of carbazole **197** in a cellular context. Finally distribution of compound **197** to other laboratories interested in the effects of PARP14 inhibition has commenced which may lead to novel phenotypes being identified for MD2 inhibition.

The outputs of this medicinal chemistry campaign described in this chapter focussed on the generation of potent PARP14 MD2 inhibitors has recently been published.[314]

4. YEATS Domain Inhibition

4.1 Introduction

4.1.1 Project Origin

The YEATS (YAf9, ENL, Af9, Taf14, Sas5) domain (YD) containing proteins are inter-species (from humans to yeast) conserved chromatin binding proteins (reader protein) which display an affinity for acylated lysine histone tails.[245] Due to the significant interest in epigenetic reader domain proteins such as bromodomains[37,76,82,150] and their roles in disease, attention has been focussed on uncovering new epigenetic reader targets. Within the Structural Genomics Consortium (Oxford), the YEATS domains were previously identified in 2013 as potential candidate protein targets for chemical probe discovery programmes. Despite the links with disease,[245] no inhibitors of YEATS domain containing proteins have been reported in the literature to date. Significant efforts were expended over five years focussed on the development of protocols involving cloning, transfection and recombinant protein production and purification. More recently, the YEATS domain containing protein ENL (MLLT1/YEATS1) has been identified as an essential protein for the carcinogenesis in Acute Myeloid Leukaemia (AML).[252,253] Due to the pathological relevance of ENL and potentially of its similar homologue, Af9 (MLLT3/YEATS3), efforts were focussed on isolation of recombinant protein for the YEATS domains of ENL and Af9, prior to the optimisation of biochemical and biophysical assays in order to begin a small molecule screening process to generate novel hit inhibitory molecules which could pose as chemical starting points for chemical probe discovery.

4.1.2 Chemical Starting Points

A medium throughput small molecule screen using the Ontario Institute of Cancer Research (OICR) small molecule library (~40k compounds) was conducted using an AlphaScreen[274]

biochemical assay. After filtering of hits, compound **206** was revealed as a single digit μM inhibitor of ENL YD (Figure 4.1).

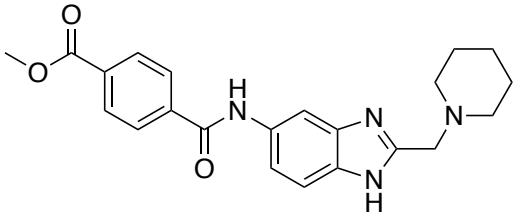

206
ENL IC_{50} 1.0 μM
ENL K_D 1.0 μM

*Figure 4.1 Compound **206** is a novel hit inhibitor of ENL YD*

Despite significant efforts to generate a co-crystal structure of benzimidazole **206** with ENL and Af9 YDs to understand the mode of binding, diffractable crystals remained elusive. Binding of compound **206** to ENL YD had been characterised by a competitive binding assay- AlphaScreen, using acetylated histone peptides as an ENL YD substrate. It could be presumed that compound **206** either directly displaces the KAc histone peptide in the YD binding site, or that there is some neighbouring allosteric site which upon binding to compound **206**, prevents binding of the KAc histone peptide substrate. Due to the lack of structural information on compound **206**: ENL YD binding, an iterative process of SAR and docking driven inhibitor design was the only available strategy based on 'chemical space sampling' around the original hit compound **206**.

4.1.3 Aims

Based on initial hit compound **206**, the aim of this research project was to advance the hit from a single digit μM inhibitor of ENL/Af9 YD to a potent (<100 nM K_D or IC_{50}), selective (>30-fold) and cell-active (target engagement at <1 μM) chemical probe.[27] In order to achieve this, an iterative process of rational inhibitor design and biochemical/biophysical characterisation of binding was employed to build an understanding around the SAR relating to compound **206**.

4.2 Chemical Methods

4.2.1 SAR/Synthesis

A previously obtained co-crystal structure of ENL YD with H3KAc27 (PDB ID 5J9S) obtained by Wan and co-workers[252] was initially used as a model to enable docking studies between ENL YD and compound **206** (Figure 4.2A). Docking studies using Molsoft ICM VLS[299] enabled predicted poses for binding with ENL YD.

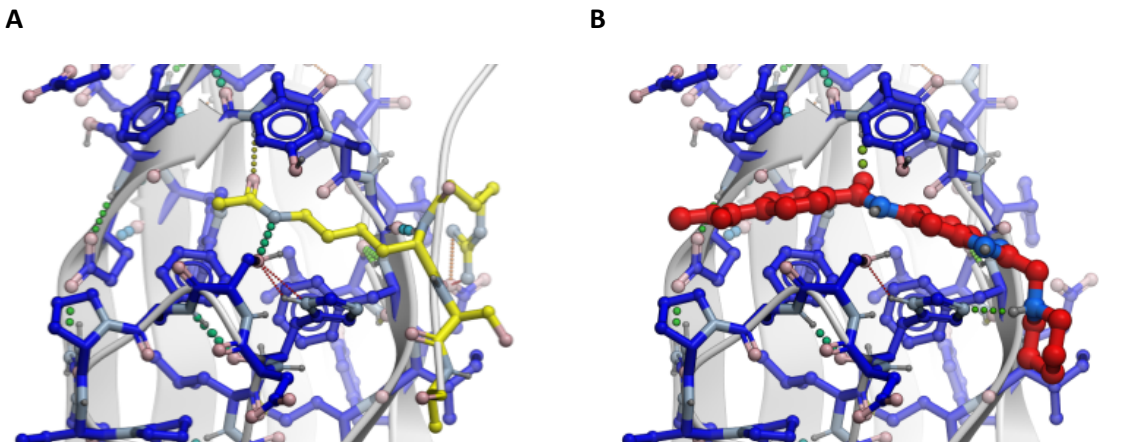

*Figure 4.2. A) Co-crystal structure of ENL YEATS domain (blue sticks) with H3KAc27 peptide(yellow sticks) bound (PDB ID 5J9S). B) Docking studies of compound **206** (red sticks) bound to ENL YD from co-crystal structure with H3KAc27 (PDB ID 5J9S).*

Docking studies revealed that compound **206** is predicted to overlay with the acetamide of H3KAc27 (Figure 4.2B). The amide bond is predicted to undergo H-bond interactions with the backbone N-Af9 of Y78 and a structural water (W312), additionally the protonated piperidine ring of **206** undergoes H-bond interactions with H56. It was rationalised that the increased potency of compound **206** for recombinant ENL YD relative to the moderate binding affinity for isolated H3KAc27 peptide (K_D 30 μM) could be due in part to the interactions around the 'aromatic sandwich' of the YD binding site. The YD binding site features an aromatic region in the form of residues F59 and Y78 which are thought to undergo a π-π-π 'sandwich stack' with crotonylated lysine residues. As depicted in Figure 4.2B, the methyl-ester substituted phenyl ring of compound **206** is predicted to be capable of intercalating the aromatic residues of F59 and

Y78 which may drive binding affinity to ENL YD. It was envisaged that 'optimisation' of the hypothetical interactions of compound **206** with ENL YD could be progressed through the deconstruction of compound **206** into three distinct components, which could be used to design new analogues (Figure 4.3).

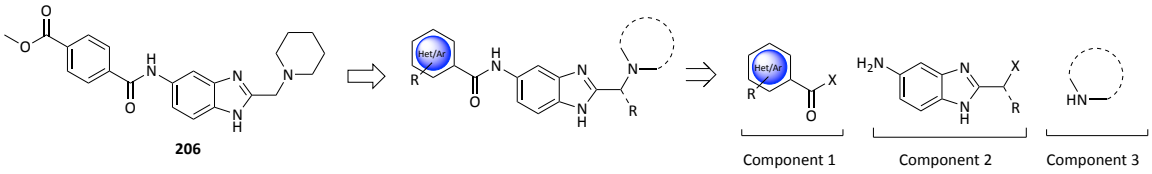

*Figure 4.3 Deconstruction of compound **206** into synthetic components 1-3.*

Due to the key interactions driving binding affinity of compound **206** with ENL YD being embedded within synthetic 'component 1' and 'component 3', initial synthetic efforts could be focussed on optimisation of these regions. The coupling of components 1, 2 and 3 in a poised fashion,[315] could be achieved using wide variety of (hetero)benzoic acids or acid chlorides (component 1) along with various commercially available amines (component 3) in a systematic approach. As found in the docking studies of compound **206** with ENL YD, optimisation of component 1 would likely hinge on generating analogues with increased capability for intercalating aromatic residues F59 and Y78. This could be achieved through the introduction of additional substituents on the phenyl ring of **206** which would decrease the electron density of the ring providing improved π-π-π stacking interactions with the relatively electron rich residues of F59 and Y78. Introduction of additional substituents on the ring of component 1 would require mindful attention to avoid the incurrence of any steric clashes with the YD binding site. However appropriately placed substituents might also be capable of identifying and engaging in new interactions not previously explored by the native substrate- acylated histone tails.

Similarly, for the optimisation of component 3, a core strategy was to foster and improve the interaction observed in docking studies of compound **206** between protonated piperidine and H56. A piperidine ring is capable of adopting a number of discrete conformations owing to

inherent flexibility in the six-membered ring (ring flipping)- however appropriately placed substituents can induce 'conformational locks' in order to avoid high energy buttressing interactions such as gauche or 1,3-diaxial interactions (Figure 4.4). It was predicted that if the piperidine ring could be 'conformationally locked' through the introduction of additional substituents, a particular conformer displaying favourable interactions to H56 may be stabilised and such a change might provide an improved structural analogue to original compound **206**. In line with this strategy, an appropriately placed substitution in the benzylic position of hit **206** may also reduce the degrees of freedom in the ligand and enhance entropically driven interactions with the protein.

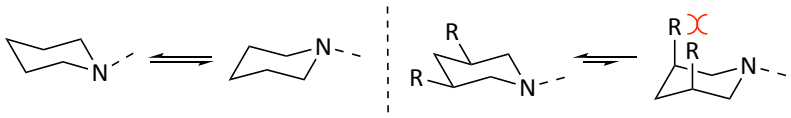

Figure 4.4 1,3-diaxial interactions confer buttressing clashes on cis-disubstituted piperidine rings shifting equilibrium towards equatorial conformers.

Whilst the synthesis of original compound **206** had not been previously described in the primary literature, owing to the intuitive disconnections of compound **206** to components 1-3, robust chemistry was employed to access analogues (Scheme 4.1).

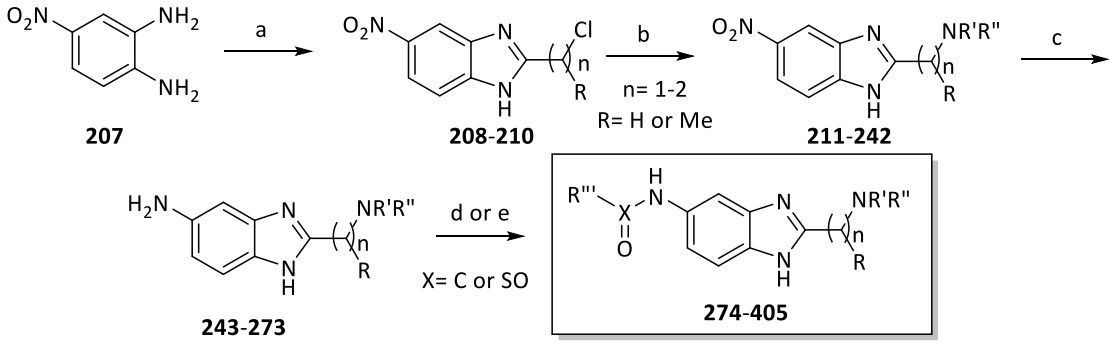

Scheme 4.1 Synthesis of ENL/Af9 benzimidazole based inhibitors. a) ethyl 2-chloroacetate, ethyl 2-chloropropanoate or ethyl 3-chloropropanoate (1.2 eq), 4N HCl (0.6 M), 16 h, 100 °C, 4-95%; b) amine (1.2-1.5 eq), Na_2CO_3 (1.5 eq), 23 °C, 3-82%; c) H_2 Pd/C (10%), MeOH, rt, 16 h, 17-88%; d) sulfonyl or acid chloride (1.2 eq), PS-DIPEA (2 eq), CH_2Cl_2, rt, 16 h or e) acid (1.2 eq), HATU (1.2 eq), PS-DIPEA (2 eq), CH_2Cl_2, rt, 16 h, 8-100%.

Synthesis of analogues commenced with a concomitant amidation and condensation of 4-nitrobenzene-1,2-diamine **207** with the corresponding ester or acid chloride affording chloro-benzimidazole compounds **208**-**210**. Chlorides **208**-**210** were then submitted into S_N2 reactions with a variety of amines to give nitro compounds **211**-**242** which were either isolated or immediately submitted to the following hydrogenation reduction step using Pd/C to give the corresponding anilines **243**-**273** which were then converted to amides or sulfonamides (examples **274**-**400**) through coupling with the corresponding acid, acid chloride or sulfonyl chloride in low to excellent yields.

4.3 Biological Methods

4.3.1 Potency

Approximately 200 lead optimisation compounds were designed and synthesised based on original hit compound **206** by the author (128 examples described in SI). Of the derivatives synthesised a number of substituents were appended onto the core of component 1 (Figure 4.5). Both electron withdrawing substituents (e.g. R= CF_3, OCF_3, Cl, Br, F, I, CN) and electron donating substituents (R= NMe_2, Me, O-alkyl, OH) in -*ortho*, -*meta* and -*para* positions were explored. Di-substituted ring analogues were also synthesised along with various heteroaromatics and bicyclic-heteroaromatics (Figure 4.5). Furthermore, a variety of substituted compounds were also synthesised with the amide motif being replaced with a sulfonamide.

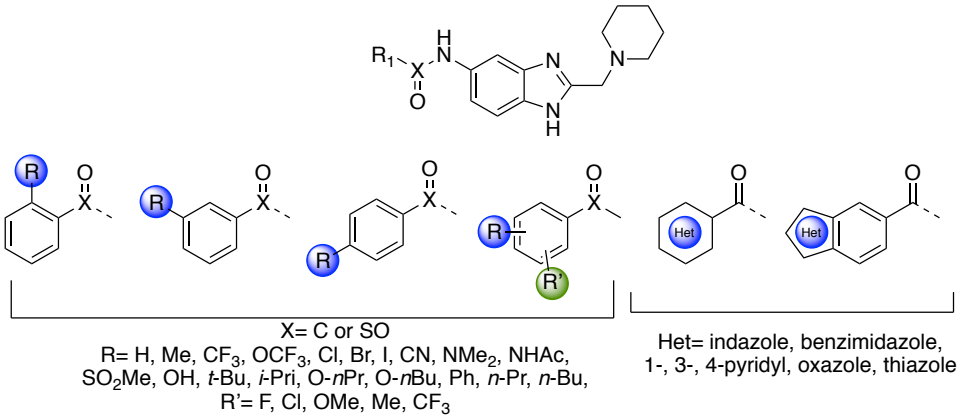

Figure 4.5 SAR Optimisation of component 1.

As a primary screen of lead optimisation analogues, AlphaScreen was employed to profile the binding activity of compounds. Promising compounds were followed up and validated by biophysical screening. Representative subsets of analogues are shown in Table 4.1 (Analogues **274**-**294**) were shown to have moderate binding.

*Table 4.1 SAR of component 1- selected analogues **274**-**294**.*

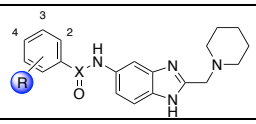

#	R	X	ENL IC_{50} (μM)
274	H	C	22
275	2-Cl	C	49
276	2-OMe	C	24
277	2-Me	C	97
278	2-CF_3	C	>50
279	2-OCF_3	C	72
280	3-Cl	C	14
281	3-F	C	9.5
282	3-OMe	C	17
283	3-CN	C	6.7
284	3-CN	SO	>50
285	3-CF_3	SO	26
286	3-CF_3	C	10
287	3-OCF_3	C	25
288	3,4-di-OMe	C	6.4
289	4-Cl	C	4.6
290	4-OMe	C	7.1
291	4-Me	C	5.9
292	4-CN	C	2.7
293	4-CF_3	C	5.3
294	4-OCF_3	C	6.5

Interestingly it was found that SAR around component 1 was largely not affected by the electronic nature of the substituent. Both EDG and EWG being tolerated to a similar extent for the same position of substitution. It was apparent from the observed SAR that compounds substituted in the 2- (*ortho*) position with both small or large substituents were the least active (compounds **275**-**279**). This may be explained by *ortho*- substituents inducing a steric clash with the protein or the influence this substitution position has on the conformation of the key amide motif. Substitutions in the 3- position were somewhat tolerated relative to original hit **206** (compounds **280**-**288**), with 4-substituted analogues being the most tolerated ENL YD binders (compounds **289**-**294**). Both electron donating (EDG) or electron withdrawing groups (EWG) placed in the *para*- position were tolerated however it seemed that binding was benefitted by introduction of more lipophilic substituents.

Having identified the 3- and 4- positions of component 1 being the position most amenable to substitution- a number of other analogues were made including the replacement of the amide motif in compound **206** with a sulfonamide. Interestingly it was found that a number of matched pair compounds bearing sulfonamide groups displayed much weaker binding activity relative to the corresponding amides (such as compounds **284**-**285**) or were completely inactive. Homologation of the methylene benzylic position in compound **206** was also explored (as in compound **296**). Additionally, substitution of the benzylic position with a methyl group (as in compound **297**) was also explored in order to minimize rotational degrees of freedom in the piperidine ring and potentially block a metabolically labile site. However, it was found that both homologation of the benzylic position and substitutions reduced the ENL YD binding affinity relative to compound **206** (compound **296** ENL YD IC_{50} 4.2 μM, compound **297** ENL YD IC_{50} 8.2 μM, Figure 4.6). Further derivatives were then designed and synthesised solely as amides with a fixed 1-carbon spacer between component 2 and the piperidine ring of component 3.

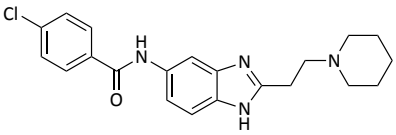

296
ENL IC_{50} 4.2 μM

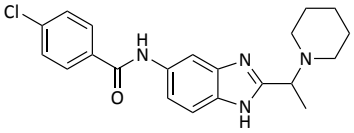

297
ENL IC_{50} 8.2 μM

*Figure 4.6 Benzimidazole derivatives **296-297***

Table 4.2 Binding activities of substituted & non-substituted heteroaromatic benzimidazole analogues.

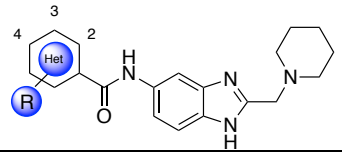

#	Het	ENL IC_{50} (μM)
298	2-Aza	24
299	3-Aza-4-Me	4.2
300	4-Aza	6.7
301	2,5-diaza	>50
302	2,3-di-Cl-4-Aza	>50

Subsequent optimisation of component 1 then focussed on exploring the inclusion of heteroaromatics and fused bicycloaromatics. Introduction of heteroatoms into the core of component 1 was carried out in order to potentially introduce new interactions with the side chains of the ENL YD binding site. Additionally, certain heteroaromatics would likely significantly influence the electron density of component 1 which may confer beneficial interactions with the lipophilic 'aromatic cage' region of the ENL YD. Both substituted and unsubstituted pyridyl rings in component 1 were tolerated without improvements in potency relative to original hit compound **206**, however the 3-aza-4-Me and 4-aza derivatives, compound **299**-**300**, displayed the most potent activity out of the heteroaromatic series.

In addition to monocyclic heteroaromatics, component 1 was also replaced with bicyclic fused and exocyclic hetero-aromatics. Component 1 was replaced with a number of fused (such as indazoles, benzimidazoles and indoles) and exocyclic (such phenyl substituted- imidazoles or pyrazoles Table 4.3) heteroaromatic analogues. There was a general trend for an increase in

potency across the various examples of fused and bicyclic hetero-aromatics. Exo-cyclic heteroaromatic compounds such as the pyridyl substituted compound **304** and 4-imidazoyl-phenyl substituted compound **307** displayed increases in binding affinity relative to the original hit compound (Table 4.3). Equally it was found that *N*-methyl-5-indazoyl analogue **312** (ENL IC_{50} 0.47 μM) displayed inhibition activity with ENL YD by AlphaScreen and was comparatively better than the corresponding 6-methyl regio-isomer (compound **309**). Increases in potency relative to initial hit compound **206** were measured for most analogues **303**-**312** with sub-μM binding achieved for most derivatives.

*Table 4.3 ENL YD Binding Affinities of exocyclic heteroaromatics **303**-**307** and bicyclic fused heteroaromatics **308**-**312***

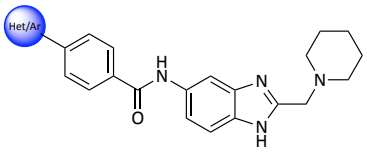

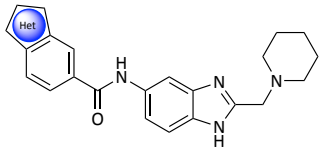

#	Het/Ar	ENL IC_{50} (μM)	#	Het	ENL IC_{50} (μM)
303		1.4	**308**	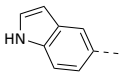	2.4
304		0.32	**309**	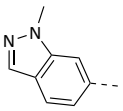	0.82
305	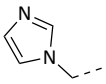	0.96	**310**	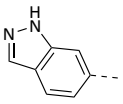	1.1
306		0.87	**311**	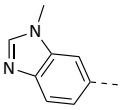	2.3
307		0.37	**312**	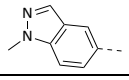	0.47

Next, equipped with knowledge regarding the beneficial substituents tolerated in 'component 1' attention was focussed on component 3 and exchanging the amine substituents in place of the piperidine ring of compound **206**. A variety of analogues were synthesised exploring substitutions on the original piperidine ring with the moderately active 4-Cl phenyl substituent chosen as a fixed component 1. Surprisingly it was found that both the 3,5-dimethyl piperidine **313** and 2,6-dimethyl piperidine **314** derivatives did not show increases in binding affinity compared to the unfunctionalised parent compound **289**. It was envisaged that the cis-

arrangement of methyl groups in these meso-configured isomers would likely incur a conformational restraint in order to minimize the potential 1,3-diaxial buttressing interactions. Additionally, conversion of the piperidine motif into the piperazines **315** and **316** did not show improvements. This may be due to a reduction in the pKa of the benzylic *N* atom due to induction of a β-heteroatom. It could also be rationalised that component 3 of original hit compound **206** is located in a more solvent exposed region of the ENL YD binding site, as such it is perhaps unsurprising that lipophilic modifications (as in compounds **316**-**318**) do not confer increases in binding affinity. It was found that contraction of the piperidine ring in compound **289** to a 2-methyl substituted pyrrolidine ring (compound **319**) showed increases in binding down to the nanomolar range (ENL YD IC_{50} 260 nM).

*Table 4.4 ENL YD Binding Affinities of compounds **289, 313**-**319**.*

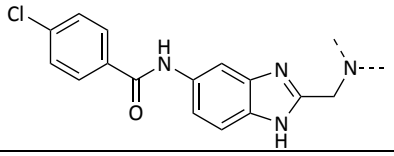

#	N--	ENL IC_{50} (μM)	#	N--	ENL IC_{50} (μM)
289		4.6	**317**	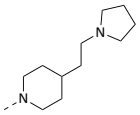	20
318	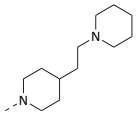	>50	**316**	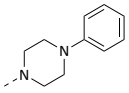	16
313	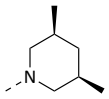	>50	**314**	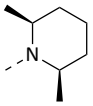	8.3
315	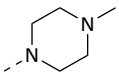	26	**319**		0.26

Encouraged by this significant result, the pyrrolidine derivative was initially synthesised as the racemate and so potentially up to 2-fold more active as a single enantiomer. It was then expected that a combination of the beneficial fused heteroaromatics in component 1 with the 2-methyl pyrrolidine of compound **319** might provide an additive effect and yield even more potent ENL YD inhibitors.

*Table 4.5 ENL YD Binding Affinities of hybrid compounds **312, 320-328**.*

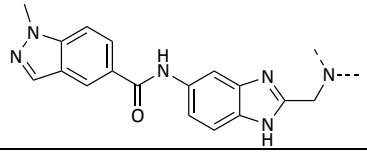

#	N--	ENL IC_{50} (μM)	#	N--	ENL IC_{50} (μM)
312		0.47	**324**	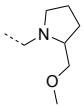	0.66
320	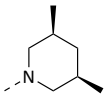	1.4	**325**	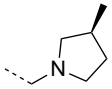	0.074
321	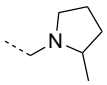	0.11	**326**	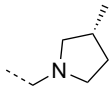	0.063
322	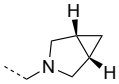	0.33	**327**	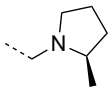	0.68
323	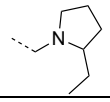	0.37	**328**	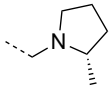	0.031

Derivatives covering a combination of these structural motifs were then synthesised and characterised for ENL YD binding affinity (selected examples **320**-**328** shown in table 4.5). In terms of both binding affinity and relative changes to logP of derivatives synthesised, the *N*-5-methyl indazole motif of compound **312** was chosen for optimal hybridisation with various amines in component 3. Whilst simple piperidine **312** displayed sub-μM activity against ENL YD (**312** ENL YD IC_{50} 0.47 μM), incorporation of cis-arranged 3,5-dimethyl groups as in compound **320**, seemed to decrease binding affinity (**320** ENL YD IC_{50} 1.4 μM). Similar to the activity of 4-chloro compound **319**, when racemic 2-methylpyrrolidine compound **321** was screened, excellent activity was observed (**321** ENL YD IC_{50} 0.11 μM). This prompted further investigation into the activity of the individual stereoisomers of compound **321**. Synthesis of both enantiomers from chiral building blocks revealed that most of the binding affinity with ENL YD lay exclusively with the (*S*) enantiomer, compound **328** (ENL YD IC_{50} 0.031 μM) whereas the (*R*) enantiomer, compound **327** was less potent (**327** ENL YD IC_{50} 0.68 μM). Elaboration of compound **277** to the corresponding 2-ethyl or 2-methylmethoxy derivatives, compounds **323** and **324** showed a decrease in binding affinity (**323** ENL YD IC_{50} 0.37 μM and **324** ENL YD 0.66

μM). Equally the 3-methylpyrrolidine derivatives compounds **325** and **326** (**325** ENL YD IC_{50} 0.074 μM and **326** ENL YD IC_{50} 0.063 μM) showed similar but less potent activity compared to compound **328**. Notably the two stereoisomers **325** and **326** showed distinctly similar binding activity whereas the potency differences between (*S*)-configured compound **328** and (*R*)-configured **327** were starkly different, allowing **327** to be used as a structurally relevant negative control compound. Although compound **328** showed excellent ENL binding in the primary assay, the AlphaScreen assay often displayed significant 'drifts' in the IC_{50} values produced and so further investigations into the binding activity were carried out using ITC which revealed potent low nanomolar binding to recombinant ENL YD. As expected, due to the high sequence homology of ENL and Af9 YD, similar levels of potency were observed for compound **328** with Af9 in both biochemical and biophysical assays (**328** Af9 YD IC_{50} 0.024 μM, Af9 K_D 0.077 μM).

*Table 4.6 Binding affinity summary of compound **328** against ENL and Af9 YDs.*

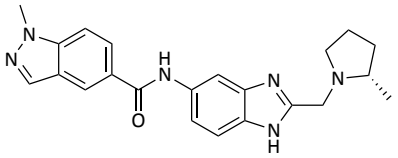 **328**	
ENL YD IC_{50} 0.031 μM	ENL YD K_D 0.129 μM
Af9 YD IC_{50} 0.024 μM	Af9 YD K_D 0.077 μM

4.3.2 Selectivity

Lead compound **328** was then profiled further for selectivity amongst the other YD containing proteins. Due to the high sequence homology of ENL and Af9 particularly within the YD (88% YD similarity) and identical residues within the characterised acyllysine binding site, it was predicted from the onset of the project that selectivity between the two target proteins may be difficult to achieve or perhaps undesired if there lies significant overlapping biology. Indeed, biophysical characterisation of compound **328** binding to both ENL and Af9 YD was measured with

equipotent activity in the sub 100 nM range (ENL K_D 129 nM, Af9 K_D 77 nM). Compound **328** was profiled against the remaining human YD containing proteins YEATS2 and YEATS4 where no measurable activity was seen by AlphaScreen (YEATS2 IC_{50} >10 μM, YEATS4 IC_{50} >10 μM).

Due to the similar binding of acyllysine histone tails (acetyl), a small panel of bromodomains were screened with compound **328** to explore selectivity over these epigenetic reading modules. Gratifyingly, no activity was observed against recombinant bromodomains BRD4(1), CBP, FALZ, BAZ2B and CECR2 (Table 4.7). Encouraged by this inherent selectivity over other acyllysine binding modules, experiments involving cells could therefore be explored.

*Table 4.7 AlphaScreen selectivity profile of compound **328** over other acyllysine reading domains.*

YEATS2	YEATS4	BRD4 (1)	CBP	FALZ	BAZ2B	CECR2
>10	>10	>10	>10	>10	>10	>10

Mean IC_{50} values reported in μM

4.3.3 Cell activity

In order to characterise compound **328** as a useful chemical probe capable of discerning the biology of ENL and Af9 YDs in a cellular context, a number of cell target engagement assays were utilised. A NanoBRET[283] assay was established exploring the ability of compound **328** and weaker enantiomeric control **327** to competitively displaced NanoLuc tagged full length ENL from Halo tagged H3.3 in HEK293 cells. Unfortunately, despite significant efforts to optimise the ENL NanoBRET assay a significant enough assay window was never obtained in order to generate meaningful data. Nonetheless, target engagement of compound **328** with Af9 was carried out using a successfully developed NanoBRET assay by colleagues in the SGC (NanoLuc tagged full length Af9 from Halo tagged H3.3 in HEK293 cells). Compound **328** displayed activity in the NanoBRET Af9 assay showing displacement in a dose dependent manner corresponding to sub-μM target engagement activity (Figure 4.7A). As expected weaker control **327** showed much poorer displacement in the Af9 NanoBRET assay pertaining to the utility of this enantiomer as a negative control (Figure 4.7B).

As an orthogonal measurement of cell target engagement, a cellular thermal shift assay (CETSA)[286] with intact MCF7 cells and HEK293 cells was explored. Cells were dosed with increasing concentrations of compound **328**, nominated control compound **327** or DMSO and heat shocked at a predetermined protein melting temperature. Compound **328** displayed a dose dependent increase in stabilisation to full length endogenous ENL which was visualised by Western Blot Analysis (Figure 4.8). The weaker enantiomeric compound **327** displayed no stabilisation at higher concentrations (2 μM and 10 μM) commensurate with the readout for the DMSO control (Figure 4.8). Taken together the orthogonal measurements of cell-target engagement pertained to the ability of compound **328** to effectively engage with both ENL and Af9 YD in a cellular context and potentially disrupt their interactions with modified chromatin.

A **B**

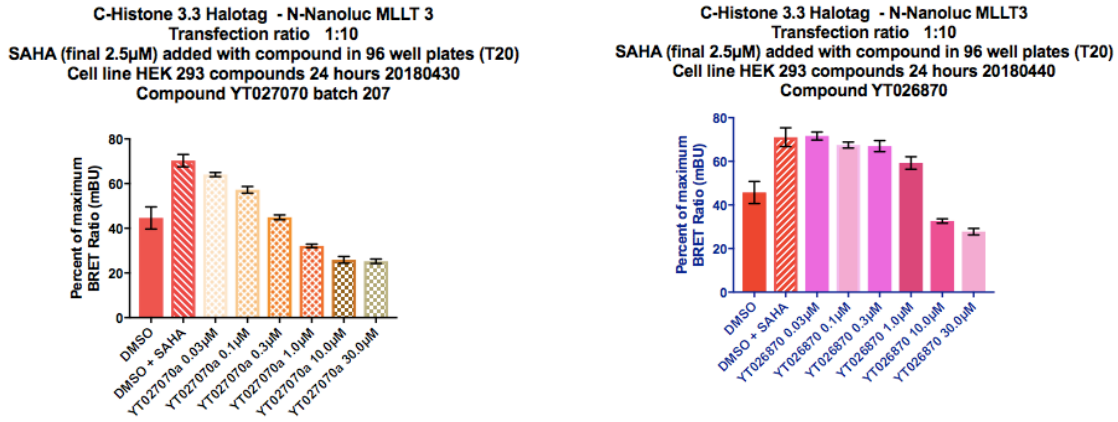

*Figure 4.7 A) Dose response NanoBRET displacement assay with Af9 and compound **328** (labelled as YT027070a). B) Dose response NanoBRET displacement assay with Af9 and compound **327** (labelled as YT026870a).*

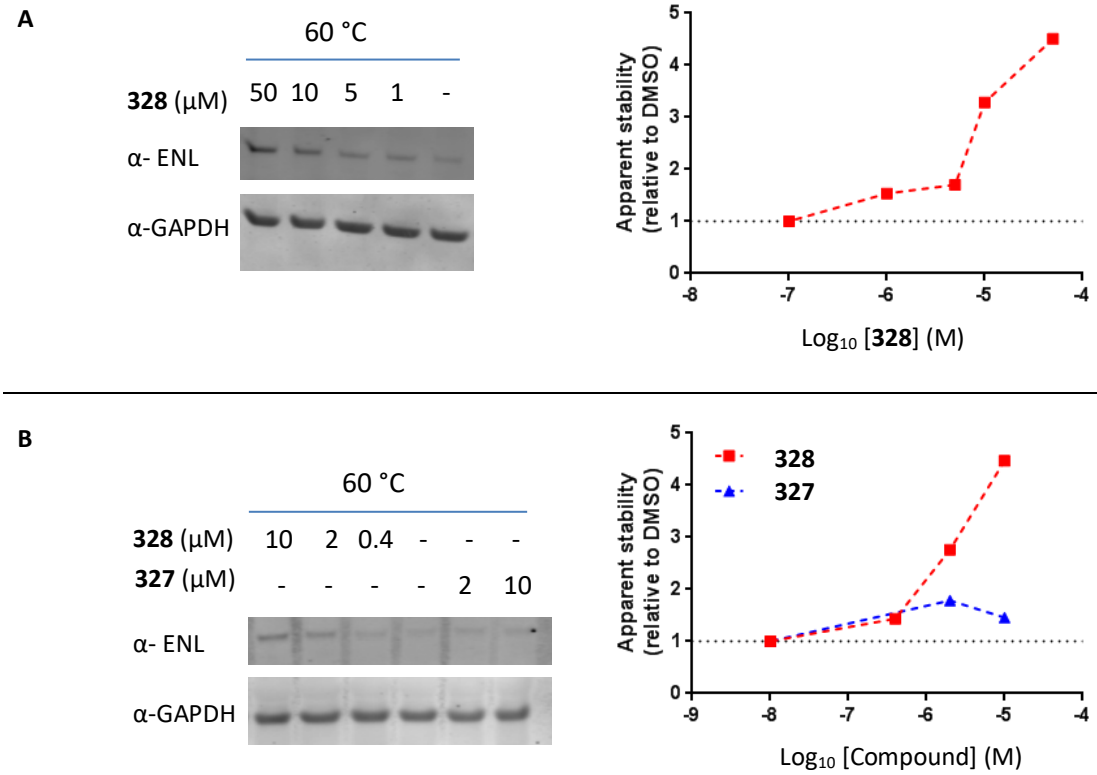

*Figure 4.8 A) Dose response stabilisation of ENL with compound **328** in HEK293 cells. B) Dose response stabilisation of ENL with compound **328** in MCF-7 cells but not with compound **327**.*

4.3.4 Cellular phenotype

Having confirmed potency and selectivity of the lead compound in both biochemical assays and biophysical assays in addition to the cell target engagement data supporting the notion that compound **328** effectively interacts with ENL and Af9 YDs in a cellular context, attention then turned to phenotypic assays. Encouraged by the confirmation of cell target engagement in multiple assays, it was rationalised that compound **328** might be a useful tool for investigating how disruption of ENL/Af9 modified chromatin interactions may affect transcriptional outcomes in disease relevant models such as leukaemia.

Following recent reports of ENL YD pharmacological inhibition sensitising cancer cells to BETi induced by treatment with the BET inhibitor, (+)-JQ1[252,253] we sought to investigate any potential synergy between the two modes of inhibition using the lead molecule **328**. Preliminary studies suggest that the lead molecule **328** does indeed sensitise AML cancer cells to BETi. At the

time of writing studies are still currently underway however preliminary results indicate that compound **328** inhibits growth of the AML relevant cancer cell line, MV4;11 cells in a dose dependent manner. Investigations are also currently underway to investigate the synergy of DOT1L inhibition with compound **328** treatment following the report from Erb *et. al.*[316] which suggested that YD inhibition of ENL may sensitize MV4;11 cells to DOT1L inhibition.

In addition to this, we profiled a number of lead compounds in the NCI-60 panel[289] to determine anti-proliferative activity induced by small molecule inhibition of ENL/Af9 YDs. Following a 72-h treatment of a number of cancer cell lines at 10 μM compound **328** failed to show cell growth inhibition across the cell lines reviewed (compound **328** cancer cell proliferation data shown in Figure 4.9). This may be due to the targets ENL and Af9 not being essential proteins in carcinogenesis within the cell lines reviewed. Or in fact it may be due to the fact that YD inhibition of these relevant targets is insufficient to abrogate the activity of ENL and Af9 within cancer cell progression. As a result, compound **328** was not chosen by the NCI for further investigations into its anti-cancer activities.

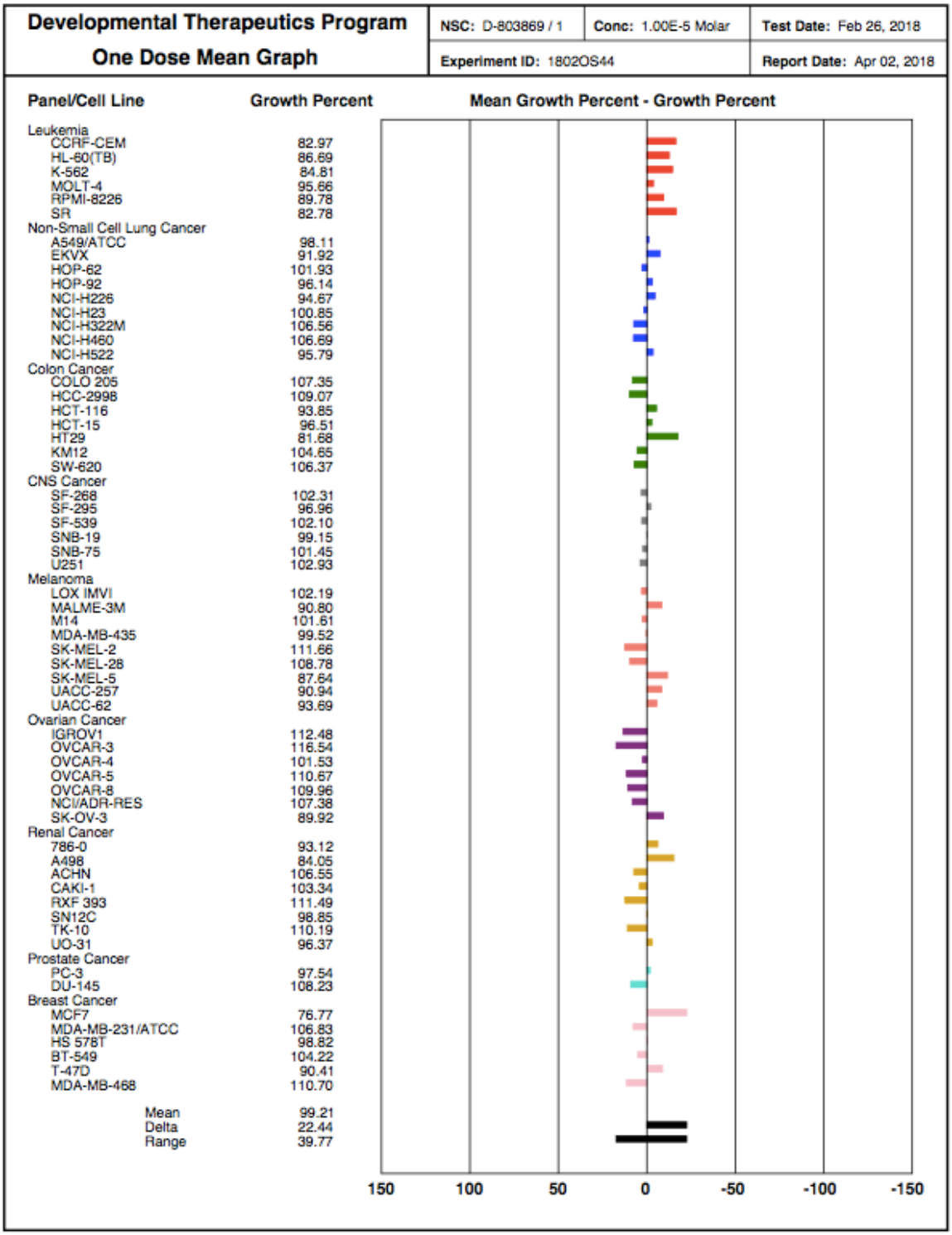

*Figure 4.9 NCI-60 Panel profile of lead compound **328**.*

4.3.5 Pharmacokinetics and metabolite identification

In order to investigate the potential of the developed ENL/Af9 YD inhibitors for use in *in vivo* studies, pharmacokinetic profiling and metabolite identification was carried out in order to ascertain metabolic stability. Compounds **328**-**332** were chosen for profiling and incubated with pooled primary human hepatocytes. It was found a major pathway for the metabolism of *N*-methylindazoles **328**-**330** was the oxidative demethylation yielding metabolite **328 M1** (Figure 4.10).

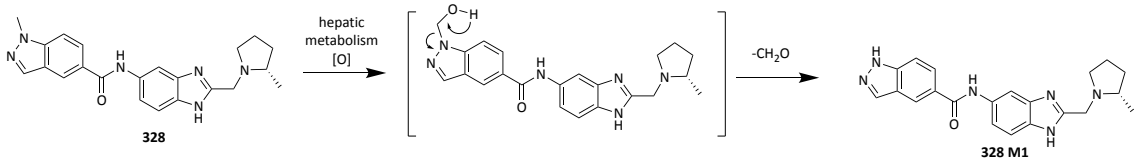

*Figure 4.10 Metabolism of lead compound **328** to dealkylated indazole **328 M1**.*

Interestingly the primary metabolite of indazole **328**, metabolite **328 M1**, was in fact synthesised separately in the YD inhibitor library as a racemate **333** and indeed displays potent binding to ENL (ENL YD IC_{50} 220 nM). However due to the superior binding of parent lead compound **328**, strategies towards mitigating the metabolic soft spot of the *N*-methylindazole were explored. A strategy towards 'blocking' the metabolic reactivity of the *N*-methyl group of **328** was via replacement with a cyclopropyl group.

Compound **334** was synthesised starting from commercially available indazole **335**, which was coupled with cyclopropyl boronic acid in a copper mediated Chan-Lam coupling in respectable yields as a single regioisomer **336**. Ester **336** was then hydrolysed with sodium hydroxide in good yields to give acid **337** which was then coupled using HATU with aniline **265** to give target material amide **334** in moderate yields (Scheme 4.2).

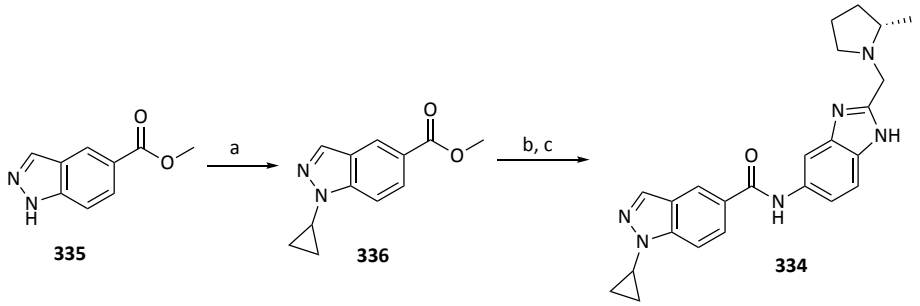

*Scheme 4.2 Synthesis of cyclopropyl- derivative **334**. a) c-PrB(OH)$_2$ (2 eq), Cu(OAc)$_2$ (1 eq), 2,2'-bipy (1 eq), 70°C, 16 h, 63%. b) NaOH (5 eq), MeOH, 65°C, 2 h, 68%. c) **265** (1 eq), HATU (1.2 eq), DIPEA-PS (2 eq), CH_2Cl_2, rt, 16 h, 42%.*

Compound **334** is currently being profiled in a similar metabolic study using pooled primary human hepatocytes. The authors envisage that compound **334** may exhibit increased metabolic resistance relative to initial hit compound **328**, with the de-cyclopropyl metabolite of **334** being less favourably formed after hepatocyte treatment. Gratifyingly compound **334** displayed potent activity against ENL YD (K_D 58 nM) compared with compound **328**. Subject to confirmation by pharmacokinetic profiling, compound **334** may represent a suitable compound for investigating ENL/Af9 YD inhibition in an *in vivo* context.

4.4 Conclusions and Future Work

This chapter has described the development of the first potent, selective and cell active chemical probe for the YEATS domains of ENL and Af9. Following a medium throughput screen of a library (~40k compounds) donated for use to the Structural Genomics Consortium/University of Oxford, an initial hit was identified using an AlphaScreen biochemical assay. This initial hit compound **206** displayed single digit μM activity against the YD of ENL (IC_{50} 1 μM). In agreement with biochemical characterisation, hit compound **206** also displayed measurable activity by ITC (ENL K_D 1 μM). Despite extensive efforts to obtain a co-crystal structure of **206** and ENL YD, diffractable crystals remained elusive.

A medicinal chemistry campaign was then initiated focussed on the development of increasingly potent inhibitors of ENL YD. After the focussed synthesis of ~200 analogues a number of nanomolar potent inhibitors were identified including lead compound **328** (ENL YD IC_{50} 0.031 μM) (additional compounds **338**-**405** within SI). The lead compound also displayed potent binding activity by ITC (ENL YD K_D 0.129 μM) and also against the highly homologous protein Af9 YD by both AlphaScreen and ITC (Af9 YD IC_{50} 0.024 μM, Af9 K_D 0.077 μM). It was then found that in addition to displaying potent binding to ENL and Af9 YD, compound **328** also displays excellent selectivity over the other two YD containing human proteins YEATS2 and GAS41 (YEATS4) (YEATS2 IC_{50} >10 μM, YEATS4 IC_{50} >10 μM). Additional reader-domain-containing protein selectivity was demonstrated for compound **328** when cross screened with a number of bromodomain proteins (BRD4(1), CBP, FALZ, CECR2, BAZ2B) demonstrating exquisite selectivity for ENL/Af9 YD. In order to demonstrate the ability of compound **328** to engage with its targets in a cellular context, a number of cell target engagement assays were developed. In a NanoBRET[283] both Nano-Luc tagged ENL YD and Nano-Luc tagged Af9 YD were shown to be competitively displaced from Halo tagged H3.3 after SAHA treatment in a dose dependent manner by compound **328**, alluding to sub-μM cellular activity.

Analogous efforts to demonstrate cell target engagement hinged upon the use of a cellular thermal shift assay (CETSA)[286], wherein dose dependent stabilisation of ENL observed following treatment of intact MCF7 cells and HEK293 cells correlating with sub μM cellular activity. In an effort to investigate the anti-cancer effects of ENL YD inhibition following recent reports[252,253] we profiled our lead compound in both MV4;11 rearranged leukemic cells in the absence and in combination with BET inhibitor (+)-JQ1 or a DOT1L inhibitor. Furthermore a number of the most potent compounds from the series were profiled in the NCI-60 panel[289] for their anti-cancer effects. Whilst preliminary studies in MV4;11 cancer cells were encouraging, surprisingly we found none of the potent ENL/Af9 inhibitors to display anti-cancer effects in any of the NCI-60

cancer cell lines investigated. This may be explained somewhat by a recent report which suggests that the essentiality of ENL YD in the context of cancer is fairly complex and indeed ENL-MLL fusions or YD mutagenesis increases the affinity for PAF1 and transforms hematopoietic cells.[265] Despite this we profiled our lead compounds further for metabolic stability in primary pooled human hepatocytes which provided insights into metabolic soft spots. In particular it was found that a number of potent *N*-methylindazole compounds **328**-**330** are readily dealkylated upon hepatocyte incubation. In order to circumvent this metabolic lability, additional compound **334** was designed and synthesised featuring an *N*-cyclopropyl motif which is expected to translate into increased metabolic stability in the same assay. It was also found that compound **334** displayed excellent potency against ENL YD and so is also considered a lead compound of development. We now seek to disseminate our lead compounds to other researchers in the epigenetic field such that the first biological studies of small molecule mediated ENL/Af9 YD inhibition can be carried out in the context of associated diseases. The work described in this chapter recently formed the basis of a manuscript being submitted as a communication article.

5. Formal Synthesis of Horsfiline

5.1 Introduction

5.1.1 Project Origin

Due in part to the increasing abundance of spiro-indolines and spiro-oxindoles presence as a structural motif in a wide variety of drug molecules, natural products and chemotherapeutics, the development of novel methods accessing these scaffolds is of significant value.[269] In 1980 Schultz et. al. reported a UV-A promoted cyclisation of aryl-enamines such as **406** to form spiroindolines **407** (Scheme 5.1).[317]

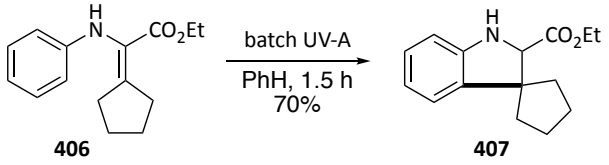

Scheme 5.1 Schultz's report of aryl-enamine cyclisation's via UV-A irradiation

The UV-A promoted cyclisation of enamine **406** is reported to proceed via a triplet di-radical mechanism (Figure 5.1) in which the double bond of aryl-enamine is promoted to an excited state following UV-A irradiation. The intermediate di-radical species is then capable of undergoing a radical cyclisation onto the aryl ring creating an intermediate dearomatised di-radical which is isoelectronic with the corresponding zwitterionic ylide which can rearomatise with a concomitant H-shift to generate the cyclised spiroindoline product (Figure 5.1).

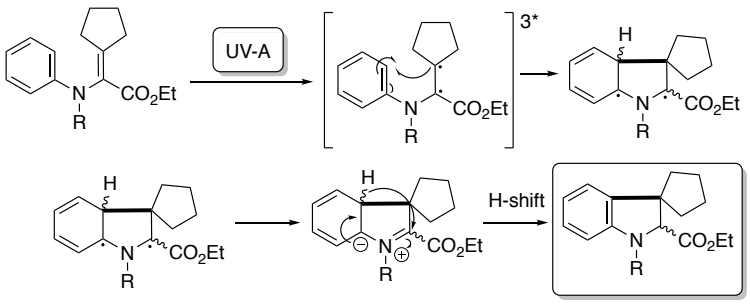

Figure 5.1 Mechanism of UV-A promoted cyclisation's of aryl-enamines to spiroindolines

Despite this seminal work describing a relatively mild and additive free transformation, there has since been few reports exploring this type of UV mediated bond activation. Previous unpublished work in the Vertex Pharmaceutical laboratories required the use of such a transformation in order to access biologically relevant molecules for medicinal chemistry campaigns. Unfortunately, when the UV-A mediated cyclisation (Scheme 5.1) was conducted using batch conditions the reactions were often impeded by sluggish reaction times, batch to batch variability and overall poor conversions of starting materials.

As the use of flow chemistry is routinely carried out for a variety of synthetic transformations in the Vertex laboratories- an initial line of inquiry was if the use of flow chemistry as applied to the UV-A mediated aryl-enamine cyclisation (Scheme 5.1) could confer practical and synthetic advantages. It has been reported that photochemistry in flow can offer a number of synthetic advantages as opposed to batch operation such as precise control over parameters such as heat, superior/consistent light penetration, controlled exposure time, inherent scalability and integration with additional parameter control.[270–272]

It was envisaged that if there existed significant synthetic advantages to the conversion of aryl-enamines to spiroindolines mediated by UV-A irradiation (Figure 5.1), it may allow for a significant investigation into the scope and utility of this underlying cyclisation. Furthermore due to the union of relatively simple starting materials and the additive free nature of the reaction, it could represent a novel and expedient method for accessing analogues of natural products[318] such as the alkaloid natural product spiro-[3,3]-oxindole horsfiline which has reported analgesic effects[273], or other compounds of biological significance[319,320] such as MDM2-p53 inhibitors (Figure 5.2).[321]

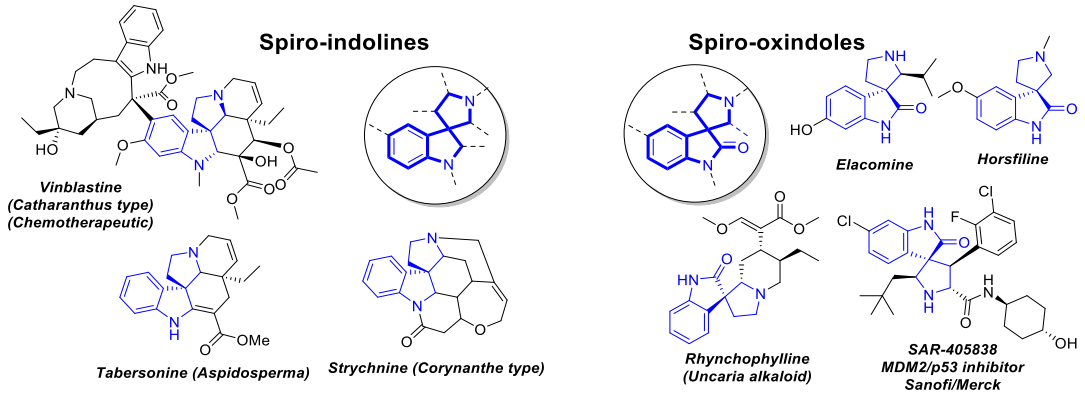

Figure 5.2 Spiroindolines and spiro-oxindoles featuring in a variety of natural product alkaloids and clinically useful drug molecules.

5.1.2 Aims

The primary line of inquiry of this research project was to explore the applicability of a flow chemistry procedure to the previously reported batch conversion of aryl-enamines to spiroindolines (Scheme 5.1). Additionally, the scope of the reaction was to be explored and its applicability to the synthesis of natural products such as horsfiline, a well-studied natural product targeted numerous times through total synthesis efforts, which could provide a platform for demonstrating the value of the transformation.

5.2 Chemical Methods

5.2.1 Method Development.

In order to investigate the applicability of a flow chemistry procedure to the cyclisation of aryl enamines to a simple model system was constructed from aniline and ethyl 2-cyclopentyl-2-oxoacetate, conditions were identified in which the corresponding condensed aryl-enamine **406** would rapidly undergo cyclisation under mild continuous flow conditions (Table 5.1) by colleagues at Vertex Pharmaceuticals.

Using a Vaportec UV photo reactor 150 flow apparatus fitted with a 10 mL reaction coil and various UV source inputs, an initial screen of UV wavelengths for the conversion of **406** to **407** was carried out. It was found that using benzene as a solvent, UV-LEDs (365 nm, entry 4, Table 5.1) proved to be superior in terms of isolated reaction yield (82%) compared with a UV-A spectral filter applied to a pan-UV lamp inserted. Pleasingly it was found that the simple translation of the reaction into flow conditions allowed the reaction to proceed to full conversion in a shorter reaction time to that previously described by batch (20 mins in flow). Whilst the previous literature report[317] describes this transformation being complete after 1.5 hours, it was found that the same reaction conducted in batch using a UV photo box equipped with UV-A bulbs required >16 hours to proceed until full conversion.

*Table 5.1 Flow optimisation of UV-photocyclisation of aryl-enamine **406** to spiroindoline **407***

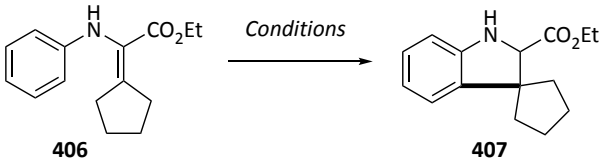

406 **407**

Entry	UV source[a]	Solvent[a]	Flow rate[b]	°C	(%)
1	UV-A	PhH	0.5	30	45
2	UV-B	PhH	0.5	30	56
3	450 nm	PhH	0.5	30	N.R.
4	**365 nm**	**PhH**	**0.5**	**30**	**82**

[a] Flow photo reactor fitted with a 10 mL reaction coil and an inserted UV lamp with a spectral filter applied or an LED insert of specified wavelength. [b] Flow rate in mL/min. [c] Temperature in °C. *Batch

It was found that the use of longer wavelengths such as entries 3 (450 nm) gave low to no conversion. Use of other solvents (MeOH, MeCN or 1,4-dioxane) also failed to facilitate the UV mediated cyclisation.

5.2.2 Formal Synthesis of (±)-horsfiline.

Equipped with the knowledge of this additive-free UV-A mediated cyclisation to form spiroindolines could be expedited using a flow protocol, it was envisaged that the method could precede a formal total synthesis of (±)-horsfiline **409** intercepting common intermediate **408** from a previous route reported by Carreira *et. al.* (Figure 5.3)[322]

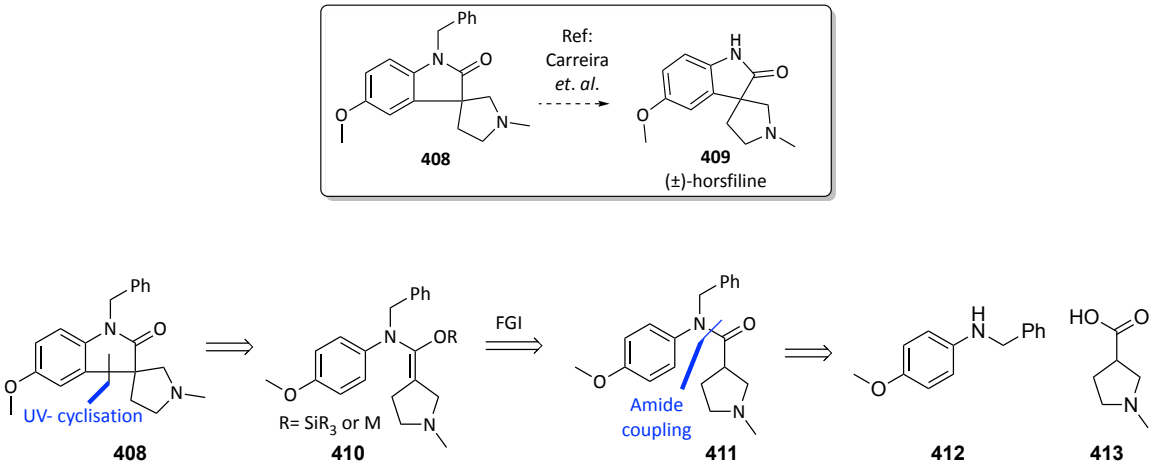

*Figure 5.3 Retrosynthesis of natural product intercept, compound **408***

It was predicted that if a final late stage UV-promoted cyclisation of a suitable silyl enol ether or enolate derivative to form **408** could be effected, this would reveal an expedient route towards the formal synthesis of horsfiline **409**. Silyl enol ether or enolate **410** could be generated from amide **411** which is disconnected to reveal commercially available fragments **412** and **413**.

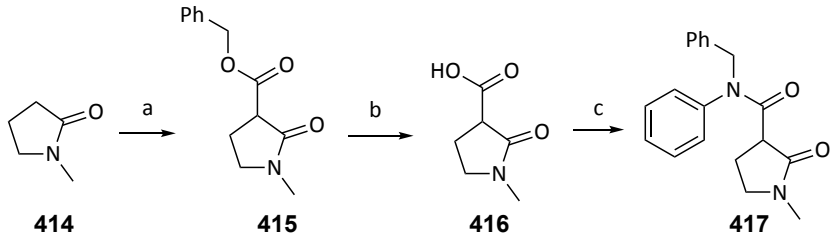

*Scheme 5.2 Synthesis of compound **417**. a) benzyl chloroformate (1.5 eq), LDA (1.5 eq), -78°C to rt, 27% b) H_2, Pd/C (10%), MeOH, rt, 16 h, quant. c) 2-chloro-1-methyl-pyridinium iodide (1.5 eq), N-benzyl-aniline (1.5 eq), DIPEA (2 eq), CH_2Cl_2, rt, 16 h, 28%.*

It was decided that a sensible model system for this particular strategy towards horsfiline **409** and related natural products would be to incorporate a lactam motif which would perhaps help to facilitate the formation of the enol ether or enolate owing to the 1,3-dicarbonyl unit embedded in the structural core depicted in Figure 5.3 (Scheme 5.2). The solvent reagent NMP **414** was acylated with benzyl chloroformate after treatment with LDA in moderate to low yields to provide 1,3-dicarbonyl **415**. Protected **415** was then hydrogenatively debenzylated to form free acid **416** in quantitative yield. Following this an amide coupling using 2-chloro-1-methyl-pyridinium iodide (CMPI) with *N*-benzyl aniline **412** and acid **416** was carried out in low isolated yields to form **417**.

After a UV cyclisation of **417** to **418** the lactam motif could then be selectively reduced following benzyl deprotection to intermediate **419** as in a previously reported total synthesis of (±)-coerulescine **420** by Kulkarni and co-workers[323] via protection as a lithium anion after treatment with BuLi and exhaustive reduction with LAH (scheme 5.3).

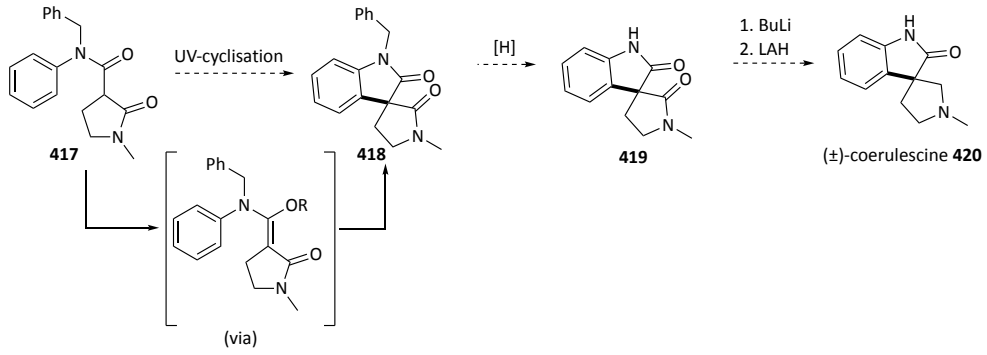

*Scheme 5.3 Lactam strategy towards spiro-oxindoles such as coerulescine **420**.*

The potential of this UV cyclisation was explored with compound **417** (with the intention of later transferring the protocol into flow). Unfortunately, it was found that despite an extensive screen of conditions including exploring a variety of bases, Lewis acids or activating agents, solvents and either irradiation with UV-A or UV-B, starting material was recovered in almost all cases (Table 5.2).

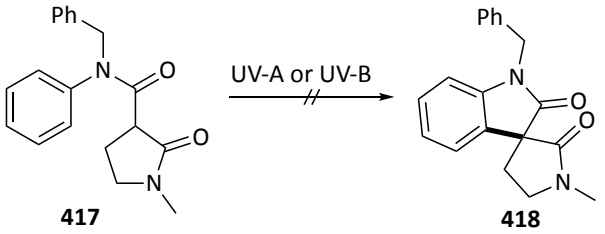

417 **418**

*Table 5.2 Conditions explored for the cyclisation of **417** to **418**.*

Bases	Lewis Acids/Activating Agents	Solvents
DBU, t-BuOK, BTTP	$Cu(OTf)_2$, TESCl, $Cu(OAc)_2$, $BF_3.OEt_2$, $AlCl_3$, TFA	MeCN, Benzene, Mesitylene, DMA

It was rationalised that the lack of reactivity in the cyclisation of **417** to **418** may be due to the fact that in order for the cyclisation to occur, the transiently formed reactive enolate or silyl enol ether would need to appropriately absorb irradiation in the UV-A or UV-B region. However, this may not overlap with the wavelength or energy required to excite the double bond to the corresponding triplet di-radical species (Figure 5.1) of the corresponding enol ether or enolate. Moreover, it was noted that in some of these trial experiments, a number of reactions were observed to be heterogeneous suspensions which may not facilitate effective light penetration into the reaction mixtures.

Instead it was decided that reintroduction of a carboxyl-ester as an electron withdrawing motif and formation of the aryl enamine via condensation onto a keto-ester might prove to be more promising, as it would be more closely aligned with the original substrate reported by Schultz.[317] The appropriate keto ester was generated starting from diethyl phosphite **421** which was reacted with ethyl-2-oxoacetate and then quenched with TBSCl to give the Horner-Wadsworth-Emmons precursor **422** in good yields. Compound **422** was then treated with LiHMDS and 1-methylpyrrolidin-3-one to give silyl enol ether **423** in moderate yield (47%) which was then deprotected using CsF to give keto ester **424** in moderate yield (58%, Scheme 5.4).

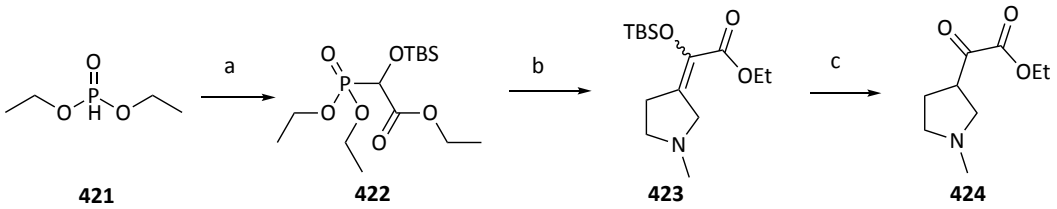

*Scheme 5.4 Synthesis of intermediate compound **424**. a) ethyl-2-oxoacetate (1 eq), TEA (1.5 eq), TBSCl (2 eq), Imidazole (1.5 eq), Toluene/DMF, 0°C to rt, 16 h, 77% b) 1. LiHMDS (1 M in THF, 1.5 eq) 2. 1-methylpyrrolidin-3-one (1.2 eq), -78°C to rt, 16 h, 47%; c) CsF (2 eq), AcOH (5 eq), 0°C, 3 h, 58%;*

Keto-ester **424** was then used and reacted with either *N*-benzyl aniline **412** or aniline to give the corresponding aryl-enamines **425** and **426** after microwave assisted condensation using a catalytic amount of TFA and $MgSO_4$ as a drying agent. Condensation to form benzyl-protected aryl enamine **425** and unsubstituted enamine **426** was found to proceed sluggishly perhaps attributable to the tertiary *N*-methyl pyrrolidine impeding the condensation through protonation with TFA. Despite this, isolated material was then submitted into the batch UV cyclisations. Interestingly the photocyclisation of **426** to form **427** proceeded in very low yield (13%), in addition the cyclisation of **425** was also found also facilitate the debenzylation of the material thus both starting materials led to the same product **427** (presumably transient production of radical species at the benzylic position may have been quenched by moisture or oxygen and facilitated the deprotection of the cyclised product). Compound **427** was found to be highly unstable and would readily undergo oxidation to side products. Compound **427** was then alkylated with benzyl bromide to give **428** in low yields. It was previously noted in unpublished research in the Vertex Laboratories that some 2-carboxyl ester indolines readily undergo decarboxylation when hydrolysed to the corresponding carboxylic acids, instead forming 2-oxindoles. It was envisaged that this reactivity could be utilised with compound **428** and so compound **428** was treated with lithium hydroxide under thermal conditions. Unfortunately, despite many attempts, decarboxylation of compound **428** never occurred, instead leading to side product formation (Scheme 5.5).

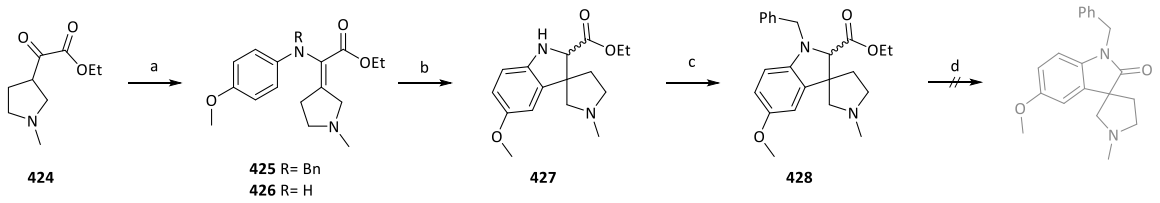

*Scheme 5.5 Synthesis of intermediate compound **428**. a) TFA (cat.), $MgSO_4$, p-anisidine (R= H) or N-benzyl-p-anisidine (R= Bn) (1.2 eq), PhH, 150°C, 30 min, R=H 25%, R=Bn 12%; b) UV-A, PhH, 16 h, R=H 13%, R=Bn 10%; c) BnBr (1.5 eq), K_2CO_3 (2 eq), MeCN, 120°C, 2 h, 38%; d) LiOH, MeOH, rt to 100°C, 0-2 h, N.R.*

It was then decided, owing to the poor yields and reactivity observed with synthetic intermediates harbouring a tertiary amine as a structural motif, that efforts be made to protect this group and later convert to the corresponding *N*-methyl group. It is well known that motifs such as tertiary amines can readily form radical cations when exposed to UV irradiation[324] and so this may have been one issue causing synthetic challenges in previous experiments.

Instead in a similar sequence, generation of silyl reagent **422** was again enabled by the addition of diethyl phosphonate **421** to ethyl glycolate (Scheme 5.6).[325] The resulting product alcohol was silylated *in situ* with TBSCl yielding silyl ether **422**. Submission of silyl ether **422** into a Horner-Wadsworth-Emmons (HWE) reaction using standard conditions with LiHMDS gave olefin **423** as an E/Z mixture in excellent yield (96%). E/Z isomers of **423** were then deprotected after treatment with caesium fluoride to furnish single keto-ester **424** in good yields (74%). Keto-ester **424** was then reacted with *N*-benzyl-*p*-anisidine **412** under microwave conditions to give condensed enamine **425** in a short reaction time (30 mins). When submitted into the previously optimised flow photocyclisation protocol, enamine **425** converted smoothly to protected spiroindoline **426** as a mixture of diastereomers in quantitative yield and short reaction time (20 mins) without the requirement for chromatographic purification upon cyclisation. Interestingly, by comparison, submission of enamine into the same cyclisation under batch conditions failed to effect the same transformation even after prolonged irradiation times.

In accordance with the previous unpublished synthetic research within the Vertex laboratories regarding the basic hydrolysis of 2-carboxyester spiroindolines which in some instances undergo

an oxidative decarboxylation to form 2-oxindoles- this transformation was explored with spiro-indoline **426**. The various 2-carboxyester spiroindolines generated in the experiments conducted had a propensity to generate oxidised by-products when exposed to air and light. Hinging on this sensitivity to undergoing oxidative degradation processes, and encouraged by similar reported transformations[326] it was envisaged that protected spiroindoline **426** could be oxidatively decarboxylated with appropriate additives (air/oxidants) to form spiro-oxindole **427** and formally intercept a route reported by Fuji and co-workers[327] towards horsfiline.

It was found that upon treatment with hydroxide, ester **426** failed to decarboxylate as previously observed for similar compounds and instead formed amino acid **428**, even with prolonged or forcing reaction conditions. Serendipitously it was observed that ester **426**, upon treatment with hydroxide under aerobic conditions and UV-A irradiation, slowly converted to the desired spiro-oxindole **427** in a modest isolated yield (22%) which underscored the completion of a formal synthesis of (±)-horsfiline **409** in five steps. By comparison the control experiments in the absence of UV-A irradiation (or using other wavelengths) led to little or no conversion to spiro-oxindole **427**.

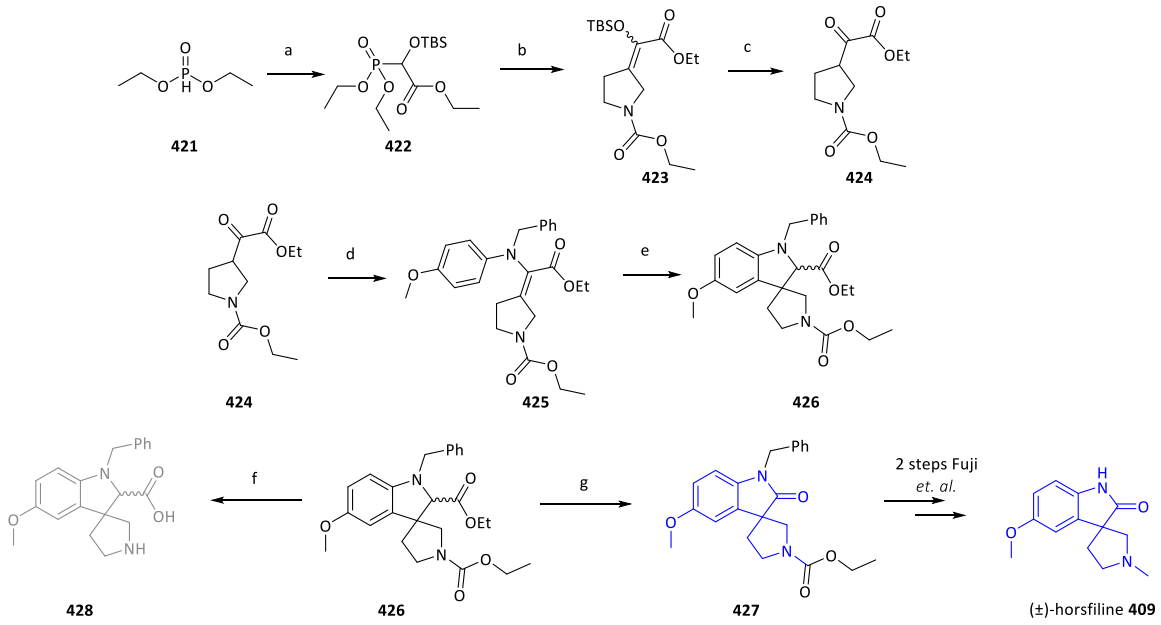

*Scheme 5.6 Formal Synthesis of (±)-horsfiline **409**. a) ethyl-2-oxoacetate (1 eq), TEA (1.5 eq), TBSCl (2 eq), Imidazole (1.5 eq), Toluene/DMF, 0°C to rt, 16 h, 77%; b) 1. LiHMDS (1 M in THF, 1.5 eq) 2. ethyl 3-oxopyrrolidine-1-carboxylate (1.2 eq), -78°C to rt, 16 h, 96%; c) CsF (2 eq), AcOH (5 eq), 0°C, 3 h, 79%; d) N-benzyl-p-anisidine (2 eq), TFA (cat.), $MgSO_4$ (anhydrous, 2 eq), 150°C, PhH, 30 min, 74%; e) UV-A LED (365 nm), 0.5 mL/min (20 min)/0.2 mmol/hr, PhH, quant; f) LiOH (2 M, 17 eq), MeOH/H_2O, rt to 100°C, quant. conversion (not isolated); g) LiOH (2 M, 17 eq), UV-A bulb, air, MeOH (2:1 H_2O:MeOH), rt, 72 h, 22%.*

Interestingly, it was noted that the formation of spiro-oxindole **427** occurred even in the absence of hydroxide (pertaining to the potential of a radical decarboxylative mechanism). This appears to be the first example of a UV-mediated oxidative decarboxylation to furnish spiro-oxindoles using mild conditions.

A potential mechanism for the formation of spiro-oxindole **427** from spiro-indoline **426** is depicted in Figure 5.4. When exposed to UV light it is presumed that hydroxyl radical species would be generated either from water (in the absence of hydroxide) or from molecular oxygen converting to superoxide radicals, peroxy radicals and then hydroxyl radicals. Sequential oxidation of spiroindoline **426** to an iminium species can be subsequently hydrolysed and decarboxylated to the corresponding ylide by water or hydroxide. The pseudo-stable ylide is

capable of radically combining with another hydroxyl radical and sequentially oxidised and tautomerised to give spiro-

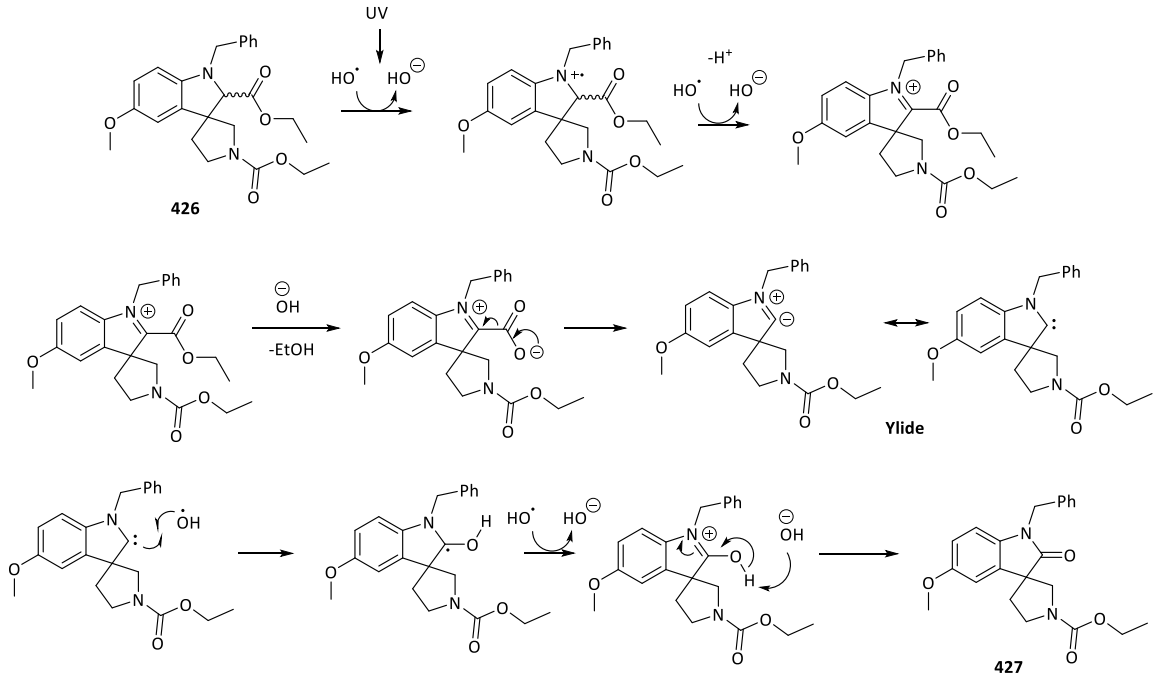

*Figure 5.4 Postulated mechanism for the oxidative decarboxylation of **426** to form **427**.*

oxindole **427** as the final product. Confirmation of the exact mechanism by which this reaction occurs requires further detailed study and the generation of experimental data to support this postulated mechanism.

5.2.3 Substrate Scope

Equipped with optimal conditions, next an investigation to the scope of the reaction was carried out in conjunction with colleagues (J. Garwin) at Vertex Pharmaceuticals. Aryl-enamines **429-440** were synthesised as reaction starting materials and submitted to the aforementioned conditions, smoothly cyclising to spiroindolines **441**-**452** in moderate to excellent yields. It was found that a variety of substituted aryl-enamines were tolerated in the reaction bearing both electron donating (OMe) and electron withdrawing (-F, -Br, -CN) groups irrespective of substitution pattern. Overall however it was found that electron withdrawing systems gave access to products in higher yields (Table 5.3). *N*-substituted aryl-enamines were also tolerated in the cyclisation (examples **450** and **451**) in addition to expanded ring-sized spiroindolines (example **452**) and the inclusion of heteroatoms in the spirocycle (compound **426**). Unfortunately, smaller ring sized (cyclopropyl or cyclobutyl) spiroindolines were inaccessible due to the instability of the corresponding starting material aryl-enamines. As an extension of the utility of this cyclisation, it was also found that aryl-enamine precursors aniline and keto-esters were also capable of undergoing an *in-situ* aryl-enamine formation/UV cyclisation. The applicability of this 'one pot' protocol was only limited by the relatively slow condensation step to access aryl-enamines.

*Table 5.3 UV-photocyclisation of aryl-enamines **429**-**440** to 2-carboxylspiroindolines **441**-**452**.*

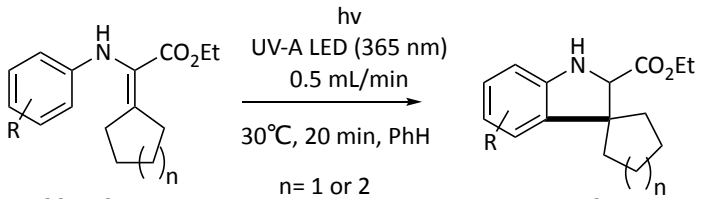

429-**440** **441**-**452**

Product[a]; Yield (%)		
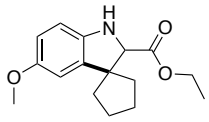	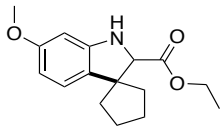	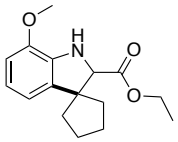
441 (40%)	**442** (43%)	**443** (61%)
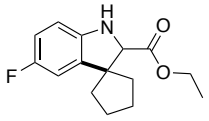	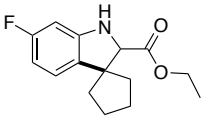	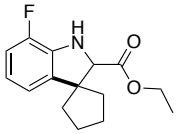
444 (79%)	**445** (70%)	**446** (69%)
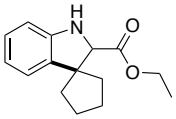	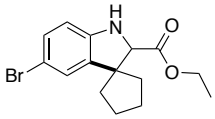	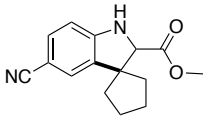
447 (82%)	**448** (76%)	**449** (68%)
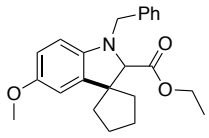	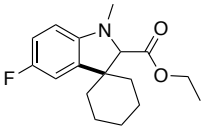	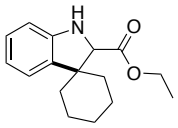
450 (51%)	**451** (88%)	**452** (45%)

[a] Flow photo reactor fitted with a 10 mL reaction coil and an inserted UV LED 365 nm. 0.5 mL/min flow rate. Reactor temperature 30°C. Solvent: PhH.

5.3 Conclusions and future work

The research carried out and described in this chapter was conducted at Vertex Pharmaceutical laboratories (Boston, USA) and was the output of a four-month PhD internship at the company. A 20th century report[317] of a UV-A mediated photocyclisation of aryl-enamines to spiroindolines was explored within the context of flow chemistry revealing unique opportunities for the

exploration of the reaction scope. Having reasonably explored the scope of the reaction using optimised conditions with colleagues at Vertex Pharmaceuticals, efforts were then applied towards the application of the method in a formal synthesis of (±)-horsfiline by the author. Through careful synthetic design a route towards intermediate **425** was developed which enabled the use of the aforementioned UV-mediated photocyclisation in flow, furnishing spiroindoline **426**. Commensurate with previous unpublished observations, an oxidative decarboxylation of spiroindoline **426** to form spiro-oxindole **427** was carried out under aerobic conditions using UV-A irradiation and LiOH treatment. This novel oxidative decarboxylation allowed for the formal intercept of a previously described route towards horsfiline **409**[327], reducing the overall synthetic step count from 16 linear steps to 5 steps. Future work involves the application of this photocyclisation in flow to other natural product syntheses and the detailed study of the oxidative decarboxylation of 2-carboxyester spiroindolines to spiro-oxindoles. A research article has been prepared for submission based on the findings of this chapter and will be submitted for publication.

6. Research conclusions and future plans

6.1 PCAF/GCN5 and *Pf*GCN5 Inhibition

The synthetic medicinal chemistry described in chapter 2 culminated in the discovery and the characterisation of the first reported chemical probe for the bromodomain containing proteins PCAF and GCN5. The probe, *L*-Moses, represents a useful tool molecule to dissect the roles of PCAF and GCN5 in their associated diseases, with particular attention to the contribution of the BRD in overall function and pathology. There remains a significant number of biological experiments that are available for inquiry using our probe- each one leading to individual research projects and potentially the subject of multiple future publications;

- Evaluation of PCAF/GCN5 BRD inhibition on acetylase activity on histone and non-histone substrates.
- Evaluation of PCAF/GCN5 BRD inhibition in relevant models of neuroinflammation and cancers.
- Evaluation of PCAF/GCN5 BRD inhibition on the onset and progression of HIV-1 infection and latency.

Additionally, in line with the observed activity of *L*-Moses against *Pf*GCN5, it is hoped that researchers in the anti-malarial research community carry out pertinent cellular experiments with our tool compound to explore the relevance of *Pf*GCN5 BRD in the life cycle of *Pf*.

6.2 PARP14 MD Inhibition

Efforts are described in chapter 3 to develop a previously reported allosteric inhibitor of the second macrodomain (MD2) of PARP14. After collaborative SAR studies with colleagues at Ludwig-Maximillans University (Munich) an improved sub-μM inhibitor is reported.

There are significant improvements that can be made to the lead molecule **197**, including improvements in potency, measurements of cell target engagement and improvements to physico-chemical properties. In addition to this, studies of how PARP14 MD2 inhibition might affect the function of other PARP14 domains is still unknown. However, the current lead molecule **197** represents a useful tool compound to explore PARP14 MD2 function in DNA damage repair and cancer cell proliferation for which full length PARP14 has been implicated in.

6.3 ENL/Af9 YD Inhibition

Chapter 4 of this thesis reports on SAR studies of an initial hit compound **206** for the YEATS domains of ENL and Af9 which was uncovered from a medium throughput biochemical screen. Extensive synthetic studies, biochemical, biophysical and cellular experiments were carried out leading to the identification of a series of potent, selective and cell active ENL/Af9 YD inhibitors.

Surprisingly it was found that when the lead molecule **328** was profiled for anti-cancer activity in the NCI-60 panel and separately against leukemic cell lines, no significant anti-proliferative effects were observed. These observations are discordant to the genetic studies reported in recent times linking ENL YD with the progression of AML.[252,253] A recent report[265] may explain the discrepancy between previous studies and our findings. However, the discrepancy may underscore the complexity of epigenetic processes and highlight the disconnect between studies using siRNA or CRISPR-Cas9 and conventional small molecule inhibition. Indeed, our probe molecule identified is a dual ENL/Af9 YD chemical probe and to date, there have not been any genetic manipulation studies examining phenotypes conferred when both ENL and Af9 are modulated simultaneously. Nonetheless, we do hope that our probe molecule can equip epigenetic researchers with a valuable tool in validating ENL/Af9 YDs for drug discovery in the context of conventional small molecule inhibition.

6.4 Formal synthesis of horsfiline

The final chapter of this thesis focusses on synthetic methodology studies utilising a UV-A promoted photocyclisation of aryl-enamines to spiroindolines. Building on seminal work in the 1980s by Schultz[317] an increased understanding about the scope of this reaction was carried out. It was then observed that carrying out this UV cyclisation under flow conditions conferred significant benefit to scope and reactivity of the reaction, A demonstration of the utility of the reaction was highlighted in a shortened formal synthesis of alkaloid natural product (±)-horsfiline conducted by the author in an expedient amount of time. This segment of doctoral research describes a significant part of the training as a synthetic chemist underscoring the work carried out in this DPhil thesis. It required intensive synthetic problem solving in a short period of time (15 weeks) in order to complete a formal synthesis route towards a natural product.

6.5. Concluding remarks

The research reported in previous chapters was largely carried out within the field of epigenetic research. It is hoped that the chemical probes and inhibitors discovered within this period of doctoral training will equip researchers to validate their cognate biological targets with improved confidence. Indeed, some of the work described in chapter 2 has already been translated into real world commercial value.[307] Moreover, the compounds reported in this thesis may serve as chemical starting points for medicinal chemistry campaigns which may then feature as motifs within the structures of future drug molecules.

7. Bibliography and Appendices

7.1 Appendix

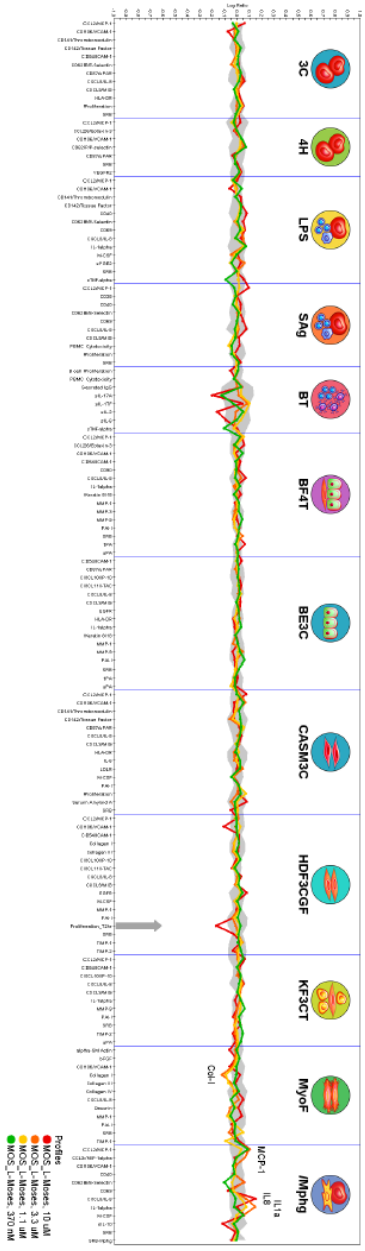

Appendix Figure 1. BioMAP Diversity PLUS panel screening of L-Moses

7.2 Bibliography

[1] P. J. Carter, G. A. Lazar, *Nat. Rev. Drug Discov.* **2017**, *17*, 197.

[2] K. Fosgerau, T. Hoffmann, *Drug Discov. Today* **2015**, *20*, 122–128.

[3] A. Beck, L. Goetsch, C. Dumontet, N. Corvaïa, *Nat. Rev. Drug Discov.* **2017**, *16*, 315.

[4] P. Agarwal, C. R. Bertozzi, *Bioconjugate Chem.* **2015**, *26*, 176–192.

[5] R. W. Carthew, E. J. Sontheimer, *Cell* **2009**, *136*, 642–655.

[6] M. Ghildiyal, P. D. Zamore, *Nat. Rev. Genet.* **2009**, *10*, 94–108.

[7] A. Reynolds, D. Leake, Q. Boese, S. Scaringe, W. S. Marshall, A. Khvorova, *Nat. Biotechnol.* **2004**, *22*, 326–330.

[8] M. T. McManus, P. A. Sharp, *Nat. Rev. Genet.* **2002**, *3*, 737–747.

[9] K. A. Whitehead, R. Langer, D. G. Anderson, *Nat. Rev. Drug Discov.* **2009**, *8*, 129–138.

[10] J. Shi, E. Wang, J. P. Milazzo, Z. Wang, J. B. Kinney, C. R. Vakoc, *Nat. Biotechnol.* **2015**, *33*, 661–667.

[11] N. Kolli, M. Lu, P. Maiti, J. Rossignol, G. L. Dunbar, *Neurochem. Int.* **2018**, *112*, 187–196.

[12] J. A. Doudna, E. Charpentier, *Science* **2014**, *346*, 1258096–1258096.

[13] J. G. Doench, *Nat. Rev. Genet.* **2018**, *19*, 67–80.

[14] R. Ferreira, F. David, J. Nielsen, *J. Ind. Microbiol. Biotechnol.* **2018**, Ahead of Print.

[15] D. C. Swinney, J. Anthony, *Nat. Rev. Drug Discov.* **2011**, *10*, 507–519.

[16] C. H. Arrowsmith, J. E. Audia, C. Austin, J. Baell, J. Bennett, J. Blagg, C. Bountra, P. E. Brennan, P. J. Brown, M. E. Bunnage, et al., *Nat. Chem. Biol.* **2015**, *11*, 536–541.

[17] J.-M. Lecerf, T. L. Shirley, Q. Zhu, A. Kazantsev, P. Amersdorfer, D. E. Housman, A. Messer, J. S. Huston, *Proc. Natl. Acad. Sci. U S A* **2001**, *98*, 4764–4769.

[18] A. M. Mhashilkar, J. Bagley, S. Y. Chen, A. M. Sziilvay, D. G. Helland, W. A. Marasco, *EMBO J.* **1995**, *14*, 1542–1551.

[19] S. L. Schreiber, *Science* **2000**, *287*, 1964–1969.

[20] J. Lamb, E. D. Crawford, D. Peck, J. W. Modell, I. C. Blat, M. J. Wrobel, J. Lerner, J.-P. Brunet, A. Subramanian, K. N. Ross, et al., *Science* **2006**, *313*, 1929–1935.

[21] K. H. Bleicher, H.-J. Boehm, K. Mueller, A. I. Alanine, *Nat. Rev. Drug Discov.* **2003**, *2*, 369–378.

[22] IFPMA, "The Pharmaceutical Industry and Global Health: Facts and Figures 2017," can be found under https://www.ifpma.org/wp-content/uploads/2017/02/IFPMA-Facts-And-Figures-2017.pdf, **2018**.

[23] Z. Wang, M. Gerstein, M. Snyder, *Nat. Rev. Genet.* **2009**, *10*, 57–63.

[24] U. Rix, G. Superti-Furga, *Nat. Chem. Biol.* **2009**, *5*, 616–624.

[25] R. Aebersold, M. Mann, *Nature* **2003**, *422*, 198–207.

[26] R. Aebersold, D. R. Goodlett, *Chem. Rev.* **2001**, *101*, 269–296.

[27] M. E. Bunnage, E. L. P. Chekler, L. H. Jones, *Nat. Chem. Biol.* **2013**, *9*, 195–199.

[28] "SGC Chemical Probes," can be found under http://www.thesgc.org/chemical-probes, **2018**.

[29] "Chemical Probes Portal," can be found under http://www.chemicalprobes.org, **2018**.

[30] J. Blagg, P. Workman, *Cancer Cell* **2017**, *32*, 9–25.

[31] S. C. R. Elgin, S. I. S. Grewal, *Curr. Biol.* **2003**, *13*, R895–R898.

[32] R. Lister, M. Pelizzola, R. H. Dowen, R. D. Hawkins, G. Hon, J. Tonti-Filippini, J. R. Nery, L. Lee, Z. Ye, Q.-M. Ngo, et al., *Nature* **2009**, *462*, 315–322.

[33] J. Chen, W. A. Weiss, *Oncogene* **2015**, *34*, 1–14.

[34] C. P. Ponting, P. L. Oliver, W. Reik, *Cell* **2009**, *136*, 629–641.

[35] J. L. Rinn, M. Kertesz, J. K. Wang, S. L. Squazzo, X. Xu, S. A. Brugmann, L. H. Goodnough, J. A. Helms, P. J. Farnham, E. Segal, et al., *Cell* **2007**, *129*, 1311–1323.

[36] J. McGrath, P. Trojer, *Pharmacol. Ther.* **2015**, *150*, 1–22.

[37] P. Filippakopoulos, S. Knapp, *Nat. Rev. Drug. Discov.* **2014**, *13*, 337–356.

[38] C. H. Waddington, *Endeavour* **1942**, *1*, 18–20.

[39] A. D. Russo, V. E. A., Martienssen, R. A., Riggs, *Epigenetic Mechanisms of Gene Regulation*, **1996**.

[40] T. C. Roloff, U. A. Nuber, *Eur. J. Cell Biol.* **2005**, *84*, 123–135.

[41] S. L. Berger, T. Kouzarides, R. Shiekhattar, A. Shilatifard, *Genes Dev.* **2009**, *23*, 781–783.

[42] K. J. Falkenberg, R. W. Johnstone, *Nat. Rev. Drug Discov.* **2014**, *13*, 673–691.

[43] S. Ackloo, P. J. Brown, S. Muller, *Epigenetics* **2017**, 1–23.

[44] S. J. Cullen, S. Ponnappan, U. Ponnappan, *Mol. Immunol.* **2009**, *47*, 600–605.

[45] P. Scaffidi, T. Misteli, M. E. Bianchi, *Nature* **2002**, *418*, 191–195.

[46] E. Nicodeme, K. L. Jeffrey, U. Schaefer, S. Beinke, S. Dewell, C. Chung, R. Chandwani, I. Marazzi, P. Wilson, H. Coste, et al., *Nature* **2010**, *468*, 1119–1123.

[47] M. K. Shanmugam, G. Sethi, *Subcell. Biochem.* **2013**, *61*, 627–657.

[48] N. H. Theodoulou, N. C. O. Tomkinson, R. K. Prinjha, P. G. Humphreys, *Curr. Opin. Chem. Biol.* **2016**, *33*, 58–66.

[49] M. Esteller, *N. Engl. J. Med.* **2008**, *358*, 1148–1159.

[50] V. Jeffers, C. Yang, S. Huang, W. J. Sullivan Jr., *Microbiol. Mol. Biol. Rev.* **2017**, *81*.

[51] Y. Revilla, A. G. Granja, *Crit. Rev. Immunol.* **2009**, *29*, 131–154.

[52] J.-S. Lee, E. Smith, A. Shilatifard, *Cell* **2010**, *142*, 682–685.

[53] S. L. Berger, *Nature* **2007**, *447*, 407–412.

[54] S. Messner, M. O. Hottiger, *Trends Cell Biol.* **2011**, *21*, 534–542.

[55] A. J. Ruthenburg, H. Li, D. J. Patel, C. D. Allis, *Nat. Rev. Mol. Cell Biol.* **2007**, *8*, 983–994.

[56] T. D. Heightman, *Curr. Chem. Genomics* **2011**, *5*, 62–71.

[57] A. Barski, S. Cuddapah, K. Cui, T.-Y. Roh, D. E. Schones, Z. Wang, G. Wei, I. Chepelev, K. Zhao, *Cell* **2007**, *129*, 823–837.

[58] C. Choudhary, B. T. Weinert, Y. Nishida, E. Verdin, M. Mann, *Nat. Rev. Mol. Cell Biol.* **2014**, *15*, 536–550.

[59] SGC, "Epigenetic Proteins and their Function in Lysine Modifications," can be found under https://www.thesgc.org/chemical-probes/epigenetics, **n.d.**

[60] M. A. Dawson, T. Kouzarides, B. J. P. Huntly, *N. Engl. J. Med.* **2012**, *367*, 647–657.

[61] W. Liu, Q. Ma, K. Wong, W. Li, K. Ohgi, J. Zhang, A. K. Aggarwal, M. G. Rosenfeld, *Cell* **2013**, *155*, 1581–1595.

[62] H. M. Chan, T. N. B. La, *J. Cell. Sci.* **2001**, *114*, 2363–2373.

[63] E. Kalkhoven, *Biochem. Pharmacol.* **2004**, *68*, 1145–1155.

[64] V. Di Cerbo, R. Schneider, *Brief. Funct. Genomics* **2013**, *12*, 231–243.

[65] M. Grunstein, *Nature* **1997**, *389*, 349–352.

[66] T. Kouzarides, *EMBO J.* **2000**, *19*, 1176–1179.

[67] D. E. Sterner, S. L. Berger, *Microbiol. Mol. Biol. Rev.* **2000**, *64*, 435–459.

[68] J. J. McClure, X. Li, C. J. Chou, *Adv. Cancer Res.* **2018**, *138*, 183–211.

[69] T. Kodadek, *Biochemistry* **2018**, *57*, 899–900.

[70] L. M. Lasko, C. G. Jakob, R. P. Edalji, W. Qiu, D. Montgomery, E. L. Digiammarino, T. M. Hansen, R. M. Risi, R. Frey, V. Manaves, et al., *Nature* **2017**, *550*, 128–132.

[71] M. R. Michaelides, A. Kluge, M. Patane, J. H. Van Drie, C. Wang, T. M. Hansen, R. M. Risi, R. Mantei, C. Hertel, K. Karukurichi, et al., *ACS Med. Chem. Lett.* **2018**, *9*, 28–33.

[72] S. Müller, S. Knapp, *Med. Chem. Commun.* **2014**, *5*, 288–296.

[73] L. R. Vidler, N. Brown, S. Knapp, S. Hoelder, *J. Med. Chem.* **2012**, *55*, 7346–7359.

[74] P. Filippakopoulos, J. Qi, S. Picaud, Y. Shen, W. B. Smith, O. Fedorov, E. M. Morse, T. Keates, T. T. Hickman, I. Felletar, et al., *Nature* **2010**, *468*, 1067–1073.

[75] W. Palmer, P. Jones, G. Liu, A. Petrocchi, N. Reyna, G. Subrumanian, J. Theroff, A. Yau, *Bromodomain Inhibitors for Treating Disease*, **2016**, WO2016033416A1.

[76] M. Moustakim, P. G. K. Clark, D. A. Hay, D. J. Dixon, P. E. Brennan, *Med. Chem. Commun.* **2016**, *7*, 2246–2264.

[77] N. H. Theodoulou, N. C. O. Tomkinson, R. K. Prinjha, P. G. Humphreys, *ChemMedChem* **2016**, *11*, 477–487.

[78] G. Zhang, S. G. Smith, M.-M. Zhou, *Chem. Rev.* **2015**, *115*, 11625–11668.

[79] M.-M. Zhou, G. Gerona-Navarro, Y. Rodriguez-Fernandez, P. Casaccia, *Small Molecule Transcription Modulators of Bromodomains*, **2015**, WO2015184257A2.

[80] F. A. Romero, A. M. Taylor, T. D. Crawford, V. Tsui, A. Cote, S. Magnuson, *J. Med. Chem.* **2016**, *59*, 1271–1298.

[81] P. Filippakopoulos, S. Picaud, M. Mangos, T. Keates, J.-P. Lambert, D. Barsyte-Lovejoy, I. Felletar, R. Volkmer, S. Muller, T. Pawson, et al., *Cell* **2012**, *149*, 214–231.

[82] S. Muller, P. Filippakopoulos, S. Knapp, *Expert Rev. Mol. Med.* **2011**, *13*, e29.

[83] A. Richters, A. N. Koehler, *Curr. Med. Chem.* **2017**, *24*, 4121–4150.

[84] Z. Nagy, L. Tora, *Oncogene* **2007**, *26*, 5341–5357.

[85] C. Dhalluin, J. E. Carlson, L. Zeng, C. He, A. K. Aggarwal, M. M. Zhou, *Nature* **1999**, *399*, 491–496.

[86] L. Zeng, Q. Zhang, G. Gerona-Navarro, N. Moshkina, M.-M. Zhou, *Structure* **2008**, *16*, 643–652.

[87] T. Yamauchi, J. Yamauchi, T. Kuwata, T. Tamura, T. Yamashita, N. Bae, H. Westphal, K. Ozato, Y. Nakatani, *Proc. Natl. Acad. Sci. U S A* **2000**, *97*, 11303–11306.

[88] H. M. Phan, A. W. Xu, C. Coco, G. Srajer, S. Wyszomierski, Y. A. Evrard, R. Eckner, S. Y. R. Dent, *Dev. Dyn.* **2005**, *233*, 1337–1347.

[89] L. Kruidenier, K. Lee, D. F. Tough, D. M. Wilson, *Inhibitors of Bromodomain-Containing Protein PCAF for the Treatment of Autoimmune and Inflammatory Diseases or for the*

Treatment of Cancer, **2014**, WO2014037362A1.

[90] B. K. Albrecht, A. Cote, T. Crawford, M. Duplessis, A. C. Good, Y. Leblanc, S. Magnuson, C. G. Nasveschuk, R. Pastor, F. A. Romero, et al., *Preparation of 1,2,4-Triazine-3,5(2H,4H)-Diones as Inhibitors of PCAF for Treating Cancer and Other PCAF-Mediated Disorders*, **2016**, WO2016036873A1.

[91] B. K. Albrecht, A. Cote, T. Crawford, M. Duplessis, A. C. Good, Y. Leblanc, S. Magnuson, C. G. Nasveschuk, R. Pastor, F. A. Romero, et al., *Preparation of Phthalazine Derivatives as PCAF and GCN5 Inhibitors for Use in the Treatment of Cancer*, **2016**, WO2016036954A1.

[92] S. Mujtaba, Y. He, L. Zeng, A. Farooq, J. E. Carlson, M. Ott, E. Verdin, M.-M. Zhou, *Mol. Cell* **2002**, *9*, 575–586.

[93] V. C. Quy, S. Pantano, G. Rossetti, M. Giacca, P. Carloni, *Biology* **2012**, *1*, 277–296.

[94] Q. Wang, R. Wang, B. Zhang, S. Zhang, Y. Zheng, Z. Wang, *MedChemComm* **2013**, *4*, 737–740.

[95] A. Dorr, V. Kiermer, A. Pedal, H.-R. Rackwitz, P. Henklein, U. Schubert, M.-M. Zhou, E. Verdin, M. Ott, *EMBO J.* **2002**, *21*, 2715–2723.

[96] T. Qu, F. Chen, J. Wang, Y. Zhang, M. Cheng, W. Sun, Y. Shen, Y. Zhang, *BMC Cancer* **2018**, *18*, 27.

[97] Y. Sunami, M. Araki, S. Kan, A. Ito, Y. Hironaka, M. Imai, S. Morishita, A. Ohsaka, N. Komatsu, *J. Biol. Chem.* **2017**, *292*, 2815–2829.

[98] H. J. Fei, L. D. Zu, J. Wu, X. S. Jiang, J. L. Wang, Y. E. Chin, G. H. Fu, *Am. J. Cancer Res.* **2016**, *6*, 2772–2786.

[99] Q. Li, Z. Liu, M. Xu, Y. Xue, B. Yao, C. Dou, Y. Jia, Y. Wang, K. Tu, X. Zheng, et al., *Cancer*

Lett. **2016**, *375*, 190–198.

[100] J. Wan, W. Xu, J. Zhan, J. Ma, X. Li, Y. Xie, J. Wang, W. G. Zhu, J. Luo, H. Zhang, *Nucleic Acids Res.* **2016**, *44*, 10662–10675.

[101] G. S. Watts, M. M. Oshiro, D. J. Junk, R. J. Wozniak, S. J. Watterson, F. E. Domann, B. W. Futscher, *Neoplasia* **2004**, *6*, 187–194.

[102] G. Xenaki, T. Ontikatze, R. Rajendran, I. J. Stratford, C. Dive, M. Krstic-Demonacos, C. Demonacos, *Oncogene* **2008**, *27*, 5785–5796.

[103] Y. Mizuguchi, S. Specht, J. G. Lunz, K. Isse, N. Corbitt, T. Takizawa, A. J. Demetris, *PLoS One* **2012**, *7*, e32449.

[104] K. Okumura, M. Mendoza, R. M. Bachoo, R. A. DePinho, W. K. Cavenee, F. B. Furnari, *J. Biol. Chem.* **2006**, *281*, 26562–26568.

[105] L. K. Linares, R. Kiernan, R. Triboulet, C. Chable-Bessia, D. Latreille, O. Cuvier, M. Lacroix, L. Le Cam, O. Coux, M. Benkirane, *Nat. Cell Biol.* **2007**, *9*, 331–338.

[106] J. E. Morgan, S. F. Greer, *Int. J. Cell Biol.* **2017**, *2017*, 11.

[107] R. L. Schiltz, Y. Nakatani, *Biochim. Biophys. Acta - Rev. Cancer* **2000**, *1470*, M37–M53.

[108] R. Kiernan, V. Brès, R. W. M. Ng, M. P. Coudart, S. El Messaoudi, C. Sardet, D. Y. Jin, S. Emiliani, M. Benkirane, *J. Biol. Chem.* **2003**, *278*, 2758–2766.

[109] R. C. M. de Jong, M. M. Ewing, M. R. de Vries, J. C. Karper, A. J. N. M. Bastiaansen, H. A. B. Peters, F. Baghana, P. J. van den Elsen, C. Gongora, J. W. Jukema, et al., *PLoS One* **2017**, *12*, e0185820.

[110] L. Yu, Z. Li, M. Fang, Y. Xu, *Biochim. Biophys. Acta - Gene Regul. Mech.* **2017**, *1860*, 839–847.

[111] P. Zhang, Y. Liu, C. Jin, M. Zhang, L. Lv, X. Zhang, H. Liu, Y. Zhou, *Stem Cells* **2016**, *34*, 2332–2341.

[112] F. Duclot, J. Meffre, C. Jacquet, C. Gongora, T. Maurice, *Neuroscience* **2010**, *167*, 850–863.

[113] T. Maurice, F. Duclot, J. Meunier, G. Naert, L. Givalois, J. Meffre, A. Célérier, C. Jacquet, V. Copois, N. Mechti, et al., *Neuropsychopharmacology* **2008**, *33*, 1584–1602.

[114] K. A. Mitchnick, S. D. Creighton, J. M. Cloke, M. Wolter, O. Zaika, B. Christen, M. Van Tiggelen, B. E. Kalisch, B. D. Winters, *Genes, Brain Behav.* **2016**, *15*, 542–557.

[115] Y. Nakatani, *Structure* **2002**, *10*, 443–4.

[116] W. Liu, Y. Xie, J. Ma, X. Luo, P. Nie, Z. Zuo, U. Lahrmann, Q. Zhao, Y. Zheng, Y. Zhao, et al., *Bioinformatics* **2015**, *31*, 3359–3361.

[117] Y. Wang, Y. R. Guo, K. Liu, Z. Yin, R. Liu, Y. Xia, L. Tan, P. Yang, J. H. Lee, X. J. Li, et al., *Nature* **2017**, *552*, 273–277.

[118] T. Li, L. Su, Y. Lei, X. Liu, Y. Zhang, X. Liu, *J. Biol. Chem.* **2015**, *290*, 11108–11118.

[119] L. Li, B. Liu, X. Zhang, L. Ye, *Biochem. Biophys. Res. Commun.* **2015**, *458*, 720–725.

[120] K. Liu, Q. Zhang, H. Lan, L. Wang, P. Mou, W. Shao, D. Liu, W. Yang, Z. Lin, Q. Lin, et al., *Int. J. Mol. Sci.* **2015**, *16*, 21897–21910.

[121] Y. W. Yin, H. J. Jin, W. Zhao, B. Gao, J. Fang, J. Wei, D. D. Zhang, J. Zhang, D. Fang, *Gene Expr.* **2015**, *16*, 187–196.

[122] M. Terreni, P. Valentini, V. Liverani, M. I. Gutierrez, C. Di Primio, A. Di Fenza, V. Tozzini, A. Allouch, A. Albanese, M. Giacca, et al., *Retrovirology* **2010**, *7*, 18.

[123] E. Col, C. Caron, D. Seigneurin-Berny, J. Gracia, A. Favier, S. Khochbin, *J. Biol. Chem.* **2001**,

276, 28179–28184.

[124] S. Salunkhe, S. V. Mishra, J. Nair, S. Ghosh, N. Choudhary, E. Kaur, S. Shah, K. Patkar, D. Anand, N. Khattry, et al., *Int. J. Cancer* **2018**, *142*, 2175–2185.

[125] T. Holmlund, M. J. Lindberg, D. Grander, A. E. Wallberg, *Leukemia* **2013**, *27*, 578–585.

[126] L. Chen, T. Wei, X. Si, Q. Wang, Y. Li, Y. Leng, A. Deng, J. Chen, G. Wang, S. Zhu, et al., *J. Biol. Chem.* **2013**, *288*, 14510–14521.

[127] L. Zhao, P. M. Loewenstein, M. Green, *Genes Cancer* **2017**, *8*, 752–761.

[128] B. Gao, Q. Kong, Y. Zhang, C. Yun, S. Y. R. Dent, J. Song, D. D. Zhang, Y. Wang, X. Li, D. Fang, *J. Immunol.* **2017**, *198*, 3927–3938.

[129] H. Kikuchi, F. Kuribayashi, H. Mimuro, S. Imajoh-Ohmi, M. Nakayama, Y. Takami, H. Nishitoh, T. Nakayama, *Biochem. Biophys. Res. Commun.* **2015**, *463*, 870–875.

[130] H. Jing, X. Su, B. Gao, Y. Shuai, J. Chen, Z. Deng, L. Liao, Y. Jin, *Cell Death Dis.* **2018**, *9*, 176.

[131] V. Martínez-Cerdeño, J. M. Lemen, V. Chan, A. Wey, W. Lin, S. R. Dent, P. S. Knoepfler, *PLoS One* **2012**, *7*, e39456.

[132] Y. C. Chen, J. R. Gatchel, R. W. Lewis, C. A. Mao, P. A. Grant, H. Y. Zoghbi, S. Y. R. Dent, *Hum. Mol. Genet.* **2012**, *21*, 394–405.

[133] D. Hatakeyama, M. Shoji, S. Yamayoshi, R. Yoh, N. Ohmi, S. Takenaka, A. Saitoh, Y. Arakaki, A. Masuda, T. Komatsu, et al., *J. Biol. Chem.* **2018**, *293*, 7126–7138.

[134] H. Kikuchi, Y. Takami, T. Nakayama, *Gene* **2005**, *347*, 83–97.

[135] M. Zhao, R. Geng, X. Guo, R. Yuan, X. Zhou, Y. Zhong, Y. Huo, M. Zhou, Q. Shen, Y. Li, et al., *Cell Rep.* **2017**, *20*, 1997–2009.

[136] A.-C. Gaupel, T. J. Begley, M. Tenniswood, *J. Cell. Biochem.* **2015**, *116*, 1982–1992.

[137] J. M. Gajer, S. D. Furdas, A. Gründer, M. Gothwal, U. Heinicke, K. Keller, F. Colland, S. Fulda, H. L. Pahl, I. Fichtner, et al., *Oncogenesis* **2015**, *4*, e137.

[138] E. A. Koutsogiannouli, N. Wagner, C. Hader, M. Pinkerneil, M. J. Hoffmann, W. A. Schulz, *Int. J. Mol. Sci.* **2017**, *18*, 1449.

[139] M. Fournier, M. Orpinell, C. Grauffel, E. Scheer, J. M. Garnier, T. Ye, V. Chavant, M. Joint, F. Esashi, A. Dejaegere, et al., *Nat. Commun.* **2016**, *7*, 13227.

[140] M. Jeitany, D. Bakhos-Douaihy, D. C. Silvestre, J. R. Pineda, N. Ugolin, A. Moussa, L. R. Gauthier, D. Busso, M.-P. Junier, H. Chneiweiss, et al., *Oncotarget* **2017**, *8*, 26269–26280.

[141] C. Armas-Pineda, F. Arenas-Huertero, M. Pérezpeñia-Diazconti, F. Chico-Ponce de León, G. Sosa-Sáinz, P. Lezama, F. Recillas-Targa, *J. Exp. Clin. cancer Res.* **2007**, *26*, 269–276.

[142] A. Saraf, S. Cervantes, E. M. Bunnik, N. Ponts, M. E. Sardiu, D.-W. D. Chung, J. Prudhomme, J. M. Varberg, Z. Wen, M. P. Washburn, et al., *J. Proteome Res.* **2016**, *15*, 2787–2801.

[143] W. Robert McMaster, C. J. Morrison, M. S. Kobor, *Trends Parasitol.* **2016**, *32*, 515–521.

[144] G. F. A. Picchi, V. Zulkievicz, M. A. Krieger, N. T. Zanchin, S. Goldenberg, L. M. F. de Godoy, *J. Proteome Res.* **2017**, *16*, 1167–1179.

[145] G. Batugedara, X. M. Lu, E. M. Bunnik, K. G. Le Roch, *Trends Parasitol.* **2017**, *33*, 364–377.

[146] J. Miao, Q. Fan, L. Cui, J. Li, J. Li, L. Cui, *Gene* **2006**, *369*, 53–65.

[147] Q. Fan, L. An, L. Cui, *Eukaryot. Cell* **2004**, *3*, 264–276.

[148] M. J. Chua, D. Robaa, T. S. Skinner-Adams, W. Sippl, K. T. Andrews, *Int. J. Parasitol. Drugs Drug Resist.* **2018**, *8*, 189–193.

[149] O. Fedorov, H. Lingard, C. Wells, O. P. Monteiro, S. Picaud, T. Keates, C. Yapp, M. Philpott, S. J. Martin, I. Felletar, et al., *J. Med. Chem.* **2014**, *57*, 462–476.

[150] J. M. Garnier, P. P. Sharp, C. J. Burns, *Expert. Opin. Ther. Pat.* **2014**, *24*, 185–199.

[151] S. G. Smith, M.-M. Zhou, *ACS Chem. Biol.* **2016**, *11*, 598–608.

[152] M. Tanaka, J. M. Roberts, H.-S. Seo, A. Souza, J. Paulk, T. G. Scott, S. L. DeAngelo, S. Dhe-Paganon, J. E. Bradner, *Nat. Chem. Biol.* **2016**, *12*, 1089–1096.

[153] F. A. Romero, A. M. Taylor, T. D. Crawford, V. Tsui, A. Côté, S. Magnuson, *J. Med. Chem.* **2016**, *59*, 1271–1298.

[154] D. Owen, *Nat. Chem. Biol.* **2016**, *12*, 991–992.

[155] O. Mirguet, Y. Lamotte, F. Donche, J. Toum, F. Gellibert, A. Bouillot, R. Gosmini, V. L. Nguyen, D. Delannée, J. Seal, et al., *Bioorganic Med. Chem. Lett.* **2012**, *22*, 2963–2967.

[156] K. Raina, J. Lu, Y. Qian, M. Altieri, D. Gordon, A. M. K. Rossi, J. Wang, X. Chen, H. Dong, K. Siu, et al., *Proc. Natl. Acad. Sci. U S A* **2016**, *113*, 7124–7129.

[157] G. Andrieu, A. C. Belkina, G. V Denis, *Drug Discov. Today Technol.* **2016**, *19*, 45–50.

[158] J. Lovén, H. A. Hoke, C. Y. Lin, A. Lau, D. A. Orlando, C. R. Vakoc, J. E. Bradner, T. I. Lee, R. A. Young, *Cell* **2013**, *153*, 320–334.

[159] J. A. Mertz, A. R. Conery, B. M. Bryant, P. Sandy, S. Balasubramanian, D. A. Mele, L. Bergeron, R. J. Sims, *Proc. Natl. Acad. Sci. U S A* **2011**, *108*, 16669–16674.

[160] C. Galdeano, A. Ciulli, *Future Med. Chem.* **2016**, *8*, 1655–1680.

[161] SGC, "NVS-1," can be found under http://www.thesgc.org/chemical-probes/NVS-1, **2018**.

[162] D. A. Hay, O. Fedorov, S. Martin, D. C. Singleton, C. Tallant, C. Wells, S. Picaud, M.

Philpott, O. P. Monteiro, C. M. Rogers, et al., *J. Am. Chem. Soc.* **2014**, *136*, 9308–9319.

[163] T. A. Popp, C. Tallant, C. Rogers, O. Fedorov, P. E. Brennan, S. Müller, S. Knapp, F. Bracher, *J. Med. Chem.* **2016**, *59*, 8889–8912.

[164] A. Hammitzsch, C. Tallant, O. Fedorov, A. O'Mahony, P. E. Brennan, D. A. Hay, F. O. Martinez, M. H. Al-Mossawi, J. de Wit, M. Vecellio, et al., *Proc. Natl. Acad. Sci. U S A* **2015**, *112*, 10768–10773.

[165] R. C. Centore, A. R. Conery, K. Gascoigne, I. I. I. R. J. Sims, *Use of Cbp/Ep300 and Bet Inhibitors for Treatment of Cancer*, **2016**, WO2016044694A1.

[166] N. A. Pegg, D. M. A. Taddei, S. T. Onions, E. S. Y. Tse, R. J. Brown, D. K. Mycock, D. Cousin, A. Patel, *Isoxazolyl-Substituted Benzimidazoles as P300 and/or CBP Modulators and Their Preparation*, **2016**, WO2016170324A1.

[167] T. D. Crawford, F. A. Romero, K. W. Lai, V. Tsui, A. M. Taylor, G. de Leon Boenig, C. L. Noland, J. Murray, J. Ly, E. F. Choo, et al., *J. Med. Chem.* **2016**, *59*, 10549–10563.

[168] F. A. Romero, J. Murray, K. W. Lai, V. Tsui, B. K. Albrecht, L. An, M. H. Beresini, G. de Leon Boenig, S. M. Bronner, E. W. Chan, et al., *J. Med. Chem.* **2017**, *60*, 9162–9183.

[169] P. G. K. Clark, L. C. C. Vieira, C. Tallant, O. Fedorov, D. C. Singleton, C. M. Rogers, O. P. Monteiro, J. M. Bennett, R. Baronio, S. Müller, et al., *Angew. Chem. Int. Ed.* **2015**, *54*, 2621–6217.

[170] D. A. Hay, C. M. Rogers, O. Fedorov, C. Tallant, S. Martin, O. P. Monteiro, S. Muller, S. Knapp, C. J. Schofield, P. E. Brennan, *MedChemComm* **2015**, *6*, 1381–1386.

[171] N. H. Theodoulou, P. Bamborough, A. J. Bannister, I. Becher, R. A. Bit, K. H. Che, C.-W. Chung, A. Dittmann, G. Drewes, D. H. Drewry, et al., *J. Med. Chem.* **2015**, *59*, 1425–1439.

[172] SGC, “TP-472,” can be found under http://www.thesgc.org/chemical-probes/TP-472, **2018**.

[173] SGC, “BI-9564,” can be found under http://www.thesgc.org/chemical-probes/BI-9564, **2018**.

[174] L. J. Martin, M. Koegl, G. Bader, X.-L. Cockcroft, O. Fedorov, D. Fiegen, T. Gerstberger, M. H. Hofmann, A. F. Hohmann, D. Kessler, et al., *J. Med. Chem.* **2016**, *59*, 4462–4475.

[175] P. Bamborough, H. A. Barnett, I. Becher, M. J. Bird, C.-W. Chung, P. D. Craggs, E. H. Demont, H. Diallo, D. J. Fallon, L. J. Gordon, et al., *ACS Med. Chem. Lett.* **2016**, *7*, 552–557.

[176] E. H. Demont, P. Bamborough, C. Chung, P. D. Craggs, D. Fallon, L. J. Gordon, P. Grandi, C. I. Hobbs, J. Hussain, E. J. Jones, et al., *ACS Med. Chem. Lett.* **2014**, *5*, 1190–1195.

[177] W. S. Palmer, G. Poncet-Montange, G. Liu, A. Petrocchi, N. Reyna, G. Subramanian, J. Theroff, A. Yau, M. Kost-Alimova, J. P. Bardenhagen, et al., *J. Med. Chem.* **2016**, *59*, 1440–1454.

[178] J. Bennett, O. Fedorov, C. Tallant, O. Monteiro, J. Meier, V. Gamble, P. Savitsky, G. A. Nunez-Alonso, B. Haendler, C. Rogers, et al., *J. Med. Chem.* **2016**, *59*, 1642–1647.

[179] M. Y. Lubula, B. E. Eckenroth, S. Carlson, A. Poplawski, M. Chruszcz, K. C. Glass, *FEBS Lett.* **2014**, *588*, 3844–3854.

[180] SGC, “PFI-4,” can be found under http://www.thesgc.org/chemical-probes/PFI-4, **2018**.

[181] N. Igoe, E. D. Bayle, C. Tallant, O. Fedorov, J. C. Meier, P. Savitsky, C. Rogers, Y. Morias, S. Scholze, H. Boyd, et al., *J. Med. Chem.* **2017**, *60*, 6998–7011.

[182] P. Bamborough, C. Chung, E. H. Demont, R. C. Furze, A. J. Bannister, K. H. Che, H. Diallo, C.

Douault, P. Grandi, T. Kouzarides, et al., *Angew. Chem. Int. Ed.* **2016**, *55*, 11382–11386.

[183] P. Bamborough, C. Chung, R. C. Furze, P. Grandi, A.-M. Michon, R. J. Sheppard, H. Barnett, H. Diallo, D. P. Dixon, C. Douault, et al., *J. Med. Chem.* **2015**, *58*, 6151–6178.

[184] A. E. Fernández-Montalván, M. Berger, B. Kuropka, S. J. Koo, V. Badock, J. Weiske, V. Puetter, S. J. Holton, D. Stöckigt, A. Ter Laak, et al., *ACS Chem. Biol.* **2017**, *12*, 2730–2736.

[185] L. Drouin, S. McGrath, L. R. Vidler, A. Chaikuad, O. Monteiro, C. Tallant, M. Philpott, C. Rogers, O. Fedorov, M. Liu, et al., *J. Med. Chem.* **2015**, *58*, 2553–2559.

[186] P. Chen, A. Chaikuad, P. Bamborough, M. Bantscheff, C. Bountra, C. Chung, O. Fedorov, P. Grandi, D. Jung, R. Lesniak, et al., *J. Med. Chem.* **2016**, *59*, 1410–1424.

[187] T. D. Crawford, V. Tsui, E. M. Flynn, S. Wang, A. M. Taylor, A. Côté, J. E. Audia, M. H. Beresini, D. J. Burdick, R. Cummings, et al., *J. Med. Chem.* **2016**, *59*, 5391–5402.

[188] L. Bouché, C. D. Christ, S. Siegel, A. E. Fernández-Montalván, S. J. Holton, O. Fedorov, A. Ter Laak, T. Sugawara, D. Stöckigt, C. Tallant, et al., *J. Med. Chem.* **2017**, *60*, 4002–4022.

[189] B. S. Gerstenberger, J. D. Trzupek, C. Tallant, O. Fedorov, P. Filippakopoulos, P. E. Brennan, V. Fedele, S. Martin, S. Picaud, C. Rogers, et al., *J. Med. Chem.* **2016**, *59*, 4800–4811.

[190] B. Vangamudi, T. A. Paul, P. K. Shah, M. Kost-Alimova, L. Nottebaum, X. Shi, Y. Zhan, E. Leo, H. S. Mahadeshwar, A. Protopopov, et al., *Cancer Res.* **2015**, *75*, 3865–3878.

[191] Z. Cui, W. Cao, J. Li, X. Song, L. Mao, W. Chen, *PLoS One* **2013**, *8*, e63887.

[192] D. P. Bondeson, A. Mares, I. E. D. Smith, E. Ko, S. Campos, A. H. Miah, K. E. Mulholland, N. Routly, D. L. Buckley, J. L. Gustafson, et al., *Nat. Chem. Biol.* **2015**, *11*, 611–617.

[193] M. Toure, C. M. Crews, *Angew. Chem. Int. Ed.* **2016**, *55*, 1966–1973.

[194] D. Remillard, D. L. Buckley, J. Paulk, G. L. Brien, M. Sonnett, H. S. Seo, S. Dastjerdi, M. Wühr, S. Dhe-Paganon, S. A. Armstrong, et al., *Angew. Chem. Int. Ed.* **2017**, *56*, 5738–5743.

[195] L. N. Gechijian, D. L. Buckley, M. A. Lawlor, J. M. Reyes, J. Paulk, C. J. Ott, G. E. Winter, M. A. Erb, T. G. Scott, M. Xu, et al., *Nat. Chem. Biol.* **2018**, *14*, 1–8.

[196] J.-C. Amé, C. Spenlehauer, G. de Murcia, *BioEssays* **2004**, *26*, 882–893.

[197] B. A. Gibson, W. L. Kraus, *Nat. Rev. Mol. Cell Biol.* **2012**, *13*, 411–424.

[198] H. Kleine, E. Poreba, K. Lesniewicz, P. O. Hassa, M. O. Hottiger, D. W. Litchfield, B. H. Shilton, B. Lüscher, *Mol. Cell* **2008**, *32*, 57–69.

[199] M. O. Hottiger, P. O. Hassa, B. Lüscher, H. Schüler, F. Koch-Nolte, *Trends Biochem. Sci.* **2010**, *35*, 208–219.

[200] S. Laing, F. Koch-Nolte, F. Haag, F. Buck, *J. Proteomics* **2011**, *75*, 169–176.

[201] O. Leidecker, J. J. Bonfiglio, T. Colby, Q. Zhang, I. Atanassov, R. Zaja, L. Palazzo, A. Stockum, I. Ahel, I. Matic, *Nat. Chem. Biol.* **2016**, *12*, 998–1000.

[202] J. J. Bonfiglio, P. Fontana, Q. Zhang, T. Colby, I. Gibbs-Seymour, I. Atanassov, E. Bartlett, R. Zaja, I. Ahel, I. Matic, *Mol. Cell* **2017**, *65*, 932–940.e6.

[203] L. J. McDonald, J. Moss, *Mol. Cell. Biochem.* **1994**, *138*, 221–226.

[204] J. A. Smith, L. A. Stocken, *Biochem. Soc. Trans.* **1974**, *2*, 95–96.

[205] D. R. Manning, B. A. Fraser, R. A. Kahn, A. G. Gilman, *J. Biol. Chem.* **1984**, *259*, 749–56.

[206] C. J. Lord, A. Ashworth, *Science* **2017**, *355*, 1152–1158.

[207] M. Posavec, G. Timinszky, M. Buschbeck, *Cell. Mol. Life Sci.* **2013**, *70*, 1509–1524.

[208] T. Yamashita, J. Ji, A. Budhu, M. Forgues, W. Yang, H.-Y. Wang, H. Jia, Q. Ye, L.-X. Qin, E. Wauthier, et al., *Gastroenterology* **2009**, *136*, 1012–1024.

[209] S. B. Bachmann, S. C. Frommel, R. Camicia, H. C. Winkler, R. Santoro, P. O. Hassa, *Mol. Cancer* **2014**, *13*, 125.

[210] V. Iansante, P. M. Choy, S. W. Fung, Y. Liu, J.-G. Chai, J. Dyson, A. Del Rio, C. D'Santos, R. Williams, S. Chokshi, et al., *Nat. Commun.* **2015**, *6*, 7882.

[211] M. Mushtaq, S. Darekar, G. Klein, E. Kashuba, *PLoS One* **2015**, *10*, e0136142.

[212] C. M. Nicolae, E. R. Aho, K. N. Choe, D. Constantin, H. J. Hu, D. Lee, K. Myung, G. L. Moldovan, *Nucleic Acids Res.* **2015**, *43*, 3143–3153.

[213] S. H. Cho, A. Raybuck, M. Wei, J. Erickson, K. T. Nam, R. G. Cox, A. Trochtenberg, J. W. Thomas, J. Williams, M. Boothby, *J. Immunol.* **2013**, *191*, 3169–3178.

[214] P. Mehrotra, J. P. Riley, R. Patel, F. Li, L. Voss, S. Goenka, *J. Biol. Chem.* **2011**, *286*, 1767–1776.

[215] P. Mehrotra, P. Krishnamurthy, J. Sun, S. Goenka, M. H. Kaplan, *Immunology* **2015**, *146*, 537–546.

[216] H. Iwata, C. Goettsch, A. Sharma, P. Ricchiuto, W. W. Bin Goh, A. Halu, I. Yamada, H. Yoshida, T. Hara, M. Wei, et al., *Nat. Commun.* **2016**, *7*, 12849.

[217] P. Krishnamurthy, S. Da-Silva-Arnold, M. J. Turner, J. B. Travers, M. H. Kaplan, *Immunology* **2017**, *152*, 451–461.

[218] A. Barbarulo, V. Iansante, A. Chaidos, K. Naresh, A. Rahemtulla, G. Franzoso, A. Karadimitris, D. O. Haskard, S. Papa, C. Bubici, *Oncogene* **2013**, *32*, 4231–4242.

[219] S. H. Cho, A. K. Ahn, P. Bhargava, C.-H. Lee, C. M. Eischen, O. McGuinness, M. Boothby,

Proc. Natl. Acad. Sci. U S A **2011**, *108*, 15972–15977.

[220] E. Wahlberg, T. Karlberg, E. Kouznetsova, N. Markova, A. Macchiarulo, A.-G. Thorsell, E. Pol, A. Frostell, T. Ekblad, D. Oncu, et al., *Nat. Biotech.* **2012**, *30*, 283–288.

[221] W. Han, X. Li, X. Fu, *Mutat. Res., Rev. Mutat. Res.* **2011**, *727*, 86–103.

[222] R. Zaffini, G. Gotte, M. Menegazzi, *Drug Des. Devel. Ther.* **2018**, *12*, 281–293.

[223] G. Caprara, E. Prosperini, V. Piccolo, G. Sigismondo, A. Melacarne, A. Cuomo, M. Boothby, M. Rescigno, T. Bonaldi, G. Natoli, *J. Immunol.* **2018**, *200*, ji1701117.

[224] D. Perina, A. Mikoč, J. Ahel, H. Ćetković, R. Žaja, I. Ahel, *DNA Repair* **2014**, *23*, 4–16.

[225] K. L. H. Feijs, P. Verheugd, B. Lüscher, *FEBS J.* **2013**, *280*, 3519–3529.

[226] D. Chen, M. Vollmar, M. N. Rossi, C. Phillips, R. Kraehenbuehl, D. Slade, P. V. Mehrotra, F. Von Delft, S. K. Crosthwaite, O. Gileadi, et al., *J. Biol. Chem.* **2011**, *286*, 13261–13271.

[227] E. Barkauskaite, G. Jankevicius, I. Ahel, *Mol. Cell* **2015**, *58*, 935–946.

[228] G. Jankevicius, M. Hassler, B. Golia, V. Rybin, M. Zacharias, G. Timinszky, A. G. Ladurner, *Nat. Struct. Mol. Biol.* **2013**, *20*, 508–514.

[229] E. Barkauskaite, A. Brassington, E. S. Tan, J. Warwicker, M. S. Dunstan, B. Banos, P. Lafite, M. Ahel, T. J. Mitchison, I. Ahel, et al., *Nat. Commun.* **2013**, *4*, 2164.

[230] M. Miwa, T. Sugimura, *J. Biol. Chem.* **1971**, *246*, 6362–6364.

[231] F. C. Peterson, D. Chen, B. L. Lytle, M. N. Rossi, I. Ahel, J. M. Denu, B. F. Volkman, *J. Biol. Chem.* **2011**, *286*, 35955–35965.

[232] F. Rosenthal, K. L. H. Feijs, E. Frugier, M. Bonalli, A. H. Forst, R. Imhof, H. C. Winkler, D. Fischer, A. Caflisch, P. O. Hassa, et al., *Nat. Struct. Mol. Biol.* **2013**, *20*, 502–507.

[233] R. Sharifi, R. Morra, C. Denise Appel, M. Tallis, B. Chioza, G. Jankevicius, M. A. Simpson, I. Matic, E. Ozkan, B. Golia, et al., *EMBO J.* **2013**, *32*, 1225–1237.

[234] D. Slade, M. S. Dunstan, E. Barkauskaite, R. Weston, P. Lafite, N. Dixon, M. Ahel, D. Leys, I. Ahel, *Nature* **2011**, *477*, 616–622.

[235] A. Sonnenblick, E. de Azambuja, H. A. Azim Jr., M. Piccart, *Nat. Rev. Clin. Oncol.* **2015**, *12*, 27–41.

[236] B. Peng, A.-G. Thorsell, T. Karlberg, H. Schüler, S. Q. Yao, *Angew. Chem. Int. Ed.* **2017**, *56*, 248–253.

[237] C. D. Andersson, T. Karlberg, T. Ekblad, A. E. G. Lindgren, A.-G. Thorsell, S. Spjut, U. Uciechowska, M. S. Niemiec, P. Wittung-Stafshede, J. Weigelt, et al., *J. Med. Chem.* **2012**, *55*, 7706–7718.

[238] P. Wang, J. Li, X. Jiang, Z. Liu, N. Ye, Y. Xu, G. Yang, Y. Xu, A. Zhang, *Tetrahedron* **2014**, *70*, 5666–5673.

[239] T. Ekblad, A. E. G. Lindgren, C. D. Andersson, R. Caraballo, A.-G. Thorsell, T. Karlberg, S. Spjut, A. Linusson, H. Schüler, M. Elofsson, *Eur. J. Med. Chem.* **2015**, *95*, 546–551.

[240] M. Yoneyama-Hirozane, S.-I. Matsumoto, Y. Toyoda, K. S. Saikatendu, Y. Zama, K. Yonemori, M. Oonishi, T. Ishii, T. Kawamoto, *Biochem. Biophys. Res. Commun.* **2017**, *486*, 626–631.

[241] J. Chen, A. T. Lam, Y. Zhang, *Anal. Biochem.* **2018**, *543*, 132–139.

[242] M. Schuller, K. Riedel, I. Gibbs-Seymour, K. Uth, C. Sieg, A. P. Gehring, I. Ahel, F. Bracher, B. M. Kessler, J. M. Elkins, et al., *ACS Chem. Biol.* **2017**, *12*, 2866–2874.

[243] N. Sen, *NeuroMolecular Med.* **2015**, *17*, 97–110.

[244] C. H. Arrowsmith, C. Bountra, P. V Fish, K. Lee, M. Schapira, *Nat. Rev. Drug Discov.* **2012**, *11*, 384–400.

[245] D. Zhao, Y. Li, X. Xiong, Z. Chen, H. Li, *J. Mol. Biol.* **2017**, *429*, 1994–2002.

[246] Q. Zhang, L. Zeng, C. Zhao, Y. Ju, T. Konuma, M. M. Zhou, *Structure* **2016**, *24*, 1606–1612.

[247] X. Xiong, T. Panchenko, S. Yang, S. Zhao, P. Yan, W. Zhang, W. Xie, Y. Li, Y. Zhao, C. D. Allis, et al., *Nat. Chem. Biol.* **2016**, *12*, 1111–1118.

[248] Y. Li, B. R. Sabari, T. Panchenko, H. Wen, D. Zhao, H. Guan, L. Wan, H. Huang, Z. Tang, Y. Zhao, et al., *Mol. Cell* **2016**, *62*, 181–193.

[249] M. Ali, K. Yan, M.-E. Lalonde, C. Degerny, S. B. Rothbart, B. D. Strahl, J. Cote, X.-J. Yang, T. G. Kutateladze, *J. Mol. Biol.* **2012**, *424*, 328–338.

[250] J. M. Schulze, A. Y. Wang, M. S. Kobor, *Biochem. Cell Biol.* **2009**, *87*, 65–75.

[251] D. Zhao, H. Guan, S. Zhao, W. Mi, H. Wen, Y. Li, Y. Zhao, C. D. Allis, X. Shi, H. Li, *Cell Res.* **2016**, *26*, 629–632.

[252] L. Wan, H. Wen, Y. Li, J. Lyu, Y. Xi, T. Hoshii, J. K. Joseph, X. Wang, Y.-H. E. Loh, M. A. Erb, et al., *Nature* **2017**, *543*, 265–269.

[253] M. A. Erb, T. G. Scott, B. E. Li, H. Xie, J. Paulk, H. S. Seo, A. Souza, J. M. Roberts, S. Dastjerdi, D. L. Buckley, et al., *Nature* **2017**, *543*, 270–274.

[254] K. Tao, J. Yang, Y. Hu, A. Deng, *Am. J. Transl. Res.* **2015**, *7*, 616–623.

[255] Y. Li, H. Wen, Y. Xi, K. Tanaka, H. Wang, D. Peng, Y. Ren, Q. Jin, S. Y. R. Dent, W. Li, et al., *Cell* **2014**, *159*, 558–571.

[256] E. J. Perlman, S. Gadd, S. T. Arold, A. Radhakrishnan, D. S. Gerhard, L. Jennings, V. Huff, J. M. G. Auvil, T. M. Davidsen, J. S. Dome, et al., *Nat. Commun.* **2015**, *6*, 10013.

[257] D. Mueller, C. Bach, D. Zeisig, M.-P. Garcia-Cuellar, S. Monroe, A. Sreekumar, R. Zhou, A. Nesvizhskii, A. Chinnaiyan, J. L. Hess, et al., *Blood* **2007**, *110*, 4445–4454.

[258] A. Yokoyama, M. Lin, A. Naresh, I. Kitabayashi, M. L. Cleary, *Cancer Cell* **2010**, *17*, 198–212.

[259] N. He, C. K. Chan, B. Sobhian, S. Chou, Y. Xue, M. Liu, T. Alber, M. Benkirane, Q. Zhou, *Proc. Natl. Acad. Sci. U S A* **2011**, *108*, E636–E645, SE636/1–SE636/2.

[260] K. M. Bernt, N. Zhu, A. U. Sinha, S. Vempati, J. Faber, A. V Krivtsov, Z. Feng, N. Punt, A. Daigle, L. Bullinger, et al., *Cancer Cell* **2011**, *20*, 66–78.

[261] S. R. Daigle, E. J. Olhava, C. A. Therkelsen, C. R. Majer, C. J. Sneeringer, J. Song, L. D. Johnston, M. P. Scott, J. J. Smith, Y. Xiao, et al., *Cancer Cell* **2011**, *20*, 53–65.

[262] A. V Krivtsov, Z. Feng, M. E. Lemieux, J. Faber, S. Vempati, A. U. Sinha, X. Xia, J. Jesneck, A. P. Bracken, L. B. Silverman, et al., *Cancer Cell* **2008**, *14*, 355–368.

[263] Y. Okada, Q. Feng, Y. Lin, Q. Jiang, Y. Li, V. M. Coffield, L. Su, G. Xu, Y. Zhang, *Cell* **2005**, *121*, 167–178.

[264] D. T. Zeisig, C. B. Bittner, B. B. Zeisig, M. P. García-Cuéllar, J. L. Hess, R. K. Slany, *Oncogene* **2005**, *24*, 5525–5532.

[265] K. Hetzner, M. P. Garcia-Cuellar, C. Buttner, R. K. Slany, *Blood* **2018**, *131*, 662–673.

[266] D. C. Wai, T. N. Szyszka, A. E. Campbell, C. Kwong, L. E. Wilkinson-White, A. P. G. Silva, J. K. K. Low, A. H. Kwan, R. Gamsjaeger, J. N. Chalmers, et al., *J. Biol. Chem.* **2018**, jbc.RA117.000678.

[267] T. Clackson, W. Yang, L. W. Rozamus, M. Hatada, J. F. Amara, C. T. Rollins, L. F. Stevenson, S. R. Magari, S. A. Wood, N. L. Courage, et al., *Proc. Natl. Acad. Sci. U S A* **1998**, *95*,

10437–10442.

[268] B. Nabet, J. M. Roberts, D. L. Buckley, J. Paulk, S. Dastjerdi, A. Yang, A. L. Leggett, M. A. Erb, M. A. Lawlor, A. Souza, et al., *Nat. Chem. Biol.* **2018**, *14*, 1–11.

[269] C. V. Galliford, K. A. Scheidt, *Angew. Chem. Int. Ed.* **2007**, *46*, 8748–8758.

[270] J. P. Knowles, L. D. Elliott, K. I. Booker-Milburn, *Beilstein J. Org. Chem.* **2012**, *8*, 2025–2052, No. 229.

[271] D. Cambie, C. Bottecchia, N. J. W. Straathof, V. Hessel, T. Noel, *Chem. Rev.* **2016**, *116*, 10276–10341.

[272] J. Wegner, S. Ceylan, A. Kirschning, *Adv. Synth. Catal.* **2012**, *354*, 17–57.

[273] A. Jossang, P. Jossang, H. A. Hadi, T. Sevenet, B. Bodo, *J. Org. Chem.* **1991**, *56*, 6527–6530.

[274] R. M. Eglen, T. Reisine, P. Roby, N. Rouleau, C. Illy, R. Bossé, M. Bielefeld, *Curr. Chem. Genomics* **2008**, *1*, 2–10.

[275] "AlphaScreen Principles Figure," can be found under http://www.perkinelmer.com/product/alphascreen-anti-c-myc-500pts-6760611c, **2018**.

[276] M. W. Pantoliano, E. C. Petrella, J. D. Kwasnoski, V. S. Lobanov, J. Myslik, E. Graf, T. Carver, E. Asel, B. A. Springer, P. Lane, et al., *J. Biomol. Screen.* **2001**, *6*, 429–440.

[277] "Fluorescence Based Thermal Shift Assay Curve Figure," can be found under http://www.bio.anl.gov/molecular_and_systems_biology/Sensor/sensor_images/assay_theory_figure.png, **2018**.

[278] F. H. Niesen, H. Berglund, M. Vedadi, *Nat. Protoc.* **2007**, *2*, 2212–2221.

[279] O. Fedorov, B. Marsden, V. Pogacic, P. Rellos, S. Mueller, A. N. Bullock, J. Schwaller, M. Sundstroem, S. Knapp, *Proc. Natl. Acad. Sci. U S A* **2007**, *104*, 20523–20528.

[280] D. Matulis, J. K. Kranz, F. R. Salemme, M. J. Todd, *Biochemistry* **2005**, *44*, 5258–5266.

[281] "ITC Figure," can be found under http://2bind.de/molecularinteractions/isothermal-titration-calorimetry/, **2018**.

[282] M. Gabourdes, V. Bourgine, G. Mathis, H. Bazin, B. Alpha-Bazin, *Anal. Biochem.* **2004**, *333*, 105–113.

[283] T. Machleidt, C. C. Woodroofe, M. K. Schwinn, J. Méndez, M. B. Robers, K. Zimmerman, P. Otto, D. L. Daniels, T. a Kirkland, K. V Wood, *ACS Chem. Biol.* **2015**, *10*, 1797–1804.

[284] Y. Xu, D. W. Piston, C. H. Johnson, *Proc. Natl. Acad. Sci. U S A* **1999**, *96*, 151–156.

[285] "NanoBRET Assay Figure," can be found under https://www.promega.co.uk/products/protein-interactions/live-cell-protein-interactions/nanobret-ppi-starter-systems/?catNum=N1821, **2018**.

[286] R. Jafari, H. Almqvist, H. Axelsson, M. Ignatushchenko, T. Lundbäck, P. Nordlund, D. M. Molina, *Nat. Protoc.* **2014**, *9*, 2100–2122.

[287] I. Pastan, M. M. Gottesman, K. Ueda, E. Lovelace, A. V Rutherford, M. C. Willingham, *Proc. Natl. Acad. Sci. U S A* **1988**, *85*, 4486–4490.

[288] E. L. Berg, J. Yang, M. A. Polokoff, *J. Biomol. Screen.* **2013**, *18*, 1260–1269.

[289] B. A. Chabner, *J. Natl. Cancer Inst.* **2016**, *108*, djv388-djv388.

[290] R. H. Shoemaker, *Nat. Rev. Cancer* **2006**, *6*, 813–823.

[291] A. J. Bannister, T. Kouzarides, *Nature* **1996**, *384*, 641–643.

[292] V. V Ogryzko, R. L. Schiltz, V. Russanova, B. H. Howard, Y. Nakatani, *Cell* **1996**, *87*, 953–959.

[293] A. J. N. M. Bastiaansen, M. M. Ewing, H. C. de Boer, T. C. van der Pouw Kraan, M. R. de Vries, E. A. B. Peters, S. M. J. Welten, R. Arens, S. M. Moore, J. E. Faber, et al., *Arter. Thromb., Vasc. Biol.* **2013**, *33*, 1902–1910.

[294] W.-G. Deng, Y. Zhu, K. K. Wu, *Blood* **2004**, *103*, 2135–2142.

[295] P. Hu, X. Wang, B. Zhang, S. Zhang, Q. Wang, Z. Wang, *ChemMedChem* **2014**, *9*, 928–931.

[296] B. K. Albrecht, D. J. Burdick, A. Cote, M. Duplessis, C. G. Nasveschuk, A. M. Taylor, *Pyridazinone Derivatives and Their Use in the Treatment of Cancer*, **2016**, WO2016112298A1.

[297] A. Chaikuad, S. Lang, P. E. Brennan, C. Temperini, O. Fedorov, J. Hollander, R. Nachane, C. Abell, S. Muller, G. Siegal, et al., *J. Med. Chem.* **2016**, *59*, 1648–1653.

[298] S. Picaud, K. Leonards, J.-P. Lambert, O. Dovey, C. Wells, O. Fedorov, O. Monteiro, T. Fujisawa, C.-Y. Wang, H. Lingard, et al., *Sci. Adv.* **2016**, *2*, e1600760.

[299] M. A. C. Neves, M. Totrov, R. Abagyan, *J. Comput. Aid. Mol. Des.* **2012**, *26*, 675–686.

[300] P. L. Southwick, J. E. Anderson, *J. Am. Chem. Soc.* **1957**, *79*, 6222–6229.

[301] E. Quinn, L. Wodicka, P. Ciceri, G. Pallares, E. Pickle, A. Torrey, M. Floyd, J. Hunt, D. Treiber, *Cancer Res.* **2013**, *73*, 4238.

[302] K. M. Johnson, M. S. Rattley, F. Sladojevich, D. M. Barber, M. G. Nuñez, A. M. Goldys, D. J. Dixon, *Org. Lett.* **2012**, *14*, 2492–2495.

[303] M. Moustakim, P. G. K. Clark, L. Trulli, A. L. Fuentes de Arriba, M. T. Ehebauer, A. Chaikuad, E. J. Murphy, J. Mendez-Johnson, D. Daniels, C.-F. D. Hou, et al., *Angew. Chem. Int. Ed.* **2017**, *56*, 827–831.

[304] P. G. Humphreys, P. Bamborough, C. Chung, P. D. Craggs, L. Gordon, P. Grandi, T. G.

Hayhow, J. Hussain, K. L. Jones, M. Lindon, et al., *J. Med. Chem.* **2017**, *60*, 695–709.

[305] R. E. Meléndez, W. D. Lubell, *Tetrahedron* **2003**, *59*, 2581–2616.

[306] B. E. Zucconi, B. Luef, W. Xu, R. A. Henry, I. M. Nodelman, G. D. Bowman, A. J. Andrews, P. A. Cole, *Biochemistry* **2016**, *55*, 3727–3734.

[307] "L-Moses," can be found under https://www.tocris.com/products/l-moses-dihydrochloride_6251, **2018**.

[308] M. Moustakim, P. G. K. Clark, L. Trulli, A. L. Fuentes de Arriba, M. T. Ehebauer, A. Chaikuad, E. J. Murphy, J. Mendez-Johnson, D. Daniels, C.-F. D. Hou, et al., *Angew. Chem. Int. Ed.* **2017**, *56*, 908.

[309] J. G. M. Rack, D. Perina, I. Ahel, *Annu. Rev. Biochem.* **2016**, *85*, 431–454.

[310] A. H. Forst, T. Karlberg, N. Herzog, A.-G. Thorsell, A. Gross, K. L. H. Feijs, P. Verheugd, P. Kursula, B. Nijmeijer, E. Kremmer, et al., *Structure* **2013**, *21*, 462–475.

[311] S. Vyas, I. Matic, L. Uchima, J. Rood, R. Zaja, R. T. Hay, I. Ahel, P. Chang, *Nat. Commun.* **2014**, *5*, 4426.

[312] T. Ekblad, P. Verheugd, A. E. Lindgren, T. Nyman, M. Elofsson, H. Schüler, *SLAS Discov.* **2018**, *23*, 353–362.

[313] M. Moustakim, K. Riedel, M. Schuller, A. P. Gehring, O. P. Monteiro, S. P. Martin, O. Fedorov, J. Heer, D. J. Dixon, J. M. Elkins, et al., *Bioorg. Med. Chem.* **2018**, *26*, 2965–2972.

[314] M. Moustakim, K. Riedel, M. Schuller, A. P. Gehring, O. P. Monteiro, S. P. Martin, O. Fedorov, J. Heer, D. J. Dixon, J. M. Elkins, et al., *Bioorg. Med. Chem.* **2018**, *26*, 2965–2972.

[315] O. B. Cox, T. Krojer, P. Collins, O. Monteiro, R. Talon, A. Bradley, O. Fedorov, J. Amin, B. D. Marsden, J. Spencer, et al., *Chem. Sci.* **2016**, *7*, 2322–2330.

[316] M. A. Erb, T. G. Scott, B. E. Li, H. Xie, J. Paulk, H. S. Seo, A. Souza, J. M. Roberts, S. Dastjerdi, D. L. Buckley, et al., *Nature* **2017**, *543*, 270–274.

[317] A. G. Schultz, C.-K. Sha, *Tetrahedron* **1980**, *36*, 1757–1761.

[318] C. Marti, E. M. Carreira, *Eur. J. Org. Chem.* **2003**, 2209–2219.

[319] K. Ding, Y. Lu, Z. Nikolovska-Coleska, G. Wang, S. Qiu, S. Shangary, W. Gao, D. Qin, J. Stuckey, K. Krajewski, et al., *J. Med. Chem.* **2006**, *49*, 3432–3435.

[320] A. K. Gupta, M. Bharadwaj, A. Kumar, R. Mehrotra, *Top. Curr. Chem.* **2017**, *375*, 1–25.

[321] S. Wang, W. Sun, Y. Zhao, D. McEachern, I. Meaux, C. Barrière, J. A. Stuckey, J. L. Meagher, L. Bai, L. Liu, et al., *Cancer Res.* **2014**, *74*, 5855–5865.

[322] F. Christian, M. Christiane, C. Erick M., *Helv. Chim. Acta* **2000**, *83*, 1175–1181.

[323] M. G. Kulkarni, A. P. Dhondge, S. W. Chavhan, A. S. Borhade, Y. B. Shaikh, D. R. Birhade, M. P. Desai, N. R. Dhatrak, *Beilstein J. Org. Chem.* **2010**, *6*, 876–879.

[324] N. Hoffmann, *Pure Appl. Chem.* **2007**, *79*, 1949.

[325] S. He, Z. Lai, D. X. Yang, Q. Hong, M. Reibarkh, R. P. Nargund, W. K. Hagmann, *Tetrahedron Lett.* **2010**, *51*, 4361–4364.

[326] G. Barman, M. Roy, J. K. Ray, *Tetrahedron Lett.* **2008**, *49*, 1405–1407.

[327] G. Lakshmaiah, T. Kawabata, M. Shang, K. Fuji, *J. Org. Chem.* **1999**, *64*, 1699–1704.

7.3 Experimental Procedures

7.3.1 Chapter 2 Bromodomain Inhibition

Appendix 7.3.1

Experimental Procedures: Chapter 2 Bromodomain Inhibition

I General Experimental

I.I Solvents and reagents

All solvents were purchased from commercial sources and used without purification (HPLC or analytical grade). Anhydrous solvents were purchased from Acros Organics stored under a nitrogen atmosphere with activated molecular sieves. Standard vacuum line techniques were used, and glassware was flame dried prior to use. Deionised water was sourced using an Elga DV 25 system. Organic solvents were dried during workup using anhydrous Na_2SO_4.

I.II Purification and chromatography

Thin Layer Chromatography (TLC) was carried out using aluminium plates coated with 60 F_{254} silica gel. Plates were visualised using UV light (254 or 365 nm) or staining with Ninhydrin (1 M, EtOH) or 1% aq. $KMnO_4$. Normal-phase silica gel chromatography was carried out using Biotage Isolera One flash column chromatography system (LPLC). Reverse-phase high pressure liquid chromatography (RP-HPLC) was performed using a Waters system equipped with a Waters 2545 Binary Gradient Module, a SecurityGuard™ ULTRA cartridges for EVO-C18 UHPLC HPLC, Kinetex 5 µM EVO C18 100 Å 100 x 3.0 mm column and a Waters SQ Detector 2 using the stated eluent system.

I.II Characterisation

Infrared spectroscopy was carried out with a Thermo Scientific Nicolet iS5 FT-IR spectrometer fitted with an iD7-ATR accessory, selected absorption maxima (ν_{max}) recorded in

wavenumbers (cm^{-1}). NMR spectra were recorded using a Bruker Avance 400 MHz spectrometer using the deuterated solvent stated. Chemical shifts (δ) quoted in parts per million (ppm) and referenced to the residual solvent peak. Multiplicities are denoted as s- singlet, d- doublet, t- triplet, q- quartet and quin- quintet and derivatives thereof (br denotes a broad resonance peak). Coupling constants recorded as Hz and round to the nearest 0.1 Hz. Two-dimensional NMR experiments (COSY, HSQC, HMBC) were used to aid the assignment of ^{1}H and ^{13}C spectra. Low Resolution mass spectra were recorded on a Waters SQ Detector 2 (LC-MS). High Resolution Mass Spectrometry (HRMS) was recorded using an Agilent 6530 QTOF. Melting points were obtained using a Stuart SMP40 apparatus and are reported uncorrected in °C. Optical rotations were recorded using a Perkin Elmer 341 polarimeter; specific optical rotations are quoted as $[\alpha]_D^T$ at 23 °C, concentration (c) is reported as g/100 mL, with a path length of 0.1 dm. Enantiomeric excesses were determined by HPLC analysis on an Agilent 1200 series instrument using chiral stationary phase columns. The same instrument was used in the separation of enantiomers using the stated semipreparative chiral stationary phase column. Compound names were generated using ChemBioDraw Ultra v14 systematic naming. Atom numbering in structures is purely for the purposes of assignment and does not reflect IUPAC numbering conventions.

II.I Synthetic Procedures

6-chloro-3-methyl-[1,2,4]triazolo[3,4-a]phthalazine (23)

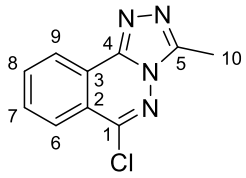

To a stirred solution of 1,4-dichlorophthalazine **24** (18.4 g, 92 mmol, 1 eq) in DMF (anhydrous) (95 mL, 0.97 M) was added acetohydrazide (12.84 g, 139 mmol, 1.5 eq). The solution was stirred at 120 °C with a reflux condenser attached for 24 h after which TLC/LCMS analysis confirmed consumption of the starting material. The reaction mixture was cooled to 4°C for 2 h after which an off-white precipitate had formed. The precipitate was filtered off, washed with EA and dried under vacuum to afford **23** (12.478 g, 57.1 mmol, 62%) as an off white solid.

Mpt: 142.0-144.0 °C; **ν_{max} (cm^{-1})** 3401, 3000, 2870, 1659, 1256, 1003, 767; **^{1}H-NMR (400 MHz, $CDCl_3$): δ** 8.69 (d, *J* = 7.8 Hz, 1H, *H*-6), 8.27 (d, *J* = 8.1 Hz, 1H, *H*-9), 8.01 (t, *J*= 8.1, 1H, *H*-8), 7.87 (t, *J*= 7.8, 1H, *H*-7); **^{13}C-NMR (100 MHz $CDCl_3$): δ** 149.8 (*C*-1), 147.8 (*C*-4), 142.3 (*C*-5), 134.8 (*C*-8), 131.2 (*C*-7), 127.5 (*C*-6), 124.1 (*C*-2), 123.6 (*C*-6), 122.0 (*C*-3), 9.8 (*C*-10); **LR-ESI-MS**: $C_{10}H_8ClN_4$ $[M+H]^+$ *m/z* found 219.27, cald 219.04; **HR-ESI-MS**: $C_{10}H_8ClN_4$ $[M+H]^+$ *m/z* found 219.0467, cald 219.0437.

1-chloro-4-hydrazinylphthalazine (26)

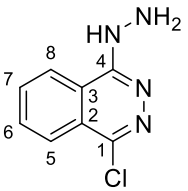

To a stirred solution of 1,4-dichlorophthalazine **24** (884 mg, 4.44 mmol, 1 eq) in EtOH (22 mL, 0.2 M) was added hydrazine.monohydrate (1.637 mL, 33.8 mmol, 7.6 eq) and the reaction mixture was warmed to 120 °C. After 10 mins the reaction mixture completely precipitated out to a yellow solid. The reaction mixture was cooled and filtered to give a yellow solid which was washed with cold Et_2O (25 mL x 3) and dried to give **26** (862 mg, 4.43 mmol, *quant*.) as a yellow solid.

Mpt: 174.5-176.5 °C; **ν_{max} (cm^{-1})** 3240, 3157, 2944, 1640, 1515, 1420, 1294, 1102, 988, 757; **^{1}H-NMR (400 MHz, DMSO-*d*^{6}): δ** 8.25 (m, 1H, *H*-8), 7.92 (m, 3H, *H*-5; *H*-6; *H*-7); **^{13}C-NMR (100 MHz DMSO-*d*^{6}): δ** 132.6 (*C*-6, *C*-7), 124.7 (*C*-2), 124.5 (*C*-5), 122.5 (*C*-3, *C*-8); **LR-ESI-MS:** $C_8H_8ClN_4$

$[M+H]^+$ *m/z* found 195.0, cald 195.0; **HR-ESI-MS:** $C_8H_8ClN_4$ $[M+H]^+$ *m/z* found 195.0096, cald 195.0437.

6-chloro-3-(trifluoromethyl)-[1,2,4]triazolo[3,4-a]phthalazine (25)

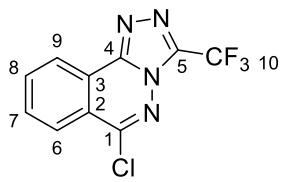

26 (860 mg, 4.42 mmol, 1 eq) was dissolved in TFA (2 mL, 26.5 mmol, 6 eq) at room temperature and stirred at 100 °C under an inert atmosphere (N_2) for 2 h. The reaction mixture was then cooled and concentrated to dryness to give a crude pink solid. The crude material was then dissolved in EA and washed with $NaHCO_3$ sat. solution (x 3). The organic layer was then washed with brine and dried over Na_2SO_4 before being concentrated and purified by Isolera Biotage LPLC (DCM/MeOH 90:10) to give **25** (519 mg, 1.903 mmol, 43%) as an off white crystalline solid.

Mpt: 170.7-172.7 °C; **ν_{max} (cm^{-1})** 1498, 1448, 1123, 1018, 962, 774, 643, 504; **^{19}F-NMR (376 MHz, $CDCl_3$): δ** -63.55; **^{1}H-NMR (400 MHz, $CDCl_3$): δ** 8.79 (dd, 1H, *J*= 7.9, 0.5 Hz, *H*-9), 8.37 (d, 1H, *J*= 8.3 Hz, *H*-6), 7.83 (td, 1H, *J*= 7.7, 1.1 Hz, *H*-8), 8.01 (m, 1H, *H*-7); **^{13}C-NMR (100 MHz $CDCl_3$): δ** 152.3 (*C*-1), 144.3 (*C*-4), 140.2 (q, *J*= 42.5 Hz, *C*-5), 135.5 (*C*-8), 132.6 (*C*-7), 127.8 (*C*-9), 124.2 (*C*-3), 123.0 (*C*-6), 122.6 (*C*-2), 117.6 (q, *J*= 271.4 Hz, *C*-10); **LR-ESI-MS:** $C_{10}H_5F_3N_4$ $[M+H]^+$ *m/z* found 272.9, cald 273.0; **HR-ESI-MS:** $C_{10}H_5F_3N_4$ $[M+H]^+$ *m/z* found 273.0172, cald 273.0155.

General Procedure A

To a stirred solution of **23** or **25** (1 eq) in EtOH (0.46 M, anhydrous) was added amine (2 eq), KI (0.1 eq) and conc. HCl (0.05 eq). The reaction mixture was then stirred at reflux for 72 h before being cooled to 4°C at which point any precipitate formed was filtered off and washed with EA/H_2O before drying to give the desired product. In the absence of precipitated product, the reaction mixture was concentrated to dryness and purified by Isolera Biotage LPLC (DCM/MeOH 90:10 then DCM/MeOH/NH_3 9:1:0.5) to furnish the desired compound.

***N*$_1$,*N*$_1$-dimethyl-*N*$_2$-(3-methyl-[1,2,4]triazolo[3,4-a]phthalazin-6-yl)ethane-1,2-diamine (27)**

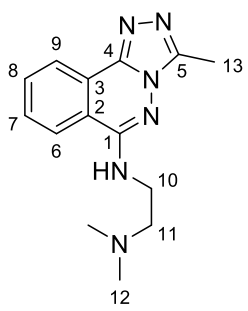

23 (100 mg, 0.457 mmol, 1 eq) and N_1,N_1-dimethylethane-1,2-diamine (81 mg, 0.915 mmol, 2 eq) were reacted according to general procedure **A**. The crude material was purified by Isolera Biotage LPLC (DCM/MeOH 90:10 then DCM/MeOH/NH_3 9:1:0.5) to give **27** (52 mg, 0.192 mmol 42%) as a white solid.

Mpt: 225.9-227.9 °C; **ν_{max} (cm^{-1})** 3227, 1566, 1519, 702; **^{1}H-NMR (400 MHz, DMSO-*d*^{6}): δ** 8.34 (dd, 1H, *J*= 7.9, 0.9 Hz, *H*-9), 8.25 (d, 1H, *J*= 8.2 Hz, *H*-6), 7.88 (m, 1H, *H*-8), 7.78 (m, 1H, *H*-7), 7.50 (m, 1H, N*H*), 3.50 (m, 2H, *H*-10), 2.57 (t, 2H, *J*= 6.9 Hz, *H*-11), 2.54 (s, 3H, *H*-13), 2.22 (s, 6H, *H*-12); **^{13}C-NMR (100 MHz, DMSO-*d*^{6}): δ** 151.1 (*C*-1), 145.9 (*C*-4), 141.1 (*C*-5), 132.8 (*C*-8), 130.1 (*C*-7), 124.1 (*C*-9), 123.3 (*C*-3), 122.5 (*C*-6), 118.2 (*C*-2), 57.0 (*C*-10), 45.3 (*C*-11; *C*-12), 9.3 (*C*-13); **LR-ESI-MS:** $C_{14}H_{19}N_6$ $[M+H]^+$ *m/z* found 271.4, cald 271.2; **HR-ESI-MS:** $C_{14}H_{19}N_6$ $[M+H]^+$ *m/z* found 271.1682, cald 371.1671.

***N*$_1$,*N*$_1$-dimethyl-*N*$_3$-(3-methyl-[1,2,4]triazolo[3,4-a]phthalazin-6-yl)propane-1,3-diamine (28)**

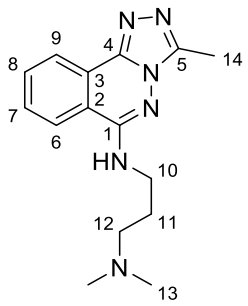

23 (200 mg, 0.915 mmol, 1 eq) and N_1,N_1-dimethylpropane-1,3-diamine (187 mg, 1.829 mmol, 2 eq) were reacted according to general procedure **A**. The crude material was purified by Isolera Biotage LPLC (DCM/MeOH 90:10 then DCM/MeOH/NH_3 9:1:0.5) to give **28** (174 mg, 0.613 mmol 67%) as a white solid.

Mpt: 118.5-120.5 °C; **ν_{max} (cm^{-1})** 3229, 2777, 1565, 1513, 1369, 1266, 1160, 783; **^{1}H-NMR (400 MHz, DMSO-*d*^{6}): δ** 8.35 (dd, 1H, *J*= 7.9, 0.9 Hz, *H*-9), 8.23 (d, 1H, *J*= 8.1 Hz, *H*-6), 7.89 (m, 1H, *H*-8), 7.79 (td, 1H, *J*= 7.7, 1.3 Hz, *H*-7), 7.73 (m, 1H, N*H*), 3.43 (m, 2H, *H*-10), 2.54 (s, 3H, *H*-14), 2.34 (t, 2H, *H*-12), 2.17 (s, 6H, *H*-13), 1.84 (m, 2H, *H*-11); **^{13}C-NMR (100 MHz, DMSO-*d*^{6}): δ** 151.2 (*C*-1), 145.9 (*C*-4), 141.1 (*C*-5), 132.7 (*C*-8), 130.1 (*C*-7), 124.0 (*C*-9), 123.3 (*C*-3), 122.4 (*C*-6), 118.3 (*C*-2), 57.3 (*C*-10), 45.2 (*C*-12; *C*-13), 25.6 (*C*-11), 9.3 (*C*-14); **LR-ESI-MS:** $C_{15}H_{21}N_6$ $[M+H]^+$ *m/z* found 285.2, cald 285.2; **HR-ESI-MS:** $C_{15}H_{21}N_6$ $[M+H]^+$ *m/z* found 285.1845, cald 285.1828.

***N*$_1$,*N*$_1$-dimethyl-*N*$_4$-(3-methyl-[1,2,4]triazolo[3,4-a]phthalazin-6-yl)butane-1,4-diamine (29)**

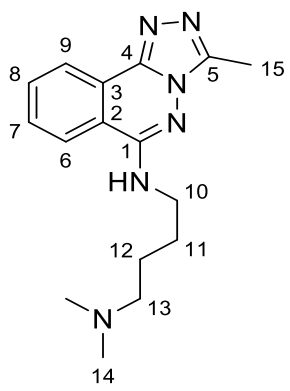

23 (200 mg, 0.915 mmol, 1 eq) and *N*$_1$,*N*$_1$-dimethylbutane-1,4-diamine (213 mg, 1.829 mmol, 2 eq) were reacted according to general procedure **A**. The crude material was purified by Isolera Biotage LPLC (DCM/MeOH 90:10 then DCM/MeOH/NH_3 9:1:0.5) to give **29** (225 mg, 0.755 mmol 83%) as a white waxy solid.

Mpt: 158.3-160.3 °C; **ν_{max} (cm^{-1})** 3261, 2865, 1591, 1512, 1476, 654; **^{1}H-NMR (400 MHz, DMSO-d^6): δ** 8.35 (dd, J = 7.9, 0.9 Hz, 1H, *H*-9), 8.30 (d, J= 8 Hz, 1H, *H*-6), 7.89 (m, 1H *H*-8), 7.79 (td, J= 7.9, 1.3 Hz, 1H *H*-7), 7.61 (t, J= 5.2 Hz, 1H, N*H*) 3.41 (m, 2H, *H*-10), 2.55 (s, 3H, *H*-15), 2.26 (m, 2H, *H*-13), 2.12 (s, 6H, *H*-14), 1.71 (quin, J= 7.3 Hz, 2H, *H*-11), 1.51 (quin, J= 7.3 Hz, 2H, *H*-12); **^{13}C-NMR (100 MHz DMSO-d^6): δ** 151.2 (*C*-1), 145.9 (*C*-4), 141.1 (*C*-5), 132.7 (*C*-8), 130.1 (*C*-7), 124.2 (*C*-9), 123.3 (*C*-3), 122.4 (*C*-6), 118.3 (*C*-2), 58.7 (*C*-13), 45.0 (*C*-14), 41.2 (*C*-10), 25.7 (*C*-11), 24.7 (*C*-12), 9.3 (*C*-15); **LR-ESI-MS:** $C_{16}H_{23}N_6$ $[M+H]^+$ m/z found 299.3, cald 299.2; **HR-ESI-MS:** $C_{16}H_{23}N_6$ $[M+H]^+$ m/z found 299.2011, cald 299.1984.

***N*$_1$,*N*$_1$-dimethyl-*N*$_2$-(3-methyl-[1,2,4]triazolo[3,4-a]phthalazin-6-yl)propane-1,2-diamine (30)**

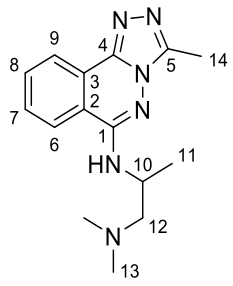

23 (200 mg, 0.915 mmol, 1 eq) and *N*$_1$,*N*$_1$-dimethylpropane-1,2-diamine (187 mg, 1.829 mmol, 2 eq) were reacted according to general procedure **A**. The crude material was purified by Isolera Biotage LPLC (DCM/MeOH 90:10 then DCM/MeOH/NH_3 9:1:0.5) to give **30** (72 mg, 0.254 mmol 28%) as a white solid.

Mpt: 142.3-144.3 °C; **ν_{max} (cm^{-1})** 3247, 2773, 1509, 1454, 1033, 699; **^{1}H-NMR (400 MHz, DMSO-d^6): δ** 8.37 (d, 2H, *J*= 8.3 Hz, *H*-6; *H*-9), 7.91 (m, 1H, *H*-8), 7.81 (m, 1H, *H*-7), 7.18 (d, 1H, *J*=7.5 Hz, N*H*), 4.28 (m, 1H, *H*-10), 2.58 (m, 1H, *H*-12"), 2.56 (s, 3H, *H*-14), 2.27 (m, 1H, *H*-12'), 2.23 (s, 6H, *H*-13), 1.3 (d, 3H, *J*= 6.5 Hz, *H*-11); **^{13}C-NMR (100 MHz, DMSO-d^6):** δ 150.6 (*C*-1), 145.9 (*C*-4), 141.0 (*C*-5), 132.8 (*C*-8), 130.0 (*C*-7), 124.3 (*C*-9), 123.4 (*C*-3), 122.4 (*C*-6), 118.2 (*C*-2), 64.0 (*C*-10),

45.6 (*C*-13), 44.8 (*C*-12), 18.4 (*C*-11), 9.3 (*C*-14); **LR-ESI-MS:** $C_{15}H_{21}N_6$ $[M+H]^+$ *m/z* found 285.2, cald 285.2; **HR-ESI-MS:** $C_{15}H_{21}N_6$ $[M+H]^+$ *m/z* found 285.1850, cald 285.1828.

(*S*)-*N*$_1$,*N*$_1$-dimethyl-*N*$_2$-(3-methyl-[1,2,4]triazolo[3,4-a]phthalazin-6-yl)propane-1,2-diamine ((*S*)-30)

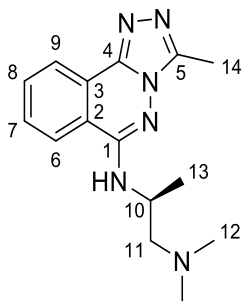

23 (300 mg, 1.372 mmol, 1 eq) and (*S*)-*N*$_1$,*N*$_1$-dimethylpropane-1,2-diamine (280 mg, 2.74 mmol, 2 eq) were reacted according to general procedure **A**. The crude material was purified by Isolera Biotage LPLC (DCM/MeOH 90:10 then DCM/MeOH/NH_3 9:1:0.5) to give **(*S*)-30** (86 mg, 0.303 mmol 22%) as a white solid.

Mpt: 147.4-149.4 °C; **ν_{max} (cm^{-1})** 3293, 2974, 2951, 2772, 1690, 1407, 1463, 1032, 700; **^{1}H-NMR (400 MHz, DMSO-*d*^{6}): δ** 8.37 (d, *J* = 8.3 Hz, 2H, *H*-9; *H*-6), 7.91 (m, 1H, *H*-8), 7.81 (m, 1H, *H*-7), 7.17 (d, *J*= 7.3 Hz, N*H*), 4.27 (spt, *J*= 6.8 Hz, 1H, *H*-10), 2.56 (m, 1H, *H*-11"), 2.55 (s, 3H, *H*-14), 2.27 (m, 1H, *H*-11'), 2.22 (s, 6H, *H*-12), 1.3 (d, *J*= 6.5 Hz, 3H, *H*-13); **^{13}C-NMR (100 MHz DMSO-*d*^{6}): δ** 150.6 (*C*-1), 145.9 (*C*-4), 141.0 (*C*-5), 132.8 (*C*-8), 130.0 (*C*-7), 124.3 (*C*-9), 123.4 (*C*-3), 122.5 (*C*-6), 118.2 (*C*-2), 64.1 (*C*-11), 45.6 (*C*-10), 44.8 (*C*-12), 18.5 (*C*-13), 9.3 (*C*-14); **LR-ESI-MS:** $C_{15}H_{21}N_6$ $[M+H]^+$ *m/z* found 285.3, cald 285.2; **HR-ESI-MS:** $C_{15}H_{21}N_6$ $[M+H]^+$ *m/z* found 285.1829, cald 285.1828.

***N*$_1$,*N*$_1$-dimethyl-*N*$_2$-(3-methyl-[1,2,4]triazolo[3,4-a]phthalazin-6-yl)butane-1,2-diamine (31)**

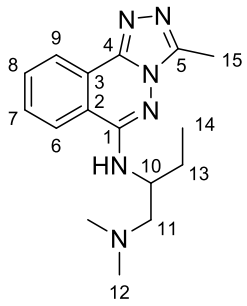

23 (400 mg, 1.829 mmol, 1 eq) and *N*$_1$,*N*$_1$-dimethylbutane-1,2-diamine (425 mg, 3.66 mmol, 2 eq) were reacted according to general procedure **A**. The crude material was purified by Isolera Biotage LPLC (DCM/MeOH 90:10 then DCM/MeOH/NH_3 9:1:0.5) to give **31** (185 mg, 0.621 mmol 34%) as a white solid.

Mpt: 153.5-155.5 °C; **ν_{max} (cm^{-1})** 3246, 2928, 2756, 1599, 1458, 1391, 1190; **^{1}H-NMR (400 MHz, DMSO-*d*^{6}): δ** 8.43 (d, *J* = 8.2 Hz, 1H, *H*-9), 8.37 (d, *J*= 7.8 Hz, 1H, *H*-6), 7.92 (m, 1H, *H*-8), 7.81 (m, 1H, *H*-7), 7.11 (d, *J*= 7.8 Hz, 1H, N*H*), 4.14 (m, 1H, *H*-10), 2.55 (m, 1H, *H*-11"), 2.54 (s, 3H, *H*-15),

2.30 (m, 1H, *H*-11'), 2.22 (s, 6H, *H*-12), 1.81 (m, 1H, *H*-13"), 1.62 (m, 1H, *H*-13'), 0.94 (m, 3H, *H*-14); **^{13}C-NMR (100 MHz, DMSO-*d*^{6}): δ** 151.2 (*C*-1), 145.9 (*C*-4), 141.0 (*C*-5), 132.7 (*C*-8), 130.0 (*C*-7), 124.3 (*C*-9), 123.3 (*C*-3), 122.5 (*C*-6), 118.3 (*C*-2), 62.7 (*C*-11), 50.6 (*C*-10), 45.7 (*C*-12), 25.1 (*C*-13), 10.8 (*C*-14), 9.3 (*C*-15); **LR-ESI-MS:** $C_{16}H_{23}N_6$ $[M+H]^+$ *m/z* found 299.2, cald 299.2; **HR-ESI-MS:** $C_{16}H_{23}N_6$ $[M+H]^+$ *m/z* found 299.2001, cald 299.1984.

***N*$_1$,*N*$_1$-4-trimethyl-*N*$_2$-(3-methyl-[1,2,4]triazolo[3,4-a]phthalazin-6-yl)pentane-1,2-diamine (32)**

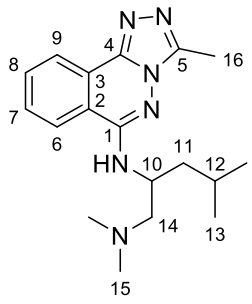

23 (300 mg, 1.372 mmol, 1 eq) and *N*$_1$, *N*$_1$,4-trimethylpentane-1,2-diamine (297 mg, 2.06 mmol, 1.5 eq) were reacted according to general procedure **A**. The crude material was purified by Isolera Biotage LPLC (DCM/MeOH 90:10 then DCM/MeOH/NH_3 9:1:0.5) to give **32** (183 mg, 0.561 mmol 41%) as a white solid.

Mpt: 172.4-174.4 °C; **ν_{max} (cm^{-1})** 3242, 2951, 2758, 1457, 1394, 1166, 1026; **^{1}H-NMR (400 MHz, $CDCl_3$): δ** 8.55 (dd, *J* = 7.9, 0.7 Hz, 1H, *H*-9), 7.85 (d, *J* = 8.2 Hz, 1H, *H*-6), 7.80 (m, 1H, *H*-8), 7.68 (m, 1H, *H*-7), 5.97 (d, *J*= 4.3 Hz, 1H, N*H*), 4.17 (m, 1H, *H*-10), 2.69 (s, 3H, *H*-16), 2.66 (m, 1H, *H*-14"), 2.51 (m, 1H, *H*-14'), 2.33 (s, 6H, *H*-15), 1.84 (m, 2H, *H*-11"; *H*-12), 1.40 (m, 1H, *H*-11'), 1.04 (d, *J*= 6.4 Hz, 3H, *H*-13"), 0.97 (d, *J*= 6.5 Hz, 3H, *H*-13'); **^{13}C-NMR (100 MHz $CDCl_3$): δ** 151.1 (*C*-1), 147.2 (*C*-4), 142.0 (*C*-5), 132.4 (*C*-8), 129.9 (*C*-7), 124.2 (*C*-9), 123.6 (*C*-3), 122.7 (*C*-6), 118.8 (*C*-2), 62.9 (*C*-14), 47.5 (*C*-10), 45.6 (*C*-15), 42.6 (*C*-11), 25.1 (*C*-12), 23.3 (*C*-13"), 22.6 (*C*-13'), 9.9 (*C*-16); **LR-ESI-MS:** $C_{18}H_{27}N_6$ $[M+H]^+$ *m/z* found 327.4, cald 327.2; **HR-ESI-MS:** $C_{18}H_{27}N_6$ $[M+H]^+$ *m/z* found 327.2319, cald 327.2297.

***N*$_1$,*N*$_1$-diethyl-*N*$_2$-(3-methyl-[1,2,4]triazolo[3,4-a]phthalazin-6-yl)propane-1,2-diamine (33)**

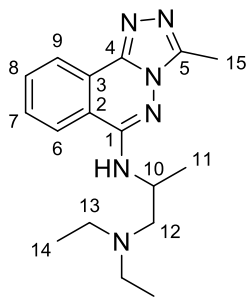

23 (400 mg, 1.829 mmol, 1 eq) and *N*$_1$, *N*$_1$-diethylpropane-1,2-diamine (477 mg, 0.571 mmol, 2 eq) were reacted according to general procedure **A**. The crude material was purified by Isolera Biotage LPLC (DCM/MeOH 90:10 then DCM/MeOH/NH_3 9:1:0.5) to give **33** (178 mg, 0.571 mmol

31%) as a white solid.

Mpt: 167.9-169.9 °C; **ν_{max} (cm^{-1})** 3243, 3070, 2965, 2930, 1592, 1293, 699; **^{1}H-NMR (400 MHz, DMSO-*d*^{6}): δ** 8.36 (m, 2H, *H*-6; *H*-9), 7.90 (m, 1H, *H*-8), 7.81 (m, 1H, *H*-7), 7.15 (s, 1H, N*H*), 4.21 (m, 1H, *H*-10), 2.63 (m, 5H, *H*-12"; *H*-13), 2.54 (s, 3H, *H*-15), 2.38 (m, 1H, *H*-12'), 1.32 (d, 3H, *J*= 6.5 Hz, *H*-11), 0.97 (s, 6H, *H*-14); **^{13}C-NMR (100 MHz, DMSO-*d*^{6}): δ** 150.7 (*C*-1), 145.9 (*C*-4), 141.0 (*C*-5), 132.7 (*C*-8), 130.0 (*C*-7), 124.3 (*C*-9), 123.4 (*C*-3), 122.4 (*C*-6), 118.3 (*C*-2), 57.7 (*C*-10), 47.2 (*C*-13), 45.5 (*C*-12), 18.3 (*C*-11), 12.0 (*C*-14), 9.3 (*C*-15); **LR-ESI-MS:** $C_{17}H_{25}N_6$ $[M+H]^+$ *m/z* found 313.3, cald 313.2; **HR-ESI-MS:** $C_{17}H_{25}N_6$ $[M+H]^+$ *m/z* found 313.2164, cald 313.2141.

***N*$_2$,*N*$_2$-dimethyl-*N*$_1$-(3-methyl-[1,2,4]triazolo[3,4-a]phthalazin-6-yl)propane-1,2-diamine (34)**

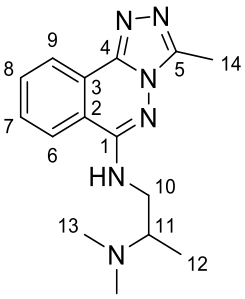

23 (200 mg, 0.915 mmol, 1 eq) and *N*$_2$,*N*$_2$-dimethylpropane-1,2-diamine (187 mg, 1.829 mmol, 2 eq) were reacted according to general procedure **A**. The crude material was purified by Isolera Biotage LPLC (DCM/MeOH 90:10 then DCM/MeOH/NH_3 9:1:0.5) to give **34** (45 mg, 0.159 mmol 17%) as a white solid.

Mpt: 227.1-229.1 °C; **ν_{max} (cm^{-1})** 3237, 3084, 2962, 1595, 1514, 770, 697; **^{1}H-NMR (400 MHz, DMSO-*d*^{6}): δ** 8.36 (d, 1H, *J*= 7.8 Hz, *H*-9), 8.29 (d, 1H, *J*= 8.1 Hz, *H*-6), 7.91 (m, 1H, *H*-8), 7.81 (m, 1H, *H*-7), 7.48 (t, 1H, *J*= 4.8 Hz, N*H*), 3.56 (dd, 1H, *J*= 12.9, 6.3 Hz, *H*-10"), 3.23 (dt, 1H, *J*= 13.1, 6.4 Hz, *H*-10'), 3.02 (m, 1H, *H*-11), 2.55 (s, 3H, *H*-14), 2.26 (s, 6H, *H*-12), 1.00 (d, 1H, *J*= 6.6 Hz, *H*-12); **^{13}C-NMR (100 MHz, DMSO-*d*^{6}): δ** 151.1 (*C*-1), 146.0 (*C*-4), 141.0 (*C*-5), 132.8 (*C*-8), 130.2 (*C*-7), 124.1 (*C*-9), 123.3 (*C*-3), 122.5 (*C*-6), 118.2 (*C*-2), 56.6 (*C*-11), 43.9 (*C*-10), 40.4 (*C*-13), 12.3 (*C*-12), 9.3 (*C*-14); **LR-ESI-MS:** $C_{15}H_{21}N_6$ $[M+H]^+$ *m/z* found 285.2, cald 285.2; **HR-ESI-MS:** $C_{15}H_{21}N_6$ $[M+H]^+$ *m/z* found 285.1841, cald 285.1828.

***N*$_2$,*N*$_2$-dimethyl-*N*$_1$-(3-methyl-[1,2,4]triazolo[3,4-a]phthalazin-6-yl)butane-1,2-diamine (35)**

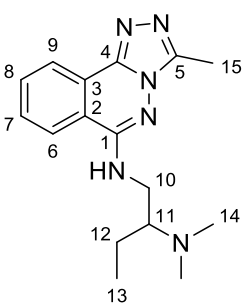

23 (200 mg, 0.915 mmol, 1 eq) and *N*$_2$,*N*$_2$-dimethylbutane-1,2-diamine (213 mg, 1.829 mmol, 2 eq) were reacted according to general procedure

A. The crude material was purified by Isolera Biotage LPLC (DCM/MeOH 90:10 then DCM/MeOH/NH_3 9:1:0.5) to give **35** (36 mg, 0.122 mmol 13%) as a white solid.

Mpt: 211.5-213.5 °C; **ν_{max} (cm^{-1})** 3227, 2927, 2776, 1510, 1451, 994, 698; **^{1}H-NMR (400 MHz, DMSO-d^6): δ** 8.37 (dd, 1H, *J*= 7.9, 0.9 Hz, *H*-9), 8.30 (d, 1H, *J*= 8.2 Hz, *H*-6), 7.91 (m, 1H, *H*-8), 7.81 (m, 1H, *H*-7), 7.52 (m, 1H, N*H*), 3.57 (m, 1H, *H*-11), 3.29 (m, 1H, *H*-10"), 2.82 (m, 1H, *H*-10'), 2.55 (s, 3H, *H*-15), 2.31 (s, 6H, *H*-14), 1.45 (m, 2H, *H*-12), 0.94 (t, 3H, *J*= 7.4 Hz, *H*-13); **^{13}C-NMR (100 MHz, DMSO-d^6): δ** 150.9 (*C*-1), 145.9 (*C*-4), 141.1 (*C*-5), 132.8 (*C*-8), 130.2 (*C*-7), 124.1 (*C*-9), 123.3 (*C*-3), 122.5 (*C*-6), 118.3 (*C*-2), 62.7 (*C*-11), 40.5 (*C*-10), 40.2 (*C*-14), 20.9 (*C*-12), 11.5 (*C*-13), 9.3 (*C*-15); **LR-ESI-MS:** $C_{16}H_{23}N_6$ $[M+H]^+$ *m/z* found 299.4, cald 299.2; **HR-ESI-MS:** $C_{16}H_{23}N_6$ $[M+H]^+$ *m/z* found 299.1990, cald 299.1984.

(*S*)-N_1,N_1-dimethyl-N2-(3-(trifluoromethyl)-[1,2,4]triazolo[3,4-a]phthalazin-6-yl)propane-1,2-diamine ((*S*)-36)

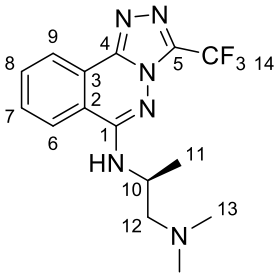

25 (85 mg, 0.312 mmol, 1 eq) and (*S*)-N_1,N_1-dimethylpropane-1,2-diamine (48 mg, 0.468 mmol, 1.5 eq) were reacted according to general procedure **A**. The crude material was purified by Isolera Biotage LPLC (DCM/MeOH 90:10 then DCM/MeOH/NH_3 9:1:0.5) to give (*S*)-**36** (67 mg, 0.199 mmol, 64%) as a white solid.

Mpt: 129.5-131.5 °C; ν_{max} (cm^{-1}) 3272, 2978, 1501, 1420, 1218, 1033, 979, 720; **^{19}F-NMR (376 MHz, $CDCl_3$): δ** -64.17; **^{1}H-NMR (400 MHz, $CDCl_3$): δ** 8.49 (dd, 1H, *J*= 8.1, 1 Hz, *H*-9), 7.90 (m, 2H, *H*-6; *H*-8), 7.82 (m, 1H, *H*-7), 6.52 (br-s, 1H, N*H*), 4.01 (m, 1H, *H*-10), 2.68 (m, 1H, *H*-12"), 2.42 (dd, 1H, *J*= 12.3, 4.9 Hz, *H*-12'), 2.33 (s, 6H, *H*-13), 1.41 (d, 3H, *J*= 6.1 Hz, *H*-11); **^{13}C-NMR (100 MHz $CDCl_3$): δ** 152.2 (*C*-1), 143.9 (*C*-4), 139.9 (q, *J*= 40.3 Hz, *C*-5), 132.9 (*C*-8), 131.3 (*C*-7), 124.3 (*C*-9), 123.1 (*C*-3), 122.9 (*C*-6), 119.2 (*C*-2), 118.6 (q, *J*= 270.0 Hz, *C*-14), 63.9 (*C*-10), 45.3 (*C*-13), 45.2 (*C*-12), 18.1 (*C*-11); **LR-ESI-MS:** $C_{15}H_{18}F_3N_6$ $[M+H]^+$ *m/z* found 339.1, cald 339.2; **HR-ESI-MS:** $C_{15}H_{18}F_3N_6$ $[M+H]^+$ *m/z* found 339.1553, cald 339.1545.

2-((3-methyl-[1,2,4]triazolo[3,4-a]phthalazin-6-yl)amino)-1-phenylethan-1-ol (74)

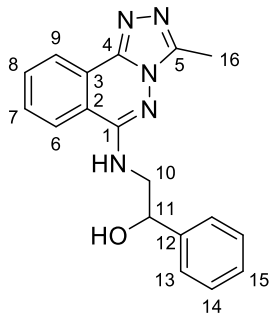

23 (10 g, 45.7 mmol, 1 eq) and 2-amino-1-phenylethan-1-ol (12.55 g, 91 mmol, 2 eq) were reacted according to general procedure **A**. After cooling to 4 °C a precipitate had formed which was washed according to **A** to give **74** as a white solid (9.6585 g, 30.2 mmol 66%).

Mpt: 172.1-174.1 °C; **ν_{max} (cm^{-1})** 3309, 3061, 1515, 1265, 1052, 759, 699, 558; **^{1}H-NMR (400 MHz, DMSO-*d*^{6}): δ** 8.37 (m, 2H, *H*-6; *H*-9), 7.92 (m, 1H, *H*-8), 7.84 (m, 2H, *H*-7; N*H*), 7.46 (d, *J*= 7.3 Hz, 2H, *H*-13), 7.35 (m, 2H, *H*-14), 7.25 (m, 1H, *H*-15), 5.55 (d, *J*= 4.3 Hz, 1H, O*H*), 5.12 (dt, *J*= 8.2, 4, 4 Hz, 1H, *H*-11), 3.71 (m, 1H, *H*-10"), 3.39 (m, 1H, *H*-10'), 2.60 (s, 3H, *H*-16); **^{13}C-NMR (100 MHz DMSO-*d*^{6}): δ** 151.1 (*C*-1), 145.9 (*C*-4), 144.1 (*C*-12), 141.1 (*C*-5), 132.8 (*C*-8), 130.2 (*C*-7), 128.1 (*C*-14), 126.9 (*C*-15), 125.8 (*C*-13), 124.3 (*C*-9), 123.3 (*C*-3), 122.4 (*C*-6), 118.3 (*C*-2), 69.4 (*C*-11), 50.0 (*C*-10), 9.4 (*C*-16); **LR-ESI-MS:** $C_{18}H_{18}N_5O$ $[M+H]^+$ *m/z* found 320.4, cald 320.2; **HR-ESI-MS:** $C_{18}H_{18}N_5O$ $[M+H]^+$ *m/z* found 320.1041, cald 320.1511.

3-methyl-*N*-((1-methylpyrrolidin-2-yl)methyl)-[1,2,4]triazolo[3,4-a]phthalazin-6-amine (75)

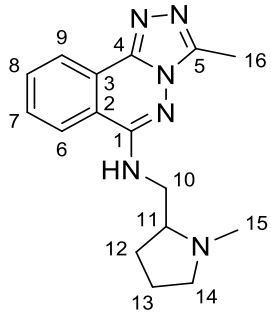

23 (200 mg, 0.915 mmol, 1 eq) and (1-methylpyrrolidin-2-yl)methanamine (209 mg, 1.829 mmol, 2 eq) were reacted according to general procedure **A**. The crude material was purified by Isolera Biotage LPLC (DCM/MeOH 90:10 then DCM/MeOH/NH_3 9:1:0.5) to give **75** (221 mg, 0.746 mmol 82%) as an off-white powder.

Mpt: 248.6-250.6 °C; ν_{max} (cm^{-1}) 3223, 3078, 2964, 2934, 2768, 1452, 698; **^{1}H-NMR (400 MHz, DMSO-*d*^{6}): δ** 8.34 (m, 2H, *H*-9; *H*-6), 7.92 (t *J*= 7.2 Hz, 1H, *H*-8), 7.82 (t, *J*= 7.2 Hz, 1H, *H*-7), 7.63 (s, 1H, N*H*), 3.68 (m, 1H, *H*-10'), 3.23 (m, 1H, *H*-10"), 3.17 (m, 1H, *H*-11), 2.98 (m, 2H, *H*-14), 2.56 (s, 3H, *H*-16), 2.41 (m, 3H, *H*-15), 2.16 (m, 1H, *H*-13'), 1.92 (m, 1H, *H*-12'), 1.66 (m, 2H, *H*-12"; *H*-13"); **^{13}C-NMR (100 MHz DMSO-*d*^{6}): δ** 151.2 (*C*-1), 145.9 (*C*-4), 141.1 (*C*-5), 132.8 (*C*-8), 130.2 (*C*-7), 124.1 (*C*-9), 123.3 (*C*-3), 122.5 (*C*-6), 118.2 (*C*-2), 63.1 (*C*-10), 56.9 (*C*-11), 45.1 (*C*-14), 40.9 (*C*-15), 29.6 (*C*-12), 22.4 (*C*-13), 9.3 (*C*-16); **LR-ESI-MS:** $C_{16}H_{21}N_6$ $[M+H]^+$ *m/z* found 297.4, cald 297.2; **HR-ESI-MS:** $C_{16}H_{21}N_6$ $[M+H]^+$ *m/z* found 297.1852, cald 297.1828.

3-methyl-*N*-(2-morpholinoethyl)-[1,2,4]triazolo[3,4-a]phthalazin-6-amine (76)

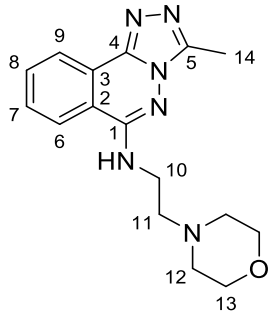

23 (200 mg, 0.915 mmol, 1 eq) and 2-morpholinoethan-1-amine (238 mg, 1.829 mmol, 2 eq) were reacted according to general procedure **A**. After cooling to 4 °C a precipitate had formed which was washed according to **A** to give **76** (58 mg, 0.185 mmol, 20%) as an off-white powder.

Mpt: 169.7-171.7 °C; **ν_{max} (cm^{-1})** 3219, 3071, 2946, 1594, 1552, 1112, 771; **^{1}H-NMR (400 MHz, DMSO-*d*^{6}): δ** 8.36 (d, *J* = 8.6 Hz, 1H, *H*-9), 8.26 (d *J*= 8.1 Hz, 1H, *H*-6), 7.90 (t, *J*= 7.2 Hz, 1H, *H*-8), 7.80 (m, 1H, *H*-7), 7.56 (t, *J*= 5.3 Hz, 1H, N*H*), 3.58 (m, 6H, *H*-10; *H*-13), 2.64 (t, *J*=7 Hz, 2H, *H*-11), 2.55 (s, 3H, *H*-14), 2.48 (m, 4H, *H*-12); **^{13}C-NMR (100 MHz DMSO-*d*^{6}): δ** 151.1 (*C*-1), 146.0 (*C*-4), 141.1 (*C*-5), 132.8 (*C*-8), 130.2 (*C*-7), 124.1 (*C*-9), 123.3 (*C*-3), 122.5 (*C*-6), 118.2 (*C*-2), 66.3 (*C*-13), 56.3 (*C*-12), 53.4 (*C*-11), 38.4 (*C*-10), 9.3 (*C*-14); **LR-ESI-MS:** $C_{16}H_{21}N_6O$ $[M+H]^+$ *m/z* found 313.4, cald 313.2; **HR-ESI-MS:** $C_{16}H_{21}N_6O$ $[M+H]^+$ *m/z* found 313.1812, cald 313.1777.

3-methyl-*N*-((tetrahydro-2H-pyran-3-yl)methyl)-[1,2,4]triazolo[3,4-a]phthalazin-6-amine (77)

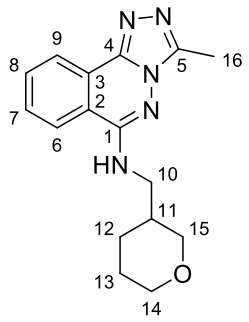

23 (100 mg, 0.457 mmol, 1 eq) and (tetrahydro-2H-pyran-3-yl)methanamine (105 mg, 0.915 mmol, 2 eq) were reacted according to general procedure **A**. The crude material was purified by Isolera Biotage LPLC (DCM/MeOH 90:10 then DCM/MeOH/NH_3 9:1:0.5) to give **77** (41 mg, 0.138 mmol 30%) as an off-white powder.

Mpt: 156.6-158.6 °C; **ν_{max} (cm^{-1})** 3250, 3923, 2849, 1567, 1483, 770; **^{1}H-NMR (400 MHz, DMSO-*d*^{6}): δ** 8.35 (t, *J* = 8.6 Hz, 2H, *H*-6; *H*-9), 7.9 (m, 1H, *H*-8), 7.8 (m, 1H, *H*-7), 7.6 (t, *J*= 5.3 Hz, 1H, N*H*), 3.87 (m, 1H, *H*-15"), 3.72 (m, 1H, *H*-15'), 3.33 (m, 1H, *H*-14"), 3.21 (m, 1H, *H*-14'), 2.55 (s, 3H, *H*-16), 2.09 (m, 1H, *H*-13"), 1.84 (m, 1H, *H*-13'), 1.61 (m, 1H, *H*-12"), 1.49 (m, 1H, *H*-12'), 1.33 (m, 1H, *H*-11); **^{13}C-NMR (100 MHz DMSO-*d*^{6}): δ** 151.3 (*C*-1), 146.0 (*C*-4), 141.1 (*C*-5), 132.7 (*C*-8), 130.1 (*C*-7), 124.2 (*C*-9), 123.3 (*C*-3), 122.4 (*C*-6), 118.2 (*C*-2), 70.9 (*C*-15), 67.5 (*C*-14), 54.9 (*C*-10),

34.8 (*C*-11), 27.4 (*C*-12), 24.9 (*C*-13), 9.3 (*C*-16); **LR-ESI-MS:** $C_{19}H_{20}N_2O$ $[M+H]^+$ *m/z* found 298.4, cald 298.2; **HR-ESI-MS:** $C_{19}H_{20}N_2O$ $[M+H]^+$ *m/z* found 298.1703, cald 298.1668.

1-methyl-3-((3-methyl-[1,2,4]triazolo[3,4-a]phthalazin-6-yl)amino)piperidin-2-one (78)

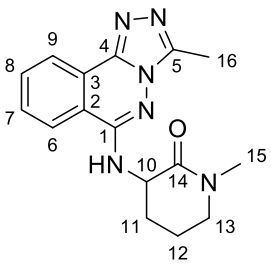

23 (100 mg, 0.457 mmol, 1 eq) and 3-amino-1-methylpiperidin-2-one (117 mg, 0.915 mmol, 2 eq) were reacted according to general procedure **A**. The crude material was purified by Isolera Biotage LPLC (DCM/MeOH 90:10 then DCM/MeOH/NH_3 9:1:0.5) to give **78** (53 mg, 0.172 mmol 38%) as a white solid.

Mpt: 229.5-231.5 °C; **ν_{max} (cm^{-1})** 3259, 3077, 2941, 1595, 1504, 1270, 658; **^{1}H-NMR (400 MHz, DMSO-*d*^{6}): δ** 8.34 (d J= 7.2 Hz, 1H, *H*-6), 8.28 (d, J= 8.2 Hz, 1H, *H*-9), 7.99 (d, J= 7.3 Hz, 1H, N*H*), 7.87 (t, J= 7.6 Hz, 1H, *H*-8), 7.76 (m, 1H, *H*-7), 4.36 (dt, J= 11.2, 6.6 Hz, 1H, *H*-10), 3.43 (m, 1H, *H*-13"), 3.37 (s, 3H, *H*-15), 3.35 (m, 1H, *H*-13'), 2.89 (s, 3H, *H*-16), 2.22 (m, 1H, *H*-12"), 2.09 (m, 1H, *H*-12'), 1.92 (m, 2H, *H*-11); **^{13}C-NMR (100 MHz DMSO-*d*^{6}): δ** 168.4 (*C*-14), 150.3 (*C*-1), 145.8 (*C*-4), 141.0 (*C*-5), 132.8 (*C*-8), 130.1 (*C*-7), 124.2 (*C*-9), 123.3 (*C*-3), 122.4 (*C*-6), 118.2 (*C*-2), 51.8 (*C*-10), 49.5 (*C*-15), 34.4 (*C*-13), 26.5 (*C*-11), 21.3 (*C*-12), 9.3 (*C*-16); **LR-ESI-MS:** $C_{16}H_{19}N_6O$ $[M+H]^+$ m/z found 311.4, cald 311.2; **HR-ESI-MS:** $C_{16}H_{19}N_6O$ $[M+H]^+$ m/z found 311.1663, cald 311.1620.

2-((3-methyl-[1,2,4]triazolo[3,4-a]phthalazin-6-yl)amino)-2-phenylethan-1-ol (79)

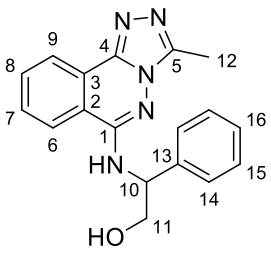

23 (100 mg, 0.457 mmol, 1 eq) and 2-amino-2-phenylethan-1-ol (125 mg, 0.915 mmol, 2 eq) were reacted according to general procedure **A**. After cooling to 4 °C a precipitate had formed which was washed according to **A** to give **79** (43 mg, 0.133 mmol, 29%).

Mpt: 171.3-173.3 °C; **ν_{max} (cm^{-1})** 3215, 2924, 1544, 1474, 1036, 760, 773; **^{1}H-NMR (400 MHz, DMSO-*d*^{6}): δ** 8.56 (d, *J* = 7.9 Hz, 1H, *H*-6), 8.36 (d, *J* = 8.9 Hz, 1H, *H*-9), 7.88 (m, 3H, N*H*; *H*-8 & *H*-7), 7.49 (d, *J*= 7.2 Hz, 2H, *H*-14), 7.31 (t, *J*=7.5 Hz, 2H, *H*-15), 7.21 (m, 1H, *H*-16), 5.12 (m, 1H, *H*-10), 5.04 (t, *J*= 5.8 Hz, 1H, O*H*), 3.91 (ddd, *J*= 11.1, 8.4, 5.7 Hz, 1H, *H*-11") 3.73 (dt, *J*= 11.1, 5.5 Hz, 1H, *H*-11'), 2.45 (s, 3H, *H*-12); **^{13}C-NMR (100 MHz DMSO-*d*^{6}): δ** 150.7 (*C*-1), 145.9 (*C*-4), 141.4 (*C*-

5), 140.9 (*C*-13), 132.9 (*C*-8), 130.1 (*C*-7), 128.0 (*C*-15), 127.3 (*C*-14), 126.9 (*C*-16), 124.6 (*C*-6), 123.3 (*C*-3), 122.5 (*C*-9), 118.2 (*C*-2), 64.5 (*C*-10), 58.3 (*C*-11), 9.2 (*C*-12); **LR-ESI-MS:** $C_{18}H_{18}N_5O$ $[M+H]^+$ *m/z* found 320.4, cald 320.2; **HR-ESI-MS:** $C_{18}H_{18}N_5O$ $[M+H]^+$ *m/z* found 320.1530, cald 320.1511.

***N*-((1-ethylpyrrolidin-2-yl)methyl)-3-methyl-[1,2,4]triazolo[3,4-a]phthalazin-6-amine (80)**

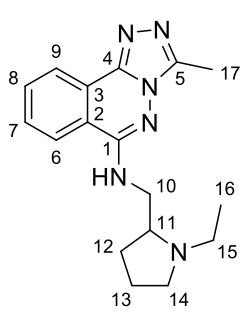

23 (200 mg, 0.915 mmol, 1 eq) and (1-ethylpyrrolidin-2-yl)methanamine (235 mg, 1.829 mmol, 2 eq) were reacted according to general procedure **A**. The crude material was purified by Isolera Biotage LPLC (DCM/MeOH 90:10 then DCM/MeOH/NH_3 9:1:0.5) to give **80** (138 mg, 0.445 mmol 49%) as a yellow solid.

Mpt: 219.4-221.4 °C; **ν_{max} (cm^{-1})** 3227, 3070, 2960, 2772, 1482, 779; **^{1}H-NMR (400 MHz, DMSO-d^6): δ** 8.36 (d, *J* = 7.8 Hz, 1H, *H*-9), 8.3 (d, *J*= 8.1 Hz, 1H, *H*-6), 7.9 (m, 1H, *H*-8), 7.8 (m, 1H, *H*-7), 7.67 (m, 1H, N*H*), 4.11 (s, 1H, *H*-10"), 3.63 (m, 1H, *H*-10'), 3.17 (m, 2H, *H*-15), 3.07 (m, 1H, *H*-11), 2.99 (m, 1H, *H*-14"), 2.91 (m, 1H, *H*-14'), 2.54 (s, 3H, *H*-17), 2.38 (m, 1H, *H*-12"), 2.18 (m, 1H, *H*-12'), 1.85 (m, 1H, *H*-13"), 1.68 (m, 1H, *H*-13'), 1.09 (t, *J*= 7.2 Hz, 3H, *H*-16); **^{13}C-NMR (100 MHz $CDCl_3$): δ** 151.2 (*C*-1), 145.9 (*C*-4), 141.1 (*C*-5), 132.8 (*C*-8), 130.2 (*C*-7), 124.1 (*C*-9), 123.3 (*C*-3), 122.5 (*C*-6), 118.2 (*C*-2), 61.2 (*C*-11), 53.3 (*C*-14), 48.6 (*C*-15), 48.3 (*C*-10), 29.1 (*C*-12), 22.5 (*C*-13), 13.8 (*C*-16), 9.3 (*C*-17); **LR-ESI-MS:** $C_{17}H_{23}N_6$ $[M+H]^+$ *m/z* found 311.4, cald 311.2; **HR-ESI-MS:** $C_{17}H_{23}N_6$ $[M+H]^+$ *m/z* found 311.2000, cald 311.1984.

(*S*)-*N*-(1-benzylpiperidin-3-yl)-3-methyl-[1,2,4]triazolo[3,4-a]phthalazin-6-amine (81)

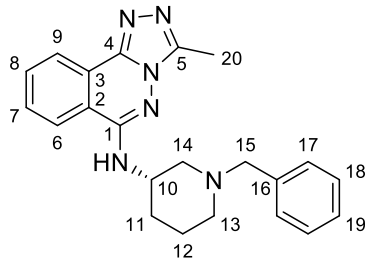

23 (400 mg, 1.829 mmol, 1 eq) and (S)-1-benzylpiperidin-3-amine (522 mg, 2.74 mmol, 1.5 eq) were reacted according to general procedure **A**. The crude material was purified by Isolera Biotage LPLC (DCM/MeOH 90:10 then DCM/MeOH/NH_3 9:1:0.5) to give **81** (200 mg, 0.537 mmol 29%) as a yellow solid.

Mpt: 132.6-134.6 °C; **ν_{max} (cm^{-1})** 3336, 2930, 2795, 1590, 1513; **^{1}H-NMR (400 MHz, DMSO-*d*^{6}): δ** 8.34 (m, 2H, *H*-9; *H*-6), 7.88 (m, 1H, *H*-8), 7.78 (td, *J* = 7.7, 1.3 Hz, 1H, *H*-8), 7.31 (m, 4H, *H*-17; *H*-18), 7.21 (m, 1H, *H*-19), 7.12 (d, *J*= 7.3 Hz, 1H, N*H*), 4.05 (m, 1H, *H*-10), 3.62 (d, *J*= 13.3 Hz, 1H, *H*-15"), 3.39 (d, *J*= 13.3 Hz, 1H, *H*-15'), 3.16 (m, 1H, *H*-14"), 2.81 (m, 1H, *H*-14'), 2.43 (s, 3H, *H*-20), 2.02 (m, 2H, *H*-13), 1.86 (t, *J*= 10 Hz, 1H, *H*-12"), 1.74 (m, 1H, *H*-11"), 1.62 (m, 1H, *H*-11'), 1.5 (m, 1H, *H*-12'); **^{13}C-NMR (100 MHz, DMSO-*d*^{6}): δ** 150.4 (*C*-1), 145.9 (*C*-4), 141.0 (*C*-5), 138.5 (*C*-16), 132.8 (*C*-8), 130.0 (*C*-7), 128.7 (*C*-17), 128.1 (*C*-18), 126.8 (*C*-19), 124.4 (*C*-9), 123.3 (*C*-3), 122.4 (*C*-6), 118.1 (*C*-2), 62.1 (*C*-15), 56.9 (*C*-14), 53.6 (*C*-13), 48.3 (*C*-10), 29.5 (*C*-11), 24.1 (*C*-12), 9.2 (*C*-20); **LR-ESI-MS:** $C_{22}H_{25}N_6$ $[M+H]^+$ *m/z* found 373.3, cald 373.2; **HR-ESI-MS:** $C_{22}H_{25}N_6$ $[M+H]^+$ *m/z* found 373.2173, cald 373.2141.

1-(3-methoxyphenyl)-4-((3-methyl-[1,2,4]triazolo[3,4-a]phthalazin-6-yl)amino)pyrrolidin-2-one (82)

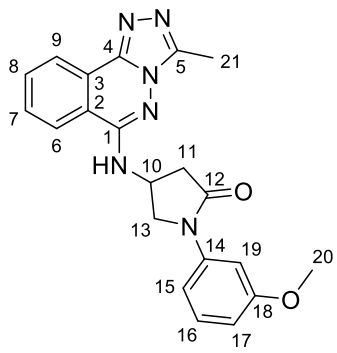

23 (400 mg, 1.829 mmol, 1 eq) and 4-amino-1-(3-methoxyphenyl)pyrrolidin-2-one (566 mg, 2.74 mmol, 1.5 eq) were reacted according to general procedure **A**. The crude material was purified by Isolera Biotage LPLC (DCM/MeOH 90:10 then DCM/MeOH/NH_3 9:1:0.5) to give **82** (61 mg, 0.157 mmol 9%) as a brown solid.

Mpt: 249.9-251.1 °C; **ν_{max} (cm^{-1})** 3250, 2929, 1697, 1592, 1498, 1317, 1212, 1043, 765, 701; **^{1}H-NMR (400 MHz, DMSO-*d*^{6}): δ** 8.34 (m, 2H, *H*-6; *H*-9), 7.88 (m, 2H, *H*-7; *H*-8), 7.76 (m, 1H, N*H*), 7.74 (m, 1H, *H*-19), 7.26 (m, 1H, *H*-16), 7.20 (m, 1H, *H*-15), 6.71 (dt, 1H, *J*= 8, 1.2 Hz, *H*-17), 4.67 (s, 1H, *H*-10), 4.30 (dd, 1H, *J*= 10.4, 7.1 Hz, *H*-13"), 3.97 (dd, 1H, *J*= 10.5, 3.2 Hz, *H*-13'), 3.73 (s, 3H, *H*-20), 3.10 (dd, 1H, *J*= 17.4, 8.4 Hz, *H*-11"), 2.81 (dd, 1H, *J*= 17.5, 3.9 Hz, *H*-11'), 2.55 (s, 3H, *H*-21); **^{13}C-NMR (100 MHz, DMSO-*d*^{6}): δ** 172.17 (*C*-12), 159.4 (*C*-18), 150.6 (*C*-1), 146.1 (*C*-4), 141.0 (*C*-5), 140.5 (*C*-14), 132.8 (*C*-8), 129.9 (*C*-7), 129.4 (*C*-19, 124.4 (*C*-9), 123.3 (*C*-3), 122.4 (*C*-6), 118.1 (*C*-2), 111.6 (*C*-16), 109.2 (*C*-15), 105.6 (*C*-17), 55.1 (*C*-20), 53.9 (*C*-10), 44.1 (*C*-11), 38.6

(*C*-13), 9.3 (*C*-21); **LR-ESI-MS:** $C_{21}H_{21}N_6O_2$ $[M+H]^+$ *m/z* found 389.2, cald 389.1; **HR-ESI-MS:** $C_{21}H_{21}N_6O_2$ $[M+H]^+$ *m/z* found 389.1742, cald 389.1726.

3-methyl-*N*-((4-methylmorpholin-3-yl)methyl)-[1,2,4]triazolo[3,4-a]phthalazin-6-amine (83)

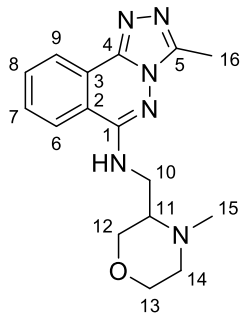

23 (200 mg, 0.915 mmol, 1 eq) and (4-methylmorpholin-3-yl)methanamine (238 mg, 1.829 mmol, 1.5 eq) were reacted according to general procedure **A**. The crude material was purified by Isolera Biotage LPLC (DCM/MeOH 90:10 then DCM/MeOH/NH_3 9:1:0.5) to give **83** (97 mg, 0.310 mmol 34%) as a white solid.

Mpt: 172.7-174.7 °C; **ν_{max} (cm^{-1})** 3224, 3069, 2924, 2857, 2792, 1565, 1513, 1124, 699; **^{1}H-NMR (400 MHz, DMSO-*d*^{6}): δ** 8.36 (d, 1H, *J*= 7.7 Hz, *H*-9), 8.29 (d, 1H, *J*= 8.1 Hz, *H*-6), 7.91 (t, 1H, *J*= 7.6 Hz, *H*-8), 7.80 (m, 1H, *H*-7), 7.61 (t, 1H, *J*= 5.4 Hz, N*H*), 3.80 (m, 2H, *H*-12"; *H*-13"), 3.66 (m, 1H, *H*-12'), 3.52 (m, 1H, *H*-13'), 3.33 (m, 1H, *H*-10"), 3.19 (m, 1H, *H*-10'), 2.66 (m, 1H, *H*-11), 2.56 (s, 3H, *H*-16), 2.51 (m, 1H, *H*-14"), 2.40 (s, 3H, *H*-15), 2.21 (m, 1H, *H*-14'); **^{13}C-NMR (100 MHz, DMSO-*d*^{6}): δ** 151.1 (*C*-1), 145.9 (*C*-4), 141.1 (*C*-5), 132.9 (*C*-8), 130.2 (*C*-7), 124.2 (*C*-9), 123.3 (*C*-3), 122.5 (*C*-6), 118.2 (*C*-2), 69.6 (*C*-12), 66.2 (*C*-13), 60.3 (*C*-11), 54.4 (*C*-14), 42.8 (*C*-10), 39.5 (*C*-15), 9.3 (*C*-16); **LR-ESI-MS:** $C_{16}H_{21}N_6O$ $[M+H]^+$ *m/z* found 313.2, cald 313.2; **HR-ESI-MS:** $C_{16}H_{21}N_6O$ $[M+H]^+$ *m/z* found 313.1797, cald 313.1777.

3-methyl-*N*-(2-(pyrrolidin-1-yl)ethyl)-[1,2,4]triazolo[3,4-a]phthalazin-6-amine acetate (84)

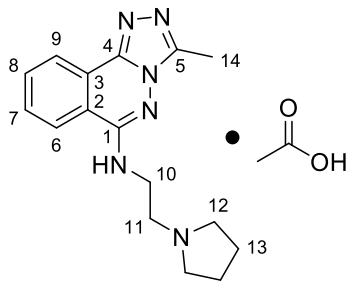

23 (200 mg, 0.915 mmol, 1 eq) and 2-(pyrrolidin-1-yl)ethan-1-amine (209 mg, 1.829 mmol, 1.5 eq) were reacted according to general procedure **A**. After cooling to 4 °C a precipitate had formed which was washed according to **A** and then co-evaporated with AcOH to give **84** as an AcOH salt (101 mg, 0.283 mmol, 31%).

Mpt: 172.4-174.4 °C; **ν_{max} (cm^{-1})** 3449, 3261, 2693, 2615, 1516, 701; **^{1}H-NMR (400 MHz, MeOD-*d*^{4}): δ** 8.33 (d, 1H, *J*= 7.9 Hz, *H*-9), 8.18 (d, 1H, *J*= 8.2 Hz, *H*-6), 7.89 (m, 1H, *H*-8), 7.81 (m, 1H, *H*-7),

3.96 (t, 2H, *J*= 5.9 Hz, *H*-10), 3.69 (t, 2H, *J*= 5.9 Hz, *H*-11), 3.50 (br s, 4H, *H*-12), 2.64 (s, 3H, *H*-14), 2.16 (s, 4H, *H*-13); **^{13}C-NMR (100 MHz, MeOD-*d*^{4}): δ** 152.1 (*C*-1), 147.2 (*C*-4), 141.8 (*C*-5), 132.9 (*C*-8), 130.8 (*C*-7), 123.8 (*C*-9), 122.7 (*C*-3), 122.6 (*C*-6), 118.6 (*C*-2), 54.1 (*C*-12), 52.9 (*C*-11), 37.7 (*C*-10), 22.6 (*C*-13), 8.1 (*C*-14); **LR-ESI-MS:** $C_{16}H_{21}N_6$ $[M+H]^+$ *m/z* found 297.2, cald 297.2; **HR-ESI-MS:** $C_{16}H_{21}N_6$ $[M+H]^+$ *m/z* found 297.1852, cald 297.1828.

3-methyl-*N*-((1-methylpiperidin-2-yl)methyl)-[1,2,4]triazolo[3,4-a]phthalazin-6-amine (85)

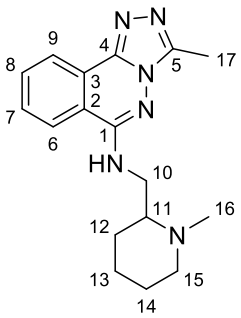

23 (200 mg, 0.915 mmol, 1 eq) and (1-methylpiperidin-2-yl)methanamine (235 mg, 1.829 mmol, 1.5 eq) were reacted according to general procedure **A**. The crude material was purified by Isolera Biotage LPLC (DCM/MeOH 90:10 then DCM/MeOH/NH_3 9:1:0.5) to give **85** (147 mg, 0.475 mmol 52%) as a white solid.

Mpt: 171.6-173.6 °C; **ν_{max} (cm^{-1})** 3231, 3071, 2928, 1565, 1511, 1267, 698; **^{1}H-NMR (400 MHz, DMSO-*d*^{6}): δ** 8.37 (dd, 1H, *J*= 7.9, 1 Hz, *H*-9), 8.31 (d, 1H, *J*= 8.2 Hz, *H*-6), 7.91 (m, 1H, *H*-8), 7.81 (td, 1H, *J*= 7.8, 1.3 Hz, *H*-7), 7.56 (t, 1H, *J*= 5 Hz, N*H*), 4.11 (s, 1H, *H*-11), 3.79 (m, 1H, *H*-10"), 3.26 (m, 1H, *H*-10'), 2.80 (d, 1H, *J*= 11.2 Hz, *H*-12"), 2.55 (s, 3H, *H*-17), 2.38 (s, 3H, *H*-16), 2.09 (m, 1H, *H*-12'), 1.8-1.1 (m, 6H, *H*-13; *H*-14; *H*-15); **^{13}C-NMR (100 MHz, DMSO-*d*^{6}): δ** 151.1 (*C*-1), 145.9 (*C*-4), 141.1 (*C*-5), 132.8 (*C*-8), 130.2 (*C*-7), 124.1 (*C*-9), 123.3 (*C*-3), 122.5 (*C*-6), 118.2 (*C*-2), 61.4 (*C*-11), 56.1 (*C*-15), 54.9 (*C*-10), 48.6 (*C*-16), 43.8 (*C*-12), 25.1 (*C*-14), 23.3 (*C*-13), 9.3 (*C*-17); **LR-ESI-MS:** $C_{17}H_{23}N_6$ $[M+H]^+$ *m/z* found 311.4, cald 311.2; **HR-ESI-MS:** $C_{17}H_{23}N_6$ $[M+H]^+$ *m/z* found 311.2006, cald 311.1984.

***N*-((1*S**, 2*S**, 4*R**)-bicyclo[2.2.1]heptan-2-yl)-3-methyl-[1,2,4]triazolo[3,4-a]phthalazin-6-amine (86)**

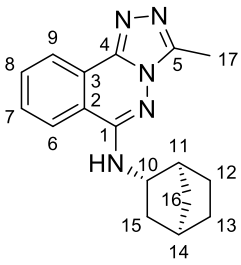

23 (100 mg, 0.457 mmol, 1 eq) and *rac*-(1*S*,2*S*,4*R*)-bicyclo[2.2.1]heptan-2-amine (102 mg, 0.915 mmol, 2 eq) were reacted according to general procedure **A**. The crude material was purified by Isolera Biotage LPLC

(DCM/MeOH 90:10 then DCM/MeOH/NH_3 9:1:0.5) to give **86** (20 mg, 0.068 mmol 15%) as a white crystalline solid.

Mpt: 256.2-258.2 °C; **ν_{max} (cm^{-1})** 3273, 2944, 1502, 769; **^{1}H-NMR (400 MHz, DMSO-d^6): δ** 8.48 (d, 1H, *J*= 8.2 Hz, *H*-9), 8.35 (dd, 1H, *J*= 7.9, 0.8 Hz, *H*-6), 7.89 (m, 1H, *H*-8), 7.79 (m, 1H, *H*-7), 7.13 (d, 1H, *J*= 5.5 Hz, N*H*), 3.75 (m, 1H, *H*-10), 2.55 (s, 3H, *H*-17), 2.46 (m, 1H, *H*-11), 2.27 (m, 1H, *H*-14), 1.8-1.4 (m, 5H, *H*-12"; *H*-15; *H*-16), 1.3-1.1 (m, 3H, *H*-12'; *H*-13); **^{13}C-NMR (100 MHz, DMSO-d^6): δ** 150.5 (*C*-1), 145.9 (*C*-4), 140.9 (*C*-5), 132.6 (*C*-8), 129.9 (*C*-7), 124.6 (*C*-9), 123.3 (*C*-3), 122.3 (*C*-6), 118.3 (*C*-2), 55.2 (*C*-10), 40.6 (*C*-15), 38.5 (*C*-12), 35.2 (*C*-14), 35.1 (*C*-11), 28.1 (*C*-13), 26.3 (*C*-16), 9.2 (*C*-17); **LR-ESI-MS:** $C_{17}H_{20}N_5$ $[M+H]^+$ *m/z* found 294.4, cald 294.2; **HR-ESI-MS:** $C_{17}H_{20}N_5$ $[M+H]^+$ *m/z* found 294.1744, cald 294.1719.

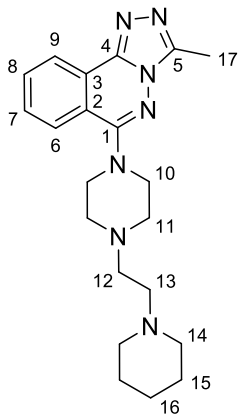

3-methyl-6-(4-(2-(piperidin-1-yl)ethyl)piperazin-1-yl)-[1,2,4]triazolo[3,4-a]phthalazine (87)

23 (200 mg, 0.915 mmol, 1 eq) and 1-(2-(piperidin-1-yl)ethyl)piperazine (361 mg, 1.829 mmol, 2 eq) were reacted according to general procedure **A**. The crude material was purified by Isolera Biotage LPLC (DCM/MeOH 90:10 then DCM/MeOH/NH_3 9:1:0.5) to give **87** (180 mg, 0.475 mmol 52%) as a white solid.

Mpt: 228.6-230.6 °C; **ν_{max} (cm^{-1})** 3254, 2932, 2643, 2550, 1654, 1477, 989, 792; **^{1}H-NMR (400 MHz, $CDCl_3$): δ** 8.60 (d, 1H, *J*= 7.7 Hz, *H*-9), 8.00 (d, 1H, *J*= 8.2 Hz, *H*-6), 7.84 (t, 1H, *J*= 7.3 Hz, *H*-8), 7.72 (m, 1H, *H*-7), 3.42 (br-s, 4H, *H*-10), 2.94 (br-s, 6H, *H*-11; *H*-12; *H*-13), 2.82 (br-s, 4H, *H*-14), 1.92 (br-s, 4H, *H*-15), 1.60 (br-s, 2H, *H*-16); **^{13}C-NMR (100 MHz, $CDCl_3$): δ** 157.5 (*C*-1), 147.6 (*C*-4), 142.5 (*C*-5), 132.9 (*C*-8), 129.9 (*C*-7), 126.3 (*C*-9), 125.0 (*C*-3), 123.8 (*C*-6), 119.9 (*C*-2), 54.5 (*C*-10), 52.9 (*C*-11), 51.1 (*C*-12; *C*-13), 26.9 (*C*-14), 23.8 (*C*-15), 22.9 (*C*-16); **LR-ESI-MS:** $C_{21}H_{30}N_7$ $[M+H]^+$ *m/z* found 380.3, cald 380.3; **HR-ESI-MS:** $C_{21}H_{30}N_7$ $[M+H]^+$ *m/z* found 380.2583, cald 380.2563.

***N*-((1-ethylpiperidin-2-yl)methyl)-3-methyl-[1,2,4]triazolo[3,4-a]phthalazin-6-amine (88)**

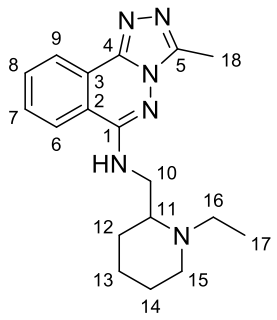

23 (200 mg, 0.915 mmol, 1 eq) and (1-ethylpiperidin-2-yl)methanamine (260 mg, 1.829 mmol, 2 eq) were reacted according to general procedure **A**. The crude material was purified by Isolera Biotage LPLC (DCM/MeOH 90:10 then DCM/MeOH/NH_3 9:1:0.5) to give **88** (99 mg, 0.307 mmol 34%) as a white solid.

Mpt: 169.0-171.0 °C; **ν_{max} (cm^{-1})** 3250, 2946, 2660, 1510, 1339, 1212, 627, 573; **^{1}H-NMR (400 MHz, DMSO-*d*^{6}): δ** 8.46 (d, 1H, *J*= 8.1 Hz, *H*-9), 8.37 (d, 1H, *J*= 7.7 Hz, *H*-6), 8.23 (m, 1H, N*H*), 7.92 (t, 1H, *J*= 7.5 Hz, *H*-8), 7.81 (m, 1H, *H*-7), 4.01 (m, 1H, *H*-11), 3.95-3.5 (m, 2H, *H*-10), 3.44 (m, 1H, *H*-15"), 3.07 (m, 1H, *H*-15'), 2.56 (s, 3H, *H*-18), 2.06 (m, 1H, *H*-12"), 2.0-1.7 (m, 4H, *H*-12'; *H*-14"; *H*-16), 1.49 (m, 1H, *H*-13"), 1.29 (m, 3H, *H*-13'; *H*-17); **^{13}C-NMR (100 MHz, DMSO-*d*^{6}): δ** 151.1 (*C*-1), 146.1 (*C*-4), 141.1 (*C*-5), 133.1 (*C*-8), 130.3 (*C*-7), 124.5 (*C*-9), 123.4 (*C*-3), 122.5 (*C*-6), 118.1 (*C*-2), 58.9 (*C*-11), 50.7 (*C*-11), 47.2 (*C*-15), 42.1 (*C*-16), 27.2 (*C*-12), 22.2 (*C*-14), 21.4 (*C*-13), 9.5 (*C*-18), 7.8 (*C*-17); **LR-ESI-MS:** $C_{18}H_{25}N_6$ $[M+H]^+$ *m/z* found 325.3, cald 325.2; **HR-ESI-MS:** $C_{18}H_{25}N_6$ $[M+H]^+$ *m/z* found 325.2160, cald 325.2141.

(*R*)-*N*-(1-benzylpiperidin-3-yl)-3-methyl-[1,2,4]triazolo[3,4-a]phthalazin-6-amine (89)

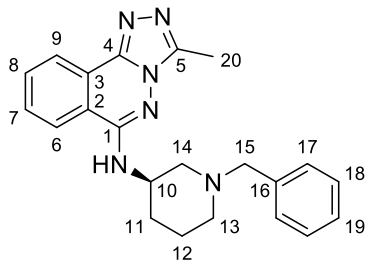

23 (400 mg, 1.829 mmol, 1 eq) and (R)-1-benzylpiperidin-3-amine (522 mg, 2.74 mmol, 1.5 eq) were reacted according to general procedure **A**. The crude material was purified by Isolera Biotage LPLC (DCM/MeOH 90:10 then DCM/MeOH/NH_3 9:1:0.5) to give **89** (153 mg, 0.411 mmol 23%) as a white solid.

Mpt: 122.5-124.5 °C; **ν_{max} (cm^{-1})** 3344, 2930, 2802, 1528, 1512, 1158, 733, 658; **^{1}H-NMR (400 MHz, DMSO-*d*^{6}): δ** 8.34 (m, 2H, *H*-6; *H*-9), 7.89 (m, 1H, *H*-8), 7.78 (td, 1H, *J*= 7.7, 1.3 Hz, *H*-7), 7.31 (m, 4H, *H*-17; *H*-18), 7.23 (m, 1H, *H*-19), 7.13 (d, 1H, *J*= 7.3 Hz, N*H*), 4.09 (m, 1H, *H*-10), 3.63 (d, 1H, *J*= 13.3 Hz, *H*-15"), 3.40 (d, 1H, *J*= 13.3 Hz, *H*-15'), 3.18 (d, 1H, *J*= 7.7 Hz, *H*-14"), 2.82 (d, 1H, *J*= 11 Hz, *H*-14'), 2.44 (s, 3H, *H*-20), 2.02 (m, 2H, *H*-13), 1.86 (m, 1H, *H*-12"), 1.74 (m, 1H, *H*-11"), 1.62 (m, 1H, *H*-11'), 1.5 (m, 1H, *H*-12'); **^{13}C-NMR (100 MHz, DMSO-*d*^{6}): δ** 150.4 (*C*-1), 145.9

(*C*-4), 141.0 (*C*-5), 138.5 (*C*-16), 132.8 (*C*-8), 130.0 (*C*-7), 128.7 (*C*-17), 128.1 (*C*-18), 126.8 (*C*-19), 124.4 (*C*-9), 123.3 (*C*-3), 122.4 (*C*-6), 118.1 (*C*-2), 62.1 (*C*-15), 56.9 (*C*-14), 53.6 (*C*-13), 48.3 (*C*-10), 29.5 (*C*-11), 24.1 (*C*-12), 9.2 (*C*-20); **LR-ESI-MS:** $C_{22}H_{24}N_6$ $[M+H]^+$ *m/z* found 373.3, cald 373.2; **HR-ESI-MS:** $C_{22}H_{24}N_6$ $[M+H]^+$ *m/z* found 373.2173, cald 373.2141.

benzyl (*R*)-3-((3-methyl-[1,2,4]triazolo[3,4-a]phthalazin-6-yl)amino)piperidine-1-carboxylate (90)

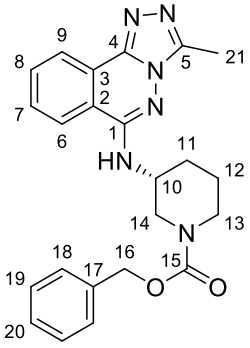

23 (300 mg, 1.372 mmol, 1 eq) and benzyl (*R*)-3-aminopiperidine-1-carboxylate (482 mg, 2.058 mmol, 1.5 eq) were reacted according to general procedure **A**. The crude material was purified by Isolera Biotage LPLC (DCM/MeOH 90:10 then DCM/MeOH/NH_3 9:1:0.5) to give **90** (93 mg, 0.223 mmol 16%) as a white solid.

Mpt: 172.2-174.2 °C; **ν_{max} (cm^{-1})** 3277, 2925, 2851, 1678, 1509, 1258, 1231, 696; **^{1}H-NMR (VT) (400 MHz, 343 K, DMSO-*d*^{6}): δ** 8.38 (m, 2H, *H*-6; *H*-9), 7.91 (td, 1H, *J*= 7.6, 1.1 Hz, *H*-8), 7.79 (ddd, 1H, *J*= 8.3, 7.2, 1.4 Hz, *H*-7), 7.27 (s, 5H, *H*-18; *H*-19, *H*-20), 6.99 (d, 1H, *J*= 6.3 Hz, N*H*), 5.07 (s, 2H, *H*-16), 4.34 (m, 1H, *H*-14"), 4.02 (m, 1H, *H*-10), 3.85 (m, 1H, *H*-14'), 3.08 (m, 2H, *H*-13), 3.03 (s, 3H, *H*-21), 2.15 (m, 1H, *H*-11"), 1.82 (m, 2H, *H*-11'; *H*-12"), 1.55 (m, 1H, *H*-12'); **^{13}C-NMR (100 MHz, DMSO-*d*^{6}): δ** 154.5 (*C*-15), 150.5 (*C*-1), 146.0 (*C*-4), 141.0 (*C*-5), 136.9 (*C*-17), 132.9 (*C*-8), 130.0 (*C*-7), 128.2 (*C*-18), 127.7 (*C*-19), 127.1 (*C*-20), 124.6 (*C*-9), 123.4 (*C*-3), 122.4 (*C*-6), 118.1 (*C*-2), 66.2 (*C*-16), 47.8 (*C*-14), 43.8 (*C*-10), 29.3 (*C*-13), 26.3 (*C*-11; *C*-12), 9.1 (*C*-21); **LR-ESI-MS:** $C_{23}H_{25}N_6O_2$ $[M+H]^+$ *m/z* found 417.2, cald 417.2; **HR-ESI-MS:** $C_{23}H_{25}N_6O_2$ $[M+H]^+$ *m/z* found 417.2064, cald 417.2039.

(1*S*, 2*S*)-*N*$_1$,*N*$_1$-dimethyl-*N*$_2$-(3-methyl-[1,2,4]triazolo[3,4-a]phthalazin-6-yl)cyclohexane-1,2-diamine (91)

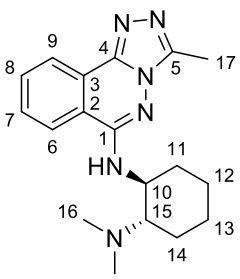

23 (300 mg, 1.372 mmol, 1 eq) and (1*S*,2*S*)-*N*$_1$,*N*$_1$-dimethylcyclohexane-1,2-diamine (390 mg, 2.74 mmol, 2 eq) were reacted according to general

procedure **A**. The crude material was purified by Isolera Biotage LPLC (DCM/MeOH 90:10 then DCM/MeOH/NH_3 9:1:0.5) to give **91** (245 mg, 0.755 mmol 55%) as a white solid.

Mpt: 183.0-185.0 °C; **ν_{max} (cm^{-1})** 3306, 2993, 1592, 1498, 791; **^{1}H-NMR (400 MHz, DMSO-*d*^{6}): δ** 8.37 (dd, 1H, *J*= 7.9, 1.0 Hz, *H*-9), 8.29 (d, 1H, *J*= 8.1 Hz, *H*-6), 7.94 (m, 1H, *H*-8), 7.81 (m, 1H, *H*-7), 7.03 (d, 1H, *J*= 6.5 Hz, N*H*), 3.92 (m, 1H, *H*-10), 2.65 (m, 1H, *H*-15), 2.55 (s, 3H, *H*-17), 2.32 (m, 1H, *H*-11"), 2.20 (s, 6H, *H*-16), 1.85 (m, 1H, *H*-11'), 1.81 (m, 1H, *H*-14"), 1.70 (m, 1H, *H*-14'), 1.28 (m, 4H, *H*-12; *H*-13); **^{13}C-NMR (100 MHz, DMSO-*d*^{6}): δ** 150.8 (*C*-1), 145.9 (*C*-4), 141.0 (*C*-5), 132.7 (*C*-8), 130.2 (*C*-7), 124.1 (*C*-9), 123.4 (*C*-3), 122.5 (*C*-6), 118.4 (*C*-2), 65.5 (*C*-15), 51.7 (*C*-10), 40.0 (*C*-16), 31.8 (*C*-11), 25.0 (*C*-12), 24.7 (*C*-14), 22.2 (*C*-13), 9.3 (*C*-17); **LR-ESI-MS:** $C_{18}H_{25}N_6$ $[M+H]^+$ *m/z* found 325.2, cald 325.2; **HR-ESI-MS:** $C_{18}H_{25}N_6$ $[M+H]^+$ *m/z* found 325.2160, cald 325.2141.

(1*R, 2*R**)-*N*$_1$,*N*$_1$-dimethyl-*N*$_2$-(3-methyl-[1,2,4]triazolo[3,4-a]phthalazin-6-yl)cyclopentane-1,2-diamine (92)**

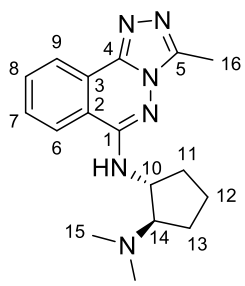

23 (300 mg, 1.372 mmol, 1 eq) and *rac*-(1*R*,2*R*)-*N*$_1$,*N*$_1$-dimethylcyclopentane-1,2-diamine (264 mg, 2.058 mmol, 1.5 eq) were reacted according to general procedure **A**. The crude material was purified by Isolera Biotage LPLC (DCM/MeOH 90:10 then DCM/MeOH/NH_3 9:1:0.5) to give **92** (120 mg, 0.387 mmol 28%) as a white solid.

Mpt: 178.3-180.3 °C; **ν_{max} (cm^{-1})** 3231, 2948, 1593, 1392, 1174, 769, 589; **^{1}H-NMR (400 MHz, DMSO-*d*^{6}): δ** 8.43 (d, 1H, *J*= 8.1 Hz, *H*-9), 8.36 (dd, 1H, *J*= 7.9, 0.9 Hz, *H*-6), 7.91 (m, 1H, *H*-8), 7.80 (td, 1H, *J*= 7.8, 1.3 Hz, *H*-7), 7.35 (d, 1H, *J*= 7.6 Hz, N*H*), 4.35 (m, 1H, *H*-10), 2.91 (q, 1H, *J*= 7.1 Hz, *H*-14), 2.56 (s, 3H, *H*-16), 2.19 (s, 6H, *H*-15), 2.13 (m, 1H, *H*-11"), 1.81 (m, 1H, *H*-13"), 1.60 (m, 4H, *H*-11'; *H*-12; *H*-13'); **^{13}C-NMR (100 MHz, DMSO-*d*^{6}): δ** 150.6 (*C*-1), 146.0 (*C*-4), 141.0 (*C*-5), 132.7 (*C*-8), 130.0 (*C*-7), 124.4 (*C*-9), 123.3 (*C*-3), 122.4 (*C*-6), 118.3 (*C*-2), 71.0 (*C*-14), 54.5 (*C*-10), 42.8 (*C*-15), 31.6 (*C*-11), 27.2 (*C*-13), 22.0 (*C*-12), 9.3 (*C*-16); **LR-ESI-MS:** $C_{17}H_{23}N_6$ $[M+H]^+$ *m/z* found 311.2, cald 311.2; **HR-ESI-MS:** $C_{17}H_{23}N_6$ $[M+H]^+$ *m/z* found 311.2006, cald 311.1984.

***N*,*N*-dimethyl-1-(3-methyl-[1,2,4]triazolo[3,4-a]phthalazin-6-yl)pyrrolidin-3-amine (93)**

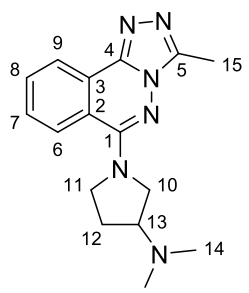

23 (200 mg, 0.915 mmol, 1 eq) and *N*,*N*-dimethylpyrrolidin-3-amine (209 mg, 1.829 mmol, 2 eq) were reacted according to general procedure **A**. The crude material was purified by Isolera Biotage LPLC (DCM/MeOH 90:10 then DCM/MeOH/NH_3 9:1:0.5) to give **93** (246 mg, 0.831 mmol 91%) as a white solid.

Mpt: 141.1-143.1 °C; **ν_{max} (cm^{-1})** 3380, 2864, 2785, 1681, 1493, 1420, 799, 704; **^{1}H-NMR (400 MHz, $CDCl_3$): δ** 8.55 (dd, 1H, *J*= 7.9, 1.0 Hz, *H*-9), 8.09 (d, 1H, *J*= 8.3 Hz, *H*-6), 7.77 (m, 1H, *H*-8), 7.65 (ddd, 1H, *J*= 8.4, 7.2, 1.3 Hz, *H*-7), 3.92 (m, 1H, *H*-13), 3.84-3.69 (m, 3H, *H*-10; *H*-11"), 2.86 (m, 1H, *H*-11'), 2.66 (s, 3H, *H*-15), 2.35 (s, 6H, *H*-14), 2.22 (m, 1H, *H*-12"), 1.97 (m, 1H, *H*-12'); **^{13}C-NMR (100 MHz, $CDCl_3$): δ** 154.3 (*C*-1), 147.1 (*C*-4), 142.2 (*C*-5), 132.1 (*C*-8), 129.3 (*C*-7), 126.5 (*C*-9), 125.0 (*C*-3), 123.5 (*C*-6), 120.1 (*C*-2), 65.4 (*C*-13), 55.8 (*C*-10), 50.3 (*C*-11), 44.3 (*C*-14), 30.2 (*C*-12), 9.7 (*C*-15); **LR-ESI-MS:** $C_{16}H_{21}N_6$ $[M+H]^+$ *m/z* found 297.2, cald 297.2; **HR-ESI-MS:** $C_{16}H_{21}N_6$ $[M+H]^+$ *m/z* found 297.1850, cald 297.1828.

3-methyl-*N*-(2-(4-methylpiperazin-1-yl)ethyl)-[1,2,4]triazolo[3,4-a]phthalazin-6-amine (94)

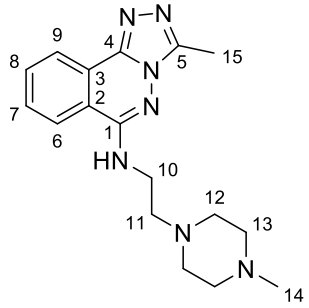

23 (200 mg, 0.915 mmol, 1 eq) and 2-(4-methylpiperazin-1-yl)ethan-1-amine (262 mg, 1.829 mmol, 2 eq) were reacted according to general procedure **A**. The crude material was purified by Isolera Biotage LPLC (DCM/MeOH 90:10 then DCM/MeOH/NH_3 9:1:0.5) to give **94** (189 mg, 0.582 mmol 64%) as an off white solid.

Mpt: 120.5-122.5 °C; **ν_{max} (cm^{-1})** 3223, 2938, 2802, 1566, 1390, 1269, 1145, 1006, 770, 698; **^{1}H-NMR (400 MHz, $CDCl_3$): δ** 8.55 (d, 1H, *J*= 7.9 Hz, *H*-9), 7.78 (m, 2H, *H*-8; *H*-6), 7.68 (m, 1H, *H*-7), 6.19 (s, 1H, N*H*), 3.56 (m, 2H, *H*-10), 2.77 (t, 2H, *J*= 6 Hz, *H*-11), 2.66 (s, 3H, *H*-15), 2.61 (m, 4H, *H*-12), 2.50 (m, 4H, *H*-13), 2.31 (s, 3H, *H*-14); **^{13}C-NMR (100 MHz, $CDCl_3$): δ** 151.0 (*C*-1), 147.1 (*C*-4), 141.9 (*C*-5), 132.3 (*C*-8), 129.9 (*C*-7), 124.1 (*C*-9), 123.6 (*C*-3), 122.3 (*C*-6), 118.4 (*C*-2), 55.5 (*C*-10), 55.2 (*C*-12), 52.6 (*C*-13), 45.9 (*C*-11), 37.8 (*C*-14), 9.7 (*C*-15); **LR-ESI-MS:** $C_{17}H_{24}N_7$ $[M+H]^+$ *m/z* found 326.2, cald 326.2; **HR-ESI-MS:** $C_{17}H_{24}N_7$ $[M+H]^+$ *m/z* found 326.2114, cald 326.2093.

3-methyl-*N*-(1-(4-methylpiperidin-1-yl)propan-2-yl)-[1,2,4]triazolo[3,4-a]phthalazin-6-amine (95)

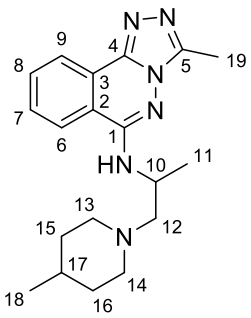

23 (200 mg, 0.915 mmol, 1 eq) and 2-(4-methylpiperazin-1-yl)ethan-1-amine (286 mg, 1.829 mmol, 2 eq) were reacted according to general procedure **A**. The crude material was purified by Isolera Biotage LPLC (DCM/MeOH 90:10 then DCM/MeOH/NH_3 9:1:0.5) to give **95** (40 mg, 0.117 mmol 13%) as an off white solid.

Mpt: 128.6-130.6 °C; **v_{max} (cm^{-1})** 3249, 2919, 1507, 1083, 699; **^{1}H-NMR (400 MHz, DMSO-d^6): δ** 8.36 (m, 2H, *H*-6; *H*-9), 7.9 (m, 1H, *H*-8), 7.8 (m, 1H, *H*-7), 7.16 (d, 1H, *J*= 6.7 Hz, N*H*), 4.28 (m, 1H, *H*-10), 3.00 (d, 1H, *J*= 9.8 Hz, *H*-12"), 2.84 (m, 1H, *H*-12'), 2.59 (m, 1H, *H*-13"), 2.54 (s, 3H, *H*-19), 2.30 (m, 1H, 13'), 1.97 (m, 2H, *H*-14), 1.52 (t, 2H, *J*= 15 Hz, *H*-15), 1.30 (d, 3H, *H*-11), 1.27 (m, 1H, *H*-17), 1.06 (m, 2H, *H*-16), 0.82 (d, 3H, *J*= 6.4 Hz, *H*-18); **^{13}C-NMR (100 MHz, DMSO-d^6): δ** 150.7 (*C*-1), 145.9 (*C*-4), 141.0 (*C*-5), 132.7 (*C*-8), 130.0 (*C*-7), 124.3 (*C*-9), 123.4 (*C*-3), 122.4 (*C*-6), 118.3 (*C*-2), 63.1 (*C*-12), 54.2 (*C*-13), 53.5 (*C*-14), 44.4 (*C*-10), 34.0 (*C*-15), 30.3 (*C*-16), 26.3 (*C*-17), 21.8 (*C*-18), 18.5 (*C*-11), 9.2 (*C*-19); **LR-ESI-MS:** $C_{19}H_{27}N_6$ $[M+H]^+$ *m/z* found 339.2, cald 339.2; **HR-ESI-MS:** $C_{19}H_{27}N_6$ $[M+H]^+$ *m/z* found 339.2320, cald 339.2297.

3-methyl-*N*-(1-(pyridin-2-yl)ethyl)-[1,2,4]triazolo[3,4-a]phthalazin-6-amine (96)

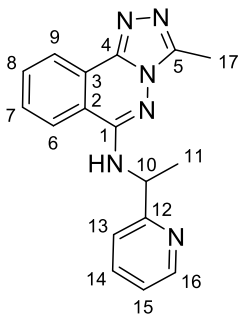

23 (300 mg, 1.372 mmol, 1 eq) and 1-(pyridin-2-yl)ethan-1-amine (335 mg, 2.74 mmol, 2 eq) were reacted according to general procedure **A**. The crude material was purified by Isolera Biotage LPLC (DCM/MeOH 90:10 then DCM/MeOH/NH_3 9:1:0.5) to give **96** (172 mg, 0.567 mmol 41%) as an off white solid.

Mpt: 143.5-145.5 °C; v_{max} (cm^{-1}) 3266, 1591, 1475, 1376, 1164, 698; **^{1}H-NMR (400 MHz, $CDCl_3$): δ** 8.60 (d, 1H, *J*= 4.6 Hz, *H*-16), 8.53 (d, 1H, *J*= 7.8 Hz, *H*-9), 7.94 (d, 1H, *J*= 8.2 Hz, *H*-6), 7.74 (m, 2H, *H*-14; *H*-8), 7.64 (m, 1H, *H*-7), 7.41 (d, 1H, *J*= 7.8 Hz, *H*-13), 7.25 (m, 1H, *H*-15), 7.15 (d, 1H, *J*= 6 Hz, N*H*), 5.29 (quin, 1H, *J*= 6.5 Hz, *H*-10), 2.65 (s, 3H, *H*-17), 1.69 (d, 3H, *J*= 6.6 Hz, *H*-11); **^{13}C-NMR**

(100 MHz, $CDCl_3$): δ 161.3 (*C*-12), 150.0 (*C*-1), 148.6 (*C*-16), 147.0 (*C*-4), 141.9 (*C*-5), 137.0 (*C*-14), 132.4 (*C*-8), 129.9 (*C*-7), 124.1 (*C*-9), 123.6 (*C*-3), 122.7 (*C*-13), 122.4 (*C*-6), 121.6 (*C*-15), 118.5 (*C*-2), 51.5 (*C*-10), 21.8 (*C*-11), 9.7 (*C*-17); **LR-ESI-MS:** $C_{17}H_{17}N_6$ $[M+H]^+$ *m/z* found 305.2, cald 305.2; **HR-ESI-MS:** $C_{17}H_{17}N_6$ $[M+H]^+$ *m/z* found 305.1556, cald 305.1515.

3-methyl-*N*-(1-(pyrazin-2-yl)ethyl)-[1,2,4]triazolo[3,4-a]phthalazin-6-amine (97)

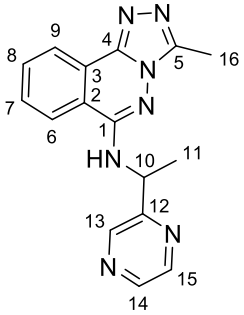

23 (300 mg, 1.372 mmol, 1 eq) and 1-(pyrazin-2-yl)ethan-1-amine (338 mg, 2.74 mmol, 2 eq) were reacted according to general procedure **A**. The crude material was purified by Isolera Biotage LPLC (DCM/MeOH 90:10 then DCM/MeOH/NH_3 9:1:0.5) to give **97** (66 mg, 0.215 mmol 16%) as an off white solid.

Mpt: 172.9-174.9 °C; **ν_{max} (cm^{-1})** 3201, 3057, 1513, 1407, 1141, 701, 629, 604; **^{1}H-NMR (400 MHz, $CDCl_3$): δ** 8.78 (d, 1H, *J*= 1.3 Hz, *H*-13), 8.59 (d, 1H, *J*= 7.3 Hz, *H*-9), 8.55 (m, 1H, *H*-15), 8.52 (m, 1H, *H*-15), 7.97 (d, 1H, *H*-6), 7.82 (m, 1H, *H*-8), 7.73 (m, 1H, *H*-7), 6.59 (d, 1H, N*H*), 5.40 (quin, 1H, *J*= 6.7 Hz, *H*-10), 2.64 (s, 3H, *H*-16), 1.75 (d, 3H, *J*= 6.7 Hz, *H*-11); **^{13}C-NMR (100 MHz, $CDCl_3$):** δ 157.2 (*C*-12), 150.0 (*C*-1), 147.1 (*C*-4), 143.9 (*C*-15), 143.8 (*C*-14), 143.5 (*C*-12), 141.7 (*C*-5), 132.8 (*C*-8), 130.3 (*C*-7), 124.0 (*C*-9; *C*-3), 122.6 (*C*-6), 118.3 (*C*-2), 49.9 (*C*-10), 21.6 (*C*-11), 9.7 (*C*-16); **LR-ESI-MS:** $C_{16}H_{16}N_7$ $[M+H]^+$ *m/z* found 306.1, cald 306.1; **HR-ESI-MS:** $C_{16}H_{16}N_7$ $[M+H]^+$ *m/z* found 306.1509, cald 306.1467.

3-methyl-6-(octahydro-2H-pyrido[1,2-a]pyrazin-2-yl)-[1,2,4]triazolo[3,4-a]phthalazine (98)

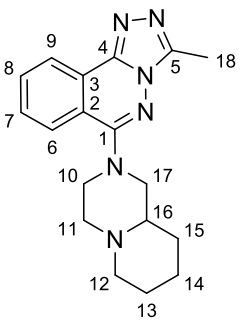

23 (200 mg, 0.915 mmol, 1 eq) and octahydro-2H-pyrido[1,2-a]pyrazine (257 mg, 1.829 mmol, 2 eq) were reacted according to general procedure **A**. The crude material was purified by Isolera Biotage LPLC (DCM/MeOH 90:10 then DCM/MeOH/NH_3 9:1:0.5) to give **98** (228 mg, 0.709 mmol 78%) as an off white solid.

Mpt: 128.7-130.7 °C; **ν_{max} (cm^{-1})** 2929, 2807, 1510, 1345, 1259, 1124, 748; **^{1}H-NMR (400 MHz, $CDCl_3$): δ** 8.60 (dd, 1H, *J*= 7.9, 0.6 Hz, *H*-9), 8.01 (d, 1H, *J*= 8.2 Hz, *H*-6), 7.83 (m, 1H, *H*-8), 7.71 (m,

1H, *H*-7), 3.70 (dd, 1H, *J*= 12.6, 2 Hz, *H*-17"), 3.57 (d, 1H, *J*= 12.6 Hz, *H*-17'), 3.37 (m, 1H, *H*-16), 2.98 (m, 3H, *H*-11; *H*-10"), 2.74 (s, 3H, *H*-18), 2.64 (m, 1H, *H*-10'), 2.30 (m, 2H, *H*-12), 1.69 (m, 6H, *H*-13; *H*-14, *H*-15); **^{13}C-NMR (100 MHz, $CDCl_3$): δ** 157.2 (*C*-1), 147.7 (*C*-4), 142.4 (*C*-5), 132.8 (*C*-8), 129.8 (*C*-7), 126.3 (*C*-9), 125.1 (*C*-3), 123.8 (*C*-6), 120.0 (*C*-2), 61.1 (*C*-16), 56.6 (*C*-17), 55.6 (*C*-11), 54.4 (*C*-10), 50.8 (*C*-12), 29.2 (*C*-15), 25.2 (*C*-13), 23.7 (*C*-14), 9.8 (*C*-18); **LR-ESI-MS:** $C_{18}H_{23}N_6$ $[M+H]^+$ *m/z* found 323.2, cald 323.2; **HR-ESI-MS:** $C_{18}H_{23}N_6$ $[M+H]^+$ *m/z* found 323.2007, cald 323.1984.

***N*-((1,4-dimethylpiperazin-2-yl)methyl)-3-methyl-[1,2,4]triazolo[3,4-a]phthalazin-6-amine (99)**

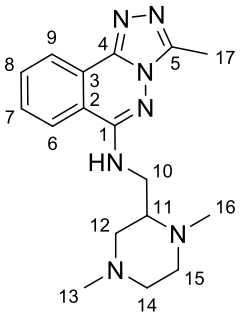

23 (200 mg, 0.915 mmol, 1 eq) and (1,4-dimethylpiperazin-2-yl)methanamine (262 mg, 1.829 mmol, 2 eq) were reacted according to general procedure **A**. The crude material was purified by Isolera Biotage LPLC (DCM/MeOH 90:10 then DCM/MeOH/NH_3 9:1:0.5) to give **99** (89 mg, 0.273 mmol 30%) as an off white solid.

Mpt: 251.6-253.6 °C; v_{max} (cm^{-1}) 3226, 3064, 2794, 1512, 1265, 1166, 697; **^{1}H-NMR (400 MHz, $CDCl_3$):** δ 8.56 (m, 1H, *H*-9), 7.80 (m, 2H, *H*-6; *H*-8), 7.69 (m, 1H, *H*-7), 6.43 (m, 1H, N*H*), 3.66 (m, 1H, *H*-10"), 3.58 (m, 1H, *H*-10'), 2.94 (dt, 1H, *J*= 11.6, 3 Hz, *H*-15"), 2.81 (m, 2H, *H*-12"; *H*-14"), 2.69 (m, 1H, *H*-15'), 2.68 (s, 3H, *H*-17), 2.53 (td, 1H, *J*= 10.9, 2.8 Hz, *H*-11), 2.41 (s, 3H, *H*-16), 2.36 (m, 2H, *H*-12'; *H*-14'), 2.29 (s, 3H, *H*-13); **^{13}C-NMR (100 MHz, $CDCl_3$): δ** 151.1 (*C*-1), 147.2 (*C*-4), 142.0 (*C*-5), 132.4 (*C*-8), 129.9 (*C*-7), 124.1 (*C*-9), 123.7 (*C*-3), 122.4 (*C*-6), 118.5 (*C*-2), 59.2 (*C*-11), 58.4 (*C*-12), 54.7 (*C*-14), 45.9 (*C*-13; *C*-16), 42.1 (*C*-15), 41.5 (*C*-10), 9.8 (*C*-17); **LR-ESI-MS:** $C_{17}H_{24}N_7$ $[M+H]^+$ *m/z* found 326.2, cald 326.2; **HR-ESI-MS:** $C_{17}H_{24}N_7$ $[M+H]^+$ *m/z* found 326.2121, cald 326.2093.

***N*,*N*-dimethyl-1-(3-methyl-[1,2,4]triazolo[3,4-a]phthalazin-6-yl)piperidin-3-amine (100)**

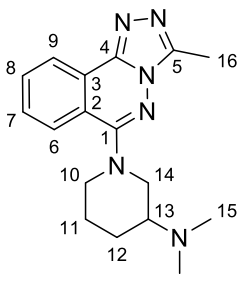

23 (200 mg, 0.915 mmol, 1 eq) and *N*,*N*-dimethylpiperidin-3-amine (235 mg, 1.829 mmol, 2 eq) were reacted according to general procedure **A**.

The crude material was purified by Isolera Biotage LPLC (DCM/MeOH 90:10 then DCM/MeOH/NH_3 9:1:0.5) to give **100** (227 mg, 0.730 mmol 80%) as an off white solid.

Mpt: 139.7-141.7 °C; **ν_{max} (cm^{-1})** 2932, 2825, 1383, 1252, 703; **^{1}H-NMR (400 MHz, $CDCl_3$): δ** 8.58 (dd, 1H, *J*= 7.9, 0.7 Hz, *H*-9), 8.00 (d, 1H, *J*= 8.1 Hz, *H*-6), 7.82 (m, 1H, *H*-8), 7.71 (m, 1H, *H*-7), 3.97 (m, 1H, *H*-14"), 3.7 (m, 1H, *H*-14'), 2.92 (m, 3H, *H*-10; *H*-13), 2.72 (s, 3H, *H*-16), 2.46 (s, 6H, *H*-15), 2.19 (m, 1H, *H*-12"), 1.98 (m, 1H, *H*-12'), 1.86 (m, 1H, *H*-11"), 1.56 (dd, 1H, *J*= 11.2, 4.1 Hz, *H*-11'); **^{13}C-NMR (100 MHz, $CDCl_3$): δ** 157.8 (*C*-1), 147.6 (*C*-4), 142.5 (*C*-5), 132.8 (*C*-8), 129.9 (*C*-7), 126.4 (*C*-9), 125.0 (*C*-3), 123.7 (*C*-6), 120.3 (*C*-2), 61.1 (*C*-13), 53.8 (*C*-14), 52.1 (*C*-10), 41.9 (*C*-15), 27.0 (*C*-12), 24.4 (*C*-11), 9.8 (*C*-16); **LR-ESI-MS:** $C_{17}H_{23}N_6$ $[M+H]^+$ *m/z* found 311.3, cald 311.2; **HR-ESI-MS:** $C_{17}H_{23}N_6$ $[M+H]^+$ *m/z* found 311.2000, cald 311.1984.

(1*S*, 2*S*)-*N*$_1$,*N*$_1$-dimethyl-*N*$_2$-(3-methyl-[1,2,4]triazolo[3,4-a]phthalazin-6-yl)cyclopentane-1,2-diamine (101)

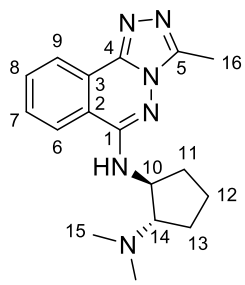

23 (200 mg, 0.915 mmol, 1 eq) and (1*S*,2*S*)-*N*$_1$,*N*$_1$-dimethylcyclopentane-1,2-diamine, 2HCl (276 mg, 1.372 mmol, 1.5 eq) were reacted according to general procedure **A** with added DIPEA (478 µL, 2.74 mmol, 3 eq). The crude material was purified by Isolera Biotage LPLC (DCM/MeOH 90:10 then DCM/MeOH/NH_3 9:1:0.5) to give **101** (48 mg, 0.155 mmol 17%) as an off white solid.

Mpt: 211.0-213.0 °C; **ν_{max} (cm^{-1})** 3238, 2954, 1561, 1551, 1264, 699; **^{1}H-NMR (400 MHz, DMSO-*d*^{6}): δ** 8.38 (m, 2H, *H*-9; *H*-6), 7.91 (t, 1H, *J*= 7.6 Hz, *H*-8), 7.80 (m, 1H, *H*-7), 7.37 (d, 1H, *J*= 7.6 Hz, N*H*), 4.34 (quin, 1H, *J*= 6.9 Hz, *H*-10), 2.92 (q, 1H, *J*= 7.3 Hz, *H*-14), 2.56 (s, 3H, *H*-16), 2.19 (s, 6H, *H*-15), 2.10 (m, 1H, *H*-11"), 1.83 (m, 1H, *H*-13"), 1.60 (m, 4H, *H*-11'; *H*-12; *H*-13'); **^{13}C-NMR (100 MHz, DMSO-*d*^{6}): δ** 151.0 (*C*-1), 146.5 (*C*-4), 141.4 (*C*-5), 133.2 (*C*-8), 130.6 (*C*-7), 124.7 (*C*-9), 123.4 (*C*-3), 122.9 (*C*-6), 118.7 (*C*-2), 71.3 (*C*-14), 54.7 (*C*-10), 43.0 (*C*-15), 31.9 (*C*-11), 27.5 (*C*-13), 22.3 (*C*-12), 9.6 (*C*-16); **LR-ESI-MS:** $C_{17}H_{23}N_6$ $[M+H]^+$ *m/z* found 311.3, cald 311.2; **HR-ESI-MS:** $C_{17}H_{23}N_6$ $[M+H]^+$ *m/z* found 311.1996, cald 311.1984.

***E/Z*-(2-nitroprop-1-en-1-yl)benzene (45)**

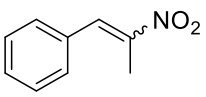

A solution of benzaldehyde **38** (20 g, 188 mmol, 1 eq) and ammonium acetate (2.91 g, 37.7 mmol, 0.2 eq) in nitroethane (314 mL, 0.6 M) was s stirred at 110 °C for 48 h. After reaction completion the mixture was cooled to 4 °C and washed with cold CH before being filtered off and dried to give *E/Z*-**45** as a 1:1 mixture (19.266 g, 118 mmol, 63%) which was submitted to the following step without further purification.

methyl *E/Z*-(2-nitroprop-1-en-1-yl)benzoate (46)

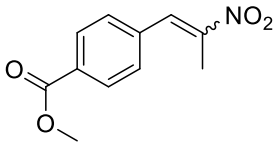

A solution of methyl 4-formylbenzoate **39** (5.31 g, 32.3 mmol, 1 eq) and ammonium acetate (0.499 g, 6.47 mmol, 0.2 eq) in nitroethane (54 mL, 0.6 M) was stirred at 110 °C for 6 days. After reaction completion the mixture was cooled to 4 °C and washed with cold CH before being filtered off and dried to give *E/Z*-**46** (6.554 g, 29.6 mmol, 92%) which was submitted to the following step without further purification.

***E/Z*-1-fluoro-4-(2-nitroprop-1-en-1-yl)benzene (47)**

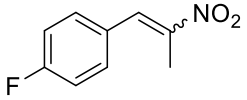

A solution of 4-fluorobenzaldehyde **40** (20 g, 161 mmol, 1 eq) and ammonium acetate (2.484 g, 32.2 mmol, 0.2 eq) in nitroethane (269 mL, 0.6 M) was stirred at 110 °C for 24 h. After reaction completion the mixture was cooled to 4 °C and washed with cold CH before being filtered off and dried to give *E/Z*-**47** (14.95 g, 83 mmol, 51%) which was submitted to the following step without further purification.

***E/Z*-1-(2-nitroprop-1-en-1-yl)-4-(trifluoromethyl)benzene (48)**

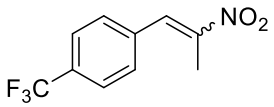

A solution of 4-(trifluoromethyl)benzaldehyde **41** (8 g, 45.9 mmol, 1 eq) and ammonium acetate (0.708 g, 9.19 mmol, 0.2 eq) in nitroethane (77 mL, 0.6 M) was stirred at 110 °C for 4 days. After reaction completion the mixture was cooled to 4 °C and washed with cold CH before being filtered off and dried to give *E/Z*-**48** (10.62 g, 45.9 mmol, *quant.*) which was submitted to the following step without further purification.

***E/Z*-1-methoxy-4-(2-nitroprop-1-en-1-yl)benzene (49)**

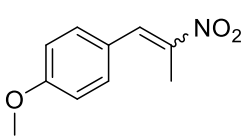

A solution of 4-methoxybenzaldehyde **42** (10 g, 73.4 mmol, 1 eq) and ammonium acetate (1.132 g, 14.69 mmol, 0.2 eq) in nitroethane (122 mL, 0.6 M) was stirred at 110 °C for 3 days. After reaction completion the mixture was cooled to 4 °C and washed with cold CH before being filtered off and dried to give *E/Z*-**49** (14.19 g, 73.4 mmol, *quant.*) which was submitted to the following step without further purification.

***E/Z*-1-chloro-4-(2-nitroprop-1-en-1-yl)benzene (50)**

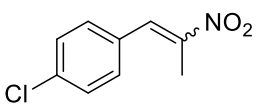

A solution of 4-chlorobenzaldehyde **43** (10 g, 71.1 mmol, 1 eq) and ammonium acetate (1.097 g, 14.23 mmol, 0.2 eq) in nitroethane (119 mL, 0.6 M) was stirred at 110 °C for 4 days. After reaction completion the mixture was cooled to 4 °C and washed with cold CH before being filtered off and dried to give *E/Z*-**50** (14.06 g, 71.1 mmol, *quant.*) which was submitted to the following step without further purification.

***E/Z*- 1-methyl-4-(2-nitroprop-1-en-1-yl)benzene (51)**

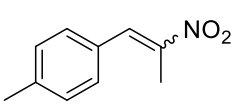

A solution of 4-methylbenzaldehyde **44** (10 g, 83 mmol, 1 eq) and ammonium acetate (1.283 g, 16.65 mmol, 0.2 eq) in nitroethane (139 mL, 0.6 M) was stirred at 110 °C for 16 h. After reaction completion the mixture was cooled to 4 °C and washed with cold CH before being filtered off and dried to give *E/Z*-**51** (14.75 g, 83 mmol, *quant.*) which was submitted to the following step without further purification.

(1*S, 2*S**)-*N*,*N*-dimethyl-2-nitro-1-phenylpropan-1-amine (52)**

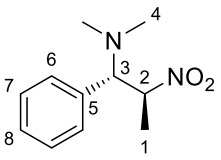

To a stirred solution of *E***/***Z*-**45** (1 g, 6.13 mmol,1 eq) in THF (15 mL, anhydrous) was added Dimethylamine 2M (in THF) (15 mL, 30.6 mmol, 5 eq) at room temperature and the solution was allowed to stir for 16 h. After reaction completion the solution was concentrated to a yellow crystalline crude material which was immediately submitted to a purification by Isolera Biotage LPLC (CH/EA 90:10 to CH/EA 2:8) to give **52** (1.0219 g, >33:1 dr, 71%) as a unstable white waxy solid.

ν_{max} (cm^{-1}) 2975, 2944, 2835, 2791, 1556, 1451, 1353, 873, 705, 614; **^{1}H-NMR (400 MHz, $CDCl_3$):** **δ** 7.39 (m, 3H, *H*-7; *H*-8), 7.11 (m, 1H, *H*-6), 5.23 (dq, 1H, *J*= 11.1, 6.6 Hz, *H*-2), 4.01 (d, 1H, *J*= 11

Hz, *H*-3), 2.15 (s, 6H, *H*-4), 1.34 (d, 1H, *J*= 6.6 Hz, *H*-1); **^{13}C-NMR (100 MHz, $CDCl_3$): δ** 131.0 (*C*-5), 129.2 (*C*-6), 128.3 (*C*-7), 128.2 (*C*-8), 83.7 (*C*-2), 72.3 (*C*-3), 40.9 (*C*-4), 17.2 (*C*-1); **LR-ESI-MS:** $C_{11}H_{17}N_2O_2$ $[M+H]^+$ *m/z* found 209.1, cald 209.1. **HR-ESI-MS:** $C_{11}H_{17}N_2O_2$ $[M+H]^+$ *m/z* found 209.0879, cald 209.1290.

methyl 4-((1*S, 2*S**)-1-(dimethylamino)-2-nitropropyl)benzoate (53)**

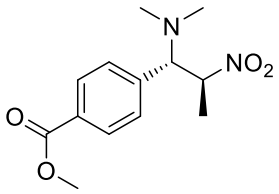

To a stirred solution of *E*/*Z*-**46** (1.133 g, 5.12 mmol,1 eq) in THF (10 mL, anhydrous) was added Dimethylamine 2M (in THF) (12.8 mL, 25.6 mmol, 5 eq) at room temperature and the solution was allowed to stir for 16 h. After reaction completion the solution was concentrated to give **53** (1.364 g, 5.12 mmol, 12:1 dr, *quant.*) as an unstable red crude material which was immediately submitted to the next step without further purification.

(1*S, 2*S**)-1-(4-fluorophenyl)-*N*,*N*-dimethyl-2-nitropropan-1-amine (54)**

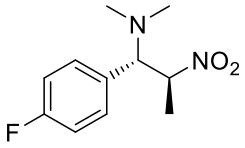

To a stirred solution of *E*/*Z*-**47** (5 g, 27.6 mmol,1 eq) in THF (20 mL, anhydrous) was added dimethylamine 2M (in THF) (69 mL, 138 mmol, 5 eq) at room temperature and the solution was allowed to stir for 16 h. After reaction completion the solution was concentrated to give **54** (6.24 g, 27.6 mmol, 15:1 dr, *quant.*) as an unstable yellow crystalline crude material which was immediately submitted to the next step without further purification.

(1*S, 2*S**)-1-(4-methoxyphenyl)-*N*,*N*-dimethyl-2-nitropropan-1-amine (55)**

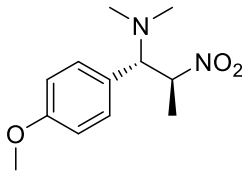

To a stirred solution of *E*/*Z*-**48** (14.19 g, 73.4 mmol,1 eq) in THF (30 mL, anhydrous) was added dimethylamine 2M (in THF) (184 mL, 367 mmol, 5 eq) at room temperature and the solution was allowed to stir for 48 h. After reaction completion the solution was concentrated to give **55** (17.5 g, 73.4 mmol, 7.5:1 dr, *quant.*) as an unstable red solid which was immediately submitted to the next step without further purification.

(1*S, 2*S**)-*N*,*N*-dimethyl-2-nitro-1-(4-(trifluoromethyl)phenyl)propan-1-amine (56)**

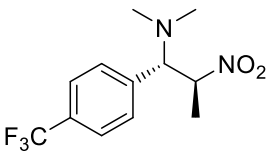

To a stirred solution of *E*/*Z*-**49** (10.62 g, 45.9 mmol,1 eq) in THF (30 mL, anhydrous) was added dimethylamine 2M (in THF) (115 mL, 230 mmol, 5 eq) at room temperature and the solution was allowed to stir for 16 h. After reaction completion the solution was concentrated to give **56** (12.69 g, 45.9 mmol, 6.8:1 dr, *quant.*) as an unstable red solid which was immediately submitted to the next step without further purification.

(1*S, 2*S**)-*N*,*N*-dimethyl-2-nitro-1-(p-tolyl)propan-1-amine (57)**

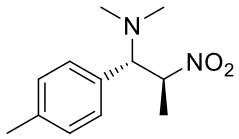

To a stirred solution of *E*/*Z*-**50** (14.75 g, 83 mmol,1 eq) in THF (30 mL, anhydrous) was added dimethylamine 2M (in THF) (208 mL, 291 mmol, 5 eq) at room temperature and the solution was allowed to stir for 16 h. After reaction completion the solution was concentrated to give **57** (18.5 g, 83 mmol, 13:1 dr, *quant.*) as an unstable dark red solid which was immediately submitted to the next step without further purification.

(1*S, 2*S**)-1-(4-chlorophenyl)-*N*,*N*-dimethyl-2-nitropropan-1-amine (58)**

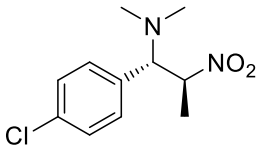

To a stirred solution of *E*/*Z*-**51** (14.06 g, 71.1 mmol,1 eq) in THF (30 mL, anhydrous) was added dimethylamine 2M (in THF) (178 mL, 249 mmol, 5 eq) at room temperature and the solution was allowed to stir for 16 h. After reaction completion the solution was concentrated to give **58** (17.27 g, 71.1 mmol, 4.6:1 dr, *quant.*) as an unstable dark red solid which was immediately submitted to the next step without further purification.

(1*S, 2*S**)-N_1,N_1-dimethyl-1-phenylpropane-1,2-diamine (59)**

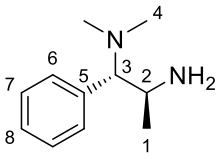

To a degassed stirred solution of **52** (4.2127 g, 20.23 mmol,1 eq) in MeOH (101 mL, 0.2 M, anhydrous) was added Pd/C (10%) (0.42 g, 0.195 eq) and atmosphere was exhanged with H_2 gas (x3). The reaction mixture was stirred under a H_2 atmsophere (double balloon, 1 bar) for 5 h. Upon reaction completion the mixture was filtered through celite, followed by filtration through a sintered frit to afford a

crude oil after drying. The oily residue was purified by Isolera Biotage LPLC (DCM/MeOH 90:10 then DCM/MeOH/NH_3 9:1:0.5) to give **59** (0.4 g, 2.244 mmol, single diastereomer, 11% over two steps) as a colourless oil.

ν_{max} (cm^{-1}) 2963, 2780, 1581, 1452, 1375, 753, 704; **^{1}H-NMR (400 MHz, $CDCl_3$): δ** 7.46 (m, 2H, *H*-7, *H*-8), 7.26 (m, 2H, *H*-6), 3.56 (m, 1H, *H*-2), 3.19 (d, 1H, *J*= 9.5 Hz, *H*-3), 2.28 (s, 6H, *H*-4), 1.03 (d, 3H, *J*= 6.2 Hz, *H*-1); **^{13}C-NMR (100 MHz DMSO-*d*^{6}): δ** 135.3 (*C*-5), 129.4 (*C*-6), 127.6 (*C*-7), 126.8 (*C*-8), 79.2 (*C*-3), 45.2 (*C*-2), 40.9 (*C*-4), 20.4 (*C*-1); **LR-ESI-MS:** $C_{11}H_{19}N_2$ $[M+H]^+$ *m/z* found 179.2, cald 179.2; **HR-ESI-MS:** $C_{11}H_{19}N_2$ $[M+H]^+$ *m/z* found 179.1549, cald 179.1548.

(1*S, 2*S**)-1-(4-fluorophenyl)-*N*$_1$,*N*$_1$-dimethylpropane-1,2-diamine (60)**

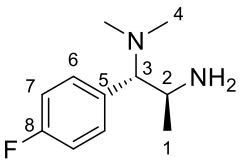

To a degassed stirred solution of **53** (6.24 g, 27.6 mmol,1 eq) in MeOH (68.9 mL, 0.4 M, anhydrous) was added Pd/C (10%) (0.646 g, 0.22 eq) and atmosphere was exhanged with H_2 gas (x3). The reaction mixture was stirred under a H_2 atmsophere (double balloon, 1 bar) for 16 h. Upon reaction completion the mixture was filtered through celite, followed by filtration through a sintered frit to afford a yellow crude oil after drying. The oily residue was purified by Isolera Biotage LPLC (DCM/MeOH 90:10 then DCM/MeOH/NH_3 9:1:0.5) to give **60** (0.569 g, 2.90 mmol, single diastereomer, 11% over two steps) as a colourless oil.

ν_{max} (cm^{-1}) 2827, 1599, 1506, 1222, 846; **^{19}F-{H}-NMR (376 MHz, $CDCl_3$): δ** -115.77; **^{1}H-{F}-NMR (400 MHz, $CDCl_3$): δ** 7.08 (d, 2H, *J*= 8.7 Hz, *H*-7), 7.02 (d, 2H, *J*= 8.7 Hz, *H*-6), 3.36 (dq, 1H, *J*= 9.8, 6.2 Hz, *H*-2), 3.03 (d, 1H, *J*= 9.2 Hz, *H*-3), 2.11 (s, 6H, *H*-4), 0.86 (d, 3H, *J*= 6.2 Hz, *H*-1); **^{13}C-NMR (100 MHz $CDCl_3$): δ** 162.0 (d, *J*= 245 Hz, *C*-8), 131.0 (d, *J*= 3.7 Hz, *C*-5), 130.8 (d, *J*= 8.1 Hz, *C*-6), 114.6 (d, *J*= 20.5 Hz, *C*-7), 76.2 (*C*-3), 46.0 (*C*-2), 41.1 (*C*-4), 20.4 (*C*-1); **LR-ESI-MS:** $C_{11}H_{18}FN_2$ $[M+H]^+$ *m/z* found 197.2, cald 197.2; **HR-ESI-MS:** $C_{11}H_{17}FN_2Na$ $[M+Na]^+$ *m/z* found 219.1363, cald 219.1273.

(1*S, 2*S**)-*N*$_1$,*N*$_1$-dimethyl-1-(p-tolyl)propane-1,2-diamine (61)**

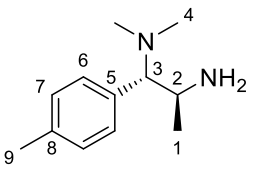

To a degassed stirred solution of **54** (1 g, 4.50 mmol,1 eq) in MeOH (30 mL, 0.15 M, anhydrous) was added Pd/C (10%) (0.144 g, 0.3 eq) and atmosphere was exhanged with H_2 gas (x3). The reaction mixture was stirred under a H_2 atmsophere (double balloon, 1 bar) for 16 h. Upon reaction completion the mixture was filtered through celite, followed by filtration through a sintered frit to afford a yellow crude oil after drying. The oily residue was purified by Isolera Biotage LPLC (DCM/MeOH 90:10 then DCM/MeOH/NH_3 9:1:0.5) to give **61** (0.153 g, 0.796 mmol, single diastereomer, 18% over two steps) as a white waxy solid.

ν_{max} (cm^{-1}) 3283, 2973, 2867, 1599, 1451, 1016, 801, 591; **^{1}H-NMR (400 MHz, $CDCl_3$): δ** 7.14 (d, 2H, *J*= 7.8 Hz, *H*-6), 6.99 (d, 2H, *J*= 8.1 Hz, *H*-7), 3.38 (dq, 1H, *J*= 9.7, 6.3 Hz, *H*-2), 3.01 (d, 1H, *J*= 9.8 Hz, *H*-3), 2.35 (s, 3H, *H*-9), 2.11 (s, 6H, *H*-4), 0.87 (d, 3H, *J*= 6.2 Hz, *H*-1); **^{13}C-NMR (100 MHz $CDCl_3$): δ** 136.6 (*C*-5), 132.0 (*C*-8), 129.4 (*C*-6), 128.4 (*C*-7), 76.5 (*C*-3), 45.8 (*C*-2), 41.2 (*C*-4), 21.0 (*C*-9), 20.4 (*C*-1); **LR-ESI-MS:** $C_{12}H_{21}N_2$ $[M+H]^+$ *m/z* found 193.3, cald 193.2; **HR-ESI-MS:** $C_{12}H_{21}N_2$ $[M+H]^+$ *m/z* found 193.1706, cald 193.1705.

(1*S, 2*S**)-1-(4-chlorophenyl)-*N*$_1$,*N*$_1$-dimethylpropane-1,2-diamine (62)**

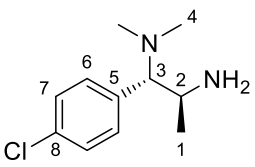

Under an inert atmsosphere (N_2) Raney Ni (2400) (0.234 g, 0.3 eq) was activated by washings with H_2O (x3) and then MeOH (x3, anhydrous) before a degassed solution of **55** (3.22 g, 13.27 mmol,1 eq) in MeOH (66 mL, 0.2 M, anhydrous) was added. The reaction vessel atmosphere was then exhanged with H_2 gas (x3). The reaction mixture was stirred under a H_2 atmsophere (double balloon, 1 bar) for 16 h. Upon reaction completion the mixture was filtered through celite, followed by filtration through a sintered frit to afford a colourless crude oil after drying. The oily residue was purified by Isolera Biotage LPLC (DCM/MeOH 90:10 then DCM/MeOH/NH_3 9:1:0.5) to give **62** (0.691 g, 3.25 mmol, single diastereomer, 25% over three steps) as a colourless oil.

ν_{max} (cm^{-1}) 2933, 2864, 2825, 2780, 1592, 1488, 1452, 1090, 1012, 842, 802, 701; **^{1}H-NMR (400 MHz, $CDCl_3$): δ** 7.30 (d, 2H, *J*= 8.6 Hz, *H*-7), 7.03 (d, 2H, *J*= 8.3 Hz, *H*-6), 3.36 (dq, 1H, *J*= 9.6, 6.3

Hz, *H*-2), 3.02 (d, 1H, *J*= 9.7 Hz, *H*-3), 2.10 (s, 6H, *H*-4), 0.86 (d, 3H, *J*= 6.2 Hz, *H*-1); **^{13}C-NMR (100 MHz $CDCl_3$): δ** 133.6 (*C*-8), 132.9 (*C*-5), 130.7 (*C*-6), 127.9 (*C*-7), 76.2 (*C*-3), 45.8 (*C*-2), 41.1 (*C*-4), 20.3 (*C*-1); **LR-ESI-MS:** $C_{11}H_{18}ClN_2$ $[M+H]^+$ *m/z* found 213.2, cald 213.1; **HR-ESI-MS:** $C_{11}H_{18}ClN_2$ $[M+H]^+$ *m/z* found 213.0792, cald 213.1159.

methyl 4-((1*S, 2*S**)-2-amino-1-(dimethylamino)propyl)benzoate (63)**

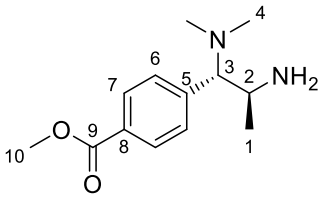

Under an inert atmsosphere (N_2) Raney Ni (2400) (0.066 g, 0.3 eq) was activated by washings with H_2O (x3) and then MeOH (x3, anhydrous) before a degassed solution of **56** (1 g, 3.76 mmol,1 eq) in MeOH (38 mL, 0.1 M, anhydrous) was added . The reaction vessel atmosphere was then exhanged with H_2 gas (x3). The reaction mixture was stirred under a H_2 atmsophere (double balloon, 1 bar) for 3 h. Upon reaction completion the mixture was filtered through celite, followed by filtration through a sintered frit to afford a colourless crude oil after drying. The oily residue was purified by Isolera Biotage LPLC (DCM/MeOH 90:10 then DCM/MeOH/NH_3 9:1:0.5) to give **63** (0.251 g, 1.062 mmol, single diastereomer, 28% over three steps) as a colourless oil.

ν_{max} (cm^{-1}) 2950, 2826, 2782, 1716, 1435, 1311, 765; **^{1}H-NMR (400 MHz, $CDCl_3$): δ** 8.01 (d, 2H, *J*= 8.1 Hz, *H*-7), 7.18 (d, 2H, *J*= 8.3 Hz, *H*-6), 3.92 (s, 3H, *H*-10), 3.42 (dq, 1H, *J*= 9.7, 6.3 Hz, *H*-2), 3.10 (d, 1H, *J*= 9.7 Hz, *H*-3), 2.13 (s, 6H, *H*-4), 0.87 (d, 3H, *J*= 6.4 Hz, *H*-1); **^{13}C-NMR (100 MHz $CDCl_3$): δ** 167.0 (*C*-9), 140.7 (*C*-5), 129.4 (*C*-7), 129.1 (*C*-8), 129.0 (*C*-6), 52.1 (*C*-3), 45.7 (*C*-2), 41.2 (*C*-4), 20.3 (*C*-1); **LR-ESI-MS:** $C_{13}H_{21}N_2O_2$ $[M+H]^+$ *m/z* found 237.2, cald 237.2; **HR-ESI-MS:** $C_{13}H_{21}N_2O_2$ $[M+H]^+$ *m/z* found 237.1560, cald 237.1603.

(1*S, 2*S**)-*N*$_1$,*N*$_1$-dimethyl-1-(4-(trifluoromethyl)phenyl)propane-1,2-diamine (64)**

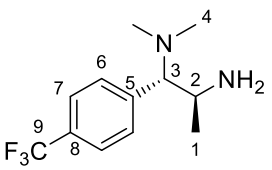

To a degassed stirred solution of **57** (2.486 g, 9 mmol,1 eq) in MeOH (60 mL, 0.15 M, anhydrous) was added Pd/C (10%) (0.287 g, 0.3 eq) and atmosphere was exhanged with H_2 gas (x3). The reaction mixture was stirred under a H_2 atmsophere (double balloon, 1 bar) for 16 h. Upon reaction completion the

mixture was filtered through celite, followed by filtration through a sintered frit to afford a colourless crude oil after drying. The oily residue was purified by Isolera Biotage LPLC (DCM/MeOH 90:10 then DCM/MeOH/NH_3 9:1:0.5) to give **64** (0.153 g, 0.796 mmol, single diastereomer, 14% over three steps) as a colourless oil.

ν_{max} (cm^{-1}) 3222, 2936, 2785, 1670, 1163, 1032, 850; **^{19}F-{H}-NMR (376 MHz, $CDCl_3$): δ** -62.44; **^{1}H-NMR (400 MHz, $CDCl_3$): δ** 7.60 (d, 2H, *J*= 8.1 Hz, *H*-7), 7.23 (d, 2H, *J*= 8.1 Hz, *H*-6), 3.42 (dq, 1H, *J*= 9.6, 6.3 Hz, *H*-2), 3.12 (d, 1H, *J*= 9.7 Hz, *H*-3), 2.13 (s, 6H, *H*-4), 0.87 (d, 3H, *J*= 6.2 Hz, *H*-1); **^{13}C-NMR (100 MHz $CDCl_3$): δ** 139.6 (*C*-5), 129.7 (*C*-7; *C*-6), 124.7 (q, *J*= 3.7 Hz, *C*-9), 76.5 (*C*-3), 45.7 (*C*-2), 41.2 (*C*-4), 20.3 (*C*-1); **LR-ESI-MS:** $C_{12}H_{18}F_3N_2$ $[M+H]^+$ *m/z* found 247.1, cald 247.1; **HR-ESI-MS:** $C_{12}H_{18}F_3N_2$ $[M+H]^+$ *m/z* found 247.1428, cald 247.1422.

(1*S, 2*S**)-1-(4-methoxyphenyl)-*N*$_1$,*N*$_1$-dimethylpropane-1,2-diamine (65)**

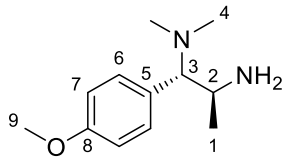

To a degassed stirred solution of **58** (2.556 g, 10.73 mmol,1 eq) in MeOH (72 mL, 0.15 M, anhydrous) was added Pd/C (10%) (0.342 g, 0.3 eq) and atmosphere was exhanged with H_2 gas (x3). The reaction mixture was stirred under a H_2 atmsophere (double balloon, 1 bar) for 16 h. Upon reaction completion the mixture was filtered through celite, followed by filtration through a sintered frit to afford a colourless crude oil after drying. The oily residue was purified by Isolera Biotage LPLC (DCM/MeOH 90:10 then DCM/MeOH/NH_3 9:1:0.5) to give **65** (0.334 g, 1.603 mmol, single diastereomer, 15% over three steps) as a colourless oil.

ν_{max} (cm^{-1}) 2931, 2825, 1608, 1509, 1246 , 1030, 840, 808, 593; **^{1}H-NMR (400 MHz, $CDCl_3$): δ** 7.02 (d, 2H, *J*= 8.7 Hz, *H*-6), 6.87 (d, 2H, *J*= 8.7 Hz, *H*-7), 3.81 (s, 3H, *H*-9), 3.35 (dq, 1H, *J*= 9.7, 6.2 Hz, *H*-2), 2.99 (d, 1H, *J*= 9.7 Hz, *H*-3), 2.10 (s, 6H, *H*-4), 0.87 (d, 3H, *J*= 6.2 Hz, *H*-1); **^{13}C-NMR (100 MHz $CDCl_3$): δ** 158.6 (*C*-8), 130.5 (*C*-6), 127.3 (*C*-5), 113.0 (*C*-7), 76.2 (*C*-3), 55.1 (*C*-9), 46.0 (*C*-2), 41.2 (*C*-4), 20.4 (*C*-1); **LR-ESI-MS:** $C_{12}H_{21}N_2O$ $[M+H]^+$ *m/z* found 209.2, cald 209.2; **HR-ESI-MS:** $C_{12}H_{21}N_2O$ $[M+H]^+$ *m/z* found 209.1295, cald 209.1654.

(1*R*, 2*S*)-2-((3-methyl-[1,2,4]triazolo[3,4-a]phthalazin-6-yl)amino)-1-phenylpropan-1-ol (102)

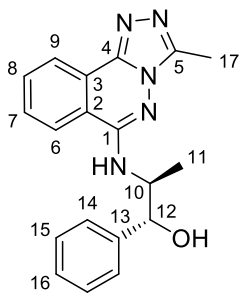

23 (1 g, 0.915 mmol, 1 eq) and (1*R*,2*S*)-(-)-Norephedrine (1.037 g, 6.86 mmol, 1.5 eq) were reacted according to general procedure **A**. The crude material was purified by Isolera Biotage LPLC (DCM/MeOH 90:10) to give **102** (0.413 g, 1.239 mmol, 27%) as a white solid.

Mpt: 239.6-241.6 °C; **ν_{max} (cm^{-1})** 3640, 3277, 2972, 1514, 1000, 701; **^{1}H-NMR (400 MHz, $CDCl_3$): δ** 8.47 (d, 1H, *J*= 8.2 Hz, *H*-9), 8.35 (d, 1H, *J*= 7.9 Hz, *H*-6), 7.89 (m, 1H, *H*-8), 7.81 (m, 1H, *H*-7), 7.49 (d, 2H, *J*= 7.3 Hz, *H*-14), 7.31 (m, 3H, *H*-15; N*H*), 7.18 (m, 1H, *H*-16, 5.45 (d, 1H, *J*= 4.8 Hz, O*H*), 5.07 (m, 1H, *H*-12), 4.32 (m, 1H, *H*-10), 1.17 (d, 3H, *J*= 6.7 Hz, *H*-11); **^{13}C-NMR (100 MHz, DMSO-*d*^{6}): δ** 150.4 (*C*-1), 146.0 (*C*-13), 143.9 (*C*-4), 141.0 (*C*-5), 132.7 (*C*-8), 130.0 (*C*-7), 127.8 (*C*-14), 126.5 (*C*-16), 125.9 (*C*-15), 124.6 (*C*-9), 123.3 (*C*-3), 122.4 (*C*-6), 118.3 (*C*-2), 72.1 (*C*-12), 53.0 (*C*-10), 13.2 (*C*-11), 9.4 (*C*-17); **LR-ESI-MS:** $C_{19}H_{20}N_5O$ $[M+H]^+$ *m/z* found 334.2, cald 334.2; **HR-ESI-MS:** $C_{19}H_{20}N_5O$ $[M+H]^+$ *m/z* found 334.1711, cald 334.1668.

(1*S, 2*S**)-1-(4-fluorophenyl)-*N*$_1$,*N*$_1$-dimethyl-*N*$_2$-(3-methyl-[1,2,4]triazolo[3,4-a]phthalazin-6-yl)propane-1,2-diamine (66)**

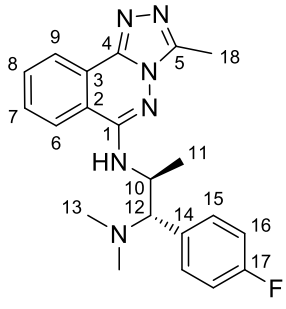

23 (365 mg, 1.669 mmol, 1 eq) and **60** (491 mg, 2.504 mmol, 1.5 eq) were reacted according to general procedure **A**. The crude material was purified by Isolera Biotage LPLC (DCM/MeOH 90:10) to give **66** (206 mg, 0.545 mmol, 33%) as an off white solid.

Mpt: 239.8-241.8 °C; **ν_{max} (cm^{-1})** 3453, 2953, 2814, 2773, 1593, 1500, 1246, 1028, 547, 695, 656, 446; **^{19}F-{H}-NMR (376 MHz, $CDCl_3$): δ** -115.67; **^{1}H-{F}-NMR (400 MHz, DMSO-*d*^{6}): δ** 8.40 (d, 1H, *J*= 7.7 Hz, *H*-9), 8.28 (d, 1H, *J*= 8.2 Hz, *H*-6), 7.94 (t, 1H, *J*= 7.7 Hz, *H*-8), 7.82 (m, 1H, *H*-7), 7.27 (d, 2H, *J*= 8.7 Hz, *H*-16), 7.18, (d, 2H, *J*= 7.2 Hz, *H*-15), 7.01 (d, 1H, *J*= 5.7 Hz, N*H*), 4.70 (m, 1H, *H*-10), 3.72 (d, 1H, *J*= 8.2 Hz, *H*-12), 2.62 (s, 3H, *H*-18), 2.13 (s, 6H, *H*-13), 1.10 (d, 3H, *J*= 6.2 Hz, *H*-11); **^{13}C-NMR (100 MHz, DMSO-*d*^{6}): δ** 161.5 (d, *J*= 242.1 Hz, *C*-17), 150.6 (*C*-1), 146.1 (*C*-4), 141.1 (*C*-5), 132.9 (*C*-8), 132.3 (*C*-14), 131.1 (d, *J*= 8.1 Hz, *C*-15), 130.2 (*C*-7), 124.2 (*C*-9), 123.4 (*C*-3), 122.6 (*C*-6), 118.3 (*C*-2), 114.5 (d, *J*= 21.3 Hz, *C*-16), 70.7 (*C*-12), 46.2

(*C*-10), 42.0 (*C*-13), 16.0 (*C*-11), 9.4 (*C*-18); **LR-ESI-MS:** $C_{21}H_{24}FN_6$ $[M+H]^+$ *m/z* found 379.3, cald 379.2; **HR-ESI-MS:** $C_{21}H_{24}FN_6$ $[M+H]^+$ *m/z* found 379.2070, cald 379.2046.

methyl 4-((1*S, 2*S**)-1-(dimethylamino)-2-((3-methyl-[1,2,4]triazolo[3,4-a]phthalazin-6-yl)amino)propyl)benzoate (67)**

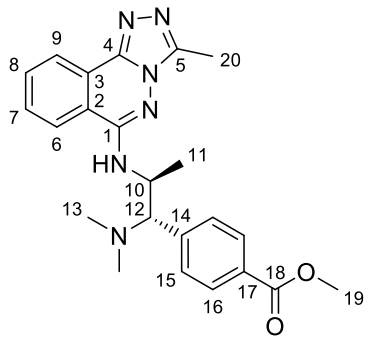

23 (156 mg, 0.713 mmol, 1 eq) and **36** (253 mg, 1.07 mmol, 1.5 eq) were reacted according to general procedure **A**. The crude material was purified by Isolera Biotage LPLC (DCM/MeOH 90:10 then DCM/MeOH/NH_3 9:1:0.5) to give **67** (83 mg, 0.198 mmol 28%) as a white solid.

Mpt: 254.3-256.3 °C; **ν_{max} (cm^{-1})** 3256, 2926, 2775, 1722, 1593, 1432, 1101, 1019, 670, 659, 542; **^{1}H-NMR (400 MHz, DMSO-*d*^{6}): δ** 8.40 (d, 1H, *J*= 7.9 Hz, *H*-9), 8.29 (d, 1H, *J*= 8.2 Hz, *H*-6), 7.94 (m, 3H, *H*-8; *H*-16), 7.81 (m, 1H, *H*-7), 7.36 (d, 2H, *J*= 8.3 Hz, *H*-15), 7.01 (d, 1H, *J*= 5.7 Hz, N*H*), 4.78 (m, 1H, *H*-10), 3.85 (s, 3H, *H*-19), 3.79 (d, 1H, *J*= 7.7 Hz, *H*-12), 2.62 (s, 3H, *H*-20), 2.15 (s, 6H, *H*-13), 1.10 (d, 3H, *J*= 6.6 Hz, *H*-11); **^{13}C-NMR (100 MHz DMSO-*d*^{6}): δ** 166.3 (*C*-18), 150.6 (*C*-1), 146.1 (*C*-4), 142.3 (*C*-14), 141.1 (*C*-5), 132.9 (*C*-8), 130.2 (*C*-7), 129.7 (*C*-16), 128.6 (*C*-15), 128.6 (*C*-17), 124.2 (*C*-9), 123.5 (*C*-3), 122.6 (*C*-6), 118.3 (*C*-2), 71.1 (*C*-12), 52.1 (*C*-19), 46.5 (*C*-10), 42.3 (*C*-13), 15.8 (*C*-11), 9.4 (*C*-20); **LR-ESI-MS:** $C_{23}H_{27}N_6O_2$ $[M+H]^+$ *m/z* found 419.4, cald 419.2; **HR-ESI-MS:** $C_{23}H_{27}N_6O_2$ $[M+H]^+$ *m/z* found 419.2233, cald 419.2195.

(1*S, 2*S**)-*N*$_1$,*N*$_1$-dimethyl-*N*$_2$-(3-methyl-[1,2,4]triazolo[3,4-a]phthalazin-6-yl)-1-(p-tolyl)propane-1,2-diamine (68)**

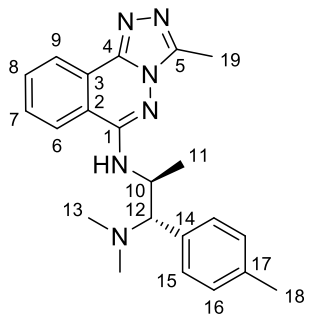

23 (75 mg, 0.343 mmol, 1 eq) and **34** (99 mg, 0.515 mmol, 1.5 eq) were reacted according to general procedure **A**. The crude material was purified by Isolera Biotage LPLC (DCM/MeOH 90:10 then DCM/MeOH/NH_3 9:1:0.5) to give **68** (43 mg, 0.115 mmol 33%) as a white solid.

Mpt: 189.6-191.6 °C; **ν_{max} (cm^{-1})** 3257, 2926, 2772, 1508, 1306, 1265, 1027, 802, 699; **^{1}H-NMR (400 MHz, $CDCl_3$): δ** 8.61 (d, 1H, *J*= 7.9 Hz, *H*-9), 7.84 (m, 2H, *H*-6; *H*-8), 7.74 (m, 1H, *H*-7), 7.26 (m, 2H, *H*-15), 7.21 (d, 2H, *J*= 7.7 Hz, *H*-16), 6.86 (s, 1H, N*H*), 4.34 (m, 1H, *H*-10), 3.66 (m, 1H, *H*-12), 2.74 (s, 3H, *H*-18), 2.41 (s, 3H, *H*-18), 2.21 (s, 6H, *H*-13), 1.26 (d, 3H, *J*= 6 Hz, *H*-11); **^{13}C-NMR (100 MHz, $CDCl_3$): δ** 151.4 (*C*-1), 147.3 (*C*-4), 142.0 (*C*-5), 136.0 (*C*-14), 132.4 (*C*-8), 130.0 (*C*-15), 129.7 (*C*-7), 128.4 (*C*-16), 124.3 (*C*-9), 123.8 (*C*-3), 122.8 (*C*-6), 119.2 (*C*-2), 73.0 (*C*-12), 47.2 (*C*-10), 40.8 (*C*-13), 21.1 (*C*-18), 17.6 (*C*-11), 9.8 (*C*-19); **LR-ESI-MS:** $C_{22}H_{27}N_6$ $[M+H]^+$ *m/z* found 375.3, cald 375.3; **HR-ESI-MS:** $C_{22}H_{27}N_6$ $[M+H]^+$ *m/z* found 375.2315, cald 375.2297.

(1*S, 2*S**)-1-(4-chlorophenyl)-*N*$_1$,*N*$_1$-dimethyl-*N*$_2$-(3-methyl-[1,2,4]triazolo[3,4-a]phthalazin-6-yl)propane-1,2-diamine (69)**

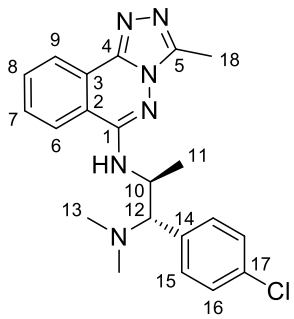

23 (410 mg, 1.875 mmol, 1 eq) and **35** (598 mg, 2.81 mmol, 1.5 eq) were reacted according to general procedure **A**. The crude material was purified by Isolera Biotage LPLC (DCM/MeOH 90:10 then DCM/MeOH/NH_3 9:1:0.5) to give **69** (43 mg, 0.115 mmol 33%) as a white solid.

Mpt: 158.8-160.8 °C; **ν_{max} (cm^{-1})** 3272, 2924, 1593, 1497, 1455, 1262, 1051, 696, 552, 461; **^{1}H-NMR (400 MHz, $CDCl_3$): δ** 8.63 (d, 1H, *J*= 7.8 Hz, *H*-9), 7.83 (m, 2H, *H*-6; *H*-8), 7.75 (m, 1H, *H*-7), 7.41 (d, 2H, *J*= 8.3 Hz, *H*-16), 7.21 (d, 2H, *J*= 8.4 Hz, *H*-15), 6.68 (s, 1H, N*H*), 4.30 (m, 1H, *H*-10), 3.61 (d, 1H, *J*= 10.1 Hz, *H*-12), 2.73 (s, 3H, *H*-18), 2.15 (s, 6H, *H*-13), 1.25 (d, 3H, *J*= 6 Hz, *H*-11); **^{13}C-NMR (100 MHz $CDCl_3$): δ** 151.2 (*C*-1), 147.3 (*C*-4), 142.0 (*C*-5), 133.9 (*C*-8), 132.5 (*C*-14), 132.0 (*C*-17), 130.9 (*C*-16), 130.0 (*C*-7), 128.4 (*C*-15), 124.3 (*C*-9), 123.8 (*C*-3), 122.5 (*C*-6), 119.1 (*C*-2), 72.7 (*C*-12), 47.1 (*C*-10), 40.9 (*C*-13), 17.4 (*C*-11), 9.8 (*C*-18); **LR-ESI-MS:** $C_{21}H_{24}ClN_6$ $[M+H]^+$ *m/z* found 395.3, cald 395.2; **HR-ESI-MS:** $C_{21}H_{24}ClN_6$ $[M+H]^+$ *m/z* found 395.1773, cald 395.1751.

(1*S, 2*S**)-*N*$_1$,*N*$_1$-dimethyl-*N*$_2$-(3-methyl-[1,2,4]triazolo[3,4-a]phthalazin-6-yl)-1-(4-(trifluoromethyl)phenyl)propane-1,2-diamine (70)**

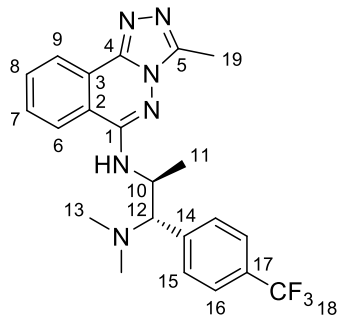

23 (170 mg, 0.778 mmol, 1 eq) and **37** (287 mg, 1.166 mmol, 1.5 eq) were reacted according to general procedure **A**. The crude material was purified by Isolera Biotage LPLC (DCM/MeOH 90:10 then DCM/MeOH/NH_3 9:1:0.5) to give **70** (53 mg, 0.124 mmol, 16%) as a white solid.

Mpt: 143.6-145.6 °C; **ν_{max} (cm^{-1})** 3286, 2958, 2820, 1505, 1320, 1066, 699, 617; **^{19}F-NMR (376 MHz, $CDCl_3$): δ** -62.53; **^{1}H-NMR (400 MHz, $CDCl_3$): δ** 8.64 (d, 1H, *J*= 7.9 Hz, *H*-9), 7.87 (m, 1H, *H*-8), 7.81 (m, 1H, *H*-6), 7.75 (m, 1H, *H*-7), 7.70 (d, 2H, *J*= 8.1 Hz, *H*-16), 7.41 (d, 2H, *J*= 8.1 Hz, *H*-15), 6.62 (s, 1H, N*H*), 4.39 (m, 1H, *H*-10), 3.71 (d, 1H, *J*= 10.3 Hz, *H*-12), 2.74 (s, 3H, *H*-18), 2.21 (s, 6H, *H*-13), 1.26 (d, 3H, *J*= 6 Hz, *H*-11); **^{13}C-NMR (100 MHz $CDCl_3$): δ** 151.2 (*C*-1), 147.3 (*C*-4), 142.0 (*C*-5), 137.8 (*C*-14), 132.5 (*C*-8), 130.0 (q, *J*= 36.7 Hz, *C*-17), 129.9 (*C*-7), 125.1 (q, *J*= 3.7 Hz, *C*-16), 124.4 (*C*-9), 124.1 (q, *J*= 105.6 Hz, *C*-18), 123.9 (*C*-3), 122.7 (*C*-15), 122.5 (*C*-6), 119.1 (*C*-2), 72.9 (*C*-12), 47.1 (*C*-10), 40.9 (*C*-13), 17.4 (*C*-11), 9.8 (*C*-19); **LR-ESI-MS:** $C_{22}H_{24}F_3N_6$ $[M+H]^+$ *m/z* found 429.2, cald 429.2; **HR-ESI-MS:** $C_{22}H_{24}F_3N_6$ $[M+H]^+$ *m/z* found 429.2061, cald 429.2015.

(1*S, 2*S**)-1-(4-methoxyphenyl)-*N*1,*N*$_1$-dimethyl-*N*$_2$-(3-methyl-[1,2,4]triazolo[3,4-a]phthalazin-6-yl)propane-1,2-diamine (71)**

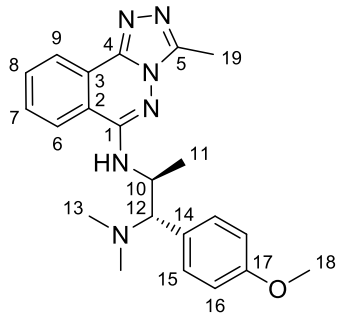

23 (234 mg, 1.07 mmol, 1 eq) and **38** (334 mg, 1.605 mmol, 1.5 eq) were reacted according to general procedure **A**. The crude material was purified by Isolera Biotage LPLC (DCM/MeOH 90:10 then DCM/MeOH/NH_3 9:1:0.5) to give **71** (330 mg, 1.07 mmol, 79%) as a white solid.

Mpt: 171.9-173.9 °C; **ν_{max} (cm^{-1})** 3318, 2929, 2778, 1509, 1263, 1177, 1028, 769; **^{1}H-NMR (400 MHz, $CDCl_3$): δ** 8.63 (d, 1H, *J*= 7.6 Hz, *H*-9), 7.84 (m, 2H, *H*-6; *H*-8), 7.75 (m, 1H, *H*-7), 7.20 (d, 2H, *J*= 8.3 Hz, *H*-15), 6.98 (d, 2H, *J*= 8.6 Hz, *H*-16), 6.85 (s, 1H, N*H*), 4.28 (m, 1H, *H*-10), 3.86 (s, 3H, *H*-18), 3.57 (d, 2H, *J*= 9.8 Hz, *H*-12), 2.74 (s, 3H, *H*-19), 2.17 (s, 6H, *H*-13), 1.26 (d, 3H, *J*= 6 Hz, *H*-11); **^{13}C-NMR (100 MHz, $CDCl_3$): δ** 159.3 (*C*-17), 151.4 (*C*-1), 147.3 (*C*-4), 142.0 (*C*-5, 132.4 (*C*-8), 130.7

(*C*-14), 130.0 (*C*-7), 125.4 (*C*-15), 124.3 (*C*-9), 123.8 (*C*-3), 122.6 (*C*-6), 119.3 (*C*-2), 113.5 (*C*-16), 72.7 (*C*-10), 55.2 (*C*-18), 47.4 (*C*-12), 40.8 (*C*-13), 17.5 (*C*-11), 9.8 (*C*-19); **LR-ESI-MS:** $C_{22}H_{27}N_6O$ $[M+H]^+$ *m/z* found 391.4, cald 391.2; **HR-ESI-MS:** $C_{22}H_{27}N_6O$ $[M+H]^+$ *m/z* found 391.2262, cald 391.2246.

(1*S, 2*S**)-*N*$_1$,*N*$_1$-dimethyl-*N*$_2$-(3-methyl-[1,2,4]triazolo[3,4-a]phthalazin-6-yl)-1-phenylpropane-1,2-diamine (72)**

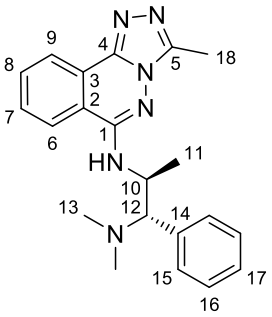

23 (110 mg, 0.503 mmol, 1 eq) and **93** (135 mg, 0.755 mmol, 1.5 eq) were reacted according to general procedure **A**. The crude material was purified by Isolera Biotage LPLC (DCM/MeOH 90:10 then DCM/MeOH/NH_3 9:1:0.5) to give **72** (34 mg, 0.095 mmol, 19%) as a white solid.

The *rac*emic mixture **72** (16 mg) was resolved by preparative chiral HPLC (Chiralpak®OG, CH/IPA 85:15, λ 220 nm, 3 mL/min) to give both enantiomers of **72** which were analysed by analytical chiral HPLC to ascertain optical purity:

***L*-72** (2.8 mg, Chiralpak®OG CH/IPA 9:1, 1 mL/min, R_t= 43.88 min, 90% *ee*) $[\alpha]_D^{20}$ -136 (0.5 *c* in $CHCl_3$)

***D*-72** (5.8 mg, Chiralpak®OG CH/IPA 9:1, 1 mL/min, R_t= 37.13 min, 99% *ee*) $[\alpha]_D^{20}$ +234 (0.5 *c* in $CHCl_3$)

Mpt: 182.7-184.7 °C; **ν_{max} (cm^{-1})** 3242, 3078, 2929, 2771, 1510, 1148, 753, 698, 546; **^{1}H-NMR (400 MHz, DMSO-*d*^{6}): δ** 8.41 (d, 1H, *J*= 7.7 Hz, *H*-9), 8.29 (d, 1H, *H*-6), 7.94 (m, 1H, *H*-8), 7.83 (m, 1H, *H*-7), 7.37 (m, 3H, *H*-15; *H*-17), 7.24 (d, 2H, *J*= 7.0 Hz, *H*-16), 7.08 (d, 1H, *J*= 5.9 Hz, N*H*), 4.71 (m, 1H, *H*-10), 3.72 (d, 1H, *J*= 8.6 Hz, *H*-12), 2.62 (s, 3H, *H*-18), 2.12 (s, 6H, *H*-13), 1.11 (d, 3H, *J*= 6.4 Hz, *H*-11); **^{13}C-NMR (100 MHz, DMSO-*d*^{6}): δ** 150.7 (*C*-1), 146.1 (*C*-4), 141.1 (*C*-5), 135.7 (*C*-14), 132.9 (*C*-8), 130.2 (*C*-7), 129.4 (*C*-15), 127.8 (*C*-16), 127.3 (*C*-17), 124.1 (*C*-9), 123.4 (*C*-3), 122.5 (*C*-6), 118.3 (*C*-2), 71.6 (*C*-12), 46.5 (*C*-10), 41.8 (*C*-13), 16.5 (*C*-11), 9.4 (*C*-18); **LR-ESI-MS**:

$C_{21}H_{25}N_6$ $[M+H]^+$ *m/z* found 361.3, cald 361.2; **HR-ESI-MS**: $C_{21}H_{25}N_6$ $[M+H]^+$ *m/z* found 361.2161, cald 361.2141.

4-((1*S, 2*S**)-1-(dimethylamino)-2-((3-methyl-[1,2,4]triazolo[3,4-a]phthalazin-6-yl)amino)propyl)benzoic acid (103)**

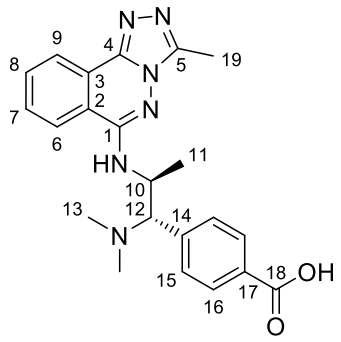

To a stirred solution of **67** (38 mg, 0.091 mmol, 1 eq) in THF/H_2O (908 µL, 2:1, 0.1 M) was added LiOH.H_2O (33 mg, 1.362 mmol, 15 eq) portion wise and allowed to stir for 16 h. Upon reaction completion the mixture was carefully quenched with 1N HCl (1.3 mL, 1.362 mmol, 15 eq) and concentrated down to dryness. The crude material was suspended in DCM/MeOH (9:1, 50 mL) and sonicated prior to being filtered through a sintered frit. The filtrate was concetrated down to give **103** (39 mg, 0.097 mmol, *quant*.) as a white solid.

Mpt: 256.3-258.3 °C; **ν_{max} (cm^{-1})** 3276, 2918, 1698, 1515, 1268, 1116, 700; **^{1}H-NMR (400 MHz, DMSO-*d*^{6}): δ** 8.42 (m, 2H, *H*-6; *H*-9), 8.05 (d, 1H, *J*= 7.9 Hz, *H*-16), 7.97 (t, 1H, *J*= 7.6 Hz, *H*-8), 7.85 (t, 1H, *J*= 7.7 Hz, *H*-7), 7.64 (m, 3H, *H*-15, N*H*), 5.15 (br-s, 1H, *H*-12), 4.85 (br-s, 1H, *H*-10), 4.78 (m, 1H, *H*-10), 3.85 (s, 3H, *H*-19), 3.79 (d, 1H, *J*= 7.7 Hz, *H*-12), 2.68 (m, 9H, *H*-13; *H*-19), 1.18 (d, 3H, *J*= 6.5 Hz, *H*-11); **^{13}C-NMR (100 MHz, DMSO-*d*^{6}): δ** 170.3 (*C*-18), 150.9 (*C*-1), 146.1 (*C*-4), 141.1 (*C*-5), 136.6 (*C*-14), 132.8 (*C*-8), 130.3 (*C*-7), 128.7 (*C*-16), 128.4 (*C*-15), 124.5 (*C*-9), 123.4 (*C*-3), 122.5 (*C*-6), 118.5 (*C*-2), 71.5 (*C*-12), 46.6 (*C*-10), 41.7 (*C*-13), 16.8 (*C*-11), 9.5 (*C*-19); **LR-ESI-MS:** $C_{22}H_{25}N_6O_2$ $[M+H]^+$ *m/z* found 405.3, cald 405.2; **HR-ESI-MS:** $C_{22}H_{25}N_6O_2$ $[M+H]^+$ *m/z* found 405.2067, cald 405.2039.

tert-butyl (4-(4-((1*S, 2*S**)-1-(dimethylamino)-2-((3-methyl-[1,2,4]triazolo[3,4-a]phthalazin-6-yl)amino)propyl)benzamido)butyl)carbamate (104)**

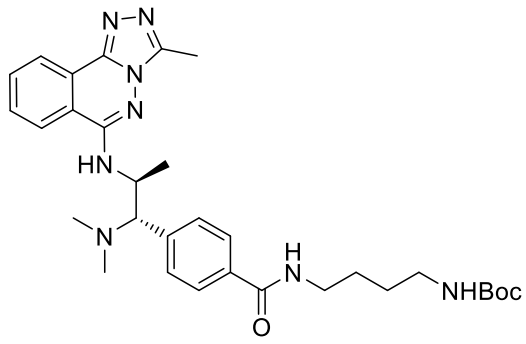

To a stirred solution of **103** (24 mg, 0.059 mmol, 1 eq) in DMF (1.1 mL, 0.05 M, anhydrous) under an

inert atmsosphere (N_2) was added TEA (19 µL, 0.142 mmol, 2.4 eq) and HATU (27 mg, 0.071 mmol, 1.2 eq). The solution was allowed to stir for 10 min before tert-butyl (4-aminobutyl)carbamate (12.5 µL, 0.065 mmol, 1.1 eq) was added. The reaction mixture was allowed to stir for 16 h before being concentrated to dryness and flushed through a silica pad with DCM/MeOH (9:1) to remove impurities and **104** was submitted to the next step without further purification.

***N*-(4-aminobutyl)-4-((1*S**, 2*S**)-1-(dimethylamino)-2-((3-methyl-[1,2,4]triazolo[3,4-a]phthalazin-6-yl)amino)propyl)benzamide (105)**

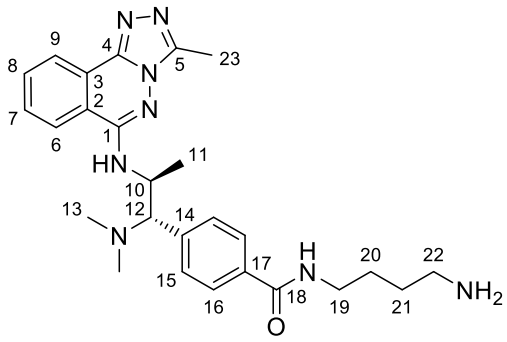

To a stirred solution of **104** (408 mg, 0.710 mmol, 1 eq) in DCM (35 mL, 0.02 M anhydrous) was added TFA (1.4 mL, 17.75 mmol, 25 eq). The reaction mixture was allowed to stir for 16 h at room temperature before being concentrated down to dryness. The crude residue was dissolved in MeOH and purified by SC-X ion exchange chromatography (MeOH to 7N NH_3 in MeOH) to give **105** (150 mg, 0.317 mmol, 45%) as a yellow oil.

ν_{max} (cm^{-1}) 2941, 1670, 1637, 1527, 1420, 1171, 1018, 704; **^{1}H-NMR (400 MHz, DMSO-*d*^{6}): δ** 8.71 (m, 1H, CON*H*), 8.45 (m, 1H, *H*-9), 8.37 (m, 1H, *H*-6), 8.01 (m, 3H, *H*-18; *H*-16), 7.91 (m, 1H, *H*-7), 7.74 (m, 2H, *H*-15), 7.60 (m, 1H, N*H*), 5.17 (m, 1H, *H*-10), 4.77 (m, 1H, *H*-12), 3.32 (d, 2H, *J*= 5.5 Hz, *H*-19), 2.90 (m, 2H, *H*-22), 2.71 (s, 3H, *H*-23), 2.54 (s, 6H, *H*-13), 1.59 (m, 4H, *H*-20; *H*-21), 1.13 (d, 3H, *J*= 6.4 Hz, *H*-11); **^{13}C-NMR (100 MHz DMSO-*d*^{6}): δ** 165.4 (*C*-18), 158.2 (*C*-, 157.9 (*C*-, 151.0 (*C*-1), 146.4 (*C*-4), 141.1 (*C*-5), 136.6 (*C*-14), 132.8 (*C*-8), 130.9 (*C*-7), 130.2 (*C*-16), 127.7 (*C*-15), 123.3 (*C*-9), 118.5 (*C*-3), 118.1 (*C*-6), 115.1 (*C*-2), 71.5 (*C*-12), 43.1 (*C*-10), 40.4 (*C*-13), 38.7 (*C*-22), 38.6 (*C*-19), 26.2 (*C*-20), 24.6 (*C*-21), 17.116.8 (*C*-11), 9.5 (*C*-23); **LR-ESI-MS:** $C_{26}H_{35}N_8O$ $[M+H]^+$ *m/z* found 475.3, cald 475.3; **HR-ESI-MS:** $C_{26}H_{35}N_8O$ $[M+H]^+$ *m/z* found 475.2390, cald 475.2934.

2-((3-methyl-[1,2,4]triazolo[3,4-a]phthalazin-6-yl)amino)-1-phenylethan-1-one (106)

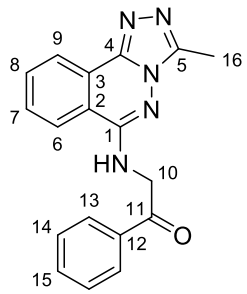

To a stirred solution of **74** (2 g, 6.26 mmol, 1 eq) in DMF (42 mL, 0.15 M, anhydrous) was added Pyridinium Dichromate (11.78 g, 31.3 mmol, 5 eq) portion wise under an inert atmosphere (N_2). The reaction mixture was stirred at room temperature for 48 h after which ice was added to the reaction mixture. A brown precipitate formed which was filtered off and dissolved in $CHCl_3$/MeOH (9:1). The mixture was then filtered through a celite plug to give ketone **106** (1.017 g, 3.20 mmol, 51%) as an off white solid.

Mpt: 156.6-158.6 °C; **ν_{max} (cm^{-1})** 3220, 3074, 2919, 1701, 1571, 1473, 1002, 965, 667; **^{1}H-NMR (400 MHz, DMSO-*d*^{6}): δ** 8.40 (d, 2H, *J*= 8.2 Hz, *H*-13), 8.28 (t, 1H, *J*= 5.6 Hz, N*H*), 8.10 (m, 2H, *H*-6; *H*-9), 7.96 (m, 1H, *H*-8), 7.88 (m, 1H, *H*-7), 7.69 (m, 1H, *H*-15), 7.59 (t, 1H, *J*= 7.9 Hz, *H*-14), 4.90 (d, 1H, *J*= 5.6 Hz, *H*-10), 2.25 (s, 3H, *H*-16); **^{13}C-NMR (100 MHz, DMSO-*d*^{6}): δ** 196.3 (*C*-11), 151.0 (*C*-1), 145.8 (*C*-4), 141.1 (*C*-5), 135.8 (*C*-12), 133.4 (*C*-15, 133.1 (*C*-8), 130.3 (*C*-7), 128.8 (*C*-13, 127.8 (*C*-14), 124.3 (*C*-9), 123.3 (*C*-3), 122.5 (*C*-6), 118.0 (*C*-2), 79.2 (*C*-10), 8.9 (*C*-16); **LR-ESI-MS:** $C_{18}H_{16}N_5O$ $[M+H]^+$ *m/z* found 318.3, cald 318.1; **HR-ESI-MS:** $C_{18}H_{16}N_5O$ $[M+H]^+$ *m/z* found 318.1387, cald 318.1355.

(1*S*, 2*S*)-*N*$_1$,*N*$_1$-dimethyl-*N*$_2$-(3-(trifluoromethyl)-[1,2,4]triazolo[3,4-a]phthalazin-6-yl)cyclohexane-1,2-diamine (107)

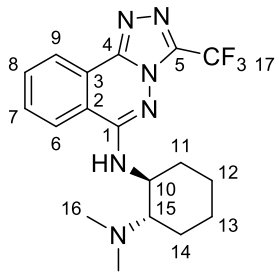

25 (300 mg, 1.1 mmol, 1 eq) and (1*S*,2*S*)-*N*$_1$,*N*$_1$-dimethylcyclohexane-1,2-diamine (313 mg, 2.201 mmol, 2 eq) were reacted according to general procedure **A**. The crude material was purified by Isolera Biotage LPLC (DCM/MeOH 90:10 then DCM/MeOH/NH_3 9:1:0.5) to give **107** (194 mg, 0.514 mmol 47%) as a white solid.

Mpt: 216.6-218.6 °C; **ν_{max} (cm^{-1})** 3312, 2939, 2864, 1530, 1477, 1125, 1024, 991, 735; **^{19}F-NMR (376 MHz, $CDCl_3$): δ** -64.22; **^{1}H-NMR (400 MHz, $CDCl_3$): δ** 8.60 (dd, 1H, *J*= 7.9, 0.7 Hz, *H*-9), 8.06 (d, 1H, *J*= 7.9 Hz, *H*-6), 7.86 (m, 1H, *H*-8), 7.79 (m, 1H, *H*-7), 7.07 (br-s, 1H, N*H*), 3.67 (t, 1H, *J*=

10.5 Hz, *H*-10), 2.87 (m, 2H, *H*-11"; *H*-15), 2.41 (s, 6H, *H*-16), 1.99 (m, 2H, *H*-14), 1.81 (d, 1H, *J*= 11 Hz, *H*-11'), 1.35 (m, 4H, *H*-12; *H*-13); **^{13}C-NMR (100 MHz $CDCl_3$): δ** 152.4 (*C*-1), 143.9 (*C*-4), 139.6 (q, *J*= 40.4 Hz, *C*-5), 132.9 (*C*-8), 131.3 (*C*-7), 124.0 (*C*-9), 123.5 (*C*-3), 122.9 (*C*-6), 119.3 (*C*-2), 118.7 (q, *J*= 270.7 Hz, *C*-17), 66.4 (*C*-15), 53.1 (*C*-10), 39.8 (*C*-16), 31.0 (*C*-11), 25.2 (*C*-14), 24.3 (*C*-13, 21.4 (*C*-12); **LR-ESI-MS:** $C_{18}H_{22}F_3N_6$ $[M+H]^+$ *m/z* found 379.2, cald 379.2; **HR-ESI-MS:** $C_{18}H_{22}F_3N_6$ $[M+H]^+$ *m/z* found 379.1913, cald 379.1858.

(1*S, 2*S**)-*N*$_1$,*N*$_1$-dimethyl-*N*$_2$-(3-(trifluoromethyl)-[1,2,4]triazolo[3,4-a]phthalazin-6-yl)cyclopentane-1,2-diamine (108)**

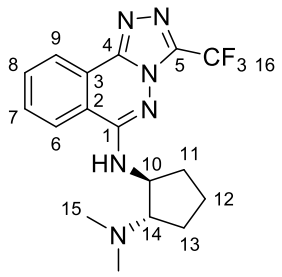

25 (300 mg, 1.1 mmol, 1 eq) and (1*S**,2*S**)-*N*$_1$,*N*$_1$-dimethylcyclopentane-1,2-diamine (212 mg, 1.651 mmol, 1.5 eq) were reacted according to general procedure **A**. The crude material was purified by Isolera Biotage LPLC (DCM/MeOH 90:10 then DCM/MeOH/NH_3 9:1:0.5) to give **108** (306 mg, 0.84 mmol, 76%) as a white solid.

Mpt: 191.1-193.1 °C; **ν_{max} (cm^{-1})** 3483, 3303, 2945, 2775, 1567, 1459, 1184, 1146, 979, 703; **^{19}F-NMR (376 MHz, DMSO-*d*^{6}): δ** -63.12; **^{1}H-NMR (400 MHz, DMSO-*d*^{6}): δ** 8.53 (d, 1H, *J*= 7.8 Hz, *H*-9), 8.49 (dd, 1H, *J*= 7.8, 1.2 Hz, *H*-6), 8.01 (m, 1H, *H*-8), 7.95 (m, 1H, *H*-7), 7.77 (d, 1H, *J*=7.7 Hz, N*H*), 4.31 (m, 1H, *H*-10), 2.97 (m, 1H, *H*-14), 2.18 (s, 6H, *H*-15), 2.08 (m, 1H, *H*-11"), 1.83 (m, 1H, *H*-13"), 1.61 (m, 1H, *H*-11'; *H*-13'; *H*-12); **^{13}C-NMR (100 MHz DMSO-*d*^{6}): δ** 151.9 (*C*-1), 143.7 (*C*-4), 138.2 (q, *J*= 39.6 Hz, *C*-5), 133.3 (*C*-8), 131.6 (*C*-7), 124.6 (*C*-9), 123.2 (*C*-3), 122.1 (*C*-6), 118.9 (*C*-2), 118.7 (q, *J*= 269.2 Hz, *C*-16), 70.7 (*C*-10), 54.6 (*C*-14), 42.5 (*C*-15), 31.3 (*C*-11), 26.9 (*C*-13), 22.0 (*C*-12); **LR-ESI-MS:** $C_{17}H_{20}F_3N_6$ $[M+H]^+$ *m/z* found 365.3, cald 365.2; **HR-ESI-MS:** $C_{17}H_{20}F_3N_6$ $[M+H]^+$ *m/z* found 365.1742, cald 365.1702.

***N*-benzyl-3-(trifluoromethyl)-[1,2,4]triazolo[3,4-a]phthalazin-6-amine (109)**

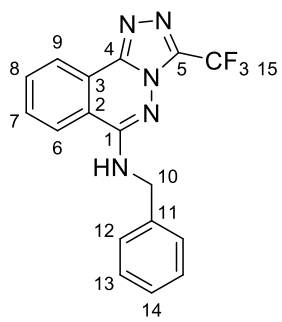

25 (200 mg, 0.734 mmol, 1 eq) and benzylamine (157 mg, 1.467 mmol, 2 eq) were reacted according to general procedure **A**. The crude material was purified by Isolera Biotage LPLC (DCM/MeOH 90:10) to give **109** (134 mg, 0.391 mmol, 53%) as a white solid.

Mpt: 166.8-168.8 °C; **ν_{max} (cm^{-1})** 3888, 1562, 1527, 1289, 1116, 1023, 973, 721, 699, 516; **^{19}F-NMR (376 MHz, $CDCl_3$): δ** -64.07; **^{1}H-NMR (400 MHz, $CDCl_3$): δ** 8.70 (d, 1H, *J*= 7.9 Hz, *H*-9), 7.92 (ddd, 1H, *J*= 8.1, 5.3, 3 Hz, *H*-6), 7.81 (m, 2H, *H*-8, *H*-7), 7.49 (d, 2H, *J*= 7.2 Hz, *H*-12), 7.38 (m, 3H, *H*-13; *H*-14), 5.61 (br-s, 1H, N*H*), 4.73 (d, 2H, *J*= 5.1 Hz, *H*-10); **^{13}C-NMR (100 MHz $CDCl_3$): δ** 151.5 (*C*-1), 143.9 (*C*-11), 137.4 (*C*-4), 133.2 (*C*-8), 131.3 (*C*-7), 128.9 (*C*-12), 128.6 (*C*-13), 128.1 (*C*-14), 126.5 (*C*-14), 124.6 (*C*-9), 123.3 (*C*-3), 122.2 (*C*-6), 118.6 (q, *J*= 269.2 Hz, *C*-15), 118.5 (*C*-2), 46.5 (*C*-10); **LR-ESI-MS:** $C_{17}H_{13}F_3N_5$ $[M+H]^+$ *m/z* found 344.1, cald 344.1; **HR-ESI-MS:** $C_{17}H_{13}F_3N_5$ $[M+H]^+$ *m/z* found 344.1142, cald 344.1123.

***N*$_1$,*N*$_1$,4-trimethyl-*N*$_2$-(3-(trifluoromethyl)-[1,2,4]triazolo[3,4-a]phthalazin-6-yl)pentane-1,2-diamine (110)**

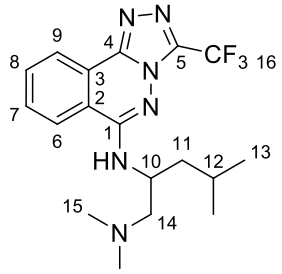

25 (300 mg, 1.1 mmol, 1 eq) and *N*$_1$,*N*$_1$-1,4-trimethylpentane-1,2-diamine (238 mg, 1.651 mmol, 1.5 eq) were reacted according to general procedure **A**. The crude material was purified by Isolera Biotage LPLC (DCM/MeOH 90:10 then DCM/MeOH/NH_3 9:1:0.5) to give **110** (108 mg, 0.283 mmol, 26%) as a white solid.

Mpt: 218.5-220.5 °C; **ν_{max} (cm^{-1})** 3286, 2957, 2821, 1552, 1493, 1148, 1044, 979, 709, 703; **^{19}F-NMR (376 MHz, DMSO-*d*^{6}): δ** -63.29; **^{1}H-NMR (400 MHz, DMSO-*d*^{6}): δ** 8.49 (m, 2H, *H*-9; *H*-6), 8.01 (m, 1H, *H*-8), 7.95 (m, 1H, *H*-7), 7.95 (m, 1H, *H*-7), 7.55 (d, 1H, *J*= 8.4 Hz, N*H*), 4.42 (m, 1H, *H*-10), 2.51 (m, 1H, *H*-14"), 2.28 (dd, 1H, *J*= 11.8, 6.8 Hz, *H*-14'), 2.18 (s, 6H, *H*-15), 1.66 (m, 2H, *H*-11"; *H*-12), 1.48 (m, 1H, *H*-11'), 0.85 (d, 6H, *J*= 7.1 Hz, *H*-13); **^{13}C-NMR (100 MHz DMSO-*d*^{6}): δ** 152.5 (*C*-1), 143.6 (*C*-4), 138.1 (q, *J*= 40.3 Hz, *C*-5), 133.4 (*C*-8), 131.6 (*C*-7), 124.5 (*C*-9), 123.3 (*C*-3), 122.2 (*C*-6), 118.7 (*C*-2), 118.7 (q, *J*= 270 Hz, *C*-16), 63.5 (*C*-10), 47.0 (*C*-14), 45.4 (*C*-15), 41.6

(*C*-11), 24.5 (*C*-12), 23.2 (*C*-13"), 21.7 (*C*-13'); **LR-ESI-MS:** $C_{18}H_{24}F_3N_6$ $[M+H]^+$ *m/z* found 381.3, cald 381.2; **HR-ESI-MS:** $C_{18}H_{24}F_3N_6$ $[M+H]^+$ *m/z* found 381.2061, cald 381.2015.

***N*$_1$,*N*$_1$-dimethyl-*N*$_2$-(3-(trifluoromethyl)-[1,2,4]triazolo[3,4-a]phthalazin-6-yl)ethane-1,2-diamine (111)**

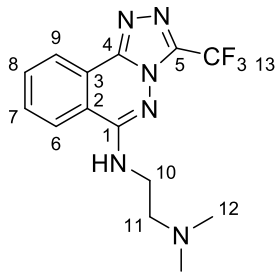

25 (300 mg, 1.1 mmol, 1 eq) and *N*$_1$,*N*$_1$-dimethylethane-1,2-diamine (146 mg, 1.651 mmol, 1.5 eq) were reacted according to general procedure **A**. The crude material was purified by Isolera Biotage LPLC (DCM/MeOH 90:10 then DCM/MeOH/NH_3 9:1:0.5) to give **111** (339 mg, 1.046 mmol, 95%) as a white solid.

Mpt: 166.1-168.1 °C; **ν_{max} (cm^{-1})** 3380, 2948, 2768, 1551, 1499, 1140, 1035, 979, 720, 693; **^{19}F-NMR (376 MHz, $CDCl_3$): δ** -64.19; **^{1}H-NMR (400 MHz, $CDCl_3$): δ** 8.64 (d, 1H, *J*= 7.9 Hz, *H*-9), 7.90 (m, 2H, *H*-6; *H*-8), 7.82 (m, 1H, *H*-7), 6.50 (br-s, 1H, N*H*), 3.61 (m, 2H, *H*-10), 2.75 (t, 2H, *J*= 5.8 Hz, *H*-11), 2.39 (s, 6H, *H*-12); **^{13}C-NMR (100 MHz $CDCl_3$): δ** 152.1 (*C*-1), 144.0 (*C*-4), 139.8 (q, *J*= 41.1 Hz, *C*-5), 133.0 (*C*-8), 131.3 (*C*-7), 124.3 (*C*-9), 123.0 (*C*-3), 122.8 (*C*-6), 118.8 (*C*-2), 118.6 (q, *J*= 270.0 Hz, *C*-16), 56.8 (*C*-10), 45.0 (*C*-11), 38.6 (*C*-12); **LR-ESI-MS:** $C_{14}H_{16}F_3N_6$ $[M+H]^+$ *m/z* found 325.3, cald 325.1; **HR-ESI-MS:** $C_{14}H_{16}F_3N_6$ $[M+H]^+$ *m/z* found 325.1396, cald 325.1389.

***N*$_1$,*N*$_1$-dimethyl-*N*$_2$-(3-(trifluoromethyl)-[1,2,4]triazolo[3,4-a]phthalazin-6-yl)butane-1,2-diamine (112)**

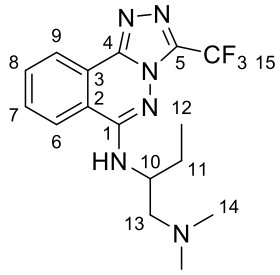

25 (300 mg, 1.1 mmol, 1 eq) and *N*$_1$,*N*$_1$-dimethylbutane-1,2-diamine (166 mg, 1.431 mmol, 1.3 eq) were reacted according to general procedure **A**. The crude material was purified by Isolera Biotage LPLC (DCM/MeOH 90:10 then DCM/MeOH/NH_3 9:1:0.5) to give **112** (299 mg, 0.849 mmol, 77%) as a white solid.

Mpt: 175.1-177.1 °C; **ν_{max} (cm^{-1})** 3298, 2937, 2821, 2773, 1554, 1492, 1287, 1136, 978, 781; **^{19}F-NMR (376 MHz, DMSO-*d*^{6}): δ** -63.35; **^{1}H-NMR (400 MHz, DMSO-*d*^{6}): δ** 8.49 (d, 1H, *J*= 8.1 Hz, *H*-9), 8.44 (d, 1H, *J*= 7.7 Hz, *H*-6), 7.95 (m, 1H, *H*-8), 7.89 (m, 1H, *H*-7), 7.49 (d, 1H, *J*= 7.8 Hz, N*H*),

4.11 (m, 1H, *H*-10), 2.54 (m, 1H, *H*-13"), 2.26 (m, 1H, *H*-13'), 2.15 (s, 6H, *H*-14), 1.76 (m, 1H, *H*-11"), 1.61 (m, 1H, *H*-11'), 0.91 (t, 3H, *J*= 7.3 Hz, *H*-12); **^{13}C-NMR (100 MHz, DMSO-*d*^{6}): δ** 152.5 (*C*-1), 143.6 (*C*-4), 138.1 (q, *J*= 39.6 Hz, *C*-5), 133.2 (*C*-8), 131.4 (*C*-7), 124.5 (*C*-9), 123.1 (*C*-3), 122.1 (*C*-6), 118.7 (*C*-2), 118.7 (q, *J*= 271.43 Hz, *C*-15), 62.5 (*C*-10), 54.8 (*C*-13), 50.9 (*C*-11), 45.4 (*C*-14), 25.0 (*C*-11), 10.6 (*C*-12); **LR-ESI-MS:** $C_{16}H_{20}F_3N_6$ $[M+H]^+$ *m/z* found 353.2, cald 353.2; **HR-ESI-MS:** $C_{16}H_{20}F_3N_6$ $[M+H]^+$ *m/z* found 353.1731, cald 353.1702.

***N*$_2$,*N*$_2$-dimethyl-*N*$_1$-(3-(trifluoromethyl)-[1,2,4]triazolo[3,4-a]phthalazin-6-yl)butane-1,2-diamine (113)**

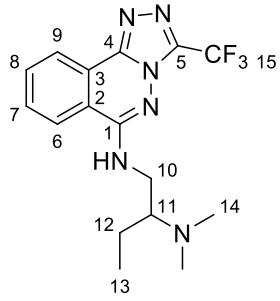

25 (300 mg, 1.1 mmol, 1 eq) and N_2,N_2-dimethylbutane-1,2-diamine (192 mg, 1.651 mmol, 1.5 eq) were reacted according to general procedure **A**. The crude material was purified by Isolera Biotage LPLC (DCM/MeOH 90:10 then DCM/MeOH/NH_3 9:1:0.5) to give **113** (247 mg, 0.702 mmol, 64%) as a white solid.

Mpt: 130.2-132.2 °C; **ν_{max} (cm^{-1})** 3263, 2930, 1565, 1501, 1454, 1178, 1074, 980, 770, 719; **^{19}F-NMR (376 MHz, DMSO-*d*^{6}): δ** -63.20; **^{1}H-NMR (400 MHz, DMSO-*d*^{6}): δ** 8.48 (d, 1H, *J*= 7.6 Hz, *H*-9), 8.36 (d, 1H, *J*= 7.9 Hz, *H*-6), 8.03 (m, 1H, *H*-8), 7.89 (m, 2H, N*H*; *H*-7), 7.49 (d, 1H, *J*= 7.8 Hz, N*H*), 4.23 (m, 1H, *H*-10"), 3.32 (m, 1H, *H*-10'), 2.78 (m, 1H, *H*-11), 2.25 (s, 6H, *H*-14), 1.52 (m, 1H, *H*-12"), 1.31 (m, 2H, *H*-12'), 0.88 (t, 3H, *J*= 7.3 Hz, *H*-13); **^{13}C-NMR (100 MHz DMSO-*d*^{6}): δ** 152.6 (*C*-1), 144.0 (*C*-4), 138.4 (q, *J*= 39.6 Hz, *C*-5), 133.6 (*C*-8), 132.0 (*C*-7), 124.5 (*C*-9), 123.5 (*C*-3), 122.3 (*C*-6), 119.1 (*C*-2), 118.9 (q, *J*= 269.20 Hz, *C*-15), 62.6 (*C*-10), 55.0 (*C*-11), 48.8 (*C*-14), 21.1 (*C*-12), 11.6 (*C*-13); **LR-ESI-MS:** $C_{16}H_{20}F_3N_6$ $[M+H]^+$ *m/z* found 353.3, cald 353.2; **HR-ESI-MS:** $C_{16}H_{20}F_3N_6$ $[M+H]^+$ *m/z* found 353.1722, cald 353.1702.

***N*$_1$,*N*$_1$-diethyl-*N*$_2$-(3-(trifluoromethyl)-[1,2,4]triazolo[3,4-a]phthalazin-6-yl)propane-1,2-diamine (114)**

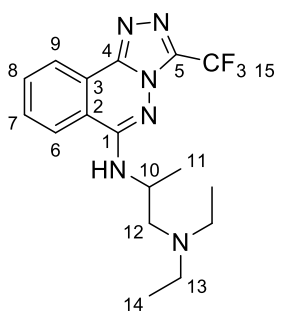

25 (300 mg, 1.1 mmol, 1 eq) and N_1,N_1-diethylpropane-1,2-diamine (215 mg, 1.651 mmol, 1.5 eq) were reacted according to general procedure **A**. The crude material was purified by Isolera Biotage LPLC (DCM/MeOH 90:10 then DCM/MeOH/NH_3 9:1:0.5) to give **114** (171 mg, 0.467 mmol, 42%) as a white solid.

Mpt: 121.1.2-123.1 °C; **ν_{max} (cm^{-1})** 3341, 2970, 2809, 1552, 1492, 1177, 1142, 703, 467; **^{19}F-NMR (376 MHz, DMSO-*d*^{6}): δ** -63.16; **^{1}H-NMR (400 MHz, DMSO-*d*^{6}): δ** 8.47 (m, 2H, *H*-9; *H*-6), 8.00 (m, 1H, *H*-8), 7.94 (m, 1H, *H*-7), 6.52 (d, 1H, *J*= 7.7 Hz, N*H*), 4.19 (m, 1H, *H*-10), 2.59 (m, 1H, *H*-12"), 2.40 (m, 1H, *H*-12'), 1.31 (d, 3H, *J*= 6.5 Hz, *H*-11), 0.93 (t, 6H, *J*= 7.1 Hz, *H*-14); **^{13}C-NMR (100 MHz DMSO-*d*^{6}): δ** 152.0 (*C*-1), 143.7 (*C*-4), 138.1 (q, *J*= 39.61 Hz, *C*-5), 133.3 (*C*-8), 131.5 (*C*-7), 124.4 (*C*-9), 123.2 (*C*-3), 122.2 (*C*-6), 118.8 (*C*-2), 118.7 (q, *J*= 269.2 Hz, *C*-15), 57.7 (*C*-10), 47.1 (*C*-12), 45.8 (*C*-13), 18.0 (*C*-11), 12.0 (*C*-14); **LR-ESI-MS:** $C_{17}H_{22}F_3N_6$ $[M+H]^+$ *m/z* found 367.3, cald 367.2; **HR-ESI-MS:** $C_{17}H_{22}F_3N_6$ $[M+H]^+$ *m/z* found 367.1884, cald 367.1858.

***N*-((1-ethylpyrrolidin-2-yl)methyl)-3-(trifluoromethyl)-[1,2,4]triazolo[3,4-a]phthalazin-6-amine (115)**

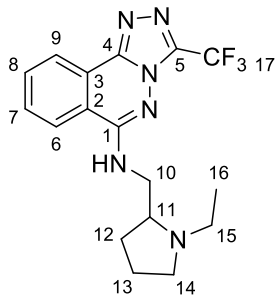

25 (300 mg, 1.1 mmol, 1 eq) and (1-ethylpyrrolidin-2-yl)methanamine (212 mg, 1.651 mmol, 1.5 eq) were reacted according to general procedure **A**. The crude material was purified by Isolera Biotage LPLC (DCM/MeOH 90:10 then DCM/MeOH/NH_3 9:1:0.5) to give **115** (336 mg, 0.929 mmol, 84%) as a white solid.

Mpt: 166.1-168.1 °C; **ν_{max} (cm^{-1})** 3404, 2932, 2800, 1562, 1497, 1526, 1137, 976, 401; **^{19}F-NMR (376 MHz, $CDCl_3$): δ** -64.18; **^{1}H-NMR (400 MHz, $CDCl_3$): δ** 8.66 (d, 1H, *J*= 7.8 Hz, *H*-9), 7.90 (m, 1H, *H*-8), 7.83 (m, 2H, *H*-6; *H*-7), 6.62 (br-s, 1H, N*H*), 3.69 (ddd, 1H, *J*= 13.6, 6.8, 2.5 Hz, *H*-10"), 3.47 (m, 1H, *H*-10'), 3.34 (dt, 1H, *J*= 9.2, 4.7 Hz, *H*-11), 2.89 (m, 2H, *H*-14), 2.35 (m, 2H, *H*-15), 2.03 (m, 1H, *H*-12"), 1.79 (m, 3H, *H*-12'; *H*-13), 1.16 (t, 3H, *J*= 7.2 Hz, *H*-16); **^{13}C-NMR (100 MHz $CDCl_3$): δ** 152.4 (*C*-1), 144.0 (*C*-4), 139.8 (q, *J*= 41.1 Hz, *C*-5), 132.9 (*C*-8), 131.4 (*C*-7), 124.3 (*C*-9), 123.1 (*C*-

3), 122.5 (*C*-6), 119.0 (*C*-2), 118.6 (q, *J*= 268.5 Hz, *C*-15), 61.8 (*C*-11), 53.5 (*C*-14), 48.0 (*C*-15), 42.1 (*C*-10), 28.8 (*C*-12), 23.0 (*C*-13), 13.9 (*C*-16); **LR-ESI-MS:** $C_{17}H_{22}F_3N_6$ $[M+H]^+$ *m/z* found 365.3, cald 365.2; **HR-ESI-MS:** $C_{17}H_{22}F_3N_6$ $[M+H]^+$ *m/z* found 365.1773, cald 365.1702.

tert-butyl ((1*R*,2*S*)-1-hydroxy-1-phenylpropan-2-yl)carbamate (118)

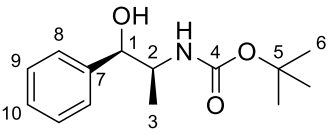

(1*R*,2*S*)-(-)-Norephedrine **117** (4.02 g, 26.6 mmol, 1 eq) was dissolved in CH_2Cl_2 (89 mL, 0.3 M, anhydrous) under an inert atmosphere (N_2). DIPEA (6.95 mL, 39.9 mmol, 1.5 eq) was then added dropwise before the solution was cooled to 0 °C and Boc_2O (9.16 mL, 39.9 mmol, 1.5 eq) was added dropwise. The solution was allowed to stir at ambient temperature for 16 h. The reaction mixture was then concentrated to dryness and the crude material was purified by Isolera Biotage LPLC (DCM/MeOH 1:0 then DCM/MeOH 9:1) to give **118** (3.374 g, 13.42 mmol, 51%) as a white solid.

Mpt: 88.9-90.9 °C; **ν_{max} (cm^{-1})** 3358, 2984, 1679, 1523, 1448, 1160, 1013, 856, 697; **^{1}H-NMR (400 MHz, $CDCl_3$):** δ 7.23 (m, 5H, *H*-8, *H*-9, *H*-10), 4.78 (br-s, 1H, *H*-1), 4.60 (br-s, 1H, N*H*), 3.94 (br-s, 1H, O*H*), 3.33 (br-s, 1H, *H*-2), 1.40 (s, 9H, *H*-6), 0.92 (d, 3H, *J*= 6.8 Hz, *H*-3) **^{13}C-NMR (100 MHz $CDCl_3$): δ** 156.4 (*C*-4), 140.8 (*C*-7), 128.1 (*C*-8), 127.4 (*C*-9), 126.3 (*C*-10), 79.8 (*C*-1), 51.9 (*C*-2), 28.4 (*C*-6), 14.8 (*C*-3); **LR-ESI-MS:** $C_{14}H_{22}NO_3$ $[M+H]^+$ *m/z* found 252.1, cald 252.2; **HR-ESI-MS:** $C_{14}H_{21}NNaO_3$ $[M+Na]^+$ *m/z* found 274.1432, cald 274.1419.

tert-butyl (4*S*,5*R*)-4-methyl-5-phenyl-1,2,3-oxathiazolidine-3-carboxylate 2,2-dioxide (119)

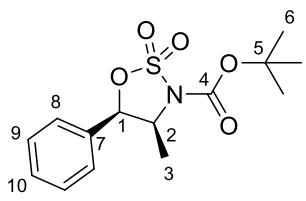

Part one:

118 (1.033g, 4.11 mmol, 1.0 eq) was dissolved in MeCN (10 mL, anhydrous) under an inert atmosphere (N_2). The solution was then added dropwise to a solution of $SOCl_2$ (373 µL, 5.14 mmol, 1.25 eq) in MeCN (10 mL, anhydrous, 0.2 M final concentration) with stirring at -40 °C. After 10 mins of stirring Pyridine (1.324 mL, 16.44 mmol, 4 eq) was then added and the mixture was stirred at -40 °C for 1 h. The mixture was then warmed to 0 °C and stirred for 1 h before H_2O (15 mL) and EtOAc (15 mL) were added. The layers were separated and the organic layers were washed with

1*N* HCl (30 mL). The combined aqueous phases were extracted with EtOAc (x3) before the organic layers were combined and washed with sat. $NaHCO_3$ (x1), brine and then dried over Na_2SO_4 before being concentrated to a brown oil.

Part two:

The residue was taken up in MeCN (20 mL) and cooled to 0 °C. The mixture then had $RuCl_3.3H_2O$ (20 mg, 0.041 mmol, 2 mol%), $NaIO_4$ (1.319 g, 6.17 mmol, 1.5 eq) and H_2O (20 mL) added sequentially before being stirred vigorously for 1 h. The mixture was then diluted with H_2O (20 mL) and Et_2O (20 mL) before the layers were separated and the organic layer was washed successively with H_2O until the brown/black colour had been completely removed. The solution was dried over Na_2SO_4 and concentrated to a residue which was triturated out of cyclohexane to give **119** (0.628 g, 2.00 mmol, 49%) as an off white solid.

Mpt: 111.3-113.3 °C; **ν_{max} (cm^{-1})** 2990, 1731, 1364, 1327, 1184, 1159, 801, 697, 629; **^{1}H-NMR (400 MHz, $CDCl_3$): δ** 7.43 (m, 3H, *H*-8, *H*-10), 7.33 (m, 2H, *H*-9), 5.97 (d, 1H, *J*= 5.3 Hz, *H*-1), 4.58 (dq, 1H, *J*= 6.7, 5.5 Hz, *H*-2), 1.58 (s, 9H, *H*-6), 1.09 (d, 3H, *J*= 6.6 Hz, *H*-3) **^{13}C-NMR (100 MHz $CDCl_3$): δ** 148.4 (*C*-4), 131.3 (*C*-7), 129.4 (*C*-8), 128.9 (*C*-9), 125.4 (*C*-10), 85.5 (*C*-1), 82.3 (*C*-5), 58.6 (*C*-2), 27.9 (*C*-6), 14.2 (*C*-3); **LR-ESI-MS:** $C_{14}H_{23}N_2O_5S$ $[M+NH_4]^+$ *m/z* found 313.1, cald 313.1; **HR-ESI-MS:** $C_{14}H_{19}NNaO_5S$ $[M+Na]^+$ *m/z* found 336.0883, cald 336.0882.

tert-butyl ((1*S*,2*S*)-1-(dimethylamino)-1-phenylpropan-2-yl)carbamate (120)

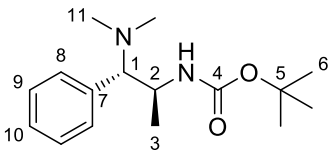

119 (0.627 g, 2.00 mmol, 1.0 eq) was dissolved in THF (2 mL, anhydrous) under an inert atmosphere (N_2) in a sealed tube. Dimethylamine (3 mL, 6.00 mmol, 3 eq, 2 M) was then added dropwise at room temperature and the mixture was allowed to stir at 80 °C for 16 h. The mixture was then concentrated down to dryness and purified by Isolera Biotage LPLC (CH/EA 9:1 then CH/EA 2:8) to give **120** (0.396 g, 1.422 mmol, 71%) as a white solid.

Mpt: 83.4-85.4 °C; **ν_{max} (cm^{-1})** 3373, 2974, 1698, 1485, 1345, 1163, 1060, 863, 703; **^{1}H-NMR (400 MHz, $CDCl_3$): δ** 7.33 (m, 3H, *H*-9, *H*-10), 7.19 (m, 2H, *H*-8), 4.97 (s, 1H, N*H*), 4.02 (m, 1H, *H*-2),

3.21 (d, 1H, *J*= 8.6 Hz, *H*-1), 2.14 (s, 6H, N(C*H*$_3$)$_2$), 1.48 (s, 9H, *H*-6), 1.02 (d, 3H, *H*-3); **^{13}C-NMR (100 MHz CDCl$_3$): δ** 156.0 (*C*-1), 135.3 (*C*-7), 129.5 (*C*-8), 127.9 (*C*-9), 127.5 (*C*-10), 79.0 (*C*-1), 73.7 (*C*-5), 46.4 (*C*-2), 41.9 (*C*-11), 28.5 (*C*-6), 17.4 (*C*-3); **LR-ESI-MS:** $C_{16}H_{27}N_2O_2$ $[M+H]^+$ *m/z* found 279.0, cald 279.2; **HR-ESI-MS:** $C_{16}H_{27}N_2O_2$ $[M+H]^+$ *m/z* found 279.2060, cald 279.2073.

(1*S*,2*S*)-*N*$_1$,*N*$_1$-dimethyl-1-phenylpropane-1,2-diamine (121)

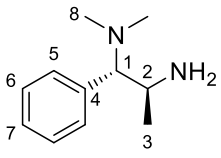

120 (0.396 g, 1.422 mmol, 1.0 eq) was dissolved in CH_2Cl_2 (3.56 mL, 0.4 M, anhydrous) under an inert atmosphere (N_2). TFA (1.09 mL, 14.22 mmol, 10 eq) was then added dropwise before the mixture was allowed to stir for 2 h. The mixture was then concentrated to dryness before being redissolved in a minimal amount of MeOH and purified by a Flash SC-X column eluting with MeOH then 7*N* in MeOH to give **121** (0.266 g, 1.492 mmol, *quant.*) as a colourless oil.

^{1}H-NMR (400 MHz, CDCl$_3$): δ 7.46 (m, 2H, *H*-7, *H*-8), 7.27 (m, 2H, *H*-6), 3.56 (m, 1H, *H*-2), 3.19 (d, 1H, *J*= 9.7 Hz, *H*-3), 2.31 (s, 6H, *H*-4), 1.03 (d, 3H, *J*= 6.2 Hz, *H*-1); **^{13}C-NMR (100 MHz CDCl$_3$): δ** 130.9 (*C*-5), 129.4 (*C*-6), 128.3 (*C*-7), 71.6 (*C*-1), 46.9 (*C*-2), 40.6 (*C*-8), 16.2 (*C*-3); **LR-ESI-MS:** $C_{11}H_{19}N_2$ $[M+H]^+$ *m/z* found 179.2, cald 179.2; *Data in agreement with that found for* **59**.

(1*S*, 2*S*)-*N*$_1$,*N*$_1$-dimethyl-*N*$_2$-(3-methyl-[1,2,4]triazolo[3,4-a]phthalazin-6-yl)-1-phenylpropane-1,2-diamine (*L*-Moses)

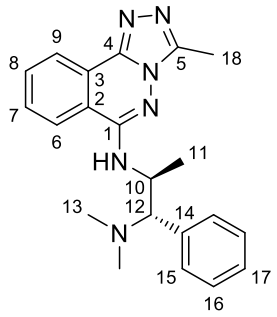

23 (35 mg, 0.160 mmol, 1 eq) and **121** (43 mg, 0.240 mmol, 1.5 eq) were reacted according to general procedure **A**. The crude material was purified by Isolera Biotage LPLC (DCM/MeOH 90:10 then DCM/MeOH/NH_3 9:1:0.5) to give ***L*-Moses** (17 mg, 0.047 mmol, 30%) as a white solid.

***L*-Moses** (Chiralpak®OG CH/IPA 8:2, 1 mL/min, R_t= 14.60 min, >99% *ee*)

^{1}H-NMR (400 MHz, DMSO-*d*^{6}): δ 8.40 (d, 1H, *J*= 7.8 Hz, *H*-9), 8.28 (d, 1H, *J*= 8.3 Hz, *H*-6), 7.93 (m, 1H, *H*-8), 7.82 (m, 1H, *H*-7), 7.37 (m, 3H, *H*-15; *H*-17), 7.22 (d, 2H, *J*= 7.2 Hz, *H*-16), 7.07 (d, 1H, *J*= 5.7 Hz, N*H*), 4.70 (m, 1H, *H*-10), 3.71 (d, 1H, *J*= 8.6 Hz, *H*-12), 2.61 (s, 3H, *H*-18), 2.11 (s, 6H, *H*-

13), 1.11 (d, 3H, *J*= 6.4 Hz, *H*-11); **^{13}C-NMR (100 MHz, DMSO-*d*^{6}): δ** 150.7 (*C*-1), 146.1 (*C*-4), 141.1 (*C*-5), 135.7 (*C*-14), 132.8 (*C*-8), 130.3 (*C*-7), 129.4 (*C*-15), 127.8 (*C*-16), 127.3 (*C*-17), 124.1 (*C*-9), 123.4 (*C*-3), 122.6 (*C*-6), 118.4 (*C*-2), 71.7 (*C*-12), 46.6 (*C*-10), 41.8 (*C*-13), 16.5 (*C*-11), 9.4 (*C*-18); **LR-ESI-MS:** $C_{21}H_{25}N_6$ $[M+H]^+$ *m/z* found 361.3, cald 361.2; *Data in agreement with that found for* **74**.

6-chloro-3-methyl-[1,2,4]triazolo[3,4-a]phthalazine (116)

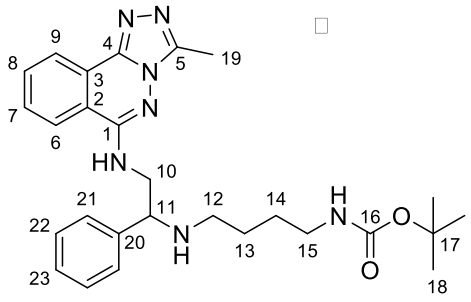

106 (163 mg, 0.514 mmol, 1 eq) was solubilised in $CHCl_3$/MeOH (5.14 mL, 2:1) under a N_2 atmosphere. tert-butyl (4-aminobutyl)carbamate (484 mg, 491 µL, 2.57 mmol, 5 eq) was then added to the solution followed by 8 drops of AcOH. $NaB(CN)H_3$ (38.7 mg, 0.616 mmol, 1.2 eq) was then added and the solution was warmed to 65 °C and allowed to stir for 24 h. Following completion the reaction mixture was concentrated to dryness and the crude material was purified by Isolera Biotage LPLC (DCM/MeOH 90:10) to give **116** (25 mg, 0.051 mmol, 10%) as a white powder.

Mpt: 212.3-214.3 °C; **ν_{max} (cm^{-1})** 3309, 3217, 3067, 2927, 1678, 1515, 1250, 669; **^{1}H-NMR (400 MHz, DMSO-*d*^{6}): δ** 8.37 (d, *J* = 8.7 Hz, 1H, *H*-9), 8.27 (d, *J* = 8.2 Hz, 1H, *H*-6), 7.91 (m, 1H, *H*-8), 7.81 (m, 1H, *H*-7), 7.74 (s, 1H, N*H*Boc), 7.74 (d, *J*= 7.3 Hz, 2H, *H*-21), 7.33 (t, *J*= 7.5 Hz, 2H, *H*-22), 7.23 (m, 1H, *H*-23), 6.73 (s, 1H, C-11-N*H*-C-12), 4.15 (s, 1H, *H*-11), 3.62 (s, 1H, H-10"), 3.46 (s, 1H, *H*-10'), 2.84 (m, 2H, *H*-15), 2.59 (s, 3H, *H*-19), 2.36 (s, 2H, *H*-12), 1.35 (m, 4H, *H*-13/*H*-14), 1.33 (s, 9H); **^{13}C-NMR (100 MHz DMSO-*d*^{6}): δ** 155.5, 151.1, 146.0, 141.1, 132.8, 130.1, 128.2, 127.1, 124.1, 123.3, 122.5, 118.2, 77.2, 60.6, 48.5, 47.0, 28.2, 27.4, 26.9, 9.3; **LR-ESI-MS:** $C_{27}H_{36}N_7O_2$ $[M+H]^+$ *m/z* found 490.6, cald 490.3; **HR-ESI-MS:** $C_{27}H_{36}N_7O_2$ $[M+H]^+$ *m/z* found 490.2962, cald 490.2930.

***N*$_1$-(2-((3-methyl-[1,2,4]triazolo[3,4-a]phthalazin-6-yl)amino)-1-phenylethyl)butane-1,4-diamine, 2xTFA (136)**

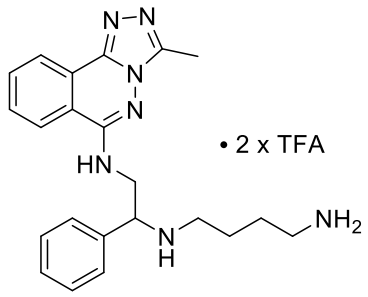

To a stirred solution of **116** (55 mg, 0.112 mmol, 1 eq) in DCM (anhydrous) (1.1 mL, 0.1 M) at room temperature was added TFA (215 µL, 2.81 mmol, 25 eq) and allowed to stir for 16 h. Upon reaction completion the reaction mixture was concentrated down to dryness to afford **136** 2xTFA salt which was submitted to the next step without further purification (66 mg, 0.108 mmol, 96%).

***N*-(4-((2-((3-methyl-[1,2,4]triazolo[3,4-a]phthalazin-6-yl)amino)-1-phenylethyl)amino)butyl)-1-(5-(2-oxohexahydro-1H-thieno[3,4-d]imidazol-4-yl)pentanamido)-3,6,9,12-tetraoxapentadecan-15-amide (73)**

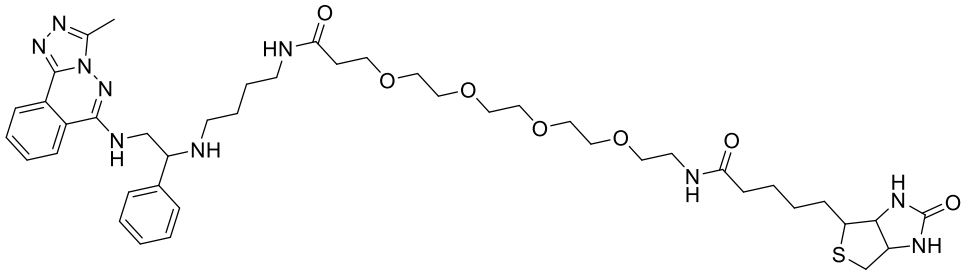

To a stirred solution of **136** (2.5 mg, 6.42 µmol, 1 eq) in DCM (642 µL, 0.01 M, anhydrous) was added 2,5-dioxopyrrolidin-1-yl 17-oxo-21-(2-oxohexahydro-1H-thieno[3,4-d]imidazol-4-yl)-4,7,10,13-tetraoxa-16-azahenicosanoate (3.8 mg, 6.42 µmol, 1 eq). The reaction mixture was stirred for 16 h after which TLC/LCMS analysis confirmed reaction completion. The reaction mixture was concentrated down to dryness and puirified via HPLC (pH 8, MeCN:H_2O) to afford **73** (2.3 mg, 2.66 µmol, 42%) as a white solid.

LR-ESI-MS: $C_{43}H_{63}N_{10}O_7S$ $[M+H]^+$ *m/z* found 864.1, cald 863.4. **ELSD-LCMS** 96% purity.

II.II Protein Expression and Purification

Human bromodomains were cloned, expressed and purified as previously described. [1]

II.III Differential Scanning Fluorimetry (DSF)

Thermal melting points were recorded using an Mx3005p Real Time PCR Machine (Stratagene). Subject proteins were buffered in 10 mM HEPES at pH 7.5, 500 mM NaCl and assayed in a 96-well plate at a final concentration of 2 µM in 20 µL volume. Compounds were then added to a final concentration of 10 µM. SPYRO Orange (Molecular Probes) was used as a fluorescent probe at a dilution of 1:1000. Excitation and emission filters for the SPYRO-Orange dye were set to 465 nm and 590 nm, respectively. The temperature was raised with a step of 3 °C/min from 25 °C to 96 °C and fluorescence readings were taken at each interval. Data was analysed as previously described.[2]

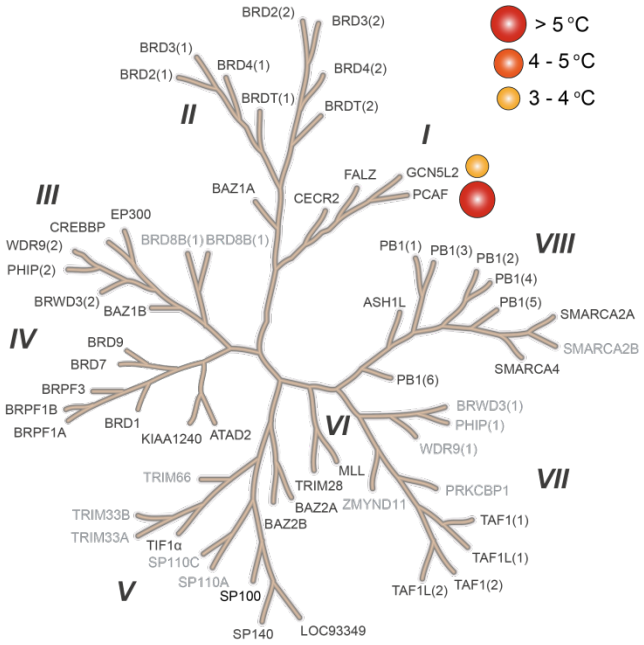

Supplemental Figure 1. *DSF Selectivity panel of L-*Moses *against 48 human Bromodomains.*

Supplemental Table 1. *DSF Selectivity panel of L-*Moses *against 48 human Bromodomains.*

Compound	PCAF ΔT_m(°C)[+]	GCN5L2 ΔT_m(°C)[+]
L-Moses	+5.4 ±0.1	+3.7 ±0.2

[+]Mean ΔT_m ± SEM (number of measurements= 2). Compound concentration: 10 µM

Supplemental Table 2. *DSF results of selected compounds against PCAF and GCN5*

# (10 µM)	PCAF ΔT_m (°C)	GCN5L2 ΔT_m (°C)
29	0.9	0.3
30	5.6	2.5
(S)-**30**	7.4	4.0
31	3.3	1.1
32	0.9	1.1
33	0	0
34	4.6	1.0
(*S*)-**36**	0.7	0.2
78	1.1	0.1
79	1.0	0
81	0.6	0.1
82	0.4	0.1
83	2.7	0.4
84	3.7	0.7
85	2.9	1.1
86	0.5	0
87	0.2	0.3
88	0.2	0
89	1.1	0.5
91	0.6	0.1
92	0.7	0.3
93	0.8	0.1
94	0.9	0
95	0	0.1
98	0.5	0.2
100	0.4	0.2
101	7.3	2.4
102	0.3	0.2
66	8.3	4.4
67	9.6	6.3
68	7.8	4.3
69	6.2	2.7
70	9.1	7.2
71	10.3	6.8
72	7.9	5.0
106	1.0	0.3
107	0.8	0
108	0.7	0.2
109	3.7	0.9
110	0.02	0.2
112	0.4	0.1
113	0.4	0.2
114	0.4	0.1
115	0.1	0.1
116	0	0.2
75	2.8	0.9
76	0.7	0.2
77	3.8	1.5

II.IV Isothermal Titration Calorimetry (ITC)

Experiments were carried out on a Nano-ITC Standard Volume Instrument (TA Instruments). All experiments were carried out at 25 °C in 20 mM HEPES pH 7.5, 150 mM NaCl, 0.5 mM TCEP and 5% glycerol. Protein solutions were buffer exchanged by gel filtration. The titrations were conducted using an initial injection of 2 µL followed by 32 injections of 8 µL. Background dilution heat was substracted from each experiment. Thermodynamic parameters were calculated using $\Delta G = \Delta H - T\Delta S = -RT\ln K_B$, where $K_D = 1/K_B$. ΔG, ΔH and ΔS are changes in free energy, enathalpy and entropy resepectively. Independent single site binding models were employed in data analysis.

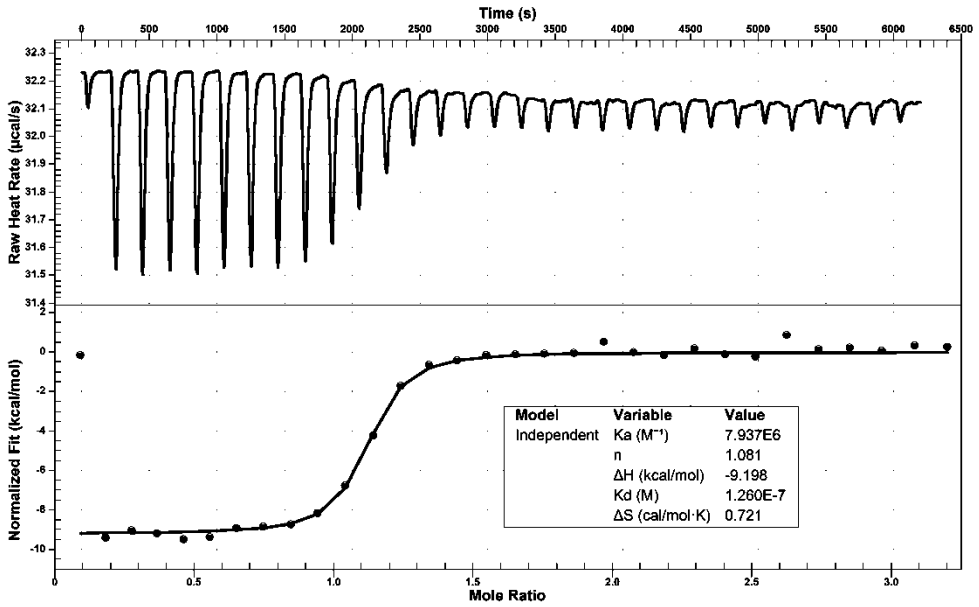

Supplemental Figure 2. *ITC trace of L-Moses and PCAF Brd*

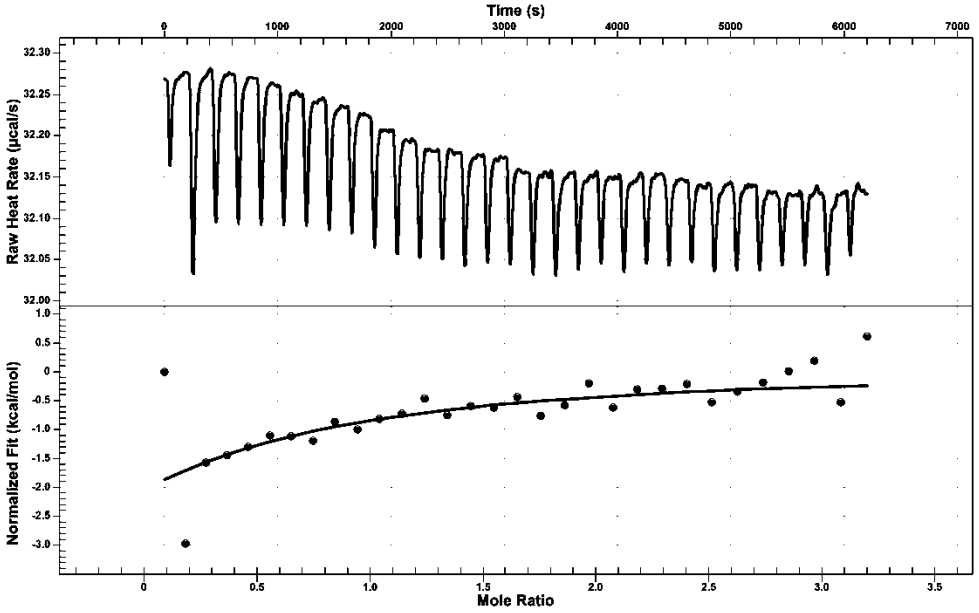

Supplemental Figure 3. *ITC trace of D-Moses and PCAF Brd*

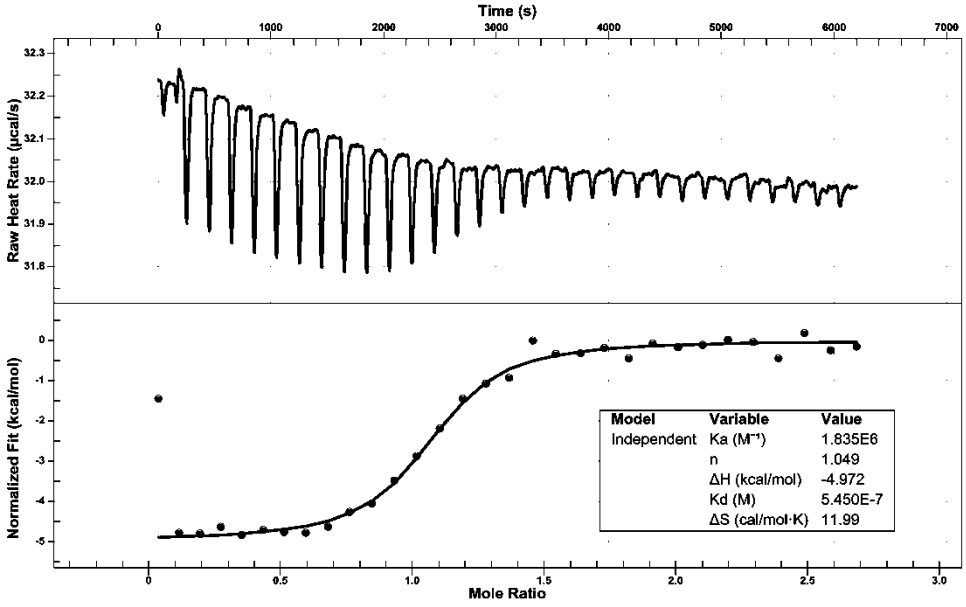

Supplemental Figure 4. *ITC trace of L-Moses and HGCN5 Brd*

ITC *Pf*GCN5

The binding of compound to the bromodomain of *Pf*GCN5 was assessed using isothermal titration calorimetry. The assay was performed at at 25 °C using a VP-ITC instrument (MicroCal,

Northanpton, MA, USA) with 0.2 mM recombinant *Pf*GCN5 and 0.01 mM *L*-Moses, both in a buffer of 20 mM HEPES, 100 mM NaCl , pH 7.5. The experimental data were fitted to a theoeretical titration curve using the software package Origin (MicroCal), resulting in a calculated K_D of (2.8 ± 0.4) x 10^{-7} M.

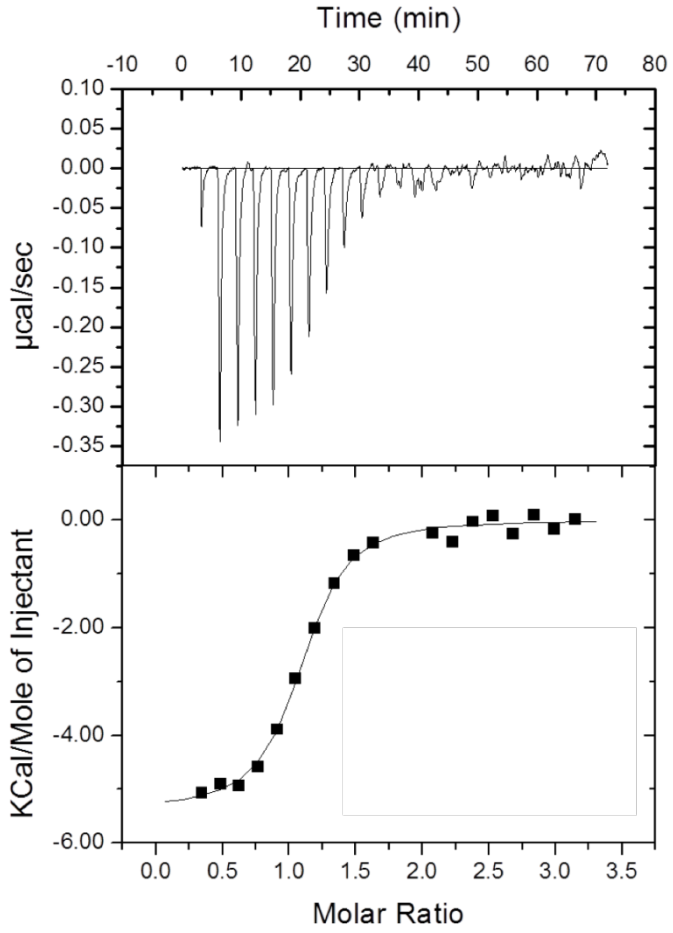

Supplemental Figure 5. *ITC trace of L-Moses and PfGCN5 BRD*

Supplemental Table 3. *Binding affinity of selected compounds (ITC).*

#	PCAF K_D (μM) [+]	
27	7.98	±0.65
28	>30	-
29	>30	-
30	0.298	±0.039
(*S*)-**30**	0.284	±0.029
31	1.76	±0.23
32	>30	-
33	>30	-
34	7.30	±1.1
35	6.90	±1.4
(S)-**36**	>30	-
81	>30	-
82	>30	-
84	4.30	±0.31
85	1.13	±0.24
87	>30	-
89	>30	-
90	>30	-
91	>30	-
92	0.321	±0.039
93	>30	-
94	>30	-
95	>30	-
96	2.3	±0.93
97	>30	-
98	>30	-
100	>30	-
101	0.168	±0.023
66	0.195	±0.040
67	0.133	±0.015
68	0.160	±0.054
69	0.223	±0.078
70	0.163	±0.117
71	0.179	±0.048
72	0.168	±0.027
107	>30	-
108	>30	-
109	>30	-
110	>30	-
111	>30	-
112	>30	-
113	>30	-
114	>30	-
115	>30	-
75	18.2	±0.13
L-**72**/L-Moses	0.126	±0.015
D-**72**/D-Moses	>30	-

[+] Compound concentration: 30 μM, Protein concentration: 280-320 μM.

II.V NanoLuciferase Bioluminescent Resonance Energy Transfer (NanoBRET) Assay

Methods

HEK293 cell (8 x 10^5) were plated in each well of a 6-well plate and co-transfected with Histone H3.3-HaloTag (NM_002107) and a NanoLuciferase fusion of the isolated bromodomain of PCAF. Twenty hours post-transfection, cells were collected, washed with PBS, and exchanged into media containing phenol red-free DMEM and 4% FBS in the absence (control sample) or the presence (experimental sample) of 100 nM NanoBRET 618 fluorescent ligand (Promega). Cell density was adjusted to 2 x 10^5 cells/ml and then re-plated in a 96-well assay white plate (Corning Costar #3917). Compounds were then added directly to media at final concentrations 5 µM or an equivalent amount of DMSO as a vehicle control, and the plates were incubated for 18 h at 37 ^oC in the presence of 5% CO_2. NanoBRET Nano-Glo substrate (Promega) was added to both control and experimental samples at a final concentration of 10 µM. Readings were performed within 5 minutes using a Glo-MAX Discover instrument (Promega) equipped with 450/8 nm bandpass and 600 nm longpass filters with a 0.3 sec reading setting. A corrected BRET ratio was calculated and is defined as the ratio of the emission at 600 nm/450 nm for experimental samples (i.e. those treated with NanoBRET fluorescent ligand) subtracted by and the emission at 600 nm/450 nm for control samples (not treated with NanoBRET fluorescent ligand). BRET ratios are expressed as milliBRET units (mBU), where 1 mBU corresponds to the corrected BRET ratio multiplied by 1000.

II.VI *In vitro* Metabolism Studies

Metabolic stability studies were carried out exposing nominated compounds to samples of liver microsomes. Compounds were analysed by LC-MS for loss of compound at 0, 5, 15, 30 and 45 minute time points. The rate of metabolic degradation of compounds was used to calculate CL_{int}, SE CL_{int}, $t_{1/2}$ (summarised in supplemental table 4.)

Supplemental Table 4. *In vitro metabolic stability of compounds DL-**72**/DL-Moses and **66***

#	Metbolic Stability (Human)				Metbolic Stability (Mouse)			
	CL_{int} (µL/min/mg protein)	SE CL_{int}	$t_{1/2}$	n	CL_{int} (µL/min/mg protein)	SE CL_{int}	$t_{1/2}$	n
DL-**72**/*DL*-Moses	35	2.2	40	5	37	2.6	38	5
66	29	2.0	48	5	21	1.3	65	5

II.VII Cytotoxicity Studies

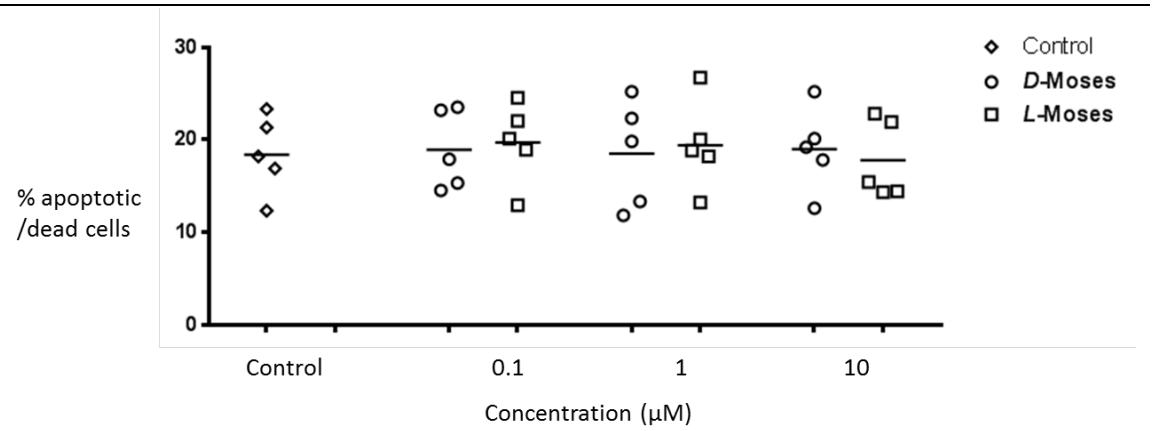

Supplemental Figure 6. *Cytotoxicity studies on PMBC cells of L-Moses and D-Moses*

Toxicity of ***D*-Moses** and ***L*-Moses** were tested on peripheral blood mononuclear cells (PBMC) obtained from 5 healthy donors. PBMC were cultured either with ***D*-Moses** or ***L*-Moses** at concentrations of 0.1, 1 and 10 µM or with a control (DMSO) for 24 hours. Viability of PBMC were then checked using LIVE/DEAD Fixable Aqua Dead Cell Stain Kit (ThermoFisher Scientific).

II.VIII High Throughput Time Resolved Fluorescence Assay (HTRF)

HTRF assay was carried out using a Cisbio Epigenous kit B (62BDBPEH) using the standard assay protocol with GST-$PCAF_{BRD}$.[3] Final assay concentrations: GST-$PCAF_{BRD}$ (20 nM), SA-XL665 (62.5 nM), α-GST donor (62.5 nM), compound **73** (500 nM). K_i was calculated using the Cheng-Prussof equation with a value of 400 nM for the K_D of compound **73**.

II.IX Crystallography

Recombinant *Pf*GCN5 (bromodomain only) was expressed in *E. coli* and purified using a previously described system [4]. The protein crystallized with the compound *L*-Moses at 293 K in 0.1M $CaCl_2$, 30% PEG 8k, 0.2 M NH_4SO_4. The concentrations of the protein sample and the

compound were 10 mg/ml and 2 mM, respectively. X-ray diffraction data for the crystal was collected at 100 K at the beamline 08ID-1 of the Canadian Macromolecular Crystallography Facility. The dataset was processed using the HKL-2000 suite [5], and the structure solved using Phaser [6], a component of the CCP4 suite [7] with molecular replacement model 4QNS. Iterative model building using the graphics program COOT [8], the refinement program Buster-TNT [9] and the validation tools of MOLPROBITY [10] led to a model with a working R value of 0.185 and a R-free value of 0.236 over a resolution range between 37.5-2.10 Å, with excellent stereochemistry.

Supplemental Table 5. *Crystallography data and refinement statistics*

PDB Code	5TPX
Data collection	
Space group	$P42_12$
Cell dimensions	
a, *b*, *c* (Å)	75.00 75.00 49.62
α, β, γ (°)	90.0, 90.0, 90.0
Resolution (Å) (highest resolution shell)	37.50-2.10 (2.14-2.10)
Measured reflections	65686
Unique reflections	8411
R_{meas}(%)	10.0(72.5)
$I/\sigma I$	20.6 (2.2)
Completeness(%)	96.0(89.0)
Redundancy	7.8(7.8)
Refinement	
Resolution (Å)	37.5-2.1
No. reflections (test set)	8368(390)
R_{work}/ R_{free} (%)	18.5/23.6
No. atoms	
Protein	870
Water	66
Heterogen	43
Average B-factors (Å^2)	
Protein	45.06
Water	49.12
Heterogen	54.5
Geometry (RMSD)	
Bond lengths (Å)	0.010
Bond angles (º)	0.67
Ramachandran plot % residues	
Favored	100.0
Additional allowed	0.0
Disallowed	0

II.X Chiral HPLC Traces

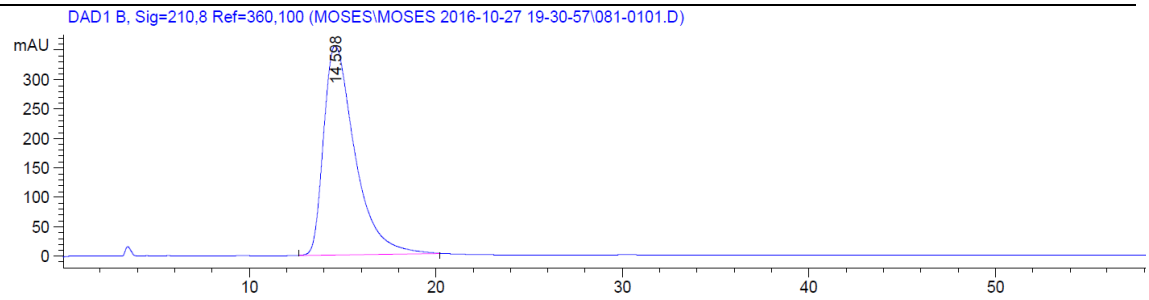

Supplemental Figure 7. *HPLC trace of L-**72**/L-Moses after asymmetric synthesis from (1R,2S)-(-)-Norephedrine **117**. (Chiralpak®OG CH/IPA 8:2, 1 mL/min, R_t= 14.59 min, >99% ee)*

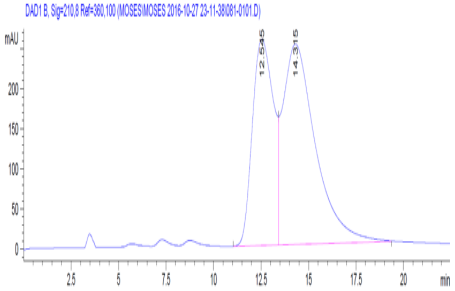

Supplemental Figure 8. *HPLC trace of **72**/DL-Moses. Chiralpak®OG CH/IPA 8:2, 1 mL/min, R_t= 12.54 min and 14.32 min, 0% ee)*

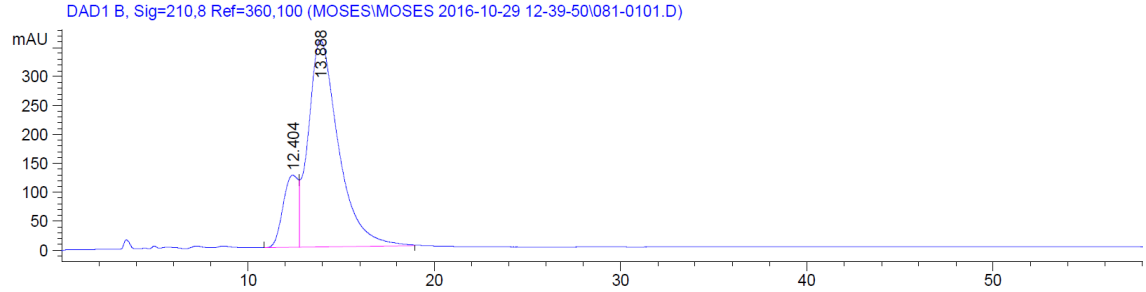

Supplemental Figure 9. *HPLC trace of L-**72**/L-Moses spiked with ~15% **72**/DL-Moses. Chiralpak®OG CH/IPA 8:2, 1 mL/min, R_t= 12.40 min and 13.88 min, 70% ee)*

III Supplemental References Chapter 2: Bromodomain Inhibition

[1] P. Filippakopoulos, S. Picaud, M. Mangos, *et al.*, *Cell* **2012**, *149*, 214-231.
[2] P. Filippakopoulos, J. Qi, S. Picaud, *et al.*, *Nature* **2010**, *468*, 1067-1073.
[3] http://www.cisbio.com/drug-discovery/epigeneous-binding-domain-assays.
[4] M. Vedadi, J. Lew, J. Artz, *et al.*, *Mol. Biochem. Parasitol.* **2007**, *151*, 100-110.
[5] Z. Otwinowski, W. Minor, et al., *Methods Enzymol.* **1997**, *276*, 307-326.
[6] A. J. McCoy, R. W. Grosse-Kunstleve, P. D. Adams, *et al.*, *J. Appl. Crystallogr.* **2007**, *40*, 658-674.
[7] M. D. Winn, C. C. Ballard, K. D. Cowtan, *et al.*, *Acta crystallogr. D, Biol. Crystallogr.* **2011**, *67*, 235-242.
[8] P. Emsley, K. Cowtan, *Acta crystallogr. D, Biol. Crystallogr.* **2004**, *60*, 2126-2132.
[9] E. Blanc, P. Roversi, C. Vonrhein, *et al.*, *Acta crystallogr. D, Biol. Crystallogr.* **2004**, *60*, 2210-2221.
[10] V. B. Chen, W. B. Arendall, 3rd, J. J. Headd, *et al.*, *Acta crystallogr. D, Biol. Crystallogr.* **2010**, *66*, 12-21

7.3.2 Chapter 3 Macrodomain Inhibition

Appendix 7.3.2

Experimental Procedures: Chapter 3 Macrodomain Inhibition

I Practical Experimental

I.I Synthetic Procedures

I.II Isothermal Titration Calorimetry (ITC)

I.I Synthetic Procedures

_N_-(2-(9_H_-carbazol-1-yl)phenyl)acetamide GeA-69 (11)

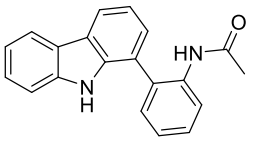

A degassed stirred solution of 1-bromo-9H-carbazole (200 mg, 0.813 mmol, 1 eq), *N*-(2-(4,4,5,5-tetramethyl-1,3,2-dioxaborolan-2-yl)phenyl)acetamide (212 mg, 0.813 mmol, 1 eq), Na_2CO_3 (258 mg, 2.44 mmol, 3 eq) and $Pd(PPh_3)_4$ (94 mg, 0.081 mmol, 0.1 eq) in a mixture of 1,4-Dioxane:EtOH:H2O (2 mL, 2:1:1, 0.4 M) under an inert N_2 atmosphere was heated with microwave irradiation at 90°C for 2 h. Following completion the crude mixture was concentrated onto silica gel and purified by Isolera Biotage LPLC (CH/EA 8:2) to give **11** (85 mg, 35%) as an off-white solid.

ν_{max} (cm^{-1}) 3397, 3309, 1686, 1574, 1516, 1453, 1442, 1287, 1238, 736; **^{1}H-NMR (400 MHz, $CDCl_3$): δ** 8.3 (d, J=8.19 Hz, 1 H), 8.2 (m, 3 H), 7.4 (m, 6 H), 7.3 (m, 2 H), 7.1 (br. s., 1 H), 1.8 (s, 3 H); **^{13}C-NMR (100 MHz $CDCl_3$): δ** 169.0, 139.6, 137.7, 135.4, 130.6, 129.0, 128.8, 126.5, 126.4, 124.9, 23.8, 123.2, 122.6, 120.4, 120.4 ,119.8, 110.9, 24.4; **LR-ESI-MS**: $C_{20}H_{17}N_2O$ $[M+H]^+$ *m/z* found 301.10, cald 301.13.

2-(9H-carbazol-1-yl)aniline (149)

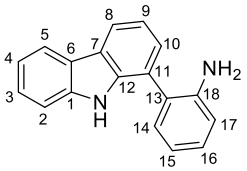

A degassed stirred solution of 1-bromo-9H-carbazole (1.0 g, 4.06 mmol, 1 eq), 2-(4,4,5,5-tetramethyl-1,3,2-dioxaborolan-2-yl)aniline (0.979 g, 4.47 mmol, 1.1 eq), Na_2CO_3 (1.292 g, 12.19 mmol, 3 eq) and $Pd(PPh_3)_4$ (0.235 g, 0.203 mmol, 0.05 eq) in a mixture of 1,4-Dioxane:EtOH:H_2O (8 mL, 2:1:1, 0.5 M) under an inert N_2 atmosphere was heated with microwave irradiation at 90°C for 2 h. Following completion the crude mixture was concentrated onto silica gel and purified by Isolera Biotage LPLC (CH/EA 8:2) to give **149** (0.752 g, 72%) as an off white solid.

ν_{max} (cm^{-1}) 3438, 3347, 3182, 1600, 1491, 1450, 743; **^{1}H-NMR (400 MHz, $CDCl_3$): δ** 8.30 (bs, 1H, N*H*), 8.13 (m, 2H, *H*-10; *H*-17), 7.45 (m, 2H, *H*-8; *H*-5), 7.41 (m, 1H, *H*-14), 7.36 (m, 2H, *H*-2; *H*-9), 7.28 (m, 2H, *H*-4; *H*-16), 6.93 (m, 2H, *H*-15; *H*-17), 3.72 (s, 2H, N*H*$_2$); **^{13}C-NMR (100 MHz $CDCl_3$): δ** 143.7, 139.6, 137.6, 131.3, 129.0, 126.8, 126.0, 124.2, 123.6, 123.5, 122.0, 120.4, 119.9, 119.5, 119.0, 115.8, 110.8; **LR-ESI-MS**: $C_{18}H_{15}N_2$ $[M+H]^+$ *m/z* found 259.07, cald 259.12

Modifications of the acylamino residue on ring D:

General Procedure A: Sulfonamide/carboxamide synthesis

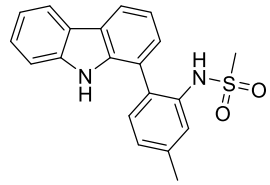

To a stirred solution of 2-(9H-carbazol-1-yl)aniline **149** (1 eq) in CH_2Cl_2 (0.1 M, anhydrous) was added pyridine (1.3 eq) followed by sulfonyl chloride or acid chloride (1.1 eq) and the solution was allowed to stir at room temperature under a nitrogen atmsophere. Upon reaction completion the crude mixture was concentrated onto silica gel and purified by Isolera Biotage LPLC (CH/EA 8:2) to afford pure sulfonamide/amide.

***N*-(2-(9H-Carbazol-1-yl)-5-methylphenyl)methanesulfonamide (138)**

2-(9H-Carbazol-1-yl)-5-methylaniline **151** (50 mg, 0.184 mmol, 1 eq) and methanesulfonyl chloride (16 µL, 0.202 mmol, 1.1 eq) were reacted according to general procedure A to give **138** (44 mg, 0.126 mmol 68%) as a white solid.

ν_{max} (cm^{-1}) 3425, 3246, 1511, 1390, 1317, 1154, 970, 749, 524; **^{1}H-NMR (400 MHz, $CDCl_3$): δ** 8.1 (t, J=7.70 Hz, 2 H), 7.9 (s, 1 H), 7.6 (s, 1 H), 7.4 (m, 1 H), 7.3 (m, 3 H), 7.2 (m, 2 H), 7.1 (m, 1 H), 6.4 (s, 1 H), 2.7 (s, 3 H), 2.4 (s, 3 H); **^{13}C-NMR (100 MHz $CDCl_3$): δ** 139.9, 139.6, 137.8, 134.6, 130.8, 126.5, 126.5, 126.4, 126.3, 124.2, 123.4, 121.6, 120.7, 120.6, 120.2, 120.1, 119.6, 111.0, 39.7, 21.5; **LR-ESI-MS**: $C_{20}H_{19}N_2O_2S$ $[M+H]^+$ *m/z* found 351.11, cald 351.12.

3-Amino-4-(9H-carbazol-1-yl)benzonitrile (139a)

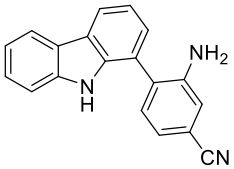

A degassed stirred solution of 1-bromo-9H-carbazole (213 mg, 0.86 mmol, 1 eq), (2-amino-4-cyanophenyl)boronic acid.HCl (189 mg, 0.95 mmol, 1.1 eq), Na_2CO_3 (275 mg, 2.60 mmol, 3 eq) and $Pd(PPh_3)_4$ (50 mg, 0.043 mmol, 0.05 eq) in a mixture of 1,4-Dioxane:EtOH:H_2O (2.5 mL, 2:1:1, 0.5 M) under an inert N_2 atmosphere was heated with microwave irradiation at 90°C for 2 h. Following completion the crude mixture was concentrated onto silica gel and purified by Isolera Biotage LPLC (CH/EA 8:2) to give **139a** (72 mg, 29%) as a red solid.

ν_{max} (cm^{-1}) 3477, 3328, 2230, 1614, 1413, 1316, 1237, 752, 619; **^{1}H-NMR (400 MHz, DMSO-d^6): δ** 10.79 (s, 1H), 8.02 - 8.33 (m, 2H), 7.50 (d, J = 8.07 Hz, 1H), 7.38 (dt, J = 1.04, 7.61 Hz, 1H), 7.24 - 7.33 (m, 3H), 7.21 (d, J = 1.59 Hz, 1H), 7.13 - 7.19 (m, 1H), 7.09 (dd, J = 1.71, 7.70 Hz, 1H), 5.19 (s, 2H); **^{13}C-NMR (100 MHz $CDCl_3$): δ** 146.7, 140.1, 137.1, 131.7, 127.3, 126.0, 125.6, 123.1, 122.4, 120.8, 120.1, 120.0, 119.5, 119.2, 118.9, 118.7, 117.3, 111.4, 110.8; **LR-ESI-MS**: $C_{19}H_{14}N_3$ $[M+H]^+$ *m/z* found 284.05, cald 284.12.

***N*-(2-(9H-Carbazol-1-yl)-5-cyanophenyl)methanesulfonamide (139)**

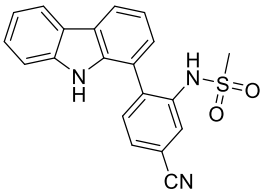

3-Amino-4-(9H-carbazol-1-yl)benzonitrile **139a** (72 mg, 0.254 mmol, 1 eq) and methanesulfonyl chloride (22 µL, 0.28 mmol, 1.1 eq) were reacted according to general procedure A to give **139** (19 mg, 0.052 mmol 21%) as a white solid.

ν_{max} (cm^{-1}) 3361, 2980, 1588, 1501, 1317, 1032, 750; **^{1}H-NMR (400 MHz, $CDCl_3$): δ** 8.2 (d, J=7.70 Hz, 1 H), 8.1 (m, 2 H), 8.0 (s, 1 H), 7.6 (d, J=0.86 Hz, 2 H), 7.4 (m, 3 H), 7.3 (m, 2 H), 6.6 (br. s., 1 H), 2.9 (s, 3 H); **^{13}C-NMR (100 MHz $CDCl_3$): δ** 139.8, 137.1, 136.2, 133.9, 132.3, 128.4, 126.9,

125.8, 124.8, 123.1, 121.8, 120.7, 120.4, 120.4, 117.9, 117.5, 113.3, 111.2, 40.5; **LR-ESI-MS**: $C_{20}H_{16}N_3O_2S$ $[M+H]^+$ *m/z* found 362.13, cald 362.09.

***N*-(2-(9*H*-Carbazol-1-yl)-3-methylphenyl)acetamide (140)**

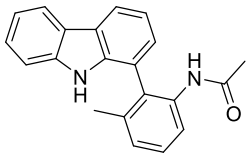

2-(9H-Carbazol-1-yl)-3-methylaniline **153** (43 mg, 0.158 mmol, 1 eq) and acetyl chloride (13 µL, 0.174 mmol, 1.1 eq) were reacted according to general procedure A to give **140** (37 mg, 0.119 mmol 75%) as a white solid.

ν_{max} (cm^{-1}) 3399, 3314, 1680, 1508, 13401, 1335, 1234, 1014, 743; **^{1}H-NMR (400 MHz, $CDCl_3$): δ** 8.1 (d, J=8.07 Hz, 1 H), 8.1 (dd, J=11.55, 7.76 Hz, 2 H), 7.9 (br. s., 1 H), 7.3 (m, 4 H), 7.2 (m, 2 H), 7.1 (d, J=7.58 Hz, 1 H), 6.8 (br. s., 1 H), 2.0 (m, 3 H), 1.6 (s, 3 H); **^{13}C-NMR (100 MHz $CDCl_3$): δ** 168.5, 139.5, 137.9, 137.8, 136.1, 128.8, 127.3, 126.5, 126.3, 126.1, 123.9, 123.3, 120.4, 120.0, 119.7, 119.0, 118.7, 110.9, 24.5, 20.3; **LR-ESI-MS**: $C_{21}H_{19}N_2O$ $[M+H]^+$ *m/z* found 315.31, cald 315.15.

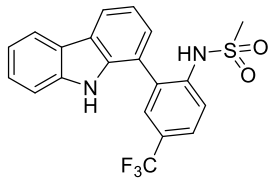

***N*-(2-(9*H*-Carbazol-1-yl)-4-(trifluoromethyl)phenyl)methanesulfonamide (150)**

2-(9H-Carbazol-1-yl)-4-(trifluoromethyl)aniline **152** (82 mg, 0.25 mmol, 1 eq) and methanesulfonyl chloride (21 µL, 0.275 mmol, 1.1 eq) were reacted according to general procedure A to give **150** (11 mg, 0.028 mmol 11%) as a white solid.

ν_{max} (cm^{-1}) 3408, 3328, 1321, 1148, 758, 750, 532; **^{19}F-{H}-NMR (376 MHz, DMSO-*d*^{6}): δ** –58.8; **^{1}H-NMR (400 MHz, $CDCl_3$): δ** 8.2 (m, 2 H), 7.9 (m, 2 H), 7.8 (m, 2 H), 7.4 (m, 3 H), 7.3 (m, 2 H), 6.6 (s, 1 H), 2.9 (s, 3 H); **^{13}C-NMR (100 MHz $CDCl_3$): δ** 139.6, 138.3, 137.3, 128.7, 128.3 (m, J=3.67 Hz), 127.1, 126.8, 126.8, 126.2, 124.7, 123.3, 121.6, 120.7, 120.5, 120.4, 119.0, 117.6, 111.1, 40.3, 26.9; **LR-ESI-MS**: $C_{20}H_{16}F_3N_2O_2S$ $[M+H]^+$ *m/z* found 405.08, cald 405.09.

2-(9*H*-Carbazol-1-yl)-5-methylaniline (151)

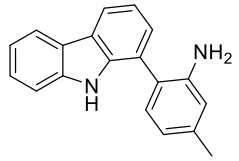

A degassed stirred solution of 1-bromo-9H-carbazole (200 mg, 0.81 mmol, 1 eq), (2-amino-4-methylphenyl)boronic acid (135 mg, 0.89 mmol, 1.1 eq), Na_2CO_3 (258 mg, 2.44 mmol, 3 eq) and $Pd(PPh_3)_4$ (47 mg, 0.041 mmol, 0.05 eq) in a mixture of 1,4-Dioxane:EtOH:H_2O (2.2 mL, 2:1:1, 0.5 M) under an inert N_2 atmosphere was heated with microwave irradiation at 90°C for 2 h. Following completion the crude mixture was concentrated onto silica gel and purified by Isolera Biotage LPLC (CH/EA 8:2) to give **151** (99 mg, 45%) as an off white solid.

ν_{max} (cm^{-1}) 3401, 3328, 1600, 1570, 1452, 1412, 742; **^{1}H-NMR (400 MHz, $CDCl_3$): δ** 8.32 (br. s., 1H), 8.12 (t, J = 7.27 Hz, 2H), 7.38 - 7.49 (m, 3H), 7.31 - 7.37 (m, 1H), 7.20 - 7.28 (m, 2H), 6.77 (d, J = 7.70 Hz, 1H), 6.73 (s, 1H), 3.67 (s, 2H), 2.40 (s, 3H); **^{13}C-NMR (100 MHz $CDCl_3$): δ** 143.5, 139.6, 139.0, 137.7, 131.1, 126.9, 125.9, 123.5, 123.5, 122.0, 121.4, 120.4, 120.0, 119.8, 119.4, 119.4, 116.5, 110.8, 21.3; **LR-ESI-MS**: $C_{19}H_{17}N_2$ $[M+H]^+$ *m/z* found 273.09, cald 273.14.

2-(9*H*-Carbazol-1-yl)-4-(trifluoromethyl)aniline (152)

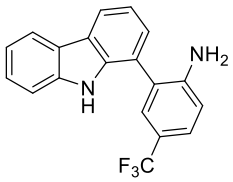

A degassed stirred solution of 1-bromo-9H-carbazole (200 mg, 0.81 mmol, 1 eq), (2-amino-5-(trifluoromethyl)phenyl)boronic acid (183 mg, 0.89 mmol, 1.1 eq), Na_2CO_3 (258 mg, 2.44 mmol, 3 eq) and $Pd(PPh_3)_4$ (47 mg, 0.041 mmol, 0.05 eq) in a mixture of 1,4-Dioxane:EtOH:H_2O (2.2 mL, 2:1:1, 0.5 M) under an inert N_2 atmosphere was heated with microwave irradiation at 90°C for 2 h. Following completion, the crude mixture was concentrated onto silica gel and purified by Isolera Biotage LPLC (CH/EA 8:2) to give **152** (102 mg, 38%) as a brown solid.

ν_{max} (cm^{-1}) 3310, 1659, 1599, 1524, 1454, 1113, 1148, 635, 590; **^{19}F-NMR (376 MHz, $CDCl_3$): δ** -61.08**; ^{1}H-NMR (400 MHz, $CDCl_3$): δ** 8.02 - 8.22 (m, 3H), 7.59 (d, J = 1.59 Hz, 1H), 7.52 (dd, J =

1.71, 8.44 Hz, 1H), 7.40 - 7.47 (m, 3H), 7.34 - 7.39 (m, 1H), 7.24 - 7.31 (m, 1H), 6.92 (d, J = 8.44 Hz, 1H), 4.01 (s, 2H); **^{13}C-NMR (100 MHz $CDCl_3$): δ** 146.7, 139.6, 137.3, 128.4 (q, J=3.7 Hz), 126.8, 126.3, 126.2, 123.8, 123.5, 123.3, 120.5, 120.3, 120.0, 119.8, 115.1, 110.9, 26.9; **LR-ESI-MS**: $C_{19}H_{12}F_3N_2$ $[M-H]^-$ *m/z* found 325.01, cald 325.09.

3-Methyl-2-(4,4,5,5-tetramethyl-1,3,2-dioxaborolan-2-yl)aniline (153a)

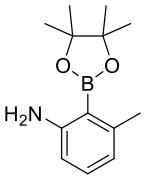

A degassed stirred solution of 2-bromo-3-methylaniline (1.0 g, 5.37 mmol, 1 eq), 4,4,4',4',5,5,5',5'-octamethyl-2,2'-bi(1,3,2-dioxaborolane) (2.73 g, 10.75 mmol, 2 eq), KOAc (1.58 g, 16.1 mmol, 3 eq) and $PdCl_2$(dppf) (197 mg, 0.269 mmol, 0.05 eq) in DMF (9 mL, 0.6 M) under an inert N_2 atmosphere was heated with microwave irradiation at 100°C for 16 h. Following completion the crude mixture was concentrated onto silica gel and purified by Isolera Biotage LPLC (CH/EA 8:2) to give a clear oil which was subsequently purified by SC-X NH_2 column (MeOH then 7*N* NH_3 in MeOH) to give **153a** (142 mg, 11%) as a clear oil.

ν_{max} (cm^{-1}) 2975, 2935, 1459, 1370, 1120, 845; **^{1}H-NMR (400 MHz, $CDCl_3$): δ** 7.1 (t, J=7.70 Hz, 4 H), 6.5 (d, J=7.46 Hz, 4 H), 6.4 (d, J=8.07 Hz, 1 H), 2.5 (s, 3 H), 1.4 (s, 12 H); **^{13}C-NMR (100 MHz $CDCl_3$): δ** 154.4, 146.9, 131.6, 119.6, 112.7, 82.9, 24.9, 23.4; **LR-ESI-MS**: $C_{13}H_{21}BNO_2$ $[M+H]^+$ *m/z* found 234.36, cald 234.17.

2-(9*H*-Carbazol-1-yl)-3-methylaniline (153)

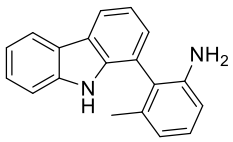

A degassed stirred solution of 1-bromo-9H-carbazole (136 mg, 0.55 mmol, 1 eq), 3-methyl-2-(4,4,5,5-tetramethyl-1,3,2-dioxaborolan-2-yl)aniline **153a** (142 mg, 0.61 mmol, 1.1 eq), Na_2CO_3 (176 mg, 1.66 mmol, 3 eq) and $Pd(PPh_3)_4$ (32 mg, 0.028 mmol, 0.05 eq) in a mixture of 1,4-Dioxane:EtOH:H2O (2 mL, 2:1:1, 0.5 M) under an inert N_2 atmosphere was heated with

microwave irradiation at 90°C for 2 h. Following completion the crude mixture was concentrated onto silica gel and purified by Isolera Biotage LPLC (CH/EA 8:2) to give **153** (69 mg, 46%) as a white solid.

ν_{max} (cm^{-1}) 3394, 3151, 1599, 1415, 801, 654; **^{1}H-NMR (400 MHz, $CDCl_3$): δ** 8.0 (m, 2 H), 7.9 (br. s., 1 H), 7.3 (m, 1 H), 7.2 (d, J=7.46 Hz, 1 H), 7.2 (m, 1 H), 7.1 (m, 2 H), 7.1 (t, J=7.76 Hz, 1 H), 6.7 (d, J= 7.5 Hz, 1H), 6.6 (d, J= 7.9 Hz, 1H), 3.3 (br. s., 2 H), 1.9 (s, 3 H); **^{13}C-NMR (100 MHz $CDCl_3$): δ** 144.7, 139.4, 138.3, 138.1, 128.8, 126.9, 125.9, 123.6, 123.5, 122.9, 120.4, 120.2, 119.9, 119.7, 119.4, 112.9, 110.7, 26.9, 20.2; **LR-ESI-MS**: $C_{19}H_{17}N_2$ $[M+H]^+$ *m/z* found 273.05, cald 273.14.

***N*-(2-(9*H*-Carbazol-1-yl)phenyl)-2-methoxyethane-1-sulfonamide (165)**

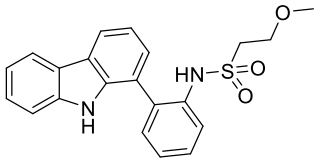

2-(9*H*-Carbazol-1-yl)aniline **149** (50 mg, 0.194 mmol, 1 eq) and 2-methoxyethane-1-sulfonyl chloride (18.71 µL, 0.232 mmol, 1.2 eq) were reacted according to general procedure **A** to give **165** (33 mg, 0.087 mmol 45%) as a white solid.

ν_{max} (cm^{-1}) 3366, 3266, 3219, 2919, 1600, 1322, 1107, 922, 740; **^{1}H-NMR (400 MHz, $CDCl_3$): δ** 8.5 (s, 1 H), 8.1 (m, 2 H), 7.8 (dd, J=8.31, 0.86 Hz, 1 H), 7.3 (m, 6 H), 7.2 (m, 2 H), 6.5 (s, 1 H), 3.5 (m, 2 H), 3.2 (td, J=5.53, 2.38 Hz, 2 H), 2.8 (s, 3 H); **^{13}C-NMR (100 MHz $CDCl_3$): δ** 139.6, 137.6, 135.3, 131.4, 129.3, 128.5, 126.9, 126.3, 124.6, 123.9, 123.3, 120.7, 120.6, 120.0, 119.8, 119.0, 110.7, 66.2, 58.5, 52.4, 26.9; **LR-ESI-MS**: $C_{21}H_{21}N_2O_3S$ $[M+H]^+$ *m/z* found 381.16, cald 381.13.

***N*-(2-(9*H*-Carbazol-1-yl)phenyl)-5-methylisoxazole-4-sulfonamide (166)**

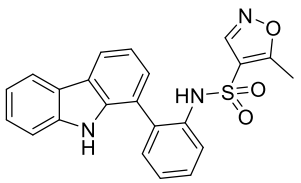

2-(9*H*-Carbazol-1-yl)aniline **149** (50 mg, 0.194 mmol, 1 eq) and 5-methylisoxazole-4-sulfonyl chloride (39 mg, 0.213 mmol, 1.1 eq) were reacted according to general procedure A to give **166** (6 mg, 0.015 mmol 8%) as a white solid.

^{1}H-NMR (400 MHz, $CDCl_3$): δ 8.1 (t, J=7.09 Hz, 2 H), 7.9 (d, J=8.07 Hz, 1 H), 7.8 (s, 1 H), 7.5 (m, 3 H), 7.4 (m, 3 H), 7.3 (t, J=7.64 Hz, 2 H), 7.0 (dd, J=7.34, 0.98 Hz, 1 H), 6.8 (br. s., 1 H), 1.9 (s, 3 H); **^{13}C-NMR (100 MHz $CDCl_3$): δ** 172.0, 148.5, 139.7, 137.3, 133.4, 131.3, 130.9, 129.6, 127.0, 126.8, 125.8, 124.3, 123.8, 123.4, 120.8, 120.6, 120.5, 119.3, 116.1, 111.4, 11.0; **LR-ESI-MS**: $C_{22}H_{18}N_3O_3S$ $[M+H]^+$ *m/z* found 404.14, cald 404.11.

***N*$_1$-(2-(9*H*-Carbazol-1-yl)phenyl)-*N*$_2$,*N*$_2$-dimethylsulfamide (167)**

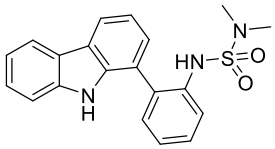

2-(9*H*-Carbazol-1-yl)aniline **149** (50 mg, 0.194 mmol, 1 eq) and dimethylsulfamoyl chloride (31 mg, 0.213 mmol, 1.1 eq) were reacted according to general procedure A to give **167** (8 mg, 0.022 mmol 12%) as a white solid.

^{1}H-NMR (400 MHz, $CDCl_3$): δ 8.0 (m, 2 H), 8.0 (s, 1 H), 7.6 (dd, J=8.25, 0.92 Hz, 1 H), 7.3 (m, 4 H), 7.3 (m, 2 H), 7.2 (m, 2 H), 6.3 (s, 1 H), 2.6 (s, 6 H); **^{13}C-NMR (100 MHz $CDCl_3$): δ** 139.6, 137.6, 135.5, 130.9, 129.3, 128.3, 126.5, 126.4, 124.5, 124.2, 123.3, 120.8, 120.6, 120.2, 119.9, 119.9, 119.6, 111.0, 37.9 **LR-ESI-MS:** $C_{20}H_{20}N_3O_2S$ $[M+H]^+$ *m/z* found 366.15, cald 366.13.

***N*-(2-(9*H*-Carbazol-1-yl)phenyl)benzenesulfonamide (168)**

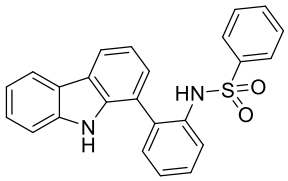

2-(9*H*-Carbazol-1-yl)aniline **149** (50 mg, 0.194 mmol, 1 eq) and benzenesulfonyl chloride (27 µL, 0.213 mmol, 1.1 eq) were reacted according to general procedure A to give **168** (66 mg, 0.165 mmol 85%) as a white solid.

^{1}H-NMR (400 MHz, $CDCl_3$): δ 8.1 (dd, J=7.64, 3.61 Hz, 2 H), 7.8 (d, J=8.07 Hz, 1 H), 7.4 (m, 5 H), 7.3 (m, 6 H), 7.1 (m, 2 H), 6.9 (dd, J=7.27, 0.92 Hz, 1 H), 6.7 (s, 1 H); **^{13}C-NMR (100 MHz $CDCl_3$): δ** 139.5, 138.6, 137.6, 134.4, 132.8, 130.5, 129.9, 129.3, 128.7, 126.9, 126.4, 125.8, 125.6, 123.9, 123.2, 122.4, 120.6, 120.5, 119.9, 119.2, 110.9; **LR-ESI-MS:** $C_{24}H_{19}N_2O_2S$ $[M+H]^+$ *m/z* found 399.12, cald 399.12.

***N*-(2-(9*H*-Carbazol-1-yl)phenyl)-2-phenylacetamide (147)**

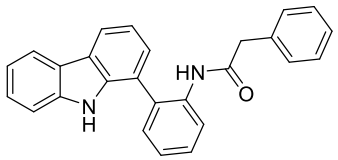

2-(9*H*-Carbazol-1-yl)aniline **149** (50 mg, 0.194 mmol, 1 eq) and 2-phenylacetyl chloride (33 mg, 0.213 mmol, 1.1 eq) were reacted according to general procedure A to give **147** (41 mg, 0.11 mmol 57%) as a white solid.

ν_{max} (cm^{-1}) 3354, 3311, 1661, 1520, 1447, 1320, 1238, 748; **^{1}H-NMR (400 MHz, $CDCl_3$): δ** 8.3 (d, J=8.19 Hz, 1 H), 8.0 (d, J=7.70 Hz, 1 H), 8.0 (d, J=7.70 Hz, 1 H), 7.9 (s, 1 H), 7.4 (m, 2 H), 7.2 (m, 3 H), 7.1 (m, 2 H), 7.0 (dd, J=7.21, 0.98 Hz, 1 H), 6.9 (br. s., 1 H), 6.8 (m, 1 H), 6.6 (t, J=7.64 Hz, 2 H), 6.5 (d, J=7.34 Hz, 2 H), 3.3 (m, 2 H); **^{13}C-NMR (100 MHz $CDCl_3$): δ** 169.6, 139.5, 137.2, 135.4, 132.9, 130.6, 128.9, 128.7, 128.6, 128.5, 127.1, 126.4, 126.2, 124.8, 123.6, 123.5, 121.3, 120.4, 120.2, 119.8, 119.7, 110.9, 44.8; **LR-ESI-MS**: $C_{26}H_{21}N_2O$ $[M+H]^+$ *m/z* found 377.21, cald 377.17.

***N*-(2-(9*H*-Carbazol-1-yl)phenyl)-1-phenylmethanesulfonamide (148)**

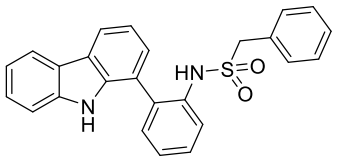

2-(9*H*-Carbazol-1-yl)aniline **149** (50 mg, 0.194 mmol, 1 eq) and phenylmethanesulfonyl chloride (41 mg, 0.213 mmol, 1.1 eq) were reacted according to general procedure A to give **148** (13 mg, 0.032 mmol 16%) as a white solid.

^{1}H-NMR (400 MHz, $CDCl_3$): δ 8.1 (d, J=7.82 Hz, 2 H), 7.9 (s, 1 H), 7.8 (dd, J=8.25, 0.67 Hz, 1 H), 7.5 (m, 4 H), 7.3 (m, 5 H), 7.2 (m, 1 H), 7.1 (m, 3 H), 6.3 (s, 1 H), 4.3 (m, 2 H); **^{13}C-NMR (100 MHz $CDCl_3$): δ** 139.5, 137.6, 135.2, 131.2, 130.5, 129.6, 128.9, 128.8, 128.1, 127.9, 126.5, 126.1,

124.6, 124.2, 123.3, 120.8, 120.6, 120.0, 119.9, 119.1, 118.7, 110.9, 57.9; **LR-ESI-MS:** $C_{25}H_{21}N_2O_2S$ $[M+H]^+$ *m/z* found 413.16, cald 413.13.

***N*-(2-(9*H*-Carbazol-1-yl)phenyl)-2-methoxybenzamide (169)**

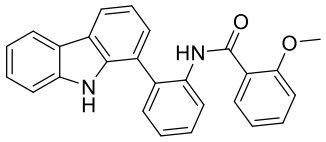

2-(9*H*-Carbazol-1-yl)aniline **149** (50 mg, 0.194 mmol, 1 eq) and 2-methoxybenzoyl chloride (32 µL, 0.213 mmol, 1.1 eq) were reacted according to general procedure A to give **169** (55 mg, 0.140 mmol 73%) as a white solid.

^{1}H-NMR (400 MHz, $CDCl_3$): δ 9.8 (s, 1 H), 8.7 (m, 1 H), 8.1 (m, 4 H), 7.4 (m, 2 H), 7.3 (m, 4 H), 7.2 (m, 3 H), 6.9 (m, 1 H), 6.5 (d, J=8.07 Hz, 1 H), 2.8 (s, 3 H); **^{13}C-NMR (100 MHz $CDCl_3$): δ** 163.7, 157.0, 139.6, 138.1, 136.9, 133.1, 132.4, 130.8, 129.1, 128.4, 127.1, 126.2, 124.2, 123.6, 123.1, 121.9, 121.4, 121.1, 121.0, 120.2, 120.0, 119.8, 119.5, 110.9, 54.9; **LR-ESI-MS**: $C_{26}H_{21}N_2O_2$ $[M+H]^+$ *m/z* found 393.14, cald 393.16.

***N*-(2-(9*H*-Carbazol-1-yl)phenyl)-3-methoxybenzamide (170)**

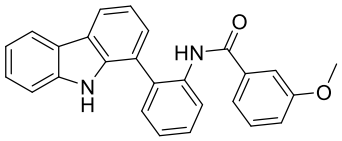

2-(9*H*-Carbazol-1-yl)aniline **149** (50 mg, 0.194 mmol, 1 eq) and 3-methoxybenzoyl chloride (30 µL, 0.213 mmol, 1.1 eq) were reacted according to general procedure A to give **170** (72 mg, 0.184 mmol 95%) as a white solid.

ν_{max} (cm^{-1}) 3391, 3281, 1655, 1485, 1026, 734, 591, 542; **^{1}H-NMR (400 MHz, $CDCl_3$): δ** 8.5 (d, J=8.07 Hz, 1 H), 8.3 (s, 1 H), 8.1 (m, 2 H), 7.8 (s, 1 H), 7.3 (m, 6 H), 7.2 (m, 2 H), 6.9 (m, 1 H), 6.7 (m, 2 H), 6.7 (m, 1 H), 3.3 (s, 3 H); **^{13}C-NMR (100 MHz $CDCl_3$): δ** 165.5, 159.6, 139.7, 137.6, 135.9, 135.7, 130.4, 129.6, 129.2, 128.4, 126.7, 126.5, 124.8, 123.9, 123.2, 121.4, 120.6, 120.4, 120.2, 120.1, 119.9, 118.9, 118.8, 111.0, 110.4, 54.9; **LR-ESI-MS**: $C_{26}H_{21}N_2O_2$ $[M+H]^+$ *m/z* found 393.16, cald 393.16.

***N*-(2-(9*H*-Carbazol-1-yl)phenyl)-4-methoxybenzamide (171)**

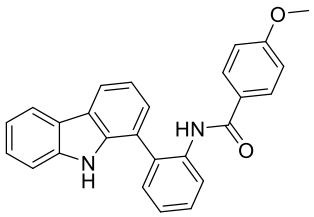

2-(9H-carbazol-1-yl)aniline **149** (50 mg, 0.194 mmol, 1 eq) and 4-methoxybenzoyl chloride (36 mg, 0.213 mmol, 1.1 eq) were reacted according to general procedure A to give **171** (56 mg, 0.142 mmol 74%) as a white solid.

ν_{max} (cm^{-1}) 3400, 3258, 1652, 1600, 1504, 1313, 1170, 801, 587; **^{1}H-NMR (400 MHz, $CDCl_3$): δ** 8.5 (m, 1 H), 8.2 (s, 1 H), 8.1 (m, 2 H), 7.8 (s, 1 H), 7.4 (m, 2 H), 7.3 (m, 4 H), 7.2 (m, 4 H), 6.5 (m, 2 H), 3.6 (s, 3 H); **^{13}C-NMR (100 MHz $CDCl_3$): δ** 165.1, 162.3, 139.6, 137.7, 135.9, 130.3, 129.2, 128.5, 128.4, 126.6, 126.6, 126.4, 124.5, 123.9, 123.2, 121.6, 120.6, 120.5, 120.2, 119.9, 119.8, 113.8, 110.9, 55.3; **LR-ESI-MS**: $C_{26}H_{21}N_2O_2$ $[M+H]^+$ *m/z* found 393.13, cald 393.16.

***N*-(2-(9*H*-Carbazol-1-yl)phenyl)-2-(pyridin-3-yl)acetamide (172)**

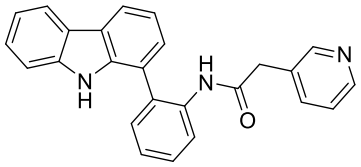

2-(9*H*-Carbazol-1-yl)aniline **149** (50 mg, 0.194 mmol, 1 eq), 2-(pyridin-3-yl)acetic acid (32 mg, 0.232 mmol, 1.2 eq) and DIPEA (162 µL, 0.929 mmol, 4.8 eq) were dissolved in DCM (2 mL, 0.1 M) and then had HATU (88 mg, 0.232 mmol, 1.2 eq) added before the solution was stirred for 16 h at room temperature. Upon reaction completion the crude mixture was concentrated onto silica gel before being purified by Isolera Biotage LPLC (CH/EA 8:2) to give **172** (22 mg, 0.057 mmol, 29%) as a white solid.

Mpt: 145.2-147.2 °C; **ν_{max} (cm^{-1})** 1675, 1498, 1240, 1015, 839, 751, 702; **^{1}H-NMR (400 MHz, DMSO-d^6): δ** 10.7 (s, 1 H), 9.2 (s, 1 H), 8.3 (m, 1 H), 8.3 (s, 1 H), 8.2 (m, 2 H), 7.8 (m, 1 H), 7.5 (d, J=8.07 Hz, 3 H), 7.4 (s, 2 H), 7.3 (m, 1 H), 7.2 (m, 3 H), 7.1 (m, 1 H), 3.4 (s, 2 H); **^{13}C-NMR (100 MHz DMSO-d^6): δ** 168.8, 164.6, 149.9, 147.5, 140.2, 137.7, 136.3, 135.6, 132.5, 131.3, 130.7,

127.9, 126.3, 125.7, 125.5, 123.2, 123.2, 122.6, 121.4, 120.0, 119.5, 118.6, 118.6, 111.5, 38.2; **LR-ESI-MS**: $C_{25}H_{18}N_3O$ $[M-H]^-$ *m/z* found 378.25, cald 378.16.

***N*-(2-(9*H*-Carbazol-1-yl)phenyl)-2-(6-methylpyridin-3-yl)acetamide (173)**

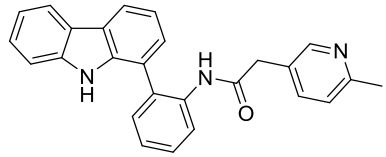

2-(9H-carbazol-1-yl)aniline **149** (50 mg, 0.194 mmol, 1 eq), 2-(6-methylpyridin-3-yl)acetic acid (35 mg, 0.232 mmol, 1.2 eq) and DIPEA (162 µL, 0.929 mmol, 4.8 eq) were dissolved in DCM (2 mL, 0.1 M) and then had HATU (88 mg, 0.232 mmol, 1.2 eq) added before the solution was stirred for 16 h at room temperature. Upon reaction completion the crude mixture was concentrated onto silica gel before being purified by Isolera Biotage LPLC (CH/EA 8:2) to give **173** (56 mg, 0.143 mmol, 74%) as a white solid.

Mpt: 126.6-128.6 °C; **ν_{max} (cm^{-1})** 2981, 1683, 1602, 1287, 1021, 839, 732; **^{1}H-NMR (400 MHz, DMSO-*d*^{6}): δ** 10.7 (s, 1 H), 9.0 (s, 1 H), 8.1 (m, 3 H), 7.8 (d, J=7.95 Hz, 1 H), 7.4 (d, J=7.09 Hz, 3 H), 7.3 (m, 2 H), 7.1 (m, 4 H), 6.8 (d, J=7.95 Hz, 1 H), 2.3 (m, 3 H); **^{13}C-NMR (100 MHz DMSO-*d*^{6}): δ** 168.9, 155.8, 149.1, 140.2, 137.6, 136.5, 135.6, 132.3, 130.7, 128.0, 126.3, 125.6, 125.3, 123.2, 122.6, 122.5, 121.3, 120.1, 119.6, 118.7, 118.6, 111.5, 23.6; **LR-ESI-MS**: $C_{26}H_{22}N_3O$ $[M+H]^+$ *m/z* found 392.26, cald 392.18.

***N*-(2-(9*H*-Carbazol-1-yl)phenyl)-2-(pyrazin-2-yl)acetamide (174)**

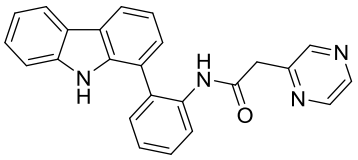

2-(9*H*-Carbazol-1-yl)aniline **149** (50 mg, 0.194 mmol, 1 eq), 2-(pyrazin-2-yl)acetic acid (40 mg, 0.29 mmol, 1.5 eq) and DIPEA (162 µL, 0.929 mmol, 4.8 eq) were dissolved in DCM (2 mL, 0.1 M) and then had HATU (88 mg, 0.232 mmol, 1.2 eq) added before the solution was stirred for 16 h at room temperature. Upon reaction completion the crude mixture was concentrated onto silica

gel before being purified by Isolera Biotage LPLC (CH/EA 8:2) to give **174** (32 mg, 0.084 mmol, 44%) as a white solid.

Mpt: 189.0-191.0 °C; **ν_{max} (cm^{-1})** 3296, 1659, 1581, 1532, 1312, 1236, 738; **^{1}H-NMR (400 MHz, $CDCl_3$): δ** 8.8 (br. s., 1 H), 8.3 (d, J=7.95 Hz, 1 H), 8.0 (m, 3 H), 7.8 (d, J=2.57 Hz, 2 H), 7.4 (m, 1 H), 7.3 (m, 5 H), 7.2 (m, 3 H), 3.5 (m, 2 H); **^{13}C-NMR (100 MHz $CDCl_3$): δ** 166.6, 149.4, 144.1, 142.8, 142.6, 139.2, 137.6, 135.5, 130.9, 129.2, 128.9, 126.9, 126.3, 125.0, 123.4, 123.1, 122.4, 120.8, 120.3, 120.0, 119.8, 119.7, 110.7, 42.9; **LR-ESI-MS**: $C_{24}H_{19}N_4O$ $[M+H]^+$ *m/z* found 379.25, cald 379.16.

***N*-(2-(9*H*-Carbazol-1-yl)phenyl)-2-(2-cyanopyridin-4-yl)acetamide (175)**

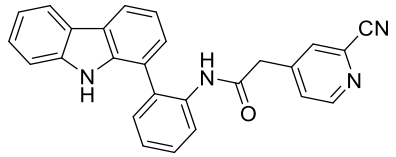

2-(9*H*-Carbazol-1-yl)aniline **149** (50 mg, 0.194 mmol, 1 eq), 2-(2-cyanopyridin-4-yl)acetic acid (38 mg, 0.232 mmol, 1.2 eq) and DIPEA (101 µL, 0.581 mmol, 3 eq) were dissolved in DCM (2 mL, 0.1 M) and then had HATU (88 mg, 0.232 mmol, 1.2 eq) added before the solution was stirred for 16 h at room temperature. Upon reaction completion the crude mixture was concentrated onto silica gel before being purified by Isolera Biotage LPLC (CH/EA 8:2) to give **175** (57 mg, 0.142 mmol, 73%) as a white solid.

Mpt: 194.1-196.1 °C; **ν_{max} (cm^{-1})** 3387, 3319, 1671, 1523, 1313, 1218, 750; **^{1}H-NMR (400 MHz, DMSO-d^6): δ** 10.7 (s, 1 H), 9.4 (s, 1 H), 8.4 (d, J=5.01 Hz, 1 H), 8.1 (dd, J=8.19, 6.60 Hz, 2 H), 7.8 (d, J=7.82 Hz, 1 H), 7.6 (s, 1 H), 7.4 (m, 5 H), 7.2 (d, J=4.03 Hz, 1 H), 7.2 (m, 3 H), 3.5 (s, 2 H); **^{13}C-NMR (100 MHz DMSO-d^6): δ** 167.7, 150.8, 146.7, 140.1, 137.6, 135.4, 133.1, 132.3, 130.8, 129.4, 128.1, 128.0, 126.2, 125.9, 125.5, 123.1, 122.4, 121.6, 120.1, 119.5, 118.6, 118.4, 117.4, 111.3, 41.2; **LR-ESI-MS**: $C_{26}H_{19}N_4O$ $[M+H]^+$ *m/z* found 403.53, cald 403.16.

***N*-(2-(9*H*-Carbazol-1-yl)phenyl)-2-(6-cyanopyridin-3-yl)acetamide (176)**

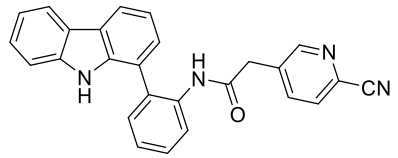

2-(9*H*-Carbazol-1-yl)aniline **149** (50 mg, 0.194 mmol, 1 eq), 2-(6-cyanopyridin-3-yl)acetic acid (38 mg, 0.232 mmol, 1.2 eq) and DIPEA (101 µL, 0.581 mmol, 3 eq) were dissolved in DCM (2 mL, 0.1 M) and then had HATU (88 mg, 0.232 mmol, 1.2 eq) added before the solution was stirred for 16 h at room temperature. Upon reaction completion the crude mixture was concentrated onto silica gel before being purified by Isolera Biotage LPLC (CH/EA 8:2) to give **176** (64 mg, 0.159 mmol, 82%) as a white solid.

Mpt: 220.3-222.3 °C; **ν_{max} (cm^{-1})** 3280, 2980, 1667, 1581, 1519, 1445, 1318, 1032, 751; **^{1}H-NMR (400 MHz, DMSO-*d*^{6}): δ** 10.6 (s, 1 H), 9.3 (s, 1 H), 8.4 (s, 1 H), 8.1 (m, 2 H), 7.8 (d, J=7.82 Hz, 1 H), 7.6 (d, J=7.95 Hz, 1 H), 7.5 (m, 3 H), 7.4 (m, 3 H), 7.2 (m, 3 H), 3.6 (s, 2 H); **^{13}C-NMR (100 MHz DMSO-*d*^{6}): δ** 167.8, 151.5, 140.1, 137.6, 137.5, 136.0, 135.4, 132.8, 130.8, 130.5, 128.3, 128.0, 126.3, 125.8, 125.5, 123.0, 122.5, 121.5, 120.0, 119.5, 118.6, 118.5, 117.5, 111.4; **LR-ESI-MS**: $C_{26}H_{19}N_4O$ $[M+H]^+$ *m/z* found 403.56, cald 403.16.

***N*-(2-(9*H*-Carbazol-1-yl)phenyl)-2-(6-oxo-1,6-dihydropyridin-3-yl)acetamide (177)**

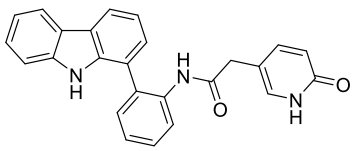

2-(9*H*-Carbazol-1-yl)aniline **149** (50 mg, 0.194 mmol, 1 eq), 2-(6-oxo-1,6-dihydropyridin-3-yl)acetic acid (36 mg, 0.232 mmol, 1.2 eq) and DIPEA (101 µL, 0.581 mmol, 3 eq) were dissolved in DCM (2 mL, 0.1 M) and then had HATU (88 mg, 0.232 mmol, 1.2 eq) added before the solution was stirred for 16 h at room temperature. Upon reaction completion the crude mixture was concentrated onto silica gel before being purified by Isolera Biotage LPLC (CH/EA 8:2) to give **177** (49 mg, 0.123 mmol, 64%) as a white solid.

Mpt: 219.4-221.4 °C; **ν_{max} (cm^{-1})** 3348, 3260, 1662, 1624, 1518, 1445, 1238, 555; **^{1}H-NMR (400 MHz, DMSO-*d*^{6}): δ** 11.3 (br. s., 1 H), 10.8 (s, 1 H), 9.0 (s, 1 H), 8.1 (m, 2 H), 7.8 (d, J=7.95 Hz, 1 H), 7.5 (m, 3 H), 7.4 (m, 2 H), 7.2 (m, 3 H), 7.0 (d, J=1.71 Hz, 1 H), 6.9 (dd, J=9.35, 2.38 Hz, 1 H), 6.0 (d, J=9.29 Hz, 1 H), 3.2 (m, 2 H); **^{13}C-NMR (100 MHz DMSO-*d*^{6}): δ** 169.2, 161.6, 142.2, 140.1, 137.6, 135.6, 134.1, 132.2, 130.6, 127.9, 126.2, 125.5, 125.5, 125.3, 123.2, 122.5, 121.3, 120.1, 119.6, 119.5, 118.6, 118.5, 112.1, 111.4, 37.9; **LR-ESI-MS**: $C_{25}H_{20}N_3O_2$ $[M+H]^+$ *m/z* found 394.56, cald 394.16.

***N*-(2-(9*H*-Carbazol-1-yl)phenyl)-1-(2-fluorophenyl)methanesulfonamide (178)**

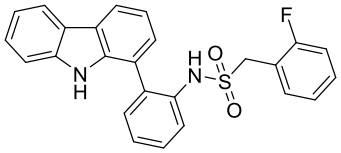

2-(9*H*-Carbazol-1-yl)aniline **149** (50 mg, 0.194 mmol, 1 eq) and (2-fluorophenyl)methanesulfonyl chloride (44 mg, 0.213 mmol, 1.1 eq) were reacted according to general procedure A to give **178** (34 mg, 0.079 mmol 41%) as a white solid.

Mpt: 176.9-178.9 °C; **ν_{max} (cm^{-1})** 3340, 1585, 1491, 1184, 1113, 748, 503; **^{19}F-{H}-NMR (376 MHz, DMSO-*d*^{6}): δ** -116.6; **^{1}H-NMR (400 MHz, DMSO-*d*^{6}): δ** 10.8 (s, 1 H), 8.8 (s, 1 H), 8.1 (m, 2 H), 7.5 (m, 4 H), 7.4 (m, 4 H), 7.3 (m, 1 H), 7.1 (m, 4 H), 4.1 (s, 2 H); **^{13}C-NMR (100 MHz DMSO-*d*^{6}): δ** 160.8 (d, J=247.96 Hz), 140.2, 138.0, 135.1, 133.7, 132.9 (d, J=2.93 Hz), 131.3, 130.5 (d, J=8.80 Hz), 128.5, 127.0, 126.0, 125.4 (d, J=22.01 Hz), 124.2 (d, J=5.13 Hz), 123.0, 122.5, 121.6, 120.0, 119.6, 118.6, 118.5, 116.7 (d, J=13.94 Hz), 115.4 (d, J=21.27 Hz), 111.4, 51.8; **LR-ESI-MS**: $C_{25}H_{20}FN_2O_2S$ $[M+H]^+$ *m/z* found 431.78, cald 431.12.

***N*-(2-(9*H*-Carbazol-1-yl)phenyl)-2-(2-fluorophenyl)acetamide (179)**

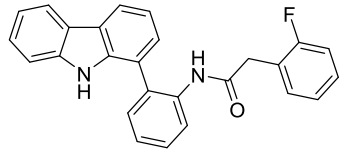

2-(9*H*-Carbazol-1-yl)aniline **149** (50 mg, 0.194 mmol, 1 eq) and 2-(2-fluorophenyl)acetyl chloride (33 µL, 0.213 mmol, 1.1 eq) were reacted according to general procedure A to give **179** (42 mg, 0.106 mmol, 55%) as a white solid.

ν_{max} (cm^{-1}) 3372, 3226, 1676, 1582, 1467, 1335, 1231, 747; **^{19}F-{H}-NMR (376 MHz, DMSO-*d*^{6}): δ** -117.5; **^{1}H-NMR (400 MHz, DMSO-*d*^{6}): δ** 10.7 (s, 1 H), 8.9 (s, 1 H), 8.1 (m, 2 H), 7.9 (d, J=7.95 Hz, 1 H), 7.5 (m, 3 H), 7.4 (m, 2 H), 7.2 (m, 4 H), 6.9 (m, 3 H), 3.5 (s, 2 H); **^{13}C-NMR (100 MHz DMSO-*d*^{6}): δ** 168.2, 161.5, 159.0, 140.2, 137.6, 135.7, 131.9, 131.3 (d, J=4.40 Hz), 130.7, 128.6 (d, J=8.07 Hz), 128.0, 126.3, 125.5, 125.3, 124.8, 124.0 (d, J=3.67 Hz), 123.2, 122.6, 122.3 (d, J=16.14 Hz), 121.2, 119.8 (d, J= 44.8 Hz), 118.6, 114.9, 114.7, 111.5, 35.8; **LR-ESI-MS**: $C_{26}H_{18}FN_2O$ $[M-H]^-$ *m/z* found 393.08, cald 393.14.

***N*-(2-(9*H*-Carbazol-1-yl)phenyl)-2-(2-chlorophenyl)acetamide (180)**

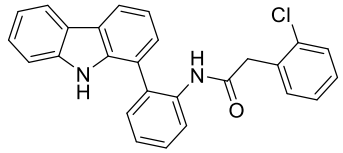

2-(9*H*-Carbazol-1-yl)aniline **149** (50 mg, 0.194 mmol, 1 eq) and 2-(2-chlorophenyl)acetyl chloride (40 mg, 0.213 mmol, 1.1 eq) were reacted according to general procedure A to give **180** (39 mg, 0.095 mmol 49%) as a white solid.

Mpt: 158.2-160.2 °C; **ν_{max} (cm^{-1})** 3351, 3241, 1671, 1522, 1445, 1235, 1052; **^{1}H-NMR (400 MHz, DMSO-*d*^{6}): δ** 10.7 (s, 1 H), 8.7 (s, 1 H), 8.1 (m, 2 H), 7.9 (s, 1 H), 7.5 (m, 3 H), 7.4 (m, 2 H), 7.2 (m, 4 H), 7.1 (m, 1 H), 7.0 (m, 2 H), 3.5 (s, 2 H); **^{13}C-NMR (100 MHz DMSO-*d*^{6}): δ** 168.0, 140.2, 137.6, 135.7, 133.3, 133.1, 131.5, 130.7, 128.8, 128.5, 128.0, 126.9, 126.4, 125.5, 125.2, 124.4, 123.2, 122.5, 121.1, 120.0, 119.6, 118.6, 111.5, 40.6; **LR-ESI-MS**: $C_{26}H_{18}ClN_2O$ $[M-H]^-$ *m/z* found 409.05, cald 409.11.

***N*-(2-(9*H*-Carbazol-1-yl)phenyl)-2-(p-tolyl)acetamide (181)**

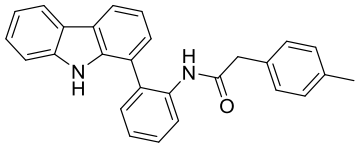

2-(9*H*-Carbazol-1-yl)aniline **149** (50 mg, 0.194 mmol, 1 eq) and 2-(p-tolyl)acetyl chloride (33 µL, 0.213 mmol, 1.1 eq) were reacted according to general procedure A to give **181** (52 mg, 0.133 mmol 69%) as a white solid.

ν_{max} (cm^{-1}) 3352, 3296, 1582, 1516, 1446, 1236, 739; **^{1}H-NMR (400 MHz, DMSO-*d*^{6}): δ** 10.7 (s, 1 H), 8.6 (s, 1 H), 8.1 (m, 2 H), 8.0 (d, J=7.95 Hz, 1 H), 7.4 (m, 4 H), 7.3 (m, 1 H), 7.2 (m, 3 H), 6.7 (m, 4 H), 3.4 (s, 2H), 2.2 (s, 3 H); **^{13}C-NMR (100 MHz DMSO-*d*^{6}): δ** 169.3, 140.2, 137.5, 135.8, 135.4, 131.9, 131.2, 130.7, 128.7, 128.6, 128.0, 126.4, 125.5, 124.9, 123.9, 123.1, 122.6, 120.9, 120.0, 119.5, 118.6, 118.5, 111.4, 42.7; **LR-ESI-MS**: $C_{27}H_{21}N_2O$ $[M-H]^-$ *m/z* found 389.12, cald 389.17.

***N*-(2-(9*H*-Carbazol-1-yl)phenyl)-2-(4-fluorophenyl)acetamide (182)**

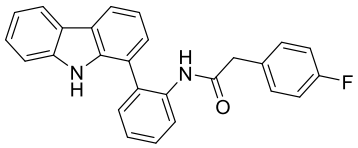

2-(9*H*-Carbazol-1-yl)aniline **149** (50 mg, 0.194 mmol, 1 eq) and 2-(4-fluorophenyl)acetyl chloride (30 µL, 0.213 mmol, 1.1 eq) were reacted according to general procedure A to give **182** (41 mg, 0.104 mmol 54%) as a white solid.

Mpt: 191.1-193.1 °C; **ν_{max} (cm^{-1})** 3354, 3313, 1664, 1521, 1219, 740; **^{19}F-{H}-NMR (376 MHz, DMSO-*d*^{6}): δ** -116.0; **^{1}H-NMR (400 MHz, DMSO-*d*^{6}): δ** 10.7 (s, 1 H), 8.8 (s, 1 H), 8.1 (m, 2 H), 7.9 (d, J=7.95 Hz, 1 H), 7.4 (m, 3 H), 7.4 (m, 2 H), 7.2 (m, 3 H), 6.9 (dd, J=8.50, 5.69 Hz, 2 H), 6.8 (m, 2 H), 3.4 (s, 2 H); **^{13}C-NMR (100 MHz DMSO-*d*^{6}): δ** 169.1, 162.0, 159.6, 140.2, 137.6, 135.7, 131.8, 131.4 (d, J=2.94 Hz), 130.7, 130.6, 128.0, 126.4, 125.5, 125.3, 124.6, 122.8 (d, J=53.55 Hz), 121.1, 120.0, 119.5, 118.6, 114.7 (d, J=21.27 Hz), 111.4, 41.9; **LR-ESI-MS**: $C_{26}H_{18}FN_2O$ $[M-H]^-$ *m/z* found 393.07, cald 393.14.

***N*-(2-(9*H*-Carbazol-1-yl)phenyl)-2-(4-methoxyphenyl)acetamide (183)**

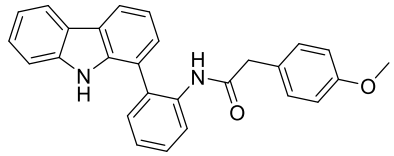

2-(9*H*-Carbazol-1-yl)aniline **149** (50 mg, 0.194 mmol, 1 eq) and 2-(4-methoxyphenyl)acetyl chloride (33 µL, 0.213 mmol, 1.1 eq) were reacted according to general procedure A to give **183** (54 mg, 0.133 mmol 69%) as a white solid.

Mpt: 191.1-193.1 °C; **ν_{max} (cm^{-1})** 3349, 3293, 1657, 1511, 1448, 762; **^{1}H-NMR (400 MHz, DMSO-*d*^{6}): δ** 10.7 (s, 1 H), 8.6 (s, 1 H), 8.1 (m, 2 H), 8.0 (d, J=7.95 Hz, 1 H), 7.4 (m, 5 H), 7.2 (m, 3 H), 6.8 (d, J=8.68 Hz, 2 H), 6.5 (d, J=8.56 Hz, 2 H), 3.7 (s, 3 H), 3.3 (s, 2H); **^{13}C-NMR (100 MHz DMSO-*d*^{6}): δ** 169.5, 157.8, 140.2, 137.6, 135.8, 131.3, 130.7, 129.8, 128.0, 126.9, 126.4, 125.5, 125.0, 124.1, 123.2, 122.6, 121.0, 120.0, 119.6, 118.7, 118.6, 113.5, 111.5, 54.9, 42.1; **LR-ESI-MS**: $C_{27}H_{23}N_2O_2$ $[M+H]^+$ *m/z* found 407.49, cald 407.18.

***N*-(2-(9*H*-Carbazol-1-yl)phenyl)-1-(4-cyanophenyl)methanesulfonamide (184)**

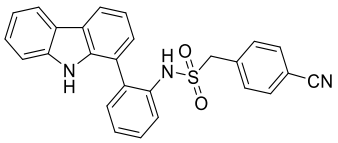

2-(9*H*-Carbazol-1-yl)aniline **149** (50 mg, 0.194 mmol, 1 eq) and (4-cyanophenyl)methanesulfonyl chloride (46 mg, 0.213 mmol, 1.1 eq) were reacted according to general procedure A to give **184** (65 mg, 0.149 mmol, 77%) as a white solid.

ν_{max} (cm^{-1}) 3348, 1503, 1415, 1333, 1152, 920, 751; **^{1}H-NMR (400 MHz, DMSO-*d*^{6}): δ** 10.8 (s, 1 H), 8.8 (s, 1 H), 8.1 (dd, J=7.09, 5.50 Hz, 2 H), 7.7 (d, J=8.31 Hz, 2 H), 7.5 (m, 4 H), 7.4 (m, 3 H), 7.3 (m, 3 H), 7.2 (m, 1 H), 4.1 (s, 2 H); **^{13}C-NMR (100 MHz DMSO-*d*^{6}): δ** 140.2, 138.0, 135.2, 135.1, 133.9, 131.9, 131.6, 131.3, 128.5, 127.0, 126.1, 125.7, 125.6, 123.0, 122.5, 121.7, 120.1, 119.7, 118.7, 118.5, 111.4, 110.8, 58.1; **LR-ESI-MS**: $C_{26}H_{18}N_3O_2S$ $[M-H]^-$ *m/z* found 436.05, cald 436.11.

***N*-(2-(9*H*-Carbazol-1-yl)phenyl)-2-(4-chlorophenyl)acetamide (185)**

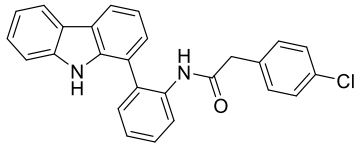

2-(9*H*-Carbazol-1-yl)aniline **149** (50 mg, 0.194 mmol, 1 eq) and 2-(4-chlorophenyl)acetyl chloride (40 mg, 0.213 mmol, 1.1 eq) were reacted according to general procedure A to give **185** (37 mg, 0.09 mmol 47%) as a white solid.

ν_{max} (cm^{-1}) 3358, 3316, 1661, 1119, 762; **^{1}H-NMR (400 MHz, DMSO-*d*^{6}): δ** 10.7 (s, 1 H), 8.8 (s, 1 H), 8.1 (m, 2 H), 7.9 (m, 1 H), 7.4 (m, 3 H), 7.4 (s, 2 H), 7.1 (m, 3 H), 7.0 (m, 2 H), 6.9 (d, J=8.31 Hz, 2 H), 3.4 (s, 2H); **^{13}C-NMR (100 MHz DMSO-*d*^{6}): δ** 168.8, 140.2 ,137.5, 135.7, 134.3, 131.9, 131.1, 130.7, 130.6, 128.0, 127.9, 126.3, 125.5, 125.3, 124.7, 123.1, 122.6, 121.2, 120.1, 119.5, 118.6, 111.4, 42.0; **LR-ESI-MS**: $C_{26}H_{18}ClN_2O$ $[M-H]^-$ *m/z* found 409.12, cald 409.11.

***N*-(2-(9*H*-Carbazol-1-yl)phenyl)-1-(4-(trifluoromethyl)phenyl)methanesulfonamide (186)**

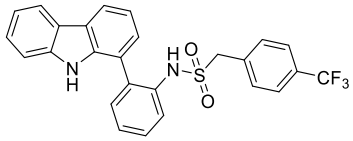

2-(9*H*-Carbazol-1-yl)aniline **149** (50 mg, 0.194 mmol, 1 eq) and (4-(trifluoromethyl)phenyl)methanesulfonyl chloride (55 mg, 0.213 mmol, 1.1 eq) were reacted according to general procedure A to give **186** (33 mg, 0.068 mmol 35%) as a white solid.

ν_{max} (cm^{-1}) 3382, 3241, 1417, 1320, 1118, 753; **^{19}F-{H}-NMR (376 MHz, DMSO-*d*^{6}): δ** -61.2; **^{1}H-NMR (400 MHz, DMSO-*d*^{6}): δ** 10.8 (s, 1 H), 8.7 (s, 1 H), 8.1 (m, 2 H), 7.5 (m, 6 H), 7.4 (m, 3 H), 7.3 (m, 3 H), 7.2 (m, 1 H), 4.1 (s, 2H); **^{13}C-NMR (100 MHz DMSO-*d*^{6}): δ** 140.2, 138.0, 135.1, 134.4, 133.7, 131.5, 131.3, 128.5, 128.4, 127.0, 126.0, 125.5, 125.4, 125.0 (m), 123.0, 122.5, 121.6, 120.1, 119.6, 118.6, 118.5, 111.4, 57.9. **LR-ESI-MS**: $C_{26}H_{18}F_3N_2O_2S$ $[M-H]^-$ *m/z* found 479.05, cald 479.10.

***N*-(2-(9*H*-Carbazol-1-yl)phenyl)-2-(3,4-dimethoxyphenyl)acetamide (187)**

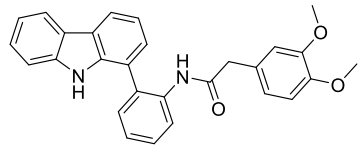

2-(9*H*-Carbazol-1-yl)aniline **149** (50 mg, 0.194 mmol, 1 eq) and 2-(3,4-dimethoxyphenyl)acetyl chloride (37 µL, 0.213 mmol, 1.1 eq) were reacted according to general procedure A to give **187** (16 mg, 0.037 mmol 19%) as a white solid.

ν_{max} (cm^{-1}) 3310, 2978, 1671, 1512, 1157, 1122, 545; **^{1}H-NMR (400 MHz, DMSO-*d*^{6}): δ** 10.7 (m, 1 H), 8.6 (m, 1 H), 8.1 (d, J=7.70 Hz, 1 H), 8.1 (d, J=7.21 Hz, 1 H), 8.0 (d, J=8.31 Hz, 1 H), 7.4 (m, 3 H), 7.4 (m, 1 H), 7.3 (m, 1 H), 7.2 (m, 1 H), 7.1 (m, 2 H), 6.6 (m, 1 H), 6.4 (m, 1 H), 6.3 (dd, J=8.19, 1.96 Hz, 1 H), 3.7 (s, 3 H), 3.5 (s, 3 H); **^{13}C-NMR (100 MHz DMSO-*d*^{6}): δ** 169.4, 148.4, 147.4, 140.1, 137.5, 135.8, 130.6, 128.0, 127.2, 126.1, 125.5, 123.8, 123.1, 122.5, 120.8, 120.0, 119.6, 118.6, 118.5, 112.7, 111.4, 111.4, 55.3, 55.1, 42.7; **LR-ESI-MS**: $C_{28}H_{23}N_2O_3$ $[M-H]^-$ *m/z* found 435.04, cald 435.17.

***N*-(2-(9*H*-Carbazol-1-yl)phenyl)-2-(benzo[d][1,3]dioxol-5-yl)acetamide (188)**

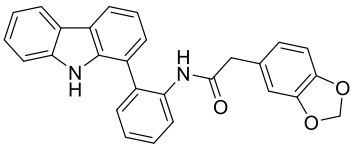

2-(9*H*-Carbazol-1-yl)aniline **149** (50 mg, 0.194 mmol, 1 eq) and 2-(benzo[d][1,3]dioxol-5-yl)acetyl chloride (38 µL, 0.213 mmol, 1.1 eq) were reacted according to general procedure A to give **188** (54 mg, 0.128 mmol, 66%) as a white solid.

ν_{max} (cm^{-1}) 3359, 3288, 1525, 1582, 1297, 742; **^{1}H-NMR (400 MHz, DMSO-*d*^{6}): δ** 10.7 (s, 1 H), 8.6 (s, 1 H), 8.1 (t, J=8.07 Hz, 2 H), 8.0 (d, J=7.95 Hz, 1 H), 7.4 (t, J=8.62 Hz, 3 H), 7.3 (m, 2 H), 7.2 (m, 2 H), 7.1 (m, 1 H), 6.5 (s, 1 H), 6.4 (m, 1 H), 6.3 (dd, J=7.89, 1.41 Hz, 1 H), 5.9 (s, 2 H), 3.3 (s, 2 H); **^{13}C-NMR (100 MHz DMSO-*d*^{6}): δ** 169.2, 146.9, 145.7, 140.2, 137.5, 135.7, 131.2, 130.6, 128.5, 128.0, 126.3, 125.5, 125.0, 123.9, 123.2, 122.6, 121.9, 120.8, 120.0, 119.6, 118.6, 111.4, 109.2, 107.8, 100.7, 42.6; **LR-ESI-MS**: $C_{27}H_{19}N_2O_3$ $[M-H]^-$ *m/z* found 419.15, cald 419.14.

***N*-(2-(9*H*-Carbazol-1-yl)phenyl)-1-(5-cyano-2-fluorophenyl)methanesulfonamide (189)**

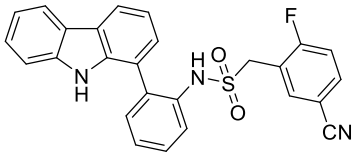

2-(9*H*-Carbazol-1-yl)aniline **149** (50 mg, 0.194 mmol, 1 eq) and (5-cyano-2-fluorophenyl)methanesulfonyl chloride (50 mg, 0.213 mmol, 1.1 eq) were reacted according to general procedure A to give **189** (68 mg, 0.149 mmol 77%) as a white solid.

Mpt: 204.4-206.4 °C; **ν_{max} (cm^{-1})** 3338, 3300, 2239, 1497, 1334, 1152, 1055, 756; **^{19}F-{H}-NMR (376 MHz, $CDCl_3$): δ** -106.2; **^{1}H-NMR (400 MHz, $CDCl_3$): δ** 8.1 (dd, J=11.98, 7.82 Hz, 2 H), 8.0 (s, 1 H), 7.7 (m, 1 H), 7.5 (m, 6 H), 7.3 (m, 4 H), 7.0 (t, J=8.74 Hz, 1 H), 6.5 (s, 1 H), 4.3 (m, 2 H); **^{13}C-NMR (100 MHz $CDCl_3$): δ** 139.6, 137.5, 136.5, 136.4, 135.0 (d, J=10.27 Hz), 134.5, 131.3, 129.7, 128.6, 126.6, 126.1, 125.4, 124.4, 123.5, 121.1, 120.7, 120.3, 120.2, 119.3, 119.0, 118.1 (d, J=16.87 Hz), 117.2, 117.0, 111.1, 50.7 (d, J=2.20 Hz); **LR-ESI-MS**: $C_{26}H_{19}FN_3O_2S$ $[M+H]^+$ *m/z* found 456.20, cald 456.12.

***N*-(2-(9*H*-Carbazol-1-yl)phenyl)-2-(2,5-dimethylphenyl)acetamide (190)**

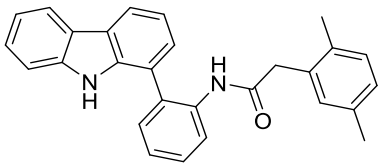

2-(9*H*-Carbazol-1-yl)aniline **149** (50 mg, 0.194 mmol, 1 eq) and 2-(2,5-dimethylphenyl)acetyl chloride (35 µL, 0.213 mmol, 1.1 eq) were reacted according to general procedure A to give **190** (52 mg, 0.129 mmol, 66%) as a white solid.

ν_{max} (cm^{-1}) 3336, 1662, 1498, 1446, 1234, 749, 574; **^{1}H-NMR (400 MHz, DMSO-d^6): δ** 10.7 (s, 1 H), 8.1 (m, 4 H), 7.4 (m, 2 H), 7.4 (m, 2 H), 7.3 (m, 1 H), 7.2 (m, 3 H), 6.6 (m, 3 H), 3.4 (s, 2 H), 2.0 (s, 3 H), 1.9 (s, 3 H); **^{13}C-NMR (100 MHz DMSO-d^6): δ** 168.9, 140.2, 137.3, 135.8, 134.5, 132.9, 132.7, 130.6, 130.3, 129.6, 128.1, 127.4, 126.1, 125.4, 124.7, 123.1, 123.0, 122.7, 120.6, 120.1, 119.8, 118.6, 118.5, 111.4, 41.2, 20.3, 18.3; **LR-ESI-MS**: $C_{28}H_{23}N_2O$ $[M-H]^-$ *m/z* found 403.16, cald 403.18.

***N*-(2-(9*H*-Carbazol-1-yl)phenyl)-2-(3,4-dichlorophenyl)acetamide (191)**

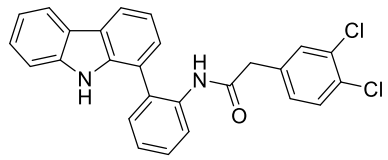

2-(9*H*-Carbazol-1-yl)aniline **149** (50 mg, 0.194 mmol, 1 eq) and 2-(3,4-dichlorophenyl)acetyl chloride (40 µL, 0.213 mmol, 1.1 eq) were reacted according to general procedure A to give **191** (65 mg, 0.146 mmol 75%) as a white solid.

ν_{max} (cm^{-1}) 3366, 3305, 1670, 1524, 1449, 670, 616; **^{1}H-NMR (400 MHz, DMSO-*d*^{6}): δ** 10.7 (s, 1 H), 9.0 (s, 1 H), 8.1 (m, 2 H), 7.8 (d, J=7.82 Hz, 1 H), 7.5 (m, 3 H), 7.4 (m, 2 H), 7.3 (d, J=1.10 Hz, 1 H), 7.1 (m, 4 H), 6.9 (dd, J=8.19, 1.71 Hz, 1 H), 3.4 (s, 2 H); **^{13}C-NMR (100 MHz DMSO-*d*^{6}): δ** 168.4, 140.1, 137.6, 136.5, 135.5, 132.3, 130.9, 130.7, 130.6, 130.1, 129.2, 127.9, 126.2, 125.5 125.2, 123.1, 122.5, 121.2, 120.0, 119.5, 118.6, 118.5, 111.4, 41.5; **LR-ESI-MS**: $C_{26}H_{17}Cl_2N_2O$ $[M-H]^-$ *m/z* found 443.05, cald 443.07.

***N*-(2-(9*H*-Carbazol-1-yl)phenyl)-2-(3-methoxyphenyl)acetamide (192)**

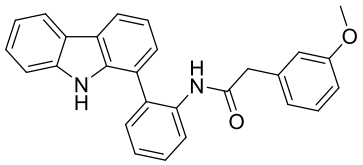

2-(9*H*-Carbazol-1-yl)aniline **149** (50 mg, 0.194 mmol, 1 eq) and 2-(3-methoxyphenyl)acetyl chloride (33 µL, 0.213 mmol, 1.1 eq) were reacted according to general procedure A to give **192** (56 mg, 0.138 mmol 71%) as a white solid.

ν_{max} (cm^{-1}) 3343, 3293, 1489, 1464, 1321, 1219, 712, 615; **^{1}H-NMR (400 MHz, DMSO-*d*^{6}): δ** 10.7 (s, 1 H), 8.8 (s, 1 H), 8.1 (m, 2 H), 7.9 (d, J=8.07 Hz, 1 H), 7.4 (m, 3 H), 7.4 (m, 2 H), 7.1 (m, 3 H), 6.9 (m, 1 H), 6.6 (m, 2 H), 6.5 (d, J=7.58 Hz, 1 H), 3.6 (s, 3 H), 3.4 (s, 2 H); **^{13}C-NMR (100 MHz DMSO-*d*^{6}): δ** 169.1, 159.0, 140.2, 137.6, 136.6, 135.7, 131.6, 130.6, 129.1, 127.9, 126.2, 125.5, 125.2, 124.6, 123.2, 122.6, 121.0, 120.0, 119.6, 118.6, 114.6, 111.9, 111.4, 54.8, 42.9; **LR-ESI-MS**: $C_{27}H_{23}N_2O_2$ $[M+H]^+$ *m/z* found 407.89, cald 407.18.

***N*-(2-(9*H*-Carbazol-1-yl)phenyl)-2-(3-fluorophenyl)acetamide (193)**

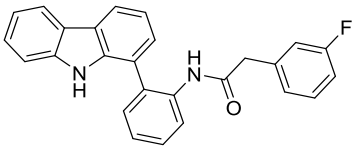

2-(9*H*-Carbazol-1-yl)aniline **149** (50 mg, 0.194 mmol, 1 eq) and 2-(3-fluorophenyl)acetyl chloride (33 µL, 0.213 mmol, 1.1 eq) were reacted according to general procedure A to give **193** (58 mg, 0.147 mmol, 76%) as a white solid.

ν_{max} (cm^{-1}) 3369, 3309, 1581, 1488, 1238, 747; **^{19}F-{H}-NMR (376 MHz, DMSO-*d*^{6}): δ** -113.6; **^{1}H-NMR (400 MHz, DMSO-*d*^{6}): δ** 10.7 (s, 1 H), 9.0 (s, 1 H), 8.1 (m, 2 H), 7.8 (d, J=7.82 Hz, 1 H), 7.5 (m, 3 H), 7.4 (m, 2 H), 7.1 (m, 4 H), 6.9 (m, 3 H), 3.4 (s, 2 H); **^{13}C-NMR (100 MHz DMSO-*d*^{6}): δ** 168.7, 163.1, 160.7, 140.2, 138.1 (d, J=8.07 Hz), 137.6, 135.6, 132.1, 130.7, 129.9 (d, J=8.07 Hz), 127.9, 126.3, 125.5, 125.4, 125.2, 125.0 (d, J= 2.2 Hz), 123.2, 122.6, 121.2, 120.0, 119.5, 118.6 (d, J=8.07 Hz), 115.8 (d, 21.3 Hz), 113.0 (d, J= 21.3 Hz), 111.4, 42.3; **LR-ESI-MS**: $C_{26}H_{18}FN_2O$ $[M-H]^-$ *m/z* found 393.07, cald 393.14.

***N*-(2-(9*H*-Carbazol-1-yl)phenyl)-1-(3-fluorophenyl)methanesulfonamide (194)**

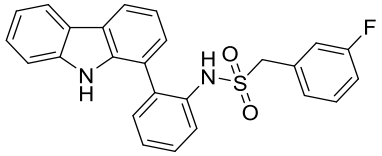

2-(9*H*-Carbazol-1-yl)aniline **149** (50 mg, 0.194 mmol, 1 eq) and (3-fluorophenyl)methanesulfonyl chloride (44 mg, 0.213 mmol, 1.1 eq) were reacted according to general procedure A to give **194** (62 mg, 0.144 mmol 74%) as a white solid.

Mpt: 75.9-77.9 °C; **ν_{max} (cm^{-1})** 3336, 2923, 2848, 1588, 1483, 1318, 1150, 921, 750, 500; **^{19}F-{H}-NMR (376 MHz, DMSO-*d*^{6}): δ** -113.5; **^{1}H-NMR (400 MHz, DMSO-*d*^{6}): δ** 10.8 (m, 1 H), 8.7 (m, 1 H), 8.1 (t, J=6.72 Hz, 2 H), 7.5 (m, 4 H), 7.3 (s, 3 H), 7.3 (s, 2 H), 7.1 (m, 2 H), 6.9 (s, 2 H), 4.0 (s, 2 H); **^{13}C-NMR (100 MHz DMSO-*d*^{6}): δ** 162.9, 160.5, 140.2, 138.0, 135.3, 133.8, 132.1 (d, J=8.07 Hz), 131.3, 130.1 (d, J=8.80 Hz), 128.5, 127.0, 126.9 (d, J=2.93 Hz), 126.0, 125.6, 123.0, 122.5, 121.8, 120.1, 119.5, 119.6, 118.6 (d, J=12.47 Hz), 117.4 (d, J=22.01 Hz), 115.0 (d, J=20.54 Hz), 111.4, 57.9; **LR-ESI-MS**: $C_{25}H_{18}FN_2O_2S$ $[M-H]^+$ *m/z* found 429.11, cald 429.11.

***N*-(2-(9*H*-Carbazol-1-yl)phenyl)-2-(3-(trifluoromethyl)phenyl)acetamide (195)**

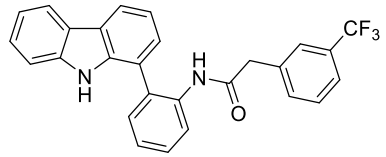

2-(9*H*-Carbazol-1-yl)aniline **149** (50 mg, 0.194 mmol, 1 eq) and 2-(3-(trifluoromethyl)phenyl)acetyl chloride (43 µL, 0.213 mmol, 1.1 eq) were reacted according to general procedure A to give **195** (58 mg, 0.130 mmol, 67%) as a white solid.

ν_{max} (cm^{-1}) 3361, 3312, 2972, 1666, 1525, 1449, 1333, 1127, 584; **^{19}F-{H}-NMR (376 MHz, DMSO-*d*^{6}): δ** -60.9; **^{1}H-NMR (400 MHz, DMSO-*d*^{6}): δ** 10.7 (s, 1 H), 9.1 (s, 1 H), 8.1 (m, 2 H), 7.8 (s, 1 H), 7.5 (m, 5 H), 7.4 (m, 2 H), 7.3 (s, 1 H), 7.2 (m, 4 H), 3.5 (s, 2 H); **^{13}C-NMR (100 MHz DMSO-*d*^{6}): δ** 168.7, 140.1, 137.6, 137.0, 135.6, 133.0, 132.4, 130.7, 129.0, 128.9, 128.7, 127.9, 126.2, 125.6 (m), 125.5, 123.2, 123.1, 123.0, 122.5, 121.3, 120.0, 119.5, 118.6, 118.4, 111.4, 42.1; **LR-ESI-MS**: $C_{27}H_{18}F_3N_2O$ $[M-H]^-$ *m/z* found 443.12, cald 443.14.

***N*-(2-(9*H*-Carbazol-1-yl)phenyl)-2-(3-cyanophenyl)acetamide (196)**

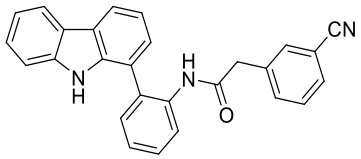

2-(9*H*-Carbazol-1-yl)aniline **149** (50 mg, 0.194 mmol, 1 eq), 2-(3-cyanophenyl)acetic acid (37 mg, 0.232 mmol, 1.2 eq) and DIPEA (81 µL, 0.465 mmol, 2.4 eq) were dissolved in DCM (2 mL, 0.1 M) and then had HATU (88 mg, 0.232 mmol, 1.2 eq) added before the solution was stirred for 16 h at room temperature. Upon reaction completion the crude mixture was concentrated onto silica gel before being purified by Isolera Biotage LPLC (CH/EA 8:2) to give **196** (56 mg, 0.139 mmol, 72%) as a white solid.

ν_{max} (cm^{-1}) 3359, 3305, 1523, 1313, 1237, 746; **^{1}H-NMR (400 MHz, $CDCl_3$): δ** 8.3 (d, J=8.19 Hz, 1 H), 8.1 (t, J=8.68 Hz, 2 H), 7.7 (s, 1 H), 7.5 (m, 2 H), 7.3 (m, 5 H), 7.2 (dd, J=7.34, 0.98 Hz, 1 H), 7.1 (d, J=7.70 Hz, 1 H), 7.0 (s, 1 H), 6.8 (m, 2 H), 6.7 (m, 1 H), 3.4 (s, 2 H); **^{13}C-NMR (100 MHz $CDCl_3$): δ** 168.0, 139.4, 137.2, 134.9, 134.6, 132.9, 131.9, 130.9, 130.6, 129.3, 129.2, 126.5, 126.4, 125.3,

123.5, 123.3, 121.7, 120.7, 120.1, 119.6, 118.0, 112.7, 110.8, 44.1; **LR-ESI-MS**: $C_{27}H_{18}N_3O$ $[M-H]^-$ *m/z* found 400.19, cald 400.15.

***N*-(2-(9*H*-Carbazol-1-yl)phenyl)-1-(3-cyanophenyl)methanesulfonamide (197)**

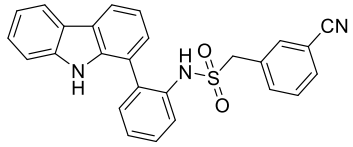

2-(9*H*-Carbazol-1-yl)aniline **149** (50 mg, 0.194 mmol, 1 eq) and (3-cyanophenyl)methanesulfonyl chloride (46 mg, 0.213 mmol, 1.1 eq) were reacted according to general procedure A to give **197** (62 mg, 0.142 mmol 73%) as a white solid.

Mpt: 88.0-90.0 °C; **ν_{max} (cm^{-1})** 3334, 2231, 1454, 1150, 920, 752, 685; **^{1}H-NMR (400 MHz, DMSO-*d*^{6}): δ** 10.8 (m, 1 H), 8.8 (s, 1 H), 8.1 (t, J=7.46 Hz, 2 H), 7.7 (m, 1 H), 7.5 (m, 5 H), 7.4 (m, 5 H), 7.3 (m, J=7.58 Hz, 1 H), 7.2 (t, J=7.46 Hz, 1 H), 4.1 (s, 2 H); **^{13}C-NMR (100 MHz DMSO-*d*^{6}): δ** 140.2, 138.0, 135.6, 135.1, 134.1, 134.0, 131.8, 131.4, 129.5, 128.5, 127.1, 126.2, 125.9, 125.6, 123.0, 122.5, 121.8, 120.1, 119.7, 118.7, 118.5, 118.4, 111.5, 111.3, 57.6; **LR-ESI-MS**: $C_{26}H_{18}N_3O_2S$ $[M+H]^+$ *m/z* found 436.09, cald 436.11.

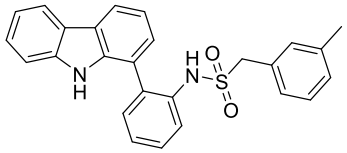

***N*-(2-(9*H*-Carbazol-1-yl)phenyl)-1-(m-tolyl)methanesulfonamide (198)**

2-(9*H*-Carbazol-1-yl)aniline **149** (50 mg, 0.194 mmol, 1 eq) and m-tolylmethanesulfonyl chloride (79 mg, 0.387 mmol, 2 eq) were reacted according to general procedure A to give *N*-(2-(9H-carbazol-1-yl)phenyl)-1-(m-tolyl)methanesulfonamide **198** (14 mg, 0.033 mmol 17%) as a white solid.

ν_{max} (cm^{-1}) 3704, 2972, 1600, 1389, 1318, 1149, 1054, 1014, 919, 636; **^{1}H-NMR (400 MHz, DMSO-*d*^{6}): δ** 10.8 (s, 1 H), 8.6 (s, 1 H), 8.1 (t, J=6.66 Hz, 2 H), 7.5 (m, 4 H), 7.4 (m, 3 H), 7.3 (m, 1 H), 7.2 (m, 1 H), 7.1 (m, 2 H), 6.8 (d, J=6.97 Hz, 1 H), 6.8 (s, 1 H), 3.9 (br. s., 2 H), 2.1 (s, 3 H); **^{13}C-NMR (100 MHz DMSO-*d*^{6}): δ** 140.2, 138.0, 137.3, 135.4, 133.7, 131.3, 131.2, 129.2, 128.6, 128.1,

127.8, 126.9, 125.9, 125.5, 123.0, 122.5, 121.8, 120.1, 119.7, 118.6, 118.5, 111.4, 58.3, 20.7; **LR-ESI-MS**: $C_{26}H_{23}N_2O_2S$ $[M+H]^+$ *m/z* found 427.39, cald 427.15.

***N*-(2-(9*H*-Carbazol-1-yl)phenyl)-3-cyanobenzenesulfonamide (199)**

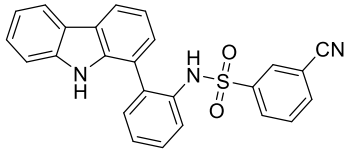

2-(9*H*-Carbazol-1-yl)aniline **149** (50 mg, 0.194 mmol, 1 eq) and 3-cyanobenzenesulfonyl chloride (43 mg, 0.213 mmol, 1.1 eq) were reacted according to general procedure A to give *N*-(2-(9H-carbazol-1-yl)phenyl)-3-cyanobenzenesulfonamide **199** (4.1 mg, 0.0097 mmol 5%) as a white solid.

ν_{max} (cm^{-1}) 3411, 3229, 1417, 1314, 1153, 752; **^{1}H-NMR (400 MHz, DMSO-*d*^{6}): δ** 10.5 (s, 1 H), 9.8 (s, 1 H), 8.1 (d, J=7.82 Hz, 1 H), 8.0 (dd, J=6.91, 1.90 Hz, 1 H), 7.4 (m, 8 H), 7.2 (m, 5 H); **^{13}C-NMR (100 MHz DMSO-*d*^{6}): δ** 141.1, 140.0, 137.7, 135.9, 134.8, 133.1, 131.3, 129.9, 129.5, 129.1, 128.9, 128.4, 127.6, 126.6, 125.4, 122.9, 122.4, 120.9, 119.9, 119.6, 118.5, 118.0, 117.3, 111.6, 111.4; **LR-ESI-MS**: $C_{25}H_{16}N_3O_2S$ $[M-H]^-$ *m/z* found 422.16, cald 422.09.

***N*-(2-(9*H*-Carbazol-1-yl)phenyl)-1-(4-fluorophenyl)methanesulfonamide (200)**

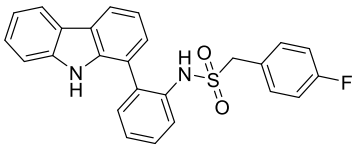

2-(9*H*-Carbazol-1-yl)aniline **149** (50 mg, 0.194 mmol, 1 eq) and (4-fluorophenyl)methanesulfonyl chloride (44 mg, 0.213 mmol, 1.1 eq) were reacted according to general procedure A to give *N*-(2-(9H-carbazol-1-yl)phenyl)-1-(4-fluorophenyl)methanesulfonamide **200** (23 mg, 0.053 mmol 28%) as a white solid.

ν_{max} (cm^{-1}) 3351, 1601, 1505, 1223, 1149, 751; **^{19}F-{H}-NMR (376 MHz, DMSO-*d*^{6}): δ** -114.0; **^{1}H-NMR (400 MHz, DMSO-*d*^{6}): δ** 10.8 (s, 1 H), 8.5 (s, 1 H), 8.1 (m, 2 H), 7.5 (m, 4 H), 7.4 (m, 3 H), 7.3 (m, 1 H), 7.2 (m, 1 H), 7.1 (m, 2 H), 7.0 (m, 2 H), 4.0 (s, 2 H); **^{13}C-NMR (100 MHz DMSO-*d*^{6}): δ** 163.2, 160.7, 140.2, 138.0, 135.2, 133.5, 132.7 (d, J=8.80 Hz), 131.3, 128.5, 127.0, 125.8, 125.5,

125.3, 123.0, 122.5, 121.7, 120.1, 119.6, 118.6, 118.5, 115.1, 114.9, 111.4, 57.4; **LR-ESI-MS**: $C_{25}H_{18}FN_2O_2S$ $[M-H]^-$ *m/z* found 429.07, cald 429.11.

***N*-(2-(9*H*-Carbazol-1-yl)phenyl)-1-phenylcyclopropane-1-carboxamide (201)**

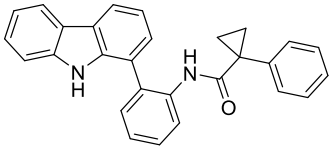

2-(9*H*-Carbazol-1-yl)aniline **149** (25 mg, 0.097 mmol, 1 eq), 1-phenylcyclopropane-1-carboxylic acid (19 mg, 0.116 mmol, 1.2 eq) and DIPEA (81 µL, 0.465 mmol, 4.8 eq) were dissolved in DCM (1 mL, 0.1 M) and then had HATU (44 mg, 0.116 mmol, 1.2 eq) added before the solution was stirred for 16 h at room temperature. Upon reaction completion the crude mixture was concentrated onto silica gel before being purified by HPLC to give *N*-(2-(9H-carbazol-1-yl)phenyl)-1-phenylcyclopropane-1-carboxamide **201** (2.4 mg, 0.006 mmol, 6%) as a white solid. **ν_{max} (cm^{-1})** 3366, 3303, 1659, 1519, 1319, 1306, 697; **^{1}H-NMR (400 MHz, DMSO-*d*^{6}): δ** 10.6 (s, 1 H), 8.4 (d, J=7.95 Hz, 1 H), 8.2 (d, J=7.83 Hz, 1 H), 8.1 (d, J=6.97 Hz, 1 H), 7.4 (m, 4 H), 7.2 (m, 5 H), 7.1 (d, J=15.04 Hz, 1 H), 7.0 (dd, J=7.27, 1.04 Hz, 1 H), 6.7 (m, 1 H), 6.6 (m, 2 H), 6.5 (m, 2 H), 1.3 (m, 2 H), 0.8 (d, J=3.30 Hz, 2 H); **^{13}C-NMR (100 MHz DMSO-*d*^{6}): δ** 171.1, 140.3, 137.4, 136.8, 136.0, 130.6, 129.4, 128.7, 128.3, 128.0, 127.2, 126.1, 125.6, 124.0, 123.1, 122.9, 120.2, 120.0, 118.9, 118.7, 111.5, 30.9, 15.4; **LR-ESI-MS**: $C_{28}H_{23}N_2O$ $[M+H]^+$ *m/z* found 403.64, cald 403.18.

***N*-(2-(9*H*-Carbazol-1-yl)phenyl)-2-(4-methylpiperazin-1-yl)acetamide (202)**

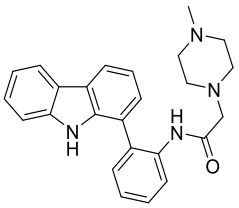

2-(9*H*-Carbazol-1-yl)aniline **149** (50 mg, 0.194 mmol, 1 eq), 2-(4-methylpiperazin-1-yl)acetic acid (37 mg, 0.232 mmol, 1.2 eq) and DIPEA (68 µL, 0.387 mmol, 2 eq) were dissolved in DCM (2 mL, 0.1 M) and then had HATU (88 mg, 0.232 mmol, 1.2 eq) added before the solution was stirred for 16 h at room temperature. Upon reaction completion the crude mixture was concentrated

onto silica gel before being purified by HPLC to give *N*-(2-(9H-carbazol-1-yl)phenyl)-2-(4-methylpiperazin-1-yl)acetamide **202** (17.2 mg, 0.043 mmol, 22%) as a white solid.

Mpt: 223.8-225.8 °C; **ν_{max} (cm^{-1})** 3290, 3206, 1671, 1521, 1449, 829, 747, 556; **^{1}H-NMR (400 MHz, DMSO-*d*^{6}): δ** 10.9 (s, 1 H), 9.2 (s, 1 H), 8.5 (d, J=8.31 Hz, 1 H), 8.2 (m, 2 H), 7.5 (m, 2 H), 7.3 (m, 5 H), 7.2 (m, 1 H), 3.6 (m, 1 H), 2.8 (s, 2 H), 2.0 (m, 7 H), 1.2 (m, 6 H); **^{13}C-NMR (100 MHz DMSO-*d*^{6}): δ** 167.9, 140.4, 137.5, 135.8, 130.8, 128.5, 128.2, 126.7, 125.8, 123.8, 123.3, 122.6, 120.6, 120.3, 119.5, 119.2, 118.9, 111.4, 61.0, 53.0, 51.6; **LR-ESI-MS**: $C_{25}H_{27}N_4O$ $[M+H]^+$ *m/z* found 399.64, cald 399.22.

***N*-(2-(9*H*-Carbazol-1-yl)phenyl)-3-(4-methylpiperazin-1-yl)propanamide (203)**

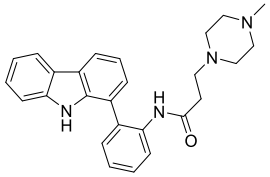

2-(9*H*-Carbazol-1-yl)aniline **149** (50 mg, 0.194 mmol, 1 eq), 3-(4-methylpiperazin-1-yl)propanoic acid.2HCl (57 mg, 0.232 mmol, 1.2 eq) and DIPEA (135 µL, 0.774 mmol, 4 eq) were dissolved in DCM (2 mL, 0.1 M) and then had HATU (88 mg, 0.232 mmol, 1.2 eq) added before the solution was stirred for 16 h at room temperature. Upon reaction completion the crude mixture was concentrated onto silica gel before being purified by Isolera Biotage LPLC (DCM/MeOH 9:1) to give *N*-(2-(9H-carbazol-1-yl)phenyl)-3-(4-methylpiperazin-1-yl)propanamide **203** (61 mg, 0.147 mmol, 76%) as a white solid.

ν_{max} (cm^{-1}) 3271, 2796, 1662, 1535, 1242, 737, 649; **^{1}H-NMR (400 MHz, DMSO-*d*^{6}): δ** 10.8 (s, 1 H), 9.5 (s, 1 H), 8.1 (m, 2 H), 8.0 (d, J=8.19 Hz, 1 H), 7.5 (m, 3 H), 7.3 (m, 2 H), 7.2 (m, 2 H), 7.1 (m, 1 H), 2.2 (m, 2 H), 2.1 (br. s., 2 H), 1.8 (m, 10 H); **^{13}C-NMR (100 MHz DMSO-*d*^{6}): δ** 170.2, 140.2, 137.8, 135.8, 131.4, 130.8, 127.9, 126.5, 125.6, 123.4, 122.5, 121.6, 120.0, 119.6, 118.7, 118.6, 111.4, 54.0, 52.9, 51.6, 45.1, 32.9; **LR-ESI-MS**: $C_{26}H_{29}N_4O$ $[M+H]^+$ *m/z* found 413.60, cald 413.23.

***N*-(2-(9*H*-Ccarbazol-1-yl)phenyl)-4-(dimethylamino)butane-1-sulfonamide (204)**

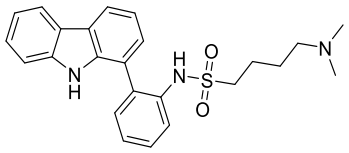

2-(9*H*-Carbazol-1-yl)aniline **149** (50 mg, 0.194 mmol, 1 eq), 4-(dimethylamino)butane-1-sulfonyl chloride.HCl (55 mg, 0.232 mmol, 1.2 eq) and DIPEA (68 µL, 0.387 mmol, 2 eq) were dissolved in DCM (2 mL, 0.1 M) and then had HATU (88 mg, 0.232 mmol, 1.2 eq) added before the solution was stirred for 16 h at room temperature. Upon reaction completion the crude mixture was concentrated onto silica gel before being purified by Isolera Biotage LPLC (DCM/MeOH 9:1) to give *N*-(2-(9H-carbazol-1-yl)phenyl)-4-(dimethylamino)butane-1-sulfonamide **204** (55 mg, 0.131 mmol, 68%) as a white solid.

ν_{max} (cm^{-1}) 3290, 1584, 1252, 1136, 978, 750, 616; **^{1}H-NMR (400 MHz, DMSO-*d*^{6}): δ** 10.7 (m, 1 H), 8.1 (t, J=7.52 Hz, 2 H), 7.5 (s, 1 H), 7.5 (m, 4 H), 7.3 (d, J=7.58 Hz, 2 H), 7.3 (d, J=7.58 Hz, 1 H), 7.2 (s, 1 H), 1.9 (s, 7 H), 1.7 (s, 2 H), 1.1 (m, 2 H), 0.8 (m, 2 H); **^{13}C-NMR (100 MHz DMSO-*d*^{6}): δ** 146.6, 140.2, 138.8, 131.7, 127.7, 126.8, 126.5, 125.2, 123.9, 122.8, 122.4, 122.2, 119.9, 118.6, 118.5, 118.4, 118.2, 111.4, 83.7, 67.5, 67.2, 52.0, 45.4, 24.2, 17.9; **LR-ESI-MS**: $C_{24}H_{28}N_3O_2S$ $[M+H]^+$ *m/z* found 422.41, cald 422.19.

***N*-(2-(9*H*-Carbazol-1-yl)phenyl)-2-(3-cyanophenyl)propanamide (205)**

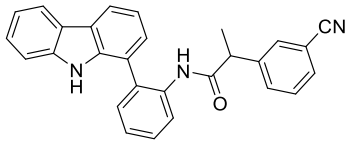

2-(9*H*-Carbazol-1-yl)aniline **149** (50 mg, 0.194 mmol, 1 eq), 2-(3-cyanophenyl)propanoic acid (41 mg, 0.232 mmol, 1.2 eq) and DIPEA (101 µL, 0.581 mmol, 3 eq) were dissolved in DCM (2 mL, 0.1 M) and then had HATU (88 mg, 0.232 mmol, 1.2 eq) added before the solution was stirred for 16 h at room temperature. Upon reaction completion the crude mixture was concentrated onto silica gel before being purified by HPLC to give *N*-(2-(9H-carbazol-1-yl)phenyl)-2-(3-cyanophenyl)propanamide **205** (10 mg, 0.024 mmol, 12%) as a white solid.

ν_{max} (cm^{-1}) 3342, 3256, 2225, 1651, 1036, 747; **^{1}H-NMR (400 MHz, DMSO-*d*^{6}): δ** 10.7 (s, 1 H), 9.0 (s, 1 H), 8.1 (m, 2 H), 7.8 (d, J=7.83 Hz, 1 H), 7.5 (m, 5 H), 7.3 (m, 4 H), 7.2 (m, 1 H), 7.0 (d, J=6.85 Hz, 2 H), 3.7 (m, 1 H), 1.2 (d, J=6.97 Hz, 3 H); **^{13}C-NMR (100 MHz DMSO-*d*^{6}): δ** 171.5, 142.7, 140.1, 137.5, 135.4, 132.6, 132.0, 130.8, 130.7, 130.3, 129.3, 127.9, 126.2, 125.6, 125.5, 123.1, 122.5, 121.3, 120.0, 119.5, 118.7, 118.6, 118.4, 111.4, 111.2, 44.7, 17.9; **LR-ESI-MS**: $C_{28}H_{23}N_2O$ $[M+H]^+$ *m/z* found 416.46, cald 416.18.

3-(9H-carbazol-1-yl)pyridin-2-amine (154a)

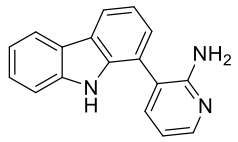

A degassed stirred solution of 1-bromo-9*H*-carbazole (0.5 g, 2.03 mmol, 1 eq), 3-(4,4,5,5-tetramethyl-1,3,2-dioxaborolan-2-yl)pyridin-2-amine (0.492 g, 2.24 mmol, 1.1 eq), Na_2CO_3 (0.646 g, 6.09 mmol, 3 eq) and $Pd(PPh_3)_4$ (117 mg, 0.102 mmol, 0.05 eq) in a mixture of 1,4-Dioxane:EtOH:H_2O (5 mL, 2:1:1, 0.5 M) under an inert N_2 atmosphere was heated with microwave irradiation at 90°C for 2 h. Following completion the crude mixture was concentrated onto silica gel and purified by Isolera Biotage LPLC (CH/EA 8:2) to give **154a** (128 mg, 0.487 mmol, 24%) as a beige solid.

ν_{max} (cm^{-1}) 3450, 3353, 1590, 1447, 1417, 1317, 1237, 849; **^{1}H-NMR (400 MHz, $CDCl_3$): δ** 8.79 (br. s., 1H), 8.04 - 8.30 (m, 3H), 7.60 (dd, J = 1.83, 7.34 Hz, 1H), 7.39 - 7.50 (m, 3H), 7.33 - 7.38 (m, 2H), 7.24 - 7.30 (m, 2H), 4.53 (br. s., 2H); **^{13}C-NMR (100 MHz $CDCl_3$): δ** 155.8, 147.9, 139.8, 139.0, 137.3, 126.7, 126.2, 123.9, 123.3, 120.4, 120.2, 119.9, 119.7, 118.8, 114.8, 110.9; **LR-ESI-MS**: $C_{17}H_{14}N_3$ $[M+H]^+$ *m/z* found 260.10, cald 260.12.

I.II ITC

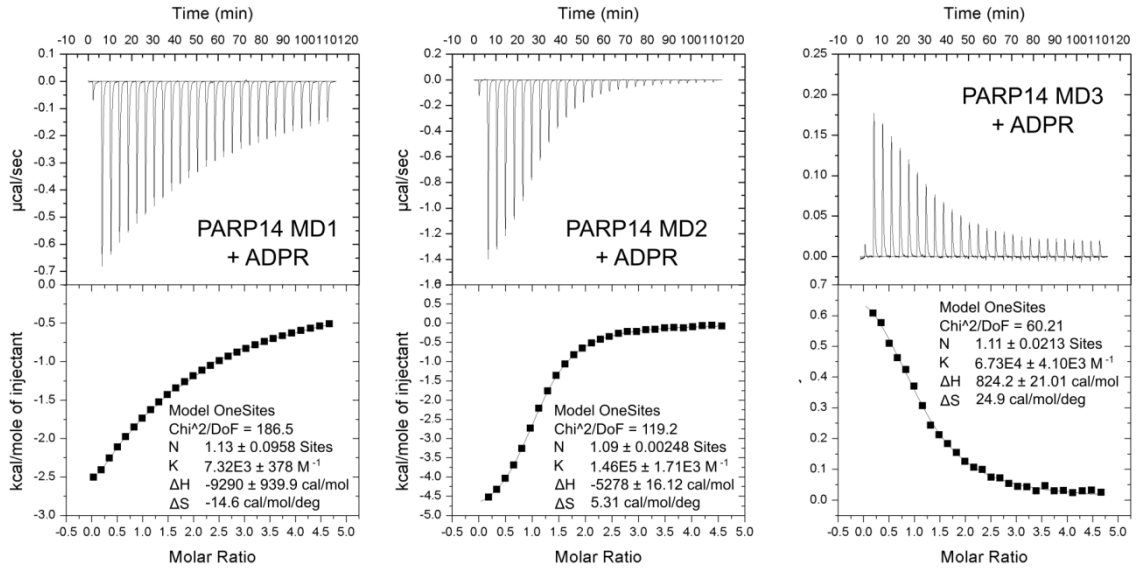

Supplemental Figure 10. *Isothermal Titration Calorimetry curves of ADPR titrated into PARP14 MD1, MD2 and MD3.*

Appendix 7.3.3

Experimental Procedures: Chapter 4 YEATS Domain Inhibition

I Practical Experimental

I.I Synthetic Procedures

I.II Biochemical/Biophysical binding characterisation

I.II.I AlphaScreen

I.II.II Selectivity

I.II.III Isothermal Titration Calorimetry (ITC)

I.III *In vitro* Metabolic Studies

I.IV Cellular Studies

I.IV.I NanoLuciferase Bioluminescence Resonance Energy Transfer (NanoBRET) Assay

I.IV.II Cellular Thermal Shift Assay (CETSA)

I.I Synthetic Procedures

2-(piperidin-1-ylmethyl)-1H-benzo[d]imidazole (338)

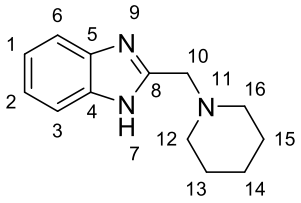

A solution of 2-(chloromethyl)-1H-benzo[d]imidazole (0.2 g, 1.2 mmol, 1 eq) in anhydrous MeCN (6 mL, 0.2 M) was stirred at room temperature as a brown suspension before piperidine (102 mg, 1.2 mmol, 1 eq) was added dropwise. The suspension was then heated conventionally at 100°C overnight. Upon reaction completion the solution was cooled to room temperature before being concentrated to a brown oil. The oil was loaded onto a KP-Sil SNAP 25 g column and eluted with CH/EA (100:0 to 0:100) to give the product as an off-white solid **338** (0.149 g, 0.69 mmol, 58%).

Mpt: 204.1-206.1 °C; **ν_{max} (cm^{-1})** 2935, 2802, 1455, 1418, 1335, 1270, 1108, 744, 487; **^{1}H NMR (400 MHz, DMSO-d_6) δ**12.23 (s, 1H, 7), 7.48 (d, *J* = 6.6 Hz, 2H, 2, 6), 7.26 – 6.92 (m, 2H, 1, 3), 3.66 (s, 2H, 10), 2.40 (t, *J* = 5.4 Hz, 4H, 12, 16), 1.52 (p, *J* = 5.6 Hz, 4H, 13, 15), 1.39 (td, *J* = 3.4, 6.8 Hz, 2H, 14); **^{13}C NMR (101 MHz, DMSO-d_6) δ**152.0 (3, 6), 121.3 (1, 2), 56.6 (10), 54.1 (12, 16), 25.4 (13, 15), 23.7 (14); **LR-ESI-MS**: $C_{13}H_{18}N_3$ $[M+H]^+$ *m/z* found 216.21, cald 216.15; **HR-ESI-MS**: $C_{13}H_{17}N_3Na$ $[M+Na]^+$ *m/z* found 238.1338, cald 238.13202.

2-((2-methylpiperidin-1-yl)methyl)-1H-benzo[d]imidazole (339)

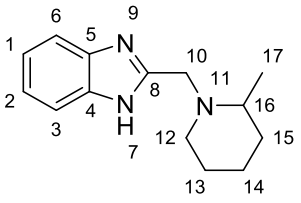

A solution of 2-(chloromethyl)-1H-benzo[d]imidazole (0.2 g, 1.2 mmol, 1 eq) in anhydrous MeCN (6 mL, 0.2 M) was stirred at room temperature as a brown suspension before 2-

methylpiperidine (119 mg, 1.2 mmol, 1 eq) was added dropwise. The suspension was then heated conventionally at 100°C overnight. Upon reaction completion the solution was cooled to room temperature before being concentrated to a brown oil. The oil was loaded onto a KP-Sil SNAP 25 g column and eluted with CH/EA (100:0 to 0:100) to give the product as an off-white solid **339** (0.081 g, 0.355 mmol, 30%).

Mpt: 204.6-206.6 °C; **ν_{max} (cm^{-1})** 2923, 2851, 1453, 1354, 1375, 1271, 1224, 742; **^{1}H NMR (400 MHz, DMSO-d_6) δ**12.1 (s, 1H, 7), 7.5 (s, 2H, 1, 2), 7.2 – 7.1 (m, 2H, 3, 6), 4.0 (d, *J* = 14.6 Hz, 1H, 10''), 3.6 (d, *J* = 14.5 Hz, 1H, 10'), 2.7 (dt, *J* = 4.0, 11.7 Hz, 1H, 16), 2.4 – 2.3 (m, 1H, 12''), 2.2 – 2.1 (m, 1H, 12'), 1.7 – 1.6 (m, 2H, 15'), 1.6 – 1.4 (m, 2H, 13''), 1.2 (tt, *J* = 5.7, 12.3 Hz, 2H, 14'), 1.1 (d, *J* = 6.1 Hz, 3H, 17); **^{13}C NMR (101 MHz, DMSO-d_6) δ**152.6 (3, 6), 122.6 – 118.5 (m, 1, 2), 55.7 , 10, 52.6 , 16, 51.8 , 12, 34.1 , 15, 25.6 , 13, 23.5 , 14, 19.0 , 17. **LR-ESI-MS:** $C_{14}H_{20}N_3$ $[M+H]^+$ *m/z* found 230.24, cald 230.17; **HR-ESI-MS**: $C_{14}H_{20}N_3$ $[M+H]^+$ *m/z* found 230.1670, cald 230.1657.

2-((3-methylpiperidin-1-yl)methyl)-1H-benzo[d]imidazole (340)

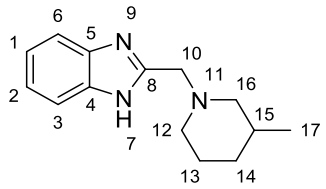

A solution of 2-(chloromethyl)-1H-benzo[d]imidazole (0.2 g, 1.2 mmol, 1 eq) in anhydrous MeCN (6 mL, 0.2 M) was stirred at room temperature as a brown suspension before 3-methylpiperidine (119 mg, 1.2 mmol, 1 eq) was added dropwise. The suspension was then heated conventionally at 100°C overnight. Upon reaction completion the solution was cooled to room temperature before being concentrated to a brown oil. The oil was loaded onto a KP-Sil SNAP 25 g column and eluted with CH/EA (100:0 to 0:100) to give the product as a yellow solid **340** (0.046 g, 0.199 mmol, 17%).

Mpt: 204.7-206.7 °C; **ν_{max} (cm^{-1})** 2924, 1453, 1421, 1339, 1271, 1043, 1020, 999; **^{1}H NMR (400 MHz, DMSO-d_6) δ**12.2 (s, 1H, 7), 7.5 (d, *J* = 24.9 Hz, 2H, 3, 6), 7.1 (dd, *J* = 2.9, 6.3 Hz, 2H, 1, 2), 3.8 – 3.5 (m, 2H, 10), 2.8 (td, *J* = 4.6, 10.3, 10.9 Hz, 2H, 12'', 16''), 2.0 (td, *J* = 3.0, 11.3 Hz, 1H, 16'),

1.8 – 1.4 (m, 5H, 12', 13, 14'', 15), 1.0 – 0.7 (m, 4H, 14', 17); **^{13}C NMR (101 MHz, DMSO-d_6) δ**152.0 (3, 6), 120.8 (1), 118.4 (2), 61.5 (16), 56.3 (10), 53.6 (12), 32.4 (14), 30.6 (15), 25.0 (13), 19.5 (17); **LR-ESI-MS:** $C_{14}H_{20}N_3$ $[M+H]^+$ *m/z* found 230.23, cald 230.17; **HR-ESI-MS**: $C_{14}H_{20}N_3$ $[M+H]^+$ *m/z* found 230.1669, cald 230.1657.

2-((4-methylpiperidin-1-yl)methyl)-1H-benzo[d]imidazole (341)

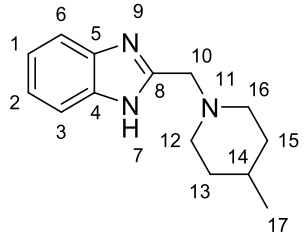

A solution of 2-(chloromethyl)-1H-benzo[d]imidazole (0.2 g, 1.2 mmol, 1 eq) in anhydrous MeCN (6 mL, 0.2 M) was stirred at room temperature as a brown suspension before 4-methylpiperidine (119 mg, 1.2 mmol, 1 eq) was added dropwise. The suspension was then heated conventionally at 100°C overnight. Upon reaction completion the solution was cooled to room temperature before being concentrated to a brown oil. The oil was loaded onto a KP-Sil SNAP 25 g column and eluted with CH/EA (100:0 to 0:100) to give the product as a white solid **341** (0.025 g, 0.11 mmol, 9%).

Mpt: 192.9-194.9 °C; **ν_{max} (cm^{-1})** 2921, 2799, 1329, 1316, 1252, 739; **^{1}H NMR (400 MHz, DMSO-d_6) δ**12.2 (s, 1H, 7), 7.5 (d, *J* = 36.3 Hz, 2H, 3, 6), 7.1 (q, *J* = 4.4 Hz, 2H, 1, 2), 3.7 (s, 2H, 10), 2.8 (dt, *J* = 3.2, 11.9 Hz, 2H, 12'', 16''), 2.0 (td, *J* = 2.5, 11.6 Hz, 2H, 12', 16'), 1.7 – 1.5 (m, 2H, 13'', 15''), 1.3 (ddd, *J* = 3.7, 6.8, 11.0 Hz, 1H, 14), 1.3 – 1.1 (m, 2H, 13', 15'), 0.9 (d, *J* = 6.4 Hz, 3H, 17); **^{13}C NMR (101 MHz, DMSO-d_6) δ**152.1 (5, 8), 121.1 – 120.5 (m, 1, 2), 118.3 (6), 111.1 (3), 56.2 (10), 53.5 (12, 16), 33.8 (13, 15), 30.0 (14), 21.8 (17); **LR-ESI-MS:** $C_{14}H_{20}N_3$ $[M+H]^+$ *m/z* found 230.24, cald 230.17; **HR-ESI-MS**: $C_{14}H_{20}N_3$ $[M+H]^+$ *m/z* found 230.1671, cald 230.1657.

***N*-(1H-benzo[d]imidazol-5-yl)benzamide (342)**

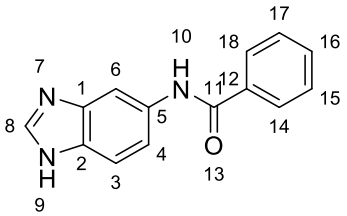

Initially a solution of 1H-benzo[d]imidazol-5-amine (0.2 g, 1.5 mmol, 1 eq), *N*,*N*-dimethylpyridin-4-amine (18 mg, 0.15 mmol, 0.1 eq) and DIPEA (314 µL, 1.8 mmol, 1.2 eq) in DCM (7.5 mL, 0.2 M) was cooled to 0°C before benzoyl chloride (209 µL, 1.8 mmol, 1.2 eq) was added dropwise. The solution was allowed to stir at ambient temperature before being concentrated onto silica gel and eluted through a KP-Sil SNAP 25 g column DCM/DCM (20% MeOH) (1:0 to 0:1) to give the product **342** as a white solid (0.013 g, 0.06 mmol, 4%).

Mpt: 288.5-290.5 °C; **ν_{max} (cm^{-1})** 2981, 2824, 1637, 1599, 1578, 1476, 1293, 1243, 807, 693, 409; **^{1}H NMR (400 MHz, DMSO-*d*$_6$) δ**12.4 (s, 1H, 9), 10.2 (s, 1H, 10), 8.3 – 8.1 (m, 1H, 8), 8.1 – 7.9 (m, 3H, 3, 4, 6), 7.7 – 7.3 (m, 5H, 14, 15, 16, 17, 18); **^{13}C NMR (101 MHz, DMSO-*d*$_6$) δ**165.4 (11), 135.2 (3), 131.3 (4, 6), 128.3 (14, 18), 127.6 (15, 17); **LR-ESI-MS**: $C_{14}H_{12}N_3O$ $[M+H]^+$ *m/z* found 238.17, cald 238.09; **HR-ESI-MS**: $C_{14}H_{12}N_3O$ $[M+H]^+$ *m/z* found 238.0984, cald 238.0980.

2-(chloromethyl)-5-nitro-1H-benzo[d]imidazole (208)

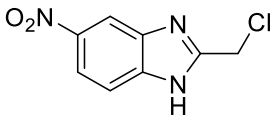

4-nitrobenzene-1,2-diamine **207** (10 g, 65.3 mmol, 1 eq) was dissolved in 4 *N* HCl solution (43.5 mL, 1.5 M) and had ethyl 2-chloroacetate (9.1 mL, 85 mmol, 1.3 eq) added dropwise before being heated to reflux for 6 hours. Upon reaction completion the mixture was cooled to 0°C with an ice bath and had ammonium hydroxide (19.3 mL, 174 mmol, 9 M) dropwise causing a red preciptate to form. The precipitate was filtered off and washed with H_2O (x 3) and dried in an oven vacuum (60°C) to give a dark red solid **208** (13.15 g, 62.1 mmol,95%) which was used without further purification.

LR-ESI-MS: $C_8H_7ClN_3O_2$ $[M+H]^+$ *m/z* found 212.20, cald 212.02.

2-(2-chloroethyl)-5-nitro-1H-benzo[d]imidazole (209)

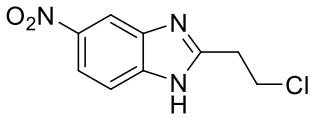

4-nitrobenzene-1,2-diamine **207** (5 g, 32.6 mmol, 1 eq) was dissolved in 4 N HCl solution (46.6 mL, 0.7 M) and had 3-chloropropanoyl chloride (6.22 g, 49.0 mmol, 1.5 eq) added dropwise before being heated to reflux for 16 hours. Upon reaction completion the mixture was cooled to 0°C with an ice bath and had ammonium hydroxide (50 mL, 450 mmol, 9 M) dropwise causing a red preciptate to form. The precipitate was filtered off and dissolved in DCM before being dried over Na_2SO_4 which was then filtered off to give a filtrate which was concentrated to red oil. The oil was then purified using a KP-Sil SNAP 25 g column to give the product **209** as an orange unstable solid (0.282 g, 1.25 mmol, 4%) which was submitted directly into the following step.

LR-ESI-MS: $C_9H_9ClN_3O_2$ $[M+H]^+$ *m/z* found 226.29, cald 226.04.

2-(1-chloroethyl)-5-nitro-1H-benzo[d]imidazole (210)

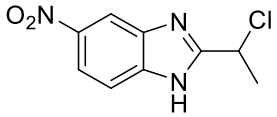

4-nitrobenzene-1,2-diamine **207** (10 g, 65.3 mmol, 1 eq) was dissolved in 4 N HCl solution (131 mL, 0.5 M) and had 2-chloropropanoyl chloride (6.86 mL, 71.8 mmol, 1.1 eq) added dropwise before being heated to reflux for 16 hours. Upon reaction completion the mixture was cooled to 0°C with an ice bath and had ammonium hydroxide (58 mL, 524 mmol, 9 M) dropwise causing a red preciptate to form. The precipitate was filtered off and washed with H_2O (x 3) and dried in an oven vacuum (60°C) to give a dark red solid **210** (4.92 g, 21.8 mmol, 33%) which was used without further purification.

LR-ESI-MS: $C_9H_9ClN_3O_2$ $[M+H]^+$ *m/z* found 226.29, cald 226.04.

2-((2-methylpiperidin-1-yl)methyl)-5-nitro-1H-benzo[d]imidazole (211)

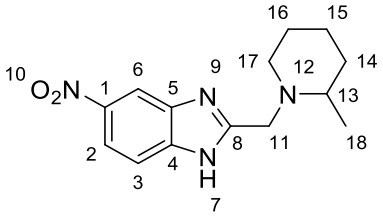

Initially a suspension of 2-(chloromethyl)-5-nitro-1H-benzo[d]imidazole **208** (3 g, 14.2 mmol, 1 eq) and Na_2CO_3 (2.25 g, 21.3 mmol, 1.5 eq) in anhydrous MeCN (43 mL, 0.33 M) had 2-methylpiperidine (3.36 mL, 28.4 mmol, 2 eq) added dropwise at room temperature. The reaction was allowed to stir at room temperature overnight. Upon reaction completion the suspension was filtered through a sintered frit and washed with acetone. The filtrate was concentrated to a residue which was purified using a Biotage MPLC KP Sil SNAP 25 g DCM/DCM (20% MeOH) 1:0 to 0:1 to give a red oil which was triturated with acetone to form a red foam **211** (1.884 g, 6.87 mmol, 48%).

Mpt: 167.8-169.8 °C; **ν_{max} (cm^{-1})** 2925, 2785, 1442, 1405, 1222, 1093, 887, 572, 541; **^{1}H NMR (400 MHz, DMSO-d_6) δ**12.8 (s, 1H, N*H*), 8.4 (d, *J* = 2.3 Hz, 1H, 6), 8.1 (dd, *J* = 2.3, 8.9 Hz, 1H, 2), 7.7 (d, *J* = 8.9 Hz, 1H, 3), 4.1 (d, *J* = 15.1 Hz, 1H, 11'), 3.7 (d, *J* = 15.1 Hz, 1H, 11''), 2.7 (dt, *J* = 4.0, 11.7 Hz, 1H, 17''), 2.4 (ddd, *J* = 2.2, 6.1, 8.8 Hz, 1H, 13), 2.2 (ddd, *J* = 3.6, 10.0, 11.5 Hz, 1H, 17'), 1.7 – 1.6 (m, 2H, 14', 16'), 1.6 – 1.4 (m, 2H, 14'', 16''), 1.4 – 1.2 (m, 2H, 15), 1.1 (d, *J* = 6.2 Hz, 3H, 18); **^{13}C NMR (101 MHz, DMSO-d_6) δ**158.3 (8), 142.2 (2, 6), 117.3 (3), 55.9 (11), 52.9 (13), 52.0 (17), 34.0 (14), 25.5 (16), 23.4 (15), 19.0 (18); **LR-ESI-MS**: $C_{14}H_{19}N_4O_2$ $[M+H]^+$ *m/z* found 275.23, cald 275.15; **HR-ESI-MS**: $C_{14}H_{19}N_4O_2$ $[M+H]^+$ *m/z* found 275.1508, cald 275.1508.

2-((3-methylpiperidin-1-yl)methyl)-5-nitro-1H-benzo[d]imidazole (212)

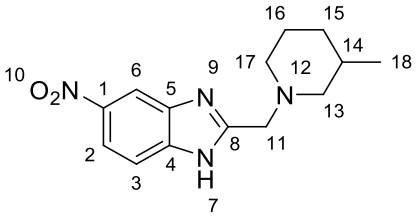

Initially a suspension of 2-(chloromethyl)-5-nitro-1H-benzo[d]imidazole **208** (3 g, 14.2 mmol, 1 eq) and Na_2CO_3 (2.25 g, 21.3 mmol, 1.5 eq) in anhydrous MeCN (43 mL, 0.33 M) had 3-

methylpiperidine (3.36 mL, 28.4 mmol, 2 eq) added dropwise at room temperature. The reaction was allowed to stir at room temperature overnight. Upon reaction completion the suspension was filtered through a sintered frit and washed with acetone. The filtrate was concentrated to a residue which was purified using a Biotage MPLC KP Sil SNAP 25 g DCM/DCM (20% MeOH) 1:0 to 0:1 to give a red oil which was triturated with acetone to form a red foam **212** (3.08 g, 11.23 mmol, 79%).

Mpt: 80.3-82.3 °C; **ν_{max} (cm^{-1})** 2925, 2796, 1466, 1449, 1332, 1309, 1117, 1064, 885, 826, 735, 688, 539; **^{1}H NMR (400 MHz, DMSO-d_6) δ**12.9 (s, 1H, 7), 8.4 (s, 1H, 6), 8.1 (dd, *J* = 2.2, 8.9 Hz, 1H, 2), 7.7 (d, *J* = 8.8 Hz, 1H, 3), 3.7 (d, *J* = 2.9 Hz, 2H, 11), 2.9 – 2.6 (m, 2H, 17), 2.1 – 1.8 (m, 1H, 13'), 1.8 – 1.4 (m, 5H, 13'', 14, 15', 16), 1.0 – 0.7 (m, 4H, 14'', 18); **^{13}C NMR (101 MHz, DMSO-d_6) δ**142.3 (2, 6), 61.5 (11), 56.2 (17), 53.6 (13), 32.3 (14), 30.6 (16), 26.3, 24.9 (15), 19.5 (18); **LR-ESI-MS**: $C_{14}H_{19}N_4O_2$ $[M+H]^+$ *m/z* found 275.23, cald 275.15; **HR-ESI-MS**: $C_{14}H_{19}N_4O_2$ $[M+H]^+$ *m/z* found 275.1508, cald 275.1508.

2-((4-methylpiperidin-1-yl)methyl)-5-nitro-1H-benzo[d]imidazole (213)

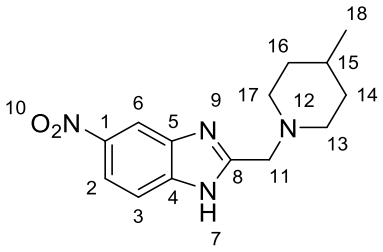

Initially a suspension of 2-(chloromethyl)-5-nitro-1H-benzo[d]imidazole **208** (3 g, 14.2 mmol, 1 eq) and Na_2CO_3 (2.25 g, 21.3 mmol, 1.5 eq) in anhydrous MeCN (43 mL, 0.33 M) had 4-methylpiperidine (3.36 mL, 28.4 mmol, 2 eq) added dropwise at room temperature. The reaction was allowed to stir at room temperature overnight. Upon reaction completion the suspension was filtered through a sintered frit and washed with acetone. The filtrate was concentrated to a residue which was purified using a Biotage MPLC KP Sil SNAP 25 g DCM/DCM (20% MeOH) 1:0 to 0:1 to give a red oil which was triturated with acetone to form a red foam **213** (2.43 g, 8.87 mmol, 63%).

Mpt: 165.6-167.6 °C; **ν_{max} (cm^{-1})** 2941, 1624, 1517, 1465, 1364, 888, 818; **^{1}H NMR (400 MHz, DMSO-d_6) δ**12.9 (s, 1H, 7), 8.4 (d, *J* = 2.3 Hz, 1H, 6), 8.1 (dd, *J* = 2.3, 8.9 Hz, 1H, 2), 7.7 (d, *J* = 8.8 Hz, 1H, 3), 3.8 (s, 2H, 11), 2.9 – 2.7 (m, 2H, 13'', 17''), 2.1 (td, *J* = 2.5, 11.6 Hz, 2H, 13', 17'), 1.7 – 1.5 (m, 2H, 14'', 16''), 1.4 – 1.3 (m, 1H, 15), 1.2 (td, *J* = 3.7, 12.2 Hz, 2H, 14', 16'), 0.9 (d, *J* = 6.4 Hz, 3H, 18); **^{13}C NMR (101 MHz, DMSO-d_6) δ**157.5 (8), 142.3 (2, 6), 117.4 (3), 56.1 (11), 53.6 (13, 17), 33.8 (14, 16), 29.9 (15), 26.3, 21.8 (18); **LR-ESI-MS**: $C_{14}H_{19}N_4O_2$ $[M+H]^+$ *m/z* found 275.24, cald 275.15; **HR-ESI-MS**: $C_{14}H_{19}N_4O_2$ $[M+H]^+$ *m/z* found 275.1505, cald 275.1508.

5-nitro-2-(piperidin-1-ylmethyl)-1H-benzo[d]imidazole (214)

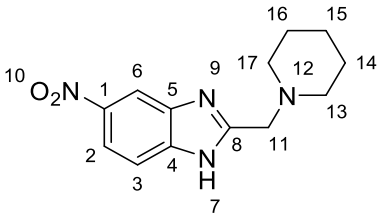

Initially a suspension of 2-(chloromethyl)-5-nitro-1H-benzo[d]imidazole **208** (5 g, 23.6 mmol, 1 eq) and Na_2CO_3 (3.76 g, 35.4 mmol, 1.5 eq) in anhydrous MeCN (72 mL, 0.33 M) had piperidine (4.67 mL, 47.3 mmol, 2 eq) added dropwise at room temperature. The reaction was allowed to stir at room temperature overnight. Upon reaction completion the suspension was filtered through a sintered frit and washed with acetone. The filtrate was concentrated to a residue which was purified using a Biotage MPLC KP Sil SNAP 25 g DCM/DCM (20% MeOH) 1:0 to 0:1 to give a red oil which was triturated with acetone to form an orange solid **214** (2.245 g, 8.62 mmol, 37%).

Mpt: 149.3-151.3 °C; **ν_{max} (cm^{-1})** 2935, 2801, 1518, 1468, 1413, 1107, 884; **^{1}H NMR (400 MHz, DMSO-d_6) δ**12.9 (s, 1H, 7), 8.4 (d, *J* = 2.3 Hz, 1H, 6), 8.1 (dd, *J* = 2.3, 8.9 Hz, 1H, 2), 7.6 (d, *J* = 8.9 Hz, 1H, 3), 3.7 (s, 2H, 11), 2.4 (t, *J* = 5.4 Hz, 4H, 13, 17), 1.5 (p, *J* = 5.6 Hz, 4H, 14, 16), 1.4 (q, *J* = 6.0 Hz, 2H, 15); **^{13}C NMR (101 MHz, DMSO-d_6) δ**206.5 (1), 157.4 (8), 142.3 (2, 6), 117.4 (3), 56.5 (11), 54.2 (13, 17), 25.4 (14, 16), 23.6 (15); **LR-ESI-MS**: $C_{13}H_{17}N_4O_2$ $[M+H]^+$ *m/z* found 261.23, cald 261.14; **HR-ESI-MS**: $C_{13}H_{17}N_4O_2$ $[M+H]^+$ *m/z* found 261.1349, cald 261.1352.

3-((5-nitro-1H-benzo[d]imidazol-2-yl)methyl)-2,3,4,5-tetrahydro-1H-benzo[d]azepine (215)

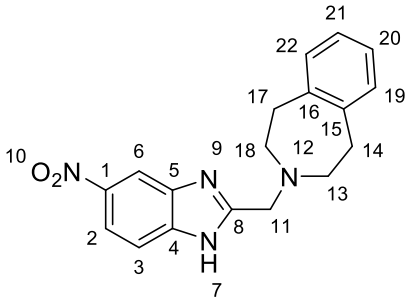

Initially a suspension of 2-(chloromethyl)-5-nitro-1H-benzo[d]imidazole **208** (0.869 g, 4.11 mmol, 1 eq) and Na_2CO_3 (0.653 g, 6.16 mmol, 1.5 eq) in anhydrous MeCN (12 mL, 0.33 M) had 2,3,4,5-tetrahydro-1H-benzo[d]azepine (907 mg, 6.16 mmol, 1.5 eq) added at room temperature. The reaction was allowed to stir at room temperature overnight. Upon reaction completion the suspension was filtered through a sintered frit and washed with acetone. The filtrate was concentrated to a residue which was purified using a Biotage MPLC KP Sil SNAP 25 g DCM/DCM (20% MeOH) 1:0 to 0:1 to give a red oil which was triturated with acetone to form a red crystalline solid **215** (1.080 g, 3.35 mmol, 82%).

Mpt: 96.5-98.5 °C; **ν_{max} (cm^{-1})** 1513, 1330, 827, 735; **^{1}H NMR (400 MHz, DMSO-d_6) δ**13.0 (s, 1H, 7), 8.4 (s, 1H, 6), 8.1 (dd, *J* = 2.3, 8.8 Hz, 1H, 2), 7.7 (d, *J* = 8.9 Hz, 1H, 3), 7.2 – 6.8 (m, 4H, 19, 20, 21, 22), 4.0 (s, 2H, 11), 2.9 (dd, *J* = 3.4, 6.6 Hz, 4H, 14, 17), 2.7 – 2.6 (m, 4H, 13, 18); **^{13}C NMR (101 MHz, DMSO-d_6) δ**142.3 (1), 141.7 (2, 6), 128.7 (20, 21), 126.1 (19, 22), 56.1 (11), 55.2 (13, 18), 35.6 (14, 17); **LR-ESI-MS**: $C_{18}H_{19}N_4O_2$ $[M+H]^+$ *m/z* found 323.26, cald 323.15; **HR-ESI-MS**: $C_{18}H_{19}N_4O_2$ $[M+H]^+$ *m/z* found 323.1502, cald 323.1508.

5-nitro-2-((4-phenylpiperazin-1-yl)methyl)-1H-benzo[d]imidazole (216)

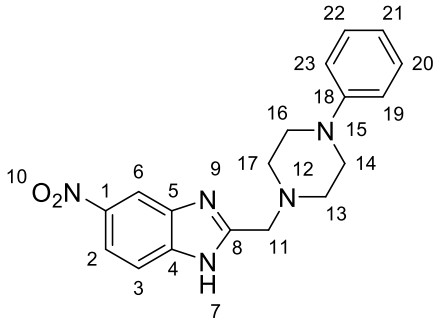

Initially a suspension of 2-(chloromethyl)-5-nitro-1H-benzo[d]imidazole **208** (0.901 g, 4.26 mmol, 1 eq) and Na_2CO_3 (0.677 g, 6.39 mmol, 1.5 eq) in anhydrous MeCN (13 mL, 0.33 M) had 1-phenylpiperazine (1.04 g, 6.39 mmol, 1.5 eq) added at room temperature. The reaction was allowed to stir at room temperature overnight. Upon reaction completion the suspension was filtered through a sintered frit and washed with acetone. The filtrate was concentrated to a residue which was purified using a Biotage MPLC KP Sil SNAP 25 g DCM/DCM (20% MeOH) 1:0 to 0:1 to give a red oil which was triturated with acetone to form a red solid **216** (0.713 g, 2.11 mmol, 50%).

Mpt: >195 °C; **ν_{max} (cm^{-1})** 2818, 1598, 1518, 1370, 1462, 1133, 1009, 737, 692, 527; **^{1}H NMR (400 MHz, DMSO-d_6) δ**13.0 (s, 1H, 7), 8.4 (s, 1H, 6), 8.1 (dd, *J* = 2.3, 8.8 Hz, 1H, 2), 7.7 (d, *J* = 8.9 Hz, 1H, 3), 7.3 – 7.1 (m, 2H, 20, 22), 7.0 – 6.9 (m, 2H, 19, 23), 6.8 (tt, *J* = 1.1, 7.3 Hz, 1H, 21), 3.9 (s, 2H, 11), 3.2 – 3.1 (m, 4H, 13, 17), 2.6 (dd, *J* = 3.7, 6.1 Hz, 4H, 14, 16); **^{13}C NMR (101 MHz, DMSO-d_6) δ**150.9 (2, 6), 142.4 (3), 128.9 (20, 22), 118.9 (21), 115.4 (19, 23), 55.6 (11), 52.8 (13, 17), 48.1 (14, 16); **LR-ESI-MS**: $C_{18}H_{20}N_5O_5$ $[M+H]^+$ *m/z* found 338.46, cald 338.16; **HR-ESI-MS**: $C_{18}H_{20}N_5O_5$ $[M+H]^+$ *m/z* found 338.1609, cald 338.1617.

5-nitro-2-((4-(2-(pyrrolidin-1-yl)ethyl)piperidin-1-yl)methyl)-1H-benzo[d]imidazole (217)

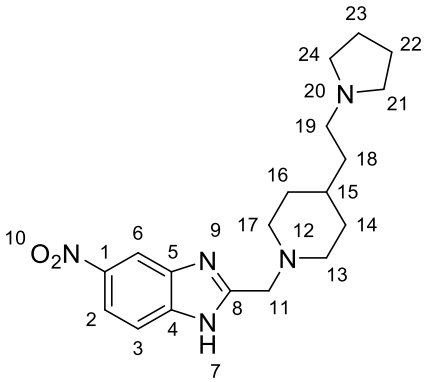

Initially a suspension of 2-(chloromethyl)-5-nitro-1H-benzo[d]imidazole **208** (0.48 g, 2.27 mmol, 1 eq) and Na_2CO_3 (0.36 g, 3.40 mmol, 1.5 eq) in anhydrous MeCN (6.8 mL, 0.33 M) had 4-(2-(pyrrolidin-1-yl)ethyl)piperidine (0.62 g, 3.40 mmol, 1.5 eq) added dropwise at room temperature. The reaction was allowed to stir at room temperature overnight. Upon reaction

completion the suspension was filtered through a sintered frit and washed with acetone. The filtrate was concentrated to a residue which was purified using a Biotage MPLC KP Sil SNAP 25 g DCM/DCM (20% MeOH) 1:0 to 0:1 to give a red oil which was triturated with acetone to form an orange solid **217** (0.241 g, 0.674 mmol, 30%).

Mpt: 88.7-90.7 °C; **ν_{max} (cm^{-1})** 2918, 2793, 1514, 1331, 1122, 1004, 828, 736; **^{1}H NMR (400 MHz, DMSO-d_6) δ**8.4 (d, *J* = 2.3 Hz, 1H, 6), 8.1 (dd, *J* = 2.3, 8.8 Hz, 1H, 2), 7.7 (d, *J* = 8.8 Hz, 1H, 3), 3.7 (s, 2H, 11), 2.9 – 2.7 (m, 2H, 19), 2.4 – 2.3 (m, 6H, 13'', 17'', 21, 24), 2.1 – 2.0 (m, 2H, 13', 17'), 1.6 (dq, *J* = 4.3, 5.6, 8.9 Hz, 6H, 14', 16', 22, 23), 1.4 – 1.1 (m, 5H, 14'', 15, 16'', 18); **^{13}C NMR (101 MHz, DMSO-d_6) δ**157.6 (8), 142.3 (2, 6), 117.4 (3), 73.8 (11), 56.1 (19), 53.6 (13, 17), 53.2 (21, 24), 35.2 (14, 16), 33.1 (22, 23), 31.9 (15), 23.0 (18); **LR-ESI-MS**: $C_{19}H_{28}N_5O_2$ $[M+H]^+$ *m/z* found 358.56, cald 358.22; **HR-ESI-MS**: $C_{19}H_{28}N_5O_2$ $[M+H]^+$ *m/z* found 358.2232, cald 358.2243.

5-nitro-2-((4-(2-(piperidin-1-yl)ethyl)piperidin-1-yl)methyl)-1H-benzo[d]imidazole (218)

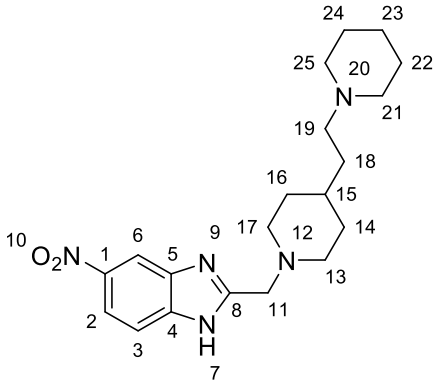

Initially a suspension of 2-(chloromethyl)-5-nitro-1H-benzo[d]imidazole **208** (0.77 g, 3.64 mmol, 1 eq) and Na_2CO_3 (0.58 g, 5.45 mmol, 1.5 eq) in anhydrous MeCN (11 mL, 0.33 M) had 1-(2-(piperidin-4-yl)ethyl)piperidine (1.07 g, 5.45 mmol, 1.5 eq) added dropwise at room temperature. The reaction was allowed to stir at room temperature overnight. Upon reaction completion the suspension was filtered through a sintered frit and washed with acetone. The filtrate was concentrated to a residue which was submitted to the next step without further purification **218** (0.592 g, 1.60 mmol, 44%).

2-((2-methylpyrrolidin-1-yl)methyl)-5-nitro-1H-benzo[d]imidazole (219)

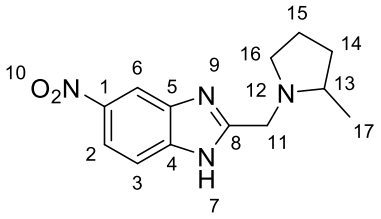

Initially a suspension of 2-(chloromethyl)-5-nitro-1H-benzo[d]imidazole **208** (1.46 g, 6.91 mmol, 1 eq) and Na_2CO_3 (1.09 g, 10.36 mmol, 1.5 eq) in anhydrous MeCN (21 mL, 0.33 M) had 2-methylpyrrolidine (0.88 g, 10.36 mmol, 1.5 eq) added dropwise at room temperature. The reaction was allowed to stir at room temperature overnight. Upon reaction completion the suspension was filtered through a sintered frit and washed with acetone. The filtrate was concentrated to a residue which was purified using a Biotage MPLC KP Sil SNAP 25 g DCM/DCM (20% MeOH) 1:0 to 0:1 to give a red oil which was triturated with acetone to form a dark red solid **219** (1.336 g, 5.13 mmol, 74%).

Mpt: 69.0-71.0 °C; **ν_{max} (cm^{-1})** 2960, 2795, 1513, 1332, 1307, 827, 735; **^{1}H NMR (400 MHz, DMSO-d_6) δ**12.9 (s, 1H, 7), 8.4 (d, *J* = 2.3 Hz, 1H, 6), 8.1 (dd, *J* = 2.3, 8.9 Hz, 1H, 2), 7.6 (d, *J* = 8.7 Hz, 1H, 3), 4.1 (d, *J* = 14.7 Hz, 1H, 11''), 3.6 (d, *J* = 14.7 Hz, 1H, 11'), 2.9 (ddd, *J* = 3.4, 7.6, 9.0 Hz, 1H, 13), 2.6 – 2.4 (m, 1H, 16'), 2.3 (q, *J* = 8.7 Hz, 1H, 16''), 1.9 (dddd, *J* = 5.5, 7.2, 9.4, 12.4 Hz, 1H, 14''), 1.7 (dddd, *J* = 4.2, 6.8, 8.9, 17.7 Hz, 2H, 14', 15''), 1.4 (dddd, *J* = 6.3, 8.4, 10.2, 12.3 Hz, 1H, 15'), 1.0 (dd, *J* = 6.1, 15.4 Hz, 3H, 17); **^{13}C NMR (101 MHz, DMSO-d_6) δ**142.2 (2, 6), 117.3 (3), 59.2 (11), 54.1 (13), 51.0 (16), 32.5 (14), 21.4 (15), 18.8 (17); **LR-ESI-MS**: $C_{13}H_{17}N_4O_2$ $[M+H]^+$ *m/z* found 261.36, cald 261.14; **HR-ESI-MS**: $C_{13}H_{17}N_4O_2$ $[M+H]^+$ *m/z* found 261.1289, cald 261.1352.

2-((cis-2,6-dimethylpiperidin-1-yl)methyl)-5-nitro-1H-benzo[d]imidazole (220)

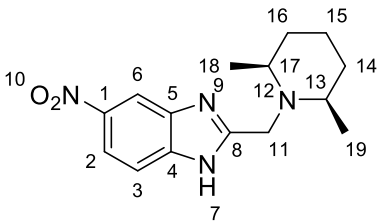

Initially a suspension of 2-(chloromethyl)-5-nitro-1H-benzo[d]imidazole **208** (1 g, 4.73 mmol, 1 eq) and Na_2CO_3 (0.751 g, 7.09 mmol, 1.5 eq) in anhydrous MeCN (14 mL, 0.33 M) had cis-2,6-

dimethylpiperidine (0.802 g, 7.09 mmol, 1.5 eq) added dropwise at room temperature. The reaction was allowed to stir at room temperature overnight. Upon reaction completion the suspension was filtered through a sintered frit and washed with acetone. The filtrate was concentrated to a residue which was purified using a Biotage MPLC KP Sil SNAP 25 g DCM/DCM (20% MeOH) 1:0 to 0:1 to give a red oil which was triturated with acetone to form red solid **220** (0.506 g, 1.76 mmol, 37%).

Mpt: 150.9-152.9 °C; **ν_{max} (cm^{-1})** 2967, 2934, 1515, 1322, 1302, 1062, 818, 738; **^{1}H NMR (400 MHz, DMSO-d_6) δ**12.6 (s, 1H, 7), 8.4 (d, *J* = 2.3 Hz, 1H, 6), 8.1 (dd, *J* = 2.3, 8.8 Hz, 1H, 2), 7.7 (d, *J* = 8.8 Hz, 1H, 3), 4.0 (s, 2H, 10''), 2.6 – 2.5 (m, 2H, 12, 16), 1.7 – 1.5 (m, 3H, 13'', 15''), 1.4 – 1.2 (m, 3H, 13', 14, 15'), 1.0 (d, *J* = 6.2 Hz, 6H, 17, 18); **^{13}C NMR (101 MHz, DMSO-d_6) δ**206.5 (8), 142.1 (2, 6), 117.1 (3), 56.9 (11), 48.6 (13), 46.9 (17), 33.6 (14, 16), 24.0 (15); **LR-ESI-MS**: $C_{15}H_{21}N_4O_2$ $[M+H]^+$ *m/z* found 289.44, cald 289.17; **HR-ESI-MS**: $C_{15}H_{21}N_4O_2$ $[M+H]^+$ *m/z* found 289.1641, cald 289.1665.

2-((4-methylpiperazin-1-yl)methyl)-5-nitro-1H-benzo[d]imidazole (221)

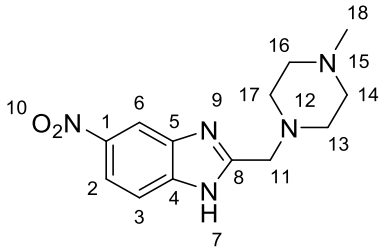

Initially a suspension of 2-(chloromethyl)-5-nitro-1H-benzo[d]imidazole **208** (1 g, 4.73 mmol, 1 eq) and Na_2CO_3 (0.751 g, 7.09 mmol, 1.5 eq) in anhydrous MeCN (14 mL, 0.33 M) had 1-methylpiperazine (0.710 g, 7.09 mmol, 1.5 eq) added dropwise at room temperature. The reaction was allowed to stir at room temperature overnight. Upon reaction completion the suspension was filtered through a sintered frit and washed with acetone. The filtrate was concentrated to a residue which was purified using a Biotage MPLC KP Sil SNAP 25 g DCM/DCM (20% MeOH) 1:0 to 0:1 to give a red oil which was triturated with acetone to form a beige solid **221** (0.424 g, 1.54 mmol, 33%).

Mpt: 140.6-142.6 °C; **ν_{max} (cm^{-1})** 3376, 2805, 1513, 1471, 1456, 1334, 1280, 821, 737; **^{1}H NMR (400 MHz, DMSO-d_6) δ**12.9 (s, 1H, 7), 8.4 (d, *J* = 2.2 Hz, 1H, 6), 8.1 (dd, *J* = 2.3, 8.9 Hz, 1H, 2), 7.7 (d, *J* = 8.9 Hz, 1H, 3), 3.8 (s, 2H, 11), 2.5 (s, 4H, 13, 17), 2.4 (s, 4H, 14, 16), 2.2 (s, 3H, 18); **^{13}C NMR (101 MHz, DMSO-d_6) δ**206.4 (8), 157.0 (1), 142.3 (2, 6), 117.4 (3), 55.6 (11), 54.5, 52.8 (14, 16), 48.6 (18), 45.7, 30.7; **LR-ESI-MS**: $C_{13}H_{18}N_5O_2$ $[M+H]^+$ *m/z* found 276.40, cald 276.15; **HR-ESI-MS**: $C_{13}H_{18}N_5O_2$ $[M+H]^+$ *m/z* found 276.1446, cald 276.1460.

***N*, *N*-dimethyl-1-(5-nitro-1H-benzo[d]imidazol-2-yl)methanamine (222)**

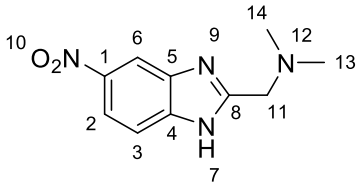

Initially a suspension of 2-(chloromethyl)-5-nitro-1H-benzo[d]imidazole **208** (1 g, 4.73 mmol, 1 eq) and Na_2CO_3 (0.751 g, 7.09 mmol, 1.5 eq) in anhydrous MeCN (14 mL, 0.33 M) had dimethylamine (3.54 mL, 7.09 mmol, 2 M in THF, 1.5 eq) added dropwise at room temperature. The reaction was allowed to stir at room temperature overnight. Upon reaction completion the suspension was filtered through a sintered frit and washed with acetone. The filtrate was concentrated to a residue which was purified using a Biotage MPLC KP Sil SNAP 25 g DCM/DCM (20% MeOH) 1:0 to 0:1 to give a red oil which was triturated with acetone to form brown solid **222** (0.761 g, 3.46 mmol, 73%).

Mpt: 148.1-150.1 °C; **ν_{max} (cm^{-1})** 2778, 1453, 1335, 1310, 1036, 823, 736; **^{1}H NMR (400 MHz, DMSO-d_6) δ**13.0 (s, 1H, 7), 8.4 (s, 1H, 6), 8.1 (dd, *J* = 2.3, 8.9 Hz, 1H, 2), 7.6 (d, *J* = 8.9 Hz, 1H, 3), 3.7 (s, 2H, 11), 2.3 (s, 6H, 13, 14); **^{13}C NMR (101 MHz, DMSO-d_6) δ**142.3 (2, 6), 117.4 (3), 56.9 (11), 45.3 (13, 14); **LR-ESI-MS**: $C_{10}H_{13}N_4O_2$ $[M+H]^+$ *m/z* found 221.31, cald 221.10; **HR-ESI-MS**: $C_{10}H_{13}N_4O_2$ $[M+H]^+$ *m/z* found 221.1029, cald 221.1039.

5-nitro-2-(2-(piperidin-1-yl)ethyl)-1H-benzo[d]imidazole (223)

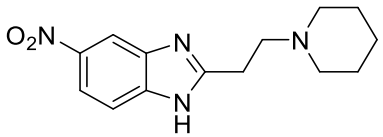

Initially a suspension of 2-(2-chloroethyl)-5-nitro-1H-benzo[d]imidazole **209** (1 g, 4.43 mmol, 1 eq) and Na_2CO_3 (0.705 g, 6.65 mmol, 1.5 eq) in anhydrous MeCN (13.4 mL, 0.33 M) had piperidine (0.657 mL, 6.65 mmol, 1.5 eq) added dropwise at room temperature. The reaction was allowed to stir at room temperature overnight. Upon reaction completion the suspension was filtered through a sintered frit and washed with acetone. The filtrate was concentrated to a residue which was purified using a Biotage MPLC KP Sil SNAP 25 g DCM/DCM (20% MeOH) 1:0 to 0:1 to give a red oil which was triturated with acetone to form an unstable orange foam **223** (0.106 g, 0.386 mmol, 9%) which was immediately submitted to the following step.

LR-ESI-MS: $C_{14}H_{19}N_4O_2$ $[M+H]^+$ *m/z* found 275.43, cald 275.15;

2-((cis-3,5-dimethylpiperidin-1-yl)methyl)-5-nitro-1H-benzo[d]imidazole (224)

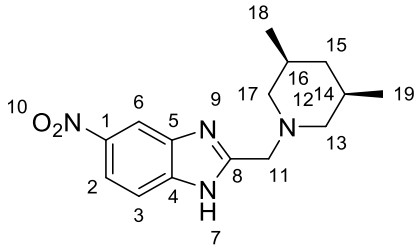

Initially a suspension of 2-(chloromethyl)-5-nitro-1H-benzo[d]imidazole **208** (1 g, 4.73 mmol, 1 eq) and Na_2CO_3 (0.751 g, 7.09 mmol, 1.5 eq) in anhydrous MeCN (13.4 mL, 0.33 M) had cis-3,5-dimethylpiperidine (0.802 g, 7.09 mmol, 1.5 eq) added dropwise at room temperature. The reaction was allowed to stir at room temperature overnight. Upon reaction completion the suspension was filtered through a sintered frit and washed with acetone. The filtrate was concentrated to a residue which was purified using a Biotage MPLC KP Sil SNAP 25 g DCM/DCM (20% MeOH) 1:0 to 0:1 to give a red oil which was triturated with acetone to form an orange foam **224** (0.979 g, 3.40 mmol, 72%).

Mpt: 108.9-110.9 °C; **ν_{max} (cm^{-1})** 2949, 1515, 1332, 1065, 880, 826, 736; **^{1}H NMR (400 MHz, DMSO-d_6) δ**12.9 (s, 1H, 7), 8.6 – 8.3 (m, 1H, 6), 8.1 (dd, *J* = 2.3, 8.8 Hz, 1H, 2), 7.7 (d, *J* = 8.9 Hz,

1H, 3), 3.8 (s, 2H, 11), 2.8 – 2.7 (m, 2H, 13'', 17''), 1.8 – 1.5 (m, 5H, 13', 14, 15, 16, 17'), 0.8 (d, *J* = 6.2 Hz, 6H, 18, 19), 0.6 – 0.4 (m, 1H, 15''); **^{13}C NMR (101 MHz, DMSO-*d*$_6$) δ**142.3 (2, 6), 61.1 (11), 55.9 (13, 17), 41.5 (14, 16), 30.6 (15), 19.4 (18, 19); **LR-ESI-MS**: $C_{15}H_{21}N_4O_2$ $[M+H]^+$ *m/z* found 289.26, cald 289.17; **HR-ESI-MS**: $C_{15}H_{21}N_4O_2$ $[M+H]^+$ *m/z* found 289.1654, cald 289.1665.

5-nitro-2-(1-(piperidin-1-yl)ethyl)-1H-benzo[d]imidazole (225)

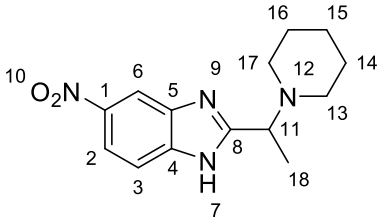

Initially a suspension of 2-(1-chloroethyl)-5-nitro-1H-benzo[d]imidazole **210** (1 g, 4.43 mmol, 1 eq) and Na_2CO_3 (0.705 g, 6.65 mmol, 1.5 eq) in anhydrous MeCN (11 mL, 0.4 M) had piperidine (0.657 mL, 6.65 mmol, 1.5 eq) added dropwise at room temperature. The reaction was allowed to stir at room temperature overnight. Upon reaction completion the suspension was filtered through a sintered frit and washed with acetone. The filtrate was concentrated to a residue which was purified using a Biotage MPLC KP Sil SNAP 25 g DCM/DCM (20% MeOH) 1:0 to 0:1 to give a red oil which was triturated with acetone to form an orange foam **225** (0.695 g, 2.53 mmol, 57%) which was used immediately in the following step.

^{1}H NMR (400 MHz, DMSO-*d*$_6$) δ12.9 (s, 1H, 7), 8.4 (s, 1H, 6), 8.1 (dd, *J* = 2.3, 8.9 Hz, 1H, 2), 7.7 (d, *J* = 8.9 Hz, 1H, 3), 3.4 – 3.3 (m, 1H, 11), 2.4 (t, *J* = 5.2 Hz, 4H, 13, 17), 1.5 (p, *J* = 5.5 Hz, 4H, 14, 16), 1.4 (d, *J* = 6.9 Hz, 3H, 18), 1.4 (q, *J* = 6.0, 6.9 Hz, 2H, 15); **^{13}C NMR (101 MHz, DMSO-*d*$_6$) δ**142.2 (2, 6), 117.3 (3), 64.9 (11), 58.5 (13), 50.2 (17), 25.8 (14, 16), 24.1 (15), 13.8 (18); **LR-ESI-MS**: $C_{14}H_{19}N_4O_2$ $[M+H]^+$ *m/z* found 275.27, cald 275.15.

2-((3-methylpyrrolidin-1-yl)methyl)-5-nitro-1H-benzo[d]imidazole (226)

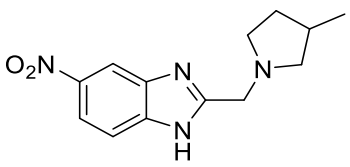

Initially a suspension of 2-(chloromethyl)-5-nitro-1H-benzo[d]imidazole **208** (1.1 g, 5.22 mmol, 1 eq) and Na_2CO_3 (1.38 g, 13.05 mmol, 2.5 eq) in anhydrous MeCN (15 mL, 0.4 M) had 3-methylpyrrolidine, HCl (0.952 g, 7.83 mmol, 1.5 eq) added at room temperature. The reaction was allowed to stir at room temperature overnight. Upon reaction completion the suspension was filtered through a sintered frit and washed with acetone. The filtrate was concentrated to a residue which was purified using a Biotage MPLC KP Sil SNAP 25 g DCM/DCM (20% MeOH) 1:0 to 0:1 to give a red oil which was triturated with acetone to form an orange foam **226** (0.04 g, 0.158 mmol, 3%) which was used immediately in the following step.

LR-ESI-MS: $C_{13}H_{17}N_4O_2$ $[M+H]^+$ *m/z* found 261.36, cald 261.14.

2-((trans-3,4-dimethylpyrrolidin-1-yl)methyl)-5-nitro-1H-benzo[d]imidazole (227)

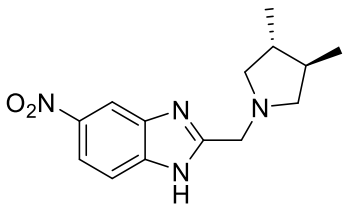

Initially a suspension of 2-(chloromethyl)-5-nitro-1H-benzo[d]imidazole **208** (0.886 g, 4.19 mmol, 1 eq) and Na_2CO_3 (1.11 g, 10.47 mmol, 2.5 eq) in anhydrous MeCN (13 mL, 0.4 M) had trans-3,4-dimethylpyrrolidine, HCl (0.852 g, 6.28 mmol, 1.5 eq) added at room temperature. The reaction was allowed to stir at room temperature overnight. Upon reaction completion the suspension was filtered through a sintered frit and washed with acetone. The filtrate was concentrated to a residue which was purified using a Biotage MPLC KP Sil SNAP 25 g DCM/DCM (20% MeOH) 1:0 to 0:1 to give a red oil which was triturated with acetone to form an unstable orange foam **227** (0.39 g, 1.42 mmol, 34%) which was used immediately in the following step.

(*R*)-2-((2-methylpyrrolidin-1-yl)methyl)-5-nitro-1H-benzo[d]imidazole (228)

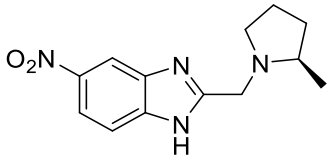

Initially a suspension of 2-(chloromethyl)-5-nitro-1H-benzo[d]imidazole **208** (1.25 g, 5.92 mmol, 1 eq) and Na_2CO_3 (1.57 g, 14.8 mmol, 2.5 eq) in anhydrous MeCN (18 mL, 0.4 M) had (*R*)-2-methylpyrrolidine, HCl (1.08 g, 8.87 mmol, 1.5 eq) added at room temperature. The reaction was allowed to stir at room temperature overnight. Upon reaction completion the suspension was filtered through a sintered frit and washed with acetone. The filtrate was concentrated to a residue which was submitted to the next step without further purification **228** (0.741 g, 2.85 mmol, 48%).

LR-ESI-MS: $C_{13}H_{17}N_4O_2$ $[M+H]^+$ *m/z* found 261.37, cald 261.14.

(*R*)-2-((3-methylpyrrolidin-1-yl)methyl)-5-nitro-1H-benzo[d]imidazole (229)

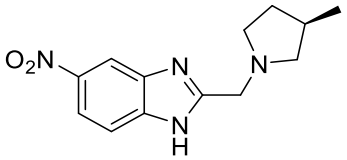

Initially a suspension of 2-(chloromethyl)-5-nitro-1H-benzo[d]imidazole **208** (0.925 g, 4.37 mmol, 1 eq) and Na_2CO_3 (1.16 g, 10.92 mmol, 2.5 eq) in anhydrous MeCN (13 mL, 0.33 M) had (*R*)-3-methylpyrrolidine, HCl (0.797 g, 6.55 mmol, 1.5 eq) added at room temperature. The reaction was allowed to stir at room temperature overnight. Upon reaction completion the suspension was filtered through a sintered frit and washed with acetone. The filtrate was concentrated to a residue which was submitted to the next step without further purification **229** (0.399 g, 1.53 mmol, 35%).

LR-ESI-MS: $C_{13}H_{17}N_4O_2$ $[M+H]^+$ *m/z* found 261.23, cald 261.14.

(*S*)-2-((3-methylpyrrolidin-1-yl)methyl)-5-nitro-1H-benzo[d]imidazole (230)

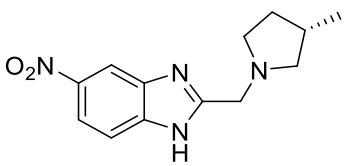

Initially a suspension of 2-(chloromethyl)-5-nitro-1H-benzo[d]imidazole **208** (0.363 g, 1.71 mmol, 1 eq) and Na_2CO_3 (0.454 g, 4.28 mmol, 2.5 eq) in anhydrous MeCN (5 mL, 0.33 M) had (*S*)-3-

methylpyrrolidine, HCl (0.250 g, 2.06 mmol, 1.2 eq) added at room temperature. The reaction was allowed to stir at room temperature overnight. Upon reaction completion the suspension was filtered through a sintered frit and washed with acetone. The filtrate was concentrated to a residue which was submitted to the next step without further purification **230** (*quant*).

LR-ESI-MS: $C_{13}H_{17}N_4O_2$ $[M+H]^+$ *m/z* found 261.22, cald 261.14.

2-((3-azabicyclo[3.1.0]hexan-3-yl)methyl)-5-nitro-1H-benzo[d]imidazole (231)

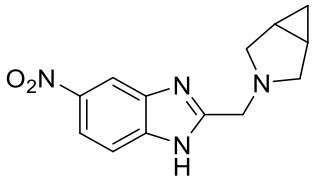

Initially a suspension of 2-(chloromethyl)-5-nitro-1H-benzo[d]imidazole **208** (1.47 g, 6.97 mmol, 1 eq) and Na_2CO_3 (1.85 g, 17.42 mmol, 2.5 eq) in anhydrous MeCN (21 mL, 0.33 M) had 3-azabicyclo[3.1.0]hexane, HCl (1 g, 8.36 mmol, 1.2 eq) added at room temperature. The reaction was allowed to stir at room temperature overnight. Upon reaction completion the suspension was filtered through a sintered frit and washed with acetone. The filtrate was concentrated to a residue which was submitted to the next step without further purification **231** (*quant*).

LR-ESI-MS: $C_{13}H_{15}N_4O_2$ $[M+H]^+$ *m/z* found 259.21, cald 259.12.

2-((3,3-difluoropyrrolidin-1-yl)methyl)-5-nitro-H-benzo[d]imidazole (232)

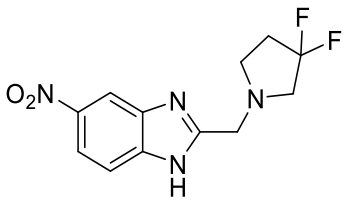

Initially a suspension of 2-(chloromethyl)-5-nitro-1H-benzo[d]imidazole **208** (0.614 g, 2.90 mmol, 1 eq) and Na_2CO_3 (0.769 g, 7.26 mmol, 2.5 eq) in anhydrous MeCN (8.8 mL, 0.33 M) had 3,3-difluoropyrrolidine, HCl (0.5 g, 3.48 mmol, 1.2 eq) added at room temperature. The reaction was allowed to stir at room temperature overnight. Upon reaction completion the suspension was filtered through a sintered frit and washed with acetone. The filtrate was concentrated to a residue which was submitted to the next step without further purification **232** (*quant*).

LR-ESI-MS: $C_{12}H_{13}F_2N_4O_2$ $[M+H]^+$ *m/z* found 283.17, cald 283.10.

(*S*)-2-((2-methylpyrrolidin-1-yl)methyl)-5-nitro-1H-benzo[d]imidazole (233)

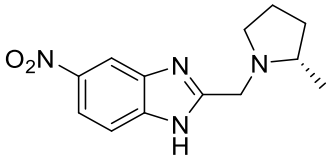

Initially a suspension of 2-(chloromethyl)-5-nitro-1H-benzo[d]imidazole **208** (1.45 g, 6.85 mmol, 1 eq) and Na_2CO_3 (1.82 g, 17.1 mmol, 2.5 eq) in anhydrous MeCN (20 mL, 0.33 M) had (*S*)-2-methylpyrrolidine, HCl (1 g, 8.22 mmol, 1.2 eq) added at room temperature. The reaction was allowed to stir at room temperature overnight. Upon reaction completion the suspension was filtered through a sintered frit and washed with acetone. The filtrate was concentrated to a residue which was submitted to the next step without further purification **233** (*quant*).

LR-ESI-MS: $C_{13}H_{17}N_4O_2$ $[M+H]^+$ *m/z* found 261.23, cald 261.14.

2-((3-methylpyrrolidin-1-yl)methyl)-5-nitro-1H-benzo[d]imidazole (234)

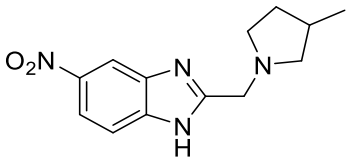

Initially a suspension of 2-(chloromethyl)-5-nitro-1H-benzo[d]imidazole **208** (1.45 g, 6.85 mmol, 1 eq) and Na_2CO_3 (1.82 g, 17.1 mmol, 2.5 eq) in anhydrous MeCN (20 mL, 0.33 M) had 3-methylpyrrolidine, HCl (1 g, 8.22 mmol, 1.2 eq) added at room temperature. The reaction was allowed to stir at room temperature overnight. Upon reaction completion the suspension was filtered through a sintered frit and washed with acetone. The filtrate was concentrated to a residue which was submitted to the next step without further purification **234** (*quant*).

LR-ESI-MS: $C_{13}H_{17}N_4O_2$ $[M+H]^+$ *m/z* found 261.23, cald 261.14.

2-((2,2-dimethylpyrrolidin-1-yl)methyl)-5-nitro-1H-benzo[d]imidazole (235)

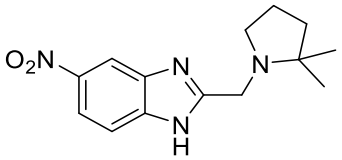

Initially a suspension of 2-(chloromethyl)-5-nitro-1H-benzo[d]imidazole **208** (1.3 g, 6.14 mmol, 1 eq) and Na_2CO_3 (1.63 g, 15.4 mmol, 2.5 eq) in anhydrous MeCN (18 mL, 0.33 M) had 2,2-dimethylpyrrolidine, HCl (1 g, 7.37 mmol, 1.2 eq) added at room temperature. The reaction was allowed to stir at room temperature overnight. Upon reaction completion the suspension was filtered through a sintered frit and washed with acetone. The filtrate was concentrated to a residue which was submitted to the next step without further purification **235** (*quant*).

LR-ESI-MS: $C_{14}H_{19}N_4O_2$ $[M+H]^+$ *m/z* found 275.35, cald 275.15.

2-((2-ethylpyrrolidin-1-yl)methyl)-5-nitro-1H-benzo[d]imidazole (236)

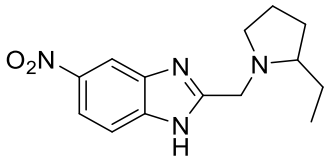

Initially a suspension of 2-(chloromethyl)-5-nitro-1H-benzo[d]imidazole **208** (1.3 g, 6.14 mmol, 1 eq) and Na_2CO_3 (1.63 g, 15.4 mmol, 2.5 eq) in anhydrous MeCN (18 mL, 0.33 M) had 2-ethylpyrrolidine, HCl (1 g, 7.37 mmol, 1.2 eq) added at room temperature. The reaction was allowed to stir at room temperature overnight. Upon reaction completion the suspension was filtered through a sintered frit and washed with acetone. The filtrate was concentrated to a residue which was submitted to the next step without further purification **236** (*quant*).

LR-ESI-MS: $C_{14}H_{19}N_4O_2$ $[M+H]^+$ *m/z* found 275.35, cald 275.15.

(1*S*,4*S*)-5-((5-nitro-1H-benzo[d]imidazol-2-yl)methyl)-2-oxa-5-azabicyclo[2.2.1]heptane (237)

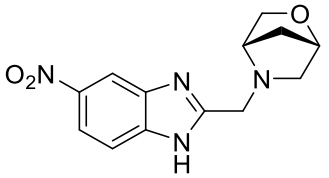

Initially a suspension of 2-(chloromethyl)-5-nitro-1H-benzo[d]imidazole **208** (1.3 g, 6.14 mmol, 1 eq) and Na_2CO_3 (1.63 g, 15.4 mmol, 2.5 eq) in anhydrous MeCN (18 mL, 0.33 M) had (1*S*,4*S*)-2-oxa-5-azabicyclo[2.2.1]heptane, HCl (1 g, 7.37 mmol, 1.2 eq) added at room temperature. The reaction was allowed to stir at room temperature overnight. Upon reaction completion the

suspension was filtered through a sintered frit and washed with acetone. The filtrate was concentrated to a residue which was submitted to the next step without further purification **237** (*quant*).

LR-ESI-MS: $C_{13}H_{15}N_4O_3$ $[M+H]^+$ *m/z* found 275.31, cald 275.11.

tert-butyl (2-(methyl((5-nitro-1H-benzo[d]imidazol-2-yl)methyl)amino)ethyl)carbamate (239)

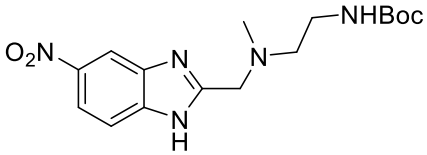

Initially a suspension of 2-(chloromethyl)-5-nitro-1H-benzo[d]imidazole **208** (0.5 g, 2.36 mmol, 1 eq) and Na_2CO_3 (0.301 g, 2.84 mmol, 2.5 eq) in anhydrous MeCN (7.2 mL, 0.33 M) had tert-butyl (2-(methylamino)ethyl)carbamate (0.494 g, 2.84 mmol, 1.2 eq) added at room temperature. The reaction was allowed to stir at room temperature overnight. Upon reaction completion the suspension was filtered through a sintered frit and washed with acetone. The filtrate was concentrated to a residue which was submitted to the next step without further purification **239** (*quant*).

LR-ESI-MS: $C_{16}H_{24}N_5O_4$ $[M+H]^+$ *m/z* found 350.28, cald 350.18.

2-((2-(methoxymethyl)pyrrolidin-1-yl)methyl)-5-nitro-1H-benzo[d]imidazole (240)

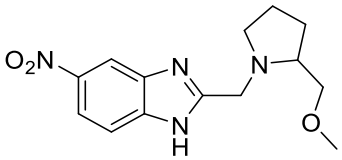

Initially a suspension of 2-(chloromethyl)-5-nitro-1H-benzo[d]imidazole **208** (0.5 g, 2.36 mmol, 1 eq) and Na_2CO_3 (0.301 g, 2.84 mmol, 2.5 eq) in anhydrous MeCN (7.2 mL, 0.33 M) had 2-(methoxymethyl)pyrrolidine (0.299 g, 2.60 mmol, 1.1 eq) added at room temperature. The reaction was allowed to stir at room temperature overnight. Upon reaction completion the suspension was filtered through a sintered frit and washed with acetone. The filtrate was concentrated to a residue which was submitted to the next step without further purification **240** (*quant*).

LR-ESI-MS: $C_{14}H_{19}N_4O_3$ $[M+H]^+$ *m/z* found 291.20, cald 291.15.

2-((2-isopropylpyrrolidin-1-yl)methyl)-5-nitro-1H-benzo[d]imidazole (241)

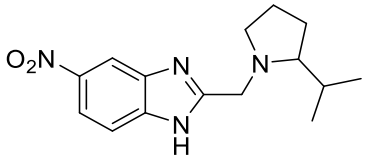

Initially a suspension of 2-(chloromethyl)-5-nitro-1H-benzo[d]imidazole **208** (0.5 g, 2.36 mmol, 1 eq) and Na_2CO_3 (0.301 g, 2.84 mmol, 2.5 eq) in anhydrous MeCN (7.2 mL, 0.33 M) had 2-isopropylpyrrolidine (0.321 g, 2.84 mmol, 1.2 eq) added at room temperature. The reaction was allowed to stir at room temperature overnight. Upon reaction completion the suspension was filtered through a sintered frit and washed with acetone. The filtrate was concentrated to a residue which was submitted to the next step without further purification **241** (*quant*).

LR-ESI-MS: $C_{15}H_{21}N_4O_2$ $[M+H]^+$ *m/z* found 289.23, cald 289.17.

5-nitro-2-((2-phenylpyrrolidin-1-yl)methyl)-1H-benzo[d]imidazole (242)

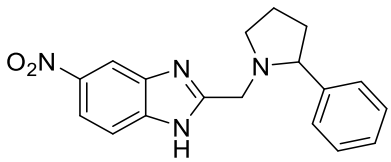

Initially a suspension of 2-(chloromethyl)-5-nitro-1H-benzo[d]imidazole **208** (1 g, 4.73 mmol, 1 eq) and Na_2CO_3 (0.601 g, 5.67 mmol, 2.5 eq) in anhydrous MeCN (14 mL, 0.33 M) had 2-phenylpyrrolidine (0.835 g, 5.67 mmol, 1.2 eq) added at room temperature. The reaction was allowed to stir at room temperature overnight. Upon reaction completion the suspension was filtered through a sintered frit and washed with acetone. The filtrate was concentrated to a residue which was submitted to the next step without further purification **242** (*quant*).

LR-ESI-MS: $C_{18}H_{19}N_4O_2$ $[M+H]^+$ *m/z* found 323.46, cald 323.15.

General Procedure A: Reduction of nitro-benzimidazoles to anilino-benzimidazoles under hydrogenative conditions

A stirred degassed solution of nitro-benzimidazole (1 eq) and Pd (10% on Carbon, 10% mass) in MeOH (0.15 M) was carefully evacuated and backfilled with H_2 atmosphere (1 bar) and finally

allowed to stir at room temperature overnight with a H_2 balloon attached. Upon reaction completion the suspension was filtered through celite with MeOH washings. The filtrate was then concentrated to an oil before being purified via Biotage LPLC using a KP-Sil-NH column eluting with mixtures of CH:EA (10% MeOH) to give the corresponding anilines or purified using an SC-X ion exchange column eluting with mixtures of MeOH and NH_3 in MeOH to give anilines which were submitted to the next step without further purification.

2-(piperidin-1-ylmethyl)-1H-benzo[d]imidazol-5-amine (243)

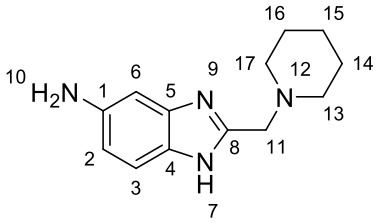

Synthesised according to general procedure **A** to give **243** (1.511 g, 6.56 mmol, 83%) as a brown crystalline solid.

Mpt: 74.1-76.1 °C; **ν_{max} (cm^{-1})** 2931, 1632, 1428, 1336, 1105, 805, 624, 432; **^{1}H NMR (400 MHz, DMSO-d_6) δ**7.2 (d, *J* = 8.5 Hz, 1H, 3), 6.6 (d, *J* = 2.1 Hz, 1H, 6), 6.5 (dd, *J* = 2.1, 8.5 Hz, 1H, 2), 3.6 (s, 2H, 11), 2.4 (d, *J* = 5.5 Hz, 4H, 13, 17), 1.5 (q, *J* = 5.6 Hz, 4H, 14, 16), 1.4 – 1.3 (m, 2H, 15); **^{13}C NMR (101 MHz, DMSO-d_6) δ**148.9 (1), 144.2 (3), 110.9 (2, 6), 56.4 (11), 54.0 (13, 17), 25.3 (14, 16), 23.6 (15); **LR-ESI-MS**: $C_{13}H_{19}N_4$ $[M+H]^+$ *m/z* found 231.21, cald 231.16; **HR-ESI-MS**: $C_{13}H_{19}N_4$ $[M+H]^+$ *m/z* found 231.1602, cald 231.1610.

2-((2-methylpiperidin-1-yl)methyl)-1H-benzo[d]imidazol-5-amine (244)

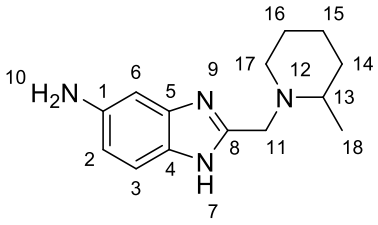

Synthesised according to general procedure **A** to give **244** (0.120 g, 0.492 mmol, 72%) as an off white solid.

Mpt: 94.0-96.0 °C; **ν_{max} (cm^{-1})** 2926, 2852, 1590, 1426, 1328, 1133, 1054, 804, 729; **^{1}H NMR (400 MHz, DMSO-d_6) δ**7.1 (d, *J* = 8.4 Hz, 1H, 3), 6.6 (d, *J* = 2.0 Hz, 1H, 6), 6.4 (dd, *J* = 2.1, 8.5 Hz, 1H, 2), 3.9 (d, *J* = 14.3 Hz, 1H, 11''), 3.5 (d, *J* = 14.3 Hz, 1H, 11'), 2.7 (dt, *J* = 4.0, 11.8 Hz, 1H, 13), 2.4 – 2.3 (m, 1H, 17'), 2.1 (td, *J* = 3.2, 11.1 Hz, 1H, 17''), 1.6 (dd, *J* = 2.7, 9.1 Hz, 2H, 14', 16'), 1.5 – 1.3 (m, 2H, 14'', 16''), 1.2 (dtd, *J* = 1.9, 6.3, 7.4, 17.1 Hz, 2H, 15), 1.1 (d, *J* = 6.2 Hz, 3H, 18); **^{13}C NMR (101 MHz, DMSO-d_6) δ**149.6 (30), 144.1 (2), 110.7 (6), 55.7 (11), 52.5 (13), 51.8 (17), 34.1 (14), 25.5 (16), 23.5 (15), 19.0 (18); **LR-ESI-MS**: $C_{14}H_{21}N_4$ $[M+H]^+$ *m/z* found 245.35, cald 245.18; **HR-ESI-MS**: $C_{14}H_{20}N_4Na$ $[M+Na]^+$ *m/z* found 267.1571, cald 267.1586.

2-((3-methylpiperidin-1-yl)methyl)-1H-benzo[d]imidazol-5-amine (245)

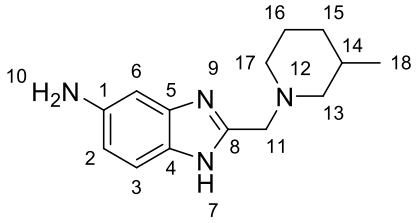

Synthesised according to general procedure **A** to give **245** (0.11 g, 0.450 mmol, 75%) as an off white solid.

Mpt: 75.5-77.5 °C; **ν_{max} (cm^{-1})** 2924, 1633, 1339, 1168, 804, 622; **^{1}H NMR (400 MHz, DMSO-d_6) δ**7.1 (d, *J* = 8.4 Hz, 1H), 6.6 (d, *J* = 2.0 Hz, 1H), 6.4 (dd, *J* = 2.1, 8.5 Hz, 1H), 3.6 – 3.5 (m, 2H, 11), 2.8 – 2.7 (m, 2H, 13'', 17'), 1.9 (td, *J* = 2.9, 11.4 Hz, 1H, 13'), 1.7 – 1.4 (m, 5H, 15, 16, 17''), 0.8 (d, *J* = 5.8 Hz, 4H, 14, 18); **^{13}C NMR (101 MHz, DMSO-d_6) δ**144.1 (3), 110.7 (2, 6), 61.4 (11), 56.4 (13), 53.6 (17), 32.4 (16), 30.6 (15), 25.0 (14), 19.6 (18); **LR-ESI-MS**: $C_{14}H_{21}N_4$ $[M+H]^+$ *m/z* found 245.34, cald 245.18; **HR-ESI-MS**: $C_{14}H_{20}N_4Na$ $[M+Na]^+$ *m/z* found 267.1574, cald 267.1586.

2-((4-methylpiperidin-1-yl)methyl)-1H-benzo[d]imidazol-5-amine (246)

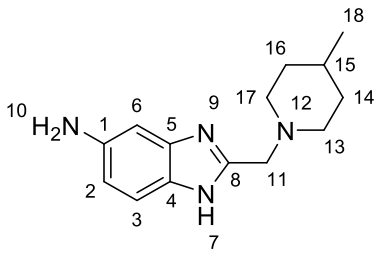

Synthesised according to general procedure **A** to give **246** (0.0492 g, 0.201 mmol, 58%) as an off white solid.

Mpt: 74.6-76.6 °C; **ν_{max} (cm^{-1})** 2916, 1632, 1332, 1254, 1112, 804, 624; **^{1}H NMR (400 MHz, DMSO-d_6) δ**7.1 (d, *J* = 8.4 Hz, 1H), 6.6 (d, *J* = 2.2 Hz, 1H), 6.4 (dd, *J* = 2.1, 8.5 Hz, 1H), 3.6 (s, 2H, 11), 2.8 (dt, *J* = 3.3, 11.8 Hz, 2H, 13'', 17''), 2.0 (td, *J* = 2.4, 11.6 Hz, 2H, 13', 17'), 1.6 – 1.5 (m, 2H, 14'', 16''), 1.3 (tdd, *J* = 4.0, 7.0, 9.9 Hz, 1H, 15), 1.2 – 1.1 (m, 2H, 14', 16'), 0.9 (d, *J* = 6.5 Hz, 3H, 18); **^{13}C NMR (101 MHz, DMSO-d_6) δ**144.1 (3), 110.7 (2, 6), 56.3 (11), 53.5 (13, 17), 33.8 (14, 16), 30.1 (15), 21.9 (18); **LR-ESI-MS**: $C_{14}H_{21}N_4$ $[M+H]^+$ *m/z* found 245.36, cald 245.18; **HR-ESI-MS**: $C_{14}H_{21}N_4$ $[M+H]^+$ *m/z* found 245.1756, cald 245.1766.

2-((1,2,4,5-tetrahydro-3H-benzo[d]azepin-3-yl)methyl)-1H-benzo[d]imidazol-5-amine (247)

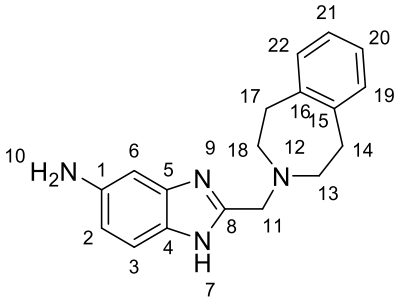

Synthesised according to general procedure **A** to give **247** (0.413 g, 1.413 mmol, 42%) as an orange foam.

Mpt: 111.8-113.8 °C; **ν_{max} (cm^{-1})** 2905, 2810, 1632, 1426, 749; **^{1}H NMR (400 MHz, DMSO-d_6) δ**11.8 (d, *J* = 44.5 Hz, 1H, 7), 7.2 (d, *J* = 8.5 Hz, 1H, 3), 7.1 (d, *J* = 1.7 Hz, 5H, 19, 20, 21, 22), 6.8 – 6.6 (m, 1H, 6), 6.4 (dd, *J* = 2.1, 8.5 Hz, 1H, 2), 4.7 (d, *J* = 76.3 Hz, 2H, 10), 3.8 (d, *J* = 36.9 Hz, 2H, 11), 2.9 (dd, *J* = 3.5, 6.6 Hz, 4H, 13, 18), 2.7 – 2.5 (m, 5H, 14, 17); **^{13}C NMR (101 MHz, DMSO-d_6) δ**149.0 (8), 144.4 (1), 141.9 (15, 16), 135.7 (5), 135.3 (4), 128.7 (20, 21), 126.1 (19, 22), 118.4 (3), 110.5 (2), 94.7 (6), 56.4 (11), 55.1 (13, 18), 35.7 (14, 17); **LR-ESI-MS**: $C_{18}H_{21}N_4$ $[M+H]^+$ *m/z* found 293.47, cald 293.18; **HR-ESI-MS**: $C_{18}H_{20}N_4Na$ $[M+Na]^+$ *m/z* found 315.1573, cald 315.1586.

2-((4-phenylpiperazin-1-yl)methyl)-1H-benzo[d]imidazol-5-amine (248)

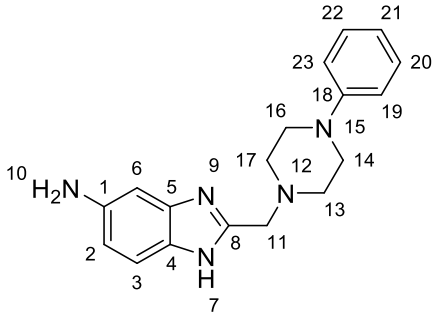

Synthesised according to general procedure **A** to give **248** (0.411 g, 1.337 mmol, 63%) as an orange solid.

Mpt: 117.2-119.2 °C; **ν_{max} (cm^{-1})** 2815, 1632, 1597, 1493, 1449, 1427, 1339, 1221, 1002, 807, 756, 690; **^{1}H NMR (400 MHz, DMSO-d_6) δ**11.7 (s, 1H, 7), 7.3 – 7.1 (m, 3H, 3, 20, 22), 7.0 – 6.8 (m, 2H, 19, 23), 6.8 (td, *J* = 1.1, 7.2 Hz, 1H, 21), 6.6 (d, *J* = 2.1 Hz, 1H, 6), 6.4 (dd, *J* = 2.1, 8.5 Hz, 1H, 2), 4.7 (s, 2H), 3.6 (s, 2H, 11), 3.1 (dd, *J* = 3.6, 6.4 Hz, 4H, 13, 17), 2.6 (t, *J* = 4.9 Hz, 4H, 14, 16); **^{13}C NMR (101 MHz, DMSO-d_6) δ**151.0 (8), 148.3 (1), 144.5 (18), 135.8 (5), 135.3 (4), 128.9 (20, 22), 118.8 (21), 118.4 (3), 115.4, 110.6 (6), 94.7 (2), 55.9 (11), 52.8 (13, 17), 48.1 (14, 16); **LR-ESI-MS**: $C_{18}H_{22}N_5$ $[M+H]^+$ *m/z* found 308.32, cald 308.19; **HR-ESI-MS**: $C_{18}H_{22}N_5$ $[M+H]^+$ *m/z* found 308.1860, cald 308.1875.

2-((4-(2-(pyrrolidin-1-yl)ethyl)piperidin-1-yl)methyl)-1H-benzo[d]imidazol-5-amine (249)

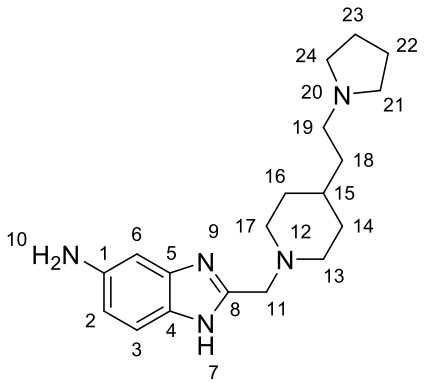

Synthesised according to general procedure **A** to give **249** (0.158 g, 0.482 mmol, 71%) as an orange solid which was purified using an SC-X ion exchange column and submitted to the next step without further purification.

LR-ESI-MS: $C_{19}H_{30}N_5$ $[M+H]^+$ *m/z* found 328.61, cald 328.25.

2-((4-(2-(piperidin-1-yl)ethyl)piperidin-1-yl)methyl)-1H-benzo[d]imidazol-5-amine (250)

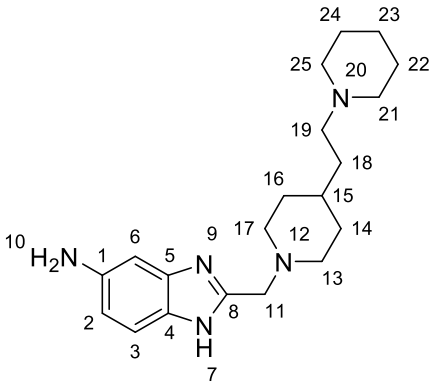

Synthesised according to general procedure **A** to give **250** (0.194 g, 0.568 mmol, 36%) which was purified using an SC-X ion exchange column and submitted to the next step without further purification.

LR-ESI-MS: $C_{20}H_{32}N_5$ $[M+H]^+$ *m/z* found 343.63, cald 342.27.

2-((cis-2,6-dimethylpiperidin-1-yl)methyl)-1H-benzo[d]imidazol-5-amine (251)

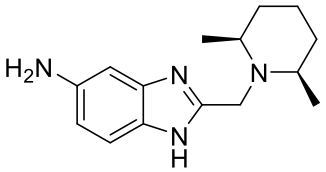

Synthesised according to general procedure **A** to give **251** (0.149 g, 0.578 mmol, 33%) as an orange solid which was purified using an SC-X ion exchange column and submitted to the next step without further purification.

LR-ESI-MS: $C_{15}H_{23}N_4$ $[M+H]^+$ *m/z* found 259.47, cald 259.19.

2-((4-methylpiperazin-1-yl)methyl)-1H-benzo[d]imidazol-5-amine (252)

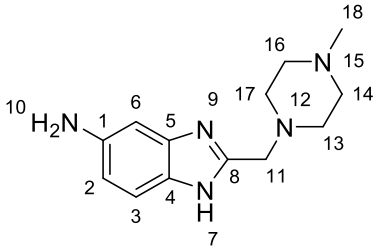

Synthesised according to general procedure **A** to give **252** (0.243 g, 0.991 mmol, 64%) as an off white solid.

Mpt: 64.8-66.8 °C; **ν_{max} (cm^{-1})** 2798, 1631, 1452, 1429, 1343, 1161, 1135, 816, 622; **^{1}H NMR (400 MHz, DMSO-d_6) δ**11.7 (d, *J* = 44.0 Hz, 1H, 7), 7.1 (dd, *J* = 8.4, 35.7 Hz, 1H, 3), 6.7 – 6.5 (m, 1H, 6), 6.5 – 6.4 (m, 1H, 2), 4.7 (d, *J* = 78.0 Hz, 2H, 10), 3.6 (d, *J* = 8.2 Hz, 2H, 11), 2.5 – 2.2 (m, 8H, 13, 14, 16, 17), 2.1 (d, *J* = 2.5 Hz, 3H, 18); **^{13}C NMR (101 MHz, DMSO-d_6) δ**148.5 (8), 144.4 (1), 135.7 (5), 135.2 (4), 118.4 (3), 110.5 (2), 94.7 (6), 55.9 (d, *J* = 9.1 Hz, 11), 54.6 (13, 17), 52.8 (14, 16), 45.8 (18); **LR-ESI-MS**: $C_{13}H_{20}N_5$ $[M+H]^+$ *m/z* found 246.44, cald 246.17; **HR-ESI-MS**: $C_{13}H_{19}N_5Na$ $[M+Na]^+$ *m/z* found 268.1528, cald 268.1538.

2-((dimethylamino)methyl)-1H-benzo[d]imidazol-5-amine (253)

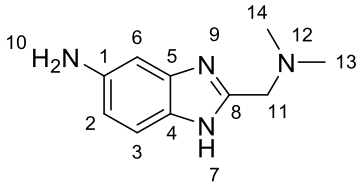

Synthesised according to general procedure **A** to give **253** (0.129 g, 0.678 mmol, 20%) as a red oil.

ν_{max} (cm^{-1}) 2773, 1632, 1435, 1345, 1170, 805, 622; **^{1}H NMR (400 MHz, DMSO-d_6) δ**11.9 – 11.6 (m, 1H, 7), 7.3 – 7.0 (m, 1H, 3), 6.8 – 6.5 (m, 1H, 6), 6.5 – 6.3 (m, 1H, 2), 5.0 – 4.5 (m, 2H, 10), 3.6 – 3.4 (m, 2H, 11), 2.2 (s, 6H, 13, 14); **^{13}C NMR (101 MHz, DMSO-d_6) δ**149.6 (8), 144.8 (1), 136.2 (5), 135.7 (4), 118.8 (3), 110.9 (2), 95.2 (6), 57.6 (11), 45.6 (13, 14); **LR-ESI-MS**: $C_{10}H_{15}N_4$ $[M+H]^+$ *m/z* found 191.35, cald 191.13; **HR-ESI-MS**: $C_{10}H_{14}N_4Na$ $[M+Na]^+$ *m/z* found 213.1108, cald 213.1116.

2-((cis-3,5-dimethylpiperidin-1-yl)methyl)-1H-benzo[d]imidazol-5-amine (254)

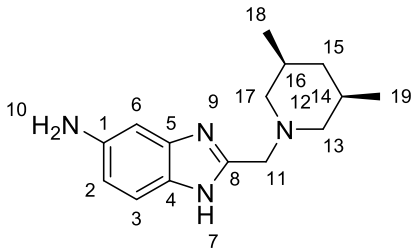

Synthesised according to general procedure **A** to give **254** (0.553 g, 2.14 mmol, 62%) as an off white solid.

Mpt: 92.5-94.5 °C; **ν_{max} (cm^{-1})** 2794, 1631, 1426, 1342, 1162, 804; **^{1}H NMR (400 MHz, DMSO-d_6) δ**7.1 (d, *J* = 8.5 Hz, 1H, 3), 6.6 (d, *J* = 2.1 Hz, 1H, 6), 6.4 (dd, *J* = 2.1, 8.4 Hz, 1H, 2), 3.6 (s, 2H, 11'), 2.8 – 2.7 (m, 2H, 13'', 17''), 1.6 (tdq, *J* = 2.7, 3.4, 6.7, 10.1 Hz, 3H, 13', 15'', 17'), 1.5 (t, *J* = 10.8 Hz, 2H, 14, 16), 0.8 (d, *J* = 6.3 Hz, 6H, 18, 19), 0.5 (td, *J* = 11.4, 13.1 Hz, 1H, 15'); **^{13}C NMR (101 MHz, DMSO-d_6) δ**149.2 (3), 144.2 (6), 110.8 (2), 61.0 (13, 17), 56.1 (11), 41.6 (15), 30.5 (14, 16), 19.5 (18, 19); **LR-ESI-MS**: $C_{15}H_{23}N_4$ $[M+H]^+$ *m/z* found 259.47, cald 259.19; **HR-ESI-MS**: $C_{15}H_{22}N_4Na$ $[M+Na]^+$ *m/z* found 281.1732, cald 281.1742.

2-(1-(piperidin-1-yl)ethyl)-1H-benzo[d]imidazol-5-amine (255)

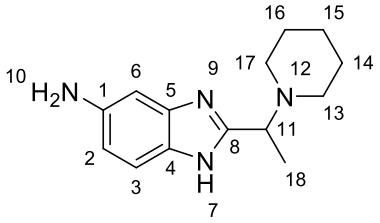

Synthesised according to general procedure **A** to give **255** (0.314 g, 1.29 mmol, 88%) as a white solid.

Mpt: 108.8-110.8 °C; **ν_{max} (cm^{-1})** 2923, 1633, 1452, 1308, 1220, 1166, 1056, 623; **^{1}H NMR (400 MHz, DMSO-d_6) δ**11.5 (d, *J* = 43.0 Hz, 1H, 7), 7.1 (dd, *J* = 8.4, 35.2 Hz, 1H, 6), 6.8 – 6.6 (m, 1H, 2), 6.5 – 6.3 (m, 1H, 3), 4.9 – 4.5 (m, 2H, 10), 3.7 (q, *J* = 6.8 Hz, 1H, 11), 2.4 (t, *J* = 5.4 Hz, 4H, 13, 17), 1.5 (p, *J* = 5.5 Hz, 4H, 14, 16), 1.3 (t, *J* = 7.4 Hz, 5H, 15, 18); **^{13}C NMR (101 MHz, DMSO-d_6) δ**152.5 (8), 144.2 (1), 135.5 (5), 135.1 (4), 118.4 (3), 110.3 (2), 94.8 (6), 64.9 (11), 58.5 (13), 50.2 (17), 25.8 (14, 16), 24.2 (15), 14.6 (18); **LR-ESI-MS**: $C_{14}H_{21}N_4$ $[M+H]^+$ *m/z* found 245.39, cald 245.18; **HR-ESI-MS**: $C_{14}H_{20}N_4Na$ $[M+Na]^+$ *m/z* found 267.1578, cald 267.1586.

2-(2-(piperidin-1-yl)ethyl)-1H-benzo[d]imidazol-5-amine (256)

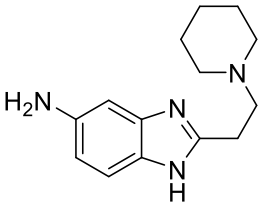

Synthesised according to general procedure **A** to give **256** (0.018 g, 0.074 mmol, 20%) as an unstable solid which was immediately used in the following step.

LR-ESI-MS: $C_{14}H_{21}N_4$ $[M+H]^+$ *m/z* found 245.43, cald 245.18.

(*R*)-2-((2-methylpyrrolidin-1-yl)methyl)-1H-benzo[d]imidazol-5-amine (257)

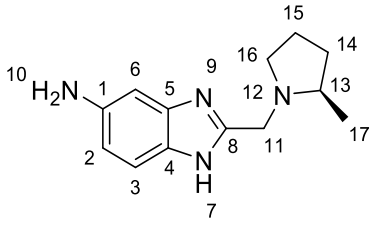

Synthesised according to general procedure **A** to give **257** (0.298 g, 1.297 mmol, 46%) as a dark green solid.

Mpt: 92.4-94.4 °C; **ν_{max} (cm^{-1})** 2958, 2794, 1632, 1426, 1165, 803, 622; **^{1}H NMR (400 MHz, DMSO-d_6) δ**11.7 (d, *J* = 44.8 Hz, 1H), 7.1 (dd, *J* = 8.5, 34.7 Hz, 1H, 3), 6.8 – 6.5 (m, 1H, 6), 6.5 – 6.4 (m, 1H, 2), 4.8 (s, 2H, 10), 3.9 (d, *J* = 13.9 Hz, 1H, 11''), 3.4 (d, *J* = 13.8 Hz, 1H, 11'), 2.9 (td, *J* = 3.2, 7.8, 8.6 Hz, 1H, 16''), 2.4 (q, *J* = 7.0 Hz, 1H, 16'), 2.2 (q, *J* = 8.8 Hz, 1H, 13), 1.9 (dddd, *J* = 5.7, 7.3, 9.4, 12.5 Hz, 1H, 14''), 1.7 – 1.5 (m, 2H, 14', 15''), 1.4 – 1.2 (m, 1H, 15'), 1.1 (d, *J* = 6.0 Hz, 3H, 17); **^{13}C NMR (101 MHz, DMSO-d_6) δ**149.7 (1), 144.3 (8), 135.7 (5), 135.3 (4), 118.3 (3), 110.4 (2), 94.8 (6), 58.8 (11), 54.0 (16), 50.9 (13), 32.5 (14), 21.3 (15), 18.9 (17); **LR-ESI-MS**: $C_{13}H_{19}N_4$ $[M+H]^+$ *m/z* found 231.30, cald 231.16; **HR-ESI-MS**: $C_{13}H_{18}N_4Na$ $[M+Na]^+$ *m/z* found 253.1429, cald 253.1418.

2-((3-methylpyrrolidin-1-yl)methyl)-1H-benzo[d]imidazol-5-amine (258)

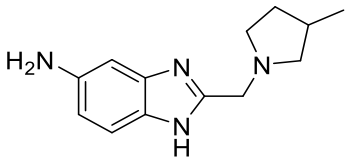

Synthesised according to general procedure **A** to give **258** (0.027 g, 0.117 mmol, 74%) as a yellow oil which was purified using an SC-X ion exchange column and submitted to the next step without further purification.

LR-ESI-MS: $C_{13}H_{19}N_4$ $[M+H]^+$ *m/z* found 231.39, cald 231.16.

2-(((3*R*, 4*R*)-3,4-dimethylpyrrolidin-1-yl)methyl)-1H-benzo[d]imidazol-5-amine (259)

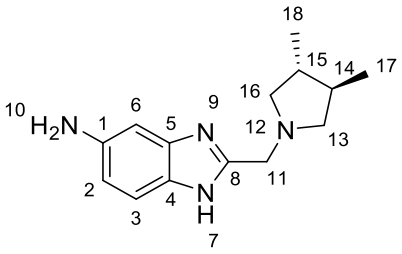

Synthesised according to general procedure **A** to give **259** (0.186 g, 0.762 mmol, 54%) as a yellow oil.

ν_{max} (cm^{-1}) 2951, 1633, 1450, 1427, 1169, 804, 623; **^{1}H NMR (400 MHz, DMSO-d_6) δ**11.9 – 11.5 (m, 1H, 7), 7.2 – 7.0 (m, 1H, 6), 6.8 – 6.5 (m, 1H, 3), 6.5 – 6.4 (m, 1H, 2), 4.8 (s, 2H, 10), 3.8 – 3.6 (m, 2H, 11), 2.8 (dd, *J* = 6.9, 8.8 Hz, 2H, 13'', 16'), 2.2 (dd, *J* = 6.6, 8.9 Hz, 2H, 13', 16''), 1.7 – 1.6 (m, 2H, 14, 15), 1.0 – 0.9 (m, 6H, 17, 18); **^{13}C NMR (101 MHz, DMSO-d_6) δ**149.5 (8), 144.3 (1), 135.7 (5), 135.2 (4), 118.4 (3), 110.5 (2), 94.8 (6), 61.7 (13, 16), 53.6 (11), 40.4 (14, 15), 18.4 (17, 18); **LR-ESI-MS**: $C_{14}H_{21}N_4$ $[M+H]^+$ *m/z* found 245.39, cald 245.18; **HR-ESI-MS**: $C_{14}H_{20}N_4Na$ $[M+Na]^+$ *m/z* found 267.1575, cald 267.1586.

2-((2-methylpyrrolidin-1-yl)methyl)-1H-benzo[d]imidazol-5-amine (260)

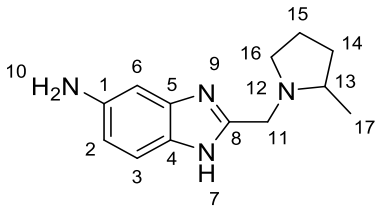

Synthesised according to general procedure **A** to give **260** (0.264 g, 1.15 mmol, 78%) as a brown oil.

ν_{max} (cm^{-1}) 2958, 2793, 1632, 1426, 1165, 804, 622; **^{1}H NMR (400 MHz, DMSO-d_6) δ**11.7 (s, 1H, 7), 7.2 (d, *J* = 8.4 Hz, 1H, 6), 6.6 (s, 1H, 3), 6.5 (d, *J* = 8.6 Hz, 1H, 2), 5.2 – 4.4 (m, 2H, 10), 3.9 (d, *J* = 13.9 Hz, 1H, 11''), 3.4 – 3.3 (m, 1H, 11'), 2.9 (ddd, *J* = 3.1, 7.7, 9.9 Hz, 1H, 13), 2.5 – 2.3 (m, 1H, 16'), 2.2 (q, *J* = 8.8 Hz, 1H, 16''), 1.9 (dddd, *J* = 3.5, 5.2, 9.4, 12.5 Hz, 1H, 14''), 1.7 – 1.5 (m, 2H, 14', 15''), 1.3 (dddd, *J* = 6.2, 8.4, 10.1, 12.2 Hz, 1H, 15'), 1.1 (d, *J* = 6.0 Hz, 3H, 17); **^{13}C NMR (101 MHz, DMSO-d_6) δ**149.8 (8), 144.3 (1), 135.7 (5), 135.3 (4), 118.3 (3), 110.5 (2), 94.9 (6), 58.9 (11),

54.0 (13), 50.9 (16), 32.6 (14), 21.4 (15), 18.9 (17); **LR-ESI-MS**: $C_{13}H_{19}N_4$ $[M+H]^+$ *m/z* found 231.40, calds 231.16; **HR-ESI-MS**: $C_{13}H_{18}N_4Na$ $[M+Na]^+$ *m/z* found 253.1419, cald 253.1429.

(*R*)-2-((3-methylpyrrolidin-1-yl)methyl)-1H-benzo[d]imidazol-5-amine (261)

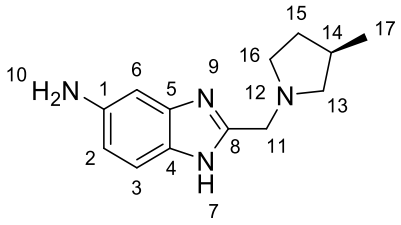

Synthesised according to general procedure **A** to give **261** (0.233 g, 1.01 mmol, 66%) as an off white solid.

Mpt: 143.2-145.2 °C; **ν_{max} (cm^{-1})** 2784, 1629, 1427, 1024, 798, 622; **^{1}H NMR (400 MHz, DMSO-d_6)** **δ**11.7 (s, 1H, 7), 7.2 (d, *J* = 8.4 Hz, 1H, 3), 6.7 – 6.5 (m, 1H, 6), 6.4 (dd, *J* = 2.1, 8.5 Hz, 1H, 2), 4.8 (s, 2H, 10), 3.9 – 3.5 (m, 2H, 11''), 2.9 – 2.7 (m, 1H, 13''), 2.6 (td, *J* = 5.7, 8.4 Hz, 1H, 16'), 2.5 (s, 1H, 16''), 2.3 – 2.1 (m, 1H, 13'), 2.1 – 1.9 (m, 2H, 15), 1.4 – 1.2 (m, 1H, 14), 1.0 (d, *J* = 6.7 Hz, 3H, 17); **^{13}C NMR (101 MHz, DMSO-d_6)** **δ**149.5 (8), 144.3 (1), 135.7 (5), 135.2 (4), 118.3 (3), 110.4 (2), 94.7 (6), 61.7 (11), 53.6 (13), 53.4 (16), 32.4 (15), 31.5 (14), 20.4 (17); **LR-ESI-MS**: $C_{13}H_{19}N_4$ $[M+H]^+$ *m/z* found 231.40, cald 231.16; **HR-ESI-MS**: $C_{13}H_{18}N_4Na$ $[M+Na]^+$ *m/z* found 253.1421, cald 253.1429.

(*S*)-2-((3-methylpyrrolidin-1-yl)methyl)-1H-benzo[d]imidazol-5-amine (262)

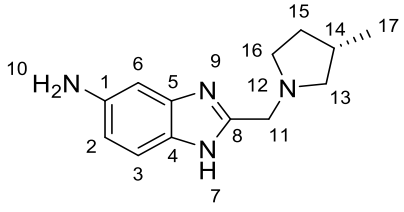

Synthesised according to general procedure **A** to give **262** (0.061 g, 0.263 mmol, 23%) as a tan oil.

ν_{max} (cm^{-1}) 2952, 1632, 1428, 805, 625; **^{1}H NMR (400 MHz, DMSO-d_6)** **δ**11.9 – 11.4 (m, 1H), 7.3 – 6.9 (m, 1H, 6), 6.8 – 6.5 (m, 1H, 3), 6.5 – 6.4 (m, 1H, 2), 4.8 (s, 2H, 10), 3.7 (s, 2H, 11'), 2.8 (dd, *J* = 7.3, 8.8 Hz, 1H, 13'), 2.6 (td, *J* = 5.8, 8.4 Hz, 1H, 16'), 2.5 – 2.4 (m, 1H, 13''), 2.2 (ddt, *J* = 6.7, 9.1,

13.5 Hz, 1H, 16''), 2.0 (dd, *J* = 6.9, 8.8 Hz, 1H, 15'), 2.0 – 1.9 (m, 1H, 14), 1.3 (ddt, *J* = 6.0, 8.4, 12.2 Hz, 1H, 15''), 1.0 (d, *J* = 6.7 Hz, 3H, 17); **^{13}C NMR (101 MHz, DMSO-d_6) δ**149.5 (8), 144.3 (1), 135.7 (5), 135.2 (4), 118.3 (3), 110.5 (2), 94.8 (6), 61.7 (13), 53.6 (16), 53.4 (11), 32.4 (14), 31.5 (15), 20.4 (17); **LR-ESI-MS**: $C_{13}H_{19}N_4$ $[M+H]^+$ *m/z* found 231.27, cald 231.16; **HR-ESI-MS**: $C_{13}H_{19}N_4$ $[M+H]^+$ *m/z* found 231.1602, cald 231.1610.

2-((3-azabicyclo[3.1.0]hexan-3-yl)methyl)-1H-benzo[d]imidazol-5-amine (263)

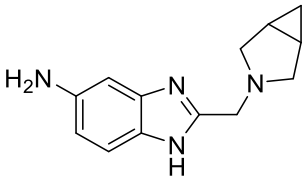

Synthesised according to general procedure **A** to give **263** (0.464 g, 2.03 mmol, 29%) as a tan solid which was purified using an SC-X ion exchange column and submitted to the next step without further purification.

LR-ESI-MS: $C_{13}H_{17}N_4$ $[M+H]^+$ *m/z* found 229.35, cald 229.15.

2-((3,3-difluoropyrrolidin-1-yl)methyl)-1H-benzo[d]imidazol-5-amine (264)

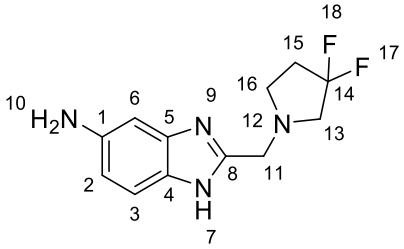

Synthesised according to general procedure **A** to give **264** (0.257 g, 1.02 mmol, 35%) as a brown solid which was purified using an SC-X ion exchange column and submitted to the next step without further purification.

LR-ESI-MS: $C_{12}H_{15}F_2N_4$ $[M+H]^+$ *m/z* found 253.32, cald 253.13.

(*S*)-2-((2-methylpyrrolidin-1-yl)methyl)-1H-benzo[d]imidazol-5-amine (265)

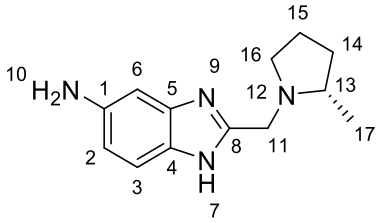

Synthesised according to general procedure **A** to give **265** (0.320 g, 1.39 mmol, 20%) as a beige solid which was purified using an SC-X ion exchange column and submitted to the next step without further purification.

LR-ESI-MS: $C_{13}H_{19}N_4$ $[M+H]^+$ *m/z* found 231.35, cald 231.16.

2-((3-methylpyrrolidin-1-yl)methyl)-1H-benzo[d]imidazol-5-amine (266)

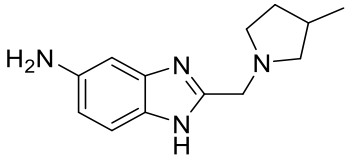

Synthesised according to general procedure **A** to give **266** (0.270 g, 1.17 mmol, 17%) as a tan solid which was purified using an SC-X ion exchange column and submitted to the next step without further purification.

LR-ESI-MS: $C_{13}H_{19}N_4$ $[M+H]^+$ *m/z* found 231.34, cald 231.16.

2-((2,2-dimethylpyrrolidin-1-yl)methyl)-1H-benzo[d]imidazol-5-amine (267)

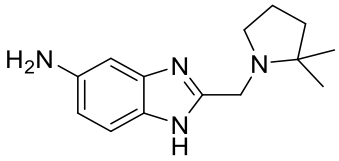

Synthesised according to general procedure **A** to give **267** (0.654 g, 2.68 mmol, 44%) as a beige solid which was purified using an SC-X ion exchange column and submitted to the next step without further purification.

LR-ESI-MS: $C_{14}H_{21}N_4$ $[M+H]^+$ *m/z* found 245.43, cald 245.18.

2-((2-ethylpyrrolidin-1-yl)methyl)-1H-benzo[d]imidazol-5-amine (268)

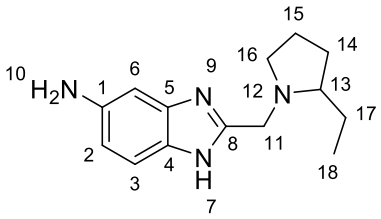

Synthesised according to general procedure **A** to give **268** (0.507 g, 2.08 mmol, 34%) as a tan solid which was purified using an SC-X ion exchange column and submitted to the next step without further purification.

LR-ESI-MS: $C_{14}H_{21}N_4$ $[M+H]^+$ *m/z* found 245.43, cald 245.18.

2-(((1*S*, 4*S*)-2-oxa-5-azabicyclo[2.2.1]heptan-5-yl)methyl)-1H-benzo[d]imidazol-5-amine (269)

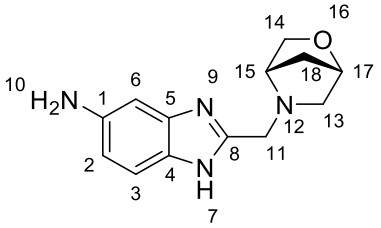

Synthesised according to general procedure **A** to give **269** (0.264 g, 1.08 mmol, 18%) as a yellow solid which was purified using an SC-X ion exchange column and submitted to the next step without further purification.

LR-ESI-MS: $C_{13}H_{17}N_4O$ $[M+H]^+$ *m/z* found 245.39, cald 245.14.

tert-butyl (2-(((5-amino-1H-benzo[d]imidazol-2-yl)methyl)(methyl)amino)ethyl)carbamate (270)

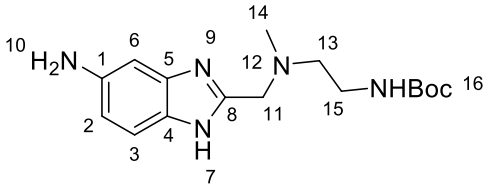

Synthesised according to general procedure **A** to give **270** (0.199 g, 0.622 mmol, 26%) as a dark brown solid.

Mpt: 88.1-90.1 °C; **ν_{max} (cm^{-1})** 3204, 2973, 1687, 1496, 1163, 806, 623; **^{1}H NMR (400 MHz, DMSO-d_6) δ**11.7 (m, 1H, 7), 7.1 (m, 1H, 3), 6.8 (t, *J* = 5.7 Hz, 1H, NHBoc), 6.6 (m, 1H, 2), 6.4 (m, 1H, 6), 4.7 (m, 2H, 10), 3.6 (m, 2H, 11), 3.1 (q, *J* = 6.4 Hz, 2H, 13), 2.4 (t, *J* = 6.7 Hz, 2H, 15), 2.2 (s,

3H, 14), 1.4 (s, 9H, 16); **^{13}C NMR (101 MHz, DMSO-d_6) δ**155.6 (-NHCO$_2$tBu), 149.3 (8), 144.4 (1), 135.6 (5), 135.3 (4), 118.4 (3), 110.4 (2), 94.7 (6), 77.6 (-O-C(CH$_3$)$_3$), 56.4 (11), 55.2 (13), 42.3 (14), 38.0 (15), 28.3 (-O-C(CH$_3$)$_3$); **LR-ESI-MS**: $C_{16}H_{26}N_5O$ $[M+H]^+$ *m/z* found 320.49, cald 320.21; **HR-ESI-MS**: $C_{16}H_{26}N_5O$ $[M+H]^+$ *m/z* found unstable Boc group failed to give identifiable [M], cald 320.2087.

2-((2-(methoxymethyl)pyrrolidin-1-yl)methyl)-1H-benzo[d]imidazol-5-amine (271)

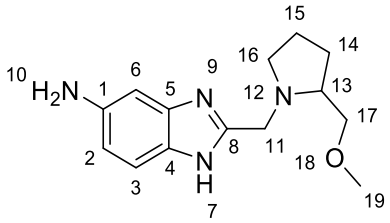

Synthesised according to general procedure **A** to give **271** (0.207 g, 0.795 mmol, 34%) as a black waxy solid.

ν_{max} (cm^{-1}) 3195, 2871, 1632, 1426, 1093, 804, 624; **^{1}H NMR (400 MHz, DMSO-d_6) δ**11.6 (s, 1H, 7), 7.2 – 7.0 (m, 1H, 3), 6.8 – 6.5 (m, 1H, 6), 6.5 – 6.3 (m, 1H, 2), 5.0 – 4.5 (m, 2H, 10), 4.1 – 4.0 (m, 1H, 11''), 3.6 – 3.5 (m, 1H, 11'), 3.4 – 3.3 (m, 1H, 17''), 3.2 (s, 4H, 17', 19), 2.9 (ddd, *J* = 3.6, 5.9, 9.4 Hz, 1H, 13), 2.8 (dt, *J* = 5.8, 8.3 Hz, 1H, 16''), 2.3 (td, *J* = 7.7, 9.1 Hz, 1H, 16'), 1.8 (dq, *J* = 8.2, 12.2 Hz, 1H, 14''), 1.6 (tt, *J* = 5.9, 8.4 Hz, 2H, 14', 15''), 1.6 – 1.4 (m, 1H, 15'); **^{13}C NMR (101 MHz, DMSO-d_6) δ**149.7 (8), 144.3 (1), 135.6 (5), 135.3 (4), 118.3 (3), 110.5 (2), 94.8 (6), 75.8 (17), 62.0 (19), 58.4, 54.3 (13), 52.2 (16), 28.4 (14), 22.6 (15); **LR-ESI-MS**: $C_{14}H_{21}N_4O$ $[M+H]^+$ *m/z* found 261.45, cald 261.17; **HR-ESI-MS**: $C_{14}H_{20}N_4NaO$ $[M+Na]^+$ *m/z* found 283.1528, cald 283.1535.

2-((2-isopropylpyrrolidin-1-yl)methyl)-1H-benzo[d]imidazol-5-amine (272)

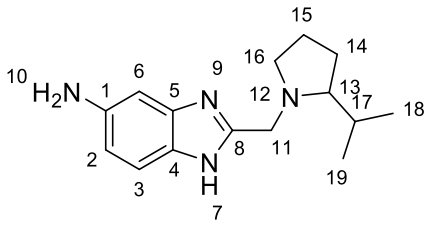

Synthesised according to general procedure **A** to give **272** (0.148 g, 0.576 mmol, 24%) as a tan solid which was purified using an SC-X ion exchange column and submitted to the next step without further purification.

LR-ESI-MS: $C_{15}H_{23}N_4$ $[M+H]^+$ *m/z* found 259.43, cald 259.19.

2-((2-isopropylpyrrolidin-1-yl)methyl)-1H-benzo[d]imidazol-5-amine (273)

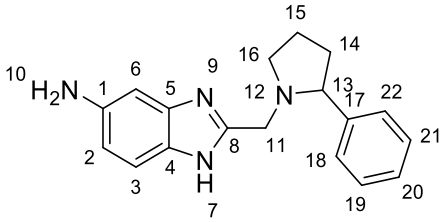

Synthesised according to general procedure **A** to give **273** which was used without further purification (0.148 g, 0.576 mmol, 24%) as a tan foam.

LR-ESI-MS: $C_{18}H_{21}N_4$ $[M+H]^+$ *m/z* found 293.42, cald 293.18.

General Procedure B: Amide Synthesis

To a stirred solution of the corresponding anilines **243**-**273** (1 eq) in CH_2Cl_2 (0.1 M, anhydrous) was added DIPEA-PS (200-400 mesh, 40% loading) (2 eq), the corresponding acid (1.2 eq) and HATU (1.2 eq). The suspension was stirred vigorously for 16 h before being concentrated onto silica gel and purified via Biotage LPLC using a mixture of DCM:DCM (20% MeOH) or CH:EA (10% MeOH). To give the products which were triturated to form solids with Et_2O or CH.

General Procedure C: Sulfonamide/Amide Synthesis

To a stirred solution of the corresponding anilines **243**-**273** (1 eq) in CH_2Cl_2 (0.1 M, anhydrous) was added DIPEA-PS (200-400 mesh, 40% loading) (3 eq) and the corresponding acid/sulfonyl chloride (1.5 eq). The suspension was stirred vigorously for 16 h before being concentrated onto silica gel and purified via Biotage LPLC using a mixture of DCM:DCM (20% MeOH) or CH:EA (10% MeOH). To give the products which were triturated to form solids with Et_2O or CH.

***N*-(2-(piperidin-1-ylmethyl)-1H-benzo[d]imidazol-5-yl)benzenesulfonamide (343)**

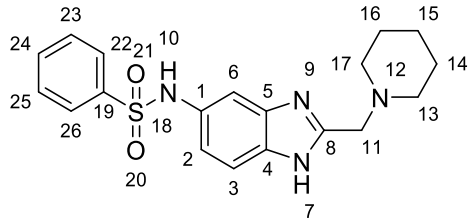

Synthesised according to general procedure **C** to give **343** (0.017 g, 0.045 mmol, 21%) as an off white solid.

Mpt: 154.5-156.5 °C; **ν_{max} (cm^{-1})** 2935, 1625, 1447, 1168, 724, 574; **^{1}H NMR (400 MHz, DMSO-d_6) δ**8.4 – 8.3 (m, 2H, 22, 26), 7.8 – 7.7 (m, 1H, 24), 7.7 – 7.6 (m, 2H, 23, 25), 7.6 (d, *J* = 8.8 Hz, 1H, 3), 6.7 (d, *J* = 2.1 Hz, 1H, 6), 6.7 (dd, *J* = 2.2, 8.8 Hz, 1H, 2), 5.1 (s, 2H, 7, 10), 3.8 (s, 2H, 11), 2.4 (s, 4H, 13, 17), 1.5 – 1.3 (m, 6H, 14, 15, 16); **^{13}C NMR (101 MHz, DMSO-d_6) δ**150.3 (8), 146.7 (5), 142.3 (1), 138.0 (24), 134.8 (19), 129.5 (22, 26), 127.3 (23, 25), 123.8 (3), 113.5 (2), 113.5 (4), 102.8 (6), 55.8 (11), 54.0 (13, 17), 25.2 (14, 16), 23.7 (15); **LR-ESI-MS**: $C_{19}H_{23}N_4O_2S$ $[M+H]^+$ *m/z* found 371.31, cald 371.15; **HR-ESI-MS**: $C_{19}H_{23}N_4O_2S$ $[M+H]^+$ *m/z* found 371.1528, cald 371.1542.

2-methoxy-*N*-(2-(piperidin-1-ylmethyl)-1H-benzo[d]imidazol-5-yl)benzamide (276)

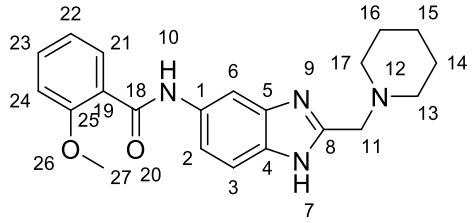

Synthesised according to general procedure **C** to give **276** (0.029 g, 0.080 mmol, 37%) as a yellow solid.

Mpt: 111.7-113.7 °C; **ν_{max} (cm^{-1})** 3356, 2936, 2359, 1661, 1599, 1249, 1020, 755; **^{1}H NMR (400 MHz, DMSO-d_6) δ**12.2 (s, 1H, 10), 10.1 (s, 1H, 7), 8.1 (s, 1H, 21), 7.7 (dd, *J* = 1.9, 7.6 Hz, 1H, 3), 7.6 – 7.1 (m, 4H, 2, 6, 23, 24), 7.1 – 6.9 (m, 1H, 22), 3.9 (s, 3H, 27), 3.6 (s, 2H, 11), 2.4 (t, *J* = 5.4 Hz, 4H, 13, 17), 1.5 (p, *J* = 5.5 Hz, 5H, 14, 16), 1.4 (q, *J* = 5.3, 6.0 Hz, 2H, 15); **^{13}C NMR (101 MHz, DMSO-d_6) δ**156.5 (18), 131.9 (21, 23), 129.7 (5), 120.5 (22), 120.0 (3), 112.3, 112.0 (24), 56.6 (11), 55.9 (27), 54.1 (13, 17), 25.5 (14, 16), 23.8 (15); **LR-ESI-MS**: $C_{21}H_{25}N_4O_2$ $[M+H]^+$ *m/z* found 365.33, cald 365.20; **HR-ESI-MS**: $C_{21}H_{25}N_4O_2$ $[M+H]^+$ *m/z* found 365.1965, cald 365.1978.

***N*-(2-(piperidin-1-ylmethyl)-1H-benzo[d]imidazol-5-yl)-3-(trifluoromethyl)benzamide (286)**

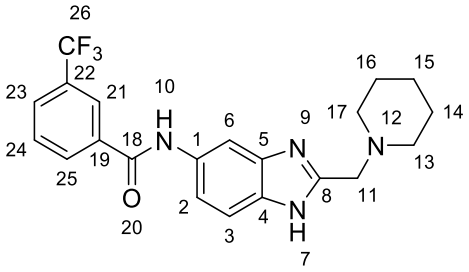

Synthesised according to general procedure **C** to give **286** (0.034 g, 0.084 mmol, 39%) as a white solid.

Mpt: 92.7-94.7 °C; **ν_{max} (cm^{-1})** 2936, 1648, 1329, 1258, 808, 650; **^{19}F NMR (376 MHz, DMSO-d_6) δ**-61.0; **^{1}H NMR (400 MHz, DMSO-d_6) δ**12.3 (s, 1H, 10), 10.5 (s, 1H, 7), 8.4 – 8.1 (m, 2H, 21, 25), 8.1 – 7.9 (m, 2H, 3, 23), 7.8 (t, *J* = 7.8 Hz, 1H, 24), 7.5 (d, *J* = 22.9 Hz, 2H, 2, 6), 3.7 (s, 2H, 11), 2.4 (t, *J* = 5.3 Hz, 4H, 13, 17), 1.5 (p, *J* = 5.5 Hz, 4H, 14, 16), 1.5 – 1.3 (m, 2H, 15); **^{13}C NMR (101 MHz, DMSO-d_6) δ**163.7 (18), 136.1 (22), 131.8 (25), 129.7 (23, 24), 124.2 (3), 56.6 (11), 54.2 (13, 17), 25.4 (14, 16), 23.8 (15); **LR-ESI-MS**: $C_{21}H_{22}F_3N_4O$ $[M+H]^+$ *m/z* found 403.30, cald 403.18; **HR-ESI-MS**: $C_{21}H_{22}F_3N_4O$ $[M+H]^+$ *m/z* found 403.1733, cald 403.1746.

4-chloro-*N*-(2-(piperidin-1-ylmethyl)-1H-benzo[d]imidazol-5-yl)benzamide (289)

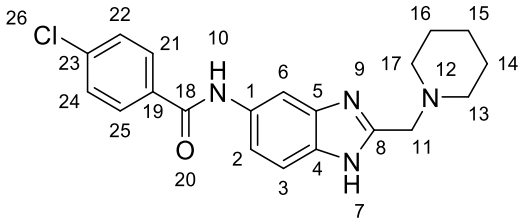

Synthesised according to general procedure **C** to give **289** (0.061 g, 0.166 mmol, 77%) as a white solid.

Mpt: 122.3-124.3 °C; **ν_{max} (cm^{-1})** 2932, 1645, 1593, 1335, 1274, 843, 749; **^{1}H NMR (400 MHz, DMSO-d_6) δ**13.2 (s, 1H, 10), 11.3 (s, 1H, 7), 9.1 – 8.8 (m, 3H, 3, 21, 25), 8.7 – 8.3 (m, 4H, 2, 6, 22, 24), 4.6 (s, 2H, 11), 3.5 (p, *J* = 1.8 Hz, 4H, 13, 17), 3.4 (t, *J* = 5.1 Hz, 4H, 14, 16), 2.4 (q, *J* = 6.0 Hz, 2H, 15); **^{13}C NMR (101 MHz, DMSO-d_6) δ**164.1 (18), 136.2 (23), 133.9 (19), 131.1 (3), 129.6 (21, 25), 128.4 (22, 24), 128.4 (2, 6), 56.6 (11), 54.1 (13, 17), 25.4 (14, 16), 23.8 (15); **LR-ESI-MS**:

$C_{20}H_{22}ClN_4O$ $[M+H]^+$ *m/z* found 369.27, cald 369.15; **HR-ESI-MS**: $C_{20}H_{22}ClN_4O$ $[M+H]^+$ *m/z* found 367.1467, cald 369.1482.

3-fluoro-*N*-(2-(piperidin-1-ylmethyl)-1H-benzo[d]imidazol-5-yl)benzamide (281)

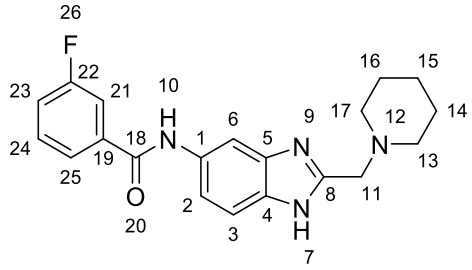

Synthesised according to general procedure **C** to give **281** (0.057 g, 0.163 mmol, 75%) as an off white solid.

Mpt: 108.8-110.8 °C; **ν_{max} (cm^{-1})** 3067, 2934, 1647, 1585, 1536, 1435, 1381, 1218, 768, 744, 665; **^{19}F NMR (376 MHz, DMSO-d_6) δ**-112.7 (td, *J* = 5.9, 9.3 Hz); **^{1}H NMR (400 MHz, DMSO-d_6) δ**12.4 (s, 0H), 10.3 (s, 1H, 10), 8.0 (s, 1H, 7), 7.9 – 7.7 (m, 2H, 21, 23), 7.7 – 7.4 (m, 5H, 2, 3, 6, 24, 25), 3.7 (s, 2H, 11), 2.4 (t, *J* = 5.4 Hz, 4H, 13, 17), 1.5 (p, *J* = 5.5 Hz, 4H, 14, 16), 1.4 (q, *J* = 6.0 Hz, 2H, 15); **^{13}C NMR (101 MHz, DMSO-d_6) δ**163.8 (18), 162.0 (d, J = 244.0 Hz, 22), 152.4 (8), 137.5 (d, J = 6.5 Hz, 19), 130.5 (d, J = 8.2 Hz, 21), 130.4 (d, J = 8.1 Hz, 24), 125.3 (d, J = 2.8 Hz, 23), 123.8 (d, J = 2.8 Hz, 25), 118.4 (5), 118.2 (4, 115.7 (3), 115.5 (1), 114.6 (6), 114.3 (2), 56.6 (11), 54.1 (13, 17), 25.4 (14, 16), 23.7 (15); **LR-ESI-MS**: $C_{20}H_{22}FN_4O$ $[M+H]^+$ *m/z* found 353.36, cald 353.18; **HR-ESI-MS**: $C_{20}H_{22}FN_4O$ $[M+H]^+$ *m/z* found 353.1765, cald 353.1778.

***N*-(2-(piperidin-1-ylmethyl)-1H-benzo[d]imidazol-5-yl)-2-(trifluoromethyl)benzamide (278)**

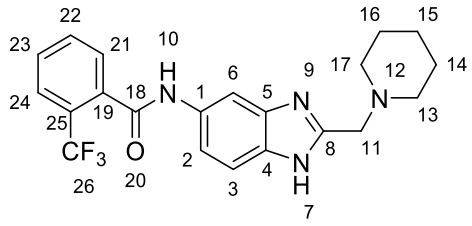

Synthesised according to general procedure **C** to give **278** (0.031 g, 0.076 mmol, 35%) as a white solid.

Mpt: 139.2-141.2 °C; **ν_{max} (cm^{-1})** 2934, 1652, 1532, 1270, 1034, 765; **^{19}F NMR (376 MHz, DMSO-d_6) δ**-57.9 , 27, 28, 29; **^{1}H NMR (400 MHz, DMSO-d_6) δ**12.4 – 12.0 (m, 1H, 7), 10.5 (s, 1H, 10), 8.0 (d, *J* = 43.9 Hz, 1H, 6), 7.9 – 7.8 (m, 1H, 24), 7.8 – 7.8 (m, 1H, 23), 7.7 (tt, *J* = 3.1, 5.2 Hz, 2H, 21, 22), 7.4 (d, *J* = 78.9 Hz, 2H, 2, 3), 3.6 (s, 2H, 11), 2.4 (t, *J* = 5.3 Hz, 4H, 13, 17), 1.5 (p, *J* = 5.6 Hz, 4H, 14, 16), 1.4 (dt, *J* = 4.6, 11.5 Hz, 2H, 15); **^{13}C NMR (101 MHz, DMSO-d_6) δ**165.3 (18), 136.6 (19), 132.6 (25), 129.9 (21), 128.6 (23), 126.3 (q, *J* = 5.0 Hz, 26), 126.0 (24), 125.7 (22), 125.2 (1), 122.5 (2), 56.6 (11), 54.1 (13, 17), 25.5 (14, 16), 23.8 (15); **LR-ESI-MS**: $C_{21}H_{22}F_3N_4O$ $[M+H]^+$ *m/z* found 403.39, cald 403.18; **HR-ESI-MS**: $C_{21}H_{22}F_3N_4O$ $[M+H]^+$ *m/z* found 403.1730, cald 403.1746.

2-chloro-*N*-(2-(piperidin-1-ylmethyl)-1H-benzo[d]imidazol-5-yl)benzamide (275)

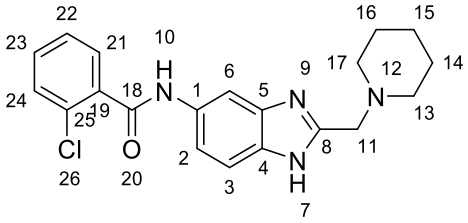

Synthesised according to general procedure **C** to give **275** (0.058 g, 0.156 mmol, 72%) as a white solid.

Mpt: 128.9-130.9 °C; **ν_{max} (cm^{-1})** 2932, 1531, 1450, 1251, 1109,1037, 859, 807, 652; **^{1}H NMR (400 MHz, DMSO-d_6) δ**12.2 (s, 1H, 10), 10.5 (s, 1H, 7), 8.0 (d, *J* = 42.8 Hz, 1H, 21), 7.7 – 7.1 (m, 6H, 2, 3, 6, 22, 23, 24), 3.6 (s, 2H, 11), 2.4 (d, *J* = 5.5 Hz, 4H, 13, 17), 1.5 (p, *J* = 5.5 Hz, 4H, 14, 16), 1.4 (q, *J* = 5.8 Hz, 2H, 15); **^{13}C NMR (101 MHz, DMSO-d_6) δ**164.6 (18), 137.3 (25), 130.9 (19), 130.0 (24), 129.6 (21), 129.0 (22, 23), 127.2 (2, 6), 56.6 (11), 54.1 (13, 17), 25.5 (14, 16), 23.8 (15); **LR-ESI-MS**: $C_{20}H_{22}ClN_4O$ $[M+H]^+$ *m/z* found 369.34, cald 369.15; **HR-ESI-MS**: $C_{20}H_{22}ClN_4O$ $[M+H]^+$ *m/z* found 369.1463, cald 369.1482.

***N*-(2-(piperidin-1-ylmethyl)-1H-benzo[d]imidazol-5-yl)benzamide (274)**

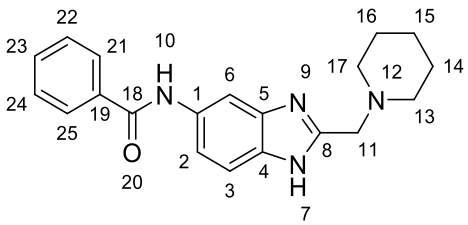

Synthesised according to general procedure **C** to give **274** (0.013 g, 0.04 mmol, 19%) as a yellow solid.

Mpt: 85.6-87.6 °C; **ν_{max} (cm^{-1})** 2933, 1600, 1527, 1277, 1108, 805, 672; **^{1}H NMR (400 MHz, DMSO-d_6) δ**12.2 (s, 1H, 10), 10.2 (s, 1H, 7), 8.1 (s, 1H, 6), 8.0 (ddd, *J* = 1.4, 2.7, 6.7 Hz, 2H, 21, 25), 7.6 – 7.5 (m, 3H, 22, 23, 24), 7.5 – 7.4 (m, 2H, 2, 3), 3.6 (s, 2H, 11), 2.4 (t, *J* = 5.1 Hz, 4H, 13, 17), 1.5 (p, *J* = 5.5 Hz, 4H, 14, 16), 1.4 – 1.3 (m, 2H, 15); **^{13}C NMR (101 MHz, DMSO-d_6) δ**165.3 (18), 135.3 (1), 131.4 (23), 129.2 (4), 129.1 (5), 128.8 (19), 128.4 (21, 25), 128.3 (2, 3), 127.6 (22, 24), 56.7 (11), 54.1 (13, 17), 25.4 (14, 16), 23.8 (15); **LR-ESI-MS**: $C_{20}H_{23}N_4O$ $[M+H]^+$ *m/z* found 335.39, cald 335.19; **HR-ESI-MS**: $C_{20}H_{23}N_4O$ $[M+H]^+$ *m/z* found 335.1857, cald 335.1872.

***N*-(2-(piperidin-1-ylmethyl)-1H-benzo[d]imidazol-5-yl)isonicotinamide (300)**

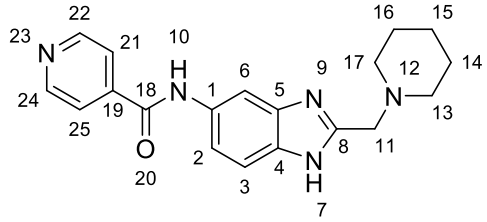

Synthesised according to general procedure **C** to give **300** (0.061 g, 0.183 mmol, 84%) as a white solid.

Mpt: 84.9-86.9 °C; **ν_{max} (cm^{-1})** 2932, 1653, 1450, 1415, 1284, 1065, 844, 809, 680, 624; **^{1}H NMR (400 MHz, DMSO-d_6) δ**12.3 (s, 1H, 7), 10.5 (s, 1H, 10), 8.8 – 8.7 (m, 2H, 22, 24), 8.1 (s, 1H, 6), 8.0 – 7.8 (m, 2H, 21, 25), 7.5 (d, *J* = 2.8 Hz, 2H, 2, 3), 3.7 (s, 2H, 11), 2.5 (s, 4H, 13, 17), 1.6 (p, *J* = 5.5 Hz, 4H, 14, 16), 1.5 – 1.4 (m, 2H, 15); **^{13}C NMR (101 MHz, DMSO-d_6) δ**163.7 (18), 150.2 (22, 24), 142.2 (19), 121.6 (21, 25), 56.3 (11), 54.0 (13, 17), 25.2 (14, 16), 23.6 (15); **LR-ESI-MS**: $C_{19}H_{22}N_5O$ $[M+H]^+$ *m/z* found 336.37, cald 336.18; **HR-ESI-MS**: $C_{19}H_{22}N_5O$ $[M+H]^+$ *m/z* found 336.1809, cald 336.1824.

***N*-(2-(piperidin-1-ylmethyl)-1H-benzo[d]imidazol-5-yl)picolinamide (298)**

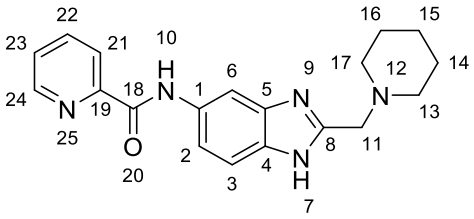

Synthesised according to general procedure **B** to give **298** (0.038 g, 0.112 mmol, 62%) as a white solid.

Mpt: 170.8-172.8 °C; **ν_{max} (cm^{-1})** 3345, 2937, 1591, 1522, 836, 807, 743, 659, 556; **^{1}H NMR (400 MHz, DMSO-d_6) δ**12.2 (s, 1H, 10), 10.6 (s, 1H, 7), 8.7 (dt, *J* = 1.4, 4.8 Hz, 1H, 24), 8.3 – 8.1 (m, 2H, 3, 21), 8.1 (td, *J* = 1.7, 7.7 Hz, 1H, 23), 7.7 (ddd, *J* = 1.3, 4.7, 7.5 Hz, 1H, 22), 7.6 (d, *J* = 8.6 Hz, 1H, 2), 7.5 (d, *J* = 8.6 Hz, 1H, 6), 3.7 (s, 2H, 11), 1.6 (p, *J* = 5.5 Hz, 4H, 13, 17), 1.4 (dd, *J* = 5.4, 10.8 Hz, 3H, 15), 1.2 (q, *J* = 6.6, 7.2 Hz, 4H, 14, 16); **^{13}C NMR (101 MHz, DMSO-d_6) δ**162.1 (18), 150.2 (19), 148.4 (22, 24), 138.1 (1), 132.8 (3), 126.8 (4, 5), 122.3 (21, 23), 115.5 (2, 6), 56.2 (11), 54.0 (13, 17), 25.2 (14, 16), 23.5 (15); **LR-ESI-MS**: $C_{19}H_{22}N_5O$ $[M+H]^+$ *m/z* found 336.38, cald 336.18; **HR-ESI-MS**: $C_{19}H_{22}N_5O$ $[M+H]^+$ *m/z* found 336.1810, cald 336.1824.

2-(3,4-dimethoxyphenyl)-*N*-(2-(piperidin-1-ylmethyl)-1H-benzo[d]imidazol-5-yl)acetamide (344)

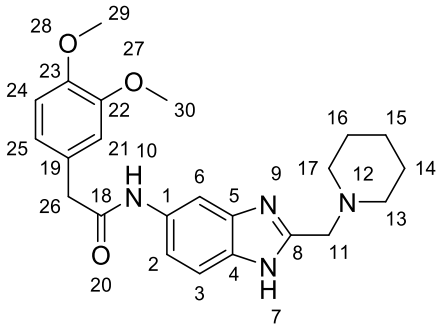

Synthesised according to general procedure **C** to give **344** (0.059 g, 0.145 mmol, 67%) as an off white solid.

Mpt: 77.4-79.4 °C; **ν_{max} (cm^{-1})** 2932, 1658, 1449, 1259, 1230, 1139, 1024, 789, 761; **^{1}H NMR (400 MHz, DMSO-d_6) δ**12.1 (s, 1H, 10), 10.1 (s, 1H, 7), 7.4 (s, 1H, 2), 7.2 (s, 1H, 6), 7.0 – 6.6 (m, 4H, 21, 24, 25), 3.7 (s, 3H, 29), 3.7 (s, 3H, 30), 3.6 (s, 2H, 26), 3.5 (s, 2H, 11), 2.4 (t, *J* = 5.3 Hz, 4H), 1.5 (p, *J* = 5.4 Hz, 4H), 1.4 (d, *J* = 7.2 Hz, 2H); **^{13}C NMR (101 MHz, DMSO-d_6) δ**173.0 (18), 169.0 (8), 148.5

(22), 147.6 (5), 128.6 (1), 127.6 (4), 121.3 (2), 121.0 (25), 113.2 (3), 113.0 (24), 111.8 (21), 111.7 (6), 56.6 (11), 55.5 (29), 55.4 (30), 54.1 (13, 17), 43.0 (26), 25.4 (14, 16), 23.8 (15); **LR-ESI-MS**: $C_{23}H_{29}N_4O_3$ $[M+H]^+$ *m/z* found 409.63, cald 409.22; **HR-ESI-MS**: $C_{23}H_{29}N_4O_3$ $[M+H]^+$ *m/z* found 409.2221, cald 409.2240.

5-methyl-*N*-(2-(piperidin-1-ylmethyl)-1H-benzo[d]imidazol-5-yl)isoxazole-3-carboxamide (345)

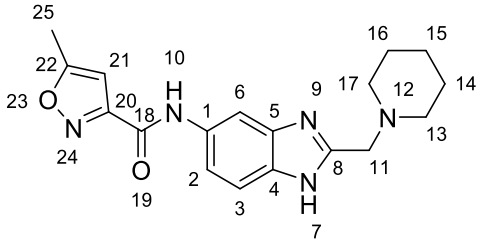

Synthesised according to general procedure **C** to give **345** (0.047 g, 0.140 mmol, 64%) as an off white solid.

Mpt: 104.0-106.0 °C; **ν_{max} (cm^{-1})** 2932, 1666, 1598, 1533, 1488, 1416, 1212, 860, 807, 610; **^{1}H NMR (400 MHz, DMSO-d_6) δ**12.2 (s, 1H, 10), 10.6 (d, *J* = 23.0 Hz, 1H, 7), 8.0 (d, *J* = 24.8 Hz, 1H, 3), 7.6 – 7.3 (m, 2H, 2, 6), 6.7 (d, *J* = 1.1 Hz, 1H, 11, 21), 3.6 (s, 2H), 2.5 (d, *J* = 1.8 Hz, 3H, 25), 2.5 – 2.3 (m, 4H, 13, 17), 1.5 (p, *J* = 5.5 Hz, 4H, 14, 16), 1.4 – 1.3 (m, 2H, 15); **^{13}C NMR (101 MHz, DMSO-d_6) δ**171.3 (22), 159.5 (20), 157.2 (18), 101.6 (2, 6), 56.6 (11), 54.1 (13, 17), 25.4 (14, 16), 23.8 (15), 11.9 (25); **LR-ESI-MS**: $C_{18}H_{22}N_5O_2$ $[M+H]^+$ *m/z* found 340.54, cald 340.18; **HR-ESI-MS**: $C_{18}H_{22}N_5O_2$ $[M+H]^+$ *m/z* found 340.1757, cald 340.1773.

4-(dimethylamino)-*N*-(2-(piperidin-1-ylmethyl)-1H-benzo[d]imidazol-5-yl)benzamide (346)

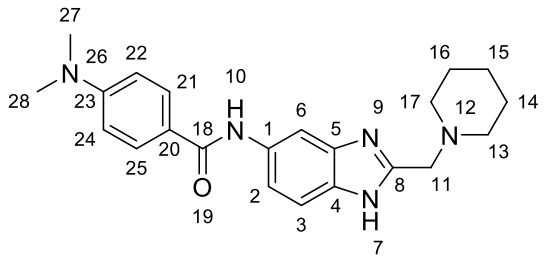

Synthesised according to general procedure **C** to give **346** (0.082 g, 0.217 mmol, 100%) as a white solid.

Mpt: >240 °C; **ν_{max} (cm^{-1})** 3290, 2932, 1639, 1605, 1441, 1193, 856; **^{1}H NMR (400 MHz, DMSO-d_6) δ**12.2 (s, 1H, 10), 9.8 (s, 1H, 7), 8.1 (s, 1H, 3), 8.0 – 7.7 (m, 2H, 21, 25), 7.4 (s, 2H, 2, 6), 6.8 – 6.6 (m, 2H, 22, 24), 3.6 (s, 2H, 11), 3.0 (s, 6H, 27, 28), 2.5 – 2.3 (m, 4H, 13, 17), 1.5 (p, *J* = 5.5 Hz, 4H, 14, 16), 1.5 – 1.3 (m, 2H, 15); **^{13}C NMR (101 MHz, DMSO-d_6) δ**172.1 (18), 165.0 (8), 152.3 (23), 130.9 (20), 129.0 (21, 25), 121.5 (2, 6), 110.8 (22, 24), 56.7 (11), 54.2 (13, 17), 25.4 (27, 28), 23.8 (14, 16), 21.1 (15); **LR-ESI-MS**: $C_{22}H_{28}N_5O$ $[M+H]^+$ *m/z* found 378.42, cald 378.23; **HR-ESI-MS**: $C_{22}H_{28}N_5O$ $[M+H]^+$ *m/z* found 378.2275, cald 378.2294.

***N*-(2-(piperidin-1-ylmethyl)-1H-benzo[d]imidazol-5-yl)benzenesulfonamide (347)**

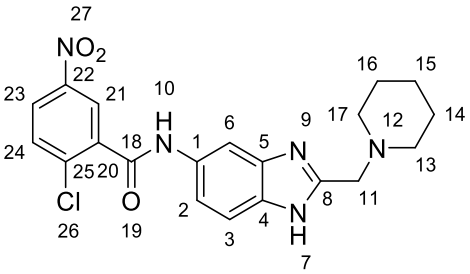

Synthesised according to general procedure **C** to give **347** (0.028 g, 0.067 mmol, 31%) as a beige solid.

Mpt: >135 °C; **ν_{max} (cm^{-1})** 2931, 1656, 1523, 1045, 738, 542; **^{1}H NMR (400 MHz, DMSO-d_6) δ**12.3 (s, 1H, 7), 10.7 (s, 1H, 10), 8.5 (d, *J* = 2.8 Hz, 1H, 21), 8.3 (dd, *J* = 2.8, 8.8 Hz, 1H, 23), 8.1 (d, *J* = 1.9 Hz, 1H, 6), 7.9 (d, *J* = 8.9 Hz, 1H, 24), 7.5 (d, *J* = 8.6 Hz, 1H, 3), 7.3 (d, *J* = 8.7 Hz, 1H, 2), 3.7 (s, 2H, 11), 2.4 (t, *J* = 5.3 Hz, 4H, 13, 17), 1.5 (q, *J* = 5.6 Hz, 4H, 14, 16), 1.4 (td, *J* = 3.6, 6.3 Hz, 2H, 15); **^{13}C NMR (101 MHz, DMSO-d_6) δ**162.5 (18), 146.2 (21), 138.1 (23), 137.2 (22), 131.3 (25), 125.6 (20), 123.9 (24), 56.5 (11), 54.1 (13, 17), 25.4 (14, 16), 23.7 (15); **LR-ESI-MS**: $C_{20}H_{21}ClN_5O_3$ $[M+H]^+$ *m/z* found 414.36, cald 414.13; **HR-ESI-MS**: $C_{20}H_{21}ClN_5O_3$ $[M+H]^+$ *m/z* found 414.1308, cald 414.1333.

***N*-(2-(piperidin-1-ylmethyl)-1H-benzo[d]imidazol-5-yl)pyrazine-2-carboxamide (301)**

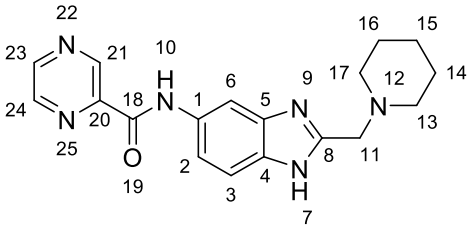

Synthesised according to general procedure **C** to give **301** (0.074 g, 0.220 mmol, 100%) as a yellow solid.

Mpt: 190.9-192.9 °C; **ν_{max} (cm^{-1})** 2931, 1669, 1524, 1419, 1106, 1018, 805, 650, 429; **^{1}H NMR (400 MHz, DMSO-d_6) δ**12.3 (s, 1H, 7), 10.7 (s, 1H, 10), 9.3 (d, *J* = 1.5 Hz, 1H, 21), 8.9 (d, *J* = 2.5 Hz, 1H, 24), 8.8 (dd, *J* = 1.5, 2.5 Hz, 1H, 23), 8.2 (s, 1H, 6), 7.7 – 7.3 (m, 2H, 2, 3), 3.7 (s, 2H, 11), 2.4 (t, *J* = 5.4 Hz, 4H, 13, 17), 1.5 (p, *J* = 5.5 Hz, 4H, 14, 16), 1.4 (q, *J* = 6.5 Hz, 2H, 15); **^{13}C NMR (101 MHz, DMSO-d_6) δ**161.3 (18), 147.5 (23), 145.4 (21), 144.0 (24), 143.2 (20), 56.6 (11), 54.1 (13, 17), 25.5 (14, 16), 23.8 (15); **LR-ESI-MS**: $C_{18}H_{21}N_6O$ $[M+H]^+$ *m/z* found 337.36, cald 337.18; **HR-ESI-MS**: $C_{18}H_{21}N_6O$ $[M+H]^+$ *m/z* found 337.1761, cald 337.1777.

2-phenoxy-*N*-(2-(piperidin-1-ylmethyl)-1H-benzo[d]imidazol-5-yl)acetamide (348)

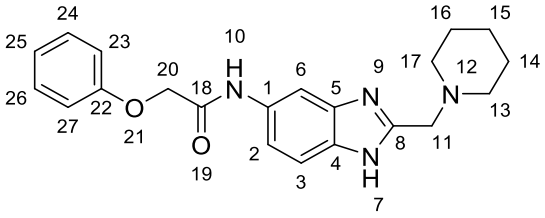

Synthesised according to general procedure **C** to give **348** (0.052 g, 0.141 mmol, 65%) as an off white solid.

Mpt: 94.6-96.6 °C; **ν_{max} (cm^{-1})** 2932, 1670, 1598, 1489, 807, 750, 689; **^{1}H NMR (400 MHz, DMSO-d_6) δ**12.4 – 12.0 (m, 1H, 10), 10.1 (s, 1H, 7), 7.9 (d, *J* = 26.9 Hz, 1H, 3), 7.6 – 7.1 (m, 4H, 2, 6, 24, 26), 7.1 – 6.8 (m, 3H, 23, 25, 27), 4.7 (s, 2H, 20), 3.6 (s, 2H, 11), 2.4 (t, *J* = 5.2 Hz, 4H, 13, 17), 1.5 (p, *J* = 5.5 Hz, 4H, 14, 16), 1.4 (q, *J* = 4.6, 6.0 Hz, 2H, 15); **^{13}C NMR (101 MHz, DMSO-d_6) δ**166.2 (18), 157.9 (8, 22), 129.5 (1, 24, 26), 121.2 (25), 114.7 (2, 3, 23, 27), 67.2 (20), 56.6 (11), 54.1 (13, 17), 25.4 (14, 16), 23.8 (15); **LR-ESI-MS**: $C_{21}H_{25}N_4O_2$ $[M+H]^+$ *m/z* found 365.58, cald 365.19; **HR-ESI-MS**: $C_{21}H_{25}N_4O_2$ $[M+H]^+$ *m/z* found 365.1960, cald 365.1978.

2-(4-chlorophenyl)-*N*-(2-(piperidin-1-ylmethyl)-1H-benzo[d]imidazol-5-yl)acetamide (349)

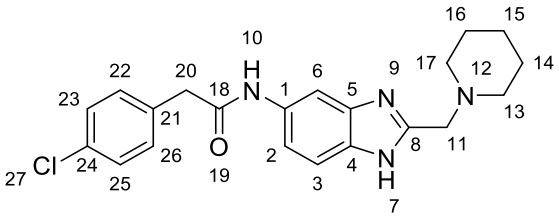

Synthesised according to general procedure **C** to give **349** (0.021 g, 0.054 mmol, 25%) as an off white solid.

Mpt: 120.6-122.6 °C; **ν_{max} (cm^{-1})** 2932, 1657, 1488, 1417, 1091, 804; **^{1}H NMR (400 MHz, DMSO-d_6) δ**12.2 (s, 1H, 10), 10.3 – 10.0 (m, 1H, 7), 8.0 – 7.8 (m, 1H, 6), 7.5 – 7.0 (m, 6H, 2, 3, 22, 23, 25, 26), 3.6 (s, 2H, 20), 3.6 (s, 2H, 11), 2.4 (t, *J* = 5.4 Hz, 4H, 13, 17), 1.5 (p, *J* = 5.5 Hz, 4H, 14, 16), 1.4 (q, *J* = 5.8 Hz, 2H, 15); **^{13}C NMR (101 MHz, DMSO-d_6) δ**168.3 (18), 152.0 (8), 139.3 (1), 135.3 (24), 134.5 (5), 133.8 (4), 131.2 (21), 131.0 (23, 25), 128.2 (22, 26), 118.2 (3), 113.8 (2), 102.0 (6), 56.6 (11), 54.1 (13, 17), 42.5 (20), 25.4 (14, 16), 23.8 (15); **LR-ESI-MS**: $C_{21}H_{24}ClN_4O$ $[M+H]^+$ *m/z* found 383.60, cald 383.16; **HR-ESI-MS**: $C_{21}H_{24}ClN_4O$ $[M+H]^+$ *m/z* found 383.1618, cald 383.1639.

***N*-(2-(piperidin-1-ylmethyl)-1H-benzo[d]imidazol-5-yl)pivalamide (350)**

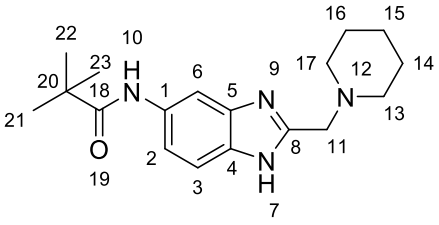

Synthesised according to general procedure **C** to give **350** (0.037 g, 0.117 mmol, 54%) as an off white solid.

Mpt: 130.0-132.0 °C; **ν_{max} (cm^{-1})** 2932, 1523, 1481, 1451, 1193, 806; **^{1}H NMR (400 MHz, DMSO-d_6) δ**12.1 (s, 1H, 10), 9.1 (s, 1H, 7), 7.9 (d, *J* = 1.8 Hz, 1H, 6), 7.4 (d, *J* = 8.6 Hz, 1H, 3), 7.3 – 7.2 (m, 1H, 2), 3.7 (s, 2H, 11), 2.4 (s, 4H, 13, 17), 1.5 (p, *J* = 5.5 Hz, 4H, 14, 16), 1.5 – 1.3 (m, 2H, 15), 1.2 (s, 9H, 21, 22, 23); **^{13}C NMR (101 MHz, DMSO-d_6) δ**176.1 (18), 56.4 (11), 54.1 (13, 17), 27.4 (14, 16), 27.0 (20), 25.2 (15), 23.6 (21, 22, 23); **LR-ESI-MS**: $C_{18}H_{27}N_4O$ $[M+H]^+$ *m/z* found 315.59, cald 315.22; **HR-ESI-MS**: $C_{18}H_{27}N_4O$ $[M+H]^+$ *m/z* found 315.2180, cald 315.2185.

3-cyano-*N*-(2-(piperidin-1-ylmethyl)-1H-benzo[d]imidazol-5-yl)benzamide (283)

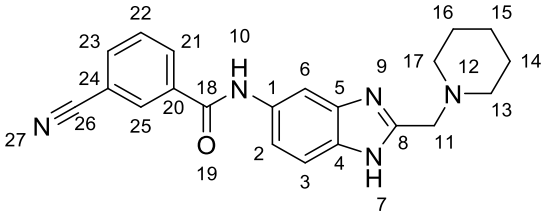

Synthesised according to general procedure **B** to give **283** (0.031 g, 0.085 mmol, 40%) as an off white solid.

Mpt: 127.7-129.7 °C; **ν_{max} (cm^{-1})** 2933, 1648, 1528, 1484, 1451, 1417, 805, 556; **^{1}H NMR (400 MHz, DMSO-d_6) δ**12.2 (s, 1H, 10), 10.4 (s, 1H, 7), 8.4 (t, *J* = 1.8 Hz, 1H, 25), 8.3 (dt, *J* = 1.5, 8.0 Hz, 1H, 21), 8.1 – 8.0 (m, 2H, 6, 23), 7.8 (t, *J* = 7.8 Hz, 1H, 22), 7.5 (t, *J* = 7.3 Hz, 2H, 2, 3), 3.7 (s, 2H, 11), 2.5 (s, 4H, 13, 17), 1.5 (p, *J* = 5.5 Hz, 4H, 14, 16), 1.4 (q, *J* = 5.9 Hz, 2H, 15); **^{13}C NMR (101 MHz, DMSO-d_6) δ**163.3 (18), 136.2 (25), 134.8 (23), 132.5 (21), 131.3 (22), 129.8 (20), 118.4 (26), 111.5 (3, 6), 56.4 (11), 54.1 (13, 17), 25.3 (14, 16), 23.6 (15); **LR-ESI-MS**: $C_{21}H_{22}N_5O$ $[M+H]^+$ *m/z* found 360.52, cald 360.18; **HR-ESI-MS**: $C_{21}H_{22}N_5O$ $[M+H]^+$ *m/z* found 360.1815, cald 360.1824.

4-cyano-*N*-(2-(piperidin-1-ylmethyl)-1H-benzo[d]imidazol-5-yl)benzamide (292)

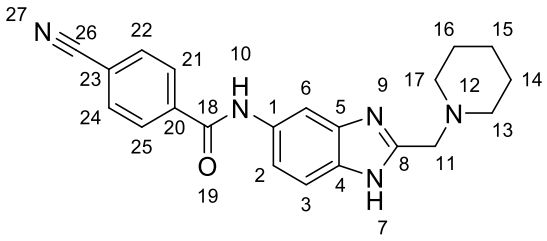

Synthesised according to general procedure **B** to give **292** (0.010 g, 0.028 mmol, 13%) as a white solid.

Mpt: 133.1-135.1 °C; **ν_{max} (cm^{-1})** 2931, 1647, 1529, 1450, 1297, 1108, 808, 756, 621; **^{1}H NMR (400 MHz, DMSO-d_6) δ**12.3 (s, 1H, 7), 10.5 (s, 1H, 10), 8.2 – 8.1 (m, 2H, 21, 25), 8.1 – 8.0 (m, 1H, 6), 8.0 – 8.0 (m, 2H, 22, 24), 7.6 – 7.3 (m, 2H, 2, 3), 3.6 (s, 2H, 11), 2.4 (t, *J* = 5.3 Hz, 4H, 13, 17), 1.5 (p, *J* = 5.5 Hz, 4H, 14, 16), 1.4 (dt, *J* = 4.7, 11.3 Hz, 2H, 15); **^{13}C NMR (101 MHz, DMSO-d_6) δ**163.8 (18), 139.3 (20), 132.5 (21, 25), 128.5 (22, 24), 118.4 (23), 113.6 (26), 56.7 (11), 54.2 (13, 17), 25.5 (14, 16), 23.8 (15); **LR-ESI-MS**: $C_{21}H_{22}N_5O$ $[M+H]^+$ *m/z* found 360.64, cald 360.18; **HR-ESI-MS**: $C_{21}H_{22}N_5O$ $[M+H]^+$ *m/z* found 360.1811, cald 360.1824.

4-methoxy-*N*-(2-(piperidin-1-ylmethyl)-1H-benzo[d]imidazol-5-yl)benzamide (290)

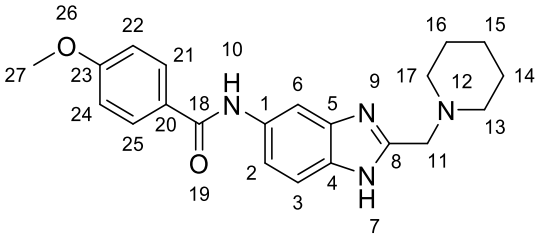

Synthesised according to general procedure **C** to give **290** (0.009 g, 0.025 mmol, 11%) as a white solid.

Mpt: 117.6-119.6 °C; **ν_{max} (cm^{-1})** 2932, 1604, 1451, 1177, 1026, 842, 760, 611; **^{1}H NMR (400 MHz, DMSO-d_6) δ**12.2 (s, 1H, 7), 10.1 (s, 1H, 10), 8.0 (s, 1H, 6), 8.0 – 7.8 (m, 2H, 21, 25), 7.4 (s, 2H, 2, 3), 7.1 – 6.7 (m, 2H, 22, 24), 3.8 (s, 3H, 27), 3.6 (s, 2H, 11), 2.4 (t, *J* = 5.3 Hz, 4H, 13, 17), 1.5 (q, *J* = 5.6 Hz, 4H, 14, 16), 1.4 – 1.3 (m, 2H, 15); **^{13}C NMR (101 MHz, DMSO-d_6) δ**164.6 (18), 161.7 (23), 129.5 (21, 25), 127.3 (20), 113.5 (22, 24), 56.7 (11), 55.4 (27), 54.2 (13, 17), 25.5 (14, 16), 23.8 (15); **LR-ESI-MS**: $C_{21}H_{25}N_4O_2$ $[M+H]^+$ *m/z* found 365.37, cald 365.19; **HR-ESI-MS**: $C_{21}H_{25}N_4O_2$ $[M+H]^+$ *m/z* found 365.1964, cald 365.1978.

***N*-(2-(piperidin-1-ylmethyl)-1H-benzo[d]imidazol-5-yl)-4-(trifluoromethyl)benzamide (293)**

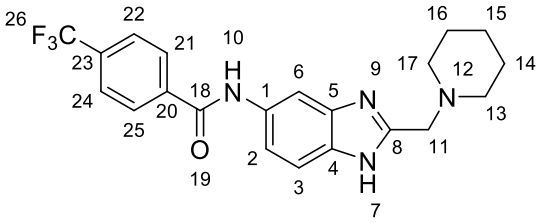

Synthesised according to general procedure **C** to give **293** (0.016 g, 0.041 mmol, 19%) as an orange solid.

Mpt: 146.6-148.6 °C; **ν_{max} (cm^{-1})** 2920, 2850, 1648, 1533, 1323, 1064, 855, 767, 689; **^{19}F NMR (376 MHz, DMSO-d_6) δ**-61.3; **^{1}H NMR (400 MHz, DMSO-d_6) δ**12.2 (s, 1H, 7), 10.5 (s, 1H, 10), 8.2 (d, *J* = 8.1 Hz, 2H, 22, 24), 8.1 (s, 1H, 6), 7.9 (d, *J* = 8.1 Hz, 2H, 21, 25), 7.5 (s, 2H, 2, 3), 3.7 (s, 2H, 11), 2.5 – 2.4 (m, 4H, 13, 17), 1.5 (q, *J* = 5.6 Hz, 4H, 14, 16), 1.4 (q, *J* = 4.9, 5.6 Hz, 2H, 15); **^{13}C NMR (101 MHz, DMSO-d_6) δ**164.1 (18), 139.1 (20), 131.3 (2), 131.0 (3), 128.6 (21, 22, 24, 25),

125.4 (q, *J* = 3.8 Hz, 26), 122.6 (6), 56.3 (11), 54.1 (13, 17), 25.2 (14, 16), 23.6 (15); **LR-ESI-MS**: $C_{21}H_{22}F_3N_4O$ $[M+H]^+$ *m/z* found 403.37, cald 403.18; **HR-ESI-MS**: $C_{21}H_{22}F_3N_4O$ $[M+H]^+$ *m/z* found 403.1733, cald 403.1746.

***N*-(2-(piperidin-1-ylmethyl)-1H-benzo[d]imidazol-5-yl)-4-(trifluoromethoxy)benzamide (294)**

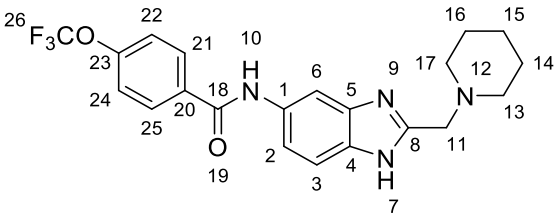

Synthesised according to general procedure **C** to give **294** (0.029 g, 0.069 mmol, 32%) as an off white solid.

Mpt: 187.0-189.0 °C; **ν_{max} (cm^{-1})** 2936, 1647, 1485, 1436, 1206, 1159, 806; **^{19}F NMR (376 MHz, DMSO-d_6) δ**-56.7; **^{1}H NMR (400 MHz, DMSO-d_6) δ**12.2 (s, 1H, 7), 10.3 (d, *J* = 22.1 Hz, 1H, 10), 8.2 – 7.9 (m, 3H, 3, 21, 25), 7.7 – 7.2 (m, 4H, 2, 6, 22, 24), 3.6 (s, 2H, 11), 2.4 (t, *J* = 5.4 Hz, 4H, 13, 17), 1.5 (p, *J* = 5.6 Hz, 4H, 14, 16), 1.4 (q, *J* = 4.6, 6.0 Hz, 2H, 15); **^{13}C NMR (101 MHz, DMSO-d_6) δ**164.1 (18), 152.3 (23), 150.3 (8), 134.4 (5), 130.0 (21, 25), 120.7 (22, 24), 118.7 (3), 118.1 (2), 115.0 (27), 103.3 (6), 56.7 (11), 54.2 (13, 17), 25.5 (14, 16), 23.8 (15); **LR-ESI-MS**: $C_{21}H_{22}F_3N_4O_2$ $[M+H]^+$ *m/z* found 419.39, cald 419.17; **HR-ESI-MS**: $C_{21}H_{22}F_3N_4O_2$ $[M+H]^+$ *m/z* found 419.1676, cald 419.1695.

2-fluoro-*N*-(2-(piperidin-1-ylmethyl)-1H-benzo[d]imidazol-5-yl)-4-(trifluoromethyl)benzamide (351)

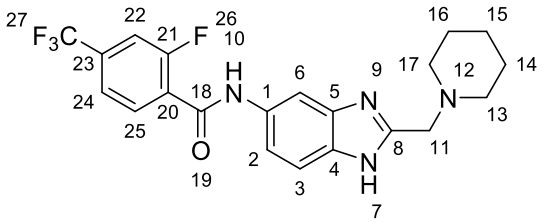

Synthesised according to general procedure **C** to give **351** (0.02 g, 0.048 mmol, 22%) as a white solid.

Mpt: 117.0-119.0 °C; **ν_{max} (cm^{-1})** 2934, 1656, 11421, 1327, 1125, 919, 745; **^{19}F NMR (376 MHz, DMSO-d_6) δ**-61.4 , 28, 29, 30, -112.5 , 26; **^{1}H NMR (400 MHz, DMSO-d_6) δ**12.3 (s, 1H, 7), 10.6 (s, 1H, 10), 8.0 (d, *J* = 27.0 Hz, 1H, 6), 8.0 – 7.8 (m, 2H, 22, 24), 7.7 (dd, *J* = 1.7, 8.2 Hz, 1H, 25), 7.6 – 7.2 (m, 2H, 2, 3), 3.6 (s, 2H, 11), 2.4 (t, *J* = 5.3 Hz, 4H, 13, 17), 1.5 (q, *J* = 5.6 Hz, 4H, 14, 16), 1.4 (q, *J* = 6.5, 7.9 Hz, 2H, 15); **^{13}C NMR (101 MHz, DMSO-d_6) δ** 161.2 (18), 158.6 (d, *J* = 250.6 Hz, 21), 131.2 (d, *J* = 3.5 Hz, 25), 129.4 (d, *J* = 16.4 Hz, 20), 124.5 (d, *J* = 2.3 Hz, 24), 121.6 (q, *J* = 3.6 Hz, 27), 114.0 (d, *J* = 3.6 Hz, 22), 113.7 (d, *J* = 3.6 Hz, 23), 56.6 (11), 54.2 (13, 17), 25.5 (14, 16), 23.8 (15); **LR-ESI-MS**: $C_{21}H_{21}F_4N_4O$ $[M+H]^+$ *m/z* found 421.36, cald 421.17; **HR-ESI-MS**: $C_{21}H_{21}F_4N_4O$ $[M+H]^+$ *m/z* found 421.1630, cald 421.1651.

3-fluoro-4-methyl-*N*-(2-(piperidin-1-ylmethyl)-1H-benzo[d]imidazol-5-yl)benzamide (352)

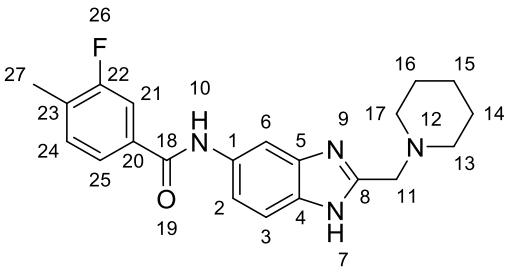

Synthesised according to general procedure **C** to give **352** (0.04 g, 0.109 mmol, 50%) as an off white solid.

Mpt: 119.1-121.1 °C; **ν_{max} (cm^{-1})** 2932, 1449, 1336, 744, 636; **^{19}F NMR (376 MHz, DMSO-d_6) δ**-117.1 (d, *J* = 39.4 Hz); **^{1}H NMR (400 MHz, DMSO-d_6) δ**10.2 (s, 1H, 10), 8.0 (s, 1H, 21), 7.8 (d, *J* = 9.2 Hz, 2H, 3, 24), 7.7 – 7.5 (m, 1H, 25), 7.5 – 7.3 (m, 3H, 2, 6, 7), 3.7 (s, 2H, 11), 2.4 (t, *J* = 5.3 Hz, 4H, 13, 17), 2.3 (dd, *J* = 1.9, 9.3 Hz, 3H, 27), 1.5 (q, *J* = 5.6 Hz, 4H, 14, 16), 1.4 (q, *J* = 6.2 Hz, 2H, 15); **^{13}C NMR (101 MHz, DMSO-d_6) δ**163.7 (18), 160.3 (d, *J* = 243.4 Hz, 22), 134.8 (d, *J* = 6.8 Hz, 24), 131.6 (d, *J* = 5.0 Hz, 23), 128.0 (d, *J* = 17.2 Hz, 25), 125.2 (d, *J* = 3.2 Hz, 20), 123.6 (d, *J* = 3.2 Hz, 2), 115.4 (d, *J* = 23.3 Hz, 3), 114.1 (d, *J* = 23.8 Hz, 21), 56.6 (11), 54.1 (13, 17), 25.4 (14, 16), 23.7 (15), 14.5 – 13.0 (m, 27); **LR-ESI-MS**: $C_{21}H_{24}FN_4O$ $[M+H]^+$ *m/z* found 367.39, cald 367.19; **HR-ESI-MS**: $C_{21}H_{24}FN_4O$ $[M+H]^+$ *m/z* found 367.1917, cald 367.1934.

2,4-dichloro-*N*-(2-(piperidin-1-ylmethyl)-1H-benzo[d]imidazol-5-yl)benzamide (353)

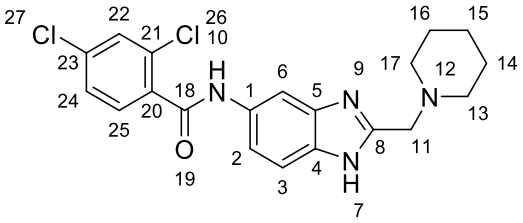

Synthesised according to general procedure **C** to give **353** (0.032 g, 0.078 mmol, 36%) as a white solid.

Mpt: 139.7-141.7 °C; **ν_{max} (cm^{-1})** 2931, 1653, 1450, 1246, 1101, 860; **^{1}H NMR (400 MHz, DMSO-d_6) δ**12.2 (s, 1H, 10), 10.5 (d, *J* = 32.4 Hz, 1H, 7), 8.2 – 7.9 (m, 1H, 22), 7.8 (d, *J* = 2.0 Hz, 1H, 6), 7.6 (d, *J* = 8.2 Hz, 1H, 3), 7.6 (dd, *J* = 2.0, 8.2 Hz, 1H, 2), 7.5 – 7.1 (m, 2H, 24, 25), 3.6 (s, 2H, 11), 2.4 (t, *J* = 5.2 Hz, 4H, 13, 17), 1.5 (t, *J* = 5.7 Hz, 4H, 14, 16), 1.4 – 1.3 (m, 2H, 15); **^{13}C NMR (101 MHz, DMSO-d_6) δ**163.7 (18), 131.3 (22), 130.4 (21, 25), 129.2 (23), 127.5 (24), 118.2 (2), 102.5 (6), 56.7 (11), 54.1 (13, 17), 25.4 (14, 16), 23.8 (15); **LR-ESI-MS**: $C_{20}H_{21}Cl_2N_4O$ $[M+H]^+$ *m/z* found 403.31, cald 403.11; **HR-ESI-MS**: $C_{20}H_{21}Cl_2N_4O$ $[M+H]^+$ *m/z* found 403.1068, cald 403.1092.

3,4-difluoro-*N*-(2-(piperidin-1-ylmethyl)-1H-benzo[d]imidazol-5-yl)benzamide (354)

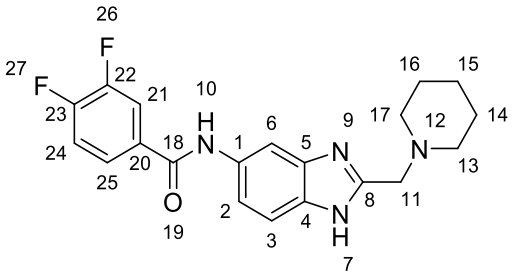

Synthesised according to general procedure **C** to give **354** (0.025 g, 0.067 mmol, 31%) as an off white solid.

Mpt: 136.0-138.0 °C; **ν_{max} (cm^{-1})** 2934, 1648, 1602, 1509, 1423, 1287, 1110, 747; **^{19}F NMR (376 MHz, DMSO-d_6) δ**-134.5 (dd, *J* = 22.1, 40.9 Hz, 27), -138.0 (d, *J* = 22.6 Hz, 26); **^{1}H NMR (400 MHz, DMSO-d_6) δ**12.2 (s, 1H, 7), 10.3 (d, *J* = 17.8 Hz, 1H, 10), 8.1 (ddd, *J* = 2.2, 7.8, 11.6 Hz, 2H, 6, 21), 7.9 (ddt, *J* = 1.6, 3.8, 8.2 Hz, 1H, 25), 7.6 (dt, *J* = 8.4, 10.6 Hz, 1H, 24), 7.6 – 7.3 (m, 2H, 2, 3), 3.6 (s, 2H, 11), 2.4 (t, *J* = 5.3 Hz, 4H, 13, 17), 1.5 (p, *J* = 5.5 Hz, 4H, 14, 16), 1.4 (q, *J* = 4.7, 6.2 Hz, 2H, 15); **^{13}C NMR (101 MHz, DMSO-d_6) δ**162.9 (18), 152.3 (8), 150.3 (dd, *J* = 12.7, 18.8 Hz, 23), 147.9

(d, *J* = 12.9 Hz, 22), 139.9 (1), 134.4 (5), 133.4 (4), 132.6 (20), 125.2 (25), 118.1 (2), 117.6 (d, *J* = 17.5 Hz, 21), 117.1 (d, *J* = 18.3 Hz, 24), 115.1 (3), 103.4 (6), 56.7 (11), 54.2 (13, 17), 25.5 (14, 16), 23.8 (15); **LR-ESI-MS**: $C_{20}H_{21}F_2N_4O$ $[M+H]^+$ *m/z* found 371.38, cald 371.17; **HR-ESI-MS**: $C_{20}H_{21}F_2N_4O$ $[M+H]^+$ *m/z* found 371.1665, cald 371.1683.

2,4-difluoro-*N*-(2-(piperidin-1-ylmethyl)-1H-benzo[d]imidazol-5-yl)benzamide (355)

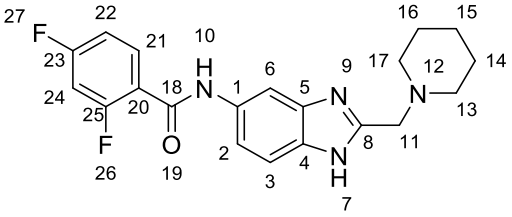

Synthesised according to general procedure **C** to give **355** (0.035 g, 0.095 mmol, 44%) as an off white solid.

Mpt: 107.3-109.3 °C; **ν_{max} (cm^{-1})** 2933, 1653, 1613, 1421, 1267, 970, 848, 807, 524; **^{19}F NMR (376 MHz, DMSO-d_6) δ**-106.6 (dd, *J* = 9.2, 34.9 Hz, 26), -109.9 (dd, *J* = 9.3, 25.4 Hz, 27); **^{1}H NMR (400 MHz, DMSO-d_6) δ**12.2 (s, 1H, 10), 10.4 (d, *J* = 33.0 Hz, 1H, 7), 8.1 – 7.9 (m, 1H, 21), 7.8 (td, *J* = 6.6, 8.4 Hz, 1H, 24), 7.5 – 7.3 (m, 2H, 3, 22), 7.3 – 7.1 (m, 2H, 2, 6), 3.6 (s, 2H, 11), 2.4 (t, *J* = 5.3 Hz, 4H, 13, 17), 1.5 (p, *J* = 5.5 Hz, 4H, 14, 16), 1.4 – 1.3 (m, 2H, 15); **^{13}C NMR (101 MHz, DMSO-d_6) δ**162.0 (18), 152.7 (25), 134.9 (5), 133.9 (21), 132.1 (dd, *J* = 4.8, 9.7 Hz), 118.7 (2), 115.9 (d, *J* = 2.6 Hz, 3), 114.8 (22), 112.3 (d, *J* = 20.0 Hz, 20), 105.1 (t, *J* = 26.1 Hz, 24), 103.1 (6), 57.1 (11), 54.6 (13, 17), 25.9 (14, 16), 24.2 (15); **LR-ESI-MS**: $C_{20}H_{21}F_2N_4O$ $[M+H]^+$ *m/z* found 371.37, cald 371.17; **HR-ESI-MS**: $C_{20}H_{21}F_2N_4O$ $[M+H]^+$ *m/z* found 371.1666, cald 371.1683.

3,4-dichloro-*N*-(2-(piperidin-1-ylmethyl)-1H-benzo[d]imidazol-5-yl)benzamide (356)

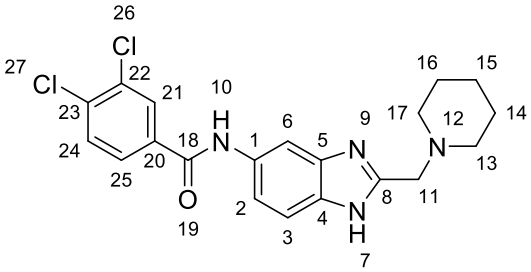

Synthesised according to general procedure **C** to give **356** (0.031 g, 0.076 mmol, 35%) as an off white solid.

Mpt: 142.2-144.2 °C; **ν_{max} (cm^{-1})** 2932, 1645, 1451, 1239, 1134, 1030, 746; **^{1}H NMR (400 MHz, DMSO-d_6) δ**12.2 (s, 1H, 10), 10.4 (d, *J* = 19.7 Hz, 1H, 7), 8.2 (d, *J* = 2.1 Hz, 1H, 21), 8.1 – 7.9 (m, 2H, 6, 24), 7.8 (d, *J* = 8.4 Hz, 1H, 25), 7.5 – 7.3 (m, 2H, 2, 3), 3.6 (s, 2H, 11), 2.4 (t, *J* = 5.1 Hz, 4H, 13, 17), 1.5 (p, *J* = 5.5 Hz, 4H, 14, 16), 1.4 (d, *J* = 7.7 Hz, 2H, 15); **^{13}C NMR (101 MHz, DMSO-d_6) δ**162.8 (18), 152.3 (8), 131.3 (21), 130.7 (25), 129.6 (23), 128.0 (22), 118.1 (3), 115.0 (2), 110.8 (6), 56.7 (11), 54.2 (13, 17), 25.4 (14, 16), 23.8 (15); **LR-ESI-MS**: $C_{20}H_{21}Cl_2N_4O$ $[M+H]^+$ *m/z* found 403.32, cald 403.11; **HR-ESI-MS**: $C_{20}H_{21}Cl_2N_4O$ $[M+H]^+$ *m/z* found 403.1072, cald 403.1092.

2-methyl-*N*-(2-(piperidin-1-ylmethyl)-1H-benzo[d]imidazol-5-yl)benzamide (277)

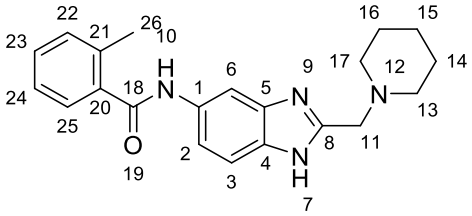

Synthesised according to general procedure **C** to give **277** (0.026 g, 0.075 mmol, 35%) as an off white solid.

Mpt: 123.1-125.1 °C; **ν_{max} (cm^{-1})** 2932, 1646, 1450, 736; **^{1}H NMR (400 MHz, DMSO-d_6) δ**12.2 (s, 1H, 10), 10.2 (d, *J* = 27.3 Hz, 1H, 7), 8.1 (d, *J* = 48.7 Hz, 1H, 6), 7.8 – 7.2 (m, 6H, 2, 3, 22, 23, 24, 25), 3.6 (s, 2H, 11), 2.4 (s, 7H, 13, 17, 26), 1.5 (p, *J* = 5.5 Hz, 4H, 14, 16), 1.4 (t, *J* = 6.0 Hz, 2H, 15); **^{13}C NMR (101 MHz, DMSO-d_6) δ**167.6 (18), 135.1 (1), 131.5 (5), 130.5 (21, 25), 130.1 (4), 129.4 (20), 127.2 (22, 24), 125.6 (23), 56.6 (11), 54.1 (13, 17), 25.4 (14, 16), 23.8 (15), 19.3 (26); **LR-ESI-MS**: $C_{21}H_{25}N_4O$ $[M+H]^+$ *m/z* found 349.42, cald 349.20; **HR-ESI-MS**: $C_{21}H_{25}N_4O$ $[M+H]^+$ *m/z* found 349.2009, cald 349.2028.

3,4-dimethyl-*N*-(2-(piperidin-1-ylmethyl)-1H-benzo[d]imidazol-5-yl)benzamide (357)

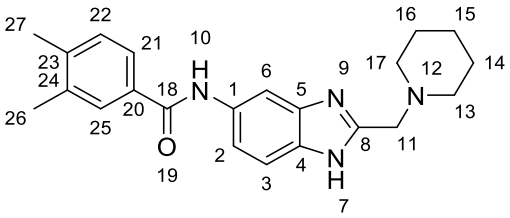

Synthesised according to general procedure **C** to give **357** (0.031 g, 0.085 mmol, 39%) as an off white solid.

Mpt: 124.0-126.0 °C; **ν_{max} (cm^{-1})** 2932, 1529, 1449, 806, 753; **^{1}H NMR (400 MHz, DMSO-d_6) δ**12.9 – 11.5 (m, 0H, 10), 10.1 (s, 1H, 7), 8.1 (s, 1H, 6), 7.8 (d, *J* = 1.9 Hz, 1H, 25), 7.7 (dd, *J* = 2.1, 7.7 Hz, 1H, 21), 7.4 (s, 2H, 2, 3), 7.2 (dd, *J* = 7.8, 21.2 Hz, 1H, 22), 3.6 (s, 2H, 11), 2.4 (t, *J* = 5.3 Hz, 4H, 13, 17), 2.3 – 2.2 (m, 7H, 26, 27), 1.5 (p, *J* = 5.5 Hz, 4H, 14, 16), 1.4 – 1.3 (m, 2H, 15); **^{13}C NMR (101 MHz, DMSO-d_6) δ**165.2 (18), 140.0 (24), 136.2 (23), 132.7 (20), 130.3 (2), 129.5 (3), 129.4 (21), 128.6 (25), 126.9 (6), 125.1 (22), 56.7 (11), 54.2 (13, 17), 25.5 (14, 16), 23.8 (15), 19.5 (27), 19.4 (26); **LR-ESI-MS**: $C_{22}H_{27}N_4O$ $[M+H]^+$ *m/z* found 363.42, cald 363.22; **HR-ESI-MS**: $C_{22}H_{27}N_4O$ $[M+H]^+$ *m/z* found 363.2169, cald 363.2185.

2-(3,4-dichlorophenyl)-*N*-(2-(piperidin-1-ylmethyl)-1H-benzo[d]imidazol-5-yl)acetamide (358)

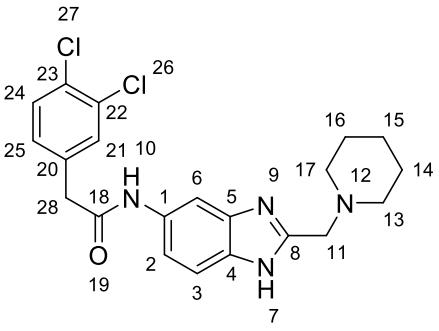

Synthesised according to general procedure **C** to give **358** (0.029 g, 0.069 mmol, 32%) as an off white solid.

Mpt: 123.6-125.6 °C; **ν_{max} (cm^{-1})** 2932, 1556, 1417, 1334, 1248, 1130, 808; **^{1}H NMR (400 MHz, DMSO-d_6) δ**12.2 (s, 1H, 10), 10.1 (d, *J* = 28.6 Hz, 1H, 7), 7.9 (d, *J* = 33.0 Hz, 1H, 3), 7.7 – 7.5 (m, 2H, 24, 25), 7.5 – 7.0 (m, 3H, 2, 6, 21), 3.7 (s, 2H, 11), 3.6 (s, 2H, 28), 2.4 (s, 4H, 13, 17), 1.5 (q, *J* = 5.6 Hz, 4H, 14, 16), 1.4 (d, *J* = 7.0 Hz, 2H, 15); **^{13}C NMR (101 MHz, DMSO-d_6) δ**167.8 (18), 137.3

(23), 131.3 (25), 130.7 (21), 130.4 (22), 129.7 (24), 129.2 (20), 56.6 (11), 54.1 (13, 17), 42.0 (28), 25.4 (14, 16), 23.8 (15); **LR-ESI-MS**: $C_{21}H_{23}Cl_2N_4O$ $[M+H]^+$ *m/z* found 417.36, cald 417.13; **HR-ESI-MS**: $C_{21}H_{23}Cl_2N_4O$ $[M+H]^+$ *m/z* found 417.1223, cald 417.1249.

1-methyl-*N*-(2-(piperidin-1-ylmethyl)-1H-benzo[d]imidazol-5-yl)-1H-benzo[d]imidazole-6-carboxamide (311)

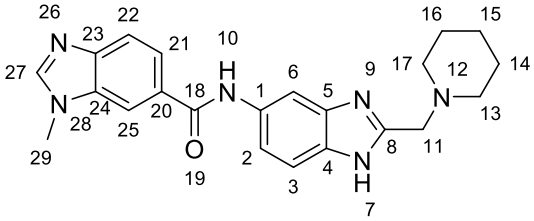

Synthesised according to general procedure **B** to give **311** (0.052 g, 0.135 mmol, 62%) as an off white solid.

Mpt: 150.2-152.2 °C; **ν_{max} (cm^{-1})** 2932, 1642, 1527, 1415, 1248, 1220, 840, 732, 434; **^{1}H NMR (400 MHz, DMSO-d_6) δ**12.2 (s, 1H, 10), 10.3 (d, *J* = 20.0 Hz, 1H, 7), 8.3 (q, *J* = 1.1 Hz, 1H, 27), 8.2 – 8.0 (m, 2H, 21, 25), 7.9 (dd, *J* = 0.8, 8.4 Hz, 1H, 3), 7.7 (dd, *J* = 1.4, 8.4 Hz, 1H, 6), 7.5 (dd, *J* = 8.4, 31.0 Hz, 2H, 2), 4.1 (s, 3H, 29), 3.7 (s, 2H, 11), 2.4 (d, *J* = 5.5 Hz, 4H, 13, 17), 1.5 (q, *J* = 5.6 Hz, 4H, 14, 16), 1.4 (d, *J* = 7.5 Hz, 2H, 15); **^{13}C NMR (101 MHz, DMSO-d_6) δ**165.5 (18), 139.1 (27), 133.0 (20), 132.5 (21), 124.9 (22), 120.7 (2), 119.7 (3), 118.0 (25), 109.6 (6), 56.7 (11), 54.2 (13, 17), 35.6 (29), 25.5 (14, 16), 23.8 (15); **LR-ESI-MS**: $C_{22}H_{25}N_6O$ $[M+H]^+$ *m/z* found 389.42, cald 389.21; **HR-ESI-MS**: $C_{22}H_{25}N_6O$ $[M+H]^+$ *m/z* found 389.2071, cald 389.2090.

3,4,5-trimethoxy-*N*-(2-(piperidin-1-ylmethyl)-1H-benzo[d]imidazol-5-yl)benzamide (359)

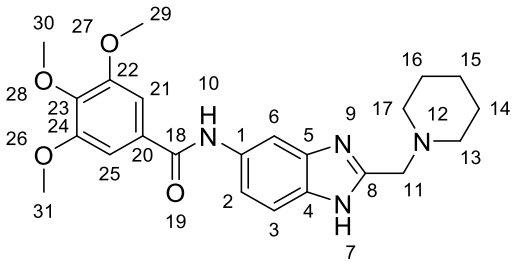

Synthesised according to general procedure **B** to give **359** (0.039 g, 0.091 mmol, 42%) as an off white solid.

Mpt: 134.2-136.2 °C; **ν_{max} (cm^{-1})** 2934, 1582, 1331, 1225, 998, 843, 727; **^{1}H NMR (400 MHz, DMSO-d_6) δ**12.2 (s, 1H, 7), 10.1 (s, 1H, 10), 8.0 (s, 1H, 6), 7.3 (d, *J* = 27.7 Hz, 4H, 2, 3, 21, 25), 3.9 (s, 6H, 29, 31), 3.7 (d, *J* = 3.5 Hz, 3H, 30), 3.7 (s, 2H, 11), 2.4 (s, 4H, 13, 17), 1.5 (t, *J* = 5.7 Hz, 4H, 14, 16), 1.4 – 1.4 (m, 2H, 15); **^{13}C NMR (101 MHz, DMSO-d_6) δ**164.6 (18), 152.6 (8), 140.1 (23), 130.3 (20), 106.5 (21, 25), 105.2 (2, 6), 60.1 (11), 56.1 (13, 17), 55.9 (30), 54.2 (29, 31), 25.4 (14, 16), 23.7 (15); **LR-ESI-MS**: $C_{23}H_{29}N_4O_4$ $[M+H]^+$ *m/z* found 425.48, cald 425.22; **HR-ESI-MS**: $C_{23}H_{29}N_4O_4$ $[M+H]^+$ *m/z* found 425.2164, cald 425.2189.

3-iodo-4-methyl-*N*-(2-(piperidin-1-ylmethyl)-1H-benzo[d]imidazol-5-yl)benzamide (360)

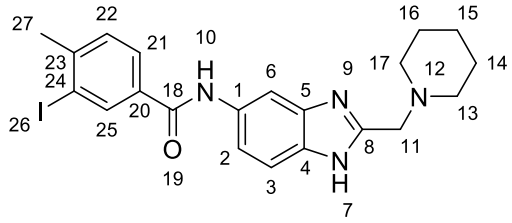

Synthesised according to general procedure **B** to give **360** (0.057 g, 0.121 mmol, 56%) as a white solid.

Mpt: 156.5-158.5 °C; **ν_{max} (cm^{-1})** 2932, 1642, 1529, 1248,746, 556; **^{1}H NMR (400 MHz, DMSO-d_6) δ**12.2 (s, 1H, 7), 10.2 (s, 1H, 10), 8.5 – 8.3 (m, 1H, 25), 8.0 (s, 1H, 3), 8.0 – 7.8 (m, 1H, 21), 7.6 – 7.3 (m, 3H, 2, 6, 22), 3.7 (s, 2H, 11), 2.5 – 2.3 (m, 7H, 13, 17, 27), 1.5 (p, *J* = 5.5 Hz, 4H, 14, 16), 1.4 (q, *J* = 6.0 Hz, 2H, 15); **^{13}C NMR (101 MHz, DMSO-d_6) δ**163.4 (18), 144.4 (25), 139.2 (5), 137.4 (21), 134.3 (23), 130.0 (4), 129.7 (20), 129.2 (22), 127.7 (2, 6), 101.1 (24), 56.6 (11), 54.1 (13, 17), 27.5 (27), 25.4 (14, 16), 23.7 (15); **LR-ESI-MS**: $C_{21}H_{24}IN_4O$ $[M+H]^+$ *m/z* found 475.30, cald 475.09; **HR-ESI-MS**: $C_{21}H_{24}IN_4O$ $[M+H]^+$ *m/z* found 475.0960, cald 475.0995.

***N*-(2-(piperidin-1-ylmethyl)-1H-benzo[d]imidazol-5-yl)-2-(pyridin-4-yl)acetamide (361)**

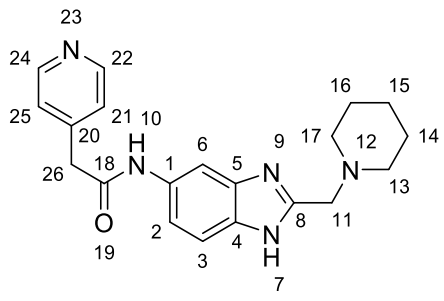

Synthesised according to general procedure **B** to give **361** (0.039 g, 0.112 mmol, 52%) as a yellow solid.

Mpt: 141.5-143.5 °C; **ν_{max} (cm^{-1})** 2932, 1600, 1418, 1125, 765; **^{1}H NMR (400 MHz, DMSO-d_6) δ**10.4 (s, 1H, 7), 8.6 – 8.2 (m, 3H, 3, 22, 24), 7.9 (d, *J* = 1.9 Hz, 1H, 10), 7.5 – 7.2 (m, 4H, 2, 6, 21, 25), 3.7 (s, 2H, 26), 3.7 (s, 2H, 11), 2.4 (t, *J* = 5.2 Hz, 4H, 13, 17), 1.5 (t, *J* = 5.7 Hz, 4H, 14, 16), 1.4 – 1.3 (m, 2H, 15); **^{13}C NMR (101 MHz, DMSO-d_6) δ**167.4 (18), 151.9 (8), 149.5 (22, 24), 148.0 (5), 145.1 (20), 139.5 (1), 134.5 (4), 133.6 (6), 127.6 (2), 124.7 (21, 25), 119.3 (3), 56.4 (11), 54.0 (13, 17), 42.5 (26), 25.3 (14, 16), 23.6 (15); **LR-ESI-MS**: $C_{20}H_{24}N_5O$ $[M+H]^+$ *m/z* found 350.40, cald 350.19; **HR-ESI-MS**: $C_{20}H_{24}N_5O$ $[M+H]^+$ *m/z* found 350.1957, cald 350.1981.

***N*-(2-(piperidin-1-ylmethyl)-1*H*-benzo[*d*]imidazol-5-yl)-3-(trifluoromethoxy)benzamide (287)**

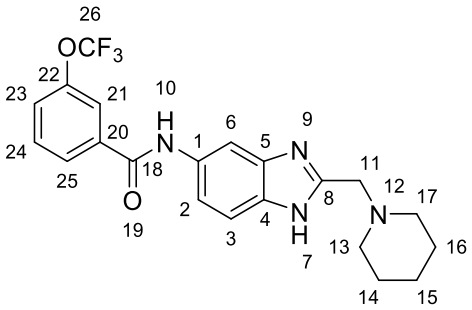

Synthesised according to general procedure **B** to give **287** (0.033 g, 0.079 mmol, 36%) as an off white solid.

Mpt: 111.6-113.6 °C; **ν_{max} (cm^{-1})** 2934, 1647, 1531, 1451, 804, 705; **^{19}F NMR (376 MHz, DMSO-d_6) δ**-56.7; **^{1}H NMR (400 MHz, DMSO-d_6) δ**12.3 (s, 1H, 7), 10.4 (s, 1H, 10), 8.1 – 8.0 (m, 2H, 21, 25), 7.9 (p, *J* = 1.2 Hz, 1H, 6), 7.7 (t, *J* = 8.0 Hz, 1H, 24), 7.6 (ddt, *J* = 1.1, 2.4, 8.1 Hz, 1H, 23), 7.5 (d, *J* = 4.7 Hz, 2H, 2, 3), 3.7 (s, 2H, 11), 2.4 (t, *J* = 5.3 Hz, 4H, 13, 17), 1.5 (p, *J* = 5.5 Hz, 4H, 14, 16), 1.4 (q, *J* = 5.8 Hz, 2H, 15); **^{13}C NMR (101 MHz, DMSO-d_6) δ**163.5 (18), 148.8 – 148.0 (m, 22), 137.4 (20), 130.6 (23), 126.8 (24), 123.9 (21), 121.4 (2), 120.2 (25), 118.8 (3), 56.6 (11), 54.1 (13, 17), 25.4 (14, 16), 23.7 (15); **LR-ESI-MS**: $C_{21}H_{22}F_3N_4O_2$ $[M+H]^+$ *m/z* found 419.62, cald 419.17; **HR-ESI-MS**: $C_{21}H_{22}F_3N_4O_2$ $[M+H]^+$ *m/z* found 419.1670, cald 419.1695.

***N*-(2-(piperidin-1-ylmethyl)-1H-benzo[d]imidazol-5-yl)-2-(trifluoromethoxy)benzamide (279)**

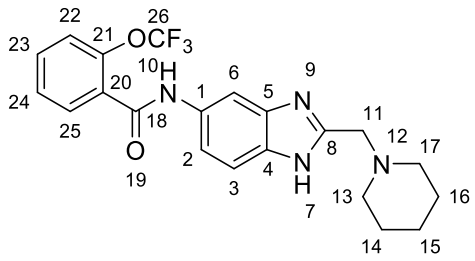

Synthesised according to general procedure **B** to give **279** (0.038 g, 0.091 mmol, 42%) as a white solid.

Mpt: 107.3-109.3 °C; **ν_{max} (cm^{-1})** 2938, 1603, 1448, 1247, 842, 761; **^{19}F NMR (376 MHz, DMSO-d_6) δ**-56.5; **^{1}H NMR (400 MHz, DMSO-d_6) δ**12.3 (s, 1H, 7), 10.4 (s, 1H, 10), 8.0 (s, 1H, 6), 7.8 (ddd, *J* = 1.8, 7.6, 51.2 Hz, 1H, 22), 7.7 – 7.6 (m, 1H, 23), 7.6 – 7.4 (m, 3H, 2, 3, 25), 7.3 (d, *J* = 8.8 Hz, 1H, 24), 3.7 (s, 2H, 11), 2.4 (t, *J* = 5.3 Hz, 4H, 13, 17), 1.5 (p, *J* = 5.5 Hz, 4H, 14, 16), 1.4 (t, *J* = 6.0 Hz, 2H, 15); **^{13}C NMR (101 MHz, DMSO-d_6) δ**163.0 (18), 152.4 (21), 144.9 – 144.7 (m, 27), 131.6 (23), 131.4 (25), 129.8 (20), 127.7 (24), 127.6 (4), 122.4 (2), 121.7 (22), 121.3 (3), 118.8 (6), 56.5 (11), 54.1 (13, 17), 25.4 (14, 16), 23.7 (15); **LR-ESI-MS**: $C_{21}H_{22}F_3N_4O_2$ $[M+H]^+$ *m/z* found 419.60, cald 419.17; **HR-ESI-MS**: $C_{21}H_{22}F_3N_4O_2$ $[M+H]^+$ *m/z* found 419.1668, cald 419.1695.

4-iodo-*N*-(2-(piperidin-1-ylmethyl)-1H-benzo[d]imidazol-5-yl)benzamide (362)

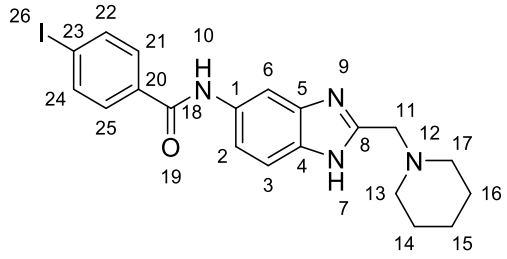

Synthesised according to general procedure **B** to give **362** (0.027 g, 0.059 mmol, 27%) as a white solid.

Mpt: 198.5-200.5 °C; **ν_{max} (cm^{-1})** 2930, 2796, 1643, 1585, 1526, 1298, 1107, 1005, 807; **^{1}H NMR (400 MHz, DMSO-d_6) δ**12.2 (s, 1H, 10), 10.3 (d, *J* = 21.2 Hz, 1H, 7), 8.0 (d, *J* = 34.1 Hz, 1H, 6), 7.9 – 7.9 (m, 2H, 21, 25), 7.8 – 7.7 (m, 2H, 22, 24), 7.5 – 7.3 (m, 2H, 2, 3), 3.6 (s, 2H, 11), 2.5 – 2.3 (m, 4H, 13, 17), 1.5 (p, *J* = 5.6 Hz, 4H, 14, 16), 1.5 – 1.3 (m, 2H, 15); **^{13}C NMR (101 MHz, DMSO-d_6) δ**164.5 (18), 152.2 (8), 137.2 (21, 25), 134.6 (5), 129.6 (22, 24), 118.0 (2), 115.0 (3), 56.7 (11),

54.2 (13, 17), 25.4 (14, 16), 23.8 (15); **LR-ESI-MS**: $C_{20}H_{22}IN_4O$ $[M+H]^+$ *m/z* found 461.43, cald 461.08; **HR-ESI-MS**: $C_{20}H_{22}IN_4O$ $[M+H]^+$ *m/z* found 461.0805, cald 461.0838.

***N*-(2-((4-methylpiperidin-1-yl)methyl)-1H-benzo[d]imidazol-5-yl)benzamide (363)**

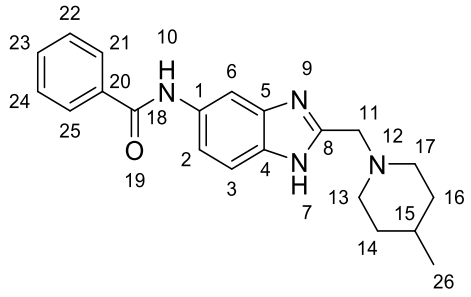

Synthesised according to general procedure **C** to give **363** (0.015 g, 0.044 mmol, 22%) as an off white solid.

Mpt: 135.5-137.5 °C; **ν_{max} (cm^{-1})** 2920, 1528, 1331, 1280, 1080, 806, 692, 626; **^{1}H NMR (400 MHz, DMSO-d_6) δ**12.2 (s, 1H, 10), 10.2 (d, *J* = 20.9 Hz, 1H, 7), 8.1 (s, 1H, 6), 8.1 – 7.9 (m, 2H, 21, 25), 7.6 – 7.3 (m, 5H, 2, 3, 22, 23, 24), 3.7 (s, 2H, 11), 2.9 – 2.7 (m, 2H, 13'', 17''), 2.0 (td, *J* = 2.4, 11.6 Hz, 2H, 13', 17'), 1.6 – 1.5 (m, 2H, 14'', 16''), 1.4 – 1.3 (m, 1H, 15), 1.2 – 1.1 (m, 2H, 14', 16'), 0.9 (d, *J* = 6.4 Hz, 3H, 26); **^{13}C NMR (101 MHz, DMSO-d_6) δ**165.3 (18), 135.3 (20), 131.4 (23), 128.4 (21, 25), 127.6 (22, 24), 56.3 (11), 53.6 (13, 17), 33.9 (14, 16), 30.1 (15), 21.9 (26); **LR-ESI-MS**: $C_{21}H_{25}N_4O$ $[M+H]^+$ *m/z* found 349.60, cald 349.20; **HR-ESI-MS**: $C_{21}H_{25}N_4O$ $[M+H]^+$ *m/z* found 349.2008, cald 349.2028.

4-chloro-*N*-(2-((1,2,4,5-tetrahydro-3*H*-benzo[*d*]azepin-3-yl)methyl)-1*H*-benzo[*d*]imidazol-5-yl)benzamide (364)

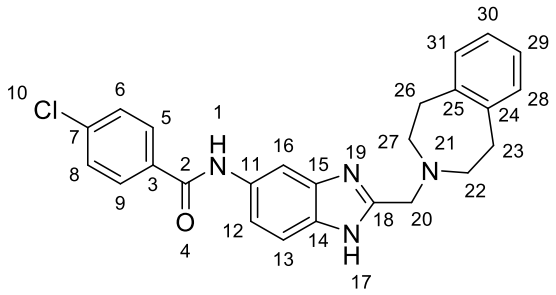

Synthesised according to general procedure **C** to give **364** (0.089 g, 0.200 mmol, 53%) as a yellow solid.

Mpt: 151.7-153.7 °C; **ν_{max} (cm^{-1})** 2929, 2812, 1643, 1596, 1433, 1302, 1269, 1089, 1013, 842, 807, 747; **^{1}H NMR (400 MHz, DMSO-d_6) δ**12.3 (s, 1H, 1), 10.3 (s, 1H, 17), 8.1 (s, 1H, 16), 8.0 – 8.0 (m, 2H, 5, 9), 7.7 – 7.6 (m, 2H, 6, 8), 7.6 – 7.4 (m, 2H, 12, 13), 7.1 – 7.0 (m, 4H, 28, 29, 30, 31), 3.9 (s, 2H, 20), 2.9 (dd, *J* = 3.4, 6.7 Hz, 4H, 23, 26), 2.7 – 2.6 (m, 4H, 22, 27); **^{13}C NMR (101 MHz, DMSO-d_6) δ**164.1 (2), 152.4 (18), 141.9 (24, 25), 136.2 (11), 133.9 (7), 129.6 (5, 9), 128.7 (6, 8), 128.4 (28, 29, 30, 31), 126.1 (3), 118.1 (12), 115.1 (13), 103.3 (16), 56.3 (20), 55.2 (22, 27), 35.7 (23, 26); **LR-ESI-MS**: $C_{25}H_{24}ClN_4O$ $[M+H]^+$ *m/z* found 431.53, cald 431.16; **HR-ESI-MS**: $C_{25}H_{24}ClN_4O$ $[M+H]^+$ *m/z* found 431.1616, cald 431.1639.

4-chloro-*N*-(2-((4-phenylpiperazin-1-yl)methyl)-1H-benzo[d]imidazol-5-yl)benzamide (316)

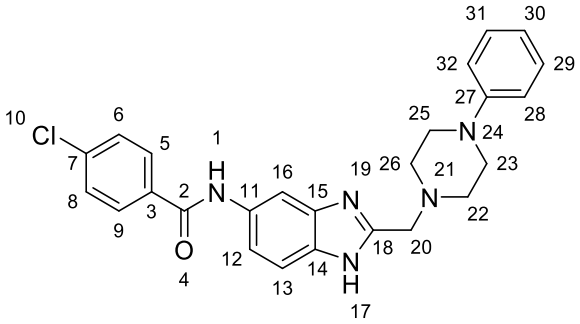

Synthesised according to general procedure **C** to give **316** (0.089 g, 0.200 mmol, 51%) as a yellow solid.

Mpt: 134.3-136.3 °C; **ν_{max} (cm^{-1})** 2812, 1647, 1596, 1448, 1333, 1227, 1089, 1013, 749; **^{1}H NMR (400 MHz, DMSO-d_6) δ**12.4 (s, 1H, 1), 10.3 (s, 1H, 17), 8.1 (s, 1H, 16), 8.0 – 8.0 (m, 2H, 5, 9), 7.7 – 7.6 (m, 2H, 6, 8), 7.5 – 7.4 (m, 2H, 12, 13), 7.3 – 7.1 (m, 2H, 29, 31), 7.0 – 6.9 (m, 2H, 28, 32), 6.8 – 6.7 (m, 1H, 30), 3.8 (s, 2H, 20), 3.3 – 3.1 (m, 4H, 22, 26), 2.6 (t, *J* = 4.9 Hz, 4H, 23, 25); **^{13}C NMR (101 MHz, DMSO-d_6) δ**164.2 (2), 151.0 (18), 136.2 (3, 7), 133.9 (14, 15), 129.6 (5, 9), 128.9 (29, 31), 128.4 (6, 8), 118.8 (12, 13), 115.4 (28, 30, 32), 55.8 (20), 52.8 (22, 26), 48.1 (23, 25); **LR-ESI-MS**: $C_{25}H_{25}ClN_5O$ $[M+H]^+$ *m/z* found 446.56, cald 446.18; **HR-ESI-MS**: $C_{25}H_{25}ClN_5O$ $[M+H]^+$ *m/z* found 446.1717, cald 446.1748.

4-chloro-*N*-(2-((4-(2-(pyrrolidin-1-yl)ethyl)piperidin-1-yl)methyl)-1H-benzo[d]imidazol-5-yl)benzamide (317)

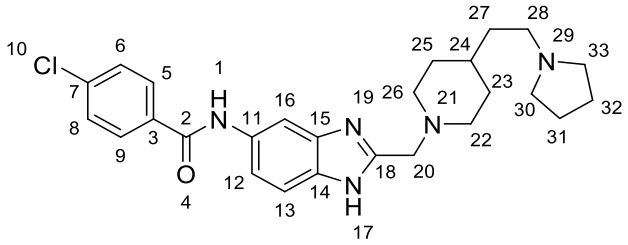

Synthesised according to general procedure **C** to give **317** (0.044 g, 0.094 mmol, 36%) as a white solid.

Mpt: 145.9-147.9 °C; **ν_{max} (cm^{-1})** 2917, 2795, 1646, 1596, 1419, 1273, 1089, 843, 807, 749; **^{1}H NMR (400 MHz, DMSO-d_6) δ**12.2 (s, 1H), 10.3 (s, 1H), 8.1 – 7.9 (m, 3H), 7.7 – 7.6 (m, 2H), 7.6 – 7.3 (m, 2H), 3.7 (s, 2H, 20), 2.9 – 2.7 (m, 2H, 28), 2.4 (dt, *J* = 4.2, 7.6 Hz, 6H, 22, 23', 25', 26), 2.0 (td, *J* = 2.3, 11.4 Hz, 2H, 23'', 25''), 1.6 (dt, *J* = 5.6, 10.6 Hz, 6H, 27, 30, 33), 1.5 – 1.1 (m, 5H, 24, 31, 32); **^{13}C NMR (101 MHz, DMSO-d_6) δ**164.1 (2), 136.2 (15), 133.9 (14), 129.6 (5, 9), 128.4 (6, 8), 56.3 (20), 53.7 (22, 26), 53.6 (30, 33), 53.2 (28), 35.2 (23, 25), 33.2 (24), 32.0 (31, 32), 23.0 (27); **LR-ESI-MS**: $C_{26}H_{33}ClN_5O$ $[M+H]^+$ *m/z* found 466.63, cald 466.24; **HR-ESI-MS**: $C_{26}H_{33}ClN_5O$ $[M+H]^+$ *m/z* found 466.2239, cald 466.2374.

4-chloro-*N*-(2-((4-(2-(piperidin-1-yl)ethyl)piperidin-1-yl)methyl)-1H-benzo[d]imidazol-5-yl)benzamide (318)

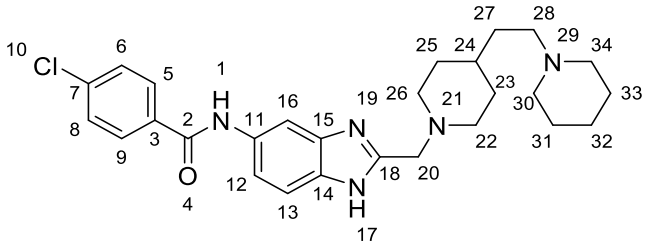

Synthesised according to general procedure **C** to give **318** (0.065 g, 0.135 mmol, 52%) as a white solid.

Mpt: 115.4-117.4 °C; **ν_{max} (cm^{-1})** 2930, 2806, 1646, 1595, 1528, 1449, 1417, 1296, 1098, 1012, 808, 749, 624; **^{1}H NMR (400 MHz, DMSO-d_6) δ**12.3 (s, 1H, 1), 10.3 (d, *J* = 19.6 Hz, 1H, 17), 8.1 (s, 1H, 16), 8.0 – 7.8 (m, 2H, 5, 9), 7.6 (d, *J* = 8.6 Hz, 2H, 6, 8), 7.5 (d, *J* = 7.7 Hz, 1H, 12), 7.4 – 7.3 (m, 1H, 13), 3.7 (s, 2H, 20), 2.5 – 2.1 (m, 17H, 22, 24, 26, 27, 28, 30, 31, 33, 34), 1.4 (p, *J* = 5.5 Hz, 4H, 23, 25), 1.3 (q, *J* = 5.9 Hz, 2H, 32); **^{13}C NMR (101 MHz, DMSO-d_6) δ**164.1 (2), 151.9 (18), 136.2

(15), 133.9 (14), 129.6 (5, 9), 128.4 (6, 8), 118.1 (12), 115.1 (13), 103.3 (16), 56.2 (20), 55.9 (28), 55.6 (30, 34), 54.5 (22, 26), 53.0 (31, 33), 53.0 (23, 25), 25.6 (24, 27), 24.1 (32); **LR-ESI-MS**: $C_{27}H_{35}ClN_5O$ $[M+H]^+$ *m/z* found 481.64, cald 480.25; **HR-ESI-MS**: $C_{27}H_{35}ClN_5O$ $[M+H]^+$ *m/z* found 481.2453, cald 480.2530.

4-chloro-*N*-(2-((2-methylpyrrolidin-1-yl)methyl)-1H-benzo[d]imidazol-5-yl)benzamide (319)

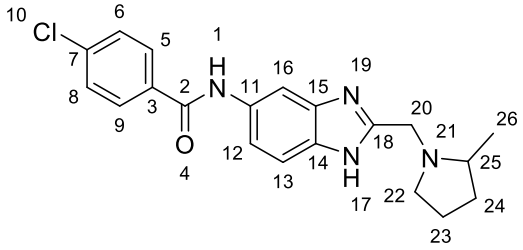

Synthesised according to general procedure **C** to give **319** (0.105 g, 0.284 mmol, 73%) as an off white solid.

Mpt: 125.8-127.8 °C; **ν_{max} (cm^{-1})** 2959, 2792, 1593, 1449, 1274, 1089, 1012, 808, 749, 528; **^{1}H NMR (400 MHz, DMSO-d_6) δ**12.3 (s, 1H, 1), 10.3 (s, 1H, 17), 8.1 – 7.9 (m, 3H, 5, 9, 16), 7.7 – 7.5 (m, 2H, 6, 8), 7.5 (s, 2H, 12, 13), 4.1 (d, *J* = 14.2 Hz, 1H, 20''), 3.6 (d, *J* = 14.2 Hz, 1H, 20'), 3.0 (ddd, *J* = 3.5, 7.5, 9.2 Hz, 1H, 25), 2.6 – 2.5 (m, 1H, 22'), 2.3 (q, *J* = 8.8 Hz, 1H, 22''), 1.9 (dddd, *J* = 5.5, 7.1, 9.3, 12.4 Hz, 1H, 23''), 1.7 (dtd, *J* = 3.0, 5.5, 6.4, 11.7 Hz, 2H, 23', 24''), 1.4 (dddd, *J* = 6.4, 8.4, 10.0, 12.2 Hz, 1H, 24'), 1.1 (d, *J* = 6.0 Hz, 3H, 26); **^{13}C NMR (101 MHz, DMSO-d_6) δ**164.1 (2), 152.8 (18), 137.5 (11), 136.2 (12), 133.9 (16), 133.3 (14, 15), 131.1 (7), 129.6 (5, 9), 128.6 (3), 128.4 (6, 8), 115.6 (13), 59.2 (20), 54.0 (22), 50.8 (25), 32.4 (24), 21.4 (23), 18.7 (26); **LR-ESI-MS**: $C_{20}H_{22}ClN_4O$ $[M+H]^+$ *m/z* found 369.49, cald 369.15; **HR-ESI-MS**: $C_{20}H_{22}ClN_4O$ $[M+H]^+$ *m/z* found 369.1460, cald 369.1482.

4-chloro-*N*-(2-(((2R,6S)-2,6-dimethylpiperidin-1-yl)methyl)-1H-benzo[d]imidazol-5-yl)benzamide (314)

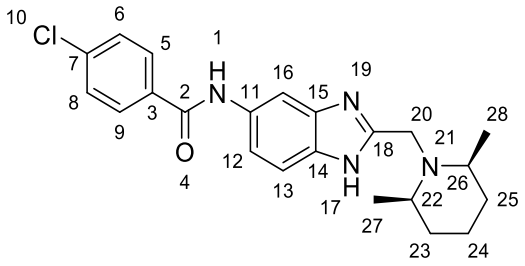

Synthesised according to general procedure **C** to give **314** (0.046 g, 0.116 mmol, 45%) as a yellow solid.

Mpt: >220 °C; **ν_{max} (cm^{-1})** 2925, 1643, 1595, 1483, 1291, 1262, 1090, 1013, 842, 807, 749; **^{1}H NMR (400 MHz, DMSO-d_6) δ**11.9 (s, 1H, 1), 10.3 (s, 1H, 17), 8.2 – 7.8 (m, 3H, 5, 9, 16), 7.7 – 7.5 (m, 2H, 6, 8), 7.5 – 7.3 (m, 2H, 12, 13), 4.0 (s, 2H, 20''), 2.6 – 2.5 (m, 2H, 22, 26), 1.7 – 1.5 (m, 3H, 23', 24', 25'), 1.4 – 1.2 (m, 3H, 23'', 24'', 25''), 1.1 (d, *J* = 6.1 Hz, 6H, 27, 28); **^{13}C NMR (101 MHz, DMSO-d_6) δ**164.2 (2), 136.1 (7), 134.0 (16), 131.1 (12, 13), 129.6 (5, 9), 128.6 (14), 128.4 (6, 8), 56.3 (20), 46.4 (22, 26), 34.1 (23, 25), 24.1 (24), 21.4 (27, 28); **LR-ESI-MS**: $C_{22}H_{26}ClN_4O$ $[M+H]^+$ *m/z* found 397.35, cald 397.18; **HR-ESI-MS**: $C_{22}H_{26}ClN_4O$ $[M+H]^+$ *m/z* found 397.1769, cald 397.1795.

4-chloro-*N*-(2-((4-methylpiperazin-1-yl)methyl)-1H-benzo[d]imidazol-5-yl)benzamide (315)

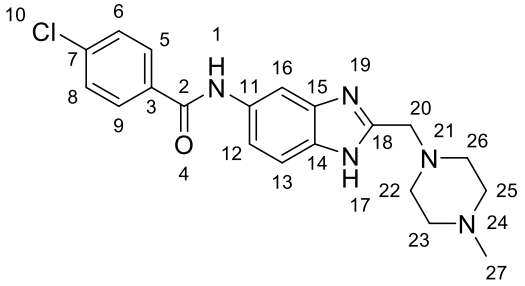

Synthesised according to general procedure **C** to give **315** (0.082 g, 0.214 mmol, 55%) as a white solid.

Mpt: 158.9-160.9 °C; **ν_{max} (cm^{-1})** 2936, 2799, 1644, 1596, 1530, 1483, 1452, 1280, 1089, 1012, 810, 749; **^{1}H NMR (400 MHz, DMSO-d_6) δ**12.3 (s, 1H, 1), 10.3 (s, 1H, 17), 8.1 – 7.9 (m, 3H, 5, 9, 16), 7.6 – 7.6 (m, 2H, 6, 8), 7.5 – 7.3 (m, 2H, 12, 13), 3.7 (s, 2H, 20), 2.5 – 2.2 (m, 8H, 22, 23, 25, 26), 2.2 (s, 3H, 27); **^{13}C NMR (101 MHz, DMSO-d_6) δ**164.1 (2), 151.9 (18), 139.8 (7), 136.2 (15),

133.9 (14), 129.6 (5, 9), 128.4, 118.1 (12), 115.1 (13), 110.7 (16), 103.3 (11), 55.8 (20), 54.6 (22, 26), 52.8 (23, 25), 45.8 (27); **LR-ESI-MS**: $C_{20}H_{23}ClN_5O$ $[M+H]^+$ *m/z* found 384.32, cald 384.16; **HR-ESI-MS**: $C_{20}H_{23}ClN_5O$ $[M+H]^+$ *m/z* found 384.1562, cald 384.1591.

4-chloro-*N*-(2-((dimethylamino)methyl)-1H-benzo[d]imidazol-5-yl)benzamide (365)

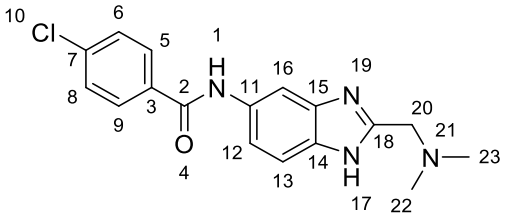

Synthesised according to general procedure **C** to give **365** (0.031 g, 0.094 mmol, 24%) as an off white solid.

Mpt: 143.2-145.2 °C; **ν_{max} (cm^{-1})** 2822, 2778, 1644, 1595, 1529, 1483, 1344, 1259, 1090, 1013, 842, 810, 741, 619; **^{1}H NMR (400 MHz, DMSO-d_6) δ**12.3 (s, 1H, 1), 10.4 – 10.2 (m, 1H, 17), 8.1 – 7.9 (m, 3H, 5, 9, 16), 7.7 – 7.6 (m, 2H, 6, 8), 7.5 – 7.3 (m, 2H, 12, 13), 3.6 (s, 2H, 20), 2.2 (s, 6H, 22, 23); **^{13}C NMR (101 MHz, DMSO-d_6) δ**164.1 (2), 152.5 (18), 139.8 (7), 136.2 (3), 134.4 (11), 133.9 (15), 133.6 (14), 129.6 (5, 9), 128.4 (6, 8), 118.1 (12), 115.1 (13), 103.3 (16), 57.1 (20), 45.2 (22, 23)s; **LR-ESI-MS**: $C_{17}H_{18}ClN_4O$ $[M+H]^+$ *m/z* found 329.25, cald 329.12; **HR-ESI-MS**: $C_{17}H_{18}ClN_4O$ $[M+H]^+$ *m/z* found 329.1144, cald 329.1169.

4-(benzyloxy)-*N*-(2-(piperidin-1-ylmethyl)-1H-benzo[d]imidazol-5-yl)benzamide (366)

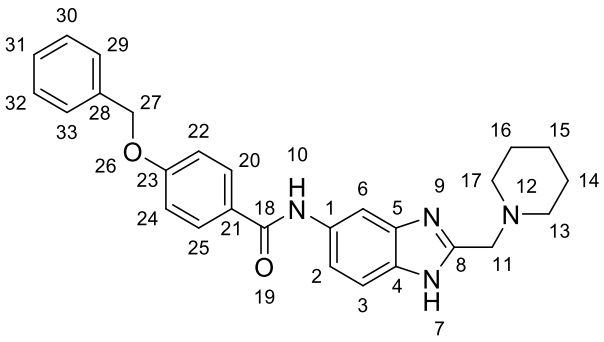

Synthesised according to general procedure **B** to give **366** (0.056 g, 0.127 mmol, 59%) as a white solid.

Mpt: 197.2-199.2 °C; **ν_{max} (cm^{-1})** 3242, 2932, 1642, 1603, 1548, 1507, 1408, 1313, 1244, 1175, 997, 839, 753, 697, 557; **^{1}H NMR (400 MHz, DMSO-*d*$_6$) δ**12.2 (s, 1H, 10), 10.1 (s, 1H, 7), 8.0 (s, 1H, 6), 8.0 – 7.9 (m, 2H, 20, 25), 7.6 – 7.3 (m, 7H, 2, 3, 29, 30, 31, 32, 33), 7.1 (d, *J* = 8.9 Hz, 2H, 22, 24), 5.2 (s, 2H, 27), 3.7 (s, 2H, 11), 2.5 – 2.3 (m, 4H, 13, 17), 1.6 – 1.5 (m, 4H, 14, 16), 1.4 – 1.4 (m, 2H, 15); **^{13}C NMR (101 MHz, DMSO-*d*$_6$) δ**164.6 (18), 160.8 (23), 136.7 (28), 129.5 (30, 32), 128.5 (20, 25), 128.0 (21), 127.8 (22, 24), 127.5 (2, 3), 114.4 (29, 31, 33), 69.4 (27), 56.6 (11), 54.1 (13, 17), 25.4 (14, 16), 23.7 (15); **LR-ESI-MS**: $C_{27}H_{29}N_4O_2$ $[M+H]^+$ *m/z* found 441.41, cald 441.23; **HR-ESI-MS**: $C_{27}H_{29}N_4O_2$ $[M+H]^+$ *m/z* found 441.2257, cald 441.2291.

5-chloro-*N*-(2-(piperidin-1-ylmethyl)-1H-benzo[d]imidazol-5-yl)picolinamide (367)

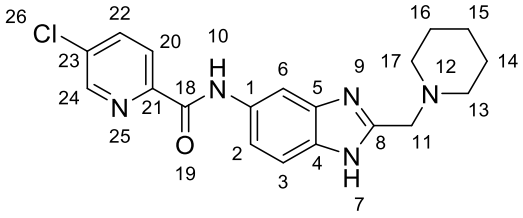

Synthesised according to general procedure **B** to give **367** (0.080 g, 0.217 mmol, 100%) as an off white solid.

Mpt: 147.4-149.4 °C; **ν_{max} (cm^{-1})** 2934, 1670, 1526, 1454, 1109, 1014, 556; **^{1}H NMR (400 MHz, DMSO-*d*$_6$) δ**8.2 (d, *J* = 2.0 Hz, 1H, 6), 2.7 – 2.5 (m, 4H), 10.6 (s, 1H, 7), 8.8 (dd, *J* = 1.0, 2.2 Hz, 1H, 24), 8.2 (dd, *J* = 1.6, 2.6 Hz, 2H, 20, 22), 7.6 (dd, *J* = 2.0, 8.7 Hz, 1H, 2), 7.5 (d, *J* = 8.7 Hz, 1H, 3), 3.9 (s, 2H, 11), 2.6 (t, *J* = 5.1 Hz, 4H, 13, 17), 1.6 (t, *J* = 5.7 Hz, 4H, 14, 16), 1.5 – 1.3 (m, 2H, 15); **^{13}C NMR (101 MHz, DMSO-*d*$_6$) δ**161.4 (18), 150.9 (8), 148.8 (24), 147.0 (21), 137.9 (22), 134.1 (23), 132.8 (5), 128.3 (1), 123.9 (20), 115.8 (2, 3), 55.7 (11), 53.8 (13, 17), 24.8 (14, 16), 23.2 (15); **LR-ESI-MS**: $C_{19}H_{21}ClN_5O$ $[M+H]^+$ *m/z* found 370.48, cald 370.14; **HR-ESI-MS**: $C_{19}H_{21}ClN_5O$ $[M+H]^+$ *m/z* found 370.1408, cald 370.1435.

***N*-(2-(piperidin-1-ylmethyl)-1H-benzo[d]imidazol-5-yl)-4-propoxybenzamide (368)**

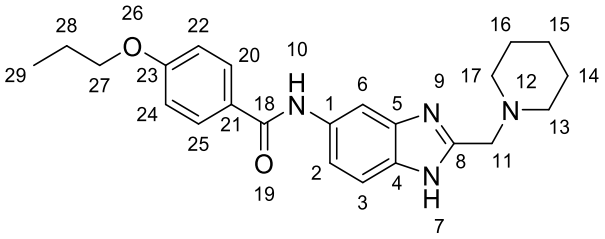

Synthesised according to general procedure **B** to give **368** (0.078 g, 0.199 mmol, 92%) as a white solid.

Mpt: 127.3-129.3 °C; **ν_{max} (cm^{-1})** 2934, 1603, 1247, 760, 555; **^{1}H NMR (400 MHz, DMSO-d_6) δ**12.2 (s, 1H, 10), 10.1 (s, 1H, 7), 8.1 (s, 1H, 6), 8.0 (d, *J* = 8.8 Hz, 2H, 20, 25), 7.4 (d, *J* = 1.3 Hz, 2H, 2, 3), 7.0 (d, *J* = 8.9 Hz, 2H, 22, 24), 4.0 (t, *J* = 6.5 Hz, 2H, 27), 3.7 (s, 2H, 11), 2.5 – 2.4 (m, 4H, 13, 17), 1.8 – 1.7 (m, 2H, 28), 1.5 (p, *J* = 5.5 Hz, 4H, 14, 16), 1.4 (p, *J* = 3.2, 4.6 Hz, 2H, 15), 1.0 (t, *J* = 7.4 Hz, 3H, 29); **^{13}C NMR (101 MHz, DMSO-d_6) δ**164.7 (18), 161.2 (23), 151.5 (8), 133.8 (1), 129.5 (20, 25), 127.1 (21), 115.7 (2), 114.0 (22, 24), 69.2 (27), 56.3 (11), 54.0 (13, 17), 25.2 (14, 16), 23.5 (15), 22.0 (28), 10.4 (29); **LR-ESI-MS**: $C_{23}H_{29}N_4O_2$ $[M+H]^+$ *m/z* found 393.58, cald 393.23; **HRS-ESI-MS**: $C_{23}H_{29}N_4O_2$ $[M+H]^+$ *m/z* found 393.2265, cald 393.2291.

***N*-(2-(piperidin-1-ylmethyl)-1H-benzo[d]imidazol-5-yl)thiophene-3-carboxamide (369)**

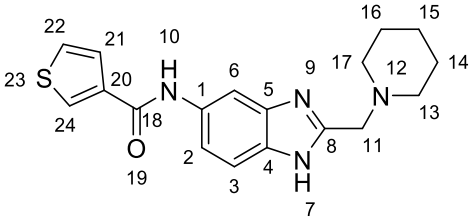

Synthesised according to general procedure **B** to give **369** (0.074 g, 0.217 mmol, 100%) as a white solid.

Mpt: 142.4-144.4 °C; **ν_{max} (cm^{-1})** 2933, 1639, 1530, 1417, 1273, 1104, 737, 555; **^{1}H NMR (400 MHz, DMSO-d_6) δ**12.3 (s, 1H, 10), 10.1 (s, 1H, 7), 8.4 (dd, *J* = 1.4, 2.8 Hz, 1H, 24), 8.1 (t, *J* = 1.4 Hz, 1H, 6), 7.7 – 7.6 (m, 2H, 21, 22), 7.5 (d, *J* = 1.3 Hz, 2H, 2, 3), 3.7 (s, 2H, 11), 2.5 (tt, *J* = 2.0, 4.8 Hz, 4H, 13, 17), 1.6 (p, *J* = 5.5 Hz, 4H, 14, 16), 1.4 (t, *J* = 4.7 Hz, 2H, 15); **^{13}C NMR (101 MHz, DMSO-d_6) δ**160.7 (18), 151.5 (8), 138.1 (22, 24), 133.5 (21), 129.4 (20), 127.3 (4), 126.8 (1), 115.7 (2, 3),

56.1 (11), 54.0 (13, 17), 25.1 (14, 16), 23.5 (15); **LR-ESI-MS**: $C_{18}H_{21}N_4OS$ $[M+H]^+$ *m/z* found 341.45, cald 341.14; **HR-ESI-MS**: $C_{18}H_{21}N_4OS$ $[M+H]^+$ *m/z* found 341.1412, cald 341.1436.

4-butyl-*N*-(2-(piperidin-1-ylmethyl)-1H-benzo[d]imidazol-5-yl)benzamide (370)

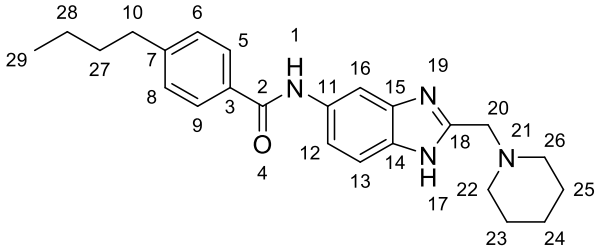

Synthesised according to general procedure **C** to give **370** (0.075 g, 0.192 mmol, 88%) as a white solid.

Mpt: 180.3-182.3 °C; **ν_{max} (cm^{-1})** 2929, 1430, 1106, 848, 808, 750, 604; **^{1}H NMR (400 MHz, DMSO-d_6) δ**12.2 (s, 1H, 1), 10.1 (s, 1H, 17), 8.1 (s, 1H, 16), 8.0 – 7.9 (m, 2H, 5, 9), 7.4 (s, 2H, 12, 13), 7.4 – 7.3 (m, 2H, 6, 8), 3.7 (s, 2H, 20), 2.7 (t, *J* = 7.7 Hz, 2H), 2.4 (d, *J* = 5.5 Hz, 4H, 22, 26), 1.6 – 1.5 (m, 6H, 23, 25, 27), 1.4 – 1.4 (m, 2H, 24), 1.3 (dt, *J* = 7.4, 14.8 Hz, 2H, 28), 0.9 (t, *J* = 7.3 Hz, 3H, 29); **^{13}C NMR (101 MHz, DMSO-d_6) δ**165.2 (2), 146.0 (7), 132.7 (14, 15), 128.2 (5, 9), 127.7 (6, 8), 56.6 (20), 54.1 (22, 26), 34.7 (10), 32.9 (27), 25.4 (23, 25), 23.8 (24), 21.7 (28), 13.8 (29); **LR-ESI-MS**: $C_{24}H_{31}N_4O$ $[M+H]^+$ *m/z* found 391.57, cald 391.25; **HR-ESI-MS**: $C_{24}H_{31}N_4O$ $[M+H]^+$ *m/z* found 391.2469, cald 391.2498.

***N*-(2-(piperidin-1-ylmethyl)-1H-benzo[d]imidazol-5-yl)-[1,1'-biphenyl]-4-carboxamide (303)**

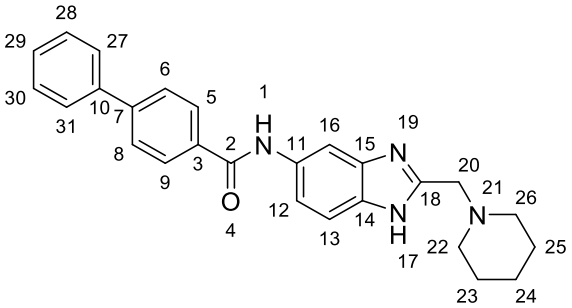

Synthesised according to general procedure **C** to give **303** (0.063 g, 0.153 mmol, 71%) as a white solid.

Mpt: 203.1-205.1 °C; **ν_{max} (cm^{-1})** 2931, 1641, 1598, 1530, 1483, 1418, 1299, 1107, 852, 694; **^{1}H NMR (400 MHz, DMSO-d_6) δ**12.3 (s, 1H, 1), 10.3 (s, 1H, 17), 8.1 – 8.0 (m, 3H, 5, 9, 16), 7.9 – 7.8 (m, 2H, 6, 8), 7.8 – 7.7 (m, 2H, 12, 13), 7.6 – 7.4 (m, 5H, 27, 28, 29, 30, 31), 3.7 (s, 2H, 20), 2.4 (t, *J* = 5.2 Hz, 4H, 22, 26), 1.5 (p, *J* = 5.5 Hz, 4H, 23, 25), 1.4 (q, *J* = 6.3 Hz, 2H, 24); **^{13}C NMR (101 MHz, DMSO-d_6) δ**164.9 (2), 142.9 (10), 139.2 (3), 134.0 (29), 129.9 (15), 129.1 (5, 9), 128.3 (28, 30), 128.1 (14), 126.9 (6, 8), 126.6 (27, 31), 56.7 (20), 54.2 (22, 26), 25.5 (23, 25), 23.8 (24); **LR-ESI-MS**: $C_{26}H_{27}N_4O$ $[M+H]^+$ *m/z* found 411.54, cald 411.22; **HR-ESI-MS**: $C_{26}H_{27}N_4O$ $[M+H]^+$ *m/z* found 411.2153, cald 411.2185.

4-butoxy-*N*-(2-(piperidin-1-ylmethyl)-1H-benzo[d]imidazol-5-yl)benzamide (371)

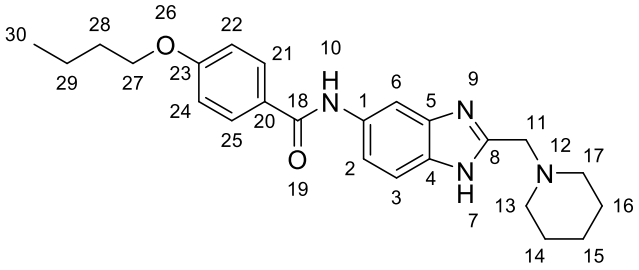

Synthesised according to general procedure **B** to give **371** (0.059 g, 0.145 mmol, 67%) as a white solid.

Mpt: 153.2-155.2 °C; **ν_{max} (cm^{-1})** 2931, 1604, 1506, 1430, 1305, 1248, 1176, 1109, 842; **^{1}H NMR (400 MHz, DMSO-d_6) δ**12.1 (s, 1H, 10), 10.1 (s, 1H, 7), 8.1 (s, 1H, 6), 8.0 (d, *J* = 8.8 Hz, 2H, 21, 25), 7.5 – 7.4 (m, 2H, 2, 3), 7.0 (d, *J* = 8.9 Hz, 2H, 22, 24), 4.1 (t, *J* = 6.5 Hz, 2H, 27), 3.7 (s, 2H, 11), 2.5 (d, *J* = 5.7 Hz, 4H, 13, 17), 1.7 (dq, *J* = 6.5, 8.5 Hz, 2H, 28), 1.5 (q, *J* = 5.6 Hz, 4H, 14, 16), 1.5 – 1.3 (m, 4H, 15, 29), 0.9 (t, *J* = 7.4 Hz, 3H, 30); **^{13}C NMR (101 MHz, DMSO-d_6) δ**164.7 (18), 161.2 (23), 129.5 (21, 25), 127.1 (20), 114.0 (22, 24), 67.4 (27), 56.4 (11), 54.1 (13, 17), 30.7 (28), 25.3 (14, 16), 23.6 (15), 18.7 (29), 13.7 (30); **LR-ESI-MS**: $C_{24}H_{31}N_4O_2$ $[M+H]^+$ *m/z* found 407.59, cald 407.25; **HR-ESI-MS**: $C_{24}H_{31}N_4O_2$ $[M+H]^+$ *m/z* found 407.2413, cald 407.2447.

***N*-(2-(((cis)-3,5-dimethylpiperidin-1-yl)methyl)-1H-benzo[d]imidazol-5-yl)-2-methylbenzo[d]oxazole-6-carboxamide (372)**

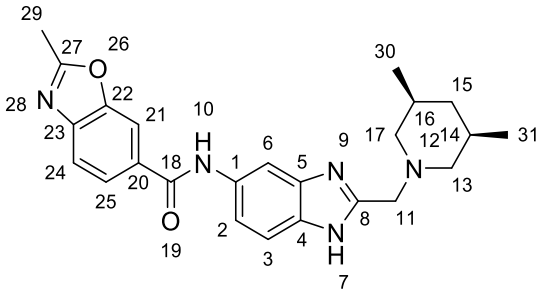

Synthesised according to general procedure **B** to give **372** (0.026 g, 0.062 mmol, 32%) as an off white solid.

Mpt: 143.8-145.8 °C; **ν_{max} (cm^{-1})** 2949, 2924, 1646, 1602, 1529, 1424, 1339, 1256, 738, 556; **^{1}H NMR (400 MHz, DMSO-d_6) δ**12.2 (s, 1H, 10), 10.3 (d, *J* = 20.4 Hz, 1H, 7), 8.3 (d, *J* = 1.6 Hz, 1H, 21), 8.1 – 7.9 (m, 2H, 6, 24), 7.8 (d, *J* = 8.3 Hz, 1H, 25), 7.5 (d, *J* = 8.3 Hz, 1H, 2), 7.5 – 7.4 (m, 1H, 3), 3.7 (s, 2H, 11'), 2.8 (dt, *J* = 2.3, 10.5 Hz, 2H, 13'', 17''), 2.7 (s, 3H, 29), 1.7 (dt, *J* = 3.9, 7.0 Hz, 3H, 13', 15', 17'), 1.6 (t, *J* = 10.7 Hz, 2H, 14, 16), 0.8 (d, *J* = 6.3 Hz, 6H, 30, 31), 0.6 – 0.4 (m, 1H, 15''); **^{13}C NMR (101 MHz, DMSO-d_6) δ**166.3 (27), 164.6 (18), 152.1 (8), 150.1 (22), 143.7 (23), 134.4 (5), 133.7 (4), 131.7 (20), 124.2 (24), 118.6 (25), 118.1 (2), 115.1 (3), 109.9 (21), 103.4 (6), 61.1 (13, 17), 56.2 (11), 41.6 (15), 30.6 (14, 16), 19.5 (29), 14.4 (30, 31); **LR-ESI-MS**: $C_{24}H_{28}N_5O_2$ $[M+H]^+$ *m/z* found 418.41, cald 418.22; **HR-ESI-MS**: $C_{24}H_{28}N_5O_2$ $[M+H]^+$ *m/z* found 418.2209, cald 418.2243.

4-chloro-*N*-(2-(((3R,5S)-3,5-dimethylpiperidin-1-yl)methyl)-1H-benzo[d]imidazol-5-yl)benzamide (313)

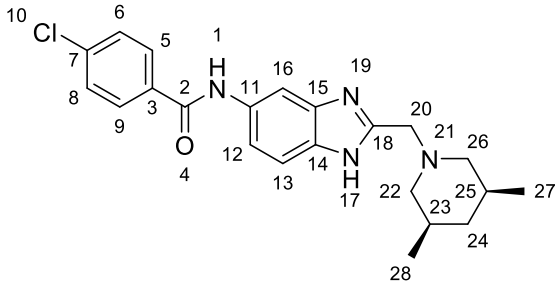

Synthesised according to general procedure **C** to give **313** (0.044 g, 0.111 mmol, 57%) as an off white solid.

Mpt: 142.2-144.2 °C; **ν_{max} (cm^{-1})** 2949, 2924, 1644, 1595, 1530, 1483, 1275, 1090, 1013, 843, 807, 749; **^{1}H NMR (400 MHz, DMSO-d_6) δ**12.3 (s, 1H, 1), 10.3 (s, 1H, 17), 8.0 (s, 1H, 16), 8.0 – 7.9 (m, 2H, 5, 9), 7.7 – 7.6 (m, 2H, 6, 8), 7.5 (d, *J* = 32.2 Hz, 2H, 12, 13), 3.7 (s, 2H, 20'), 2.8 – 2.7 (m, 2H, 22'', 26''), 1.7 – 1.6 (m, 3H, 22', 24', 26'), 1.5 (t, *J* = 10.7 Hz, 2H, 23, 25), 0.8 (d, *J* = 6.3 Hz, 6H, 27, 28), 0.5 (dt, *J* = 12.1, 14.0 Hz, 1H, 24''); **^{13}C NMR (101 MHz, DMSO-d_6) δ**164.1 (2), 136.2 (7), 133.9 (3), 129.6 (5, 9), 128.4 (6, 8), 61.1 (20), 56.1 (22, 26), 41.6 (24), 30.6 (23, 25), 19.5 (27, 28); **LR-ESI-MS**: $C_{22}H_{26}ClN_4O$ $[M+H]^+$ *m/z* found 397.48, cald 397.18; **HR-ESI-MS**: $C_{22}H_{26}ClN_4O$ $[M+H]^+$ *m/z* found 397.1768, cald 397.1795.

***N*-(2-(piperidin-1-ylmethyl)-1H-benzo[d]imidazol-5-yl)-4-(pyridin-4-yl)benzamide (304)**

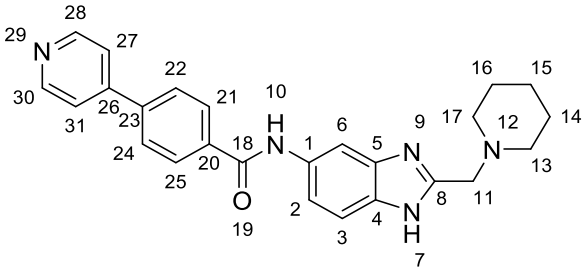

Synthesised according to general procedure **B** to give **304** (0.027 g, 0.066 mmol, 30%) as a white solid.

Mpt: >230 °C; **ν_{max} (cm^{-1})** 2931, 1645, 1597, 1534, 1483, 1414, 817, 757; **^{1}H NMR (400 MHz, DMSO-d_6) δ**12.3 (s, 1H, 10), 10.4 (s, 1H, 7), 8.7 – 8.6 (m, 2H, 28, 30), 8.2 – 8.0 (m, 3H, 6, 21, 25), 8.0 – 7.9 (m, 2H, 22, 24), 7.9 – 7.7 (m, 2H, 27, 31), 7.6 – 7.3 (m, 2H, 2, 3), 3.7 (s, 2H, 11), 2.4 (t, *J* = 5.3 Hz, 4H, 13, 17), 1.5 (p, *J* = 5.5 Hz, 4H, 14, 16), 1.4 (q, *J* = 6.2 Hz, 2H, 15); **^{13}C NMR (101 MHz, DMSO-d_6) δ**164.6 (18), 150.4 (28, 30), 146.0 (26), 139.8 (23), 135.7 (20), 128.5 (21, 25), 126.8 (22, 24), 121.4 (27, 31), 56.6 (11), 54.2 (13, 17), 25.5 (14, 16), 23.8 (15); **LR-ESI-MS**: $C_{25}H_{26}N_5O$ $[M+H]^+$ *m/z* found 412.40, cald 412.21; **HR-ESI-MS**: $C_{25}H_{26}N_5O$ $[M+H]^+$ *m/z* found 412.2106, cald 412.2137.

4-chloro-*N*-(2-(1-(piperidin-1-yl)ethyl)-1H-benzo[d]imidazol-5-yl)benzamide (297)

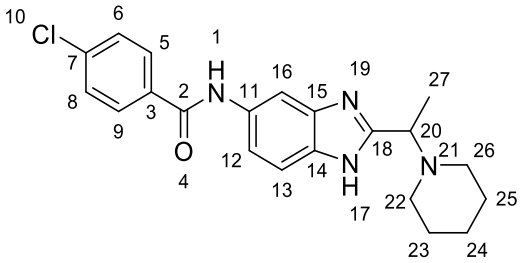

Synthesised according to general procedure **C** to give **297** (0.063 g, 0.165 mmol, 80%) as a white solid.

Mpt: 144.8-146.8 °C; **ν_{max} (cm^{-1})** 2932, 2851, 1595, 1526, 1449 1413, 1303, 1090, 843, 808, 750, 530; **^{1}H NMR (400 MHz, DMSO-*d*$_6$) δ**12.2 (s, 1H, 1), 10.3 (s, 1H, 17), 8.1 (s, 1H, 16), 8.0 (d, *J* = 8.6 Hz, 2H, 5, 9), 7.7 – 7.5 (m, 2H, 6, 8), 7.5 (d, *J* = 8.8 Hz, 2H, 12, 13), 3.9 (q, *J* = 6.8 Hz, 1H, 20), 2.5 (t, *J* = 5.2 Hz, 4H, 22, 26), 1.5 (t, *J* = 5.9 Hz, 4H, 23, 25), 1.4 (d, *J* = 6.9 Hz, 3H, 27), 1.4 – 1.3 (m, 2H, 24); **^{13}C NMR (101 MHz, DMSO-*d*$_6$) δ**164.2 (2), 136.2 (7), 133.9 (3), 131.2 (14), 129.6 (5, 9), 128.7 (15), 128.4 (6, 8), 58.5 (20), 50.3 (22, 26), 25.6 (23, 25), 24.0 (24), 14.5 (27); **LR-ESI-MS**: $C_{21}H_{24}ClN_4O$ $[M+H]^+$ *m/z* found 383.49, cald 383.16; **HR-ESI-MS**: $C_{21}H_{24}ClN_4O$ $[M+H]^+$ *m/z* found 383.1610, cald 383.1639.

***N*-(2-(1-(piperidin-1-yl)ethyl)-1H-benzo[d]imidazol-5-yl)-4-(trifluoromethyl)benzamide (373)**

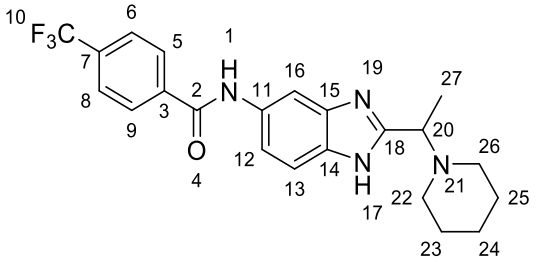

Synthesised according to general procedure **C** to give **373** (0.043 g, 0.103 mmol, 50%) as a white solid.

Mpt: 148.2-150.2 °C; **ν_{max} (cm^{-1})** 2933, 1648, 1547, 1450, 1322, 1165, 1064, 855, 688; **^{19}F NMR (376 MHz, DMSO-*d*$_6$) δ**-61.3; **^{1}H NMR (400 MHz, DMSO-*d*$_6$) δ**12.1 (s, 1H, 1), 10.5 (s, 1H, 16), 8.2 (d, *J* = 8.1 Hz, 2H, 6, 8), 8.1 (s, 1H, 15), 7.9 (d, *J* = 8.1 Hz, 2H, 5, 9), 7.5 (d, *J* = 17.6 Hz, 2H, 11, 12), 3.9 (d, *J* = 7.0 Hz, 1H, 19), 2.4 (s, 4H, 21, 25), 1.5 (q, *J* = 5.7 Hz, 4H, 22, 24), 1.4 (d, *J* = 6.9 Hz, 3H, 26), 1.4 (td, *J* = 4.7, 8.0, 9.0 Hz, 2H, 23); **^{13}C NMR (101 MHz, DMSO-*d*$_6$) δ**164.1 (2), 139.1 (3),

131.2 (q, *J* = 32.1 Hz, 27), 128.6 (5, 9), 125.4 (q, *J* = 3.7 Hz, 6, 8), 122.6 (7), 58.5 (19), 50.3 (21, 25), 25.7 (22, 24), 24.1 (23), 14.5 (26); **LR-ESI-MS**: $C_{22}H_{24}F_3N_4O$ $[M+H]^+$ *m/z* found 417.53, cald 417.19; **HR-ESI-MS**: $C_{22}H_{24}F_3N_4O$ $[M+H]^+$ *m/z* found 417.1875, cald 417.1902.

***N*-(2-(piperidin-1-ylmethyl)-1H-benzo[d]imidazol-5-yl)-2-naphthamide (374)**

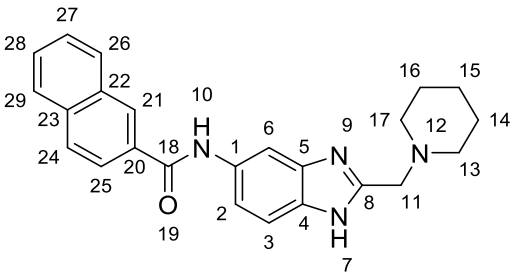

Synthesised according to general procedure **B** to give **374** (0.063 g, 0.164 mmol, 76%) as an off white solid.

Mpt: 135.7-137.7 °C; **ν_{max} (cm^{-1})** 2932, 1644, 1485, 1288, 773, 556, 474; **^{1}H NMR (400 MHz, DMSO-*d*$_6$) δ**12.3 (s, 1H, 10), 10.4 (s, 1H, 7), 8.6 (d, *J* = 1.5 Hz, 1H, 6), 8.2 – 7.9 (m, 5H, 21, 24, 25, 26, 29), 7.7 – 7.6 (m, 2H, 27, 28), 7.6 – 7.5 (m, 2H, 2, 3), 3.7 (s, 2H, 11), 2.5 (d, *J* = 5.2 Hz, 4H, 13, 17), 1.5 (p, *J* = 5.5 Hz, 4H, 14, 16), 1.4 (q, *J* = 4.6, 5.9 Hz, 2H, 15); **^{13}C NMR (101 MHz, DMSO-*d*$_6$) δ**165.8 (18), 134.7 (20), 133.0 (21), 132.6 (25), 129.4 (23), 128.4 (26), 128.3 (28), 128.2 (22), 128.1 (24), 127.3 (29), 125.0 (27), 56.9 (11), 54.5 (13, 17), 25.8 (14, 16), 24.1 (15); **LR-ESI-MS**: $C_{24}H_{25}N_4O$ $[M+H]^+$ *m/z* found 385.52, cald 385.20; **HR-ESI-MS**: $C_{24}H_{25}N_4O$ $[M+H]^+$ *m/z* found 385.1994, cald 385.2028.

***N*-(2-(piperidin-1-ylmethyl)-1H-benzo[d]imidazol-5-yl)quinoline-6-carboxamide (375)**

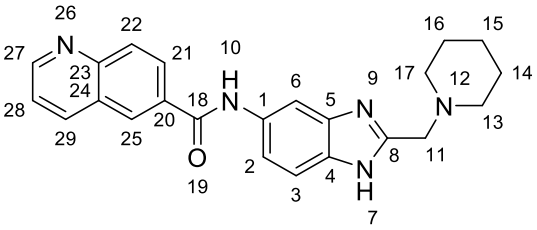

Synthesised according to general procedure **B** to give **375** (0.057 g, 0.148 mmol, 68%) as an off white solid.

Mpt: 166.5-168.5 °C; **ν_{max} (cm^{-1})** 2931, 1646, 1530, 1485, 1417, 1335, 781, 556; **^{1}H NMR (400 MHz, DMSO-d_6) δ**12.3 (s, 1H, 10), 10.5 (s, 1H, 7), 9.0 (dd, *J* = 1.7, 4.2 Hz, 1H, 29), 8.7 (d, *J* = 2.0 Hz, 1H, 25), 8.6 – 8.5 (m, 1H, 21), 8.3 (dd, *J* = 2.0, 8.8 Hz, 1H, 27), 8.1 (d, *J* = 8.8 Hz, 2H, 6, 22), 7.6 (dd, *J* = 4.2, 8.3 Hz, 1H, 28), 7.5 (s, 2H, 2, 3), 3.7 (s, 2H, 11), 2.4 (t, *J* = 5.3 Hz, 4H, 13, 17), 1.5 (q, *J* = 5.6 Hz, 4H, 14, 16), 1.4 (t, *J* = 5.5 Hz, 2H, 15); **^{13}C NMR (101 MHz, DMSO-d_6) δ**165.3 (18), 152.6 (27), 149.2 (29), 137.6 (25), 133.5 (21), 129.5 (22), 128.8 (20), 128.6 (24), 127.6 (28), 122.7 (23), 57.1 (11), 54.6 (13, 17), 25.9 (14, 16), 24.2 (15); **LR-ESI-MS**: $C_{23}H_{24}N_5O$ $[M+H]^+$ *m/z* found 386.52, cald 386.20; **HR-ESI-MS**: $C_{23}H_{24}N_5O$ $[M+H]^+$ *m/z* found 386.1948, cald 386.1981.

1-methyl-*N*-(2-(piperidin-1-ylmethyl)-1H-benzo[d]imidazol-5-yl)-1H-indazole-6-carboxamide (309)

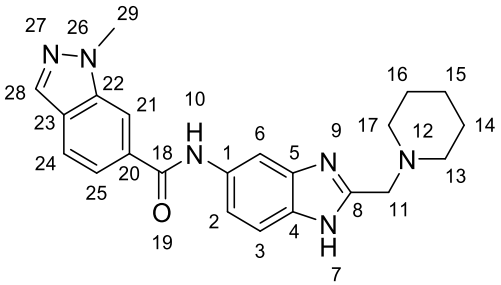

Synthesised according to general procedure **B** to give **309** (0.058 g, 0.151 mmol, 69%) as a white solid.

Mpt: 160.5-162.5 °C; **ν_{max} (cm^{-1})** 2932, 1644, 1527, 1450, 1250, 1108, 556; **^{1}H NMR (400 MHz, DMSO-d_6) δ**12.3 (s, 1H, 10), 10.3 (s, 1H, 7), 8.3 (q, *J* = 1.1 Hz, 1H, 28), 8.1 (d, *J* = 0.9 Hz, 1H, 21), 8.1 (s, 1H, 6), 7.9 (dd, *J* = 0.8, 8.4 Hz, 1H, 25), 7.7 (dd, *J* = 1.4, 8.5 Hz, 1H, 24), 7.5 (s, 2H, 2, 3), 4.1 (s, 3H, 29), 3.7 (s, 2H, 11), 2.4 (d, *J* = 5.5 Hz, 4H, 13, 17), 1.5 (q, *J* = 5.6 Hz, 4H, 14, 16), 1.4 (t, *J* = 5.9 Hz, 2H, 15); **^{13}C NMR (101 MHz, DMSO-d_6) δ**166.0 (18), 139.6 (28), 133.4 (25), 132.9 (21), 125.4 (24), 121.1 (20), 120.2 (23), 110.1 (22), 57.1 (11), 54.6 (13, 17), 36.1 (29), 25.9 (14, 16), 24.2 (15); **LR-ESI-MS**: $C_{22}H_{25}N_6O$ $[M+H]^+$ *m/z* found 389.58, cald 389.21; **HR-ESI-MS**: $C_{22}H_{25}N_6O$ $[M+H]^+$ *m/z* found 389.2063, cald 389.2090.

1-methyl-*N*-(2-(piperidin-1-ylmethyl)-1H-benzo[d]imidazol-5-yl)-1H-indazole-5-carboxamide (312)

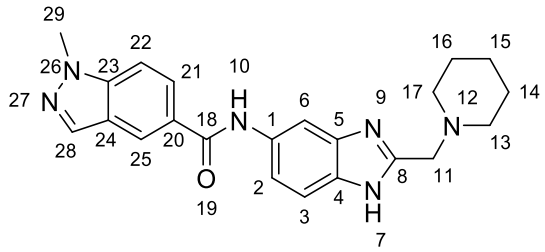

Synthesised according to general procedure **B** to give **312** (0.073 g, 0.188 mmol, 87%) as an off white solid.

Mpt: 162.2-164.2 °C; **ν_{max} (cm^{-1})** 2932, 1641, 1529, 1484, 1450, 1108, 838, 666; **^{1}H NMR (400 MHz, DMSO-d_6) δ**12.2 (s, 1H, 10), 10.3 (s, 1H, 7), 8.5 (dd, *J* = 0.8, 1.6 Hz, 1H, 25), 8.2 (d, *J* = 0.9 Hz, 1H, 28), 8.1 (s, 1H, 6), 8.0 (dd, *J* = 1.7, 8.8 Hz, 1H, 21), 7.8 (dt, *J* = 0.9, 8.9 Hz, 1H, 22), 7.5 (s, 2H, 2, 3), 4.1 (s, 3H, 29), 3.7 (s, 2H, 11), 2.5 – 2.3 (m, 4H, 13, 17), 1.5 (q, *J* = 5.6 Hz, 4H, 14, 16), 1.4 – 1.3 (m, 2H, 15); **^{13}C NMR (101 MHz, DMSO-d_6) δ**165.4 (18), 140.6 (28), 133.9 (23), 127.6 (20), 125.6 (25), 123.0 (21), 121.3 (24), 109.5 (22), 56.6 (11), 54.2 (13, 17), 35.6 (29), 25.4 (14, 16), 23.8 (15); **LR-ESI-MS**: $C_{22}H_{25}N_6O$ $[M+H]^+$ *m/z* found 389.51, cald 389.21; **HR-ESI-MS**: $C_{22}H_{25}N_6O$ $[M+H]^+$ *m/z* found 389.2065, cald 389.2090.

3-(1-methyl-1H-indol-5-yl)-*N*-(2-(piperidin-1-ylmethyl)-1H-benzo[d]imidazol-5-yl)propanamide (376)

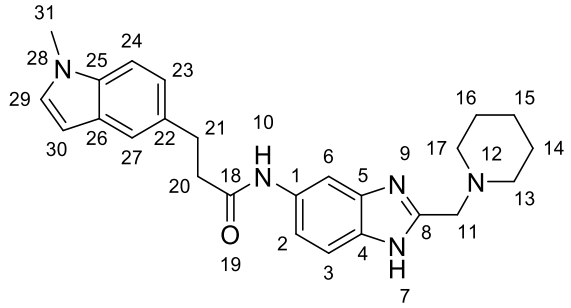

Synthesised according to general procedure **B** to give **376** (0.066 g, 0.159 mmol, 73%) as a white solid.

Mpt: 136.3-138.3 °C; **ν_{max} (cm^{-1})** 2932, 1656, 1529, 1488, 1447, 1335, 718, 556; **^{1}H NMR (400 MHz, DMSO-d_6) δ**12.2 (s, 1H, 10), 9.9 (s, 1H, 7), 8.0 – 7.9 (m, 1H, 6), 7.4 – 7.4 (m, 2H, 24, 27), 7.3 (d, *J* = 8.4 Hz, 1H, 2), 7.3 (d, *J* = 3.0 Hz, 1H, 29), 7.2 – 7.1 (m, 1H, 3), 7.1 (dd, *J* = 1.6, 8.4 Hz, 1H, 23), 6.3 (dd, *J* = 0.9, 3.1 Hz, 1H, 30), 3.7 (s, 3H, 31), 3.7 (s, 2H, 11), 3.0 (dd, *J* = 6.7, 8.7 Hz, 2H, 21),

2.6 (dd, *J* = 6.9, 8.6 Hz, 2H, 20), 2.4 (t, *J* = 5.3 Hz, 4H, 13, 17), 1.5 (t, *J* = 5.7 Hz, 4H, 14, 16), 1.5 – 1.3 (m, 2H, 15); **^{13}C NMR (101 MHz, DMSO-*d*$_6$) δ**170.3 (18), 135.1 (29), 131.6 (25), 129.6 (22), 128.2 (23), 121.9 (27), 119.4 (26), 109.5 (24), 99.9 (30), 56.5 (11), 54.1 (13, 17), 32.5 (31), 31.3 (21), 25.3 (14, 16), 23.7 (15), 18.8 (20); **LR-ESI-MS**: $C_{25}H_{30}N_5O$ $[M+H]^+$ *m/z* found 416.54, cald 416.25; **HR-ESI-MS**: $C_{25}H_{30}N_5O$ $[M+H]^+$ *m/z* found 416.2419, cald 416.2450.

4-chloro-*N*-(2-(2-(piperidin-1-yl)ethyl)-1H-benzo[d]imidazol-5-yl)benzamide (296)

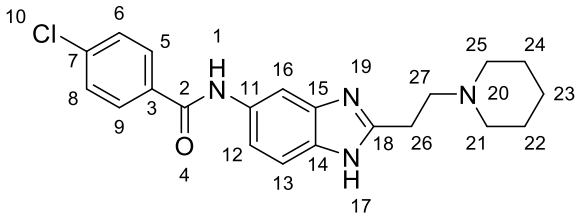

Synthesised according to general procedure **C** to give **296** (0.015 g, 0.04 mmol, 49%) as an off white solid.

Mpt: 124.7-126.7 °C; **ν_{max} (cm^{-1})** 3192, 2932, 1651, 1597, 1526, 1288, 1014, 810, 761, 656; **^{1}H NMR (400 MHz, DMSO-*d*$_6$) δ**12.0 (s, 1H, 1), 10.3 (s, 1H, 17), 8.1 – 8.0 (m, 3H, 5, 9, 16), 7.7 – 7.6 (m, 2H, 6, 8), 7.4 (d, *J* = 1.6 Hz, 2H, 12, 13), 3.0 (dd, *J* = 6.8, 8.4 Hz, 2H, 27), 2.8 (t, *J* = 7.6 Hz, 2H, 26), 2.5 – 2.4 (m, 4H, 21, 25), 1.5 (q, *J* = 5.6 Hz, 4H, 22, 24), 1.4 (q, *J* = 6.2 Hz, 2H, 23); **^{13}C NMR (101 MHz, DMSO-*d*$_6$) δ**164.1 (2), 154.0 (18), 136.2 (7), 133.9 (14, 15), 133.1 (3), 129.6 (5, 9), 128.4 (6, 8), 115.3 (12, 13), 56.5 (27), 53.6 (21, 25), 26.3 (26), 25.3 (22, 24), 23.8 (23); **LR-ESI-MS**: $C_{21}H_{24}ClN_4O$ $[M+H]^+$ *m/z* found 383.50, cald 383.16; **HR-ESI-MS**: $C_{21}H_{24}ClN_4O$ $[M+H]^+$ *m/z* found 383.1611, cald 383.1639.

***N*-(2-(piperidin-1-ylmethyl)-1H-benzo[d]imidazol-5-yl)-2,3-dihydrobenzofuran-5-carboxamide (377)**

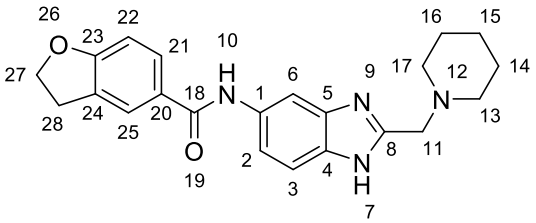

Synthesised according to general procedure **B** to give **377** (0.067 g, 0.178 mmol, 82%) as a white solid.

Mpt: 143.8-145.8 °C; **ν_{max} (cm^{-1})** 2932, 1640, 1608, 1528, 1484, 1241, 1106, 980, 839, 756, 556; **^{1}H NMR (400 MHz, DMSO-d_6) δ**12.2 (s, 1H, 10), 10.0 (s, 1H, 7), 8.0 (s, 1H, 6), 7.9 (d, *J* = 1.8 Hz, 1H, 25), 7.8 (dd, *J* = 2.0, 8.3 Hz, 1H, 21), 7.4 (s, 2H, 2, 3), 6.9 (d, *J* = 8.4 Hz, 1H, 22), 4.6 (t, *J* = 8.7 Hz, 2H, 27), 3.7 (s, 2H, 11), 3.3 (t, *J* = 8.7 Hz, 2H, 28), 2.4 (d, *J* = 5.4 Hz, 4H, 13, 17), 1.5 (q, *J* = 5.6 Hz, 4H, 14, 16), 1.4 (q, *J* = 6.0 Hz, 2H, 15); **^{13}C NMR (101 MHz, DMSO-d_6) δ**164.8 (18), 162.4 (23), 128.5 (25), 127.6 (21), 127.4 (20), 124.9 (24), 108.4 (22), 71.8 (27), 56.5 (11), 54.1 (13, 17), 28.6 (28), 25.4 (14, 16), 23.7 (15); **LR-ESI-MS**: $C_{22}H_{25}N_4O_2$ $[M+H]^+$ *m/z* found 377.54, cald 377.19; **HR-ESI-MS**: $C_{22}H_{25}N_4O_2$ $[M+H]^+$ *m/z* found 377.1955, cald 377.1978.

***N*-(2-(1-(piperidin-1-yl)ethyl)-1H-benzo[d]imidazol-5-yl)-4-(pyridin-4-yl)benzamide (378)**

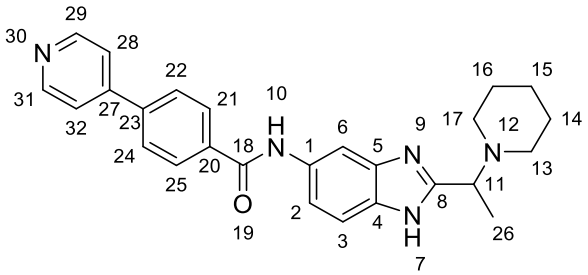

Synthesised according to general procedure **B** to give **378** (0.062 g, 0.146 mmol, 71%) as a white solid.

Mpt: 192.2-194.2 °C; **ν_{max} (cm^{-1})** 2933, 1650, 1599, 1544, 1485, 1302, 555; **^{1}H NMR (400 MHz, DMSO-d_6) δ**12.1 (s, 1H, 10), 10.3 (s, 1H, 7), 8.8 – 8.6 (m, 2H, 29, 31), 8.1 (t, *J* = 6.7 Hz, 3H, 6, 21, 25), 8.0 (d, *J* = 8.5 Hz, 2H, 22, 24), 7.8 – 7.7 (m, 2H, 28, 32), 7.5 (s, 2H, 2, 3), 3.9 (d, *J* = 7.2 Hz, 1H, 11), 2.5 – 2.4 (m, 4H, 13, 17), 1.5 (t, *J* = 5.8 Hz, 4H, 14, 16), 1.4 (d, *J* = 6.9 Hz, 3H, 26), 1.4 (dd, *J* = 3.8, 8.5 Hz, 2H, 15); **^{13}C NMR (101 MHz, DMSO-d_6) δ**164.7 (18), 150.4 (29, 31), 146.0 (27), 139.8 (23), 135.7 (20), 128.5 (21, 25), 126.8 (22, 24), 121.4 (28, 32), 58.6 (11), 50.3 (13, 17), 25.6 (14, 16), 24.0 (15), 14.5 (26). **LR-ESI-MS**: $C_{26}H_{28}N_5O$ $[M+H]^+$*m/z* found 426.61, cald 426.23; **HR-ESI-MS**: $C_{26}H_{28}N_5O$ $[M+H]^+$ *m/z* found 426.2260, cald 426.2294.

4-cyano-*N*-(2-(((3R,5S)-3,5-dimethylpiperidin-1-yl)methyl)-1H-benzo[d]imidazol-5-yl)benzamide (379)

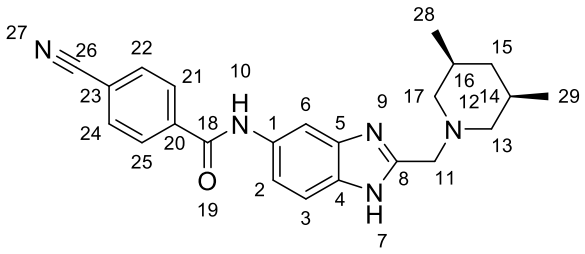

Synthesised according to general procedure **B** to give **379** (0.052 g, 0.134 mmol, 69%) as an off white solid.

Mpt: 148.3-150.3 °C; **ν_{max} (cm^{-1})** 2949, 2923, 2229, 1647, 1600, 1529, 1485, 1452, 1416, 1278, 806, 756, 568; **^{1}H NMR (400 MHz, DMSO-d_6) δ**12.3 (s, 1H, 10), 10.5 (s, 1H, 7), 8.2 – 8.1 (m, 2H, 21, 25), 8.1 (s, 1H, 6), 8.0 – 7.9 (m, 2H, 22, 24), 7.5 (d, *J* = 20.5 Hz, 2H, 2, 3), 3.7 (s, 2H, 11'), 2.9 – 2.7 (m, 2H, 13'', 17''), 1.7 (tt, *J* = 4.4, 5.8, 8.5 Hz, 3H, 13', 15', 17'), 1.5 (t, *J* = 10.7 Hz, 2H, 14, 16), 0.8 (d, *J* = 6.2 Hz, 6H, 28, 29), 0.5 (dt, *J* = 12.1, 13.9 Hz, 1H, 15''); **^{13}C NMR (101 MHz, DMSO-d_6) δ**163.8 (18), 139.3 (20), 132.5 (21, 25), 128.5 (22, 24), 118.4 (23), 113.7 (26), 61.1 (13, 17), 56.1 (11), 41.6 (15), 30.6 (14, 16), 19.5 (28, 29); **LR-ESI-MS**: $C_{23}H_{26}N_5O$ $[M+H]^+$ *m/z* found 388.57, cald 388.21; **HR-ESI-MS**: $C_{23}H_{26}N_5O$ $[M+H]^+$ *m/z* found 388.2113, cald 388.2137.

4-(benzyloxy)-*N*-(2-(((cis)-3,5-dimethylpiperidin-1-yl)methyl)-1H-benzo[d]imidazol-5-yl)benzamide (380)

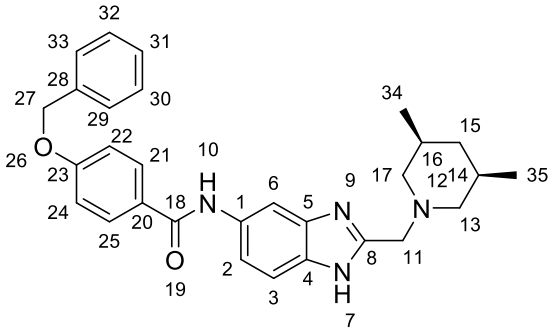

Synthesised according to general procedure **B** to give **380** (0.035 g, 0.075 mmol, 39%) as an off white solid.

Mpt: >225 °C; **ν_{max} (cm^{-1})** 2922, 1641, 1603, 1452, 1174, 1000, 734, 695, 613; **^{1}H NMR (400 MHz, DMSO-d_6) δ**12.2 (s, 1H, 10), 10.1 (s, 1H, 7), 8.1 (s, 1H, 6), 8.0 (d, *J* = 8.8 Hz, 2H, 21, 25), 7.5 – 7.3

(m, 7H, 2, 3, 29, 30, 31, 32, 33), 7.2 – 7.0 (m, 2H, 22, 24), 5.2 (s, 2H, 27''), 3.7 (s, 2H, 11'), 2.9 – 2.7 (m, 2H, 13'', 17''), 1.8 – 1.6 (m, 3H, 13', 15'', 17'), 1.5 (t, *J* = 10.7 Hz, 2H, 14, 16), 0.8 (d, *J* = 6.3 Hz, 6H, 34, 35), 0.6 – 0.4 (m, 1H, 15'); **^{13}C NMR (101 MHz, DMSO-d_6) δ**164.6 (18), 160.8 (23), 136.7 (28), 129.5 (21, 25), 128.5 (30, 32), 128.0 (31), 127.8 (29, 33), 127.5 (20), 114.4 (22, 24), 69.4 (27), 61.1 (13, 17), 56.1 (11), 41.6 (15), 30.6 (14, 16), 19.5 (34, 35); **LR-ESI-MS**: $C_{29}H_{33}N_4O_2$ $[M+H]^+$ *m/z* found 469.41, cald 469.26; **HR-ESI-MS**: $C_{29}H_{33}N_4O_2$ $[M+H]^+$ *m/z* found 469.2570, cald 469.2604.

N-(2-(((cis)-3,5-dimethylpiperidin-1-yl)methyl)-1H-benzo[d]imidazol-5-yl)-1-methyl-1H-indazole-5-carboxamide (320)

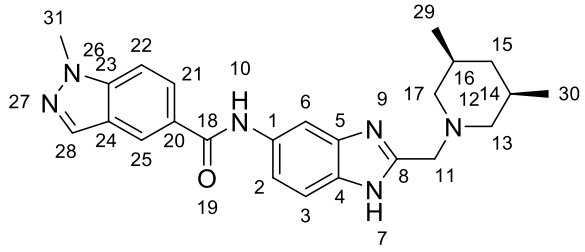

Synthesised according to general procedure **B** to give **320** (0.039 g, 0.094 mmol, 48%) as a white solid.

Mpt: 156.6-158.6 °C; **ν_{max} (cm^{-1})** 2948, 2923, 1599, 1484, 1339, 1250, 1191, 843, 622; **^{1}H NMR (400 MHz, DMSO-d_6) δ**12.2 (s, 1H, 10), 10.3 (s, 1H, 7), 8.5 (dd, *J* = 0.8, 1.7 Hz, 1H, 28), 8.2 (d, *J* = 0.9 Hz, 1H, 25), 8.1 (s, 1H, 6), 8.0 (dd, *J* = 1.6, 8.9 Hz, 1H, 21), 7.8 (dt, *J* = 0.9, 8.9 Hz, 1H, 22), 7.5 (s, 2H, 2, 3), 4.1 (s, 3H, 31), 3.7 (s, 2H, 11), 2.8 (dt, *J* = 2.3, 10.6 Hz, 2H, 13'', 17''), 1.8 – 1.6 (m, 3H, 13', 15'', 17'), 1.6 (t, *J* = 10.7 Hz, 2H, 14, 16), 0.8 (d, *J* = 6.3 Hz, 6H, 29, 30), 0.6 – 0.4 (m, 1H, 15'); **^{13}C NMR (101 MHz, DMSO-d_6) δ**165.4 (18), 140.6 (23), 133.9 (21), 127.6 (28), 125.6 (25), 123.0 (24), 121.3 (20), 109.5 (22), 61.1 (13, 17), 56.1 (11), 41.6 (31), 35.6 (15), 30.6 (14, 16), 19.5 (29, 30); **LR-ESI-MS**: $C_{24}H_{29}N_6O$ $[M+H]^+$ *m/z* found 417.42, cald 417.24; **HR-ESI-MS**: $C_{24}H_{29}N_6O$ $[M+H]^+$ *m/z* found 417.2367, cald 417.2403.

3-(*N*-(4-chlorobenzyl)sulfamoyl)-4-methoxy-*N*-(2-(piperidin-1-ylmethyl)-1H-benzo[d]imidazol-5-yl)benzamide (381)

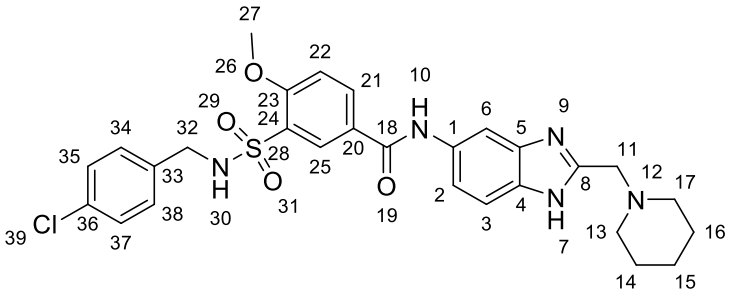

Synthesised according to general procedure **B** to give **381** (0.066 g, 0.116 mmol, 54%) as a clear oil.

ν_{max} (cm^{-1}) 2933, 1647, 1600, 1488, 1322, 1267, 1150, 1066, 842, 556; **^{1}H NMR (400 MHz, DMSO-d_6) δ**12.2 (s, 1H), 10.3 (s, 1H), 8.3 (d, *J* = 2.3 Hz, 1H, 25), 8.2 (dd, *J* = 2.3, 8.7 Hz, 1H, 21), 8.1 – 8.0 (m, 2H, 6), 7.5 – 7.4 (m, 2H, 35, 37), 7.3 – 7.1 (m, 5H, 2, 3, 22, 34, 38), 4.1 (d, *J* = 6.3 Hz, 2H, 32), 3.9 (s, 3H, 27), 3.7 (s, 2H, 11), 2.5 – 2.4 (m, 4H, 13, 17), 1.5 (p, *J* = 5.5 Hz, 4H, 14, 16), 1.4 – 1.4 (m, 2H, 15); **^{13}C NMR (101 MHz, DMSO-d_6) δ**163.6 (18), 158.3 (23), 136.9 (36), 133.7 (25), 131.6 (21), 129.4 (35, 37), 129.2 (20), 128.1 (33), 127.9 (34, 38), 126.6 (24), 112.3 (22), 56.5 (11), 56.3 (27), 54.1 (13, 17), 45.4 (32), 25.6 (14, 16), 23.8 (15); **LR-ESI-MS**: $C_{28}H_{31}ClN_5O_4S$ $[M+H]^+$ *m/z* found 568.58, cald 568.18; **HR-ESI-MS**: $C_{28}H_{31}ClN_5O_4S$ $[M+H]^+$ *m/z* found 569.3997, cald 568.1785.

***N*-(2-((2-methylpyrrolidin-1-yl)methyl)-1H-benzo[d]imidazol-5-yl)-4-(pyridin-4-yl)benzamide (382)**

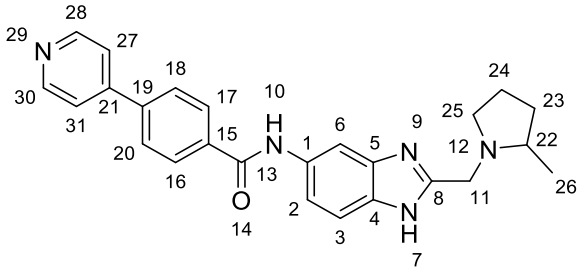

Synthesised according to general procedure **B** to give **382** (0.017 g, 0.042 mmol, 19%) as a white solid.

Mpt: 222.0-224.0 °C; **ν_{max} (cm^{-1})** 2962, 2787, 1641, 1549, 1408, 1307, 809, 758, 557; **^{1}H NMR (400 MHz, DMSO-d_6) δ**12.2 (s, 1H, 10), 10.3 (s, 1H, 7), 8.7 – 8.6 (m, 2H, 28, 30), 8.2 – 8.1 (m, 2H, 16, 17), 8.1 (s, 1H, 6), 8.0 – 7.9 (m, 2H, 18, 20), 7.9 – 7.8 (m, 2H, 27, 31), 7.5 (s, 2H, 2, 3), 4.1 (d, *J* = 14.2 Hz, 1H, 11''), 3.6 (d, *J* = 14.2 Hz, 1H, 11'), 3.0 (d, *J* = 9.5 Hz, 1H, 22), 2.7 – 2.5 (m, 1H, 25'),

2.3 (d, *J* = 9.0 Hz, 1H, 25''), 2.0 – 1.9 (m, 1H, 23''), 1.8 – 1.6 (m, 2H, 23', 24''), 1.5 – 1.3 (m, 1H, 24'), 1.2 – 1.0 (m, 3H, 26); **^{13}C NMR (101 MHz, DMSO-d_6) δ**164.7 (13), 150.4 (28, 30), 146.0 (21), 139.8 (19), 135.7 (15), 128.5 (16, 17), 126.8 (18, 20), 121.4 (27, 31), 59.3 (11), 54.0 (22), 50.8 (25), 32.4 (23), 21.4 (24), 18.7 (26); **LR-ESI-MS**: $C_{25}H_{26}N_5O$ $[M+H]^+$ *m/z* found 412.56, cald 412.21; **HR-ESI-MS**: $C_{25}H_{26}N_5O$ $[M+H]^+$ *m/z* found 412.2102, cald 412.2137.

1-methyl-*N*-(2-((2-methylpyrrolidin-1-yl)methyl)-1H-benzo[d]imidazol-5-yl)-1H-indazole-5-carboxamide (319)

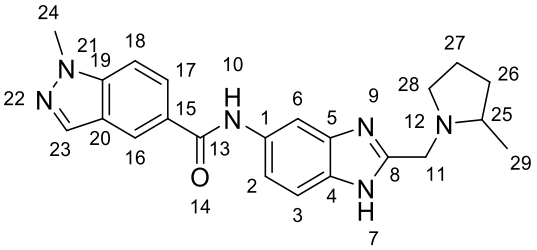

Synthesised according to general procedure **B** to give **319** (0.075 g, 0.193 mmol, 89%) as a white solid.

Mpt: 179.4-181.4 °C; **ν_{max} (cm^{-1})** 2962, , 1619, 1485, 1450, 1192, 836, 759, 555; **^{1}H NMR (400 MHz, DMSO-d_6) δ**10.3 (s, 1H, 7), 8.5 (dd, *J* = 0.8, 1.7 Hz, 1H, 6), 8.2 (d, *J* = 0.9 Hz, 1H, 16), 8.1 (dd, *J* = 0.8, 1.7 Hz, 1H, 23), 8.0 (dd, *J* = 1.6, 8.8 Hz, 1H, 17), 7.8 – 7.7 (m, 1H, 18), 7.6 – 7.4 (m, 2H, 2, 3), 4.2 (d, *J* = 14.2 Hz, 1H, 11''), 4.1 (s, 3H, 24), 3.7 (d, *J* = 14.2 Hz, 1H, 11'), 3.1 (ddd, *J* = 4.0, 7.3, 9.6 Hz, 1H, 25), 2.8 – 2.6 (m, 1H, 28''), 2.5 (s, 1H, 28'), 2.0 – 1.9 (m, 1H, 26''), 1.8 – 1.6 (m, 2H, 26', 27'), 1.5 – 1.4 (m, 1H, 27''), 1.1 (d, *J* = 6.1 Hz, 3H, 29); **^{13}C NMR (101 MHz, DMSO-d_6) δ**165.5 (13), 151.6 (8), 140.7 (23), 134.9 – 133.5 (4, 19), 127.9 (20), 127.6 (16), 125.7 (17), 123.0 (15), 121.4 (1), 119.6 (2), 115.8 (3), 109.5 (6, 18), 59.8 (11), 53.9 (25), 50.4 (28), 35.6 (24), 32.2 (26), 21.3 (27), 18.2 (29); **LR-ESI-MS**: $C_{22}H_{25}N_6O$ $[M+H]^+$ *m/z* found 389.50, cald 389.21; **HR-ESI-MS**: $C_{22}H_{25}N_6O$ $[M+H]^+$ *m/z* found 389.2062, cald 389.2090.

4-((6-methylpyrazin-2-yl)oxy)-*N*-(2-((2-methylpyrrolidin-1-yl)methyl)-1H-benzo[d]imidazol-5-yl)benzamide (331)

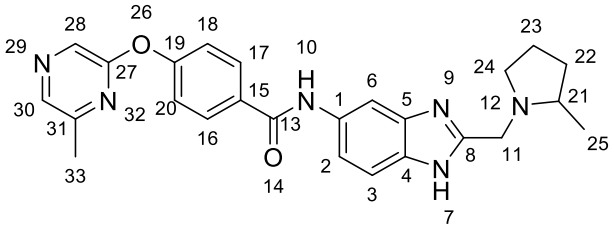

Synthesised according to general procedure **B** to give **331** (0.053 g, 0.120 mmol, 55%) as an off white solid .

Mpt: 101.3-103.3 °C; **ν_{max} (cm^{-1})** 2962, 1646, 1532, 1400, 1290, 1249, 1167, 837, 555; **^{1}H NMR (400 MHz, DMSO-d_6) δ**10.3 (s, 1H, 7), 8.4 – 8.3 (m, 2H, 28, 30), 8.1 – 8.1 (m, 1H, 6), 8.1 – 8.0 (m, 2H, 16, 17), 7.5 (d, *J* = 1.9 Hz, 2H, 2, 3), 7.4 – 7.3 (m, 2H, 18, 20), 4.2 (d, *J* = 14.3 Hz, 1H, 11''), 3.7 (d, *J* = 14.2 Hz, 1H, 11'), 3.1 (q, *J* = 4.0, 7.0 Hz, 1H, 21), 2.8 – 2.7 (m, 1H, 24''), 2.4 (s, 3H, 33), 2.1 – 1.9 (m, 1H, 24'), 1.8 – 1.6 (m, 2H, 22'', 23''), 1.5 – 1.4 (m, 1H, 22'), 1.3 – 1.1 (m, 4H, 23', 25); **^{13}C NMR (101 MHz, DMSO-d_6) δ**164.6 (13), 158.3 (27), 155.7 (31), 151.1 (8), 138.9 (28, 30), 132.4 (4), 131.8 (5), 131.3 (15), 129.6 (16, 17), 120.6 (18, 20), 60.0 (21), 54.0 (11), 50.4 (24), 32.1 (22), 21.3 (23), 20.6 (33), 18.1 (25); **LR-ESI-MS**: $C_{25}H_{27}N_6O_2$ $[M+H]^+$ *m/z* found 443.52, cald 443.22; **HR-ESI-MS**: $C_{25}H_{27}N_6O_2$ $[M+H]^+$ *m/z* found 443.2161, cald 443.2195.

***N*-(2-((2-methylpyrrolidin-1-yl)methyl)-1H-benzo[d]imidazol-5-yl)-1H-indazole-5-carboxamide (333)**

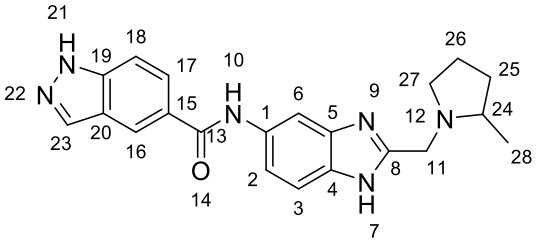

Synthesised according to general procedure **B** to give **333** (0.018 g, 0.048 mmol, 22%) as a white solid.

Mpt: 197.8-199.8 °C; **ν_{max} (cm^{-1})** 3129, 1623, 1530, 1485, 1376, 942, 843; **^{1}H NMR (400 MHz, DMSO-d_6) δ**13.4 (s, 1H, 21), 12.2 (s, 1H, 10), 10.3 (s, 1H, 7), 8.6 – 8.4 (m, 1H, 23), 8.3 – 8.2 (m, 1H, 16), 8.1 (s, 1H, 6), 8.0 (ddd, *J* = 1.6, 8.8, 23.1 Hz, 1H, 17), 7.7 – 7.6 (m, 1H, 18), 7.5 – 7.4 (m, 2H, 2, 3), 4.1 (d, *J* = 14.1 Hz, 1H, 11''), 3.6 (d, *J* = 14.1 Hz, 1H, 11'), 2.9 (ddd, *J* = 3.4, 7.5, 9.1 Hz,

1H, 24), 2.5 (s, 1H, 27''), 2.3 (q, *J* = 8.8 Hz, 1H, 27'), 2.0 – 1.9 (m, 1H, 25''), 1.7 (dtd, *J* = 2.4, 5.3, 5.8, 14.8 Hz, 2H, 25', 26''), 1.4 – 1.3 (m, 1H, 26'), 1.1 (d, *J* = 6.0 Hz, 3H, 28); **^{13}C NMR (101 MHz, DMSO-d_6) δ**165.6 (13), 127.6 (16), 126.7 (20), 125.7 (17), 123.7 (15), 122.3 (23), 121.1 (2), 109.9 (18), 59.1 (11), 54.0 (24), 50.9 (27), 32.5 (25), 21.4 (26), 18.8 (28); **LR-ESI-MS**: $C_{21}H_{23}N_6O$ $[M+H]^+$ *m/z* found 375.49, cald 375.19; **HR-ESI-MS**: $C_{21}H_{23}N_6O$ $[M+H]^+$ *m/z* found 375.1905, cald 375.1933.

***N*$_1$-isopropyl-*N*$_4$-(2-(piperidin-1-ylmethyl)-1H-benzo[d]imidazol-5-yl)terephthalamide (383)**

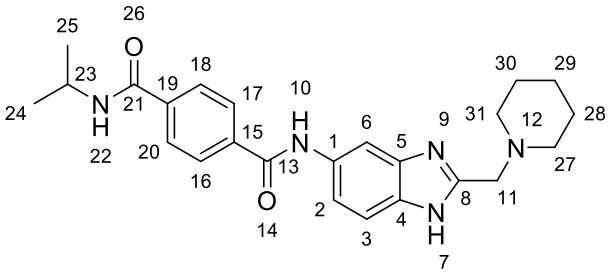

Synthesised according to general procedure **B** to give **383** (0.055 g, 0.131 mmol, 60%) as an off white solid.

Mpt: 186.6-188.6 °C; **ν_{max} (cm^{-1})** 2933, 1633, 1531, 1279, 1172, 840, 555; **^{1}H NMR (400 MHz, DMSO-d_6) δ**12.2 (s, 1H, 10), 10.3 (s, 1H, 7), 8.4 (d, *J* = 7.8 Hz, 1H, 22), 8.1 – 8.0 (m, 3H, 6, 16, 17), 8.0 – 7.9 (m, 2H, 18, 20), 7.5 (s, 2H, 2, 3), 4.1 (dt, *J* = 6.5, 7.8 Hz, 1H, 23), 3.7 (s, 2H, 11), 2.4 (d, *J* = 6.0 Hz, 4H, 27, 31), 1.5 (p, *J* = 5.4 Hz, 4H, 28, 30), 1.5 – 1.3 (m, 2H, 29), 1.2 (d, *J* = 6.6 Hz, 6H, 24, 25); **^{13}C NMR (101 MHz, DMSO-d_6) δ**164.7 (21), 164.6 (13), 137.2 (15, 19), 127.5 (16, 17), 127.3 (18, 20), 56.5 (11), 54.1 (27, 31), 41.2 (23), 25.3 (28, 30), 23.7 (29), 22.3 (24, 25); **LR-ESI-MS**: $C_{24}H_{30}N_5O_2$ $[M+H]^+$ *m/z* found 420.57, cald 420.24; **HR-ESI-MS**: $C_{24}H_{30}N_5O_2$ $[M+H]^+$ *m/z* found 420.2367, cald 420.2400.

***N*-(2-(piperidin-1-ylmethyl)-1H-benzo[d]imidazol-5-yl)-1H-indole-6-carboxamide (384)**

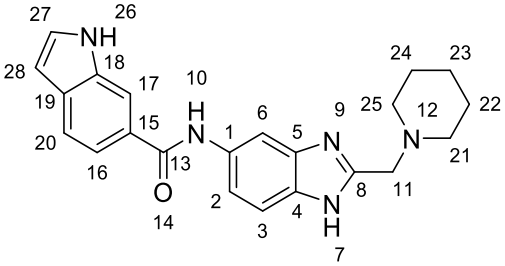

Synthesised according to general procedure **B** to give **384** (0.065 g, 0.174 mmol, 80%) as an off white solid.

Mpt: >215.0 °C; **ν_{max} (cm^{-1})** 3399, 3150, 2934, 1623, 1526, 1451, 1107, 831, 555; **^{1}H NMR (400 MHz, DMSO-d_6) δ**11.5 (t, *J* = 2.3 Hz, 1H, 26), 10.2 (s, 1H, 7), 8.1 (dd, *J* = 1.6, 8.5 Hz, 2H, 6, 27), 7.7 – 7.6 (m, 2H, 16, 17), 7.6 – 7.4 (m, 3H, 2, 3, 20), 6.5 (ddd, *J* = 0.9, 1.9, 3.0 Hz, 1H, 28), 3.7 (s, 2H, 11), 2.5 (dt, *J* = 3.7, 9.2 Hz, 4H, 21, 25), 1.5 (t, *J* = 5.7 Hz, 4H, 22, 24), 1.5 – 1.3 (m, 2H, 23); **^{13}C NMR (101 MHz, DMSO-d_6) δ**167.7 (13), 153.0 (8), 136.7 (1), 135.6 (5), 131.5 (27), 129.7 (4), 129.3 (15), 120.9 (16), 119.9 (17), 117.1 (2, 3, 6), 113.1 (20), 102.8 (28), 57.7 (11), 55.5 (21, 25), 26.6 (22, 24), 25.0 (23); **LR-ESI-MS**: $C_{22}H_{24}N_5O$ $[M+H]^+$ *m/z* found 374.35, cald 374.19; **HR-ESI-MS**: $C_{22}H_{24}N_5O$ $[M+H]^+$ *m/z* found 374.1958, cald 374.1981.

4-cyclopropyl-*N*-(2-(piperidin-1-ylmethyl)-1H-benzo[d]imidazol-5-yl)benzamide (385)

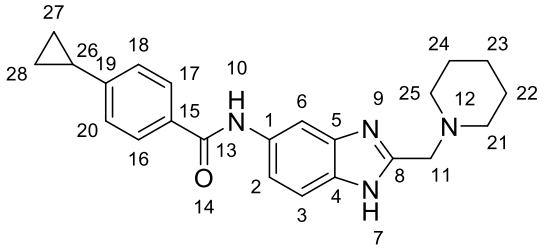

Synthesised according to general procedure **B** to give **385** (0.056 g, 0.150 mmol, 69%) as an off white solid.

Mpt: 147.8-149.8 °C; **ν_{max} (cm^{-1})** 2934, 1609, 1451, 837, 555; **^{1}H NMR (400 MHz, DMSO-d_6) δ**12.3 (s, 1H, 10), 10.1 (s, 1H, 7), 8.1 (t, *J* = 1.4 Hz, 1H, 6), 7.9 (d, *J* = 8.4 Hz, 2H, 16, 17), 7.5 (d, *J* = 1.3 Hz, 2H, 2, 3), 7.2 (d, *J* = 8.4 Hz, 2H, 18, 20), 3.8 (s, 2H, 11), 2.5 (p, *J* = 1.9 Hz, 4H, 21, 25), 2.0 (tt, *J* = 5.0, 8.3 Hz, 1H, 26), 1.5 (q, *J* = 5.6 Hz, 4H, 22, 24), 1.4 (d, *J* = 6.1 Hz, 2H, 23), 1.1 – 1.0 (m, 2H, 27', 28'), 0.8 – 0.7 (m, 2H, 27'', 28''); **^{13}C NMR (101 MHz, DMSO-d_6) δ**165.1 (13), 151.4 (8), 147.8 (19), 133.7 (6), 132.1 (4, 5), 127.7 (16, 17), 125.1 (18, 20), 115.7 (2, 3), 56.1 (11), 54.0 (21, 25), 25.1 (22, 24), 23.5 (23), 15.2 (26), 10.2 (27, 28); **LR-ESI-MS**: $C_{23}H_{27}N_4O$ $[M+H]^+$ *m/z* found 375.38, cald 375.22; **HR-ESI-MS**: $C_{23}H_{27}N_4O$ $[M+H]^+$ *m/z* found 375.2158, cald 375.2185.

4-(1H-imidazol-1-yl)-*N*-(2-(piperidin-1-ylmethyl)-1H-benzo[d]imidazol-5-yl)benzamide (307)

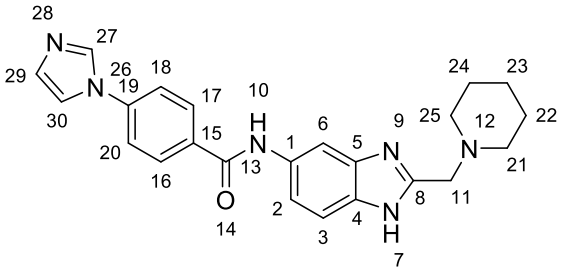

Synthesised according to general procedure **B** to give **307** (0.013 g, 0.032 mmol, 15%) as a clear yellow oil.

ν_{max} (cm^{-1}) 3116, 2932, 1646, 1552, 1484, 1301, 1248, 1055, 809; **^{1}H NMR (400 MHz, DMSO-d_6) δ**12.3 (s, 1H, 10), 10.3 (s, 1H, 7), 8.4 (d, *J* = 1.2 Hz, 1H, 27), 8.2 – 8.1 (m, 2H, 16, 17), 8.1 (s, 1H, 6), 7.9 (t, *J* = 1.5 Hz, 1H, 29), 7.9 – 7.8 (m, 2H, 18, 20), 7.5 (s, 2H, 2, 3), 7.3 – 7.1 (m, 1H, 30), 3.7 (s, 2H, 11), 2.5 – 2.3 (m, 4H, 21, 25), 1.5 (q, *J* = 5.6 Hz, 4H, 22, 24), 1.4 (q, *J* = 6.0 Hz, 2H, 23); **^{13}C NMR (101 MHz, DMSO-d_6) δ**164.2 (13), 139.0 (19), 135.7 (27), 133.1 (15), 130.3 (29), 129.4 (16, 17), 119.5 (18, 20), 117.9 (30), 56.6 (11), 54.1 (21, 25), 25.4 (22, 24), 23.8 (23); **LR-ESI-MS**: $C_{23}H_{25}N_6O$ $[M+H]^+$ *m/z* found 401.63, cald 401.21; **HR-ESI-MS**: $C_{23}H_{25}N_6O$ $[M+H]^+$ *m/z* found 401.2056, cald 401.2090.

4-((1H-pyrrol-1-yl)methyl)-*N*-(2-(piperidin-1-ylmethyl)-1H-benzo[d]imidazol-5-yl)benzamide (386)

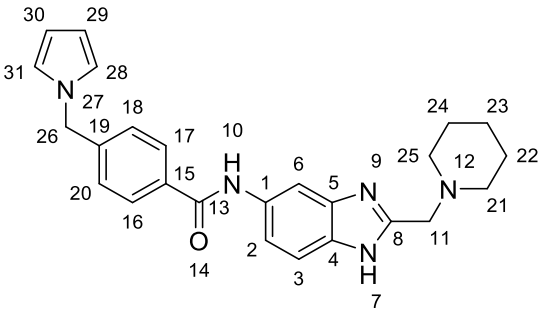

Synthesised according to general procedure **B** to give **386** (0.027 g, 0.064 mmol, 30%) as a clear oil.

ν_{max} (cm^{-1}) 2933, 1644, 1529, 1417, 1276, 842, 719, 556; **^{1}H NMR (400 MHz, DMSO-d_6) δ**12.2 (s, 1H, 10), 10.2 (s, 1H, 7), 8.0 (s, 1H, 6), 8.0 – 7.9 (m, 2H, 18, 20), 7.4 (s, 2H, 2, 3), 7.3 – 7.2 (m, 2H, 16, 17), 6.8 (t, *J* = 2.1 Hz, 2H, 28, 31), 6.0 (t, *J* = 2.1 Hz, 2H, 29, 30), 5.2 (s, 2H, 26), 3.7 (s, 2H, 11),

2.5 – 2.3 (m, 4H, 21, 25), 1.5 (p, *J* = 5.5 Hz, 4H, 22, 24), 1.4 (t, *J* = 6.0 Hz, 2H, 23); **^{13}C NMR (101 MHz, DMSO-d_6) δ**165.0 (13), 142.5 (19), 134.3 (15), 127.9 (16, 17), 127.0 (18, 20), 121.1 (28, 31), 108.2 (29, 30), 56.5 (11), 54.1 (21, 25), 51.8 (26), 25.4 (22, 24), 23.7 (23); **LR-ESI-MS**: $C_{25}H_{28}N_5O$ $[M+H]^+$ *m/z* found 414.56, cald 414.23; **HR-ESI-MS**: $C_{25}H_{28}N_5O$ $[M+H]^+$ *m/z* found 414.2263, cald 414.2294.

4-((dimethylamino)methyl)-*N*-(2-(piperidin-1-ylmethyl)-1H-benzo[d]imidazol-5-yl)benzamide (387)

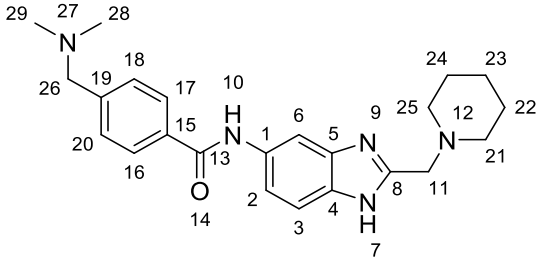

Synthesised according to general procedure **B** to give **387** (0.019 g, 0.049 mmol, 22%) as a white solid.

Mpt: 175.0-177.0 °C; **ν_{max} (cm^{-1})** 2933, 2777, 1643, 1418, 806, 749; **^{1}H NMR (400 MHz, DMSO-d_6) δ**12.2 (s, 1H, 10), 10.3 – 10.1 (m, 1H, 7), 8.2 – 8.0 (m, 1H, 6), 8.0 – 7.9 (m, 2H, 16, 17), 7.6 – 7.3 (m, 4H, 2, 3, 18, 20), 3.6 (s, 2H, 11), 3.5 (s, 2H, 26), 2.4 (t, *J* = 5.3 Hz, 4H, 21, 25), 2.2 (s, 6H, 28, 29), 1.5 (p, *J* = 5.4 Hz, 4H, 22, 24), 1.4 – 1.3 (m, 2H, 23); **^{13}C NMR (101 MHz, DMSO-d_6) δ**165.1 (13), 152.1 (19), 142.6 (5), 134.4 (1), 133.9 (4), 128.5 (16, 17), 127.6 (18, 20), 118.0 (2), 115.0 (3), 103.2 (6), 63.0 (26), 56.7 (11), 54.2 (21, 25), 45.0 (28, 29), 25.5 (22, 24), 23.8 (23); **LR-ESI-MS**: $C_{23}H_{30}N_5O$ $[M+H]^+$ *m/z* found 392.57, cald 392.25; **HR-ESI-MS**: $C_{23}H_{30}N_5O$ $[M+H]^+$ *m/z* found 392.2415, cald 392.2450.

***N*-(2-(piperidin-1-ylmethyl)-1H-benzo[d]imidazol-5-yl)-4-(pyridin-3-yloxy)benzamide (388)**

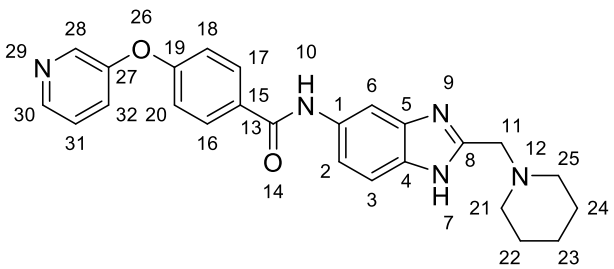

Synthesised according to general procedure **B** to give **388** (0.019 g, 0.089 mmol, 41%) as an off white solid.

Mpt: 143.5-145.5 °C; **ν_{max} (cm^{-1})** 2933, 1646, 1604, 1500, 1423, 1235, 1168, 839, 555; **^{1}H NMR (400 MHz, DMSO-d_6) δ**12.2 (s, 1H, 10), 10.2 (s, 1H, 7), 8.5 – 8.4 (m, 2H, 28, 30), 8.1 – 8.0 (m, 3H, 6, 16, 17), 7.6 (ddd, *J* = 1.4, 2.9, 8.4 Hz, 1H, 31), 7.5 – 7.4 (m, 3H, 2, 3, 32), 7.2 (d, *J* = 8.8 Hz, 2H, 18, 20), 3.7 (s, 2H, 11), 2.5 – 2.4 (m, 4H, 21, 25), 1.5 (t, *J* = 5.7 Hz, 4H, 22, 24), 1.4 (d, *J* = 5.6 Hz, 2H, 23); **^{13}C NMR (101 MHz, DMSO-d_6) δ**164.4 (13), 158.9 (27), 152.4 (19), 145.4 (30), 141.6 (28), 130.5 (15), 130.0 (16, 17), 126.8 (31), 124.9 (32), 117.7 (18, 20), 56.4 (11), 54.1 (21, 25), 25.2 (22, 24), 23.6 (23); **LR-ESI-MS**: $C_{25}H_{26}N_5O_2$ $[M+H]^+$ *m/z* found 428.51, cald 428.21; **HR-ESI-MS**: $C_{25}H_{26}N_5O_2$ $[M+H]^+$ *m/z* found 428.2056, cald 428.2087.

4-isobutyl-*N*-(2-(piperidin-1-ylmethyl)-1H-benzo[d]imidazol-5-yl)benzamide (389)

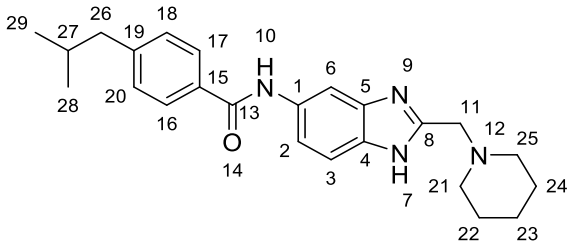

Synthesised according to general procedure **B** to give **389** (0.035 g, 0.090 mmol, 41%) as a tan oil.

ν_{max} (cm^{-1}) 2931, 1644, 1529, 1452, 835, 750, 555; **^{1}H NMR (400 MHz, DMSO-d_6) δ**12.2 (s, 1H, 10), 10.2 (s, 1H, 7), 8.2 – 8.0 (m, 1H, 6), 7.9 (d, *J* = 8.3 Hz, 2H, 16, 17), 7.5 (d, *J* = 1.4 Hz, 2H, 2, 3), 7.4 – 7.3 (m, 2H, 18, 20), 3.8 (s, 2H, 11), 2.6 – 2.5 (m, 6H, 21, 25, 26), 1.9 (dt, *J* = 6.8, 13.5 Hz, 1H, 27), 1.6 (p, *J* = 5.5 Hz, 4H, 22, 24), 1.4 (d, *J* = 6.5 Hz, 2H, 23), 0.9 (d, *J* = 6.6 Hz, 6H, 28, 29); **^{13}C NMR (101 MHz, DMSO-d_6) δ**165.3 (13), 144.9 (19), 133.8 (4, 5), 132.7 (15), 128.9 (16, 17), 127.5 (18, 20), 115.8 (2, 3), 55.8 (11), 53.9 (21, 25), 44.4 (26), 29.6 (27), 24.9 (22, 24), 23.3 (23), 22.1 (28, 29); **LR-ESI-MS**: $C_{24}H_{31}N_4O$ $[M+H]^+$ *m/z* found 391.60, cald 391.25; **HR-ESI-MS**: $C_{24}H_{31}N_4O$ $[M+H]^+$ *m/z* found 391.2473, cald 391.2498.

4-(acrylamidomethyl)-*N*-(2-(piperidin-1-ylmethyl)-1H-benzo[d]imidazol-5-yl)benzamide (390)

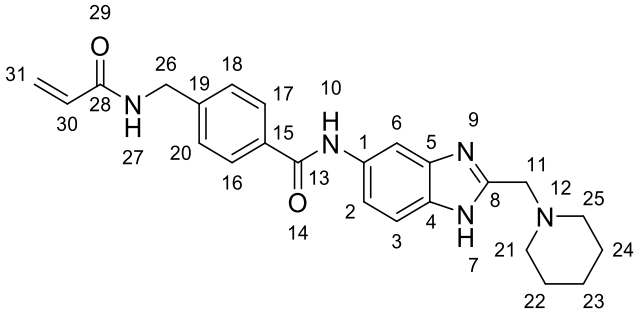

Synthesised according to general procedure **B** to give **390** (0.044 g, 0.108 mmol, 50%) as an off white solid.

Mpt: 151.7-153.7 °C; **ν_{max} (cm^{-1})** 2935, 1652, 1530, 1246, 838, 556; **^{1}H NMR (400 MHz, DMSO-*d*$_6$) δ**12.3 (s, 1H, 10), 10.2 (s, 1H, 7), 8.7 (t, *J* = 6.1 Hz, 1H, 27), 8.1 (s, 1H, 6), 8.0 – 7.8 (m, 2H, 16, 17), 7.6 – 7.2 (m, 4H, 2, 3, 18, 20), 6.3 (dd, *J* = 10.2, 17.1 Hz, 1H, 31''), 6.1 (dd, *J* = 2.3, 17.1 Hz, 1H, 31'), 5.6 (dd, *J* = 2.2, 10.1 Hz, 1H, 30), 4.4 (d, *J* = 6.1 Hz, 2H, 26), 3.7 (s, 2H, 11), 2.4 (t, *J* = 5.5 Hz, 4H, 21, 25), 1.5 (t, *J* = 5.7 Hz, 4H, 22, 24), 1.4 (d, *J* = 6.0 Hz, 2H, 23); **^{13}C NMR (101 MHz, DMSO-*d*$_6$) δ**165.0 (28), 164.8 (13), 142.9 (19), 133.8 (31), 131.6 (15), 127.8 (16, 17), 127.2 (18, 20), 125.6 (30), 56.5 (11), 54.1 (21, 25), 25.3 (22, 24), 23.7 (23); **LR-ESI-MS**: $C_{24}H_{28}N_5O_2$ $[M+H]^+$ *m/z* found 418.34, cald 418.22; **HR-ESI-MS**: $C_{24}H_{28}N_5O_2$ $[M+H]^+$ *m/z* found 418.2213, cald 418.2243.

4-((2-oxopyrrolidin-1-yl)methyl)-*N*-(2-(piperidin-1-ylmethyl)-1H-benzo[d]imidazol-5-yl)benzamide (391)

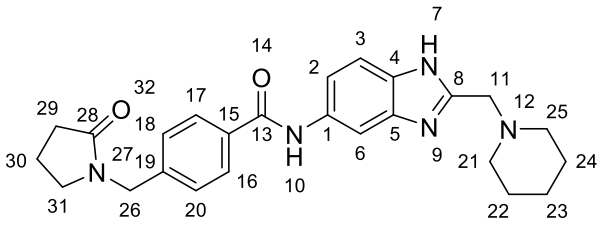

Synthesised according to general procedure **B** to give **391** (0.042 g, 0.097 mmol, 45%) as a yellow solid.

Mpt: 155.5-157.5 °C; **ν_{max} (cm^{-1})** 2934, 1651, 1531, 1266, 836, 556; **^{1}H NMR (400 MHz, DMSO-*d*$_6$) δ**12.3 (s, 1H, 10), 10.2 (s, 1H, 7), 8.1 (s, 1H, 6), 7.9 (d, *J* = 8.3 Hz, 2H, 16, 17), 7.5 (s, 2H, 2, 3), 7.4 (d, *J* = 8.3 Hz, 2H, 18, 20), 4.5 (s, 2H, 26), 3.7 (s, 2H, 11), 3.3 (t, *J* = 7.0 Hz, 2H, 31), 2.5 (t, *J* = 4.4 Hz, 4H, 21, 25), 2.3 (t, *J* = 8.1 Hz, 2H, 29), 1.9 (dq, *J* = 7.3, 10.9 Hz, 2H, 30), 1.5 (p, *J* = 5.5 Hz,

4H, 22, 24), 1.4 (q, *J* = 5.3, 5.7 Hz, 2H, 23); **^{13}C NMR (101 MHz, DMSO-d_6) δ**174.2 (28), 165.0 (13), 140.6 (19), 134.2 (15), 129.6 (1), 128.0 (16, 17), 127.6 (4), 127.5 (18, 20), 56.3 (11), 54.0 (21, 25), 46.2 (26), 45.2 (31), 30.2 (29), 25.2 (22, 24), 23.5 (23), 17.4 (30); **LR-ESI-MS**: $C_{25}H_{30}N_5O_2$ $[M+H]^+$ *m/z* found 432.66, cald 432.24; **HR-ESI-MS**: $C_{25}H_{30}N_5O_2$ $[M+H]^+$ *m/z* found 432.2373, cald 432.2400.

***N*-(2-(piperidin-1-ylmethyl)-1H-benzo[d]imidazol-5-yl)-4-(pyridin-3-ylmethoxy)benzamide (392)**

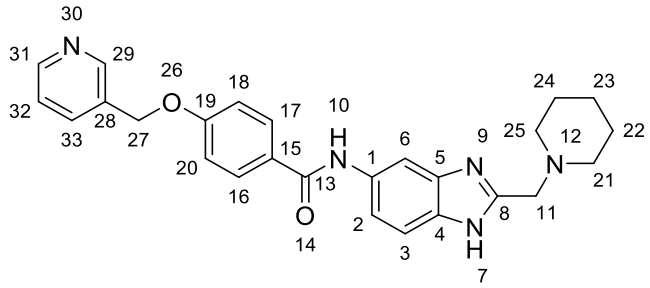

Synthesised according to general procedure **B** to give **392** (0.031 g, 0.07 mmol, 32%) as an off white solid.

Mpt: 163.2-165.2 °C; **ν_{max} (cm^{-1})** 2934, 1640, 1604, 1506, 1427, 1244, 1179, 837, 556; **^{1}H NMR (400 MHz, DMSO-d_6) δ**12.2 (s, 1H, 10), 10.1 (s, 1H, 7), 8.7 (d, *J* = 2.2 Hz, 1H, 29), 8.6 – 8.5 (m, 1H, 31), 8.1 (s, 1H, 6), 8.0 – 7.9 (m, 2H, 16, 17), 7.9 (dt, *J* = 2.0, 7.8 Hz, 1H, 33), 7.5 – 7.3 (m, 3H, 2, 3, 32), 7.2 – 7.1 (m, 2H, 18, 20), 5.3 (s, 2H, 27), 3.7 (s, 2H, 11), 2.5 (s, 4H, 21, 25), 1.5 (q, *J* = 5.6 Hz, 4H, 22, 24), 1.4 (q, *J* = 5.8 Hz, 2H, 23); **^{13}C NMR (101 MHz, DMSO-d_6) δ**164.6 (13), 160.5 (19), 149.3 (31), 149.2 (29), 135.8 (15), 132.3 (33), 129.6 (16, 17), 127.7 (28), 123.7 (32), 114.4 (18, 20), 67.1 (27), 56.4 (11), 54.1 (21, 25), 25.3 (22, 24), 23.6 (23); **LR-ESI-MS**: $C_{26}H_{28}N_5O_2$ $[M+H]^+$ *m/z* found 442.54, cald 442.22; **HR-ESI-MS**: $C_{26}H_{28}N_5O_2$ $[M+H]^+$ *m/z* found 442.2211, cald 442.2243.

4-((1H-imidazol-1-yl)methyl)-*N*-(2-(piperidin-1-ylmethyl)-1H-benzo[d]imidazol-5-yl)benzamide (305)

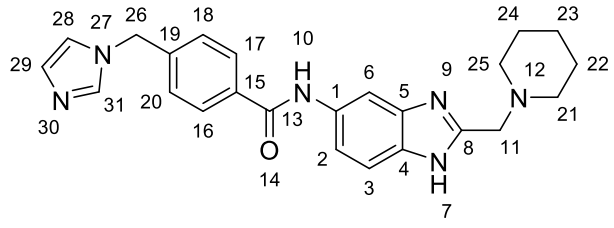

Synthesised according to general procedure **B** to give **305** (0.014 g, 0.034 mmol, 16%) as an off white solid.

Mpt: 127.7-129.7 °C; **ν_{max} (cm^{-1})** 2932, 1646, 1534, 1484, 807, 722; **^{1}H NMR (400 MHz, DMSO-d_6) δ**12.3 (s, 1H, 10), 10.2 (s, 1H, 7), 8.0 (s, 1H, 6), 8.0 (d, *J* = 8.3 Hz, 2H, 16, 17), 7.8 (d, *J* = 1.2 Hz, 1H, 31), 7.4 (s, 2H, 2, 3), 7.4 – 7.3 (m, 2H, 18, 20), 7.2 (d, *J* = 1.3 Hz, 1H, 28), 6.9 (d, *J* = 1.1 Hz, 1H, 29), 5.3 (s, 2H, 26), 3.6 (s, 2H, 11), 2.5 – 2.3 (m, 4H, 21, 25), 1.5 (p, *J* = 5.5 Hz, 4H, 22, 24), 1.4 (q, *J* = 5.9 Hz, 2H, 23); **^{13}C NMR (101 MHz, DMSO-d_6) δ**164.9 (13), 141.1 (31), 137.6 (29), 134.6 (15), 128.8 (19), 128.0 (16, 17), 127.3 (18, 20), 119.6 (28), 56.6 (11), 54.1 (21, 25), 49.1 (26), 25.4 (22, 24), 23.8 (23); **LR-ESI-MS**: $C_{24}H_{27}N_6O$ $[M+H]^+$ *m/z* found 415.53, cald 415.23; **HR-ESI-MS**: $C_{24}H_{26}N_6NaO$ $[M+Na]^+$ *m/z* found 437.2026, cald 437.2066.

4-(2-(dimethylamino)ethyl)-*N*-(2-(piperidin-1-ylmethyl)-1H-benzo[d]imidazol-5-yl)benzamide (393)

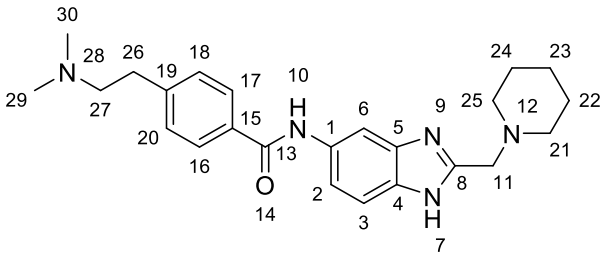

Synthesised according to general procedure **B** to give **393** (0.051 g, 0.126 mmol, 58%) as a tan solid.

Mpt: 217.9-219.9 °C; **ν_{max} (cm^{-1})** 3292, 2940, 2798, 1636, 1451, 813; **^{1}H NMR (400 MHz, DMSO-d_6) δ**12.2 (s, 1H, 10), 10.1 (s, 1H, 7), 8.2 – 7.9 (m, 1H, 6), 7.9 (d, *J* = 8.3 Hz, 2H, 16, 17), 7.6 – 7.2 (m, 4H, 2, 3, 18, 20), 3.6 (s, 2H, 11), 2.8 (t, *J* = 7.5 Hz, 2H, 27), 2.5 – 2.5 (m, 2H, 26), 2.4 (t, *J* = 5.1 Hz, 4H, 21, 25), 2.2 (s, 6H, 29, 30), 1.5 (p, *J* = 5.5 Hz, 4H, 22, 24), 1.4 – 1.3 (m, 2H, 23); **^{13}C NMR (101 MHz, DMSO-d_6) δ**165.2 (13), 144.3 (19), 132.9 (15), 128.6 (16, 17), 127.6 (18, 20), 60.5 (27), 56.7 (11), 54.2 (21, 25), 45.1 (29, 30), 33.1 (26), 25.5 (22, 24), 23.8 (23); **LR-ESI-MS**: $C_{24}H_{32}N_5O$ $[M+H]^+$ *m/z* found 406.40, cald 406.26; **HR-ESI-MS**: $C_{24}H_{32}N_5O$ $[M+H]^+$ *m/z* found 406.2581, cald 406.2607.

***N*$_1$, *N*$_1$-dimethyl-*N*$_4$-(2-(piperidin-1-ylmethyl)-1H-benzo[d]imidazol-5-yl)terephthalamide (394)**

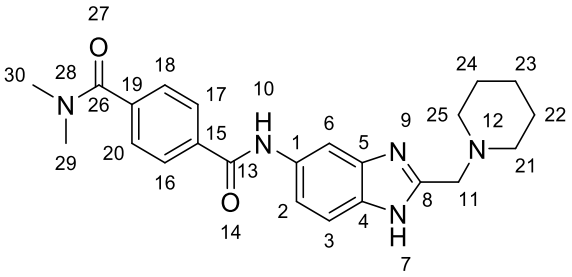

Synthesised according to general procedure **B** to give **394** (0.030 g, 0.074 mmol, 34%) as a white solid.

Mpt: 143.0-145.0 °C; **ν_{max} (cm^{-1})** 2930, 1611, 1264, 859, 724; **^{1}H NMR (400 MHz, DMSO-*d*$_6$) δ**12.2 (s, 1H, 10), 10.3 (s, 1H, 7), 8.1 (s, 1H, 6), 8.0 – 7.9 (m, 2H, 16, 17), 7.5 (d, *J* = 8.3 Hz, 2H, 18, 20), 7.5 (s, 2H, 2, 3), 3.7 (s, 2H, 11), 3.0 (s, 3H, 29), 2.9 (s, 3H, 30), 2.4 (t, *J* = 5.4 Hz, 4H, 21, 25), 1.5 (q, *J* = 5.6 Hz, 4H, 22, 24), 1.4 – 1.3 (m, 2H, 23); **^{13}C NMR (101 MHz, DMSO-*d*$_6$) δ**169.5 (26), 164.7 (13), 139.2 (15), 135.8 (19), 127.7 (16, 17), 126.9 (18, 20), 56.6 (11), 54.1 (21, 25), 34.7 (29, 30), 25.4 (22, 24), 23.7 (23); **LR-ESI-MS**: $C_{23}H_{28}N_5O_2$ $[M+H]^+$ *m/z* found 406.59, cald 406.22; **HR-ESI-MS**: $C_{23}H_{28}N_5O_2$ $[M+H]^+$ *m/z* found 406.2223, cald 406.2243.

4-((2-methoxyethoxy)methyl)-*N*-(2-(piperidin-1-ylmethyl)-1H-benzo[d]imidazol-5-yl)benzamide (395)

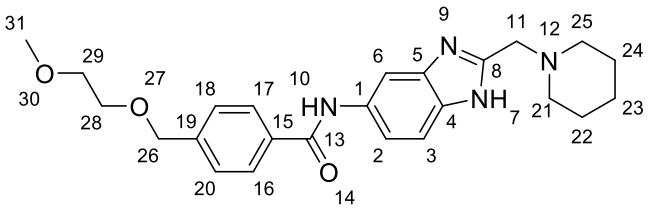

Synthesised according to general procedure **B** to give **395** (0.056 g, 0.133 mmol, 61%) as an orange solid.

Mpt: 101.4-103.4 °C; **ν_{max} (cm^{-1})** 2932, 1646, 1529, 1449, 1081, 836, 555; **^{1}H NMR (400 MHz, DMSO-*d*$_6$) δ**12.2 (s, 1H, 10), 10.2 (s, 1H, 7), 8.1 (d, *J* = 1.3 Hz, 1H, 6), 8.0 (d, *J* = 8.3 Hz, 2H, 16, 17), 7.5 – 7.4 (m, 4H, 2, 3, 18, 20), 4.6 (s, 2H, 26), 3.8 (s, 2H, 11), 3.6 – 3.5 (m, 2H, 28), 3.5 – 3.4 (m, 2H, 29), 3.3 (s, 3H, 31), 2.6 (d, *J* = 6.3 Hz, 4H, 21, 25), 1.6 (t, *J* = 5.7 Hz, 4H, 22, 24), 1.4 (d, *J* = 5.9 Hz, 2H, 23); **^{13}C NMR (101 MHz, DMSO-*d*$_6$) δ**165.1 (13), 150.6 (8), 142.1 (19), 134.2 (15), 133.8

(5), 128.4 (4), 127.7 (16, 17), 127.1 (18, 20), 120.2 (3), 115.8 (2), 71.5 (26), 71.3 (28), 69.2 (29), 58.2 (31), 55.7 (11), 53.8 (21, 25), 24.8 (22, 24), 23.2 (23); **LR-ESI-MS**: $C_{24}H_{31}N_4O_3$ $[M+H]^+$ *m/z* found 423.58, cald 423.24; **HR-ESI-MS**: $C_{24}H_{31}N_4O_3$ $[M+H]^+$ *m/z* found 423.2370, cald 423.2396.

4-(2-hydroxyethoxy)-*N*-(2-(piperidin-1-ylmethyl)-1H-benzo[d]imidazol-5-yl)benzamide (396)

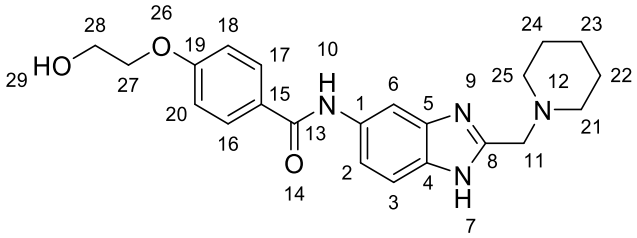

Synthesised according to general procedure **B** to give **396** (0.015 g, 0.039 mmol, 18%) as an off white solid.

Mpt: 147.3-149.3 °C; **ν_{max} (cm^{-1})** 2930, 1603, 1246, 1178, 807, 622; **^{1}H NMR (400 MHz, DMSO-d_6) δ**12.2 (s, 1H, 10), 10.1 (s, 1H, 7), 8.0 (s, 1H, 6), 8.0 – 7.9 (m, 2H, 16, 17), 7.4 (s, 2H, 2, 3), 7.2 – 7.0 (m, 2H, 18, 20), 5.0 (t, *J* = 5.5 Hz, 1H, 29), 4.1 (t, *J* = 4.9 Hz, 2H, 28), 3.7 (d, *J* = 4.8 Hz, 2H, 27), 3.7 (s, 2H, 11), 2.5 – 2.3 (m, 4H, 21, 25), 1.5 (p, *J* = 5.5 Hz, 4H, 22, 24), 1.4 (q, *J* = 6.0 Hz, 2H, 23); **^{13}C NMR (101 MHz, DMSO-d_6) δ**164.7 (13), 161.2 (19), 129.5 (16, 17), 127.2 (15), 114.0 (18, 20), 69.8 (28), 59.5 (27), 56.6 (11), 54.1 (21, 25), 25.4 (22, 24), 23.7 (23); **LR-ESI-MS**: $C_{22}H_{27}N_4O_3$ $[M+H]^+$ *m/z* found 395.53, cald 395.21; **HR-ESI-MS**: $C_{22}H_{27}N_4O_3$ $[M+H]^+$ *m/z* found 395.2059, cald 395.2083.

4-((methylsulfonyl)methyl)-*N*-(2-(piperidin-1-ylmethyl)-1H-benzo[d]imidazol-5-yl)benzamide (397)

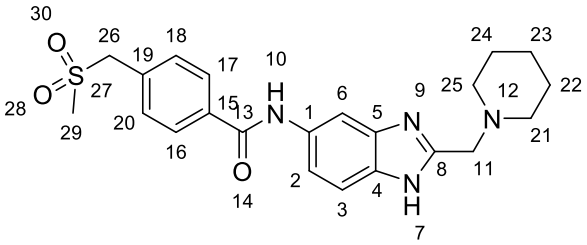

Synthesised according to general procedure **B** to give **397** (0.033 g, 0.077 mmol, 36%) as a white solid.

Mpt: 163.4-165.4 °C; **ν_{max} (cm^{-1})** 2931, 1647, 1530, 1292, 839, 556; **^{1}H NMR (400 MHz, DMSO-d_6) δ**12.2 (s, 1H, 10), 10.3 (s, 1H, 7), 8.1 (s, 1H, 6), 8.0 – 7.9 (m, 2H, 16, 17), 7.6 (d, *J* = 8.4 Hz, 2H, 18, 20), 7.4 (s, 2H, 2, 3), 4.6 (s, 2H, 26), 3.7 (s, 2H, 11), 2.9 (s, 3H, 29), 2.4 (t, *J* = 5.4 Hz, 4H, 21, 25), 1.5 (t, *J* = 5.7 Hz, 4H, 22, 24), 1.4 – 1.3 (m, 2H, 23); **^{13}C NMR (101 MHz, DMSO-d_6) δ**165.0 (13), 135.3 (19), 132.4 (15), 130.9 (16, 17), 127.8 (18, 20), 59.1 (26), 56.5 (11), 54.1 (21, 25), 30.7 (29), 25.4 (22, 24), 23.7 (23); **LR-ESI-MS**: $C_{22}H_{27}N_4O_3S$ $[M+H]^+$ *m/z* found 427.49, cald 427.18; **HR-ESI-MS**: $C_{22}H_{27}N_4O_3S$ $[M+H]^+$ *m/z* found 427.1777, cald 427.1804.

(*R*)-1-methyl-*N*-(2-((2-methylpyrrolidin-1-yl)methyl)-1H-benzo[d]imidazol-5-yl)-1H-indazole-5-carboxamide (327)

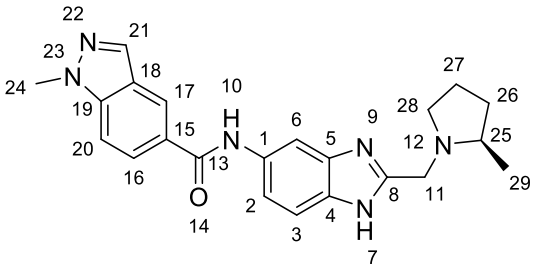

Synthesised according to general procedure **B** to give **327** (0.058 g, 0.149 mmol, 69%) as an orange solid.

Mpt: 149.0-151.0 °C; **ν_{max} (cm^{-1})** 2960, 1618, 1529, 1378, 1191, 840, 759, 556; **^{1}H NMR (400 MHz, DMSO-d_6) δ**12.2 (s, 1H, 10), 10.3 (s, 1H, 7), 8.5 (dd, *J* = 0.8, 1.6 Hz, 1H, 21), 8.2 (d, *J* = 0.9 Hz, 1H, 17), 8.1 (s, 1H, 6), 8.1 – 7.9 (m, 1H, 16), 7.8 (dt, *J* = 0.9, 8.8 Hz, 1H, 20), 7.5 – 7.4 (m, 2H, 2, 3), 4.2 – 4.0 (m, 4H, 11'', 24), 3.6 (d, *J* = 14.2 Hz, 1H, 11'), 3.0 (ddd, *J* = 3.5, 7.4, 9.2 Hz, 1H, 25), 2.5 (d, *J* = 6.8 Hz, 1H, 28'), 2.3 (q, *J* = 8.8 Hz, 1H, 28''), 1.9 (dddd, *J* = 5.7, 7.3, 9.2, 12.4 Hz, 1H, 26''), 1.7 (dtd, *J* = 4.2, 8.0, 8.8, 15.0 Hz, 2H, 26', 27''), 1.4 (dddd, *J* = 6.4, 8.5, 10.0, 12.3 Hz, 1H, 27'), 1.1 (d, *J* = 6.0 Hz, 3H, 29); **^{13}C NMR (101 MHz, DMSO-d_6) δ**165.4 (13), 140.6 (19), 133.9 (16), 127.6 (21), 125.6 (17), 122.9 (15), 121.3 (18), 109.5 (20), 59.3 (11), 54.0 (25), 50.8 (28), 35.6 (24), 32.4 (26), 21.4 (27), 18.7 (29); **LR-ESI-MS**: $C_{22}H_{25}N_6O$ $[M+H]^+$ *m/z* found 389.58, cald 389.21; **HR-ESI-MS**: $C_{22}H_{25}N_6O$ $[M+H]^+$ *m/z* found 389.2069, cald 389.2090.

(*R*)-*N*-(2-((2-methylpyrrolidin-1-yl)methyl)-1H-benzo[d]imidazol-5-yl)-4-(pyridin-4-yl)benzamide (398)

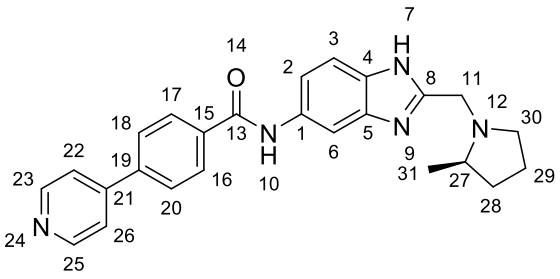

Synthesised according to general procedure **B** to give **398** (0.051 g, 0.124 mmol, 57%) as a salmon pink solid.

Mpt: 162.4-164.4 °C; **ν_{max} (cm^{-1})** 2959, 2796, 1645, 1597, 1532, 1483, 1415, 843, 817, 756; **^{1}H NMR (400 MHz, DMSO-d_6) δ**12.2 (s, 1H, 10), 10.3 (s, 1H, 7), 8.8 – 8.6 (m, 2H, 23, 25), 8.1 (d, *J* = 8.5 Hz, 2H, 16, 17), 8.1 (s, 1H, 6), 8.0 – 7.9 (m, 2H, 18, 20), 7.8 – 7.7 (m, 2H, 22, 26), 7.5 (s, 2H, 2, 3), 4.1 (d, *J* = 14.1 Hz, 1H, 11''), 3.6 (d, *J* = 14.3 Hz, 1H, 11'), 3.0 – 2.9 (m, 1H, 27), 2.5 (s, 1H, 30'), 2.3 (d, *J* = 8.9 Hz, 1H, 30''), 2.0 – 1.9 (m, 1H, 28''), 1.7 (ddt, *J* = 6.4, 8.9, 12.6 Hz, 2H, 28', 29''), 1.4 (dddd, *J* = 6.3, 8.4, 9.9, 12.2 Hz, 1H, 29'), 1.1 (d, *J* = 6.0 Hz, 3H, 31); **^{13}C NMR (101 MHz, DMSO-d_6) δ**164.6 (13), 150.4 (23, 25), 146.0 (21), 139.8 (19), 135.7 (15), 128.5 (16, 17), 126.8 (18, 20), 121.4 (22, 26), 59.2 (11), 54.0 (27), 50.8 (30), 32.5 (28), 21.4 (29), 18.7 (31); **LR-ESI-MS**: $C_{25}H_{26}N_5O$ $[M+H]^+$ *m/z* found 412.61, cald 412.21; **HR-ESI-MS**: $C_{25}H_{26}N_5O$ $[M+H]^+$ *m/z* found 412.2110, cald 412.2137.

***N*-(2-(((trans)-3,4-dimethylpyrrolidin-1-yl)methyl)-1H-benzo[d]imidazol-5-yl)-1-methyl-1H-indazole-5-carboxamide (329)**

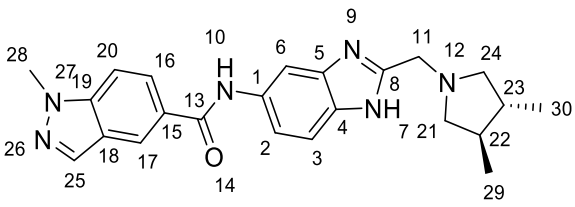

Synthesised according to general procedure **B** to give **329** (0.039 g, 0.097 mmol, 47%) as an off white solid.

Mpt: 136.0-138.0 °C; **ν_{max} (cm^{-1})** 2954, 1618, 1450, 1191, 837, 556; **^{1}H NMR (400 MHz, DMSO-d_6) δ**12.2 (s, 1H, 10), 10.3 (s, 1H, 7), 8.5 (dd, *J* = 0.8, 1.7 Hz, 1H, 17), 8.2 (d, *J* = 0.9 Hz, 1H, 25), 8.1 (s, 1H, 6), 8.0 (dd, *J* = 1.6, 8.9 Hz, 1H, 16), 7.8 (dt, *J* = 0.9, 8.9 Hz, 1H, 20), 7.5 (d, *J* = 2.2 Hz, 2H, 2, 3), 4.1 (s, 3H, 28), 4.1 – 3.9 (m, 2H, 11''), 3.0 (t, *J* = 8.1 Hz, 2H, 21'', 24'), 2.5 (t, *J* = 8.8 Hz, 2H, 21', 24''), 1.8 – 1.6 (m, 2H, 22, 23), 1.0 (d, *J* = 6.2 Hz, 6H, 29, 30); **^{13}C NMR (101 MHz, DMSO-d_6) δ**165.4 (13), 140.6 (19), 133.9 (25), 127.6 (17), 125.6 (16), 122.9 (15), 121.3 (18), 109.5 (20), 61.4 (11), 53.1 (21), 40.0 (23), 35.6 (28), 17.5 (29, 30); **LR-ESI-MS**: $C_{23}H_{27}N_6O$ $[M+H]^+$ *m/z* found 403.41, cald 403.23; **HR-ESI-MS**: $C_{23}H_{27}N_6O$ $[M+H]^+$ *m/z* found 403.2223, cald 403.2246.

***N*-(2-(((trans)-3,4-dimethylpyrrolidin-1-yl)methyl)-1H-benzo[d]imidazol-5-yl)-4-(pyridin-4-yl)benzamide (399)**

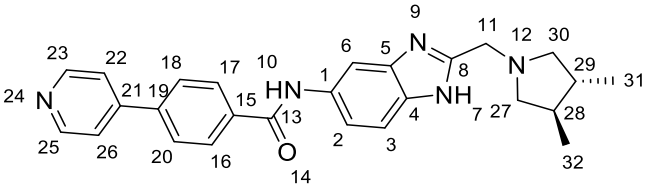

Synthesised according to general procedure **B** to give **399** (0.029 g, 0.07 mmol, 34%) as a white solid.

Mpt: 211.5-213.5 °C; **ν_{max} (cm^{-1})** 3302, 2947, 1638, 1594, 1573, 1283, 813, 752, 650; **^{1}H NMR (400 MHz, DMSO-d_6) δ**12.3 (d, *J* = 11.1 Hz, 1H, 10), 10.5 – 10.2 (m, 1H, 7), 8.7 (q, *J* = 5.7 Hz, 2H, 23, 25), 8.3 – 8.1 (m, 3H, 16, 17), 8.1 – 7.9 (m, 2H, 22, 26), 7.8 (q, *J* = 5.7 Hz, 2H, 18, 20), 7.7 – 7.3 (m, 2H, 2, 3), 3.9 – 3.7 (m, 2H, 11''), 2.9 – 2.7 (m, 2H, 27'', 30''), 2.3 (p, *J* = 8.0 Hz, 2H, 27', 30'), 1.7 (tt, *J* = 6.1, 10.9 Hz, 2H, 28, 29), 1.0 (q, *J* = 6.0 Hz, 6H, 31, 32); **^{13}C NMR (101 MHz, DMSO-d_6) δ**164.6 (13), 150.4 (23, 25), 146.0 (21), 139.8 (19), 135.7 (15), 134.4 (5), 133.7 (4), 128.5 (16, 17), 126.8 (18, 20), 121.4 (22, 26), 118.1 (2), 115.1 (3), 103.3 (6), 61.7 (27, 30), 53.6 (11), 40.4 (28, 29), 18.3 (31, 32); **LR-ESI-MS**: $C_{26}H_{28}N_5O$ $[M+H]^+$ *m/z* found 426.44, cald 426.23; **HR-ESI-MS**: $C_{26}H_{28}N_5O$ $[M+H]^+$ *m/z* found 426.2267, cald 426.2294.

(*R*)-1-methyl-*N*-(2-((3-methylpyrrolidin-1-yl)methyl)-1H-benzo[d]imidazol-5-yl)-1H-indazole-5-carboxamide (326)

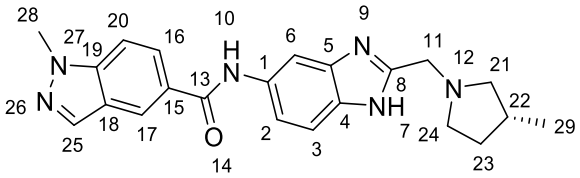

Synthesised according to general procedure **B** to give **326** (0.028 g, 0.07 mmol, 33%) as an off white solid.

Mpt: 167.0-169.0 °C; **ν_{max} (cm^{-1})** 2954, 1619, 1530, 1485, 1452, 834, 556; **^{1}H NMR (400 MHz, DMSO-d_6) δ**12.2 (s, 1H, 10), 10.3 (s, 1H, 7), 8.5 (dd, *J* = 0.8, 1.7 Hz, 1H, 17), 8.2 (d, *J* = 0.9 Hz, 1H, 25), 8.1 (s, 1H, 6), 8.0 (dd, *J* = 1.6, 8.9 Hz, 1H, 16), 7.8 (dt, *J* = 1.0, 8.9 Hz, 1H, 20), 7.5 (s, 2H, 2, 3), 4.1 (s, 3H, 28), 3.9 (s, 2H, 11), 2.9 (s, 1H, 21'), 2.8 (t, *J* = 7.7 Hz, 1H, 24'), 2.7 (q, *J* = 4.0, 5.6 Hz, 1H, 21''), 2.2 (q, *J* = 6.2, 7.1 Hz, 2H, 22, 24''), 2.1 – 1.9 (m, 1H, 23'), 1.4 (ddt, *J* = 6.1, 8.1, 12.4 Hz, 1H, 23''), 1.0 (d, *J* = 6.3 Hz, 3H, 29); **^{13}C NMR (101 MHz, DMSO-d_6) δ**165.4 (13), 140.6 (25), 133.9 (16), 127.6 (19), 125.6 (17), 122.9 (15), 121.3 (18), 109.5 (20), 61.5 (11), 53.8 (24), 53.0 (21), 35.6 (28), 32.2 (22), 31.5 (23), 19.9 (29); **LR-ESI-MS**: $C_{22}H_{25}N_6O$ $[M+H]^+$ *m/z* found 389.39, cald 389.21; **HR-ESI-MS**: $C_{22}H_{25}N_6O$ $[M+H]^+$ *m/z* found 389.2071, cald 389.2090.

***N*-(2-(piperidin-1-ylmethyl)-1H-benzo[d]imidazol-5-yl)-4-(pyrrolidin-1-ylmethyl)benzamide (400)**

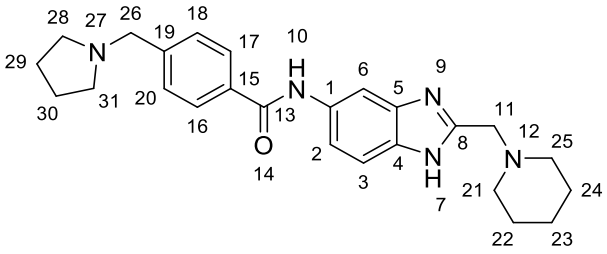

Synthesised according to general procedure **B** to give **400** (0.078 g, 0.187 mmol, 86%) as a yellow solid.

Mpt: 137.7-139.7 °C; **ν_{max} (cm^{-1})** 2930, 2790, 1642, 1529, 1277, 1107, 852, 805; **^{1}H NMR (400 MHz, DMSO-d_6) δ**12.2 (s, 1H, 10), 10.2 (d, *J* = 22.2 Hz, 1H, 7), 8.0 (d, *J* = 35.6 Hz, 1H, 6), 7.9 (d, *J* = 8.2 Hz, 2H, 16, 17), 7.4 (dd, *J* = 8.6, 17.5 Hz, 4H, 2, 3, 18, 20), 3.6 (s, 4H, 11, 26), 2.5 – 2.3 (m, 8H, 21, 25, 28, 31), 1.8 – 1.7 (m, 4H, 29, 30), 1.5 (p, *J* = 5.6 Hz, 4H, 22, 24), 1.4 (q, *J* = 4.7, 6.1 Hz, 2H,

23); **^{13}C NMR (101 MHz, DMSO-d_6) δ**165.2 (13), 152.1 (8), 143.1 (19), 139.6 (5), 134.4 (4), 133.7 (15), 128.3 (16, 17), 127.6 (18, 20), 118.0 (3), 115.0 (2), 103.2 (6), 59.3 (26), 56.7 (11), 54.2 (21, 25), 53.5 (28, 31), 25.5 (22, 24), 23.8 (23), 23.2 (29, 30); **LR-ESI-MS**: $C_{25}H_{32}N_5O$ $[M+H]^+$ *m/z* found 418.59, cald 418.26; **HR-ESI-MS**: $C_{25}H_{32}N_5O$ $[M+H]^+$ *m/z* found 418.2580, cald 418.2607.

(*R*)-4-(1H-imidazol-1-yl)-*N*-(2-((3-methylpyrrolidin-1-yl)methyl)-1H-benzo[d]imidazol-5-yl)benzamide (401)

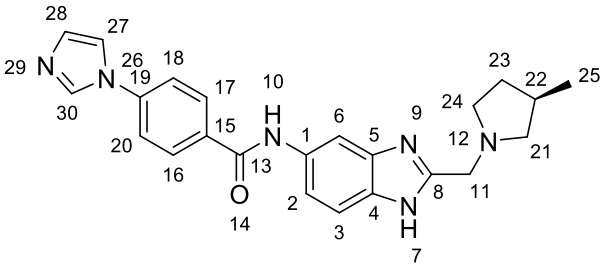

Synthesised according to general procedure **B** to give **401** (0.037 g, 0.09 mmol, 100%) as a yellow solid.

Mpt: 285.2-287.2 °C; **ν_{max} (cm^{-1})** 2955, 1646, 1606, 1517, 1483, 1425, 1300, 1244, 1058, 815; **^{1}H NMR (400 MHz, DMSO-d_6) δ**12.3 (s, 1H, 10), 10.3 (s, 1H, 7), 8.4 (t, *J* = 1.2 Hz, 1H, 30), 8.1 (d, *J* = 8.8 Hz, 2H, 16, 17), 8.1 (d, *J* = 14.1 Hz, 1H, 6), 7.9 (t, *J* = 1.4 Hz, 1H, 28), 7.9 – 7.8 (m, 2H, 18, 20), 7.5 (s, 2H, 2, 3), 7.2 (t, *J* = 1.2 Hz, 1H, 27), 3.8 (d, *J* = 1.6 Hz, 2H, 11'), 2.8 (dd, *J* = 7.2, 8.8 Hz, 1H, 21'), 2.7 – 2.7 (m, 1H, 21''), 2.6 (td, *J* = 5.9, 8.7 Hz, 1H, 24'), 2.2 (qd, *J* = 2.2, 6.7 Hz, 1H, 24''), 2.2 – 2.1 (m, 1H, 23''), 2.1 – 1.9 (m, 1H, 22), 1.3 (ddd, *J* = 2.3, 6.2, 12.4 Hz, 1H, 23'), 1.0 (d, *J* = 6.7 Hz, 3H, 25); **^{13}C NMR (101 MHz, DMSO-d_6) δ**164.2 (13), 139.0 (30), 135.7 (19), 133.1 (15), 131.0 (1), 130.3 (28), 129.4 (16, 17), 119.7 (2, 3), 119.5 (18, 20), 117.8 (27), 61.6 (11), 53.7 (21), 53.2 (24), 32.4 (22), 31.5 (23), 20.2 (25); **LR-ESI-MS**: $C_{23}H_{25}N_6O$ $[M+H]^+$ *m/z* found 401.54, cald 401.21; **HR-ESI-MS**: $C_{23}H_{25}N_6O$ $[M+H]^+$ *m/z* found 401.2063, cald 401.2090.

***N*-(2-(((trans)-3,4-dimethylpyrrolidin-1-yl)methyl)-1H-benzo[d]imidazol-5-yl)-4-(1H-imidazol-1-yl)benzamide (402)**

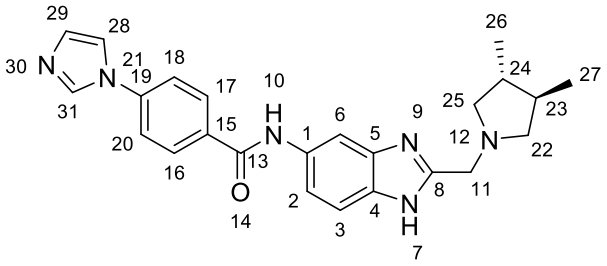

Synthesised according to general procedure **B** to give **402** (0.026 g, 0.063 mmol, 73%) as an off white solid.

Mpt: 165.0-167.0 °C; **ν_{max} (cm^{-1})** 2953, 1608, 1514, 1302, 1249, 839, 555; **^{1}H NMR (400 MHz, DMSO-d_6) δ**12.3 (s, 1H, 10), 10.3 (s, 1H, 7), 8.4 (d, *J* = 1.2 Hz, 1H, 31), 8.1 (d, *J* = 8.7 Hz, 2H, 16, 17), 8.1 (s, 1H, 6), 7.9 (t, *J* = 1.4 Hz, 1H, 28), 7.9 (d, *J* = 8.7 Hz, 2H, 18, 20), 7.5 (s, 2H, 2, 3), 7.2 (t, *J* = 1.1 Hz, 1H, 29), 3.9 – 3.8 (m, 2H, 11), 3.0 – 2.8 (m, 2H, 22'', 25'), 2.3 (dd, *J* = 6.7, 9.1 Hz, 2H, 22', 25''), 1.8 – 1.6 (m, 2H, 23, 24), 1.0 (d, *J* = 6.2 Hz, 6H, 26, 27); **^{13}C NMR (101 MHz, DMSO-d_6) δ**164.2 (13), 139.0 (31), 135.7 (19), 133.1 (29), 130.3 (15), 129.4 (16, 17), 119.5 (18, 20), 117.9 (28), 61.6 (22, 25), 53.4 (11), 40.3 (23, 24), 18.1 (26, 27); **LR-ESI-MS**: $C_{24}H_{27}N_6O$ $[M+H]^+$ *m/z* found 415.58, cald 415.23; **HR-ESI-MS**: $C_{24}H_{26}N_6NaO$ $[M+H]^+$ *m/z* found 437.2025, cald 437.2066.

(*S*)-1-methyl-*N*-(2-((3-methylpyrrolidin-1-yl)methyl)-1H-benzo[d]imidazol-5-yl)-1H-indazole-5-carboxamide (325)

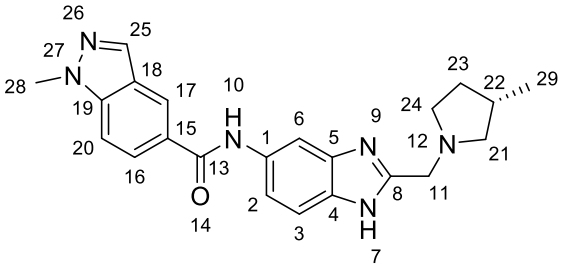

Synthesised according to general procedure **B** to give **325** (0.016 g, 0.041 mmol, 38%) as an off white solid.

Mpt: 144.1-146.1 °C; **ν_{max} (cm^{-1})** 2952, 2922, 1640, 1618, 1482, 1450, 1191, 842, 807, 758, 621; **^{1}H NMR (400 MHz, DMSO-d_6) δ**12.3 (s, 1H, 10), 10.3 (s, 1H, 7), 8.5 (d, *J* = 1.6 Hz, 1H, 17), 8.2 (d, *J* = 0.9 Hz, 1H, 25), 8.1 (s, 1H, 6), 8.0 (dd, *J* = 1.6, 8.8 Hz, 1H, 20), 7.8 (d, *J* = 8.8 Hz, 1H, 16), 7.5 (s, 2H, 2, 3), 4.1 (s, 3H, 28), 3.9 – 3.7 (m, 2H, 11''), 2.8 (dd, *J* = 7.3, 8.8 Hz, 1H, 21'), 2.7 – 2.6 (m, 1H,

24'), 2.6 (td, *J* = 5.9, 8.7 Hz, 1H, 21''), 2.3 – 2.2 (m, 1H, 24''), 2.1 – 2.1 (m, 1H, 22), 2.0 – 1.9 (m, 1H, 23''), 1.3 (ddt, *J* = 6.2, 8.3, 12.3 Hz, 1H, 23'), 1.0 (d, *J* = 6.7 Hz, 3H, 29); **^{13}C NMR (101 MHz, DMSO-d_6) δ**165.4 (13), 140.6 (19), 133.9 (25), 127.6 (18), 125.6 (16), 122.9 (15), 121.3 (17), 109.5 (20), 61.7 (11), 53.7 (24), 53.3 (21), 35.6 (28), 32.4 (23), 31.5 (22), 20.3 (29); **LR-ESI-MS**: $C_{22}H_{25}N_6O$ $[M+H]^+$ *m/z* found 389.54, cald 389.21; **HR-ESI-MS**: $C_{22}H_{25}N_6O$ $[M+H]^+$ *m/z* found 389.2070, cald 389.2090.

***N*-(2-(((cis)-3-azabicyclo[3.1.0]hexan-3-yl)methyl)-1H-benzo[d]imidazol-5-yl)-1-methyl-1H-indazole-5-carboxamide (322)**

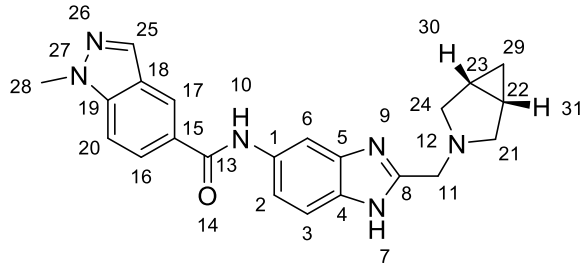

Synthesised according to general procedure **B** to give **X** (0.013 g, 0.033 mmol, 15%) as a yellow solid.

Mpt: 135.6-137.6 °C; **ν_{max} (cm^{-1})** 2794, 1640, 1529, 1450, 1315, 839, 556; **^{1}H NMR (400 MHz, DMSO-d_6) δ**12.1 (s, 1H, 10), 10.3 (s, 1H, 7), 8.6 – 8.4 (m, 1H, 25), 8.2 (d, *J* = 0.9 Hz, 1H, 17), 8.1 (s, 1H, 6), 8.0 (dd, *J* = 1.6, 8.9 Hz, 1H, 16), 7.8 (dd, *J* = 1.0, 8.8 Hz, 1H, 20), 7.5 (d, *J* = 2.5 Hz, 2H, 2, 3), 4.1 (s, 3H, 28), 3.8 (s, 2H, 11'), 2.9 (d, *J* = 8.7 Hz, 2H, 21', 24'), 2.5 (p, *J* = 1.9 Hz, 2H, 21'', 24''), 1.4 (dt, *J* = 2.9, 7.3 Hz, 2H, 30, 31), 0.8 (t, *J* = 3.8 Hz, 1H, 29'), 0.4 (td, *J* = 3.9, 7.7 Hz, 1H, 29''); **^{13}C NMR (101 MHz, DMSO-d_6) δ**165.4 (13), 140.6 (19), 133.9 (25), 127.6 (15), 125.6 (16), 122.9 (17), 121.3 (18), 109.5 (20), 54.3 (21, 24), 51.6 (11), 35.6 (28), 15.2 (22, 23), 6.5 (29); **LR-ESI-MS**: $C_{22}H_{23}N_6O$ $[M+H]^+$ *m/z* found 387.49, cald 387.19; **HR-ESI-MS**: $C_{22}H_{23}N_6O$ $[M+H]^+$ *m/z* found 387.1913, cald 387.1933.

(*S*)-1-methyl-*N*-(2-((2-methylpyrrolidin-1-yl)methyl)-1H-benzo[d]imidazol-5-yl)-1H-indazole-5-carboxamide (328)

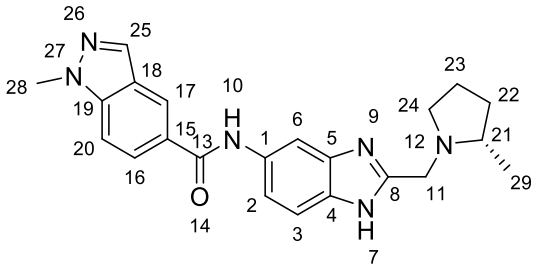

Synthesised according to general procedure **B** to give **328** (0.076 g, 0.196 mmol, 52%) as an off white solid.

Mpt: 176.7-178.7 °C; **ν_{max} (cm^{-1})** 2960, 1619, 837, 556; **^{1}H NMR (400 MHz, DMSO-d_6) δ**12.2 (s, 1H, 10), 10.2 (d, *J* = 21.8 Hz, 1H, 7), 8.5 (t, *J* = 1.1 Hz, 1H, 17), 8.2 (d, *J* = 0.9 Hz, 1H, 20), 8.1 (s, 1H, 25), 8.0 (dd, *J* = 1.7, 8.8 Hz, 1H, 16), 7.8 (d, *J* = 8.9 Hz, 1H, 3), 7.6 – 7.3 (m, 2H, 2, 6), 4.1 (s, 3H, 28), 4.0 (d, *J* = 14.2 Hz, 1H, 11''), 3.5 (d, *J* = 14.1 Hz, 1H, 11'), 2.9 (ddd, *J* = 3.3, 7.5, 9.0 Hz, 1H, 21), 2.5 (s, 1H, 24''), 2.3 (q, *J* = 8.7 Hz, 1H, 24'), 1.9 (dddd, *J* = 5.6, 7.2, 9.4, 12.5 Hz, 1H, 22''), 1.7 – 1.6 (m, 2H, 22', 23''), 1.5 – 1.3 (m, 1H, 23'), 1.1 (d, *J* = 6.0 Hz, 3H, 29); **^{13}C NMR (101 MHz, DMSO-d_6) δ**165.4 (8, 13), 140.6 (1, 5), 133.9 (4, 19), 127.6 (25), 125.6 (15, 17), 122.9 (16), 121.3 (18), 117.9 (2), 115.1 (20), 109.5 (3), 103.2 (6), 59.0 (11), 54.0 (21), 51.0 (24), 35.6 (28), 32.6 (22), 21.4 (23), 18.9 (29); **LR-ESI-MS**: $C_{22}H_{25}N_6O$ $[M+H]^+$ *m/z* found 389.35, cald 389.21; **HR-ESI-MS**: $C_{22}H_{25}N_6O$ $[M+H]^+$ *m/z* found 389.2069, cald 389.2090.

***N*-(2-((2-ethylpyrrolidin-1-yl)methyl)-1H-benzo[d]imidazol-5-yl)-1-methyl-1H-indazole-5-carboxamide (323)**

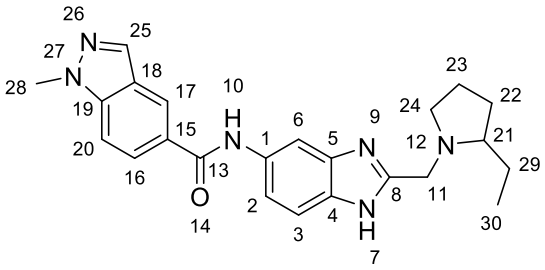

Synthesised according to general procedure **B** to give **323** (0.017 g, 0.043 mmol, 21%) as a yellow solid.

Mpt: 211.5-213.5 °C; **ν_{max} (cm^{-1})** 2958, 1641, 1529, 1450, 1414, 1191, 808, 758; **^{1}H NMR (400 MHz, DMSO-d_6) δ**12.1 (s, 1H, 10), 10.2 (d, *J* = 20.9 Hz, 1H, 7), 8.5 (dd, *J* = 0.8, 1.6 Hz, 1H, 17), 8.2

(d, *J* = 0.9 Hz, 1H, 25), 8.1 (d, *J* = 11.9 Hz, 1H, 6), 8.0 (dd, *J* = 1.6, 8.8 Hz, 1H, 16), 7.8 (dt, *J* = 0.9, 8.8 Hz, 1H, 20), 7.5 (qq, *J* = 8.6, 17.2 Hz, 2H, 2, 3), 4.1 (s, 3H, 28), 4.1 (d, *J* = 14.2 Hz, 1H, 11''), 3.5 (d, *J* = 14.2 Hz, 1H, 11'), 3.0 – 2.8 (m, 1H, 21), 2.4 – 2.2 (m, 2H, 24), 1.9 (dq, *J* = 7.7, 12.2 Hz, 1H, 23''), 1.7 (dtd, *J* = 3.5, 5.9, 6.6, 14.0 Hz, 3H, 22, 23'), 1.4 (dt, *J* = 7.7, 12.2 Hz, 1H, 29''), 1.3 – 1.2 (m, 1H, 29'), 0.9 – 0.7 (m, 3H); **^{13}C NMR (101 MHz, DMSO-*d*$_6$) δ**165.4 (13), 140.6 (19), 139.7 (1), 133.9 (25), 127.6 (15), 125.6 (16), 122.9 (17), 121.3 (18), 117.9 (2), 115.1 (3), 109.5 (20), 103.2 (6), 65.0 (11), 54.3 (21), 51.4 (24), 35.6 (28), 29.5 (22), 26.0 (23), 21.8 (29), 10.3 (30); **LR-ESI-MS**: $C_{23}H_{27}N_6O$ $[M+H]^+$ *m/z* found 403.51, cald 403.23; **HR-ESI-MS**: $C_{23}H_{27}N_6O$ $[M+H]^+$ *m/z* found 403.2225, cald 403.2246.

***N*-(2-(((1*S*,4*S*)-2-oxa-5-azabicyclo[2.2.1]heptan-5-yl)methyl)-1H-benzo[d]imidazol-5-yl)-1-methyl-1H-indazole-5-carboxamide (330)**

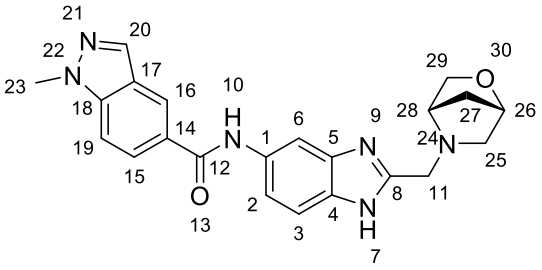

Synthesised according to general procedure **B** to give **330** (0.034 g, 0.084 mmol, 41%) as an off white solid.

Mpt: 146.7-148.7 °C; **ν_{max} (cm^{-1})** 2954, 1644, 1193, 950; **^{1}H NMR (400 MHz, DMSO-*d*$_6$) δ**12.2 (s, 1H, 10), 10.2 (s, 1H, 7), 8.5 (dd, *J* = 0.8, 1.7 Hz, 1H, 16), 8.2 (d, *J* = 0.9 Hz, 1H, 20), 8.1 (d, *J* = 9.4 Hz, 1H, 6), 8.0 (dd, *J* = 1.6, 8.9 Hz, 1H, 15), 7.8 (dt, *J* = 0.9, 8.9 Hz, 1H, 19), 7.5 (s, 2H, 2, 3), 4.4 (t, *J* = 2.0 Hz, 1H, 29'), 4.1 (s, 3H, 23), 4.0 – 3.8 (m, 3H, 11'', 26, 29''), 3.6 – 3.5 (m, 2H, 11', 28), 2.8 (dd, *J* = 1.7, 9.9 Hz, 1H, 25''), 2.6 (d, *J* = 10.0 Hz, 1H, 25'), 1.8 (dd, *J* = 2.1, 9.8 Hz, 1H, 27''), 1.7 – 1.6 (m, 1H, 27'); **^{13}C NMR (101 MHz, DMSO-*d*$_6$) δ**165.4 (12), 140.6 (18), 133.9 (15), 127.6 (20), 125.6 (16), 122.9 (14), 121.3 (17), 109.5 (19), 76.2 (26), 69.4 (29), 61.2 (28), 60.6 (25), 51.7 (11), 35.6 (23), 34.4 (27); **LR-ESI-MS**: $C_{22}H_{23}N_6O_2$ $[M+H]^+$ *m/z* found 403.47, cald 403.19; **HR-ESI-MS**: $C_{22}H_{23}N_6O_2$ $[M+H]^+$ *m/z* found 403.1860, cald 403.1882.

***N*-(2-((2,2-dimethylpyrrolidin-1-yl)methyl)-1H-benzo[d]imidazol-5-yl)-4-(1H-imidazol-1-yl)benzamide (403)**

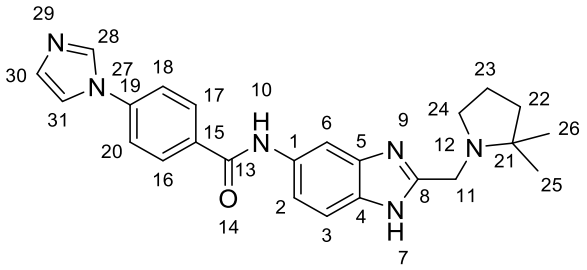

Synthesised according to general procedure **B** to give **403** (0.0054 g, 0.013 mmol, 6%) as a yellow film.

ν_{max} (cm^{-1}) 2958, 1608, 1514, 1483, 1301, 1249, 1054, 962, 848, 809, 655; **^{1}H NMR (400 MHz, DMSO-*d*$_6$) δ**12.0 (s, 1H, 10), 10.3 (s, 1H, 7), 8.4 (t, *J* = 1.2 Hz, 1H, 28), 8.2 – 8.0 (m, 2H, 6, 16, 17), 7.9 (t, *J* = 1.4 Hz, 1H, 30), 7.9 – 7.8 (m, 2H, 18, 20), 7.4 (d, *J* = 17.6 Hz, 2H, 2, 3), 7.2 (d, *J* = 1.2 Hz, 1H, 31), 3.7 (s, 2H, 11), 2.7 (t, *J* = 6.8 Hz, 3H, 24), 1.8 – 1.6 (m, 4H, 22, 23), 1.1 (s, 6H, 25, 26); **^{13}C NMR (101 MHz, DMSO-*d*$_6$) δ**139.0 (28), 135.7 (30), 133.1 (15), 130.3 (19), 129.4 (16, 17), 119.5 (18, 20), 117.8 (31), 59.8 (21, 24), 51.3 (11), 46.8 (22), 22.7 (25, 26), 20.2 (23); **LR-ESI-MS**: $C_{24}H_{27}N_6O$ $[M+H]^+$ *m/z* found 415.51, cald 415.23; **HR-ESI-MS**: $C_{24}H_{26}N_6NaO$ $[M+H]^+$ *m/z* found 437.2027, cald 437.2066.

***N*-(2-((2-(methoxymethyl)pyrrolidin-1-yl)methyl)-1H-benzo[d]imidazol-5-yl)-1-methyl-1H-indazole-5-carboxamide (324)**

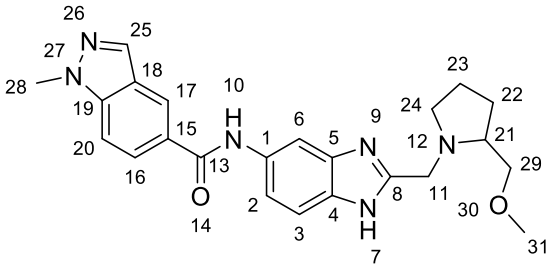

Synthesised according to general procedure **B** to give **324** (0.034 g, 0.081 mmol, 21%) as an orange foam.

Mpt: 126.5-128.5 °C; **ν_{max} (cm^{-1})** 2871, 1617, 1449, 1252, 1191, 1107, 808, 759; **^{1}H NMR (400 MHz, DMSO-*d*$_6$) δ**12.1 (s, 1H, 10), 10.2 (d, *J* = 22.1 Hz, 1H, 7), 8.5 (dd, *J* = 0.8, 1.7 Hz, 1H, 17), 8.2

(d, *J* = 1.0 Hz, 1H, 25), 8.1 (d, *J* = 10.6 Hz, 1H, 6), 8.0 (dd, *J* = 1.6, 8.9 Hz, 1H, 20), 7.8 (dt, *J* = 1.0, 8.9 Hz, 1H, 16), 7.5 (td, *J* = 16.3, 23.5, 24.7 Hz, 2H, 2, 3), 4.2 (d, *J* = 14.4 Hz, 1H, 11''), 4.1 (s, 3H, 28), 3.7 (d, *J* = 14.3 Hz, 1H, 11'), 3.4 (dd, *J* = 5.3, 9.4 Hz, 1H, 21), 3.2 (s, 4H, 29'', 31), 2.9 (ddd, *J* = 3.9, 5.8, 9.4 Hz, 1H, 29'), 2.8 – 2.7 (m, 1H, 24''), 2.4 (td, *J* = 7.8, 9.0 Hz, 1H, 24'), 1.9 (dq, *J* = 8.2, 12.3 Hz, 1H, 22''), 1.7 (tt, *J* = 3.1, 7.4, 9.2 Hz, 2H, 22', 23''), 1.5 (ddd, *J* = 6.6, 12.4, 13.8 Hz, 1H, 23'); **^{13}C NMR (101 MHz, DMSO-*d*$_6$) δ**165.4 (13), 152.9 (8), 140.6 (19), 133.9 (16), 127.6 (25), 125.6 (17), 122.9 (18), 121.3 (15), 118.0 (2), 115.1 (3), 109.5 (20), 103.2 (6), 75.8 (29), 62.1 (31), 58.4 (21), 54.4 (11), 52.2 (24), 38.3 (28), 35.6 (22), 28.3 (23); **LR-ESI-MS**: $C_{23}H_{27}N_6O_2$ $[M+H]^+$ *m/z* found 419.52, cald 419.22; **HR-ESI-MS**: $C_{23}H_{27}N_6O_2$ $[M+H]^+$ *m/z* found 419.2172, cald 419.2195.

***N*-(2-((2-isopropylpyrrolidin-1-yl)methyl)-1H-benzo[d]imidazol-5-yl)-1-methyl-1H-indazole-5-carboxamide (404)**

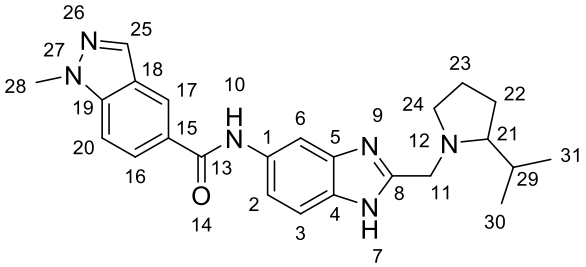

Synthesised according to general procedure **B** to give **404** (0.019 g, 0.044 mmol, 15%) as an off white solid.

Mpt: 256.8-258.8 °C; **ν_{max} (cm^{-1})** 2954, 2794, 1640, 1544, 1411, 1314, 1190, 1109, 810, 759, 616; **^{1}H NMR (400 MHz, DMSO-*d*$_6$) δ**12.1 (s, 1H, 10), 10.3 (s, 1H, 7), 8.5 (dd, *J* = 0.8, 1.6 Hz, 1H, 17), 8.2 (d, *J* = 0.9 Hz, 1H, 25), 8.1 (s, 1H, 6), 8.0 (dd, *J* = 1.7, 8.8 Hz, 1H, 16), 7.8 (dt, *J* = 0.9, 8.9 Hz, 1H, 20), 7.5 (d, *J* = 19.1 Hz, 2H, 2, 3), 4.1 (s, 3H, 28), 4.0 (d, *J* = 14.3 Hz, 1H, 11''), 3.5 (d, *J* = 14.1 Hz, 1H, 11'), 2.9 (ddd, *J* = 2.1, 6.2, 8.2 Hz, 1H, 21), 2.5 (s, 1H, 29), 2.4 (dd, *J* = 2.8, 6.9 Hz, 1H, 24'), 2.3 (dtd, *J* = 2.6, 6.5, 9.2 Hz, 1H, 24''), 1.9 (td, *J* = 4.4, 6.8 Hz, 1H, 22''), 1.7 – 1.4 (m, 3H, 22', 23), 0.9 (dd, *J* = 2.5, 6.8 Hz, 6H, 30, 31); **^{13}C NMR (101 MHz, DMSO-*d*$_6$) δ**165.9 (13), 141.1 (19), 134.3 (16), 128.1 (25), 126.1 (18), 123.4 (15), 121.8 (17), 109.9 (20), 68.7 (21), 55.0 (11), 52.2 (24), 36.0

(28), 28.8 (23), 24.7 (22), 23.0 (29), 20.7 (30), 16.0 (31); **LR-ESI-MS**: $C_{24}H_{29}N_6O$ $[M+H]^+$ *m/z* found 417.54, cald 417.24; **HR-ESI-MS**: $C_{24}H_{29}N_6O$ $[M+H]^+$ *m/z* found 417.2378, cald 417.2403.

2-(((trans)-2,5-dimethylpyrrolidin-1-yl)methyl)-5-nitro-1*H*-benzo[*d*]imidazole (405a)

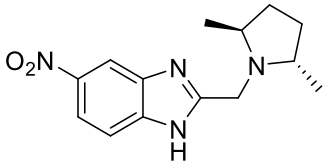

Initially a suspension of 2-(chloromethyl)-5-nitro-1H-benzo[d]imidazole **208** (1.3 g, 6.14 mmol, 1 eq) and Na_2CO_3 (1.563 g, 14.75 mmol, 2.4 eq) in anhydrous MeCN (8 mL, 0.8 M) had 2,5-dimethylpyrrolidine, HCl (1 g, 7.37 mmol, 1.2 eq) added at room temperature. The reaction was allowed to stir at room temperature overnight. Upon reaction completion the suspension was filtered through a sintered frit and washed with acetone. The filtrate was concentrated to a residue which was immediately submitted to the next step without further purification as **405a**.

2-(((trans)-2,5-dimethylpyrrolidin-1-yl)methyl)-1*H*-benzo[*d*]imidazol-5-amine (405b)

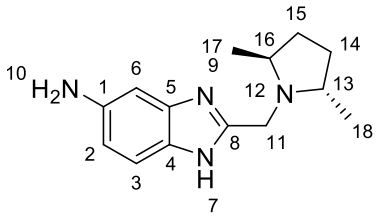

Synthesised according to general procedure **A** to give **405b** (0.089 g, 0.36 mmol, 32%) as a white solid.

Mpt: 171.31-173.3 °C; **ν_{max} (cm^{-1})** 3356, 2955, 1631, 1422, 1221, 1013, 800, 434; **^{1}H NMR (400 MHz, $CDCl_3$) δ** 7.46 – 7.22 (m, 1H, 6), 6.76 (s, 1H, 3), 6.59 (dd, *J* = 8.5, 2.2 Hz, 1H, 2), 3.87 (s, 2H, 11), 2.78 – 2.49 (m, 2H, 13, 16), 1.94 – 1.70 (m, 2H, 14', 15'), 1.48 – 1.23 (m, 2H, 14'', 15''), 0.97 (dd, *J* = 6.2, 1.9 Hz, 6H, 17, 18). **^{13}C NMR (101 MHz, $CDCl_3$) δ** 153.7 (8), 142.1 (6), 112.0 (2, 3), 62.10 (11), 50.6 (13, 16), 31.3 (14, 15), 20.6 (17, 18); **LR-ESI-MS**: $C_{14}H_{21}N_4$ $[M+H]^+$ *m/z* found 245.47, cald 245.17; **HR-ESI-MS**: $C_{14}H_{20}N_4Na$ $[M+Na]^+$ *m/z* found 267.1574, cald 267.1586.

***N*-(2-(((trans)-2,5-dimethylpyrrolidin-1-yl)methyl)-1*H*-benzo[*d*]imidazol-5-yl)-1-methyl-1*H*-indazole-5-carboxamide (405)**

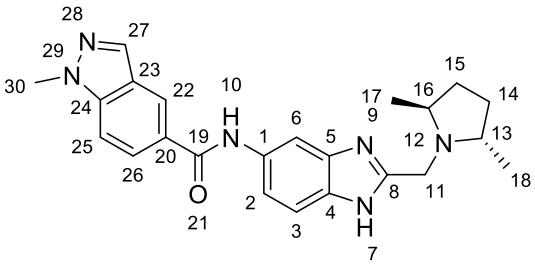

Synthesised according to general procedure **B** to give **405** (0.037 g, 0.093 mmol, 60%) as a white solid.

Mpt: 149.3-151.3 °C; **ν_{max} (cm^{-1})** 2958, 1599, 1484, 1415, 1310, 1192, 840, 556; **^{1}H NMR (400 MHz, DMSO-*d*^{6}) δ** 12.09 (s, 1H, 8), 10.25 (s, 1H, 7), 8.48 (d, *J*=1.6, 1H, 26), 8.25 (d, *J*=0.9, 1H, 29), 8.10 (s, 1H, 6), 8.02 (dd, *J*=8.8, 1.6, 1H, 22), 7.76 (d, *J*=8.8, 1H, 23), 7.47 (s, 2H, 2, 3), 4.10 (s, 3H, 30), 3.92 (s, 2H, 11''), 2.92 – 2.57 (m, 2H, 13, 16), 1.82 (s, 2H, 14'', 15''), 1.48 – 1.25 (m, 2H, 14', 15'), 1.14 – 0.88 (m, 6H, 17, 18); **^{13}C NMR (101 MHz, DMSO-*d*^{6}) δ** 165.4 (19), 140.6 (29), 133.9 (22), 127.6 (6), 125.6 (26), 122.9 (23), 121.3 (2), 109.5 (3), 64.9 (11), 59.7 (13, 16), 47.9 (30), 35.6 (17, 18), 19.8 (15), 15.2 (14); **LR-ESI-MS**: $C_{23}H_{27}N_6O$ $[M+H]^+$ *m/z* found 403.49, cald 403.23; **HR-ESI-MS**: $C_{23}H_{27}N_6O$ $[M+H]^+$ *m/z* found 403.2246, cald 403.2246.

methyl 1-cyclopropyl-1*H*-indazole-5-carboxylate (336)

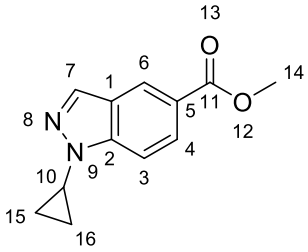

Initially methyl 1H-indazole-5-carboxylate **335** (0.828 g, 4.70 mmol, 1 eq), cyclopropylboronic acid (0.807 g, 9.40 mmol, 2 eq), $Cu(OAc)_2$ (0.854 g, 4.70 mmol, 1 eq) and 2,2'-bipyridine (0.734 g, 4.70 mmol, 1 eq) were dissolved in 1, 2-Dichloroethane (42 mL, 0.11 M) and heated to 70°C for 16 h under a blanket of air. Upon reaction completion the mixture was filtered through a bed of celite and the filtrate was concentrated to a residue which was purified via Biotage LPLC eluting with CH:EA (1:0 to 1:1) to give the product **336** as a yellow solid (0.641 g, 2.96 mmol, 63%).

Mpt: 76.0-78.0 °C; **ν_{max} (cm^{-1})** 1714, 1617, 1438, 1311, 1251, 1086, 761, 452; **^{1}H NMR (400 MHz, DMSO-*d*^{6}) δ** 8.44 (dd, *J*=1.6, 0.8, 1H, 7), 8.18 (d, *J*=0.9, 1H, 6), 7.95 (dd, *J*=8.8, 1.6, 1H, 4), 7.74 (dt, *J*=8.9, 0.9, 1H, 3), 3.86 (s, 3H, 14), 3.79 (tt, *J*=6.7, 4.0, 1H, 10), 1.20 – 0.95 (m, 4H, 15, 16); **^{13}C NMR (101 MHz, DMSO-*d*^{6}) δ** 166.5 (11), 141.9 (7), 134.5 (4), 126.4 (6), 124.2 (5), 123.6 (2), 122.4 (1), 109.9 (3), 52.0 (14), 29.4 (10), 6.2 (15, 16); **LR-ESI-MS**: $C_{12}H_{13}N_2O_2$ $[M+H]^+$ *m/z* found 217.20, cald 217.10; **HR-ESI-MS**: $C_{12}H_{13}N_2O_2$ $[M+H]^+$ *m/z* found 217.0967, cald 217.0977.

1-cyclopropyl-1*H*-indazole-5-carboxylic acid (337)

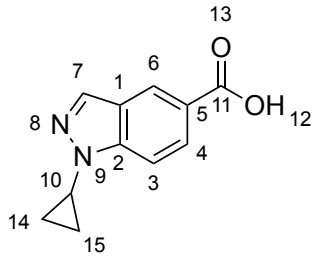

Initially compound **336** (0.573 g, 2.65 mmol, 1 eq) was dissolved in MeOH (4 mL, 0.6 M) and had crushed NaOH pellets (0.53 g, 13.25 mmol, 5 eq) added before being stirred at 65°C for 2 h. Upon reaction completion the mixture was concentrated to dryness and then dissolved in water. The aqueous mixture was carefully acidified with 2 *N* HCl (until pH 4-5) until the product began to precipitate, which was then filtered off, washed with water and dried in a vacuum oven to give the product **337** as a pale yellow solid (0.366 g, 1.81 mmol, 68%).

Mpt: 174.6-176.6 °C; **ν_{max} (cm^{-1})** 2783, 1701, 1618, 1243, 1175, 765, 687, 603, 481; **^{1}H NMR (400 MHz, DMSO-*d*^{6}) δ**12.84 (s, 1H, 12), 8.57 – 8.39 (m, 1H, 7), 8.18 (s, 1H, 6), 7.98 (dd, *J*=8.8, 1.6, 1H, 4), 7.73 (d, *J*=8.8, 1H, 3), 3.92 – 3.69 (m, 1H, 10), 1.13 (tt, *J*=6.3, 2.4, 4H, 14, 15); **^{13}C NMR (101 MHz, DMSO-*d*^{6}) δ** 167.6 (11), 141.9 (7), 134.4 (4), 126.8 (6), 124.1 (1), 123.6 (2), 123.6 (5), 109.7 (3), 29.4 (10), 6.2 (14, 15); **LR-ESI-MS**: $C_{11}H_{11}N_2O_2$ $[M+H]^+$ *m/z* found 203.37, cald 203.08; **HR-ESI-MS**: $C_{11}H_{11}N_2O_2$ $[M+H]^+$ *m/z* found 203.0808, cald 203.0821.

(*S*)-1-cyclopropyl-*N*-(2-((2-methylpyrrolidin-1-yl)methyl)-1*H*-benzo[*d*]imidazol-5-yl)-1*H*-indazole-5-carboxamide (334)

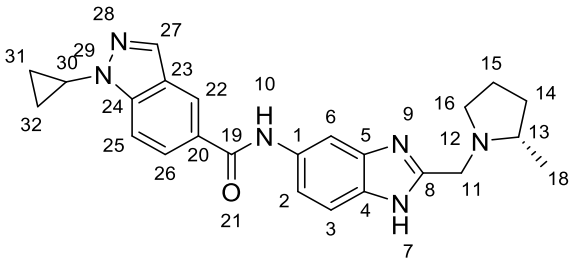

Synthesised according to general procedure **B** to give **334** (0.038 g, 0.091 mmol, 42%) as a beige solid.

Mpt: 170.0-172.0 °C; **ν_{max} (cm^{-1})** 3406, 2925, 1644, 1485, 1312, 1252, 838, 556; **^{1}H NMR (400 MHz, DMSO-*d*^{6}) δ**12.19 (s, 1H, 7), 10.26 (s, 1H, 10), 8.48 (d, *J*=1.6, 1H, 22), 8.21 (s, 1H, 27), 8.13 – 7.99 (m, 2H, 6, 26), 7.79 (d, *J*=8.8, 1H, 25), 7.56 – 7.33 (m, 2H, 2, 3), 4.09 (d, *J*=14.2, 1H, 11''), 3.83 (tt, *J*=7.1, 4.0, 1H, 30), 3.59 (d, *J*=14.1, 1H, 11'), 3.06 – 2.88 (m, 1H, 13), 2.34 (d, *J*=9.1, 1H, 16'), 1.94 (dtd, *J*=12.5, 7.7, 7.1, 4.2, 1H, 16''), 1.77 – 1.61 (m, 2H, 14', 15''), 1.47 – 1.30 (m, 2H, 14'', 15'), 1.26 – 1.00 (m, 8H, 18, 31, 32); **^{13}C NMR (101 MHz, DMSO-*d*^{6}) δ** 165.4 (19), 141.3 (27), 134.0 (22), 128.1 (26), 125.9 (6), 123.4 (3), 121.5 (2), 109.6 (25), 54.0 (11), 50.8 (13, 16), 32.4 (30), 29.4 (14), 26.4 (15), 21.4 (18), 6.3 (31, 32); **LR-ESI-MS**: $C_{24}H_{27}N_6O$ $[M+H]^+$ *m/z* found 415.53, cald 415.23; **HR-ESI-MS**: $C_{24}H_{27}N_6O$ $[M+H]^+$ *m/z* found 415.2228, cald 415.2246.

I.II Biochemical/Biophysical binding characterisation

I.II.I AlphaScreen

Supplementary Table 6. *Inhibition data of selected additional compounds with ENL YD.*

Compound	ENL IC_{50} (μM)	Compound	ENL IC_{50} (μM)	Compound	ENL IC_{50} (μM)
286	10	**362**	5.1	**384**	5.0
281	14	**364**	14	**385**	2.4
278	>50	**316**	16	**386**	ND
274	22	**317**	20	**387**	3.6
300	6.7	**318**	>50	**388**	1.8
298	ND	**319**	0.26	**389**	2.2
344	>50	**315**	26	**390**	1.4
345	20	**365**	0.33	**391**	2.4
346	8.4	**366**	10	**392**	1.7
347	>50	**367**	3.1	**305**	0.96
301	>50	**368**	1.4	**393**	2.7
348	40	**369**	4.8	**394**	6.6
349	>50	**370**	2.1	**395**	2.3
350	>50	**303**	1.3	**396**	1.5
283	6.7	**371**	2.4	**397**	>50
292	2.7	**372**	4.5	**398**	0.50
293	5.3	**313**	>50	**329**	0.065
294	6.5	**304**	0.32	**399**	0.049
351	5.7	**373**	6.4	**400**	1.9
352	8.2	**374**	0.74	**401**	0.037
353	22	**376**	25	**402**	0.043
354	8.2	**377**	5.2	**330**	>50
355	12	**378**	3.3	**403**	0.204
277	>50	**379**	2.4	**404**	0.283
358	>50	**380**	11	**338**	>50
311	2.3	**381**	13	**339**	>50
359	>50	**382**	0.19	**340**	>50
360	3.9	**331**	0.61	**341**	>50
361	ND	**333**	0.22	**342**	>50
279	>50	**383**	>50	**328**	0.026

ND- not determined

I.II.II Selectivity

Supplemental Table 7. *AlphaScreen selectivity screen of compound* ***328*** *over other acyllysine reading domains.*

YEATS2 IC_{50} (μM)	YEATS4 IC_{50} (μM)	BRD4 (1) IC_{50} (μM)	CECR2 (2) IC_{50} (μM)	FALZ IC_{50} (μM)	BAZ2B IC_{50} (μM)	CBP IC_{50} (μM)
>10	>10	>10	>10	>10	>10	>10

I.II.III Isothermal Titration Calorimetry (ITC)

Experiments were carried out on a Nano-ITC Standard Volume Instrument (TA Instruments). All experiments were carried out at 25 °C in 20 mM HEPES pH 7.5, 150 mM NaCl, 0.5 mM TCEP and 5% glycerol. Protein solutions were buffer exchanged by gel filtration. The titrations were conducted using an initial injection of 2 µL followed by 32 injections of 8 µL. Background dilution heat was subtracted from each experiment. Thermodynamic parameters were calculated using $\Delta G = \Delta H - T\Delta S = -RTlnK_B$, where $K_D = 1/K_B$. ΔG, ΔH and ΔS are changes in free energy, enthalpy and entropy respectively. Independent single site binding models were employed in data analysis.

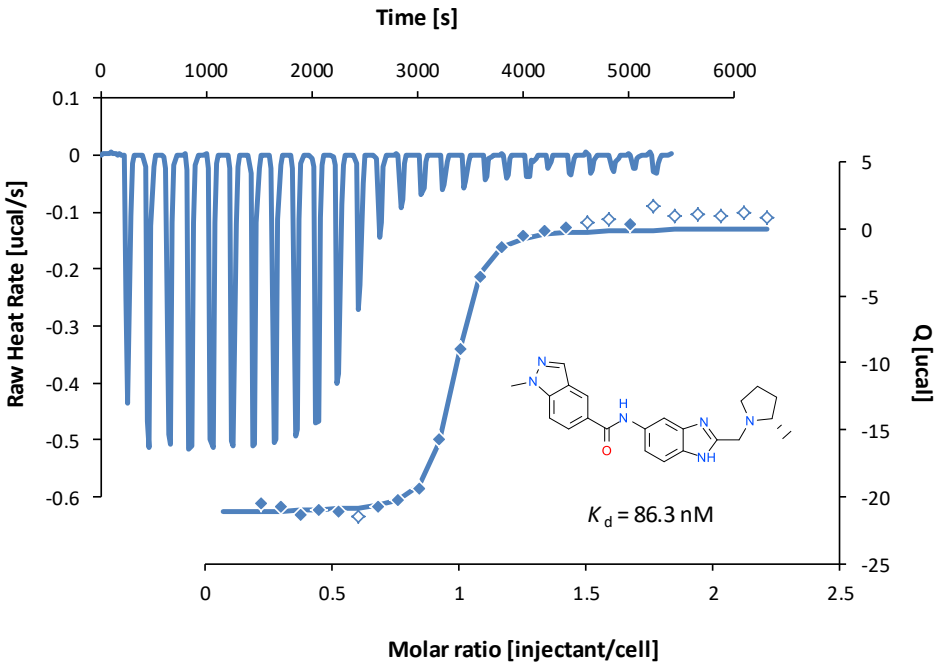

Supplementary Figure 11. *ITC trace of compound* ***328*** *and ENL YD*

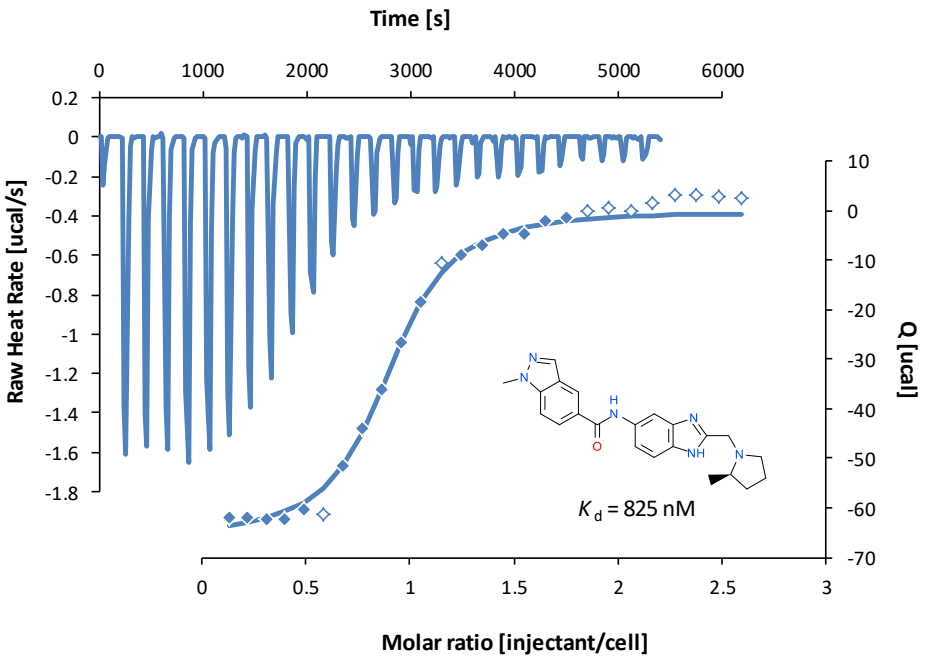

Supplementary Figure 12. *ITC trace of compound* ***327*** *and Af9 YD*

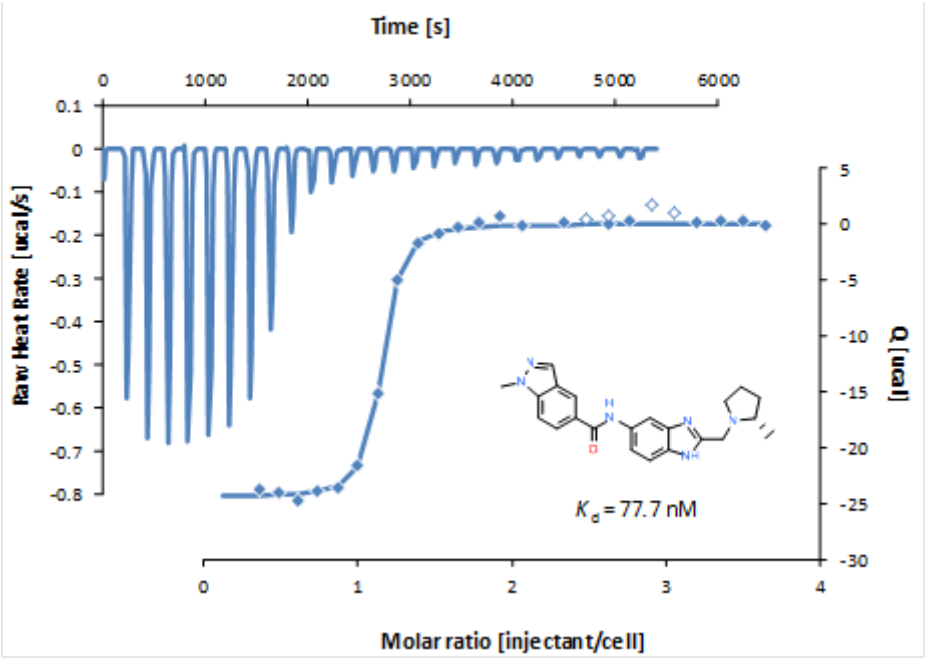

Supplementary Figure 13. *ITC trace of compound* ***328*** *and Af9 YD*

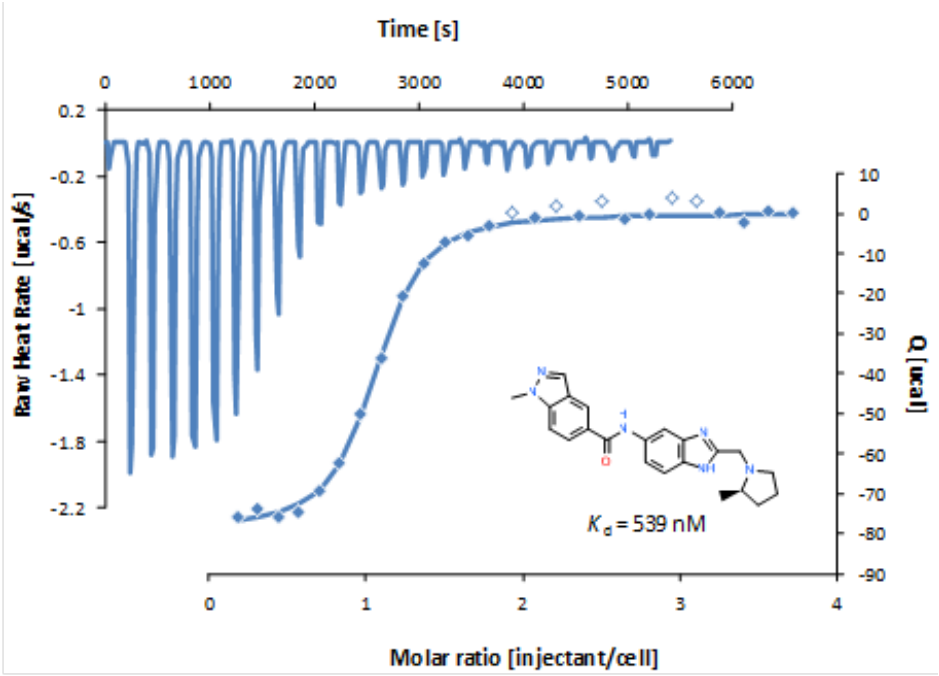

Supplementary Figure 14. *ITC trace of compound* ***327*** *and Af9 YD*

I.III *In vitro* Metabolism Studies

Metabolic stability studies were carried out exposing nominated compounds to samples of primary human hepatocytes. Compounds were analysed by LC-MS for loss of parent compound at 0, 10, 30, 60 and 120-minute time points and analysis of metabolites formed. The rate of metabolic degradation of parent compound was used to calculate, $t_{1/2}$ (summarised in Supplementary Figure 15).

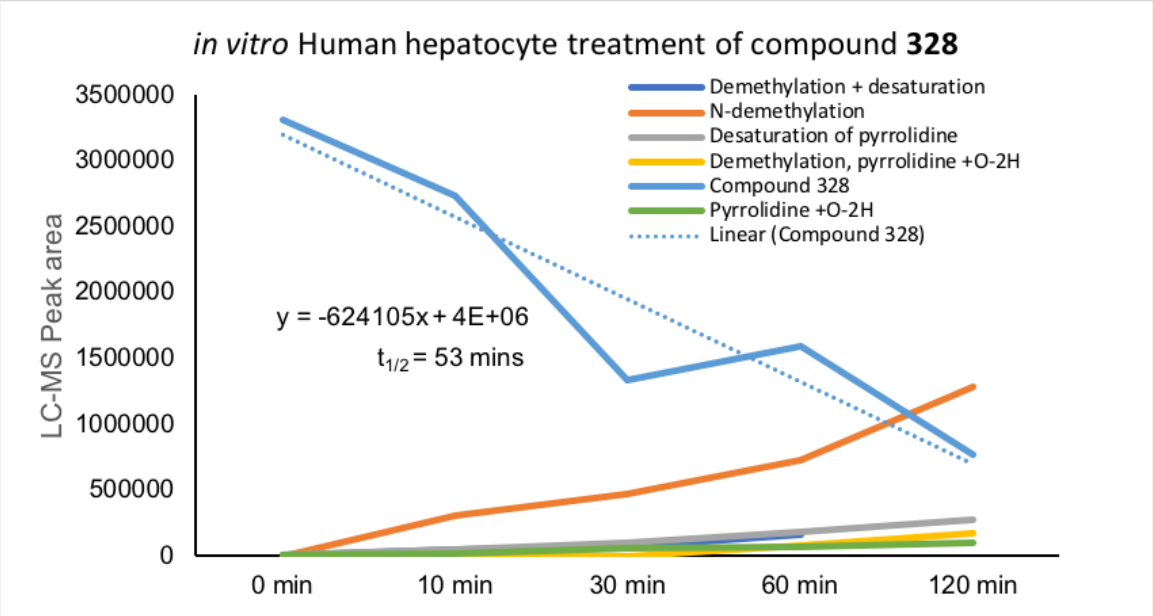

Supplementary Figure 15. *In vitro metabolic stability of compound* ***328****.*

I.IV Cellular Assays

I.IV.I NanoLuciferase Bioluminescent Resonance Energy Transfer (NanoBRET) Assay[283]

Methods

HEK293 cell (8 x 10^5) were plated in each well of a 6-well plate and co-transfected with Histone H3.3-HaloTag (NM_002107) and a NanoLuciferase fusion of ENL. Twenty hours post-transfection, cells were collected, washed with PBS, and exchanged into media containing phenol red-free DMEM and 4% FBS in the absence (control sample) or the presence (experimental sample) of 100 nM NanoBRET 618 fluorescent ligand (Promega). Cell density was adjusted to 2 x 10^5 cells/ml and then re-plated in a 96-well assay white plate (Corning Costar #3917). Compounds were then added directly to media at final concentrations 5 µM or an equivalent amount of DMSO as a vehicle control, and the plates were incubated for 18 h at 37 °C in the presence of 5% CO_2. NanoBRET Nano-Glo substrate (Promega) was added to both control and experimental samples at a final concentration of 10 µM. Readings were performed within 5 minutes using a Glo-MAX Discover instrument (Promega) equipped with 450/8 nm bandpass and

600 nm longpass filters with a 0.3 sec reading setting. A corrected BRET ratio was calculated and is defined as the ratio of the emission at 600 nm/450 nm for experimental samples (i.e. those treated with NanoBRET fluorescent ligand) subtracted by and the emission at 600 nm/450 nm for control samples (not treated with NanoBRET fluorescent ligand). BRET ratios are expressed as milliBRET units (mBU), where 1 mBU corresponds to the corrected BRET ratio multiplied by 1000.

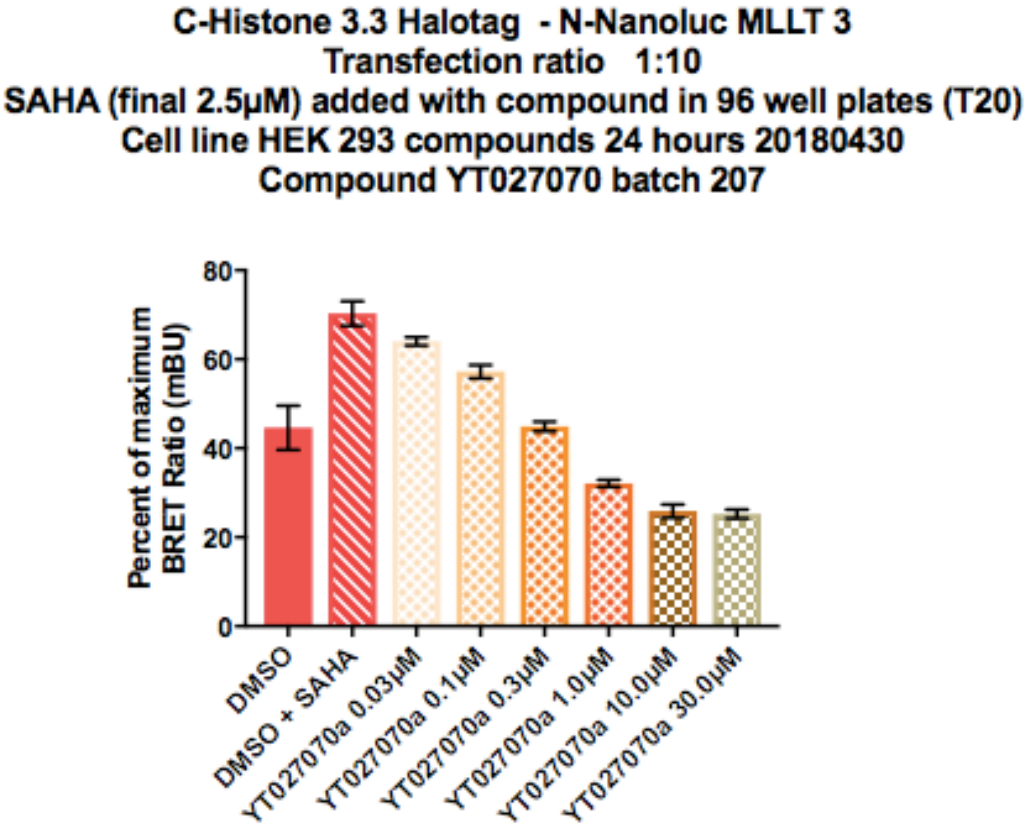

Supplementary Figure 16. *Displacement of Halotagged H3.3 from NanoLuc-ENL in HEK293 cells using the NanoBRET™ assay by compound* ***328*** *(YT027070a).*

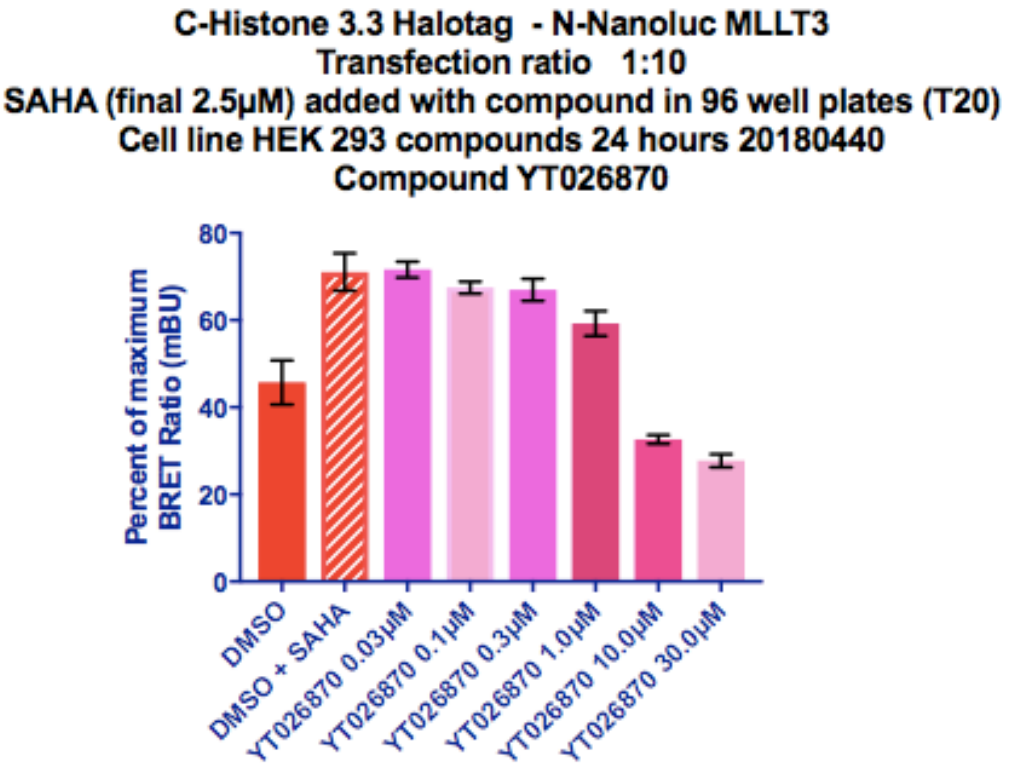

Supplementary Figure 17. *Displacement of Halotagged H3.3 from NanoLuc-ENL in HEK293 cells using the NanoBRET™ assay by compound* ***327*** *(YT026870a).*

I.IV.II Cellular Thermal Shift Assay (CETSA)

Methods

HEK293 and MV4;11 cells were cultured at 37 °C in a humidified 5% CO2 atmosphere in DMEM Medium containing 10% FBS and Iscove's Modified Dulbecco's Medium containing 10% FBS, respectively. Cells were grown until approximately 80% confluency and treated with indicated concentrations of compound **328** or **327** (0.5% DMSO final concentration) for 30 minutes. Cells were then collected, washed with PBS, transferred in PCR tubes, and pelleted by centrifugation (300 *g*, 3 min, RT.) The PBS was removed and the cell pellets heated at the indicated temperature for 3 minutes in a PCR machine (UNO96, VMR) and then placed on ice. Lysis buffer (50 mM Tris pH 7.5, 0.8% v/v NP-40, 5% v/v glycerol, 1.5 mM $MgCl_2$, 100 mM NaCl, 25 mM NaF,

1mM Na_3VO_4, 1mM PMSF, 1mM DTT, 10 µg/mL TLCK, 1 µg/mL Leupeptin, 1 µg/mL Aprotinin, 1 µg/mL soy bean trypsin, ≥250 units/mL Benzonase) was added and the cells lysed by 3 freeze-thaw cycles in liquid nitrogen. Aggregated proteins were removed by centrifugation (17000 *g*, 20 min, 4 °C) and the protein concentration of the retained soluble fraction determined. 4× sample loading buffer (Bio-Rad) containing 20% v/v DTT was added and samples were heated for 6 min at 90 °C prior to separation by SDS-PAGE. Proteins were transferred to nitrocellulose blotting membrane (Amersham, GE healthcare) and membranes were blocked with blocking buffer (2.5% (m/v) BLOT-QuickBlocker (Merck) in PBST (Phosphate-buffered saline with 0.05% (v/v) Tween 20) before probing with antibodies. Blots were imaged on an Odyssey CLx imager (LI-COR), with quantitative analysis performed using ImageQuant software. Antibodies: anti-ENL (Cell Signalling Technology, 14893, 1:500 dilution); anti-GAPDH (Santa Cruz Technology, sc-365062, 1:1000 dilution); anti-rabbit alexa fluor 680 (LI-COR, A-21109, 1:10,000 dilution); anti-mouse alexa fluor 750 (LI-COR, A-21037, 1:10,000 dilution).

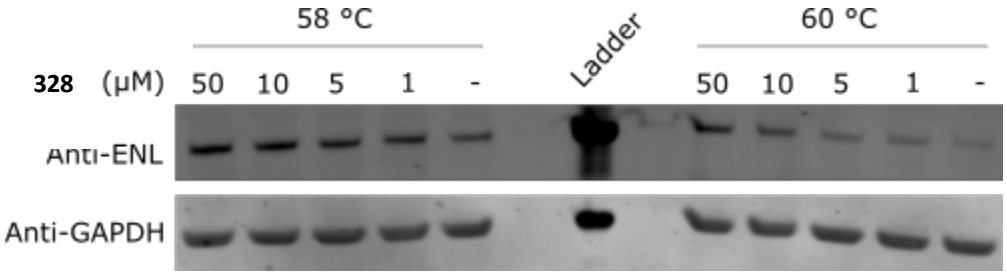

Supplementary Figure 18. *Western blot showing dose dependent heat shock stabilisation of endogenous ENL in HEK293 cells by compound* ***328****.*

Appendix 7.3.4

Experimental Procedures: Chapter 5 Formal Synthesis of Horsfiline

I Practical Experimental

I.I Synthetic Procedures

I.I Synthetic Procedures

Ethyl 2-((tert-butyldimethylsilyl)oxy)-2-(diethoxyphosphoryl)acetate (422)

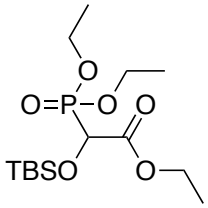

Initially 1-ethoxyphosphonoyloxyethane **421** (10 mL, 77.62 mmol) was dissolved in Toluene (17 mL) and had TEA (approximately 11.78 g, 16.23 mL, 116.4 mmol) added at 0°C over a period of 5 minutes. Ethyl 2-oxoacetate (15.39 mL, 77.62 mmol) was then added dropwise and the solution was allowed to stir for 1 hour at room temperature. The solution was then cooled to 0°C and imidazole (7.924 g, 116.4 mmol) followed by a solution of TBSCl (approximately 23.39 g, 28.88 mL, 155.2 mmol) in DMF (50 mL) was added dropwise before the white suspension was warmed to room temperature and allowed to stir overnight. Upon reaction completion, the suspension was filtered to and the resulting salts were washed with DCM (x3). The solute was then washed with ammonium chloride sat. (x2), H_2O (x2) and brine (x1) before being dried over Na_2SO_4, filtered and concentrated to a clear colourless oil. The crude oil was purified via FCC Isco Telsedyne eluting with Heptane/EA (1:0 to 4:6) to give a clear colourless oil **422** (21.1 g, 30.75 mmol, 77%).

^{1}H-NMR (400 MHz, $CDCl_3$): δ 4.58 (d, J = 18.0 Hz, 1H), 4.31 – 3.99 (m, 6H), 1.41 – 1.19 (m, 9H), 0.91 (s, 9H), 0.10 (s, 6H); **^{13}C-NMR (100 MHz $CDCl_3$): δ** 168.7, 168.7, 71.7, 70.1, 63.6, 63.6, 63.5, 61.8, 32.0, 29.2, 25.7, 22.8, 18.5, 16.6, 14.2, -5.2, -5.4; **LR-ESI-MS**: $C_{14}H_{32}O_6PSi$ $[M+H]^+$ *m/z* found 355.23, cald 355.17;

Ethyl 3-(1-((tert-butyldimethylsilyl)oxy)-2-ethoxy-2-oxoethylidene)pyrrolidine-1-carboxylate (423)

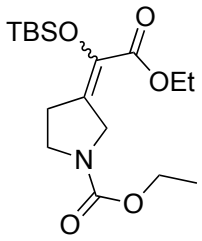

Initially a solution of ethyl 2-[tert-butyl(dimethyl)silyl]oxy-2- diethoxyphosphoryl-acetate **422** (1.111 g, 3.134 mmol) in THF (5 mL) under a N_2 atmosphere was cooled to -78°C before LiHMDS (4.7 mL, 4.70 mmol, 1.5 eq, 1 M in THF) was added dropwise over 5 minutes. The solution was stirred for 20 minutes before a solution of ethyl 3-oxopyrrolidine-1-carboxylate (0.59 g, 3.76 mmol, 1.2 eq) in THF (2 mL) was added dropwise at -78°C and allowed to stir for 30 minutes before being warmed to ambient temperature and stirred for 16 hours. Upon reaction completion the mixture was concentrated onto silica and purified via FCC Isco Telsedyne eluting with Heptane/EA (1:0 to 0:1) to give a clear yellow oil **423** (1.081 g, 3.03 mmol, 96%).

^{1}H-NMR (400 MHz, $CDCl_3$): δ 4.35 (s, 1H), 4.27 – 4.07 (m, 4H), 3.66 – 3.33 (m, 2H), 3.05 – 2.64 (m, 2H), 1.29 (m, 6H), 0.95 (s, 9H), 0.14 (s, 6H); **^{13}C-NMR (100 MHz $CDCl_3$): δ** 164.3, 164.2, 155.2, 135.4, 134.0, 133.7, 61.2, 61.0, 49.3, 44.5, 29.5, 26.0, 18.6, 14.9, 14.4, -3.9.; **LR-ESI-MS**: $C_{17}H_{32}NO_5Si$ $[M+H]^+$ *m/z* found 358.04, cald 358.21; **HR-ESI-MS**: $C_{17}H_{32}NO_5Si$ $[M+H]^+$ *m/z* found 358.2046, cald 358.2044.

Ethyl 3-(2-ethoxy-2-oxoacetyl)pyrrolidine-1-carboxylate (424)

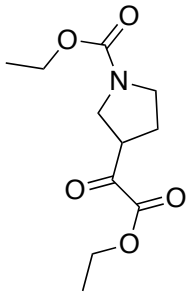

Initially Ethyl 3-(1-((tert-butyldimethylsilyl)oxy)-2-ethoxy-2-oxoethylidene)pyrrolidine-1-carboxylate **423** (609 mg, 1.703 mmol, 1.0 eq) was dissolved in acetonitrile (10.17 mL) and cooled to 0°C before AcOH (0.484 mL, 8.515 mmol, 5 eq) was added followed by CsF (517.4 mg,

3.406 mmol, 2 eq). The reaction was then allowed to stir at 0°C for 2 hours and then stirred at room temperature for 1 hour before being quenched by the addition of silica. The slurry was then concentrated to dryness and purified via FCC Isco Telsedyne eluting with Heptane/EA (1:0 to 0:1) to give a clear colourless oil **424** (0.33 g, 1.36 mmol, 80%).

^{1}H-NMR (400 MHz, $CDCl_3$): δ 4.33 (q, J = 7.1 Hz, 2H), 4.12 (q, J = 7.1 Hz, 2H), 3.97 – 3.20 (m, 4H), 2.39 – 1.95 (m, 2H), 1.37 (t, J = 7.1 Hz, 3H), 1.24 (t, J = 7.1 Hz, 3H).; **^{13}C-NMR (100 MHz $CDCl_3$): δ** 193.1, 192.9, 174.6, 160.6, 154.9, 62.8, 61.2, 27.6, 27.2, 14.8, 14.0; **LR-ESI-MS**: $C_{11}H_{18}NO_5$ $[M+H]^+$ *m/z* found 244.22, cald 244.12; **HR-ESI-MS**: $C_{11}H_{18}NO_5$ $[M+H]^+$ *m/z* found 244.1182, cald 244.1180.

Ethyl 3-(1-(benzyl(4-methoxyphenyl)amino)-2-ethoxy-2-oxoethylidene)pyrrolidine-1-carboxylate (425)

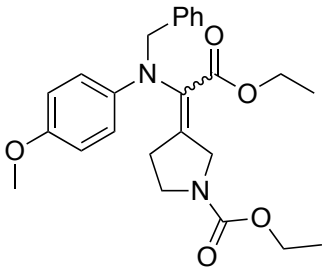

Initially ethyl 3-(2-ethoxy-2-oxo-acetyl)pyrrolidine-1-carboxylate **424** (203 mg, 0.8345 mmol), $MgSO_4$ (anhydrous) (200 mg, 2 eq), *N*-benzyl-4-methoxy-aniline **412** (267 mg, 1.252 mmol, 2 eq) and TFA (1 drop) were dissolved in benzene (4.1 mL, 0.2 M) before being stirred with microwave irradiation at 150°C for 30 minutes. The brown mixture was then filtered and concentrated onto silica before being purified via FCC Isco Telsedyne eluting with Heptane/EA (1:0 to 0:1) to give a clear yellow oil **425** (0.27 g, 0.63 mmol, 75%).

^{1}H-NMR (400 MHz, $CDCl_3$): δ 7.37 – 7.20 (m, 5H), 6.81 – 6.68 (m, 2H), 6.60 (d, J = 8.7 Hz, 2H), 4.67 – 4.46 (m, 3H), 4.26 – 3.95 (m, 5H), 3.73 (s, 3H), 3.51 (d, J = 70.6 Hz, 2H), 2.92 (dt, J = 190.7, 7.6 Hz, 2H), 2.04 (s, 1H), 1.36 – 1.01 (m, 8H); **^{13}C-NMR (100 MHz $CDCl_3$): δ** 171.3, 155.1, 155.0, 152.8, 152.7, 141.9, 128.6, 127.6, 127.4, 127.1, 127.1, 114.9, 114.7, 114.7, 61.3, 61.3, 60.9, 60.8,

60.5, 56.2, 55.8, 55.7, 44.1, 21.2, 15.0, 14.9, 14.3; **LR-ESI-MS**: $C_{25}H_{31}N_2O_5$ $[M+H]^+$ *m/z* found 439.45, cald 439.22; **HR-ESI-MS**: $C_{25}H_{31}N_2O_5$ $[M+H]^+$ *m/z* found 439.2233, cald 439.2228.

Diethyl 1-benzyl-5-methoxyspiro[indoline-3,3'-pyrrolidine]-1',2-dicarboxylate (426)

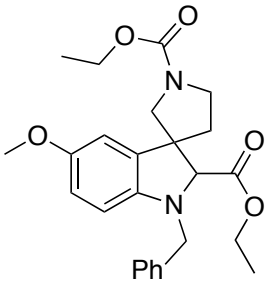

Initially Ethyl 3-(1-(benzyl(4-methoxyphenyl)amino)-2-ethoxy-2-oxoethylidene)pyrrolidine-1-carboxylate **425** (57 mg, 0.13 mmol) was dissolved in benzene (1.3 mL) and sparged with N_2 in a sealed tube for 15 minutes before being irradiated by UV-A LEDs (365 nm) in a UV-150 photoreactor (Vaportec) flow (0.25 mL/min, 30°C, 1 bar, 10 mL reaction coil, 40 min residence time). Upon completion the collected fraction was concentrated to a yellow oil and used without further purification as a mixture of rotameric diastereomers **426** (57 mg, 0.13 mmol, *quant.*)

^{1}H-NMR (400 MHz, $CDCl_3$): δ 7.40 – 7.22 (m, 5H), 6.62 (d, J = 2.0 Hz, 2H), 6.43 – 6.30 (m, 1H), 4.51 – 4.36 (m, 1H), 4.25 – 3.94 (m, 5H), 3.85 – 3.30 (m, 7H), 2.37 – 1.88 (m, 2H), 1.36 – 1.10 (m, 7H); **^{13}C-NMR (100 MHz $CDCl_3$): δ** 170.7, 170.5, 170.4, 155.2, 155.1, 155.1, 153.6, 144.9, 144.7, 144.7, 137.5, 137.5, 133.9, 133.8, 133.2, 133.0, 128.7, 128.2, 128.1, 127.5, 127.5, 113.2, 112.9, 112.7, 110.0, 109.8, 108.2, 108.1, 107.7, 75.4, 74.2, 73.8, 61.3, 61.2, 61.1, 56.3, 56.1, 54.5, 54.1, 53.7, 53.2, 52.8, 52.7, 52.5, 52.3, 52.1, 45.3, 45.0, 44.8, 44.4, 38.8, 37.6, 33.5, 32.6, 14.9, 14.9, 14.4, 14.2; **LR-ESI-MS**: $C_{25}H_{31}N_2O_5$ [M+H]+ m/z found 439.40, cald 439.22; **HR-ESI-MS**: $C_{25}H_{31}N_2O_5$ $[M+H]^+$ *m/z* found 439.2234, cald 439.2228.

Ethyl 1-benzyl-5-methoxy-2-oxospiro[indoline-3,3'-pyrrolidine]-1'-carboxylate (427)

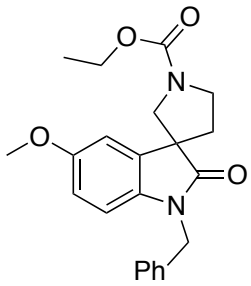

Initially Diethyl 1-benzyl-5-methoxy-spiro[indoline-3,3'-pyrrolidine]-1',2-dicarboxylate **426** (50 mg, 0.1140 mmol) was dissolved in MeOH (300 µL) in a quartz glass vial and then had a solution of LiOH (0.97 mL, 2 M aqueous, 1.938 mmol, 17 eq) added. The suspension was stirred for 72 hours with UV-A (365 nm) irradiation using a UV-photobox. The mixture was then concentrated onto Si-amine gel and purified via FCC Isco Telsedyne Silica-NH_2 eluting with Heptane/EA (1:0 to 8:2) to give a clear wax **427** (10.3 mg, 0.024 mmol, 22%).

^{1}H-NMR (400 MHz, $CDCl_3$): δ 7.38 – 7.19 (m, 5H), 6.84 – 6.77 (m, 1H), 6.70 (d, J = 8.7 Hz, 1H), 6.63 (dd, J = 8.5, 3.0 Hz, 1H), 4.90 (s, 2H), 4.27 – 4.09 (m, 2H), 4.02 – 3.49 (m, 6H), 2.48 (dt, J = 12.9, 8.3 Hz, 1H), 2.24 – 1.94 (m, 1H), 1.32 (t, J = 7.0 Hz, 3H); **^{13}C-NMR (100 MHz $CDCl_3$): δ** 177.4, 177.1, 175.8, 156.3, 155.0, 135.7, 128.8, 127.7, 127.2, 112.3, 112.0, 110.5, 110.2, 109.6, 109.6, 61.3, 55.8, 55.8, 54.5, 54.1, 53.3, 52.3, 45.6, 45.2, 43.9, 36.4, 35.6, 29.7, 14.8; **LR-ESI-MS**: $C_{22}H_{25}N_2O_4$ $[M+H]^+$ *m/z* found 381.30, cald 381.18; **HR-ESI-MS**: $C_{22}H_{25}N_2O_4$ $[M+H]^+$ *m/z* found 381.1810, cald 381.1809.

1'-benzyl-5'-methoxyspiro[cyclopentane-1,3'-indolin]-2'-one (453)

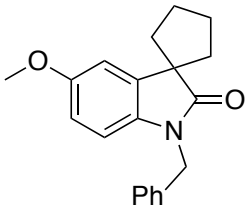

Initially ethyl 1'-benzyl-5'-methoxy-spiro[cyclopentane-1,3'-indoline]-2'-carboxylate (74 mg, 0.241 mmol, 1 eq) was dissolved in MeOH (2.4 mL) and had a solution of $LiOH.H_2O$ (1.2 mL, 2 M, 10 eq) added dropwise before the suspension was warmed to 125°C for 1 hour in a microwave. Upon reaction completion the mixture was concentrated onto silica gel and purified via purified

via FCC Isco Telsedyne eluting with DCM/MeOH (1:0 to 8:2) to give a clear colourless oil **453** (18.5 mg, 0.062 mmol, 25%).

^{1}H-NMR (400 MHz, $CDCl_3$): δ 7.35 – 7.20 (m, 5H), 6.82 (d, J = 2.4 Hz, 1H), 6.63 (dd, J = 8.5, 2.5 Hz, 1H), 6.57 (d, J = 8.5 Hz, 1H), 4.89 (s, 2H), 3.75 (s, 3H), 2.31 – 2.17 (m, 2H), 2.17 – 2.05 (m, 2H), 2.04 – 1.94 (m, 2H), 1.93 – 1.83 (m, 2H); **^{13}C-NMR (100 MHz $CDCl_3$): δ** 181.9, 156.2, 138.3, 136.4, 135.6, 128.9, 127.6, 127.3, 111.1, 110.4, 109.1, 55.9, 54.5, 43.9, 38.7, 26.9; **LR-ESI-MS**: $C_{20}H_{22}NO_2$ $[M+H]^+$ *m/z* found 308.24, cald 308.17; **HR-ESI-MS**: $C_{20}H_{22}NO_2$ $[M+H]^+$ *m/z* found 308.164, cald 308.1645.

Ethyl 1'-benzyl-5'-methoxyspiro[cyclopentane-1,3'-indoline]-2'-carboxylate (450)

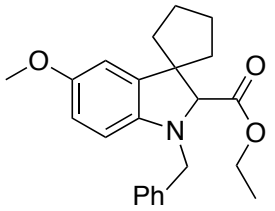

Initially ethyl 5'-methoxyspiro[cyclopentane-1,3'-indoline]-2'-carboxylate (518 mg, 1.88 mmol, 1 eq) was dissolved in MeCN (12.5 mL, 0.15 M) and had K_2CO_3 (390 mg, 2.82 mmol, 1.5 eq) added before BnBr (290 µL, 2.45 mmol, 1.3 eq) was added dropwise and the solution was heated to 120°C for 2 hours in a microwave with stirring. Upon reaction completion the mixture was concentrated onto silica gel and purified via FCC Isco Telsedyne eluting with Heptane/EA (1:0 to 1:1) to give a clear yellow oil **450** (352 mg, 0.963 mmol, 51%).

^{1}H-NMR (400 MHz, $CDCl_3$): δ 7.35 – 7.15 (m, 5H), 6.57 (d, J = 2.6 Hz, 1H), 6.51 (dd, J = 8.4, 2.6 Hz, 1H), 6.24 (d, J = 8.4 Hz, 1H), 4.37 (d, J = 15.1 Hz, 1H), 4.11 (qd, J = 7.1, 0.6 Hz, 2H), 4.00 (d, J = 15.1 Hz, 1H), 3.92 (s, 1H), 3.67 (s, 3H), 2.13 – 1.99 (m, 1H), 1.95 – 1.84 (m, 1H), 1.84 – 1.56 (m, 4H), 1.19 (t, J = 7.1 Hz, 3H); **LR-ESI-MS**: $C_{23}H_{28}NO_3$ $[M+H]^+$ *m/z* found 366.31, cald 366.21.

Ethyl 5'-methoxyspiro[cyclopentane-1,3'-indoline]-2'-carboxylate (441)

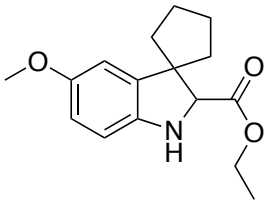

Ethyl 2-cyclopentylidene-2-((4-methoxyphenyl)amino)acetate **429** (1.27g, 4.58 mmol, 1 eq) was dissolved in benzene (15 mL, 0.3 M) and sparged with a N_2 balloon for 15 minutes before the solution was irradiated with UV-A LEDs (365 nm) in a UV-150 photoreactor (Vaportec) flow (0.25 mL/min, 30°C, 1 bar, 10 mL reaction coil, 40 min residence time). Upon reaction completion the solution was concentrated onto silica gel and purified via FCC Isco Telsedyne eluting with Heptane/EA (1:0 to 0:1) to give a clear colourless oil **441** (518 mg, 1.88 mmol, 40%).

^{1}H-NMR (400 MHz, $CDCl_3$): δ 6.74 – 6.57 (m, 3H), 4.28 – 4.15 (m, 4H), 3.75 (s, 3H), 2.16 – 1.91 (m, 2H), 1.84 (ddd, J = 5.3, 2.2, 0.9 Hz, 2H), 1.79 – 1.63 (m, 2H), 1.30 (t, J = 7.1 Hz, 3H); **^{13}C-NMR (100 MHz $CDCl_3$): δ** 173.0, 154.5, 142.6, 139.5, 112.2, 111.1, 109.5, 71.6, 61.1, 57.4, 56.1, 40.5, 35.9, 25.4, 25.2, 14.4; **HR-ESI-MS**: $C_{16}H_{22}NO_3$ $[M+H]^+$ *m/z* found 276.1593, cald 276.1594.

Ethyl 2-cyclopentylidene-2-((4-methoxyphenyl)amino)acetate (429)

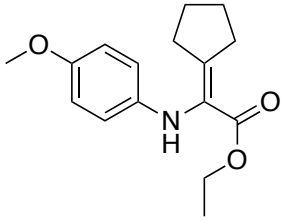

To a suspension of *p*-anisidine **412** (2.24 g, 18.2 mmol, 2 eq), ethyl 2-cyclopentyl-2-oxo-acetate (1.55 g, 9.1 mmol, 1 eq) and $MgSO_4$ anhy. (1.5 g) in benzene (12 mL, 0.8 M) was added one drop of TFA. The suspension was then heated in the microwave at 150°C for 30 minutes before being concentrated down onto silica gel and purified via FCC Isco Telsedyne eluting with Heptane/EA (1:0 to 0:1) to give a clear yellow oil **429** (1.30 g, 4.71 mmol, 52%).

^{1}H-NMR (400 MHz, $CDCl_3$): δ 6.76 (d, J = 9.0 Hz, 2H), 6.62 – 6.52 (m, 2H), 5.12 (s, 1H), 4.19 (q, J = 7.1 Hz, 2H), 3.74 (s, 3H), 2.89 – 2.74 (m, 2H), 2.33 (tt, J = 7.1, 1.5 Hz, 2H), 1.84 – 1.68 (m, 2H),

1.70 – 1.51 (m, 2H), 1.25 (t, J = 7.1 Hz, 3H); **LR-ESI-MS**: $C_{16}H_{22}NO_3$ $[M+H]^+$ *m/z* found 276.28, cald 276.16;

Ethyl 2-cyclopentylidene-2-((3-methoxyphenyl)amino)acetate (430)

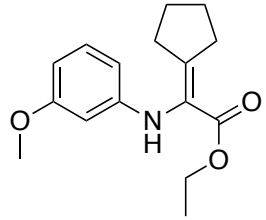

To a suspension of *m*-anisidine (290 mg, 2.35 mmol, 2 eq), ethyl 2-cyclopentyl-2-oxo-acetate (200 mg, 1.18 mmol, 1 eq) and MgSO4 anhy. (300 mg) in benzene (4 mL, 0.29 M) was added one drop of TFA. The suspension was then heated in the microwave at 150°C for 30 minutes before being concentrated down onto silica gel and purified via FCC Isco Telsedyne eluting with Heptane/EA (1:0 to 0:1) to give a clear yellow oil **430** (221 mg, 0.80 mmol, 68%).

^{1}H-NMR (400 MHz, $CDCl_3$): δ 7.07 (t, J = 8.1 Hz, 1H), 6.32 (ddd, J = 8.2, 2.4, 0.9 Hz, 1H), 6.22 (ddd, J = 8.1, 2.2, 0.9 Hz, 1H), 6.14 (t, J = 2.3 Hz, 1H), 5.29 (s, 1H), 4.19 (q, J = 7.1 Hz, 2H), 3.74 (s, 3H), 2.86 (tt, J = 7.3, 1.3 Hz, 2H), 2.40 (tt, J = 7.2, 1.4 Hz, 2H), 1.83 – 1.72 (m, 2H), 1.70 – 1.59 (m, 2H), 1.25 (t, J = 7.1 Hz, 3H); **^{13}C-NMR (100 MHz $CDCl_3$): δ** 166.0, 160.7, 157.4, 146.8, 129.8, 121.8, 107.3, 103.7, 100.3, 60.6, 55.1, 34.1, 33.0, 27.1, 25.5, 14.3; LR-ESI-MS: $C_{16}H_{22}NO_3$ [M+H]+ m/z found 276.28, cald 276.16; **HR-ESI-MS**: $C_{16}H_{22}NO_3$ $[M+H]^+$ *m/z* found 276.1597, cald 276.1594.

Ethyl 2-cyclopentylidene-2-((2-methoxyphenyl)amino)acetate (431)

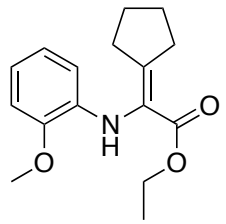

To a suspension of *o*-anisidine (290 mg, 2.35 mmol, 2 eq), ethyl 2-cyclopentyl-2-oxo-acetate (200 mg, 1.18 mmol, 1 eq) and MgSO4 anhy. (300 mg) in benzene (4 mL, 0.29 M) was added one drop of TFA. The suspension was then heated in the microwave at 150°C for 30 minutes before

being concentrated down onto silica gel and purified via FCC Isco Telsedyne eluting with Heptane/EA (1:0 to 0:1) to give a clear yellow oil **431** (211 mg, 0.76 mmol, 65%).

^{1}H-NMR (400 MHz, $CDCl_3$): δ 6.88 – 6.76 (m, 2H), 6.73 (td, J = 7.7, 1.7 Hz, 1H), 6.39 (dd, J = 7.7, 1.6 Hz, 1H), 5.68 (s, 1H), 4.19 (q, J = 7.1 Hz, 2H), 3.89 (s, 3H), 2.99 – 2.81 (m, 2H), 2.43 (tt, J = 7.1, 1.4 Hz, 2H), 1.88 – 1.72 (m, 2H), 1.72 – 1.61 (m, 2H), 1.24 (t, J = 7.1 Hz, 3H); **^{13}C-NMR (100 MHz $CDCl_3$): δ** 166.0, 157.3, 147.3, 135.0, 121.7, 120.7, 117.8, 111.6, 110.0, 60.5, 55.5, 33.9, 33.0, 27.2, 25.5, 14.3; LR-ESI-MS: $C_{16}H_{22}NO_3$ [M+H]+ m/z found 276.28, cald 276.16; **HR-ESI-MS**: $C_{16}H_{22}NO_3$ $[M+H]^+$ *m/z* found 276.1597, cald 276.1594.

Ethyl 6'-methoxyspiro[cyclopentane-1,3'-indoline]-2'-carboxylate (442)

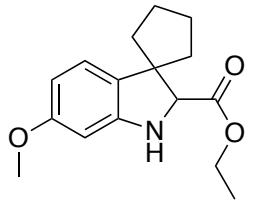

Ethyl 2-cyclopentylidene-2-((3-methoxyphenyl)amino)acetate **430** (78 mg, 0.29 mmol, 1 eq) was dissolved in benzene (3 mL, 0.1 M) and sparged with a N2 balloon for 15 minutes before the solution was irradiated with UV-A LEDs (365 nm) in a UV-150 photoreactor (Vaportec) flow (0.25 mL/min, 30°C, 1 bar, 10 mL reaction coil, 40 min residence time). Upon reaction completion the solution was concentrated onto silica gel and purified via FCC Isco Telsedyne eluting with Heptane/EA (1:0 to 0:1) to give a clear colourless oil **442** (34 mg, 0.12 mmol, 43%).

^{1}H-NMR (400 MHz, $CDCl_3$): δ 6.91 (dd, J = 7.8, 0.7 Hz, 1H), 6.36 – 6.28 (m, 2H), 4.30 – 4.18 (m, 3H), 3.77 (s, 3H), 2.15 – 2.03 (m, 1H), 1.99 – 1.67 (m, 7H), 1.32 (t, J = 7.1 Hz, 3H); **^{13}C-NMR (100 MHz $CDCl_3$): δ** 173.0, 160.1, 150.4, 129.5, 122.5, 104.7, 96.7, 71.4, 61.0, 56.4, 55.5, 40.9, 35.8, 25.0, 24.8, 14.4; **LR-ESI-MS**: $C_{16}H_{22}NO_3$ $[M+H]^+$ *m/z* found 276.28, cald 276.16; **HR-ESI-MS**: $C_{16}H_{22}NO_3$ $[M+H]^+$ *m/z* found 276.1594, cald 276.1594.

Ethyl 7'-methoxyspiro[cyclopentane-1,3'-indoline]-2'-carboxylate (443)

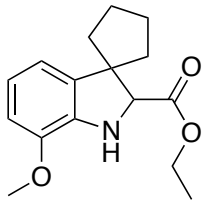

Ethyl 2-cyclopentylidene-2-((2-methoxyphenyl)amino)acetate **431** (84 mg, 0.30 mmol, 1 eq) was dissolved in benzene (3 mL, 0.1 M) and sparged with a N_2 balloon for 15 minutes before the solution was irradiated with UV-A LEDs (365 nm) in a UV-150 photoreactor (Vaportec) flow (0.25 mL/min, 30°C, 1 bar, 10 mL reaction coil, 40 min residence time). Upon reaction completion the solution was concentrated onto silica gel and purified via FCC Isco Telsedyne eluting with Heptane/EA (1:0 to 0:1) to give a clear colourless oil **443** (51 mg, 0.18 mmol, 61%).

^{1}H-NMR (400 MHz, $CDCl_3$): δ 6.80 – 6.73 (m, 1H), 6.68 (t, J = 1.3 Hz, 1H), 6.66 (dd, J = 2.5, 1.1 Hz, 1H), 4.33 – 4.13 (m, 3H), 3.83 (s, 3H), 2.20 – 2.06 (m, 1H), 1.97 (dd, J = 13.1, 6.7 Hz, 1H), 1.91 – 1.78 (m, 4H), 1.77 – 1.64 (m, 2H), 1.30 (t, J = 7.1 Hz, 3H); **^{13}C-NMR (100 MHz $CDCl_3$): δ** 172.8, 145.5, 138.1, 137.8, 120.5, 114.6, 109.5, 71.5, 61.0, 57.7, 55.5, 40.7, 35.7, 25.3, 25.1, 14.4; **LR-ESI-MS**: $C_{16}H_{22}NO_3$ $[M+H]^+$ *m/z* found 276.28, cald 276.16; **HR-ESI-MS**: $C_{16}H_{22}NO_3$ $[M+H]^+$ *m/z* found 276.1593, cald 276.1594.